Nanotechnology and Drug Delivery

Volume 1

Nanoplatforms in Drug Delivery

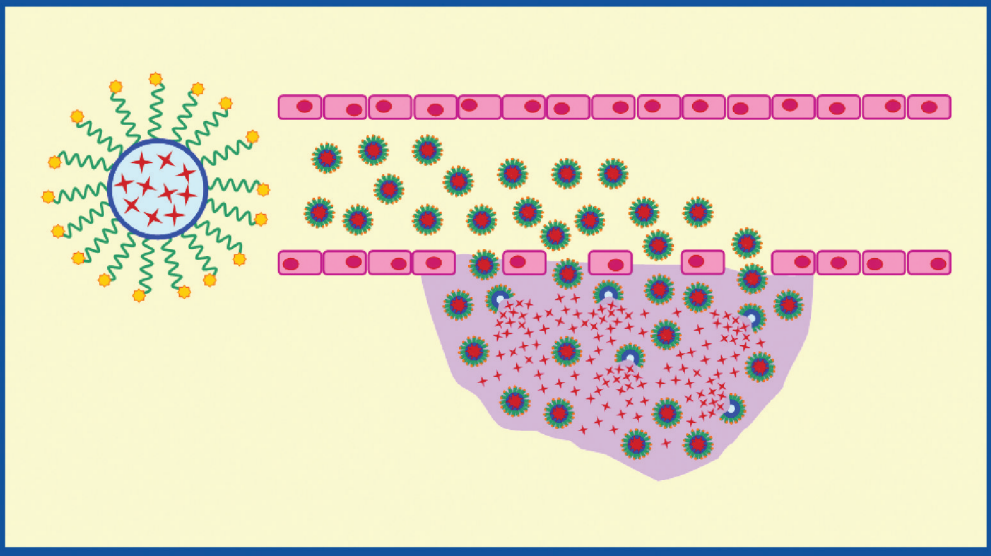

Editor

José L. Arias

CRC Press
Taylor & Francis Group
A SCIENCE PUBLISHERS BOOK

Nanotechnology and Drug Delivery

Volume 1: Nanoplatforms in Drug Delivery

Nanotechnology and Drug Delivery

Volume 1: Nanoplatforms in Drug Delivery

Editor

Professor Dr. José L. Arias

Department of Pharmacy and Pharmaceutical Technology
Faculty of Pharmacy
University of Granada
Campus Universitario de Cartuja s/n
18071 Granada, Spain

CRC Press
Taylor & Francis Group
Boca Raton London New York

CRC Press is an imprint of the
Taylor & Francis Group, an **informa** business

A SCIENCE PUBLISHERS BOOK

CRC Press
Taylor & Francis Group
6000 Broken Sound Parkway NW, Suite 300
Boca Raton, FL 33487-2742

© 2015 by Taylor & Francis Group, LLC
CRC Press is an imprint of Taylor & Francis Group, an Informa business

No claim to original U.S. Government works
Version Date: 20140715

International Standard Book Number-13: 978-1-4665-9948-2 (eBook - PDF)

This book contains information obtained from authentic and highly regarded sources. Reasonable efforts have been made to publish reliable data and information, but the author and publisher cannot assume responsibility for the validity of all materials or the consequences of their use. The authors and publishers have attempted to trace the copyright holders of all material reproduced in this publication and apologize to copyright holders if permission to publish in this form has not been obtained. If any copyright material has not been acknowledged please write and let us know so we may rectify in any future reprint.

Except as permitted under U.S. Copyright Law, no part of this book may be reprinted, reproduced, transmitted, or utilized in any form by any electronic, mechanical, or other means, now known or hereafter invented, including photocopying, microfilming, and recording, or in any information storage or retrieval system, without written permission from the publishers.

For permission to photocopy or use material electronically from this work, please access www.copyright.com (http://www.copyright.com/) or contact the Copyright Clearance Center, Inc. (CCC), 222 Rosewood Drive, Danvers, MA 01923, 978-750-8400. CCC is a not-for-profit organization that provides licenses and registration for a variety of users. For organizations that have been granted a photocopy license by the CCC, a separate system of payment has been arranged.

Trademark Notice: Product or corporate names may be trademarks or registered trademarks, and are used only for identification and explanation without intent to infringe.

Visit the Taylor & Francis Web site at
http://www.taylorandfrancis.com

and the CRC Press Web site at
http://www.crcpress.com

Preface to The Book Series

Pharmacotherapy is frequently associated with inefficacy and toxicity problems limiting disease treatment and prognosis and the quality of life of patients. Such incidences have been described even during the clinical use of new drug molecules, dosage forms and more sophisticated treatment schedules. To beat the challenge, recent advances in drug therapy have involved the introduction of nanotechnology in the development of medicines. In fact, drug-loaded nanoplatforms (the so-called nanomedicines) are expected to become the definitive step toward a successful pharmacotherapy. These nanocarriers are wisely engineered to maximize drug accumulation into non-healthy tissues and cells, thus optimizing the pharmacokinetics and pharmacodynamics of active molecules, while minimizing their systemic side effects. In addition, new synthesis methodologies in nanomedicine formulation, the theranosis conceptualization, have made possible to combine disease diagnosis and therapy, thus opening the door to "personalized" medicines.

In line with all these revolutionary progresses in the drug delivery field, "Nanotechnology and Drug Delivery" is a series of two volumes analyzing the fundaments and more advanced aspects in the development of nanomedicines. The selected book chapter contributions have been written by well-known experts in the field, and comprise insights into the most promising moves toward superior drug-loaded nanoplatforms. Original concepts derived from advanced materials science, physical chemistry and medicinal chemistry with critical applicability into the clinic are emphasized in the book series.

The first volume "Nanoplatforms in Drug Delivery" is focused on the physicochemical engineering of nanomedicines, their pharmacokinetics, biocompatibility and biodegradability aspects, representative nanoplatforms (based on lipids, polymers, cyclodextrins, metals, carbon, silica, iron oxides, etc.) for an efficient drug delivery, and advanced nano-engineering strategies for passive, ligand-mediated and/or stimuli-sensitive drug targeting. As an ideal complement to this book, the second volume "Nano-Engineering Strategies and Nanomedicines against Severe Diseases" further discusses the possibilities of nanotechnology, in the context of nanomedicine, for

oral, dental, topical and transdermal, pulmonary and nasal, ocular and otic, vaginal and brain drug delivery and targeting. Furthermore, an updated point of view is given to nanomedicines against severe diseases, i.e., cancer, cardiovascular diseases, neurodegenerative disorders, infectious diseases, chronic inflammatory diseases and metabolic diseases. Gene delivery and the recent concept of nanotheranosis are also analyzed in the book.

In my opinion, the book series will give a complete overview on the current state of the art, including more revolutionary conceptualizations, and future perspectives in nanotechnology and drug delivery. It will also be a vast source of knowledge not only to non-expert but also to senior researchers in the field of advanced drug delivery to severe diseases. Last but not least, I would like to thank all the contributors to the book series for the excellent work accomplished. It has been a privilege to work with them.

Professor Dr. José L. Arias

Preface to Volume 1

The development of platforms for drug delivery purposes have been classically based on the engineering of micro- and nano-particulate systems that can optimize the specificity of any given active agent for the disease site. However, conventional drug carriers were found unable to perfectly meet the challenge, mainly given their inadequate pharmacokinetic properties (rapid plasma clearance and elimination by the reticuloendothelial system) and poor drug vehiculization capabilities (low loading values and rapid release). As a consequence, there was a huge demand for new ideas revolutionizing the *status quo* in the drug delivery arena. In this line, recently published research articles have described the benefits coming from engineering nanoplatforms with excellent drug vehiculization properties, and capable of perfectly controlling the biological fate of drug molecules: maximization of drug levels into non-healthy tissues and/or cells (drug efficacy), while drug biodistribution into non-targeted sites is kept to a very minimum (drug safety).

In line with this reconceptualization of drug delivery, the first volume "Nanoplatforms in Drug Delivery" of the book series "Nanotechnology and Drug Delivery" is devoted to the analysis and discussion of the most representative physicochemical engineering approaches to the formulation of nanocarriers with the best drug vehiculization characteristics and controllable biological fate. In this respect, an important factor to be considered is the material to be used in nanoplatform development, i.e., polymers, cyclodextrins, lipids, carbon, silica, metals, iron oxides, etc. In fact, only an intelligent design and chemical engineering of the particulate structure will assure a satisfactory drug loading and release, an efficient *in vivo* behavior, biocompatibility and biodegradability and adequate pharmacokinetic properties. Even more, engineering strategies for passive, ligand-mediated and/or stimuli-sensitive drug targeting clearly depend on the materials used in the formulation of the nanomedicine.

The selected book chapters included in this book comprise insights into the most promising moves toward conventional and more advanced conceptualizations in nanomedicine formulation coming from physical chemistry, materials science, and medicinal chemistry. Chapter 1 (Key Aspects in Nanotechnology and Drug Delivery) could be considered as

an interesting introduction to the design and synthesis of drug-loaded nanoplatforms which updates the current state of the art and future perspectives in the field. Essential elements to be included in the preparation of competent drug delivery systems are analyzed, including basic nanotoxicity concepts, and particular attention is given to the description of formulation strategies facilitating the control over nanoparticle biodistribution, and the development of theranostic nanotools.

At this point in the book, the reader will be able to gain access to chapters devoted to the most representative materials selected for the synthesis of efficient drug-loaded nanoplatforms. Concretely, Chapters 2 (Drug Delivery and Release from Polymeric Nanomaterials) and 3 (Nano-Sized Polymeric Drug Carrier Systems) by Prof. Vasile and co-workers discuss the fundaments and recent advances in the preparation of polymer-based drug delivery systems. The authors also describe the most important aspects related to their rational design and (bio)evaluation, i.e., stability, drug vehiculization capacity (loading and release properties), correlation between design and drug release properties, interconnection between the route of administration and mechanism of drug release, kinetics/pharmacokinetics and biodistribution.

The contribution by the research group of Prof. Lam (Chapter 4: Reversible Cross-Linked Polymeric Nanoplatform in Drug Delivery) discuss the promising development of reversibly cross-linked polymeric micelles for targeted drug delivery. These nanoplatforms are characterized by a superior structural stability, and the capability to respond to endogenous and/or exogenous stimuli that can modulate drug release. The chapter is further focused on the strategies used for the design, preparation and cross-linking, stimuli-responsive capability and triggered drug release. *In vitro* and *in vivo* evidence demonstrating the effectiveness of reversibly cross-linked micelles is also presented and, of course, biomedical applications and future perspectives in their development are explored.

The potential use of cyclodextrins in drug delivery is carefully analyzed by Prof. Bilensoy and co-worker (Chapter 5: Cyclodextrins in Drug Delivery). This chapter provides an interesting overview on the most important characteristics (i.e., stability, drug solubility and dissolution, bioavailability and safety), and use of cyclodextrins and their derivatives as excipients in drug formulation and in the design of advanced drug delivery systems, e.g., liposomes, microspheres, microcapsules and nanoparticles.

Recent developments and future perspectives related to the technology of biodegradable nano-sized drug carriers made of tyrosine-derived amphiphilic block copolymers are examined in Chapter 6 [Drug Delivery Systems Based on Tyrosine-derived Nanospheres (TyroSpheres™)] by Prof. Michniak-Kohn and co-workers. TyroSpheres™ are vehicles for lipophilic drugs made of tyrosine dipeptide derivatives, naturally occurring diacid

and poly(ethylene glycol), while the hydrophobic segments of polymers are based on naturally occurring metabolites. It is justified in the chapter how chemical composition determines the physicochemical properties and core-shell structure of these drug delivery systems and, thus, the drug vehiculization properties and *in vivo* fate. In addition, the potential use of TyroSpheres™ for the topic and intravenous delivery of drug molecules in the treatment of skin diseases and breast cancer is discussed.

Recent achievements in the formulation of carbon nanotubes for drug delivery purposes are very carefully described by Prof. Rosen and co-worker in Chapter 7 (Carbon Nanotubes for Drug Delivery Applications). Their large surface area, high aspect ratio and extraordinary electrical and mechanical characteristics have called the attention of scientists. Synthesis methodologies, toxicological aspects and applications of carbon nanotubes, ranging from cancer therapy to gene therapy, are also commented on in the chapter.

Chapter 8 (Metallic Nanoparticulate Drug Delivery Systems) by the research group of Prof. Pokharkar analyzes the introduction and possibilities of metal- and metal oxide-based nanoparticulate tools in targeted drug delivery. More relevant synthesis procedures, biological and design aspects, and surface engineering approaches in nanoparticulate development are also the objective of this contribution. As well, the most significant properties, characterization methodologies, regulatory perspectives and biomedical applications of metallic nanomaterials are emphasized in the chapter.

Prof. Trewyn and co-worker focus on recent efforts in the development of porous silica-based drug delivery systems, as well as investigations on their *in vitro* and *in vivo* applications (Chapter 9: Porous Silica Nanoparticles for Drug Delivery and Controlled Release). The contribution reviews the more interesting approaches to the synthesis and characterization of versatile porous silica nanoparticles, and current progress in their functionalization with specific cell and antigen targeting moieties, organic components and inorganic nanoparticles. It is also highlighted that a triggered drug release from these nanoplatforms is possible by physical, chemical or biological external or internal stimuli. Finally, this chapter also includes an analysis of the investigations on the biocompatibility and on the internalization efficiency of porous silica nanoparticles by cells.

The contributions written by Prof. Sahoo and co-worker (Chapter 10: Iron Oxides in Drug Delivery), and Prof. Misra (Chapter 11: Nanoengineered Magnetic Field-Induced Targeted Drug Delivery System with Stimuli Responsive Release) extend the interest of the book to the use of iron oxides in drug (and gene) delivery and hyperthermia. In fact, Chapter 10 is devoted to the analysis of the more representative preparation procedures to obtain iron oxide nanoparticles. Interestingly, the improvement of drug

delivery by these nanotools on the basis of passive and/or active targeting strategies is described. Finally, the possibilities of hybrid (i.e., gold-coated, silica-coated and platinum-containing) magnetic nanoparticles in drug delivery are commented. With respect to Chapter 11, all aspects related to the development of a magnetic core/shell nanoparticulate system are carefully described. This is based on the analysis of recent research by the author. The structure of this nanoplatform is typically characterized by a magnetic core surrounded by a shell where the drug is loaded. It is demonstrated in the chapter that a clever engineering of the nanocomposite allows the introduction of temperature- and pH-responsive functionalities for a controllable drug delivery and release. The focus of the contribution further explores additional characteristics exhibited by the magnetic nanoparticulate system, i.e., tumor targeting, carrier imaging and monitoring, localized and targeted heat and controlled drug release.

The selected book chapter contributions to the first volume "Nanoplatforms in Drug Delivery" of the book series "Nanotechnology and Drug Delivery" will be a plentiful source of updated background information and conceptualization to scientists involved in the formulation and clinical development of nanomedicines. To end with, I would like to thank all the authors for the outstanding contributions to this volume.

Professor Dr. José L. Arias

Contents

Preface to The Book Series **v**

Preface to Volume 1 **vii**

1. **Key Aspects in Nanotechnology and Drug Delivery** **1**
   José L. Arias

2. **Drug Delivery and Release from Polymeric Nanomaterials** **28**
   Cornelia Vasile, Ana Maria Oprea, Manuela Tatiana Nistor and *Anca-Maria Cojocariu*

3. **Nano-Sized Polymeric Drug Carrier Systems** **81**
   Cornelia Vasile, Manuela Tatiana Nistor and *Anca-Maria Cojocariu*

4. **Reversible Cross-Linked Polymeric Nanoplatform in Drug Delivery** **142**
   Yuanpei Li, Kai Xiao and *Kit S. Lam*

5. **Cyclodextrins in Drug Delivery** **178**
   Nazlı Erdoğar and *Erem Bilensoy*

6. **Drug Delivery Systems Based on Tyrosine-derived Nanospheres (TyroSpheres™)** **210**
   Zheng Zhang, Tannaz Ramezanli, Pei-Chin Tsai and *Bozena B. Michniak-Kohn*

7. **Carbon Nanotubes for Drug Delivery Applications** **233**
   Yitzhak Rosen and *Pablo Gurman*

8. **Metallic Nanoparticulate Drug Delivery Systems** **249**
   Varsha B. Pokharkar, Vividha V. Dhapte and *Shivajirao S. Kadam*

9. **Porous Silica Nanoparticles for Drug Delivery and Controlled Release** **290**
   Xiaoxing Sun and *Brian G. Trewyn*

10. **Iron Oxides in Drug Delivery** **328**
    Fahima Dilnawaz and *Sanjeeb Kumar Sahoo*

11. Nanoengineered Magnetic Field-Induced Targeted Drug Delivery System with Stimuli-Responsive Release **344**
R. Devesh K. Misra

Color Plate Section **365**

CHAPTER 1

Key Aspects in Nanotechnology and Drug Delivery

José L. Arias

ABSTRACT

Drug inefficacy and toxicity are frequently encountered problems with drug therapy failure. In order to overcome these limitations, new drug dosage forms have been developed by taking advantage of nanoparticulate drug delivery systems. The so-called nanomedicines are engineered to maximize drug concentration into the targeted site while keeping to a very minimum the drug adverse effects. To this aim, nanoplatforms should basically exhibit appropriate drug vehiculization capabilities and a perfect control on the biological fate of drug molecules. It is unquestionably accepted that only the wise engineering of the drug nanocarrier will meet these requisites.

This chapter is devoted to the analysis of the essential elements to be included in the formulation of drug-loaded nanoparticulate systems. These are the nanoplatform, therapeutic molecule and the functionalization moieties. Particular attention is given to the compilation and explanation of more advanced formulation strategies facilitating the control over the *in vivo* fate of the nanomedicine. In addition, recent developments in nanoplatform formulation for simultaneous disease imaging and image-guided drug delivery will be analyzed. Finally, basic nanotoxicity concepts in nanomedicine development are also discussed.

Department of Pharmacy and Pharmaceutical Technology, Faculty of Pharmacy, University of Granada, Campus Universitario de Cartuja s/n, 18071 Granada, Spain.
Email: jlarias@ugr.es

List of abbreviations after the text.

Introduction

Recent investigations in pharmacotherapy have focused on the identification of new molecular targets and potent active agents to be included in the disease arena. As a consequence, disease therapy has been enriched by the clinical use of novel dosage forms and drugs, and refined treatment regimes. Unfortunately, drug therapy failure frequently occurs due to the unfavorable pharmacokinetics and pharmacodynamics of drug molecules (Couvreur 2013, Arias 2011a).

Many reasons could be given to justify pharmacotherapy failure (Arias 2008, 2009, Iyer et al. 2013). Principally, inadequate physical chemistry of drug molecules (high electrical charge and hydrophobic character), the unfavorable pharmacokinetic characteristics (intense and rapid metabolism and plasma clearance) and the development of resistance mechanisms at the cell and/or tissue levels. Furthermore, the activity of a therapeutic agent can be severely conditioned by a non-specific biological fate: non-selective biodistribution and accumulation into healthy targeted sites, where the drug carries out undesirable actions. All these reasons can determine drug inefficacy and toxicity problems, and further justify why many therapeutic molecules become ineffective and toxic *in vivo*, despite the promising *in vitro* activity being exhibited.

Fortunately, the recent introduction of nanotechnology conceptualizations in the development of new drug dosage forms is generating promising (nano) tools in the continuous fight against diseases (Jain et al. 2013, Kumar et al. 2013). Drug-loaded nanoparticulate systems, the so-called nanomedicines or nanodrugs, have started to generate interesting results related to drug efficacy and the absence of collateral toxicities. In fact, such nanocarriers can optimize drug concentration into the site of action, thus resulting in a prolonged and deeper contact between the active agent and the non-healthy tissue/cells. An additional benefit coming from the vehiculization (and *in vitro* and *in vivo* protection) of drug molecules into these nanoplatforms is the enhancement of their pharmacokinetic and pharmacodynamic profiles. As a consequence, new treatments are emerging with improved efficacy and minimal toxicity (Ehmann et al. 2013, van der Meel et al. 2013).

However, despite preclinical (and some clinical) reports highlighting the interesting possibilities associated to the use of nanodrugs, the *in vivo* activity of drug-loaded nanoplatforms can be severely limited. In fact, the number of (conventional) nanomedicines marketed is conditioned by limitations mainly associated to their engineering (Fig. 1.1). Thus, additional research in nanoplatform design and development is needed before it is possible to the complete introduction of nanodrugs into the clinic.

In this line, this contribution explores the basic components to be included in the formulation of drug nanocarriers. Special emphasis is

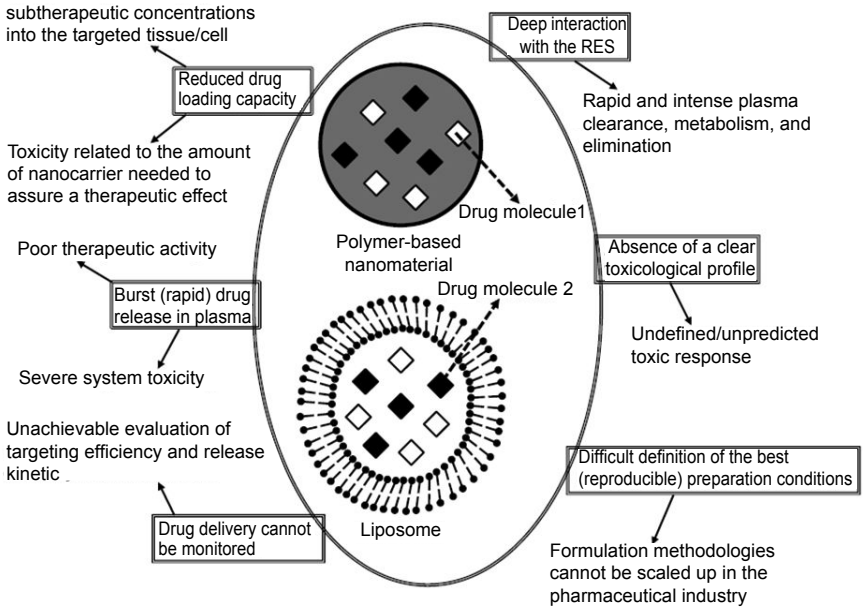
subtherapeutic concentrations into the targeted tissue/cell
Reduced drug loading capacity
Toxicity related to the amount of nanocarrier needed to assure a therapeutic effect
Poor therapeutic activity
Burst (rapid) drug release in plasma
Severe system toxicity
Unachievable evaluation of targeting efficiency and release kinetic
Drug delivery cannot be monitored
Deep interaction with the RES
Rapid and intense plasma clearance, metabolism, and elimination
Drug molecule1
Polymer-based nanomaterial
Drug molecule 2
Liposome
Absence of a clear toxicological profile
Undefined/unpredicted toxic response
Difficult definition of the best (reproducible) preparation conditions
Formulation methodologies cannot be scaled up in the pharmaceutical industry

Figure 1.1. Common limits to the clinical use of nanomedicines. Conventional nanoplatforms often formulated for drug delivery purposes, i.e., lipid (liposome)- and polymer-based, are schematized in the figure. The biodegradable nanocarrier should assure both the efficient delivery of therapeutic molecules to the non-healthy site and a negligible toxicity. The deep interaction nanomedicine—reticuloendothelial system (RES) determines the natural tendency of the nanocarrier to accumulate into this system, which can be advantageously used against diseases exclusively located into RES tissues and organs (e.g., bone marrow, lungs, liver and spleen): the nanodrug would move toward these locations to display its therapeutic effect. In addition, the need for predictive models facilitating the evaluation of the toxic response to the nanomedicine is accepted.

given to the discussion of more elaborated formulation strategies that may control the biological fate of these nanomedicines. In addition, the revolution introduced into the disease arena by theranostic nanoparticles (NPs), and basic nanotoxicity conceptualizations in nanodrug development are also analyzed.

Fundamentals of Nanomedicine Design and Development

The formulation of nanomedicines involves the satisfactory integration of physical, chemical and physicochemical factors. It is accepted that any given drug-loaded nanoplatform must fulfill some basic requisites to display efficient *in vitro* and *in vivo* activities (Table 1.1) (Arias 2012, 2013).

In general, and despite recent investigations have emphasized the need for advanced modifications in the nanoplatform structure (based on passive and/or active drug delivery strategies), it is accepted that a

Table 1.1. Requisites that need to be fulfilled by a nanoplatform for efficient drug delivery. Advanced engineering approaches (functionalization on the basis of passive and active drug targeting strategies) are beginning to be considered as basic requisites to optimize the therapeutic effect.

Requisite	**Significance to the therapeutic activity**
Biodegradability, biocompatibility and negligible antigenicity	Null toxicity
Appropriate geometry: spherical shape and size < 100 nm	Extended biodistribution, thus reaching the small capillaries irrigating the disease site. Uniform perfusion through the small gaps between endothelial cells of the capillaries
Zero or negligible surface electrical charge and hydrophilic character	Delayed plasma clearance: opsonization processes leading to recognition by macrophages are retarded
Physicochemical stability	Lack of aggregation and precipitation under storage conditions and after administration. Inadequate biodistribution and embolization will be avoided
Suitable drug vehiculization capabilities: high loading values and sustained and triggered release	Negligible burst release immediately upon administration. Protection of drug molecules from biodegradation. Prolonged therapeutic effect thanks to an extended contact drug - targeted tissue/ cell. The body will not be overloaded with foreign material
Advanced functionalization of particle structure	Targetable pharmacokinetic and biodistribution profile. Enhanced residence time of the drug in plasma and improved intracellular loading. Minimization of the toxicity associated to an extended drug biodistribution

nanomedicine is made of two basic components: the nanoplatform and the therapeutic molecule. In the latter case, the active agent could be a drug (Ma and Mumper 2013), a gene (Kanasty et al. 2013) and/or additional engineering elements which can develop a therapeutic activity or could be used in combination with the preceding components for complementary therapy, i.e., photodynamic (Gamal-Eldeen et al. 2013, Reshetov et al. 2013), photothermal (Guo et al. 2013, Zhou et al. 2013) and/or hyperthermia (Rodrigues et al. 2013, Yoo et al. 2013) therapies. As well, an imaging agent can further be introduced into the nanomedicine structure for additional disease imaging functionalities, e.g., a Magnetic Resonance Imaging (MRI) probe (Arias et al. 2011a), a luminophore (Marpu et al. 2010) and/or a radionuclide (Rangger et al. 2012). In this case, the delivery of therapeutic and imaging molecules inside one nanoplatform has led to the revolutionary conceptualization of theranosis for the simultaneous and selective disease diagnosis and pharmacotherapy (Arias 2011b, Terreno et al. 2012).

The nanoplatform

The visionary concept of "magic bullet" introduced by Dr. Paul Ehrlich (Prüll 2003) can be considered as a starting point to the beginning of the numerous efforts developing colloidal systems that can optimize drug delivery to the disease site. In fact, the number of preclinical and clinical investigations has grown exponentially (Couvreur 2013), and the interesting preclinical results reported have contributed to the introduction of these nanoformulations into the clinic. In fact, we can easily think of some examples of marketed nanomedicines: Myocet®, Lipoplatin®, Depocyte®, DaunoXome® and Doxil®, to cite just a few. Thus, it is accepted with no doubt that nanocarriers have optimized the way of administering drugs and biomacromolecules to patients (Arias 2013).

A successful drug delivery by using nanoplatforms strongly relies on their structure and formulation methodologies. Not considering more advanced engineering and functionalization approaches to the nanoplatform (to be described in another section of this chapter), the nature and physical chemistry of the nanomaterial can influence the *in vitro* behavior and biological fate of the nanomedicine (Lazzari et al. 2012, Zhu et al. 2013). Table 1.1 compiles all the basic requisites to be satisfied by a nanoplatform for an efficient drug delivery. Biodegradable and biocompatible nanoplatforms for drug delivery purposes are recurrently based on inorganic materials (Kim et al. 2013), organic matrices (Vauthier and Bouchemal 2009), or hybrid (inorganic/organic, core/shell) structures (Feng et al. 2013) (Fig. 1.2). Notably, the nanoplatform should undergo a rapid and complete metabolism and elimination when their *in vivo* activity is finished. Otherwise, the organism would be overloaded with foreign material (resulting in toxicity) when the nanomedicine-based treatment is administered to the patient during long periods of time.

Regarding the synthesis methodology chosen for the formulation of such nanoparticulate systems, it can define the platform structure (Vauthier and Bouchemal 2009). In essence, nanoplatforms can be formulated in the form of a reservoir-type system (nanocapsule) or alternatively, a matrix-type system (nanosphere). Additional (advanced) modifications that can be introduced into the particle structure allow a better control over the *in vivo* fate of the nanomedicine and a more efficient drug activity (Arias 2011a, Clares et al. 2012), as it will be discussed in another section of this chapter. They characteristically involve covalently attachment of targeting ligands onto the particle surface for a more selective drug delivery toward the non-healthy site, and/or, as previously indicated, the functionalization of the particle structure with advanced materials (i.e., inorganic cores, stimuli-sensitive polymers) for multidrug delivery (including high drug loading values and sustained and triggered drug release), multimodality imaging possibilities,

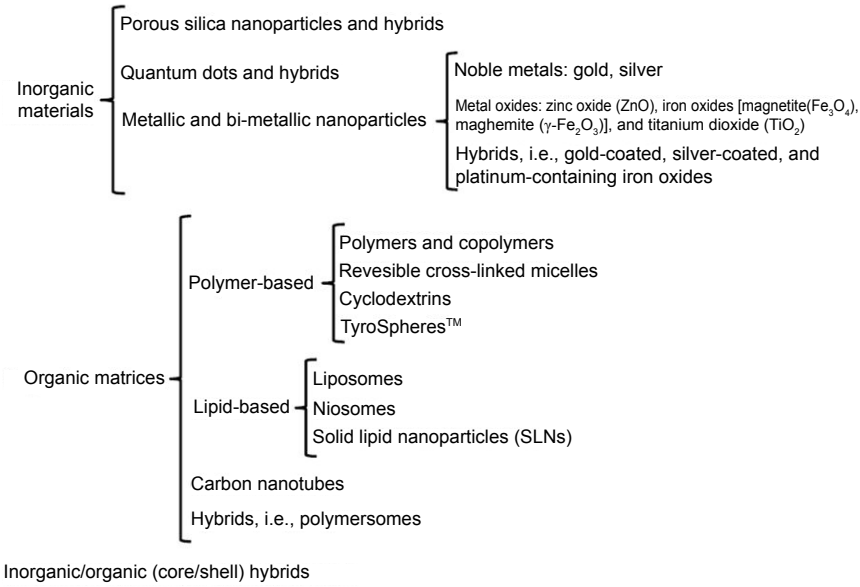

Figure 1.2. Representative examples of nanoplatforms intended for drug delivery applications. Inorganic nanoparticulate systems can be based on quantum dots (Savla et al. 2011, Rejinold et al. 2013), metals (Wang et al. 2012, Sánchez-Paradinas et al. 2013), mesoporous silica (Lin et al. 2013, Shen et al. 2014) or hybrids (Yang et al. 2009, Fahmi et al. 2011). These inorganic materials offer additional functionalities given their potential use as contrast agents in MRI, iridotomy, near infrared tomography, optical coherence tomography, photoacoustic tomography (PAT), fluorescence imaging or confocal imaging (Arias 2011b). On the contrary, organic platforms are generally made of lipid-based nanostructures [remarkably, liposomes (Türker et al. 2008, Takahama et al. 2013), niosomes (Kaur et al. 2007, Hasan et al. 2013), and solid lipid nanoparticles (SLNs) (Thakkar et al. 2007, Yang et al. 2013)], biodegradable polymers [e.g., poly(D,L-lactide-*co*-glycolide) (PLGA) (Valizadeh et al. 2012, Sabzevari et al. 2013), chitosan (Arias et al. 2011a, Md et al. 2012), poly(ε-caprolactone) (PCL) (Arias et al. 2010, Ortiz et al. 2012), poly(ethyleneimine) (PEI) (Zhan et al. 2012, Liu et al. 2013a) and poly(alkylcyanoacrylates) (Hillaireau et al. 2006, Arias et al. 2009a)], carbon nanotubes (Singh et al. 2013, Shao et al. 2013), or hybrids (Li et al. 2011, Lin et al. 2012). More interestingly, inorganic/organic (core/shell) nanocomposites can combine different therapeutic molecules and complementary treatment functionalizations (e.g., hyperthermia, photodynamic or photothermal therapies) into the particle structure (Tian et al. 2011, Chen et al. 2013a). The main features related to the use of all these nanoplatforms in drug delivery are comprehensively revised in the selected contributions to this first volume "Nanoplatforms in Drug Delivery" of the book series "Nanotechnology and Drug Delivery".

plus additional treatment options (i.e., photothermal, hyperthermia, or photodynamic therapies) (Arias 2011b). For instance, a nanoplatform structure may consist of (Reddy et al. 2012, Amiri et al. 2013, Lorenzato et al. 2013): *i*) inorganic cores as imaging agents and/or as functionalization structures for active drug targeting, e.g., superparamagnetic iron oxides as MRI contrast agents and magnetic responsiveness functionalities for drug

delivery and hyperthermia; and, *ii*) the organic matrix where the signal emitter, photosensitizer agent and/or drug molecules are loaded, and where the inorganic cores are generally embedded.

The therapeutic molecule

Numerous drug molecules, with very different chemical structures and physical chemistries, have been loaded to nanocarriers for an efficient, triggered and prolonged therapeutic activity (Table 1.2). Drug loading to nanoplatforms may fundamentally happen by: *i*) absorption, being incorporated the drug molecules mainly onto the particle surface; or, more interestingly if high loading values and a controlled release are the objectives, *ii*) absorption, being embedded in the active agent into the particle matrix. Additionally, the loading of the drug dose to the nanoparticulate system can be possible by taking advantage of physicochemical interactions, i.e., covalent linkages established between the drug molecule and chemical groups of the nanocarrier structure (e.g., ester, disulfide, amide, hydrazone and/or thioether). In the case of hydrophobic drugs, non-covalent links involving hydrophobic interactions can lead to the loading (Sahana et al. 2008, Men et al. 2012). Idyllically, the nanomedicine should contain more than one therapeutic agent (drug, gene and/or supplementary engineering components for hyperthermia, photodynamic or photothermal therapies) in order to make possible complementary therapeutic activities (Arias 2011b, 2013, Reddy et al. 2012).

Several investigations have highlighted that the best drug vehiculization results (high drug loading efficiency and controlled/prolonged drug release) are normally obtained when the molecules of an active agent are incorporated (absorbed) within the particle structure (Arias et al. 2011b,c, Santos et al. 2011). In this line, the (sustained) drug release pattern generally fits to a biphasic process with an initial fast (burst) drug release, the remaining drug molecules being released in a sustained manner. The rapid release during the first phase is most likely the consequence of the leakage of the surface-associated and/or poorly entrapped drug, which easily diffuses into the release medium. After that, the rate of drug release falls as the principal mechanism is generally changed to drug diffusion through the particle matrix. However, an essential aspect in nanomedicine development is the need for an adequately triggered/controlled drug release if a complete concentration of the drug dose into the disease site is intended (Arias 2010, Fleige et al. 2012, Loh et al. 2012). In this way, external (ultrasounds, light excitation, alternating magnetic gradients) and/or environmental (temperature, enzymes, pH) stimulus could be used to specifically activate drug release into the non-healthy tissue/cells.

Table 1.2. Illustrative examples of drug molecules incorporated to nanoplatforms for an efficient treatment of severe diseases.

Disease	Active agent	Nanoplatform	Reference
Cancer	Gemcitabine	Chitosan, carbon nanotube	Arias et al. 2011a, Singh et al. 2013
	Paclitaxel	Poly(ethylene glycol) (PEG)-*b*-PCL, PLGA	Gong et al. 2012, Chen et al. 2013b
	5-fluorouracil	PCL, magnetoliposome, chitosan	Ortiz et al. 2012, Clares et al. 2013, Honary et al. 2013
	Methotrexate	Liposome, chitosan	Kuznetsova et al. 2012, Nogueira et al. 2013
	Doxorubicin	Carboxymethyl dextran-cyclodextrin conjugate, gold	Sivasubramanian et al. 2013, Sun et al. 2014
Cardiovascular diseases, i.e., atherosclerosis and thrombosis	Nebivolol	Eudragit® RS100	Jana et al. 2013
	Amiodarone	Liposome	Takahama et al. 2013
	Enoxaparin	Alginate-coated chitosan	Bagre et al. 2013
	Rosiglitazone	Polyvinyl alcohol (PVA)-coated PLGA	Di Mascolo et al. 2013
Chronic inflammatory diseases, i.e., arthritis, inflammatory bowel disease, chronic lung inflammatory diseases (e.g., allergic asthma), and uveitis	Diclofenac sodium	Liposome, iron/ethylcellulose (core/shell), PCL	Türker et al. 2008, Arias et al. 2009b, 2010
	Celecoxib	Niosome, SLN	Kaur et al. 2007, Thakkar et al. 2007
	Tacrolimus	PLGA, Eudragit® P-4135F	Lamprecht et al. 2005, Meissner et al. 2006
	5-aminosalicylic acid	PLGA, silica, and composites of them	Pertuit et al. 2007, Moulari et al. 2008
	Theophylline	Thiolated chitosan	Lee et al. 2006
	Betamethasone disodium 21-phosphate	Poly(D,L-lactide) (PLA), PEG-*b*-PLA copolymer	Matsuo et al. 2009, Sakai et al. 2011
	Piroxicam	Eudragit® RS100	Adibkia et al. 2007
	Triamcinolone acetonide	PLGA	Sabzevari et al. 2013
	Dexamethasone	Sialyl-Lewis X-conjugated liposome	Hashida et al. 2008
Metabolic diseases, i.e., diabetes	Insulin	Gold, cationic liposome, chitosan-coated SLN, PLGA	Joshi et al. 2006, Park et al. 2011, Fonte et al. 2012, Reix et al. 2012
	Nicotinamide	Carbon nanotube	Ilie et al. 2013
	Metformin	Niosome, chitosan-coated liposome	Hasan et al. 2013, Manconi et al. 2013
	Andrographolide	SLN	Yang et al. 2013

Table 1.2. contd....

Table 1.2. contd.

Disease	Active agent	Nanoplatform	Reference
Neurodegenerative diseases, i.e., Alzheimer's disease and Parkinson's disease	Dopamine	Chitosan	De Giglio et al. 2011, Trapani et al. 2011
	Bromocriptine	SLN, chitosan	Esposito et al. 2008, Md et al. 2012
	Olanzapine	SLN, PLGA	Vivek et al. 2007, Seju et al. 2011
Infectious diseases	Amoxicillin	Chitosan-alginate polyelectrolyte complex, PEG-*b*-poly(ethylcyanoacrylate)	Arora et al. 2011, Fontana et al. 2001
	Ciprofloxacin	Niosome, liposome	Moazeni et al. 2010, Ong et al. 2012
	Amphotericin B	PLGA, silica	Van de Ven et al. 2012, Paulo et al. 2013
	Clarithromycin	PLGA	Mohammadi et al. 2011, Valizadeh et al. 2012

This controllable drug release will be possible by a perfect engineering of the NP structure, i.e., by introducing a temperature-responsive polymer [poly(*N*-isopropylacrylamide) (PNiPAAm)] (Lue et al. 2013).

The imaging agent

Monitoring the *in vivo* fate of nanomedicines by a non-invasive methodology has been identified as a very significant challenge in the development of an efficient nanoparticulate-based drug therapy. In fact, it has been stated that the optimization of drug transport to targeted non-healthy sites could only be possible by a real-time analysis of the efficacy of the drug targeting strategy (Arias 2011b, Couvreur 2013). In this line, several investigations (involving the development of theranostic conceptualizations) have reported the benefits coming from the inclusion of imaging agents into a drug-loaded nanoparticulate system (Table 1.3) (Janib et al. 2010, Arias 2011b, Ding and Wu 2012, Terreno et al. 2012). As a consequence, new advances in nanomedicine engineering (and disease diagnosis and therapy) have been possible thanks to the information coming from image-assisted biodistribution characterizations based on MRI, radionuclides [Single Photon Emission Computed Tomography (SPECT), and Positron Emission Tomography (PET)], optical imaging [Near Infrared Fluorescence (NIRF), and bioluminescence], PAT, and Fluorescence-Mediated Tomography (FMT).

For instance, a recent investigation reported the development of a multifunctional nanoplatform for targeted molecular Computed

Table 1.3. More significant benefits associated to the formulation of theranostic nanoplatforms.

Benefit	**Clinical utility**
Real-time (and non-invasive) monitoring of the *in vivo* fate of the drug nanocarrier	Prediction/analysis of the pharmacokinetics and pharmacodynamics of the (drug) nanomedicine. Development of efficient and less toxic (nano) pharmacotherapy regimens
Trigger (and quantify) drug release from the nanoparticulate system	Complete release of the drug dose into the targeted tissue/cell
Estimate drug responses	Detection of patients that will respond to the (nano) pharmacotherapy. Identification of biomarkers for the choice of therapy. Individualization of clinical protocols
Real-time assessment of therapy outcomes	Longitudinal investigation of disease progression (and response to therapy). Very interesting when drug resistances can occur

Tomography (CT) imaging and drug therapy of prostate cancer (Kim et al. 2010). The nanocarrier was based on gold NPs loaded with doxorubicin and surface decorated with a Prostate-Specific Membrane Antigen (PSMA) Ribonucleic Acid (RNA) aptamer that binds to PSMA. It was demonstrated that the nanomedicine was capable of selectively imaging LNCaP prostate cancer cells that express the PSMA protein (> 4-fold greater CT intensity compared to non-targeted PC3 cells). In addition, the nanomedicine was significantly more potent against LNCaP cells in comparison to non-targeted PC3 cells.

It is worth noting that, multimodality imaging techniques (involving the incorporation of more than one signal emitter/imaging agent into the same nanoplatform structure), e.g., MRI-optical imaging (Kaimal et al. 2011), MRI-PET (Cowger and Xie 2013), or PET-NIRF-MRI (Xie et al. 2010), have been proposed in an attempt to overcome the limitations typically associated to all these imaging modalities (e.g., lack of targeted molecular imaging, resolution, limited sensitivity, short imaging time and toxicity). Of course optical, magnetic and/or radioactive characteristics of the signal emitter/imaging agent must be taken into consideration in order to guarantee the best image signal. In fact, such properties can define physicochemical modifications that the molecule undergoes upon exposure to the stimulus directed to the non-healthy tissues/cells. Thereafter, changes in the amplitude or composition of the emitted signal will be detected by an external receiver and reconstructed to form images. Similar to drug incorporation into a nanoparticulate system, the loading of the signal emitter/imaging agent to the nanocarrier is possible on the basis of physicochemical interactions.

Advanced Engineering Strategies for a Controllable Biological Fate

Despite numerous research (and review) articles having emphasized the benefits coming from the use of nanomedicines in the management of severe diseases, conventional drug-loaded nanoplatforms have found significant limitations during development or when tested *in vitro* and/or *in vivo*. Mostly, poor drug vehiculization characteristics [i.e., low drug loading values and very rapid ("burst") drug release after the administration of the nanomedicine] (Moog et al. 2002, Jiang et al. 2005, Yang et al. 2006, Esmaeilia et al. 2010), and the unfeasibility to be cost-effectively scaled up in the pharmaceutical industry (according to good manufacturing practices standards) given the difficulty in defining easy synthesis methodologies. In addition, the typical biological fate reported in the case of these conventional nanomedicines (intense interaction with the RES leading to a rapid plasma clearance by macrophages, biodegradation and elimination; plasma half life < 5 minutes) will be a limiting factor when other tissue or cell targets (non-related to the RES) are concerned (Maeda et al. 2009). Even more, marketed nanomedicines can develop a limited therapeutic efficacy and/or severe toxicity when introduced into the clinic. It is hypothesized that this could be the result of nanomedicine interaction with the RES, vasculature walls, enzymatic systems, etc. (Barraud et al. 2005, Pirollo and Chang 2008, Arias 2009, 2010). Some frequent limitations to the clinical use of nanomedicines were previously compiled in Fig. 1.1. In addition, even if the nanodrug fulfill several basic prerequisites to assure efficient *in vitro* and *in vivo* activities (Table 1.1), supplementary research in nanoplatform engineering is required before its total (safe and efficient) introduction into the clinic.

Providentially, more elaborated formulation strategies have provided additional benefits related to the control (and optimization) of the biological fate (and efficacy) of the nanomedicine (Arias 2011a,b, Couvreur 2013). Figure 1.3 displays the general structure of a multifunctional nanoplatform developed for drug delivery purposes on the basis of passive and active targeting strategies, along with the fundaments of such approaches.

Briefly, passive drug targeting strategies are based on the EPR effect which is commonly developed by non-healthy organs and tissues (e.g., inflammatory tissues and tumor interstitium) (Maeda 2013, Maeda et al. 2013). These strategies generally involve the engineering of long-circulating nanomedicines by functionalization of the NP surface with hydrophilic macromolecules (Moghimi et al. 2001, Huynh et al. 2010). For instance, poloxamines, poloxamers, polyethylene oxides or polysaccharides, can be incorporated by chemical conjugation and/or physical adsorption. The creation of non-fouling shells onto the particle surface will supply a shielding effect (the so-called "stealth" characteristic) (Fig. 1.3b). Up to

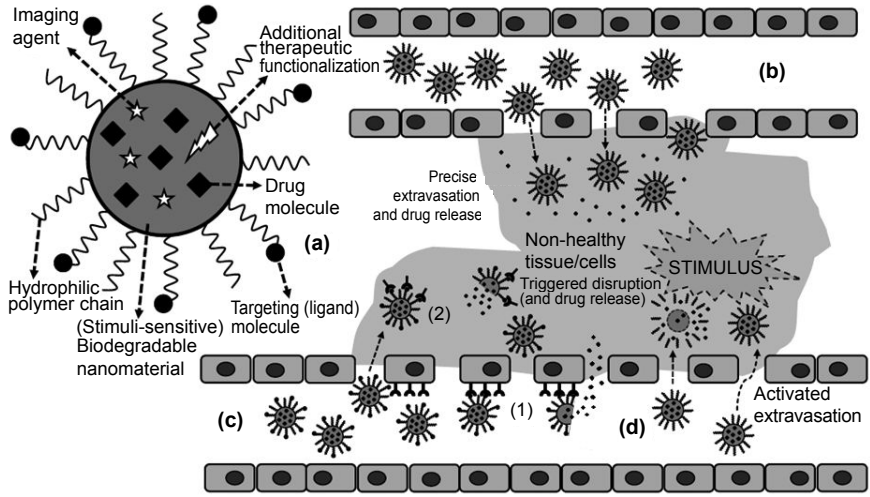

Figure 1.3. (a) Nanomedicine formulated on the basis of passive and active drug targeting strategies. Advanced engineering elements to be introduced in the NP structure are: hydrophilic macromolecules onto the surface for passive targeting capabilities (i.e., PEG, by the so-called PEGylation techniques), targeting moieties for ligand-mediated targeting, and stimuli-responsive moieties to drive the nanodrug to the targeted site and/or to trigger drug release exclusively within the non-healthy tissues/cells. Complementary engineering elements could be further introduced to obtain additional therapeutic activities, e.g., photodynamic, photothermal and/or hyperthermia therapies. Furthermore, one or more signal emitters/imaging agents (for MRI, optical imaging, PET, NIRF, etc.) could be found into the nanoplatform to visualize and quantify drug (gene) delivery (image guided delivery/theranosis conceptualizations). (b) Long-circulating nanomedicines can specifically accumulate into the targeted site upon reaching the leaky vasculature irrigating the disease site. The "stealth" nanodrug will then exploit the structural irregularities of the vessels irrigating the non-healthy tissue and/or cells, undergoing a selective extravasation by passive diffusion or convection through the hyperpermeable endothelium. This phenomenon is known as the Enhanced Permeability and Retention (EPR) effect. An adequate decoration of the nanomedicine surface with hydrophilic moieties will retard particle opsonization (and plasma clearance). Blood recirculation should contribute to the complete concentration of the long-circulating nanomedicine into the targeted tissue/cells. (c) Long-circulating nanomedicines surface functionalized with targeting moieties for molecular recognition processes (ligand-receptor interactions) leading to: (1) NP adhesion onto the vascular endothelium irrigating the targeted site; and/or, (2) NP internalization into the non-healthy tissue (and cells). Subsequent drug release (by particle biodegradation/disruption) will provide high therapeutic concentrations. (d) Long-circulating nanomedicines formulated to be stimuli-sensitive. After administration to the patient, the stimulus will drive/attract the responsive nanodrug toward the non-healthy tissue/cells. After that, drug release will be triggered exclusively within the disease site by inducing particle disruption.

now, PEG is by far considered the most adequate hydrophilic polymer to prevent the rapid systemic clearance of nanomedicines by the RES (in essence retarding the *in vivo* recognition by opsonization).

The effect of PEG shells on the *in vitro*/*in vivo* properties of topotecan-loaded liposomes (Dadashzadeh et al. 2008) have been investigated. To this

aim, PEGylated and conventional liposomes were formulated by following the lipid film hydration procedure (mean size of both formulations ≈ 100 nm). Pharmacokinetic characteristics of topotecan were evaluated in Wistar rats after intravenous injection of the drug formulated in phosphate buffered saline (PBS, pH 7.4), in conventional liposomes or in PEGylated liposomes. Results showed that both conventional and PEGylated liposomes increased the total concentration of topotecan in plasma. However, the initial concentration, and the values of area under the plasma drug concentration-time curve (AUC) and Mean Residence Time (MRT) were significantly greater ($p < 0.001$) for the PEGylated liposomes than for the conventional liposomes or for the free topotecan. In fact, PEGylated liposomes resulted in 52-fold and 2-fold increases in AUC in comparison with that of free drug and conventional liposomes, respectively.

Recently, some preclinical studies have reported the phenomenon of "accelerated blood clearance" when PEGylated particles are repeatedly injected to rats (Laverman et al. 2001, Ishida and Kiwada 2008). This process determined a decrease in plasma circulation time (rapid systemic elimination) of the second and/or subsequent doses of PEGylated NPs. Therefore, these observations should be seriously considered when engineering a "stealth" nanomedicine.

With respect to active/specific drug targeting strategies, these can be based on the surface functionalization of nanomedicines with biomacromolecules for receptor- or ligand-mediated drug delivery (Clares et al. 2012, Holgado et al. 2012), and/or on the formulation of nanodrugs by using stimuli-sensitive materials (Torchilin 2009). Both approaches facilitate a more selective (and intense) biodistribution into the site of action.

The former active drug targeting strategy relies on the formulation of nanomedicines surface decorated with (bio)molecules that can bind specifically to ligands (over) expressed by non-healthy tissues and/or cells. The subsequent ligand-receptor interaction will commonly result in a receptor-mediated internalization process (and cytosolic accumulation) by endocytosis (Fig. 1.3c). The targeting moieties can be conjugated directly onto the particle surface and/or through the hydrophilic moieties (e.g., PEG chains) determining the "stealth" properties of the nanomedicine. Some typical examples of these targeting moieties are compiled in Table 1.4.

An illustrative example of the benefits coming from this advanced engineering strategy was recently published (Ditto et al. 2012). Briefly, L-tyrosine polyphosphate NPs were surface decorated with PEG chains previously conjugated to Folic Acid (FA) moieties. Under simulated physiological flow, the resulting nanoplatform (mean size: 100–500 nm) demonstrated a 10-fold greater attachment to HeLa cervical cancer cells in comparison with non-decorated (plain) NPs. It was hypothesized that such encouraging results were the consequence of a receptor-ligand

Table 1.4. Representative examples of targeting moieties that have been chemically conjugated to nanomedicines for ligand- or receptor-mediated drug targeting.

Targeting moiety	**Targeted biomolecule**
Monoclonal antibodies: OX26, TfRscFv, anti-CD33, MRK-16, trastuzumab	Human epidermal growth factor receptor-2, P-glycoprotein, transferrin receptor
Peptides: CREKA, vasoactive intestinal peptide, H2009.1, arginine-glycine-aspartic acid (RGD), PR_b, PH1, LyP-1	Integrin $\alpha_v\beta_6$, integrin $\alpha_v\beta_3$, integrin $\alpha_5\beta_1$
Aptamers: A10 2′-fluoropyrimidine RNA aptamer, PSMA RNA aptamer	Extracellular domain of the PSMA
Folate	Folate-binding protein
Transferrin	Transferrin receptor

binding, given the fact that a competition study with free FA inhibited the nanoplatform attachment. In addition, when the nanoplatform was loaded with a silver-based drug (the silver-carbene complex 22, SCC_{22}), the toxicity of this antitumor agent against HeLa cells was significantly higher as compared to the non-decorated SCC_{22}-loaded NPs ($p = 0.004$) or the free drug ($p = 0.006$). In fact, it was found that the viability of HeLa cells incubated with the SCC_{22}-loaded nanoplatform was dramatically reduced to ≈ 55%, while plain SCC_{22}-loaded NPs determined greater cell viability (≈ 93%).

Active drug targeting strategies can also be based on the design of nanomedicines with stimuli-responsive characteristics. The main objective is, again, to enhance the selectivity of the nanodrug for the non-healthy tissue/cells (Fig. 1.3d). To this aim, the nanoplatforms are built by using materials that can easily modify their physicochemical properties (e.g., undergoing a disruption or swelling process) under exposure to a biological or externally controlled stimulus (Arias 2011a). As a result, drug (gene) release from the nanocarrier can be specifically triggered into the site of action, by the damage caused by the applied stimulus into the NP structure (leading to nanodrug degradation). Alternatively, pulsatile drug release can be possible when the drug nanocarrier act as a multi-switchable system by undergoing reversible structural changes when cycles of stimulus on/off (i.e., light/dark) are applied. The stimulus can also activate cytotoxic molecules or trigger the release of endocytosed macromolecules into the cytosol. Finally, the stimulus could also be advantageously used to: i) activate the imaging agent inside the nanoplatform or to trigger its release into the disease site, thus gaining access to disease imaging functionalities or even more, indirectly facilitating the quantification of drug delivery (Arias 2011b); and/or, ii) drive/attract the nanomedicine toward the non-healthy site, i.e., magnetically responsive nanodrugs (Arias et al. 2011a, Reddy et al. 2012, Cui et al. 2013). Drug nanocarriers made of iron oxide nuclei can

be magnetically guided to the site of action, keeping them there until the drug dose is completely released/accumulated (magnetic targeting).

Representative examples of stimulus triggering drug release from a stimuli-sensitive nanocarrier are enzymatic systems, pH, temperature, light and ultrasounds. Briefly, nanomedicines can be engineered to be selectively disrupted by enzymes overexpressed into non-healthy tissues/cells (Andresen et al. 2005, Su et al. 2013), e.g., sphingomyelinase, alkaline phosphatase, phospholipase C, secretory phospholipase A_2, elastase and transglutaminase. pH-sensitive nanodrugs typically contain pH-sensitive functional groups into their structure (Rao et al. 2012, Cheng et al. 2013), i.e., acidic sulfonic acid, carboxylic acid, sulphonamide and ammonium salts. Temperature-sensitive drug nanocarriers are frequently engineered with thermosensitive polymers (Kono et al. 2011, Ayano et al. 2012), i.e., PNiPAAm and derivatives. In the case of light-sensitive drug delivery nanosystems, near infrared light is frequently used to activate drug release (Lv et al. 2012, Cao et al. 2013). Finally, ultrasound-mediated drug delivery basically consists on the exposition of non-healthy sites to ultrasounds, hence leading to an increased extravasation and cellular uptake of the nanodrug (upon disruption of the cell membrane permeability), and nanomedicine degradation and drug release (Ibsen et al. 2011, Liu et al. 2013b).

For instance, nanocomposites consisting of a γ-Fe_2O_3 core and a stimuli-responsive polymer shell [made of a poly(acrylic acid)-*b*-PVA copolymer] were recently designed for multi-stimuli triggered drug release purposes (Liu et al. 2013c). The coating permitted the release of the cationic model drug methylene blue under exposure to acidic environments, and improved the biocompatibility and circulation time of the iron oxide NPs. In addition, local heating generated by the iron oxide core under the influence of an alternating magnetic field further triggered drug release. Finally, the possible use of the nanocomposites as MRI agents was confirmed by relaxivity measurements and acquisition of T_2-weighted images.

In line with this example, several research reports have emphasized the benefits coming from the formulation of nanodrugs on the basis of all these advanced engineering approaches (passive targeting + ligand-mediated drug delivery + stimuli-sensitive drug delivery) (Arias 2011a,b). This will lead to the development of the "definitive" nanomedicine (multifunctional nanoplatform with optimal therapeutic effect and null toxicity, Fig. 1.3a), capable of evading the RES, reaching the non-healthy site. As a result, the drug (gene) dose and the amount of imaging agent will be completely concentrated into the site of action. Such conceptualization has led to the design of theranostic NPs for simultaneous and selective disease diagnosis and pharmacotherapy (Arias 2011b, Terreno et al. 2012).

An interesting exemplification of this revolutionary idea was devoted to the formulation of tamoxifen-loaded FA-armed PEGylated magnetic

NPs (average size ≈ 40 nm) (Heidari Majd et al. 2013). In this study, Fe_3O_4 NPs were prepared through thermal decomposition of tris(acetylacetonate) iron(III). PEGylation of iron oxide NPs was possible by treating the bromoacetyl-terminal PEG silane complex with protected ethylene diamine to form a bifunctional PEG compound containing triethoxysilane at one end and an amino group at the other end. Self-assembly of this complex with Fe_3O_4 NPs led to the formation of PEGylated magnetic NPs, while the terminal amino groups of the nanostructure were conjugated with FA, and then the NP was loaded with tamoxifen. Drug loading efficiency was ≈ 49%, while drug molecules were sustainably released (90% release in 72 hours). Finally, cytotoxicity analysis resulted in significant growth inhibition in MCF-7 human breast cancer cells (that express folate receptors). In fact, fluorescence microcopy and flow cytometry analyses revealed substantial interaction of the NPs with MCF-7 cells.

Nanotoxicity and Nanomedicine Development

When any given nanomedicine enters the bloodstream, intensive bio-interactions occur determining the *in vivo* fate of the nanoparticulate system and immunoresponse reactions. These (nano)immuno-interactions may induce toxicity effects associated to, i.e., granuloma formation, oxidative stress, and/or enzyme function. Moreover, tissue inflammation and irregular function or cell death may take place when the nanodrug enters the cell (Kunzmann et al. 2011, Sharma et al. 2014). It is suggested that the incidence and severity of the adverse side effects are related to products coming from nanodrug (bio)degradation, and to the biocompatibility and biodegradability of the nanomedicine, method of administration, dose, cellular dose (internalized mass), delivered dose (mass per cell or cm^3), pharmacokinetics, biodistribution and physical chemistry (chemical structure and composition, surface area, surface charge and thermodynamics, purity, solubility and reactivity) (Kuempel et al. 2012, El-Ansary et al. 2013, Sun et al. 2013). In addition, very little is known about the long-term toxicological impact of exposure to NPs.

In order to prepare nanomedicines with safe quantitative/qualitative compositions, the exhaustive analysis of the data coming from physicochemical, preclinical and clinical investigations is of great significance. By analyzing the information coming from these studies, it should be possible to select the more adequate nanomaterial to formulate the nanodrug, and to determine relevant doses and concentrations, identify relevant models, target sites and endpoints and develop alternatives to animal testing (Johnston et al. 2013). Such rational engineering will provide the finest therapeutic effect and toxicity profile to the nanomedicine.

In this line, predictive models to analyze the experimental data and to define the toxic response to the nanomedicine are needed (Cattaneo et al. 2010). For example, multigene expression-based models have been proposed to establish toxicity profiles of nanomaterials and consequent potential human health risks (Snyder-Talkington et al. 2012). Efficient methodologies for nanotoxicity screening are under development, e.g., inductively coupled plasma optical emission spectroscopy (Simpson et al. 2013), and synchrotron radiation-based techniques (Wang et al. 2010). With respect to current toxicity tests and risk assessment methods, these should be adapted to fit to the unique features related to nanomaterials, and appropriate controls and reference materials should further be appropiatedly established (Kuempel et al. 2012, Dusinska et al. 2013). In addition, validated procedures are needed to obtain sensitive and quantitative measurements of exposure to nanomaterials during their formulation and use in the preparation of nanomedicines, while validation methods for exposure controls and standardized criteria to categorize hazard data are additional challenges (Kuempel et al. 2012).

Finally, nanomedicines have attracted the attention of international regulatory agencies (Kimbrell 2009, United States Government Accountability Office 2010). These organisms generally suggest treating nanodrugs as additives with potential side effects. Therefore, apart from updating existing laws, safety regulations/requirements to be met by manufacturers and standardized approaches (e.g., predictive models, monitoring protocols) to define the risk associated to nanomedicine exposure must be also developed.

Conclusions

Nanomedicines can improve the therapeutic effect of drug molecules while minimizing the associated toxicity. Important progress has been made in nanodrug design thanks to advanced engineering strategies capable of controlling the pharmacokinetic and pharmacodynamic characteristics. Nevertheless, the complete introduction of nanomedicines into the clinic and long-term use rely on a better knowledge of (bio)disorders causing the disease, the engineering of biocompatible and biodegradable nanomaterials with optimized drug delivery capabilities and the clarification of the toxicity associated to their use (nanotoxicity). Thus, additional research efforts are needed to perfectly define (and optimize) the *in vivo* fate, viability, nanotoxicity and effectiveness of these drug-loaded nanoplatforms which, from a preclinical point of view, are really promising. The scientific community has recently established the definitive step toward the perfect management of diseases by engineering theranostic nanoplatforms

which may provide the efficient combination of disease diagnosis and pharmacotherapy.

Abbreviations

AUC	:	area under the plasma drug concentration-time curve
CT	:	computed tomography
EPR	:	enhanced permeability and retention
FA	:	folic acid
γ-Fe_2O_3	:	maghemite
Fe_3O_4	:	magnetite
FMT	:	fluorescence-mediated tomography
MRI	:	magnetic resonance imaging
MRT	:	mean residence time
NIRF	:	near infrared fluorescence
NP	:	nanoparticle
PAT	:	photoacoustic tomography
PEI	:	poly(ethyleneimine)
PBS	:	phosphate buffered saline
PEG	:	poly(ethylene glycol)
PET	:	positron emission tomography
PLA	:	poly(D,L-lactide)
PLGA	:	poly(D,L-lactide-*co*-glycolide)
PNiPAAm	:	poly(*N*-isopropylacrylamide)
PSMA	:	prostate-specific membrane antigen
PVA	:	polyvinyl alcohol
RES	:	reticuloendothelial system
RGD	:	arginine-glycine-aspartic acid
RNA	:	ribonucleic acid
SCC_{22}	:	silver-carbene complex 22
SLN	:	solid lipid nanoparticle
SPECT	:	single photon emission computed tomography
TiO_2	:	titanium dioxide
ZnO	:	zinc oxide

References

Adibkia, K. and M.R. Siahi Shadbad, A. Nokhodchi, A. Javadzedeh, M. Barzegar-Jalali, J. Barar, G. Mohammadi and Y. Omidi. 2007. Piroxicam nanoparticles for ocular delivery: physicochemical characterization and implementation in endotoxin-induced uveitis. J. Drug. Target. 15: 407–416.

Amiri, H. and K. Saeidi, P. Borhani, A. Manafirad, M. Ghavami and V. Zerbi. 2013. Alzheimer's disease: pathophysiology and applications of magnetic nanoparticles as MRI theranostic agents. ACS Chem. Neurosci. 4: 1417–1429.

Andresen, T.L. and S.S. Jensen, T. Kaasgaard and K. Jørgensen. 2005. Triggered activation and release of liposomal prodrugs and drugs in cancer tissue by secretory phospholipase A2. Curr. Drug Deliv. 2: 353–362.

Arias, J.L. 2008. Novel strategies to improve the anticancer action of 5-fluorouracil by using drug delivery systems. Molecules. 13: 2340–2369.

Arias, J.L. Micro- and nano-particulate drug delivery systems for cancer treatment. pp. 1–85. *In*: P. Spencer and W. Holt [eds.]. 2009. Anticancer Drugs: Design, Delivery and Pharmacology. Nova Science Publishers, Inc., New York, USA.

Arias, J.L. 2010. Drug Targeting by Magnetically Responsive Colloids. Nova Science Publishers, Inc., New York, USA.

Arias, J.L. 2011a. Drug targeting strategies in cancer treatment: an overview. Mini Rev. Med. Chem. 11: 1–17.

Arias, J.L. 2011b. Advanced methodologies to formulate nanotheragnostic agents for combined drug delivery and imaging. Expert Opin. Drug Deliv. 8: 1589–1608.

Arias, J.L. Nano-strategies in the delivery of antitumor drugs to cancer. pp. 268–289. *In*: R. Srirajaskanthan and V.R. Preedy [eds.]. 2012. Nanomedicine and Cancer. Science Publishers, New Hampshire, USA.

Arias, J.L. 2013. Liposomes in drug delivery: a patent review (2007-present). Expert Opin. Ther. Pat. 23: 1399–1414.

Arias, J.L. and L.H. Reddy and P. Couvreur. 2009a. Polymeric nanoparticulate system augmented the anticancer therapeutic efficacy of gemcitabine. J. Drug Target. 17: 586–598.

Arias, J.L. and M. López-Viota, J. López-Viota and A.V. Delgado. 2009b. Development of iron/ethylcellulose (core/shell) nanoparticles loaded with diclofenac sodium for arthritis treatment. Int. J. Pharm. 382: 270–276.

Arias, J.L. and M. López-Viota, E. Sáez-Fernández and M.A. Ruiz. 2010. Formulation and physicochemical characterization of poly(epsilon-caprolactone) nanoparticles loaded with ftorafur and diclofenac sodium. Colloids Surf. B Biointerfaces. 75: 204–208.

Arias, J.L. and L.H. Reddy, M. Othman, B. Gillet, D. Desmaële, F. Zouhiri, F. Dosio, R. Gref and P. Couvreur. 2011a. Squalene based nanocomposites: a new platform for the design of multifunctional pharmaceutical theragnostics. ACS Nano. 5: 1513–1521.

Arias, J.L. and L.H. Reddy and P. Couvreur. 2011b. Superior preclinical efficacy of gemcitabine developed as chitosan nanoparticulate system. Biomacromolecules. 12: 97–104.

Arias, J.L. and G. Cebrián-Torrejón, E. Poupon, A. Fournet and P. Couvreur. 2011c. Biodegradable polymeric nanoformulation based on the antiprotozoal canthin-6-one. J. Nanopart. Res. 13: 6737–6746.

Arora, S. and S. Gupta, R.K. Narang and R.D. Budhiraja. 2011. Amoxicillin loaded chitosan-alginate polyelectrolyte complex nanoparticles as mucopenetrating delivery system for h. Pylori. Sci. Pharm. 79: 673–694.

Ayano, E. and M. Karaki, T. Ishihara, H. Kanazawa and T. Okano. 2012. Poly(N-isopropylacrylamide)-PLA and PLA blend nanoparticles for temperature-controllable drug release and intracellular uptake. Colloids Surf. B Biointerfaces. 99: 67–73.

Bagre, A.P. and K. Jain and N.K. Jain. 2013. Alginate coated chitosan core shell nanoparticles for oral delivery of enoxaparin: *in vitro* and *in vivo* assessment. Int. J. Pharm. 456: 31–40.

Barraud, L. and P. Merle, E. Soma, L. Lefrançois, S. Guerret, M. Chevallier, C. Dubernet, P. Couvreur, C. Trépo and L. Vitvitski. 2005. Increase of doxorubicin sensitivity by doxorubicin-loading into nanoparticles for hepatocellular carcinoma cells *in vitro* and *in vivo*. J. Hepatol. 42: 736–743.

Cao, J. and S. Huang, Y. Chen, S. Li, X. Li, D. Deng, Z. Qian, L. Tang and Y. Gu. 2013. Near-infrared light-triggered micelles for fast controlled drug release in deep tissue. Biomaterials. 34: 6272–6283.

Cattaneo, A.G. and R. Gornati, E. Sabbioni, M. Chiriva-Internati, E. Cobos, M.R. Jenkins and G. Bernardini. 2010. Nanotechnology and human health: risks and benefits. J. Appl. Toxicol. 30: 730–744.

Chen, T. and T. Zhao, D. Wei, Y. Wei, Y. Li and H. Zhang. 2013a. Core-shell nanocarriers with ZnO quantum dots-conjugated Au nanoparticle for tumor-targeted drug delivery. Carbohydr. Polym. 92: 1124–1132.

Chen, Y. and Z. Yang, C. Liu, C. Wang, S. Zhao, J. Yang, H. Sun, Z. Zhang, D. Kong and C. Song. 2013b. Synthesis, characterization, and evaluation of paclitaxel loaded in six-arm star-shaped poly(lactic-co-glycolic acid). Int. J. Nanomedicine. 8: 4315–4326.

Cheng, F.F. and J.J. Zhang, F. Xu, L.H. Hu, E.S. Abdel-Halim and J.J. Zhu. 2013. pH-sensitive polydopamine nanocapsules for cell imaging and drug delivery based on folate receptor targeting. J. Biomed. Nanotechnol. 9: 1155–1163.

Clares, B. and M.A. Ruiz, V. Gallardo and J.L. Arias. 2012. Drug delivery to inflammation based on nanoparticles surface decorated with biomolecules. Curr. Med. Chem. 19: 3203–3211.

Clares, B. and R.A. Biedma-Ortiz, E. Sáez-Fernández, J.C. Prados, C. Melguizo, L. Cabeza, R. Ortiz and J.L. Arias. 2013. Nano-engineering of 5-fluorouracil-loaded magnetoliposomes for combined hyperthermia and chemotherapy against colon cancer. Eur. J. Pharm. Biopharm. 85: 329–338.

Couvreur, P. 2013. Nanoparticles in drug delivery: past, present and future. Adv. Drug Deliv. Rev. 65: 21–23.

Cowger, T. and J. Xie. 2013. Polyaspartic acid coated iron oxide nanoprobes for PET/MRI imaging. Methods Mol. Biol. 1025: 225–235.

Cui, Y. and Q. Xu, P.K. Chow, D. Wang and C.H. Wang. 2013. Transferrin-conjugated magnetic silica PLGA nanoparticles loaded with doxorubicin and paclitaxel for brain glioma treatment. Biomaterials. 34: 8511–8520.

Dadashzadeh, S. and A.M. Vali and M. Rezaie. 2008. The effect of PEG coating on *in vitro* cytotoxicity and *in vivo* disposition of topotecan loaded liposomes in rats. Int. J. Pharm. 353: 251–259.

De Giglio, E. and A. Trapani, D. Cafagna, L. Sabbatini and S. Cometa. 2011. Dopamine-loaded chitosan nanoparticles: formulation and analytical characterization. Anal. Bioanal. Chem. 400: 1997–2002.

Di Mascolo, D. and C.J. Lyon, S. Aryal, M.R. Ramirez, J. Wang, P. Candeloro, M. Guindani, W.A. Hsueh and P. Decuzzi. 2013. Rosiglitazone-loaded nanospheres for modulating macrophage-specific inflammation in obesity. J. Control. Release. 170: 460–468.

Ding, H. and F. Wu. 2012. Image guided biodistribution of drugs and drug delivery. Theranostics. 2: 1037–1039.

Ditto, A.J. and K.N. Shah, N.K. Robishaw, M.J. Panzner, W.J. Youngs and Y.H. Yun. 2012. The Interactions between L-tyrosine based nanoparticles decorated with folic acid and cervical cancer cells under physiological flow. Mol. Pharm. 9: 3089–3098.

Dusinska, M. and Z. Magdolenova and L.M. Fjellsbø. 2013. Toxicological aspects for nanomaterial in humans. Methods Mol. Biol. 948: 1–12.

Ehmann, F. and K. Sakai-Kato, R. Duncan, D. Hernán Pérez de la Ossa, R. Pita, J.M. Vidal, A. Kohli, L. Tothfalusi, A. Sanh, S. Tinton, J.L. Robert, B. Silva Lima and M.P. Amati. 2013. Next-generation nanomedicines and nanosimilars: EU regulators' initiatives relating to the development and evaluation of nanomedicines. Nanomedicine (Lond.). 8: 849–856.

El-Ansary, A. and S. Al-Daihan, A.B. Bacha and M. Kotb. 2013. Toxicity of novel nanosized formulations used in medicine. Methods Mol. Biol. 1028: 47–74.

Esmaeilia, F. and R. Dinarvand, M.H. Ghahremani, S.N. Ostad, H. Esmaily and F. Atyabi. 2010. Cellular cytotoxicity and *in vivo* biodistribution of docetaxel poly(lactide-co-glycolide) nanoparticles. Anticancer Drugs. 21: 43–52.

Esposito, E. and M. Fantin, M. Marti, M. Drechsler, L. Paccamiccio, P. Mariani, E. Sivieri, F. Lain, E. Menegatti, M. Morari and R. Cortesi. 2008. Solid lipid nanoparticles as delivery systems for bromocriptine. Pharm. Res. 25: 1521–1530.

Fahmi, A. and D. Appelhans, N. Cheval, T. Pietsch, C. Bellmann, N. Gindy and B. Voit. 2011. Hybrid nanoalloy: nanofibers fabricated by self-assembling dendrimers mediate *in situ* CdSe quantum dots and their metallization with discrete gold nanoparticles. Adv. Mater. 23: 3289–3293.

Feng, L. and C. Zhu, H. Yuan, L. Liu, F. Lv and S. Wang. 2013. Conjugated polymer nanoparticles: preparation, properties, functionalization and biological applications. Chem. Soc. Rev. 42: 6620–6633.

Fleige, E. and M.A. Quadir and R. Haag. 2012. Stimuli-responsive polymeric nanocarriers for the controlled transport of active compounds: concepts and applications. Adv. Drug Deliv. Rev. 64: 866–884.

Fontana, G. and M. Licciardi, S. Mansueto, D. Schillaci and G. Giammona. 2001. Amoxicillin-loaded polyethylcyanoacrylate nanoparticles: influence of PEG coating on the particle size, drug release rate and phagocytic uptake. Biomaterials. 22: 2857–2865.

Fonte, P. and F. Andrade, F. Araújo, C. Andrade, Jd. Neves and B. Sarmento. 2012. Chitosan-coated solid lipid nanoparticles for insulin delivery. Methods Enzymol. 508: 295–314.

Gamal-Eldeen, A.M. and S.M. El-Daly, I.H. Borai, H.A. Wafay and A.R. Abdel-Ghaffar. 2013. Photodynamic therapeutic effect of indocyanine green entrapped in polymeric nanoparticles and their anti-EGFR-conjugate in skin cancer in CD1 mice. Photodiagnosis Photodyn. Ther. 10: 446–459.

Gong, C. and Y. Xie, Q. Wu, Y. Wang, S. Deng, D. Xiong, L. Liu, M. Xiang, Z. Qian and Y. Wei. 2012. Improving anti-tumor activity with polymeric micelles entrapping paclitaxel in pulmonary carcinoma. Nanoscale. 4: 6004–6017.

Guo, Y. and Z. Zhang, D.H. Kim, W. Li, J. Nicolai, D. Procissi, Y. Huan, G. Han, R.A. Omary and A.C. Larson. 2013. Photothermal ablation of pancreatic cancer cells with hybrid iron-oxide core gold-shell nanoparticles. Int. J. Nanomedicine. 8: 3437–3446.

Hasan, A.A. and H. Madkor and S. Wageh. 2013. Formulation and evaluation of metformin hydrochloride-loaded niosomes as controlled release drug delivery system. Drug Deliv. 20: 120–126.

Hashida, N. and N. Ohguro, N. Yamazaki, Y. Arakawa, E. Oiki, H. Mashimo, N. Kurokawa and Y. Tano. 2008. High-efficacy site-directed drug delivery system using sialyl-Lewis X conjugated liposome. Exp. Eye Res. 86: 138–149.

Heidari Majd, M. and D. Asgari, J. Barar, H. Valizadeh, V. Kafil, A. Abadpour, E. Moumivand, J.S. Mojarrad, M.R. Rashidi, G. Coukos and Y. Omidi. 2013. Tamoxifen loaded folic acid armed PEGylated magnetic nanoparticles for targeted imaging and therapy of cancer. Colloids Surf. B Biointerfaces. 106: 117–125.

Hillaireau, H. and T. Le Doan, M. Besnard, H. Chacun, J. Janin and P. Couvreur. 2006. Encapsulation of antiviral nucleotide analogues azidothymidine-triphosphate and cidofovir in poly(iso-butylcyanoacrylate) nanocapsules. Int. J. Pharm. 324: 37–42.

Holgado, M.A. and L. Martin-Banderas, J. Alvarez-Fuentes, M. Fernandez-Arevalo and J.L. Arias. 2012. Drug targeting to cancer by nanoparticles surface functionalized with special biomolecules. Curr. Med. Chem. 19: 3188–3195.

Honary, S. and P. Ebrahimi and R. Hadianamrei. 2013. Optimization of size and encapsulation efficiency of 5-fu loaded chitosan nanoparticles by response surface methodology. Curr. Drug Deliv. 10: 742–752.

Huynh, N.T. and E. Roger, N. Lautram, J.P. Benoît and C. Passirani. 2010. The rise and rise of stealth nanocarriers for cancer therapy: passive versus active targeting. Nanomedicine (Lond.). 5: 1415–1433.

Ibsen, S. and M. Benchimol, D. Simberg, C. Schutt, J. Steiner and S. Esener. 2011. A novel nested liposome drug delivery vehicle capable of ultrasound triggered release of its payload. J. Control. Release. 155: 358–366.

Ilie, I. and R. Ilie, T. Mocan, F. Tabaran, C. Iancu and L. Mocan. 2013. Nicotinamide-functionalized multiwalled carbon nanotubes increase insulin production in pancreatic beta cells via MIF pathway. Int. J. Nanomedicine. 8: 3345–3353.

Ishida, T. and H. Kiwada. 2008. Accelerated blood clearance (ABC) phenomenon upon repeated injection of PEGylated liposomes. Int. J. Pharm. 354: 56–62.
Iyer, A.K. and A. Singh, S. Ganta and M.M. Amiji. 2013. Role of integrated cancer nanomedicine in overcoming drug resistance. Adv. Drug Deliv. Rev. 65: 1784–1802.
Jain, S. and A.S. Doshi, A.K. Iyer and M.M. Amiji. 2013. Multifunctional nanoparticles for targeting cancer and inflammatory diseases. J. Drug Target. 21: 888–903.
Jana, U. and A.K. Mohanty, P.K. Manna and G.P. Mohanta. 2013. Preparation and characterization of nebivolol nanoparticles using Eudragit® RS100. Colloids Surf. B Biointerfaces. 113C: 269–275.
Janib, S.M. and A.S. Moses and J.A. MacKay. 2010. Imaging and drug delivery using theranostic nanoparticles. Adv. Drug Deliv. Rev. 62: 1052–1063.
Jiang, B. and L. Hu, C. Gao and J. Shen. 2005. Ibuprofen-loaded nanoparticles prepared by a co-precipitation method and their release properties. Int. J. Pharm. 304: 220–230.
Johnston, H. and G. Pojana, S. Zuin, N.R. Jacobsen, P. Møller, S. Loft, M. Semmler-Behnke, C. McGuiness, D. Balharry, A. Marcomini, H. Wallin, W. Kreyling, K. Donaldson, L. Tran and V. Stone. 2013. Engineered nanomaterial risk. Lessons learnt from completed nanotoxicology studies: potential solutions to current and future challenges. Crit. Rev. Toxicol. 43: 1–20.
Joshi, H.M. and D.R. Bhumkar, K. Joshi, V. Pokharkar and M. Sastry. 2006. Gold nanoparticles as carriers for efficient transmucosal insulin delivery. Langmuir. 22: 300–305.
Kaimal, V. and Z. Chu, Y.Y. Mahller, B. Papahadjopoulos-Sternberg, T.P. Cripe, S.K. Holland and X. Qi. 2011. Saposin C coupled lipid nanovesicles enable cancer-selective optical and magnetic resonance imaging. Mol. Imaging Biol. 13: 886–897.
Kanasty, R. and J.R. Dorkin, A. Vegas and D. Anderson. 2013. Delivery materials for siRNA therapeutics. Nat. Mater. 12: 967–977.
Kaur, K. and S. Jain, B. Sapra and A.K. Tiwary. 2007. Niosomal gel for site-specific sustained delivery of anti-arthritic drug: *in vitro-in vivo* evaluation. Curr. Drug Deliv. 4: 276–282.
Kim, D. and Y.Y. Jeong and S. Jon. 2010. A drug-loaded aptamer-gold nanoparticle bioconjugate for combined CT imaging and therapy of prostate cancer. ACS Nano. 4: 3689–3696.
Kim, K.M. and J.H. Kang, A. Vinu, J.H. Choy and J.M. Oh. 2013. Inorganic nanomedicines and their labeling for biological imaging. Curr. Top. Med. Chem. 13: 488–503.
Kimbrell, G.A. 2009. Governance of nanotechnology and nanomaterials: principles, regulation, and renegotiating the social contract. J. Law Med. Ethics. 37: 706–723.
Kono, K. and S. Nakashima, D. Kokuryo, I. Aoki, H. Shimomoto, S. Aoshima, K. Maruyama, E. Yuba, C. Kojima, A. Harada and Y. Ishizaka. 2011. Multi-functional liposomes having temperature-triggered release and magnetic resonance imaging for tumor-specific chemotherapy. Biomaterials. 32: 1387–1395.
Kuempel, E.D. and C.L. Geraci and P.A. Schulte. 2012. Risk assessment and risk management of nanomaterials in the workplace: translating research to practice. Ann. Occup. Hyg. 56: 491–505.
Kumar, A. and F. Chen, A. Mozhi, X. Zhang, Y. Zhao, X. Xue, Y. Hao, X. Zhang, P.C. Wang and X.J. Liang. 2013. Innovative pharmaceutical development based on unique properties of nanoscale delivery formulation. Nanoscale. 5: 8307–8325.
Kunzmann, A. and B. Andersson, T. Thurnherr, H. Krug, A. Scheynius and B. Fadeel. 2011. Toxicology of engineered nanomaterials: focus on biocompatibility, biodistribution and biodegradation. Biochim. Biophys. Acta. 1810: 361–373.
Kuznetsova, N.R. and C. Sevrin, D. Lespineux, N.V. Bovin, E.L. Vodovozova, T. Mészáros, J. Szebeni and C. Grandfils. 2012. Hemocompatibility of liposomes loaded with lipophilic prodrugs of methotrexate and melphalan in the lipid bilayer. J. Control. Release. 160: 394–400.
Lamprecht, A. and H. Yamamoto, H. Takeuchi and Y. Kawashima. 2005. Nanoparticles enhance therapeutic efficiency by selectively increased local drug dose in experimental colitis in rats. J. Pharmacol. Exp. Ther. 315: 196–202.

Laverman, P. and M.G. Carstens, O.C. Boerman, E.T. Dams, W.J. Oyen, N. van Rooijen, F.H. Corstens and G. Storm. 2001. Factors affecting the accelerated blood clearance of polyethylene glycol-liposomes upon repeated injection. J. Pharmacol. Exp. Ther. 298: 607–612.

Lazzari, S. and D. Moscatelli, F. Codari, M. Salmona, M. Morbidelli and L. Diomede. 2012. Colloidal stability of polymeric nanoparticles in biological fluids. J. Nanopart. Res. 14: 920.

Lee, D.W. and S.A. Shirley, R.F. Lockey and S.S. Mohapatra. 2006. Thiolated chitosan nanoparticles enhance anti-inflammatory effects of intranasally delivered theophylline. Respir. Res. 7: 112.

Li, C. and K. Yang, Y. Zhang, H. Tang, F. Yan, L. Tan, Q. Xie and S. Yao. 2011. Highly biocompatible multi-walled carbon nanotube-chitosan nanoparticle hybrids as protein carriers. Acta Biomater. 7: 3070–3077.

Lin, Y.L. and Y.K. Liu, N.M. Tsai, J.H. Hsieh, C.H. Chen, C.M. Lin and K.W. Liao. 2012. A lipo-PEG-PEI complex for encapsulating curcumin that enhances its antitumor effects on curcumin-sensitive and curcumin-resistance cells. Nanomedicine. 8: 318–327.

Lin, Y.C. and L.Y. Lin, M.Y. Gao and Y.P. Fang. 2013. Mesoporous silica nanoparticles synthesized from liquid crystal display manufacturing extracts as a potential candidate for a drug delivery carrier: evaluation of their safety and biocompatibility. Int. J. Nanomedicine. 8: 3833–3842.

Liu, C. and F. Liu, L. Feng, M. Li, J. Zhang and N. Zhang. 2013a. The targeted co-delivery of DNA and doxorubicin to tumor cells via multifunctional PEI-PEG based nanoparticles. Biomaterials. 34: 2547–2564.

Liu, T.Y. and M.Y. Wu, M.H. Lin and F.Y. Yang. 2013b. A novel ultrasound-triggered drug vehicle with multimodal imaging functionality. Acta Biomater. 9: 5453–5463.

Liu, J. and C. Detrembleur, A. Debuigne, M.C. De Pauw-Gillet, S. Mornet, L. Vander Elst, S. Laurent, C. Labrugère, E. Duguet and C. Jérôme. 2013c. Poly(acrylic acid)-block-poly(vinyl alcohol) anchored maghemite nanoparticles designed for multi-stimuli triggered drug release. Nanoscale. 5: 11464–11477.

Loh, X.J. and J. del Barrio, P.P. Toh, T.C. Lee, D. Jiao, U. Rauwald, E.A. Appel and O.A. Scherman. 2012. Triply triggered doxorubicin release from supramolecular nanocontainers. Biomacromolecules. 13: 84–91.

Lorenzato, C. and A. Cernicanu, M.E. Meyre, M. Germain, A. Pottier, L. Levy, B.D. de Senneville, C. Bos, C. Moonen and P. Smirnov. 2013. MRI contrast variation of thermosensitive magnetoliposomes triggered by focused ultrasound: a tool for image-guided local drug delivery. Contrast Media Mol. Imaging. 8: 185–192.

Lue, S.J. and B.W. Chen, C.M. Shih, F.Y. Chou, J.Y. Lai and W.Y. Chiu. 2013. Micron- and nano-sized poly(N-isopropylacrylamide-co-acrylic acid) latex syntheses and their applications for controlled drug release. J. Nanosci. Nanotechnol. 13: 5305–5315.

Lv, C. and Z. Wang, P. Wang and X. Tang. 2012. Photodegradable polyurethane self-assembled nanoparticles for photocontrollable release. Langmuir. 28: 9387–9394.

Ma, P. and R.J. Mumper. 2013. Anthracycline nano-delivery systems to overcome multiple drug resistance: a comprehensive review. Nano Today. 8: 313–331.

Maeda, H. 2013. The link between infection and cancer: tumor vasculature, free radicals, and drug delivery to tumors via the EPR effect. Cancer Sci. 104: 779–789.

Maeda, H. and G.Y. Bharate and J. Daruwalla. 2009. Polymeric drugs for efficient tumor-targeted drug delivery based on EPR-effect. Eur. J. Pharm. Biopharm. 71: 409–419.

Maeda, H. and H. Nakamura and J. Fang. 2013. The EPR effect for macromolecular drug delivery to solid tumors: improvement of tumor uptake, lowering of systemic toxicity, and distinct tumor imaging *in vivo*. Adv. Drug Deliv. Rev. 65: 71–79.

Manconi, M. and A. Nácher, V. Merino, M. Merino-Sanjuan, M.L. Manca, C. Mura, S. Mura, A.M. Fadda and O. Diez-Sales. 2013. Improving oral bioavailability and pharmacokinetics of liposomal metformin by glycerolphosphate-chitosan microcomplexation. AAPS Pharm. Sci. Tech. 14: 485–496.

Marpu, S. and Z. Hu and M.A. Omary. 2010. Brightly phosphorescent, environmentally responsive hydrogels containing a water-soluble three-coordinate gold(I) complex. Langmuir. 26: 15523–15531.

Matsuo, Y. and T. Ishihara, J. Ishizaki, K. Miyamoto, M. Higaki and N. Yamashita. 2009. Effect of betamethasone phosphate loaded polymeric nanoparticles on a murine asthma model. Cell Immunol. 260: 33–38.

Md, S. and R.A. Khan, G. Mustafa, K. Chuttani, S. Baboota, J.K. Sahni and J. Ali. 2012. Bromocriptine loaded chitosan nanoparticles intended for direct nose to brain delivery: pharmacodynamic, pharmacokinetic and scintigraphy study in mice model. Eur. J. Pharm. Sci. 48: 393–405.

Meissner, Y. and Y. Pellequer and A. Lamprecht. 2006. Nanoparticles in inflammatory bowel disease: particle targeting versus pH-sensitive delivery. Int. J. Pharm. 316: 138–143.

Men, K. and W. Liu, L. Li, X. Duan, P. Wang, M. Gou, X. Wei, X. Gao, B. Wang, Y. Du, M. Huang, L. Chen, Z. Qian and Y. Wei. 2012. Delivering instilled hydrophobic drug to the bladder by a cationic nanoparticle and thermo-sensitive hydrogel composite system. Nanoscale. 4: 6425–6433.

Moazeni, E. and K. Gilani, F. Sotoudegan, A. Pardakhty, A.R. Najafabadi, R. Ghalandari, M.R. Fazeli and H. Jamalifar. 2010. Formulation and *in vitro* evaluation of ciprofloxacin containing niosomes for pulmonary delivery. J. Microencapsul. 27: 618–627.

Moghimi, S.M. and A.C. Hunter and J.C. Murray. 2001. Long-circulating and target-specific nanoparticles: theory to practice. Pharmacol. Rev. 53: 283–318.

Mohammadi, G. and A. Nokhodchi, M. Barzegar-Jalali, F. Lotfipour, K. Adibkia, N. Ehyaei and H. Valizadeh. 2011. Physicochemical and anti-bacterial performance characterization of clarithromycin nanoparticles as colloidal drug delivery system. Colloids Surf. B Biointerfaces. 88: 39–44.

Moog, R. and A.M. Burger, M. Brandl, J. Schüler, R. Schubert, C. Unger, H.H. Fiebig and U. Massing. 2002. Change in pharmacokinetic and pharmacodynamic behaviour of gemcitabine in human tumor xenografts upon entrapment in vesicular phospholipid gels. Cancer Chemother. Pharmacol. 49: 356–366.

Moulari, B. and D. Pertuit, Y. Pellequer and A. Lamprecht. 2008. The targeting of surface modified silica nanoparticles to inflamed tissue in experimental colitis. Biomaterials. 29: 4554–4560.

Nogueira, D.R. and L. Tavano, M. Mitjans, L. Pérez, M.R. Infante and M.P. Vinardell. 2013. *In vitro* antitumor activity of methotrexate via pH-sensitive chitosan nanoparticles. Biomaterials. 34: 2758–2772.

Ong, H.X. and D. Traini, D. Cipolla, I. Gonda, M. Bebawy, H. Agus and P.M. Young. 2012. Liposomal nanoparticles control the uptake of ciprofloxacin across respiratory epithelia. Pharm. Res. 29: 3335–3346.

Ortiz, R. and J. Prados, C. Melguizo, J.L. Arias, M.A. Ruiz, P.J. Alvarez, O. Caba, R. Luque, A. Segura and A. Aránega. 2012. 5-Fluorouracil-loaded poly(ε-caprolactone) nanoparticles combined with phage E gene therapy as a new strategy against colon cancer. Int. J. Nanomedicine. 7: 95–107.

Park, S.J. and S.G. Choi, E. Davaa and J.S. Park. 2011. Encapsulation enhancement and stabilization of insulin in cationic liposomes. Int. J. Pharm. 415: 267–272.

Paulo, C.S. and M.M. Lino, A.A. Matos and L.S. Ferreira. 2013. Differential internalization of amphotericin B-conjugated nanoparticles in human cells and the expression of heat shock protein 70. Biomaterials. 34: 5281–5293.

Pertuit, D. and B. Moulari, T. Betz, A. Nadaradjane, D. Neumann, L. Ismaïli, B. Refouvelet, Y. Pellequer and A. Lamprecht. 2007. 5-amino salicylic acid bound nanoparticles for the therapy of inflammatory bowel disease. J. Control. Release. 123: 211–218.

Pirollo, K.F. and E.H. Chang. 2008. Does a targeting ligand influence nanoparticle tumor localization or uptake? Trends Biotechnol. 26: 552–558.

Prüll, C.R. 2003. Part of a scientific master plan? Paul Ehrlich and the origins of his receptor concept. Med. Hist. 47: 332–356.

Rangger, C. and A. Helbok, E. von Guggenberg, J. Sosabowski, T. Radolf, R. Prassl, F. Andreae, G.C. Thurner, R. Haubner and C. Decristoforo. 2012. Influence of PEGylation and RGD loading on the targeting properties of radiolabeled liposomal nanoparticles. Int. J. Nanomedicine. 7: 5889–5900.

Rao, N.V. and S.R. Mane, A. Kishore, J. Das Sarma and R. Shunmugam. 2012. Norbornene derived doxorubicin copolymers as drug carriers with pH responsive hydrazone linker. Biomacromolecules. 13: 221–230.

Reddy, L.H. and J.L. Arias, J. Nicolas and P. Couvreur. 2012. Magnetic nanoparticles: design and characterization, toxicity and biocompatibility, pharmaceutical and biomedical applications. Chem. Rev. 112: 5818–5878.

Reix, N. and A. Parat, E. Seyfritz, R. Van der Werf, V. Epure, N. Ebel, L. Danicher, E. Marchioni, N. Jeandidier, M. Pinget, Y. Frère and S. Sigrist. 2012. *In vitro* uptake evaluation in Caco-2 cells and *in vivo* results in diabetic rats of insulin-loaded PLGA nanoparticles. Int. J. Pharm. 437: 213–220.

Rejinold, N.S. and T. Baby, S.V. Nair and R. Jayakumar. 2013. Paclitaxel loaded fibrinogen coated CdTe/ZnTe core shell nanoparticles for targeted imaging and drug delivery to breast cancer cells. J. Biomed. Nanotechnol. 9: 1657–1671.

Reshetov, V. and H.P. Lassalle, A. François, D. Dumas, S. Hupont, S. Gräfe, V. Filipe, W. Jiskoot, F. Guillemin, V. Zorin and L. Bezdetnaya. 2013. Photodynamic therapy with conventional and PEGylated liposomal formulations of mTHPC (temoporfin): comparison of treatment efficacy and distribution characteristics *in vivo*. Int. J. Nanomedicine. 8: 3817–3831.

Rodrigues, H.F. and F.M. Mello, L.C. Branquinho, N. Zufelato, E.P. Silveira-Lacerda and A.F. Bakuzis. 2013. Real-time infrared thermography detection of magnetic nanoparticle hyperthermia in a murine model under a non-uniform field configuration. Int. J. Hyperthermia. 29: 752–767.

Sabzevari, A. and K. Adibkia, H. Hashemi, A. Hedayatfar, N. Mohsenzadeh, F. Atyabi, M.H. Ghahremani and R. Dinarvand. 2013. Polymeric triamcinolone acetonide nanoparticles as a new alternative in the treatment of uveitis: *in vitro* and *in vivo* studies. Eur. J. Pharm. Biopharm. 84: 63–71.

Sahana, D.K. and G. Mittal, V. Bhardwaj and M.N. Kumar. 2008. PLGA nanoparticles for oral delivery of hydrophobic drugs: influence of organic solvent on nanoparticle formation and release behavior *in vitro* and *in vivo* using estradiol as a model drug. J. Pharm. Sci. 97: 1530–1542.

Sakai, T. and T. Ishihara, M. Higaki, G. Akiyama and H. Tsuneoka. 2011. Therapeutic effect of stealth-type polymeric nanoparticles with encapsulated betamethasone phosphate on experimental autoimmune uveoretinitis. Invest. Ophthalmol. Vis. Sci. 52: 1516–1521.

Sánchez-Paradinas, S. and M. Pérez-Andrés, M.J. Almendral-Parra, E. Rodríguez-Fernández, A. Millán, F. Palacio, A. Orfao, J.J. Criado and M. Fuentes. 2013. Enhanced cytotoxic activity of bile acid cisplatin derivatives by conjugation with gold nanoparticles. J. Inorg. Biochem. 131C: 8–11.

Santos, D.P. and M.A. Ruiz, V. Gallardo, M.V.B. Zanoni and J.L. Arias. 2011. Multifunctional antitumor magnetite/chitosan-L-glutamic acid (core/shell) nanocomposites. J. Nanopart. Res. 13: 4311–4323.

Savla, R. and O. Taratula, O. Garbuzenko and T. Minko. 2011. Tumor targeted quantum dot-mucin 1 aptamer-doxorubicin conjugate for imaging and treatment of cancer. J. Control. Release. 153: 16–22.

Seju, U. and A. Kumar and K.K. Sawant. 2011. Development and evaluation of olanzapine-loaded PLGA nanoparticles for nose-to-brain delivery: *in vitro* and *in vivo* studies. Acta Biomater. 7: 4169–4176.

Shao, W. and A. Paul, B. Zhao, C. Lee, L. Rodes and S. Prakash. 2013. Carbon nanotube lipid drug approach for targeted delivery of a chemotherapy drug in a human breast cancer xenograft animal model. Biomaterials. 34: 10109–10119.

Sharma, G. and V. Kodali, M. Gaffrey, W. Wang, K.R. Minard, N.J. Karin, J.G. Teeguarden and B.D. Thrall. 2014. Iron oxide nanoparticle agglomeration influences dose rates and

modulates oxidative stress-mediated dose-response profiles *in vitro*. Nanotoxicology. 8: 663–675.

Shen, J. and G. Song, M. An, X. Li, N. Wu, K. Ruan, J. Hu and R. Hu. 2014. The use of hollow mesoporous silica nanospheres to encapsulate bortezomib and improve efficacy for non-small cell lung cancer therapy. Biomaterials. 35: 316–326.

Simpson, C.A. and B.J. Huffman and D.E. Cliffel. 2013. *In vivo* testing for gold nanoparticle toxicity. Methods Mol. Biol. 1026: 175–186.

Singh, R. and N.K. Mehra, V. Jain and N.K. Jain. 2013. Gemcitabine-loaded smart carbon nanotubes for effective targeting to cancer cells. J. Drug Target. 21: 581–592.

Sivasubramanian, M. and T. Thambi, V.G. Deepagan, G. Saravanakumar, H. Ko, Y.M. Kang and J.H. Park. 2013. Carboxymethyl dextran-cyclodextrin conjugate as the carrier of doxorubicin. J. Nanosci. Nanotechnol. 13: 7271–7278.

Snyder-Talkington, B.N. and Y. Qian, V. Castranova and N.L. Guo. 2012. New perspectives for *in vitro* risk assessment of multiwalled carbon nanotubes: application of coculture and bioinformatics. J. Toxicol. Environ. Health B Crit. Rev. 15: 468–492.

Su, C.W. and S.Y. Chen and D.M. Liu. 2013. Polysaccharide-lecithin reverse micelles with enzyme-degradable triglyceride shell for overcoming tumor multidrug resistance. Chem. Commun. (Camb.). 49: 3772–3774.

Sun, J. and Q. Zhang, Z. Wang and B. Yan. 2013. Effects of nanotoxicity on female reproductivity and fetal development in animal models. Int. J. Mol. Sci. 14: 9319–9337.

Sun, T.M. and Y.C. Wang, F. Wang, J.Z. Du, C.Q. Mao, C.Y. Sun, R.Z. Tang, Y. Liu, J. Zhu, Y.H. Zhu, X.Z. Yang and J. Wang. 2014. Cancer stem cell therapy using doxorubicin conjugated to gold nanoparticles via hydrazone bonds. Biomaterials. 35: 836–845.

Takahama, H. and H. Shigematsu, T. Asai, T. Matsuzaki, S. Sanada, H.Y. Fu, K. Okuda, M. Yamato, H. Asanuma, Y. Asano, M. Asakura, N. Oku, I. Komuro, M. Kitakaze and T. Minamino. 2013. Liposomal amiodarone augments anti-arrhythmic effects and reduces hemodynamic adverse effects in an ischemia/reperfusion rat model. Cardiovasc. Drugs Ther. 27: 125–132.

Terreno, E. and F. Uggeri and S. Aime. 2012. Image guided therapy: the advent of theranostic agents. J. Control. Release. 161: 328–337.

Thakkar, H. and R. Kumar Sharma and R.S. Murthy. 2007. Enhanced retention of celecoxib-loaded solid lipid nanoparticles after intra-articular administration. Drugs R D. 8: 275–285.

Tian, B. and W.T. Al-Jamal, K.T. Al-Jamal and K. Kostarelos. 2011. Doxorubicin-loaded lipid-quantum dot hybrids: surface topography and release properties. Int. J. Pharm. 416: 443–447.

Torchilin, V. 2009. Multifunctional and stimuli-sensitive pharmaceutical nanocarriers. Eur. J. Pharm. Biopharm. 71: 431–444.

Trapani, A. and E. De Giglio, D. Cafagna, N. Denora, G. Agrimi, T. Cassano, S. Gaetani, V. Cuomo and G. Trapani. 2011. Characterization and evaluation of chitosan nanoparticles for dopamine brain delivery. Int. J. Pharm. 419: 296–307.

Türker, S. and S. Erdoğan, Y.A. Ozer, H. Bilgili and S. Deveci. 2008. Enhanced efficacy of diclofenac sodium-loaded lipogelosome formulation in intra-articular treatment of rheumatoid arthritis. J. Drug Target. 16: 51–57.

United States Government Accountability Office. 2010. United States Government Accountability Office report on nanotechnology: nanomaterials are widely used in commerce, but EPA faces challenges in regulating risk. Int. J. Occup. Environ. Health. 16: 525–539.

Valizadeh, H. and G. Mohammadi, R. Ehyaei, M. Milani, M. Azhdarzadeh, P. Zakeri-Milani and F. Lotfipour. 2012. Antibacterial activity of clarithromycin loaded PLGA nanoparticles. Pharmazie. 67: 63–68.

Van de Ven, H. and C. Paulussen, P.B. Feijens, A. Matheeussen, P. Rombaut, P. Kayaert, G. Van den Mooter, W. Weyenberg, P. Cos, L. Maes and A. Ludwig. 2012. PLGA nanoparticles

and nanosuspensions with amphotericin B: potent *in vitro* and *in vivo* alternatives to Fungizone and AmBisome. J. Control. Release. 161: 795–803.

van der Meel, R. and L.J. Vehmeijer, R.J. Kok, G. Storm and E.V. van Gaal. 2013. Ligand-targeted particulate nanomedicines undergoing clinical evaluation: current status. Adv. Drug Deliv. Rev. 65: 1284–1298.

Vauthier, C. and K. Bouchemal. 2009. Methods for the preparation and manufacture of polymeric nanoparticles. Pharm. Res. 26: 1025–1058.

Vivek, K. and H. Reddy and R.S. Murthy. 2007. Investigations of the effect of the lipid matrix on drug entrapment, *in vitro* release, and physical stability of olanzapine-loaded solid lipid nanoparticles. AAPS Pharm. Sci. Tech. 8: E83.

Wang, B. and Z. Wang, W. Feng, M. Wang, Z. Hu, Z. Chai and Y. Zhao. 2010. New methods for nanotoxicology: synchrotron radiation-based techniques. Anal. Bioanal. Chem. 398: 667–676.

Wang, Y. and B.B. Newell and J. Irudayaraj. 2012. Folic acid protected silver nanocarriers for targeted drug delivery. J. Biomed. Nanotechnol. 8: 751–759.

Xie, J. and K. Chen, J. Huang, S. Lee, J. Wang, J. Gao, X. Li and X. Chen. 2010. PET/NIRF/MRI triple functional iron oxide nanoparticles. Biomaterials. 31: 3016–3022.

Yang, J. and S.B. Park, H.G. Yoon, Y.M. Huh and S. Haam. 2006. Preparation of poly ε-caprolactone nanoparticles containing magnetite for magnetic drug carrier. Int. J. Pharm. 324: 185–190.

Yang, Y.J. and X. Tao, Q. Hou and J.F. Chen. 2009. Fluorescent mesoporous silica nanotubes incorporating CdS quantum dots for controlled release of ibuprofen. Acta Biomater. 5: 3488–3496.

Yang, T. and H.H. Sheng, N.P. Feng, H. Wei, Z.T. Wang and C.H. Wang. 2013. Preparation of andrographolide-loaded solid lipid nanoparticles and their *in vitro* and *in vivo* evaluations: characteristics, release, absorption, transports, pharmacokinetics, and antihyperlipidemic activity. J. Pharm. Sci. 102: 4414–4425.

Yoo, D. and H. Jeong, S.H. Noh, J.H. Lee and J. Cheon. 2013. Magnetically triggered dual functional nanoparticles for resistance-free apoptotic hyperthermia. Angew. Chem. Int. Ed. Engl. 52: 13047–13051.

Zhan, C. and X. Wei, J. Qian, L. Feng, J. Zhu and W. Lu. 2012. Co-delivery of TRAIL gene enhances the anti-glioblastoma effect of paclitaxel *in vitro* and *in vivo*. J. Control. Release. 160: 630–636.

Zhou, J. and Z. Lu, X. Zhu, X. Wang, Y. Liao, Z. Ma and F. Li. 2013. NIR photothermal therapy using polyaniline nanoparticles. Biomaterials. 34: 9584–9592.

Zhu, M. and G. Nie, H. Meng, T. Xia, A. Nel and Y. Zhao. 2013. Physicochemical properties determine nanomaterial cellular uptake, transport, and fate. Acc. Chem. Res. 46: 622–631.

CHAPTER 2

Drug Delivery and Release from Polymeric Nanomaterials

Cornelia Vasile,[a,] Ana Maria Oprea,[b] Manuela Tatiana Nistor[c]* and *Anca-Maria Cojocariu[d]*

ABSTRACT

Controlled drug delivery technology represents one of the most rapidly advancing areas of science in which chemists and chemical engineers are contributing to human health care. The rational design and evaluation of drug formulation is based on the kinetics and mechanism of release as they are interconnected. As nano-sized polymeric systems are continuously developing, the interrelation between design and release behavior should be very well understood and adapted to new investigated systems. Nano-sized delivery systems offer numerous advantages compared to conventional dosage forms including improved efficacy, reduced toxicity and improved patient compliance and convenience. Nano-sized carriers based on natural and synthetic polymers allow treatments that would not otherwise be possible, which are now in conventional use.

This chapter examines the mechanism, kinetics/pharmacokinetics, biodistribution and bioevaluation of polymeric nanomaterials and also their main administration routes.

"Petru Poni" Institute of Macromolecular Chemistry, Department of Physical Chemistry of Polymers, 41A Grigore Ghica Voda Alley, R0 700487, Iasi, Romania.
[a] Email: cvasile@icmpp.ro
[b] Email: aoprea@icmpp.ro
[c] Email: manuela.pintilie@icmpp.ro
[d] Email: ancuta_cojocariu@yahoo.com
* Corresponding author

List of abbreviations after the text.

Introduction

Drug vehiculization capability (loading and release properties) determines the performance of drug delivery systems. Entrapment or conjugation of an active agent to a polymeric system may protect the drug molecules from inactivation and help to store its activity for prolonged durations, decrease its toxicity as well as may achieve administration flexibility. Drug release is the reverse process by which drug molecules are liberated from the solid phase, and become available for absorption and pharmacological action. Thus, drug loading and release are related to each other because they depend on the physical chemistry of both the matrix and the drug, and on the interaction between the matrix, the drug and the environment. An adequate engineering of a polymer-based nanoparticulate drug delivery system further relies on the pharmacokinetic and biodistribution profiles, and on the transition process from blood to the tissue/organ. The administration route may play a decisive role in the development of the therapeutic activity.

In line with the formulation of an efficient drug delivery system, this chapter is devoted to the study of the most significant aspects related to their design and (bio)evaluation. These are mainly the drug vehiculization capacity, the interconnection between route of administration and drug release, and the pharmacokinetics and biodistribution of the polymeric nanocarrier.

Drug Loading

Drug loading and release are two important properties for the performance of drug delivery systems. Entrapment or conjugation of a drug to a polymeric system may protect the drug from inactivation and help to store its activity for prolonged durations, decrease its toxicity, as well as may achieve administration flexibility.

Drug loading is the process of incorporation of the drug into a polymeric matrix or capsule. Drug loading can be done by two methods: *i*) incorporating at the time of Nanoparticles (NPs) production (incorporation method); or, *ii*) adsorption of the drug after formation of NPs by incubating the carrier with a concentrated drug solution (adsorption technique) (Allémann et al. 1993). If preformed NPs are incubated in a drug solution for drug loading, the drug can be extensively adsorbed to their large surface area which in turn can result in initial burst release, which is more pronounced in smaller particles (Chorny et al. 2002, Lecaroz et al. 2006). Furthermore, this method generally results in lower drug loading (Bapat and Boroujerdi 1992, Lopes et al. 2000, Soppimath et al. 2001). The time of incubation can also influence drug loading, and the incubation time has to be sufficient to

reach equilibrium for maximum loading (Lopes et al. 2000). Drug loading (or drug content, %) is defined as: (mass of drug loaded to the NPs/mass of NPs) × 100. Drug entrapment efficiency (%) is defined as: (mass of drug loaded to the NPs/initial mass of drug used to load the NPs) × 100.

Drug release is the reverse process by which drug molecules are liberated from the solid phase, and become available for absorption and pharmacological action. Drug loading and release are related to each other because both depend on the physicochemical properties of the matrix, the physicochemical properties of the drug and the interaction between the matrix, the drug and the environment.

In the delivery of bioactive agents, generally the agent is dissolved, entrapped, adsorbed, encapsulated or attached to a polymeric matrix that has a micro- or nano-dimension. The drug can be incorporated into NPs by hydrogen bonding, ionic interaction, dipole interaction, physical entrapment (or encapsulation), precipitation, covalent bonding or be adsorbed onto the surface. In most drug delivery systems, more than one loading mechanism can be involved.

Common drug-loading procedures are: simple equilibrium, dialysis, water-in-oil (w/o) emulsion, solution casting and freeze-drying. Drug loading depends on the type of NPs (nanocapsule, dendrimer, polymeric micelle, nanoemulsion and nanogel) and the preparation methodology. In *nanocapsules* as vesicular systems, the drug is trapped in the central cavity which is surrounded by a polymeric membrane, whereas in nanospheres, the drug is physically and uniformly dispersed in the matrix. An exhaustive list of examples of drug loading can be found in the excellent review published by Judefeind and de Villiers (2009). The drugs can be loaded in *nanospheres* by: double emulsion/solvent evaporation, cation-induced controlled gelification, nanoprecipitation, incubation in buffer solution, instantaneous precipitation using supercritical CO_2 and encapsulation of drug in matrix by anhydrous solid-oil technique, melting-sonication or polymerization with drug added before or after completion of polymerization.

Drug loading to *dendrimers* is achieved by: equilibrium dialysis method, incubation, separation, conjugation of drug to end groups of the dendrimer or to the surface end groups of the dendrimer with different spacers. Alternatively, the drug can be chemically incorporated into the dendrimer structure. Drug entrapment in dendrimers can be increased with higher generations (Kojima et al. 2000, Kolhe et al. 2003), different types of dendrimers, their surface modification (Tripathi et al. 2002, Bhadra et al. 2006, Dutta et al. 2007), different spacers used for drug conjugation onto the surface end group of the dendrimer (Wiwattanapatapee et al. 2003) and the polarity of the drug (Dhanikula and Hildgen 2006).

Polymeric micelles can be loaded by: dialysis method, solvent/co-solvent evaporation method with different co-solvent compositions and sequences of adding.

Drug loading of *nanoemulsions* and *nanocapsules* habitually uses: solvent displacement method, loading during interfacial deposition, nanoprecipitation, spontaneous emulsification or interfacial polymerization. The right selection of polymer, copolymer (molecular weight, existence of functional groups, charge, and monomer ratio), functional groups on polymers, molecular weight of the polymer/copolymer (Gaspar et al. 1998, Pandey et al. 2005, Pfeifer et al. 2005), drug nature (acidic, base, or salt form), loading conditions [modification in pH (Tripathi et al. 2002, Asthana et al. 2005), temperature, sequence of adding excipients], nominal drug loading, etc., are crucial for optimizing drug entrapment (Govender et al. 1999). With increasing interactions (mainly ionic interaction) with the carrier system rather than with the surrounding medium, drug loading as well as entrapment efficiency increase. However, the release rate could decline (Gaspar et al. 1998, Govender et al. 2000, Bhattarai et al. 2006, Opanasopit et al. 2006).

Macromolecules or proteins show the greatest loading efficiency when they are loaded at or near their isoelectric point when it has minimum solubility and maximum adsorption. If the drug is loaded by the incorporation method, the system has a relatively small burst effect and better sustained release characteristics. If the NPs are coated by a polymer, the release is then controlled by diffusion of the drug from the core across the polymeric membrane. The membrane coating acts as a barrier to release, therefore, drug solubility and diffusivity in polymeric membrane becomes the determining factor in drug release. When the drug is involved in interaction with auxiliary ingredients to form a less water-soluble complex, then the drug release can be very slow with almost no burst release effect; whereas if the addition of auxiliary ingredients, e.g., ethylene oxide-propylene oxide block copolymer (PEO-PPO) to Chitosan (CS), reduces the interaction of Bovine Serum Albumin (BSA) with the CS matrix due to competitive electrostatic interaction of PEO-PPO with CS, then an increase in drug release could be observed.

Both water-soluble and water-insoluble drugs can be loaded into CS-based particulate systems. Water-soluble drugs (sodium diclofenac) and drugs that can precipitate in acidic pH solutions can be loaded after the formation of particles by soaking of the preformed particles with the saturated solution of drug. Percentage loading of drug decreased with increasing cross-linking due to decreased swelling. Water-insoluble drugs can also be loaded using the multiple emulsion technique. Sometimes, drugs can be dispersed into CS solution by using a surfactant to get the suspension. The resulting droplets can be hardened by using a suitable cross-linking

agent (Agnihotri et al. 2004). The conjugated doxorubicin (DOX)-poly(D,L-lactic-*co*-glycolic acid) (PLGA) and DOX-loaded PLGA NPs prepared by spontaneous emulsion solvent diffusion method showed an encapsulation efficiency of 3.5 and 96.6%, respectively (Yoo et al. 1999).

Biological agents can be incorporated in *nanogels* by: physical entrapment, covalent conjugation, or controlled self-assembly (Table 2.1). Generally, drug loading capacities that can be expected for hydrophilic nanogels are greater than those normally observed for other nano-sized pharmaceutical carriers such as polymeric micelles, liposomes and biodegradable NPs. The main reason for this is that swollen nanogels are mainly comprised of water and therefore provide for a larger cargo space for incorporation of solutes, which is important for low molecular weight drugs and especially, for biomacromolecules. Furthermore, the high loading in nanogels can be achieved by self-assembly via combinations of electrostatic and hydrophobic interactions and in relatively mild conditions compared to other carriers, which is very important for preservation of the biological activity of labile drugs and biomacromolecules, such as proteins and polypeptides (Vinogradov 2007). Binding of drugs induces collapse of nanogel, which usually decreases the volume by at least one order of magnitude. However, drug-nanogel particles remain dispersed due to the lyophilizing effect of nanogel hydrophilic polymer chains, such as poly(ethylene glycol) (PEG) exposed onto the surface. During the collapse of the drug-nanogel complex, such polymers become exposed to the surface and form a protective hydrophilic layer around the nanogel that prevents phase-separation. Functional groups at the nanogel surface can be additionally modified with various targeting moieties for site specific drug delivery in the body. Various nanogels were shown to deliver their payload inside cells and across biological barriers.

Mechanisms of Drug Release from Polymeric Nanocarriers

Long-term sustained drug delivery is a desired property which is affected by the diffusion kinetics of the drug and matrix degradation which controls the rate of drug release. It is possible to extend this period from hours to months.

Some characteristics differentiate nano-sized drug delivery systems from the others. It is well known that the surface to volume ratio is increased for NPs, and therefore higher drug amount is located at the surface compared to the core (Redhead et al. 2001). Additionally, the diffusion distance is reduced, therefore a higher initial burst release from NPs was observed comparatively with drug release from microparticles. Gref et al. (2001) and Lecaroz et al. (2006) found that drug loading as well as entrapment efficiency was higher for microparticles compared to NPs.

Table 2.1. Principal methods to load biological agents into nanogels.

Loading method	Drug	System	Observation	Reference
Physical entrapment	Insulin	Cholesterol-modified pullulan nanogel		Akiyoshi et al. 1998
	*si*RNA	Thiol-conjugated hyaluronic acid nanogel		Lee et al. 2007
	Prostaglandin E2	Solubilized in cholesterol-modified pullulan nanogel		Kato et al. 2007
	DOX	Amphiphilic cross-linked nanogel based on Pluronic® F-127		Missirlis et al. 2005
	DOX	Poly[oligo(ethylene oxide)-methyl methacrylate]		Oh et al. 2007
Covalent attachment	Cisplatin	Carboxyl group containing nanogels made of cross-linked (core-shell) PMA-*b*-PEG	Drug reacts with carboxylic groups in the nanogel core	Bronich et al. 2006, Jin et al. 2007
	Protein	Modification of enzyme molecules with *N*-hydroxysuccinimidoacrylate followed by polymerization of acrylamide in dilute aqueous solutions		Yan et al. 2006, 2007
	α-chymotrypsin	Polyacrylamide nanogel	Covalently bounded protein with increased thermostability	Khmelnitsky et al. 1992, Hong et al. 2007
Controlled self-assembly of polyelectrolyte-based nanogel with oppositely charged solutes	Charged and amphiphilic biological agents, e.g., sodium oleate, indomethacin, and retinoic acid	Binding of sodium tetradecyl sulfate, an anionic surfactant with cationic PEG-*cl*-PEI nanogel	High loading, high binding cooperativity, and efficiency. Stable at physiological pHs and ionic strength. It can be lyophilized, stored, and then re-dispersed	Bronich et al. 2001
	5′-triphosphates of nucleoside analogs	Cationic nanogel		Vinogradov et al. 2005
	Biomacromolecules of opposite charge	Weakly cross-linked polyelectrolyte nanogel	Interpolyelectrolyte complex	Kabanov et al. 2004, Oh et al. 2007
	Antisense polynucleotides, oligonucleotide	Cationic nanogel of PEG-*cl*-PEI	"Collapse" of the nanogel volume. Loading capacity: 15–30% by weight	Vinogradov et al. 1998, 1999, McAllister et al. 2002

Mechanisms of drug release are mainly based on the dissolution phenomenon, which is a diffusion-controlled process (Judefeind and de Villiers 2009). *In vitro* dissolution rate of a drug formulation with different particle sizes (namely particle diameter and the thickness of the diffusion boundary layer, which are inversely related to the dissolution rate) affect the drug dissolution rate mainly in the case of nano-sized particles (Tinke et al. 2005). The increase in dissolution rate with decreasing particle size was higher than that expected from the increase in surface area alone, because of a decrease in the diffusion boundary layer thickness with decreasing drug particle radius (Bisrat and Nystrom 1988). Mihranyan and Strømme (2007) derived a relationship between fractal surface dimension and solubility and predicted a higher solubility for particles with a rough surface compared to particles with a smooth surface.

A decreased particle size causes a higher curvature resulting in higher surface free energy and, therefore, higher drug solubility. The solubility is increased by decreased particle size up to a certain radius below which the solubility is decreased again (Knapp 1922, Mihranyan and Strømme 2007). By the increase in the free surface energy (smaller particles), the particles tend to agglomerate (Ostwald ripening), and the surface area, taking part in the dissolution process, is decreased and can be overestimated (Bisrat and Nyström 1988).

The effect of surface tension and wettability of NPs was investigated by Sdobnyakov and Samsonov (2005). For very small droplets (2–10 nm in radius) the surface tension decreases with size, whereas above a critical radius the surface tension approaches the one of the macroscopic planar interface. The wettability of NPs (> 1 nm in radius) can be described by the Young's equation for high surface tension interfaces (Powell et al. 2002).

It is generally accepted that the dissolution of a drug from small particles occurs in two steps (Crisp et al. 2007): *i*) the solute-solvent interaction resulting in dissociation of drug molecules (solvation step); and, *ii*) diffusion of the drug molecule into the bulk dissolution media. Usually, the diffusion is the rate-limiting step (Bisrat et al. 1992), which is described by Fickian diffusion laws. The dissolution rate described as a diffusional process is directly proportional to surface area, drug solubility and indirectly proportional to the diffusion boundary layer. Extrapolation of this finding to NPs showed that for particles in the range of 100–1000 nm, the solvation step (surface kinetic constant, k_S) controls the dissolution, rather than the diffusion of the drug molecules into the bulk medium (Shekunov et al. 2006, Crisp et al. 2007). The process of dissolution not only is important for drug delivery systems but can also be used to evaluate nanomaterials (Borm et al. 2006).

The following types of controlled drug release systems have been identified: *i*) dissolution controlled systems as encapsulation dissolution or

matrix dissolution; *ii*) diffusion controlled systems as reservoir controlled or matrix controlled; *iii*) dissolution and diffusion controlled release systems; *iv*) water penetration controlled systems by swelling or osmotic; *v*) chemically controlled release systems as erodible or to pendent chain; *vi*) nanohydrogels; and, *vii*) ion-exchange resin controlled release systems.

For the first type of controlled drug release systems, the rate controlling step is dissolution. The drug is embedded either in slowly dissolving or erodible matrix, or by coating with slowly dissolving substances. In the first category, drug-loaded particles are coated or encapsulated by microencapsulation techniques with slowly dissolving materials like cellulose, PEGs, polymethacrylates, waxes, etc. The dissolution rate of the coating depends upon its solubility and thickness. Waxes such as, beeswax, carnauba wax, hydrogenated castor oil, etc., control drug dissolution by controlling the rate of dissolution fluid penetration into the matrix, by their properties and the thickness of the dissolving layer.

Diffusion controlled release systems are characterized by a drug release rate dependent on its diffusion through an inert water-insoluble membrane barrier (Modesti et al. 2009) (Fig. 2.1a). In matrix diffusion systems the drug core is encased in a partially soluble membrane [e.g., a mixture of ethyl cellulose with poly(*N*-vinylpyrrolidone) (PVP), or methyl cellulose]. Due to dissolution of parts, the membrane pores are created which permit entry of aqueous medium into the core, drug dissolution then takes place and also its diffusion out of the system (Fig. 2.1b). Polakovic et al. (1999) found that the diffusion model could be used to describe the release from

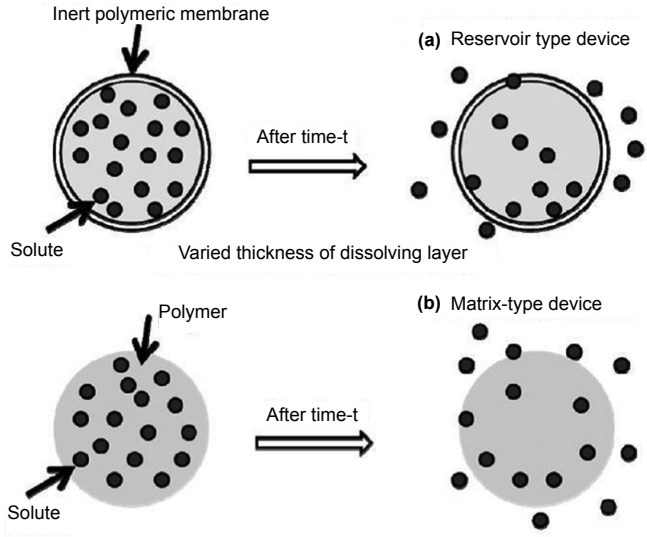

Figure 2.1. (a) Reservoir- and (b) matrix-type controlled drug delivery devices.

NPs with a low drug loading where the drug was molecularly dispersed. On the contrary, if the drug was in the crystallized form at higher drug loading, the release rate was controlled by dissolution.

In water penetration controlled delivery systems, water permeation into the matrix can be a prerequisite for drug release (e.g., swelling of the matrix to enable drug diffusion, or dissolving the drug in the matrix prior to diffusion). Initially, the dry system is placed in the body when it absorbs water or other body fluids and swells. Swelling increases the aqueous solvent content within the formulation as well as the polymer mesh size, enabling the drug to diffuse through the swollen network into the external environment (Ferrero et al. 2010).

Solute transport from non-degradable polymeric systems is mainly considered as diffusion driven. Non-degradable polymers can be fabricated into reservoir- and matrix-type devices. By definition, reservoir-type devices refer to those having an inert coating material, which functions as a rate-controlling membrane. The release rate remains relatively constant and is not affected by the concentration gradient, but depends on the thickness and permeability of the polymeric membrane. In contrast for matrix-type devices, drug release is more likely to be Fickian diffusion driven, which is associated with concentration gradient, diffusion distance and the degree of swelling.

Osmotically controlled release systems are fabricated by encapsulating an osmotic drug core containing an osmotically active drug (or a combination of an osmotically inactive drug with an osmotically active salt, e.g., NaCl) within a semi-permeable membrane made from a biocompatible polymer (i.e., cellulose acetate), so a gradient of osmotic pressure is created, under which the drug solutes are continuously pumped out over a prolonged period of time through the delivery orifice. This type of drug system dispenses drug solutes continuously at a zero order rate.

Chemically controlled release systems change their chemical structure, when exposed to biological fluid. In erodible systems, the mechanism of drug release occurs by erosion which can be a bulk erosion process, and/or a surface erosion process (polyorthoesters and polyanhydrides). Biodegradable polymers are generally designed to degrade as a result of hydrolysis of polymeric chains into biologically safe and progressively smaller moieties. On the other hand, in bulk erosion polymer degradation may occur through bulk hydrolysis. For instance, pendent chain systems consist of linear homopolymers or copolymers [e.g., *N*-(2-hydroxypropyl) methacrylamide] with the drug attached to the backbone chains. The drug is released from the polymer by hydrolysis or enzymatic degradation of some linkages. The cleavage of the drug is the rate controlling mechanism of zero order.

Drug release from hydrogels and nanogels can be: diffusion-, swelling-, chemically-controlled or environmentally responsive systems. The most important factors to be taken into account when formulating hydrophilic matrices such as hydrogels are: solubility, drug particle size, type of polymer, drug loading, viscosity, polymer particle size, percentage and mixtures of polymers, drug/polymer ratio and the amount of water entering the matrix (Maderuelo et al. 2011).

Ion-exchange resins controlled release systems are designed to provide the controlled release of an ionic (or ionizable) drug (e.g., codeine base in Amberlite™). A cationic/anionic drug forms a complex with an anionic/cationic ion-exchange resin, e.g., a resin with a SO_3^- group or a $N(CH_3)_3^+$ group, respectively. In the Gastrointestinal (GI) tract, hydrogen ion (H^+ or chloride ion Cl^-) penetrates the system and drug release takes place.

Drug Release Kinetics from Polymeric Nanocarriers

Because qualitative and quantitative changes in a formulation may alter drug release and *in vivo* performance, developing tools that facilitate product development by reducing the necessity of bio-studies is always desirable. In this regard, the use of *in vitro* drug dissolution data to predict *in vivo* bio-performance can be considered as the rational development of controlled release formulations (Wagner 1969, Dressman and Fleisher 1986, Ozturk et al. 1988, Costa and Lobo 2001). Another advantage of the kinetics is to represent several release data with one or two parameters.

The methods to investigate drug release kinetics in controlled release formulations can be classified into three categories:

- Statistical methods [exploratory data analysis method, repeated measures design, multivariate approach (MANOVA/ANOVA: multivariate analysis of variance)]. Time is the repeated factor and percent dissolved is the dependent variable. The dissolution profile data are given in both graphical and numerical manner (Polli et al. 1997).
- Model dependent methods are based on different mathematical functions, which describe the dissolution profile. The model that gives the highest correlation coefficient *r* value is considered as the best fitted for the drug release data. Once a suitable function has been selected, the dissolution profiles are evaluated depending on the derived model parameters. The model dependent approaches included zero order, first order, Higuchi, Hixson-Crowell, Korsmeyer-Peppas, Baker-Lonsdale, Weibull, Hopfenberg, Gompertz and regression models, to cite just a few (Shah et al. 1997, Costa and Lobo 2001) (Table 2.2).

Table 2.2. Some kinetic models used for analysis of drug release data from nanoparticulate systems (Polakovic et al. 1999, Jo et al. 2004, Cruz et al. 2006, Fu and Kao 2010).

Model	Equation	Application as and to:
Zero order (Serra et al. 2006)	$F = k_o t$, or $Q_t = Q_0 + K_0 \cdot t$, or $\frac{M_t}{M_\infty} = k_d t$	*Graph:* time on *x*-axis, and the cumulative percentage of drug release on *y*-axis. It describes systems where drug release rate is independent of the concentration of dissolved substance. Drug dissolution from dosage forms that do not disaggregate as transdermal systems, matrix tablets with low soluble drugs in coated forms, osmotic systems
First order	$\ln(1\text{-}F) = -k_f t$, or $\log Q_t = \log Q_0 + (K_t/2.303)$	*Graph:* time on *x*-axis, and log cumulative percentage of drug remaining to be released on *y*-axis. Drug release rate depends on its concentration, drug absorption and/or elimination or drug dissolution in pharmaceutical dosage forms such as those containing water-soluble drugs in porous matrices
Higuchi (Higuchi 1963)	$F = k_H t^{1/2}$, or $Q = K_H t^{1/2}$	*Graph:* the square root of time taken on *x*-axis, and the cumulative percentage of drug release on *y*-axis. The Higuchi equation suggests drug release by diffusion, transdermal systems, and matrix tablets with water-soluble drugs
Power law Korsmeyer-Peppas, or Ritger-Peppas (Ritger and Peppas 1987a,b)	$\ln F = \ln k_p + p \ln t$, or $F = (M_t/M) = K_m \cdot t^n$	*Graph*: log time taken on *x*-axis, and log cumulative percentage of drug release on *y*-axis. First 60% drug release data *n* is estimated from linear regression of log (M_t/M) *vs*. log *t*. Release transport can be classified according to the diffusional exponent which takes different values for the various swellable as well as non-swellable carrier systems. For the case of cylindrical tablets, $0.45 \leq n$ corresponds to a Fickian diffusion mechanism, $0.45 < n < 0.89$ anomalous diffusion or non-Fickian diffusion/transport, $n = 0.89$ to case II (relaxational—zero order release) transport, and $n > 0.89$ to super case II transport. Anomalous diffusion or non-Fickian diffusion refers to combination of both diffusion and erosion controlled release. Case II relaxation or super case II transport refers to the erosion of the polymeric chain
Peppas-Sahlin (Peppas and Sahlin 1989)	$\frac{M_t}{M_\infty} = k_1 t^m + k_2 t^{2m}$	Non-Fickian diffusion

Alfrey et al. 1966	$\frac{M_t}{M_\infty} = k_1 t + k_2 \sqrt{t}$	Non-Fickian diffusion (sigmoid)
Hixson-Crowell	$1 - \sqrt[3]{1-F} = k_{1/3} t$, or $\sqrt[3]{Q_0} - \sqrt[3]{Q_t} = K_{HC} t$	*Graph*: time on *x*-axis, and the cube root of the initial concentration minus the cube root of percent remaining on *y*-axis It describes drug release by dissolution, and release with the changes in surface area and diameter of particles or tablets
Square root of mass	$1 - \sqrt{1-F} = k_{1/2} t$	
Weibull	$\ln[-\ln(1-F)] = (-\beta \cdot \ln t_d) + (\beta \ln t)$	Widely applied to release data of both rapid and extended release drug delivery systems; is more useful for comparing the release profiles of matrix type drug delivery. The time, when 50% (w/w) and 90% (w/w) of drug being in each formulation was released, was calculated using the inverse function of the Weibull
Gompertz model	$X(t) = X_{\max}^{-\alpha e^{\beta \log t}}$	Drugs having good solubility and intermediate release rate
Linear probability	$Z = Z_0 + qt$	
Linear or first order regression model	$Y = \beta_0 + \beta_1 X_1 + \beta_2 X_2$, or $Y = \beta_0 + \beta_1 X_1 + \beta_2 X_2 + \beta_{12} X_1$	Multiple linear regression technique by adding interaction terms to the first order linear model
Quadratic model or second order regression model	$Y = \beta_0 + \beta_1 X_1 + \beta_2 X_2 + \beta_{11} X_1^2 + \beta_{22} X_2^2 + \beta_{12} X_1 X_2$	
Log-probability	$Z = Z'_0 + q't$	
Non conventional order 1	$1-(1-F)^{1-n} = (1-n) k_{1-n} t$	
Non conventional order 2	$\frac{1}{(1-F)^{n-1}} - 1 = (n-1) k_{n-1}$	
Reciprocal powered time	$\left(\frac{1}{F} - 1\right) = \frac{m}{t^b}$	

- Model independent methods use the difference factor, the similarity factor as a criterion for assessment of similarity between two *in vitro* dissolution profiles and Rescigno index (Moore and Flanner 1996, Costa 2001).

The parameters of these models k_0, k_f, k_H, p, k_P, $k_{1/3}$, $k_{1/2}$, $k_{2/3}$, t_d, β, Z_0, Z'_0, q, q', n, $k_{1\text{-}n}$, $k_{n\text{-}1}$, m, and b can be obtained by linear regression or non-linear regression. F denotes the fraction of drug released up to time t. Z and Z' are probits of the fraction of drug released at any time. Z_0 and Z'_0 are the values of Z and Z' when $t = 0$ and $t = 1$, respectively. The relationships between Z and Z' with F are given by:

$$F = (2\pi)^{-\frac{1}{2}} \int_{-\infty}^{Z} \exp\left[\frac{-Z^2}{2}\right] dZ \tag{1}$$

$$F = (2\pi)^{-\frac{1}{2}} \int_{-\infty}^{Z'} \exp\left[\frac{-Z'^2}{2}\right] dZ' \tag{2}$$

where $Z = (t - t_{50\%})/\sigma$ and $Z' = (\log t - \log t_{50\%})/\sigma'$. σ and σ' are relevant standard deviations.

Q_0 is the initial amount of drug, Q_t is the cumulative amount of drug release at time t, K_0 is the zero order release constant, t is the time in hour, K_1 is the first order release constant, K_{HC} is the Hixson Crowell release constant, K_H is the Higuchi constant, F is the fraction of drug released at time t, M_t is the amount of drug released at time t, M is the total amount of drug in the dosage form, K_m is the Korsmeyer-Peppas kinetic constant, n is the diffusion or release exponent, X(t) is the percent of drug dissolved at time t divided by 100, X_{max} is the maximum dissolution, α determines the undissolved proportion at time $t = 1$ and it is described as location or scale parameter, and β is the dissolution rate per unit of time described as shape parameter.

Barzegar-Jalali et al. (2008) analyzed the release data of 32 drugs from 106 nanoparticulate formulations gathered from various research articles using 10 well known models, as well as three models developed by them. They demonstrated that Weibull and Wagner's log-probability models were superior to the rest of models. Among the models the novel Reciprocal Powered Time (RPT), Weibull and log-probability ones produced overall mean percent error (OE) values of 6.47, 6.39 and 6.77%, respectively. The OE values of other models were higher than 10%. Considering the accuracy criteria, the RPT model could be suggested as a general model for analysis of multi-mechanistic drug release from NPs.

Regardless of the mechanism involved in drug release, its rate under sink conditions can be expressed by a single general equation, as follows:

$$\frac{dw}{dt} = \left(\frac{D}{h}\right) \cdot S \cdot C_S \tag{3}$$

where w is the amount of drug released up to time t, and dw/dt is the rate of release. D, S, C_s, and h are the drug diffusion coefficient, effective surface area of drug with the release medium, drug solubility in the medium and the length of diffusion path, respectively. This equation represents both the Noyes-Whitney law of dissolution (Noyes and Whitney 1897) applied for dissolution rate limited release, as well as the Fick's first law of diffusion used for diffusion rate limited release processes. For a complex system, such as NPs, this equation does not seem to include all other factors influencing the release rate, such as penetration rate of liquid into the system and hydration, swelling, relaxation, erosion and dissolution of polymer.

Drug release rates from NPs typically depend upon: *i*) desorption of the surface-bound or adsorbed drug; *ii*) diffusion through the NP matrix; *iii*) diffusion (in the case of nanocapsules) through the polymer wall; *iv*) NP matrix erosion; and, *v*) combined erosion-diffusion process. Thus, diffusion and biodegradation govern the drug release process (Soppimath et al. 2001).

Factors influencing drug release kinetics are classified depending on:

- Matrix: composition, structure, swelling, degradation, cross-linking, morphology, size and density of the particulate system.
- Release medium: pH, temperature, ionic strength, enzymes, polarity and presence of adjuvants. For example, the dendrimer-methotrexate (Patri et al. 2005) or ibuprofen (Kolhe et al. 2003) inclusion complex released drug in buffer, while no drug was released when water was used.
- Drug: solubility, stability, charge, interaction with matrix and physicochemical properties.
- The interaction between the drug and the carrier matrix: conjugation or adsorption which not only affects drug loading, but also influences the release rate as well as the extent of release. Sometimes, this interaction has to be neutralized by, e.g., introducing ions (buffer solutions) to enable the release from the carrier.

In general, the release from nanocarriers follows a biphasic pattern with an initial burst release of adsorbed and weakly bound drug from the surface, followed by a slower release rate attributed to the diffusion of entrapped drug through the matrix. This fact implies that drug distribution within the NP influences the release pattern: a higher amount of drug close to the surface or adsorbed onto the surface increases the initial burst effect. In contrast, if the drug is more uniformly distributed or a higher amount

is entrapped inside the NP, the initial rapid release rate is reduced. The burst release is an important issue that has to be taken into account for drug delivery nanosystems because of the high surface to volume ratio (Quaglia et al. 2006, Zhang et al. 2006). For instance, BSA-containing nanospheres prepared by the double emulsion method showed an elevated burst release, compared to particles prepared by a novel method employing thermosensitive Pluronic® F-127 gel (Leo et al. 2006). Concretely, particles prepared following the double emulsion method yielded a higher BSA adsorption compared to particles synthesized following the other method where the drug could be entrapped into their core.

Methods to study the *in vitro* release are: *i*) side-by-side diffusion cells with artificial or biological membranes; *ii*) dialysis bag diffusion technique; *iii*) reverse dialysis sac technique; *iv*) ultracentrifugation; *v*) ultrafiltration; or, *vi*) centrifugal ultrafiltration (Magenheim and Benita 1991, D'Souza and DeLuca 2006).

If a drug is uniformly dispersed in a polymer matrix system (nanospheres) which is non-biodegradable or the degradation of the polymer only occurs much later than drug release (drug is not released by matrix erosion), the drug has to dissolve and diffuse from the polymeric matrix to reach the surface and to partition into the surrounding medium through a diffusion-controlled release transport, described by the well-known Higuchi equation (Higuchi 1963). For a porous matrix, the Higuchi equation is extended by the porosity of the matrix and the tortuosity of the capillary system. The Higuchi's equation indicates that the release rate is directly proportional to the surface area, the total amount of drug incorporated into the matrix (drug loading), drug solubility in the matrix, and the diffusion coefficient of the drug in the matrix. The interaction between the drug and the polymer leads to an alteration of the diffusion coefficient: the higher the interaction , results in lower the diffusion coefficient. For example, Chorny et al. (Chorny et al. 2002, Cruz et al. 2006) investigated the release kinetics of indomethacin and indomethacin ethyl ester from different nanocarriers: nanocapsules, nanoemulsions and nanospheres. No differences were discovered in the release patterns from these nanocarriers when the drug (indomethacin) was adsorbed onto the NPs. However, if the drug (indomethacin ethyl ester) was entrapped into the nanocarrier, all these delivery systems exhibited different release kinetics.

Drug delivery is generally accomplished through oral administration or by injection, and follows first order kinetics. Costa and Lobo (2003) showed that transdermal drug delivery mechanisms follow the Higuchi model. Entrapping or encapsulating the drug within a polymer allows for greater control of its pharmacokinetics. The drug can be released with a more ideal, near zero order kinetic profile, which establishes a more constant flow of the drug out of the carrier. This pharmacokinetic behavior maintains more

appropriate steady drug levels at the targeted site. In contrast, conventional oral drug delivery typically follows first order release kinetics, where the drug release rate is proportional to the amount of drug remaining in the carrier. In another research report, NP-coated tablets with hydroxypropyl methylcellulose phthalate showed a decrease in release rate and a migration towards zero order release kinetics, as the particle size was decreased (Kim et al. 2003).

Drug release from an erodible polymeric matrix

Hopfenberg developed a mathematical model to correlate drug release from surface eroding polymers, so long as the surface area remains constant during the degradation process where a zero order surface detachment of the drug is the rate limiting release step (Kalam et al. 2007, Fu and Kao 2010). The equation is valid for spheres, cylinders and slabs:

$$\frac{M_t}{M_\infty} = 1 - \left(1 - \frac{k_0 t}{c_0 a}\right)^n \tag{4}$$

where M_t and M_∞ are the cumulative amounts of drug released at time t and at a infinite time, k_0 refers to the erosion rate constant, c_0 denotes the initial drug concentration within the matrix, a is the radius of a cylinder or sphere or the half-thickness of a slab, n is a "shape" factor representing the spherical (n = 3), cylindrical (n = 2), or slab geometry (n = 1). Katzhendler et al. (1997) developed a general mathematical model for drug release from an erodible matrix, which takes into account radial and axial erosion:

$$\frac{M_t}{M_\infty} = 1 - \left(1 - \frac{k_a t}{c_0 a_0}\right)^2 \left(1 - \frac{2k_b t}{C_0 b_0}\right) \tag{5}$$

where k_a is the radial erosion rate constant, k_b is the axial erosion rate constant, and a_0 and b_0 are the tablets' initial radius and thickness, respectively. When $k_a \approx k_b$, the release profiles of theophylline from a cylindrical tablet could be well described by this equation. Karasulu et al. (2000) and Rothstein et al. (2009) developed a unified model for both surface- and bulk-eroding materials. This model combines diffusion-reaction equations, taking into account the system's hydration kinetics, dissolution, and pore formation to compute drug release (Lao et al. 2011), by equation:

$$\frac{\partial C_w}{\partial t} = \nabla\left(D_w \nabla C_w\right) - kC_w M_w \tag{6}$$

The kinetics of hydrolysis can be described by the following equation:

$$\frac{\delta M_w}{\delta t} = -kC_w M_w \tag{7}$$

where C_w is the time-dependent concentration of water, D_w is the diffusivity of water in the polymer matrix, k is the degradation rate constant and M_w is the molecular weight of the polymer.

The cumulative fraction of drug released at time t was described as:

$$\frac{M_t}{M_\infty} = 1 - \left(1 - \frac{k_0 t}{c_L a}\right)^n \tag{8}$$

where k_0 is the zero order rate constant describing the polymer degradation (surface erosion) process, C_L is the initial drug loading throughout the system, a is the half thickness of the system (i.e., the radius for a sphere or cylinder), and n is an exponent that varies with geometry with numerical values of 1, 2, and 3 for slab (flat), cylindrical and spherical geometry, respectively. This model is used to identify the mechanism of release from the optimized spheres using data derived from the composite profile, which essentially displayed site-specific biphasic release kinetics.

In hydrophilic matrix systems, the surface initially hydrates during dissolution to generate an outer viscous gel layer. This phase is then sequentially followed by matrix bulk hydration, swelling and erosion (Nagarwal et al. 2010). The overall dissolution rate is controlled by the rate of matrix swelling, drug diffusion through the gel layer (Harland et al. 1988) and/or matrix erosion (Bain et al. 1991). Water-soluble drugs are released primarily by diffusion of the dissolved molecules across the gel layer, while poorly soluble drugs are released predominantly by matrix erosion. The contribution of each mechanism in the overall drug release process is influenced by the drug solubility, drug geometry, drug ionization and by the physical and mechanical properties of the gel barrier formed. Costa and Lobo (2001) and Panyam et al. (2003) found that the degradation rate of PLGA during the initial phase was higher for 100 nm-sized particles than for 1 or 10 nm-sized particles. For these systems different release mechanisms can occur simultaneously (Siepmann and Gopferich 2001, von Burkersroda et al. 2002, Chen and Ma 2006).

Drug release through polymeric shells

If a drug is encapsulated into nanocapsules, the drug has to traverse the capsule shell prior to reaching the surrounding medium. Drug release can occur by permeation through the capsule wall, erosion of the shell or

diffusion through pores. Depending on the formulation type, the drug is released by one or a combination of several mechanisms: desorption of adsorbed drug, diffusion through the polymeric matrix, diffusion through the polymeric membrane shell in the case of nanocapsules and polymer degradation and erosion (Jain 2000, Soppimath et al. 2001, Mainardes and Silva 2004).

The mass rate of permeation (dM/dt) of a drug through the capsule shell can be written according to the first Fick's law under sink conditions:

$$\frac{dM}{dt} = \frac{DKAC_D}{h} \tag{9}$$

where D is the diffusion coefficient of the drug in the capsule shell, A is the surface area, K is the partitioning coefficient of the drug between capsule core and shell, C_D is the solubility (solid) or concentration (dissolved) of the drug in the interior of the capsule and h is the thickness of the capsule shell.

The permeability coefficient, also known as permeability P, is used to compare various systems as it is independent of the surface area and the concentration of the drug on the donor side C_D. The permeability coefficient, of a polymer shell is described as follows:

$$P = \frac{DK}{h} \tag{10}$$

Nanocapsules and nanospheres differ in their release profiles due to the nature of the active agent containment. Drug release from the matrix occurs through diffusion as well as erosion of the matrix itself. If diffusion occurs more quickly than degradation, then the process is diffusion dependent, otherwise the process of degradation is highly influential (Niwa et al. 1993). Matrix-type NPs usually exhibit first order kinetics (Fresta et al. 1995, Radwan 1995). Reservoir-like morphology of the nanocapsules theoretically leads to zero order kinetics of release (Calvo et al. 1996, Lu et al. 1999).

In conclusion, diffusion and biodegradation govern the process of drug release and the release rates from NPs depend upon: *i*) desorption of the surface-bound or adsorbed drug; *ii*) diffusion through the NP matrix; *iii*) diffusion (in case of nanocapsules) through the polymer wall; *iv*) NP matrix erosion; and, *v*) a combined erosion/diffusion process.

Kinetics and Mechanism of Drug Release from Hydrogels/Nanogels

The biological agents can be released from nanogels as a result of: *i*) simple diffusion; *ii*) nanogel degradation; *iii*) pH shift; *iv*) displacement by counterions present in the environment; *v*) transitions induced by

the external energy source; or, *vi*) response to environmental changes (Kim et al. 1992). For example, Tan et al. (2008) synthesized via emulsion polymerization, pH-responsive nanogels consisting of methacrylic acid-ethylacrylate cross-linked with di-allyl phthalate. The mathematical fitting to the Berens and Hopfenberg model allowed the parameters describing the contributions of chain relaxation and diffusion process to be determined. A balance between chain relaxation and Fickian diffusion process controlled drug release from these pH-responsive nanogels. Several examples of drug release from stimuli-responsive nanogels are collected in Table 2.3. Nanogels can be modified to eliminate the burst release or even to achieve zero order drug release kinetics (Zhang et al. 2007).

Table 2.3. Drug release from stimuli-responsive nanogels.

Mechanism	Active agent	System	Reference
Diffusion	DOX	Pluronic-based hydrogels	Missirlis et al. 2006
Reductive agent		PEG-*cl*-PEI nanogel with disulfide cross-links rapidly degraded in presence of reductive agents	Vinogradov et al. 2006, Kohli et al. 2007
Degradation	Rhodamine 6G, DOX	Poly[oligo(ethylene oxide)-methyl methacrylate] nanogel with disulfide cross-links degraded by glutathione tripeptides found in cells	Oh et al. 2007
External agent	*si*RNA	Dissolution of disulfide cross-linked HA nanogels by glutathione	Lee et al. 2007
Environmental changes	Protein	pH-sensitive nanogel based on PAA	Varga et al. 2006, Yu et al. 2006, Chang et al. 2007, Oishi et al. 2007

Pharmacokinetics

Pharmacokinetics is concerned with the fate of external substances introduced into the body, specifically the extent and rate of absorption, distribution, metabolism and excretion of compounds. Chemical and physical properties of NPs, including size, surface charge and surface chemistry, are important factors that determine their pharmacokinetics and biodistribution (Yang et al. 2010).

The maximum plasma concentration (C_{max}) and the time to reach C_{max} relative to the time of dosing (t_{max}) can be determined from plasma concentration *vs*. time profiles. The biological half-life ($t_{1/2}$) can be calculated by using the formula $t_{1/2} = 0.6931/K_e$, where K_e is the elimination rate constant, i.e., the rate at which a drug is removed from the body. The total area under the concentration *vs*. time curve (AUC_{0-t}) can be obtained by linear trapezoidal method.

In pharmacology, bioavailability (F_{abs}) is a subcategory of absorption, one of the principal pharmacokinetic properties of drugs, which it is used to describe the fraction of an administered dose of unchanged drug that reaches the systemic circulation. More explicitly, the ratio of the amount of drug "absorbed" from a test formulation to the amount "absorbed" after administration of a standard formulation. Frequently, the "standard formulation" used in assessing bioavailability is the aqueous solution of the drug given intravenously. By definition, when a medicine is administered intravenously, its bioavailability is 100%. However, when it is administered via other routes, such as orally, its bioavailability generally decreases (due to incomplete absorption and first-pass metabolism) or may vary from patient to patient. Bioavailability is one of the essential tools in pharmacokinetics, as it must be considered when calculating dosages for non-intravenous routes of administration. The "amount absorbed" is conventionally measured by one of two criteria, either the area under the time-plasma concentration curve (AUC) or the total (cumulative) amount of drug excreted in the urine following drug administration which linearly depend on each other. Alinearity of the relationship between AUC and dose may occur if, for example, the absorption process is a saturable one, or if drug fails to reach the systemic circulation because of, e.g., binding of drug in the intestine or biotransformation in the liver during the drug's first transit through the portal system. Obviously, it depends on such factors as disintegration and dissolution properties of the dosage form, and the rate of biotransformation relative to rate of absorption. Dosage forms containing identical amounts of active drug may differ markedly in their abilities to make drug available and, therefore, in their abilities to permit the drug to manifest the expected pharmacodynamic and therapeutic properties.

Absolute bioavailability compares the bioavailability of the active drug in systemic circulation following non-intravenous administration (i.e., after oral, rectal, transdermal, subcutaneous or sublingual administration), with the bioavailability of the same drug following intravenous administration. In order to determine the absolute bioavailability of a drug, a pharmacokinetic study must be done to obtain a plasma drug concentration *vs*. time plot after both intravenous and extravascular (non-intravenous, i.e., oral) administration. The absolute bioavailability is the dose-corrected non-intravenous AUC divided by the intravenous AUC. For example, the formula for calculating F_{abs} for a drug administered by the oral route (peroral, po) is given below (where D_{iv} and D_{po} are the amounts of drug administered intravenously and perorally, respectively).

$$F_{abs} = \frac{AUC_{po} D_{iv}}{AUC_{iv} D_{po}} \times 100 \tag{11}$$

Therefore, a drug given by the intravenous route will have an absolute bioavailability of 100% (F_{abs} = 1), whereas drugs given by other routes usually have a F_{abs} < 1. Alternatively, comparative bioavailability can be estimated by comparing drug bioavailability of two different dosage forms having the same active ingredients. Summary of drug release kinetics and transport mechanisms of polymeric delivery devices is given in Table 2.4.

Polyanhydrides are a group of surface-erosion dominated biodegradable materials (Park et al. 1998). Drug release from pH- and enzyme-sensitive polymeric delivery systems is mainly attributed to stimuli-triggered degradation. A zero order release of BSA in the presence of human neutrophil elastase has been observed. Poly(ortho ester amides) degradation is triggered by acids. Both the mass loss kinetics of poly(ortho ester amides) in physiological aqueous buffers and the release of fluorescently labeled dextran followed the near zero order pattern, suggesting the release was predominantly driven by surface restricted polymer erosion.

Polysaccharides, such as hydroxypropyl methylcellulose (HPMC), cyclodextrin, dextran, gellan gum, remain stable under physiological pH and temperature, but will undergo hydrolysis at extreme pH and temperatures. Solute transport from polysaccharide-based systems could be driven by diffusion and/or dissolution.

Biodistribution and Bioevaluation of Polymeric Nanomaterials

Pharmacokinetic and biodistribution characteristics are important parameters to consider when designing and testing novel NPs and their transition from circulating blood to the tissue (Peer et al. 2007, Desai 2012). Nanomaterials may have different toxicity profiles due to the differences in chemical, optical, magnetic and structural properties (Garnett et al. 2006), thus leading to harmful side effects (Service et al. 2004, Kipen et al. 2005). Toxicity has been thought to originate from particle geometry, surface area and composition as reviewed by Lanone and Boczkowski (2006). Due to their small size and enhanced reactivity, some NPs readily travel throughout the body, deposit in targeted organs, penetrate cell membranes, lodge in sub-cellular compartments such as mitochondria (maybe triggering injurious responses) and affect the mode of endocytosis and the efficiency of particle processing in the endocytic pathway (Lanone and Boczkowski 2006).

The NP surface is more reactive on itself (aggregation) and to its surrounding environment (biological components). The NPs can induce bigger inflammatory responses and increased lung toxicity, compared with larger particles with the same chemical composition at equivalent mass dose (Kreyling et al. 2006, Lanone and Boczkowski 2006).

Table 2.4. Summary of release kinetics and transport mechanisms of polymeric delivery devices.

Material	Device	Drug	Burst release	Release kinetic	Transport mechanism	Reference
Non-degradable polymer-based delivery device						
Segmented polyurethane (Cardiomat® 610)	Drug-eluting stent	1,3-dipropyl-8-cyclopentyl xanthine	1 d	Near linear release (≈ 20 d)	Non-Fickian diffusion	Kang et al. 2009
Elast-Eon™	Drug-eluting stent	Dexamethasone acetate		Biphasic pattern	Fickian diffusion	Simmons et al. 2008
Polyurethane (Walopur®)	Disk-shaped matrices	Flucloxacillin sodium, fosfomycin, gentamicin	1 d	Near linear (2–5 d)	Matrix-controlled	Schierholz et al. 1997
PEGylated polyurethane	Dermal patch	Thiamazole, diclofenac sodium, ibuprofen	12 hr	Biphasic pattern (≈ 48 hr)	–	Chen et al. 2009
Polydimethylsiloxane	Rod (matrix *vs.* reservoir)	Ivermectin	–	Matrix: first order (50 d). Reservoir: zero order (84 d)	Matrix: diffusion Reservoir: case II transport	Maeda et al. 2003
Polydimethylsiloxane	Intravaginal ring (reservoir)	TMC120, prior to polymerization or via equilibrium absorption after polymerization	1–2 d	Biphasic, near zero order release (30 d)	Case II transport	Woolfson et al. 2006
Polydimethylsiloxane	Reservoir devices. Intravaginal ring (core-type). Hydrophilic lactose	TMC120	–	Zero order (71 d). Concentration-dependent manner	Case II transport	Malcolm et al. 2005
Polydimethylsiloxane	Reservoir- and matrix-type devices. Strip (10 × 20 mm)	Metronidazole		Higuchi (linear *vs.* $t^{1/2}$)	Fickian diffusion	Riggs et al. 1999, Malcolm et al. 2004
Poly(ethylene-*co*-vinyl acetate) (40% vinyl acetate content)	Membrane	Quinupramine		Higuchi (linear *vs.* $t^{1/2}$)	Fickian diffusion	Kim et al. 2006

Table 2.4. contd....

Table 2.4. contd.

Material	Device	Drug	Burst release	Release kinetic	Transport mechanism	Reference
Poly(ethylene-*co*-vinyl acetate)	Thin film	Acyclovir, chlorhexidine diacetate	–	Near zero order (≈ 8 d)	Non-Fickian diffusion	Tallury et al. 2007
Poly(ethylene-*co*-vinyl acetate)	Drug-eluting stent coating	5-FU		Biphasic pattern (≈ 20 d)	Fickian diffusion	de Queiroz et al. 2006
Poly(ethylene-*co*-vinyl acetate) (40% vinyl acetate content)	Disk-shaped film	Chlorhexidine diacetate		Near zero order (≈ 7 d)	Non-Fickian diffusion	Arnold et al. 2008
Poly(ethylene-*co*-vinyl acetate) (40% vinyl acetate content)	Membrane	Furosemide		Higuchi (linear *vs.* $t^{1/2}$)	Fickian diffusion	Cho et al. 2005
Degradable polymer-based delivery devices						
Methacrylated dextran	Hydrogel	Vitamin E	≈ 3 hr	Biphasic	Swelling	Cassano et al. 2009
PLGA	NP	Estradiol		Zero order (up to 31–54 d). Chain scission and polymer erosion	Diffusion-cum-degradation. Degradation becomes the dominant driving force, thus determining the drug release kinetic	Wang et al. 2006, Biondi et al. 2008, Sahana et al. 2008
PEG hydrogel with degradable cross-links	Disk	BSA	–	Zero order in the presence of human neutrophil elastase	Triggered degradation	Aimetti et al. 2009
Poly(ortho ester amide) copolymer	Not available	Fluorescein isothiocyanate-dextran	–	Near zero order	Erosion	Tang et al. 2009
HPMC	Tablet	Adinazolam mesylate		Near zero order (10 hours)	Swelling and dissolution	Ju et al. 1995

Biodistribution

Nanomaterials are capable of entering the human body by inhalation, ingestion, skin penetration or by intravenous injections and medical devices. Then, they can be translocated to other parts of the body by blood circulation. The studies on rodent models *in vivo* strongly indicate that most nanomaterials tend to accumulate in the liver (Zhou et al. 2006, Kamruzzaman et al. 2007, Sadauskas et al. 2007), leading to tissue injury (Wang et al. 2007).

Factors which can affect NP blood circulation and organ specific accumulation include interactions with biological barriers and tunable NP parameters, i.e., composition (type, hydrophobic character and biodegradation profile), size, core properties, surface modifications (PEGylation and surface charge), drug loading techniques (e.g., adsorption or incorporation) and finally, targeting ligand functionalization (Elsabahy and Wooley 2012). All these factors affect the NP biodistribution by reducing the level of non-specific uptake, delaying opsonization, and increasing the extent of tissue specific accumulation (Duguet et al. 2006, Alexis et al. 2008, Mahapatro and Singh 2011). Biodistribution in non-healthy organs can be improved through passive enhanced permeation and retention (EPR) and active targeting (ligand functionalization). Biodistribution into the liver and spleen typically occurs by phagocytic uptake and hepatic filtration, while optimizing the NP circulation half life can be achieved by particle sizes under 100 nm and negative or neutral surface charge. In this way, avoiding kidney uptake, which occurs by excretion, can be possible when particle size is ≤ 10 nm.

NPs should ideally have a hydrophilic surface to escape from macrophage capture. This can be achieved in two ways: coating the NP surface with a hydrophilic polymer, such as PEG, which protects from opsonization by repelling plasma proteins. Alternatively, NPs can be formed from block copolymers with hydrophilic and hydrophobic domains (Cho et al. 2008).

There are several biological barriers to NP distribution, such as, epithelium, living organisms (bacteria, viruses and protozoa), opsonins (antibodies and complement factors which facilitate NP binding to phagocytic cells, particularly macrophages and neutrophiles which take them up), and vascular endothelium (Garnett and Kallinteri 2006). The active delivery of targeted NPs across the vascular endothelium could significantly increase the therapeutic index and decrease the associated toxicity of nanoparticulate drug delivery systems. In fact, the use of active transendothelial transport pathways (i.e., caveolae) may provide an effective solution to NP targeting and delivery (Chrastina et al. 2011).

Many types of systemically injected NPs are rapidly cleared from the blood stream by the Reticuloendothelial System (RES) and the Mononuclear Phagocytic System (MPS), mainly through the liver, spleen and bone marrow resulting in low therapeutic indexes. Development of NPs that avoid rapid clearance is a necessary requirement for sufficient delivery to the desired target (Alexis et al. 2008). Choi et al. (2011) developed NP-based therapeutics for targeting diseases that involve the mesangium of the kidney. The encapsulation of different drugs in NPs (70–200 nm in size) significantly reduced the apparent body clearance compared with the free drug (Kadam et al. 2012).

Biodegradable polymers

The effect of surface PLGA coating with different concentrations of polymeric surfactants (PEG and Pluronic® F-127) was studied after intravenously administration (Kumari et al. 2010). *In vivo*, 1% PEG and 1% Pluronic® F-127 coated particles presented similar biodistribution profiles in various tissues over seven days, and the amount of coated particles detected in plasma was higher than that of uncoated PLGA particles. In another biodistribution study, it was shown that cytarabine-loaded PEGylated PLGA NPs were present in significantly higher concentrations in blood circulation as well as in the brain and bones, and avoided RES uptake as compared to the free drug (Yadav et al. 2011a). Endostar®, a novel recombinant human endostatin has a broad spectrum of activity against solid tumors. Endostar-loaded PEG-modified PLGA NPs have a longer elimination half life, caused a slower growth of tumor cell xenografts, and prolonged tumor doubling times (Hu and Zhang 2010). In another investigation, antacid-insulin co-encapsulated PLGA NPs increase six-fold in oral bioavailability to that of plain insulin in healthy rats. Both subcutaneous insulin and oral insulin-loaded NPs partially attenuated hyperglycemia-induced inflammation (Sharma et al. 2011). The Pluronic® F-68-coated PLGA NPs demonstrated the greatest cellular uptake and achieved highest fluorescence concentration in the brain tissues over those with Tween® 80 and Pluronic® F-127 surface modification (Kulkarni and Feng 2011).

Cisplatin-loaded NPs obtained by harnessing a novel PEG-functionalized poly-isobutylene-maleic acid copolymeric NPs exhibited *in vivo* significantly improved antitumor efficacy in a 4T1 breast cancer model, with limited nephrotoxicity, which can be explained by preferential biodistribution into the tumor with reduced kidney concentrations (Paraskar et al. 2011). Etoposide-loaded PLGA NPs (105 nm in size) were present in blood, after intravenous administration, at higher concentrations up to 24 hours and were able to reduce their RES uptake, as compared to that of etoposide-loaded PLGA-NPs (160 nm in size) and pure drug. Moreover, 105 nm-sized

NPs had greater uptake in bones and the brain, in which the concentration of free drug and 160 nm-sized NPs was negligible. It was then concluded that NPs of size ≤ 100 nm could be used for long-term circulation without the need for surface modification (Yadav et al. 2011b). In another research report, it was analyzed the biodistribution behavior of plain and hepatitis B surface antigen (HBsAg)-coated ^{99m}Tc-tagged PLGA NPs after intravenous injection. Seventy five percent of the radioactivity was recovered in the liver after 4 hours of injection that was nearly 3-fold greater than the plain PLGA NPs (Giri et al. 2011).

Biodistribution of poly(D,L-lactic acid) (PLA) is safe and no major toxicity has been found owing to its biocompatibility and biodegradability (Kumari et al. 2010).

DOX-loaded poly(butylcyanoacrylate) (PBCA) NPs significantly enhanced the elimination half life and mean residence time of DOX in blood after intravenous injection, and greatly reduced the distribution of DOX to the heart after injection (Reddy and Murthy 2004).

NPs of a gelatinase-cleavage peptide with PEG and poly(ε-caprolactone) (PCL) have been developed as novel "intelligent" structures for tumor-targeted docetaxel NPs (DOC-TNPs) (Mahapatro and Singh 2011). *In vivo* biodistribution study demonstrated that targeted DOC-TNPs could accumulate and remain into tumor regions, whereas non-targeted DOC-NPs were rapidly eliminated from the tumor tissues (Liu et al. 2012). In another study, paclitaxel-loaded PCL-*b*-PVP NPs with satisfactory drug loading content (15%) and encapsulation efficiency (> 90%) accumulated into the tumor site and showed enhanced penetration into tumor tissues (Zhu et al. 2011).

PEGylated and non-PEGylated poly(γ-benzyl-L-glutamate) (PBLG) NPs were prepared with polymeric mixtures containing PBLG-fluorescein isothiocyanate and imaged by fluorescence microscopy to measure their accumulation in liver and spleen tissues of rats after intravenous administration. It was observed that PEGylated NPs could be useful for active targeting of drugs while reducing systemic side effects (Ozcan et al. 2010).

Natural polymers

Surface modification of CS NPs with synthetic polymers like PEG, poly(vinylalcohol) or polysaccharide can enhance solubility of hydrophobic materials, minimize non-specific binding, prolong circulation time and enhance tumor specific targeting (Sheng et al. 2009). The biodistribution of thiolated CS NPs of tizanidine HCl has been evaluated across monolayer of RPMI 2650 cells (a human nasal septum carcinoma cell line) after intranasal administration. High mucoadhesion and drug permeation were observed for thiolated

CS NPs with least toxicity to nasal epithelial cells. Brain uptake and antinociceptive effect of the drug were significantly enhanced after thiolation of CS NPs (Patel et al. 2012). Monoclonal antibodies against the transferrin receptor, which is highly expressed on the brain capillary endothelium, were conjugated to CS NPs via biotin-streptavidin bonds. It was shown that the activation of the transferrin receptor by the NP-antibody complex induced transcytosis, and thus delivered the loaded drug to the brain. Consequently, *N*-benzyloxycarbonyl-Asp(OMe)-Glu(OMe)-Val-Asp(OMe)-fluoromethyl ketone-loaded CS NPs rapidly released their contents within brain parenchyma and inhibited ischemia-induced caspase-3 activity, thereby providing neuroprotection (Yemişci et al. 2012).

CS-conjugated iron oxide core NPs have been developed to deliver targeted anticancer therapeutics, and as an imaging agent for visualizing tumors in mice. Binding patterns in the liver and spleen suggested macrophage uptake, and high concentration of NPs was revealed in the spleen white pulp (Pirollo and Chang 2008, Veiseh et al. 2009). Biodistribution studies demonstrated the localization in kidney, spleen, and liver for both targeted and non-targeted NPs. High uptake by MPS in the liver and spleen are one of the greatest challenges of using NPs for tumor targeting (Lee et al. 2010). Functional NPs of CS/poly(γ-glutamic acid) (γPGA)-diethylene triamine pentaacetic acid (DTPA) (CS/γPGA-DTPA) for oral insulin delivery were pH-responsive: they disintegrated at pHs > 7. CS/γPGA-DTPA NPs could promote insulin absorption throughout the entire small intestine. It was shown that the absorbed insulin was clearly identified in the kidney and bladder. The relative oral bioavailability of insulin was ≈ 20% (Su et al. 2012).

A biodistribution investigation of a pulmonary delivery system for antibiotic (tobramycin)-loaded PLGA-modified alginate (ALG) NPs showed that the NPs reached the deep lung, while CS-modified NPs were found in great amounts in the upper airways, lining lung epithelial surfaces (Ungaro et al. 2012). The biodistribution, toxicity and antitumor activity liver cancer of DOX-loaded glycyrrhetinic acid (GA)-modified ALG NPs was studied in Kunming mice. The concentration of DOX in the liver reached 67.8 ± 4.9 μg/g after intravenous administration, which was 2.8-fold and 4.7-fold higher compared to non-GA-modified NPs and free DOX, respectively (Zhang et al. 2012).

Dendrimers

To systematically elucidate the effect of surface charge on the cellular uptake and *in vivo* fate of PEG-oligocholic acid-based micellar NPs, the distal PEG termini of monomeric PEG-oligocholic acid dendrimers (telodendrimers) were each derivatized with different number (n = 0, 1, 3, and 6) of anionic

aspartic acids (negative charge) or cationic lysines (positive charge). Under aqueous conditions, these telodendrimers self-assembled to form a series of micellar NPs with various surface charges, but with similar particle size. NPs with high surface charge, either positive or negative, were taken up more efficiently by RAW 264.7 murine macrophages after opsonization in fresh mouse serum. After cellular uptake, the majority of NPs were found to localize into the lysosome. *In vivo* biodistribution studies demonstrated that undesirable liver uptake was very high for highly positively or negatively charged NPs, which was likely due to active phagocytosis by macrophages (Küpffer cells) in the liver. In contrast, liver uptake was very low, but tumor uptake was very high when the surface charge of NPs was slightly negative. Slightly negative charged NPs could reduce the undesirable clearance by the RES, thus improving blood compatibility and the delivery of anticancer drugs (Xiao et al. 2011).

Nanoparticles for oral drug delivery

Insulin-loaded poly(isobutylcyanoacrylate) (PIBCA) NPs have preserved insulin activity and produced blood glucose reduction in diabetic rats for up to 14 days following oral administration (Mahapatro and Singh 2011).

pH-sensitive NPs based on a poly(methylacrylic acid and methacrylate) copolymer can increase the oral bioavailability of drugs like cyclosporine A (CsA) by releasing their load at a specific pH within the GI tract (Mahapatro and Singh 2011).

Nanoparticles for vaccine/gene delivery

Echogenic (amenable to destruction by ultrasound) PLGA NPs are an attractive strategy for ultrasound-mediated gene delivery (Figueiredo and Esenaliev 2012). NPs loaded with plasmid DNA could also serve as an efficient sustained release gene delivery system due to their rapid escape from the degradative endo-lysosomal compartment to the cytoplasmic compartment (Mahapatro and Singh 2011).

Nanoparticles for ocular drug delivery

It has been developed a nanoformulation made of CsA incorporated into cationic Eudragit® RS 100 NPs aiming ocular application on sheep. *In vivo* results demonstrated the prolonged residence time of CsA in deeper layers (vitreous humor) of the eye with positively charged Eudragit® RS 100 NPs (Başaran et al. 2011).

Nanoparticles for drug delivery into the brain

The central nervous system is well protected by the Brain-Blood-Barrier (BBB) which maintains its homeostasis. Due to this barrier many potential drugs for the treatment of diseases associated to the central nervous system cannot reach the brain in sufficient concentrations (Wohlfart et al. 2011). Modification of NP surfaces with covalently attached targeting ligands or by coating with certain surfactants enabling the adsorption of specific plasma proteins could be of interest for receptor-mediated brain uptake (Wohlfart et al. 2011). PBCA NPs were able to deliver hexapeptide dalargin, DOX, and other agents into the brain. The successful delivery of several drugs through the BBB using polysorbate 80-coated poly(alkylcyanoacrylate) (PACA) NPs (Kreuter 2001) has been demonstrated. The effects of polysorbate-80 on transport through the BBB were confirmed with PLA NPs. PLGA-glycoheptapetide-conjugated NPs are able to cross the BBB. Loperamide and rhodamine-123 (model drugs unable to cross the BBB) were loaded into NPs, composed of a mixture of PLGA, differently modified with glycoheptapetide or with a random sequence of the same aminoamides. Electron photomicrographs showed the ability of NPs in crossing the BBB. NPs of *n*-butyl-2-cyanoacrylate (BCA) have been developed to cross the BBB to facilitate the early diagnosis of Alzheimer's disease (Kulkarni et al. 2010, Tosi et al. 2011).

Protein binding is one of the key elements that affect biodistribution of the NPs throughout the body. Understanding the NP-protein complex allows for improved engineering of NPs with favorable bioavailability and biodistribution (Aggarwal et al. 2009). Biodistribution results of PEG-coated gold NPs (Au NPs) (5–60 nm in size) showed that 5 nm- and 10 nm-sized particles accumulated in the liver, and that 30 nm-sized particles accumulated in the spleen, while the 60 nm-sized particles did not accumulate to an appreciable extent in one of these locations. Peptide capping significantly increased hepatic uptake, showing the influence of Au NPs functionalization in their biodistribution (Morais et al. 2012). To increase Au NP cell uptake and circulation half life, and to improve its biodistribution, Au NPs were coated with PEG and 1-palmitoyl-2-oleoyl-*sn*-glycero-3-phospho-(1'-rac-glycerol) (sodium salt) (POPG). Under the same incubation conditions, POPG-coated Au NPs were uptaken by cells quicker and in higher amount than PEGylated Au NPs, the maximum uptake was 8 hours *vs*. 16 hours after incubation (Hao et al. 2012).

Bioevaluation

Techniques that can be used to assess toxicity of nanomaterials include: *i*) *in vitro* assays for cell viability/proliferation, mechanistic assays (reactive

oxygen species generation, apoptosis, necrosis, DNA damaging potential); *ii*) microscopic evaluation of intracellular localization (including scanning electron microscopy-energy dispersive X-ray spectroscopy, transmission electron microscopy, atomic force microscopy, fluorescence spectroscopy, magnetic resonance imaging, video-enhanced differential interference contrast microscopy); *iii*) gene expression analysis, high-throughput systems; *iv*) *in vitro* haemolysis; and, *v*) genotoxicity.

Usually nanotoxicology studies have used cell monocultures that are specific to organs of the body. Epithelial, macrophage and dendritic cells are commonly used. Additionally, specific cells such as C3A and HepG2 cells are also used for the liver, the PC12 cell line for the brain, whilst there are also numerous tumor cell lines, such as mesothelioma cell lines (e.g., IST-Mes3/2P cells) that can also be used.

Very recently, there have been increased efforts to establish more realistic models to study the toxicity of NPs. Rothen-Rutishauser et al. (2005) proposed the triple cell co-culture system composed of epithelial cell line (A549 or 16HBE14o$^-$), human monocyte-derived macrophages, and dendritic cells, thus simulating the most important barrier functions of the epithelial airway. This model provides a clear basis for investigating the interaction of NPs with the lung (Rothen-Rutishauser et al. 2005, 2008), as well as at the air-liquid interface (Blank et al. 2006, 2007, Alfaro-Moreno et al. 2008, Bhabra et al. 2009). Alfaro-Moreno et al. (2008) proposed is a "quad-culture" containing epithelial, endothelial, macrophage and mast cells, while Bhabra et al. (2009) used a bi-culture of BeWo (placental) and human fibroblast cells (Arora et al. 2012).

The potential dangers of the exclusive use of *in vitro* testing have been documented by Donaldson et al. (2009), who stated that cells in culture do not experience the range of pathogenic effects that are likely to be observed *in vivo*, which are partly related to issues of translocation, toxicokinetics and coordinated tissue responses. Monteiro-Riviere et al. (2009) observed that classical dye-based assays such as tetrazolium reduction assay and neutral red to determine cell viability produced invalid results with some nanomaterials, due to interactions and/or adsorption of the dye/dye products. Cells in culture are sensitive to changes in their environment, such as fluctuations in temperature, pH, nutrient and waste concentrations. Kroll et al. (2011) tested 23 engineered nanomaterials using 10 different cell lines in three different assays concluding that a combination of assays is often required.

Nanomaterial toxicity can occur through a variety of mechanisms in the body. There are reports on the association of protein with NPs and the formation of a "protein corona" (Bihari et al. 2008, Lynch and Dawson 2008), thereby influencing their biodistribution and interactions with cells and biostructures and triggering conformational changes in protein folding, that

alters its biological function and affects the signaling pathways activated by NPs (Dhawan and Sharma 2010).

A general understanding of the impact of NP-protein interactions is yet lacking (Chithrani and Chan 2007, Ehrenberg et al. 2009, Casals et al. 2010, Oberdörster 2010). *In vivo*, specific binding of proteins may affect NP biodistribution (Dobrovolskaia et al. 2008, Ehrenberg et al. 2009, Moghimi et al. 2001), thus promoting phagocytosis with removal of the NPs from the bloodstream (Ishida et al. 2001, Owens 3rd and Peppas 2006), while binding of dysopsonins like Human Serum Albumin (HSA), apolipoproteins, etc. promotes prolonged blood circulation times (Camner et al. 2002).

Inside the cell, NPs can remain structurally unaltered, can be modified or can be metabolized. Ideally, once they have exerted their function, it would be desirable for NP secretion or degradation without any associated toxicity. Approaches to this end are to coat NPs with biodegradable polymeric materials already used in biomedicine (Choi et al. 2007), or to design novel nanoparticulate systems with biodegradable polymers (Gref et al. 1994, Owens 3rd and Peppas 2006, Sanvicens and Marco 2008).

The main molecular mechanism of *in vivo* nanotoxicity is the induction of oxidative stress by free radical formulation (Lanone and Boczkowski 2006). In excess, free radicals cause damage to biological components through oxidation of lipids, proteins and DNA. Slow clearance and tissue accumulation of potential free radical producing nanomaterials, as well as prevalence of numerous phagocytic cells in RES organs, makes liver, kidney, lung and the spleen main targets of oxidative stress (Hoet et al. 2004, Vega-Villa et al. 2008). For instance, the intravenous administration of PIBCA (biodegradable) or polystyrene (PS, non-biodegradable) NPs resulted in depletion of reduced glutathione and oxidized glutathione, as well as inhibition of superoxide dismutase activity, and a slight increase in catalase activity in the liver (Hoet et al. 2004).

Interactions of nanomaterials with mitochondria and cell nucleus are being considered as main sources of toxicity (Lanone and Boczkowski 2006), while the interaction with blood components can lead to haemolysis and thrombosis, and interactions with the immune system increases immunotoxicity (Lanone and Boczkowski 2006, Dobrovolskaia and McNeil 2007, Aillon et al. 2009).

A higher degree of control over the relationship material architecture-biodistribution, cellular internalization, toxicity and elimination could reduce undesired side effects. For instance, cylindrical particles (100 nm in size) can be internalized to a lesser extent than larger cylindrical particles (150 nm in size). Worm-like PS particles exhibited negligible phagocytosis compared with conventional spherical particles of equal volume (Champion and Mitragotri 2009). HepG2 liver cancer cells have been described to take

up smaller methoxy poly(ethylene glycol)-poly(ε-caprolactone) (MePEG-PCL) NPs more efficiently than their larger counterparts (Hu et al. 2007).

Degradability of the material is also key-factor determining acute and long-term toxicity. Non-biodegradable nanomaterials can accumulate in organs and also intracellularly where they can cause detrimental effects to the cell, similar to that associated to lysosomal storage diseases (Garnett and Kallinteri 2006). In contrast, biodegradable nanomaterials can lead to unpredicted toxicity due to unexpected toxic degradation products (Fischer and Chan 2007). Information on their potential adverse health effects is very limited at the present time.

Administration Routes

The administration routes for polymeric NPs are mainly transdermal, oral, respiratory, parenteral and ocular.

Transdermal administration

Currently, there is little evidence that nanomaterials can penetrate through the skin barrier into the living tissue (i.e., dermal compartment) (Kezic and Nielsen 2009), and on possible adverse local or systemic effects even if they do penetrate skin (Santos et al. 2002, Berry et al. 2004, Gupta and Curtis 2004, Münster et al. 2005, Rouse et al. 2007, Kuntsche et al. 2008).

The topical antimicrobial chlorhexidine-loaded PCL nanocapsules decreased the percutaneous absorption through stripped skin (Lboutounne et al. 2004). In the hairy Guinea pig skin, minoxidil encapsulated in a diblock PCL-*b*-PEG nanocapsules (40 nm in size) permeated 1.5-fold higher in the epidermal layer and 1.7-fold higher in the receptor solution, compared to larger NPs (130 nm in size) (Shim et al. 2004). The flufenamic acid lipophilic drug transport from PLGA NPs into excised human skin has been enhanced (Luengo et al. 2006). Indomethacin-loaded PBCA nanocapsules penetrated intact through the rat skin (Miyazaki et al. 2003, Guterres et al. 2007).

Oral administration

Drug bioavailability can be improved by controlling particle size, along with prolonging the residence time of drug carrier systems in the GI tract (Takeuchi et al. 2001). Adhesive properties of NPs were reported to increase bioavailability, and reduce or minimize erratic absorption (Ponchel et al. 1997). Absorption of NPs occurs through mucosa of the intestine by several mechanisms, namely through the Peyer's patches, intracellular uptake or paracellular pathway.

Blood glucose levels were reduced in diabetic rats following oral administration of insulin-loaded NPs (Damge et al. 1990). Limiting nano-sized particles to less than 500 nm in diameter seemed to be a key factor in permitting their transport through the intestinal mucosa, most probably by an endocytotic mechanism (Jani et al. 1990). McClean et al. (1998) showed that ≈ 10% of PLA NPs administered orally were absorbed by the apical membrane of the gut in animals. The absorption mechanism was predominately transcellular.

Strong interactions were found between rat intestinal epithelium and CS NPs several hours after oral administration, promoting an increase in peptide bioavailability (Pan et al. 2002). Ovalbumin was adsorbed onto the surface of CS particles to enhance their uptake by the M cells of Peyer's patches. Coating the particles with sodium ALG prevented the burst release of the loaded antigen and improved NP stability in GI fluid (Borges et al. 2005). ALG-modified trimethyl CS NPs were prepared for protein delivery. NPs with a lower degree of quaternarization showed an increase in particle size, a decrease in zeta potential, and a slower drug release profile, whereas for ALG-modified particles a smaller size and lower zeta potential were observed (Chen et al. 2007).

Valproic acid (VA) in PEG-*cl*-poly(ethylenimine) (PEI) nanogels was studied in a cellular model of the BBB (bovine brain microvessel endothelial cells monolayers). At least 70% increase in the transcellular transport of VA in nanogel across cell monolayers was observed compared to the free drug (Vinogradov et al. 2004). PACA nanocapsules and nanospheres are efficient to improve the oral bioavailability of peptides such as insulin (Damgé et al. 1988, 1990, Lowe and Temple 1994, Pinto-Alphandary et al. 2003), octeotride (Damgé et al. 1997), CsA (Allémann et al. 1998), and calcitonin (Lowe and Temple 1994).

Respiratory administration

Nasal drug delivery may not need protection against enzymatic degradation. Drugs may be administered as solution or powder with absorption enhancing agents to slow down mucociliary clearance processes, and thereby prolong the contact time between the formulation and nasal tissue. However, nanoparticulate systems have shown interesting properties. For instance, PLGA NPs and surface-functionalized PLGA NPs sustained drug levels in the lungs (Pandey et al. 2003, Sharma et al. 2004). Natural polymer sodium ALG formulated along with CS into NPs encapsulating the three antitubercular drugs (rifampicin, isoniazid and pyrazinamide) have shown enhanced efficacy in pulmonary treatments (Ahmad et al. 2005).

Parenteral administration

DOX-loaded CS NPs showed regression in tumor growth and enhanced survival rate of tumor-implanted rats after intravenous administration (Brasseur et al. 1980). In addition, CS NPs (< 100 nm in size) showed to be RES evading and circulate in blood for a considerable amount of time.

Oligonucleotides were bound to PACA nanospheres, being protected from nucleases *in vitro* (Chavany et al. 1992), and their intracellular uptake was increased (Chavany et al. 1994). Antisense oligonucleotides formulated in this way were able specifically to inhibit mutated Ha-ras-mediated cell proliferation and tumorigenicity in nude mice (Schwab et al. 1994). PIBCA nanospheres were able to inhibit PKCα neoexpression in cultured Hep G6 cells (Lambert et al. 1998).

Nanospheres containing oligonucleotides have also been formulated with ALG, which forms a gel in the presence of calcium ions, providing a high loading yield and good protection against nucleases (Aynie et al. 1999). The linkage of ampicillin to poly(isohexylcyanoacrylate) (PIHCA) nanospheres increased its efficacy in treating *Salmonella typhimurium* infection in C57BL/6 mice (Fattal et al. 1989) or listeriosis (Youssef et al. 1988). In an attempt to kill both dividing and non-dividing bacteria a fluoroquinolone antibiotic, ciprofloxacin, has been associated with PIBCA and PIHCA nanospheres (Page-Clisson et al. 1998). A single subcutaneous dose of PLGA NPs loaded with rifampicin, isoniazid and pyrazinamide maintained therapeutic drug levels in plasma for 32 days, and in lungs/spleen for 36 days (Pandey and Khuller 2004, Gelperina et al. 2005).

Ocular administration

Various types of NPs tend to adhere to the ocular epithelial surface (Wood et al. 1985). CS NPs could be used as a CsA vehicle to enhance the therapeutic index of clinically challenging drugs with potential application at the extraocular level (De Campos et al. 2001, Agnihotri et al. 2004). CS-coated NPs can also be utilized to enhance corneal penetration (Calvo et al. 1997).

PCL nanocapsules could specifically penetrate the corneal epithelium by an endocytic process without causing any damage to cells (Calvo et al. 1994), in contrast with PIBCA NPs, the uptake of which was associated with cellular lysis (Zimmer et al. 1991). Le Bourlais et al. (1997) proposed an alternative preparation of CsA-loaded nanocapsules based on PACA dispersed in a poly(acrylic acid) (PAA) gel able to reduce drastically PACA toxicity on the cornea, and to promote drug absorption. Ibuprofen-loaded polymeric NPs (≈ 100 nm in size and positively charged) made from Eudragit® RS 100 were shown to be suitable for ophthalmologic applications (Pignatello et al. 2002). Intravitreous injection of PLA NPs resulted in

transretinal movement, with a preferential localization in retinal pigmented epithelial cells (Bourges el al. 2003).

Neuroprotective effects of PLGA nanospheres to encapsulate pigment epithelium-derived factor peptides have been evaluated in induced retinal ischemic injury (Li et al. 2006). PLGA NPs incorporating flurbiprofen improved the availability of the drug for the prevention of inflammation caused by ocular surgery (Vega et al. 2006). Intraocular injection in rats of a hydrophobic cyanoacrylate-*co*-hexadecyl cyanoacrylate coupled to hydrophilic PEG chains to produce tamoxifen-loaded NPs resulted in a significant inhibition of experimentally induced autoimmune uveoretinitis (De Kozak et al. 2004).

Formulations Containing Nanoparticles

Technically, NP formulations refer to series of processing steps that are needed to obtain drug-loaded NPs into the final dosage form with ideal properties for application. Physical and chemical properties of the base polymers, chemical reactions, purification steps and excipients have to be considered in order to ensure the quality and integrity of the final product (Hasanovic et al. 2009, Kaewprapan et al. 2012).

Nanoparticulate formulations with applications in drug release show interest directly for pharmaceutical technology. In production of products based on NPs, the manufacturing step should not affect the therapeutic agent, the polymeric component and others excipients and storage conditions must ensure the desired therapeutic effect. Also, the compatibility of the therapeutic agent with excipients is essential. Excipients play a specific functional role in the modulation of solubility, and optimize the stability, bioavailability, safety and/or efficacy. Additionally, excipients must not present toxicity at contact with the biological environment and should not influence the biopharmaceutical characteristics of the therapeutic agent. The surfactant type and stabilizer, the electric charge of the particle in solution, NP stability and aggregation and the uniformity of size distribution are several parameters to be taken into consideration in the preparation of drug delivery nanoformulations. These formulations are related to the cost-effective manufacturing process and possible modulation of drug release profiles.

NP stabilization can be performed with surfactants (e.g., sodium lauryl sulfate, polyethoxylated castor oil or Cremophor® EL or polysorbate 80 or Tween® 80), grafted polymeric chains, soluble block chains, adsorbed polymeric chains or ionic groups. Hydrophilic ascorbic acid derivatives are used as antioxidants and as pharmaceutical excipients to increase drug solubilization in NP formulations. In addition, pH regulators, antimicrobial preservatives, anti-foaming agents, humectants, solvents and emulsifiers are

used to decrease of the NP surface tension. Other common excipients for NP formulation are lactose monohydrate, HPMC and sodium starch glycolate. The formulation of NPs in lyophilized form requires a cryoprotectant agent such as sucrose, mannitol or glucose. Several formulations are presented in Table 2.5 for commercial drugs or new drugs that are in clinical trials [http://www.cancer.gov/drugdictionary].

Conclusions

This chapter focuses on basic principles of drug release kinetics from nano-sized polymeric systems. Meanwhile, the literature is growing by the day, the explanation of the transport mechanism calls for further theoretical analysis. Only a little is known about the release kinetics and mechanism from "smart" drug delivery nanosystems in various conditions.

Nanopharmaceuticals are complex drug delivery systems which are beneficial for therapeutic use because of their targetability and improved bioavailability. The kinetics and pharmacokinetics is controlled by complex and interrelated physicochemical, anatomical, pathophysiological, immunobiological factors and dosing regimen, thus theoretical basis should be continuously updated and improved.

Acknowledgement

Financial support from Romanian UEFISCDI by 164/2012 BIONANOMED Project.

Abbreviations

Au NPs	:	gold nanoparticles
ALG	:	alginate
AUC	:	area under the time-plasma concentration curve
BBB	:	brain-blood-barrier
BCA	:	*n*-butyl-2-cyanoacrylate
BSA	:	bovine serum albumin
C_{max}	:	maximum plasma concentration
CS	:	chitosan
CsA	:	cyclosporine A
CS/γPGA-DTPA	:	chitosan/poly(γ-glutamic acid)-diethylene triamine pentaacetic acid
DOC	:	docetaxel
DOC-TNPs	:	tumor-targeted docetaxel nanoparticles
DOX	:	doxorubicin
EPR	:	enhanced permeation and retention

Table 2.5. Formulations containing nano-sized polymeric components.

Generic/Brand name	Polymer	Therapeutic agent	Other excipients/Activity
Abraxane®	HSA-bound (130 nm in size)	Paclitaxel (100 mg)	900 mg of HSA (containing sodium caprylate and sodium acetyltryptophanate)/chemotherapeutic
Feridex®	Mannitol, dextran	Imaging contrast media (ferumoxide injectable solution)	1 mL of Feridex® = 11.2 mg of iron, and 61.3 mg of mannitol, dextran (5.6–9.1 mg/mL), and citrate (0.25–0.53 mg/mL)
GastroMARK®, Lumirem®	Poly[*N*-(2-aminoethyl)-3-aminopropyl] siloxane-coated particles of non-stoichiometric magnetite	Imaging agent (ferumoxil oral suspension)	Methyl parahydroxybenzoate (E218), propyl arahydroxybenzoate (E216), carmellose sodium, sunset yellow S (E110), orange flavor (limonene, linalol, terpinene, octanal, decanal, citral, myrcene, terpineol, pinene), ammonium glycyrrhizinate, saccharin sodium, crystallizable sorbitol 70%, sodium chloride, NaOH
NC-6004 Nanoplatin®	PEG-poly(glutamic acid) block copolymer	Cisplatin	Chemotherapeutic
XMT-1107	Poly(hydroxymethylethylene hydroxymethyl formal)	Fumagillin	Antiangiogenic and chemotherapeutic
Genexol®-PM	PEG-PLA	Paclitaxel	Chemotherapeutic (recommended therapeutic dose: 300 mg/m^2)
Davanat® (galactomannan derivative)	Carbohydrate polymer composed of mannose and galactose	5-FU	Chemotherapeutic
Feraheme®	Non-stoichiometric magnetite (superparamagnetic iron oxide) coated with polyglucose sorbitol carboxymethylether	Ferumoxytol imaging agents	Feraheme® solution has anti-anemic and imaging properties. Feraheme® injection is formulated with mannitol, without preservatives, and has an osmolality of 270–330 mOsm/Kg. 1 mL of the sterile colloidal solution contains 30 mg of elemental iron and 44 mg of mannitol. Isotonic formulation

Sinerem® (Foreign brand name)/Combidex® (US brand name)	Dextran-coated superparamagnetic iron oxide	Ferumoxtran-10. Imaging agent	Molecular resonance imaging contrast agent. Sinerem® injection is formulated by suspending the powder in an isotonic glucose solution for a dose of 2.6 mg Fe/Kg
IMF-001 (CHP-NY-ESO-1	Complexed cholesteryl hydrophobized pullulan	Cancer-testis antigen NY-ESO-1 protein	Immunostimulating and chemotherapeutic
ABI-008	Albumin	DOC. Semi-synthetic second-generation taxane derived	Chemotherapeutic, immunomodulatory and pro-inflammatory
Quaternary ammonium PEI	Quaternary ammonium PEI		Antibacterial. NPs can be incorporated into dental composite resins or silicon obturator prostheses, and may prevent or delay bacterial growth
NK012	Self-assembly amphiphilic PEG-poly(α-glutamic acid) block copolymer	Irinotecan metabolite SN-38 loaded polymeric micelles (7-ethyl-10-hydroxy-camptothecin)	Chemotherapeutic
Transdrug®	PIHCA	DOX	Treatment of hepatocarcinoma
VivaGel™	L-lysine dendrimer		Vaginal microbicide gel. Prevention of sexually transmitted infections

F_{abs}	:	bioavailability
5-FU	:	5-fluorouracil
GA	:	glycyrrhetinic acid
GI	:	gastrointestinal
HBsAg	:	hepatitis B surface antigen
HPMC	:	hydroxypropyl methylcellulose
HSA	:	human serum albumin
LPS	:	lipopolysaccharide
MePEG-PCL	:	methoxy poly(ethylene glycol)-poly(ε-caprolactone)
MPS	:	mononuclear phagocitic system
NPs	:	nanoparticles
OE	:	overall mean percent error
OMC	:	octyl methoxycinnamate
PAA	:	poly(acrylic acid)
PACA	:	poly(alkylcyanoacrylates)
PBCA	:	poly(butylcyanoacrylate)
PBLG	:	poly(γ-benzyl-L-glutamate)
PCL	:	poly(ε-caprolactone)
PEG	:	poly(ethylene glycol)
PEG-FOL	:	poly(ethylene glycol)-folate
PEI	:	poly(ethylenimine)
PEO-PPO	:	ethylene oxide-propylene oxide
PIBCA	:	poly(isobutylcyanoacrylate)
PIHCA	:	poly(isohexylcyanoacrylate)
PIMA	:	poly-isobutylene-maleic acid
PLA	:	poly(D,L-lactic acid)
PLGA	:	poly(D,L-lactic-*co*-glycolic acid)
po	:	peroral
POPG	:	1-palmitoyl-2-oleoyl-sn-glycero-3-phospho-(1'-rac-glycerol) (sodium salt)
PS	:	polystyrene
PVP	:	poly(*N*-vinylpyrrolidone)
RES	:	reticuloendothelial system
RPT	:	reciprocal powered time
VA	:	valproic acid
w/o	:	water-in-oil

References

Aggarwal, P. and J.B. Hall, C.B. McLeland, M.A. Dobrovolskaia and S.E. McNeil. 2009. Nanoparticle interaction with plasma proteins as it relates to particle biodistribution, biocompatibility and therapeutic efficacy. Adv. Drug. Deliv. Rev. 61: 428–437.

Agnihotri, S.A. and N.N. Mallikarjuna and T.M. Aminabhavi. 2004. Recent advances on chitosan based micro- and nanoparticles in drug delivery. J. Control. Release. 100: 5–28.

Ahmad, Z. and S. Sharma and G.K. Khuller. 2005. Inhalable alginate nanoparticles as antitubercular drug carriers against experimental tuberculosis. Int. J. Antimicrob. Agents. 26: 298–303.

Aillon, K.L. and Y. Xie, N. El-Gendy, C.J. Berkland and M.L. Forrest. 2009. Effects of nanomaterial physicochemical properties on *in vivo* toxicity. Adv. Drug Deliv. Rev. 61: 457–466.

Aimetti, A.A. and A.J. Machen and K.S. Anseth. 2009. Poly(ethylene glycol) hydrogels formed by thiol-ene photopolymerization for enzyme-responsive protein delivery. Biomaterials. 30: 6048–6054.

Akiyoshi, K. and S. Kobayashi, S. Shichibe, D. Mix, M. Baudys, S.W. Kim and J. Sunamoto. 1998. Self-assembled hydrogel nanoparticle of cholesterol-bearing pullulan as a carrier of protein drugs: complexation and stabilization of insulin. J. Control. Release. 54: 313–320.

Alexis, F. and E. Pridgen, L.K. Molnar and O.C. Farokhzad. 2008. Factors affecting the clearance and biodistribution of polymeric nanoparticles. Mol. Pharm. 5: 505–515.

Alfaro-Moreno, E. and T.S. Nawrot, B.M. Vanaudenaerde, M.F. Hoylaerts, J.A. Vanoirbeek, B. Nemery and P.H. Hoet. 2008. Co-cultures of multiple cell types mimic pulmonary cell communication in response to urban PM10. Eur. Respir. J. 32: 1184–1194.

Alfrey, T. Jr and E.F. Gurnee and W.G. Lloyd. 1966. Diffusion in glassy polymers. J. Polymer Sci. C Polymer Symposia. 12: 249–261.

Allémann, E. and R. Gurny and E. Doelker. 1993. Drug-loaded nanoparticles. Preparation methods and drug targeting issues. Eur. J. Pharm. Biopharm. 39: 173–191.

Allémann, E. and J.C. Leroux and R. Gurny. 1998. Polymeric nano- and microparticles for the oral delivery of peptides and peptidomimetics. Adv. Drug Deliv. Rev. 34: 171–189.

Arnold, R.R. and H.H. Wei, E. Simmons, P. Tallury, D.A. Barrow and S. Kalachandra. 2008. Antimicrobial activity and local release characteristics of chlorhexidine diacetate loaded within the dental copolymer matrix, ethylene vinyl acetate. J. Biomed. Mater. Res. B Appl. Biomater. 86: 506–513.

Asthana, A. and A.S. Chauhan, P.V. Diwan and N.K. Jain. 2005. Poly(amidoamine) (PAMAM) dendritic nanostructures for controlled site-specific delivery of acidic anti-inflammatory active ingredient. AAPS Pharm. Sci. Tech. 6: E536–E542.

Aynié, I. and C. Vauthier, H. Chacun, E. Fattal and P. Couvreur. 1999. Spongelike alginate nanoparticles as a new potential system for the delivery of antisense oligonucleotides. Antisense Nucleic Acid Drug Dev. 9: 301–312.

Bain, J.C. and S.B. Tan, D. Gandarton and M.C. Solomon. 1991. Comparison of the *in vitro* release characteristics of a wax matrix and a hydrogel sustained release diclofenac sodium tablet. Drug Develop. Ind. Pharm. 17: 215–232.

Bapat, N. and M. Boroujerdi. 1992. Uptake capacity and adsorption isotherms of doxorubicin on polymeric nanoparticles: effect of methods of preparation. Drug Develop. Ind. Pharm. 18: 65–77.

Barzegar-Jalali, M. and K. Adibkia, H. Valizadeh, M.R. Shadbad, A. Nokhodchi, Y. Omidi, G. Mohammadi, S.H. Nezhadi and M. Hasan. 2008. Kinetic analysis of drug release from nanoparticles. J. Pharm. Pharm. Sci. 11: 167–177.

Başaran, E. and M. Demirel, B. Sirmagül and Y. Yazan. 2011. Polymeric cyclosporine-A nanoparticles for ocular application. J. Biomed. Nanotechnol. 7: 714–723.

Berry, C.C. and S. Wells, S. Charles, G. Aitchison and A.S. Curtis. 2004. Cell response to dextran-derivatised iron oxide nanoparticles post internalisation. Biomaterials. 25: 5405–5413.

Bhadra, D. and S. Bhadra and N.K. Jain. 2006. PEGylated peptide dendrimeric carriers for the delivery of antimalarial drug chloroquine phosphate. Pharm. Res. 23: 623–633.

Bhabra, G. and A. Sood, B. Fisher, L. Cartwright, M. Saunders, W.H. Evans, A. Surprenant, G. Lopez-Castejon, S. Mann, S.A. Davis, L.A. Hails, E. Ingham, P. Verkade, J. Lane, K. Heesom, R. Newson and C.P. Case. 2009. Nanoparticles can cause DNA damage across a cellular barrier. Nat. Nanotechol. 4: 876–883.

Bhattarai, N. and H.R. Ramay, S.H. Chou and M. Zhang. 2006. Chitosan and lactic acid-grafted chitosan nanoparticles as carriers for prolonged drug delivery. Int. J. Nanomed. 1: 181–187.

Bihari, P. and M. Vippola, S. Schultes, M. Praetner, A.G. Khandoga, C.A. Reichel, C. Coester, T. Tuomi, M. Rehberg and F. Krombach. 2008. Optimized dispersion of nanoparticles for biological *in vitro* and *in vivo* studies. Part. Fibre Toxicol. 5: 14.

Biondi, M. and F. Ungaro, F. Quaglia and P.A. Netti. 2008. Controlled drug delivery in tissue engineering. Adv. Drug Deliv. Rev. 60: 229–242.

Bisrat, M. and C. Nyström. 1988. Physicochemical aspects of drug release. VIII. The relation between particle size and surface specific dissolution rate in agitated suspensions. Int. J. Pharm. 47: 223–231.

Blank, F. and B.M. Rothen-Rutishauser, S. Schurch and P. Gehr. 2006. An optimized *in vitro* model of the respiratory tract wall to study particle cell interactions. J. Aerosol Med. 19: 392–405.

Blank, F. and B. Rothen-Rutishauser and P. Gehr. 2007. Dendritic cells and macrophages form a transepithelial network against foreign particulate antigens. Am. J. Respir. Cell Mol. Biol. 36: 669–677.

Borges, O. and G. Borchard, J.C. Verhoef, A. de Sousa and H.E. Junginger. 2005. Preparation of coated nanoparticles for a new mucosal vaccine delivery system. Int. J. Pharm. 299: 155–166.

Borm, P. and F.C. Klaessig, T.D. Landry, B. Moudgil, J. Pauluhn, K. Thomas, R. Trottier and S. Wood. 2006. Research strategies for safety evaluation of nanomaterials, part V: role of dissolution in biological fate and effects of nanoscale particles. Toxicol. Sci. 90: 23–32.

Bourges, J.L. and S.E. Gautier, F. Delie, R.A. Bejjani, J.C. Jeanny, R. Gurny, D. BenEzra and F.F. Behar-Cohen. 2003. Ocular drug delivery targeting the retina and retinal pigment epithelium using polylactide nanoparticles. Invest. Ophthalmol. Vis. Sci. 44: 3562–3569.

Brasseur, F. and P. Couvreur, B. Kante, L. Deckers-Passau, M. Roland, C. Deckers and P. Speiser. 1980. Actinomycin D absorbed on polymethylcyanoacrylate nanoparticles: increased efficiency against an experimental tumor. Eur. J. Cancer. 16: 1441–1445.

Bronich, T.K. and S.V. Vinogradov and A.V. Kabanov. 2001. Interaction of nanosized copolymer networks with oppositely charged amphiphilic molecules. Nano Lett. 1: 535–540.

Bronich, T.K. and S. Bontha, L.S. Shlyakhtenko, L. Bromberg, T.A. Hatton and A.V. Kabanov. 2006. Template-assisted synthesis of nanogels from Pluronic-modified poly(acrylic acid). J. Drug Target. 14: 357–366.

Calvo, P. and C. Thomas, M.J. Alonso, J.L. Vila-Jato and J.R. Robinson. 1994. Study of the mechanism of interaction of poly(ε-caprolactone) nanocapsules with the cornea by confocal laser scanning microscopy. Int. J. Pharm. 103: 283–291.

Calvo, P. and J.L. Vila-Jato and M.J. Alonso. 1996. Comparative *in vitro* evaluation of several colloidal systems, nanoparticles, nanocapsules, and nanoemulsions, as ocular drug carriers. J. Pharm. Sci. 85: 530–536.

Calvo, P. and J.L. Vila-Jato and M.J. Alonso. 1997. Evaluation of cationic polymer-coated nanocapsules as ocular drug carriers. Int. J. Pharm. 153: 41–50.

Camner, P. and M. Lundborg, L. Låstbom, P. Gerde, N. Gross and C. Jarstrand. 2002. Experimental and calculated parameters on particle phagocytosis by alveolar macrophages. J. Appl. Physiol. 92: 2608–2616.

Casals, E. and T. Pfaller, A. Duschl, G.J. Oostingh and V. Puntes. 2010. Time evolution of the nanoparticle protein corona. ACS Nano. 4: 3623–3632.

Cassano, R. and S. Trombino, R. Muzzalupo, L. Tavano and N. Picci. 2009. A novel dextran hydrogel linking trans-ferulic acid for the stabilization and transdermal delivery of vitamin E. Eur. J. Pharm. Biopharm. 72: 232–238.

Champion, J.A. and S. Mitragotri. 2009. Shape induced inhibition of phagocytosis of polymer particles. Pharm. Res. 26: 244–249.

Chang, C. and Z.C. Wang, C.Y. Quan, H. Cheng, S.X. Cheng, X.Z. Zhang and R.X. Zhuo. 2007. Fabrication of a novel pH-sensitive glutaraldehyde cross-linked pectin nanogel for drug delivery. J. Biomater. Sci. Polym. Ed. 18: 1591–1599.

Chavany, C. and T. Le Doan, P. Couvreur, F. Puisieux and C. Hélène. 1992. Polyalkylcyanoacrylate nanoparticles as polymeric carriers for antisense oligonucleotides. Pharm. Res. 9: 441–449.

Chavany, C. and T. Saison-Behmoaras, T. Le Doan, F. Puisieux, P. Couvreur and C. Hélène. 1994. Adsorption of oligonucleotides onto polyisohexylcyanoacrylate nanoparticles protects them against nucleases and increases their cellular uptake. Pharm. Res. 11: 1370–1378.

Chen, V.J. and P.X. Ma. 2006. The effect of surface area on the degradation rate of nano-fibrous poly(L-lactic acid) foams. Biomaterials. 27: 3708–3715.

Chen, F. and Z.R. Zhang and Y. Huang. 2007. Evaluation and modification of N-trimethyl chitosan chloride nanoparticles as protein carriers. Int. J. Pharm. 336: 166–173.

Chen, X. and W. Liu, Y. Zhao, L. Jiang, H. Xu and X. Yang. 2009. Preparation and characterization of PEG-modified polyurethane pressure-sensitive adhesives for transdermal drug delivery. Drug Dev. Ind. Pharm. 35: 704–711.

Chithrani, B.D. and W.C.W Chan. 2007. Elucidating the mechanism of cellular uptake and removal of protein-coated gold nanoparticles of different sizes and shapes. Nano Lett. 7: 1542–1550.

Cho, C.W. and J.S. Choi and S.C. Shin. 2005. Controlled release of furosemide from the ethylene-vinyl acetate matrix. Int. J. Pharm. 299: 127–133.

Cho, K. and X. Wang, S. Nie, Z.G. Chen and D.M. Shin. 2008. Therapeutic nanoparticles for drug delivery in cancer. Clin. Cancer Res. 14: 1310–1316.

Choi, H.S. and W. Liu, P. Misra, E. Tanaka, J.P. Zimmer, B.I. Ipe, M.G. Bawendi and J.V. Frangioni. 2007. Renal clearance of quantum dots. Nat. Biotechnol. 25: 1165–1170.

Chorny, M. and I. Fishbein, H.D. Danenberg and G. Golomb. 2002. Study of the drug release mechanism from tyrphostin AG-1295-loaded nanospheres by *in situ* and external sink methods. J. Control. Release. 83: 401–414.

Chrastina, A. and K.A. Massey and J.E. Schnitzer. 2011. Overcoming *in vivo* barriers to targeted nanodelivery. Wiley Interdiscip. Rev. Nanomed. Nanobiotechnol. 3: 421–437.

Costa, P. 2001. An alternative method to the evaluation of similarity factor in dissolution testing. Int. J. Pharm. 220: 77–83.

Costa, P. and J.M.S. Lobo. 2001. Modelling and comparison of dissolution profiles. Eur. J. Pharm. Sci. 13: 123–133.

Costa, P. and J.M.S. Lobo. 2003. Evaluation of mathematical models describing drug release from estradiol transdermal systems. Drug Dev. Ind. Pharm. 29: 89–97.

Crisp, M.T. and C.J. Tucker, T.L. Rogers, R.O. Williams 3rd and K.P. Johnston. 2007. Turbidimetric measurement and prediction of dissolution rates of poorly soluble drug nanocrystals. J. Control. Release. 117: 351–359.

Cruz, L. and L.U. Soares, T.D. Costa, G. Mezzalira, N.P. da Silveira, S.S. Guterres and A.R. Pohlmann. 2006. Diffusion and mathematical modelling of release profiles from nanocarriers. Int. J. Pharm. 313: 198–205.

D'Souza, S.S. and P.P. DeLuca. 2006. Methods to assess *in vitro* drug release from injectable polymeric particulate systems. Pharm. Res. 23: 460–474.

Damgé, C. and C. Michel, M. Aprahamian and P. Couvreur. 1988. New approach for oral administration of insulin with poly-alkylcyanoacrylate nanocapsules as drug carrier. Diabetes. 37: 246–251.

Damgé, C. and C. Michael, M. Aprahamian, P. Couvreur and J.P. Devissaguet. 1990. Nanocapsules as carriers for oral peptide delivery. J. Control. Release. 13: 233–239.

Damgé, C. and J. Vonderscher, P. Marbach and M. Pinget. 1997. Poly(alkylcyanoacrylate) nanocapsules as a delivery system in the rat for octeotride, a long-acting somatostatin analogue. J. Pharm. Pharmacol. 49: 949–954.

De Campos, A.M. and A. Sánchez and M.J. Alonso. 2001. Chitosan nanoparticles: a new vehicle for the improvement of the delivery of drugs to the ocular surface. Application to cyclosporin A. Int. J. Pharm. 224: 159–168.

de Kozak, Y. and K. Andrieux, H. Villarroya, C. Klein, B. Thillaye-Goldenberg, M.C. Naud, E. Garcia and P. Couvreur. 2004. Intraocular injection of tamoxifen-loaded nanoparticles: a new treatment of experimental autoimmune uveoretinitis. Eur. J. Immunol. 34: 3702–3712.

de Queiroz, A.A. and G.A. Abraham and O.Z. Higa. 2006. Controlled release of 5-fluorouridine from radiation-crosslinked poly(ethylene-co-vinyl acetate) films. Acta Biomater. 2: 641–650.

Desai, N. 2012. Challenges in development of nanoparticle-based therapeutics. AAPS J. 14: 282–295.

Dhanikula, R.S. and P. Hildgen. 2006. Synthesis and evaluation of novel dendrimers with a hydrophilic interior as nanocarriers for drug delivery. Bioconjug. Chem. 17: 29–41.

Dhawan, A. and V. Sharma. 2010. Toxicity assessment of nanomaterials: methods and challenges. Anal. Bioanal. Chem. 398: 589–605.

Dobrovolskaia, M.A. and S.E. McNeil. 2007. Immunological properties of engineered nanomaterials. Nat. Nanotechnol. 2: 469–478.

Dobrovolskaia, M.A. and P. Aggarwal, J.B. Hall and S.E. McNeil. 2008. Preclinical studies to understand nanoparticle interaction with the immune system and its potential effects on nanoparticle biodistribution. Mol. Pharm. 5: 487–495.

Donaldson, K. and P.J. Borm, V. Castranova and M. Gulumian. 2009. The limits of testing particle-mediated oxidative stress *in vitro* in predicting diverse pathologies; relevance for testing of nanoparticles. Part. Fibre Toxicol. 6: 13–20.

Dressman, J.B. and D. Fleisher. 1986. Mixing-tank model for predicting dissolution rate control of oral absorption. J. Pharm. Sci. 75: 109–114.

Duguet, E. and S. Vasseur, S. Mornet and J.M. Devoisselle. 2006. Magnetic nanoparticles and their applications in medicine. Nanomedicine (Lond.). 1: 157–168.

Dutta, T. and H.B. Agashe, M. Garg, P. Balakrishnan, M. Kabra and N.K. Jain. 2007. Poly(propyleneimine) dendrimer based nanocontainers for targeting of efavirenz to human monocytes/macrophages *in vitro*. J. Drug Target. 15: 89–98.

Ehrenberg, M.S. and A.E. Friedman, J.N. Finkelstein, G. Oberdörster and J.L. McGrath. 2009. The influence of protein adsorption on nanoparticle association with cultured endothelial cells. Biomaterials. 30: 603–610.

Elsabahy, M. and K.L. Wooley. 2012. Design of polymeric nanoparticles for biomedical delivery applications. Chem. Soc. Rev. 41: 2545–2561.

Fattal, E. and M. Youssef, P. Couvreur and A. Andremont. 1989. Treatment of experimental salmonellosis in mice with ampicillin-bound nanoparticles. Antimicrob. Agents Chemother. 33: 1540–1543.

Ferrero, C. and D. Massuelle and E. Doelker. 2010. Towards elucidation of the drug release mechanism from compressed hydrophilic matrices made of cellulose ethers. II. Evaluation of a possible swelling-controlled drug release mechanism using dimensionless analysis. J. Control. Release 141: 223–233.

Figueiredo, M. and R. Esenaliev. 2012. PLGA nanoparticles for ultrasound-mediated gene delivery to solid tumors. J. Drug Deliv. 2012: 767839.

Fischer, H.C. and W.C. Chan. 2007. Nanotoxicity: the growing need for *in vivo* study. Curr. Opin. Biotechnol. 18: 565–571.

Fresta, M. and G. Puglisi, G. Giammona, G. Cavallaro, N. Micali and P.M. Furneri. 1995. Pefloxacine mesilate- and ofloxacin-loaded polyethylcyanoacrylate nanoparticles: characterization of the colloidal drug carrier formulations. J. Pharm. Sci. 84: 895–902.

Fu, Y. and W.J. Kao. 2010. Drug release kinetics and transport mechanisms of non-degradable and degradable polymeric delivery systems. Expert Opin. Drug Deliv. 7: 429–444.

Garnett, M.C. and P. Kallinteri. 2006. Nanomedicines and nanotoxicology: some physiological principles. Occup. Med. (Lond.). 56: 307–311.

Gaspar, M.M. and D. Blanco, M.E. Cruz and M.J. Alonso. 1998. Formulation of L-asparaginase-loaded poly(lactide-co-glycolide) nanoparticles: influence of polymer properties on enzyme loading, activity and *in vitro* release. J. Control. Release 52: 53–62.

Gelperina, S. and K. Kisich, M.D. Iseman and L. Heifets. 2005. The potential advantages of nanoparticle drug delivery systems in chemotherapy of tuberculosis. Am. J. Respir. Crit. Care Med. 172: 1487–1490.

Giri, N. and P. Tomar, V.S. Karwasara, R.S. Pandey and V.K. Dixit. 2011. Targeted novel surface-modified nanoparticles for interferon delivery for the treatment of hepatitis B. Acta Biochim. Biophys. Sin. (Shanghai). 43: 877–883.

Govender, T. and S. Stolnik, M.C. Garnett, L. Illum and S.S. Davis. 1999. PLGA nanoparticles prepared by nanoprecipitation: drug loading and release studies of a water soluble drug. J. Control. Release. 57: 171–185.

Govender, T. and T. Riley, T. Ehtezazi, M.C. Garnett, S. Stolnik, L. Illum and S.S. Davis. 2000. Defining the drug incorporation properties of PLA-PEG nanoparticles. Int. J. Pharm. 199: 95–110.

Gref, R. and Y. Minamitake, M.T. Peracchia, V. Trubetskoy, V. Torchilin and R. Langer. 1994. Biodegradable long-circulating polymeric nanospheres. Science. 263: 1600–1603.

Gref, R. and P. Quellec, A. Sanchez, P. Calvo, E. Dellacherie and M.J. Alonso. 2001. Development and characterization of CyA-loaded poly(lactic acid)-poly(ethylene glycol) PEG micro- and nanoparticles. Comparison with conventional PLA particulate carriers. Eur. J. Pharm. Biopharm. 51: 111–118.

Gupta, A.K. and A.S. Curtis. 2004. Surface modified superparamagnetic nanoparticles for drug delivery: interaction studies with human fibroblasts in culture. J. Mater. Sci. Mater. Med. 15: 493–496.

Guterres, S.S. and M.P. Alves and A.R. Pohlmann. 2007. Polymeric nanoparticles, nanospheres and nanocapsules, for cutaneous applications. Drug Target Insights. 2: 147–157.

Hao, Y. and X. Yang, S. Song, M. Huang, C. He, M. Cui and J. Chen. 2012. Exploring the cell uptake mechanism of phospholipid and polyethylene glycol coated gold nanoparticles. Nanotechnology. 23: 045103.

Harland, R.S. and A. Gazzaniga, M.E. Sangalli, P. Colombo and N.A. Peppas. 1988. Drug/polymer matrix swelling and dissolution. Pharm. Res. 5: 488–494.

Hasanovic, A. and M. Zehl, G. Reznicek and C. Valenta. 2009. Chitosan-tripolyphosphate nanoparticles as a possible skin drug delivery system for aciclovir with enhanced stability. J. Pharm. Pharmacol. 61: 1609–1616.

Higuchi, T. 1963. Mechanism of sustained-action medication. Theoretical analysis of rate of release of solid drugs dispersed in solid matrices. J. Pharm. Sci. 52: 1145–1149.

Hoet, P.H. and I. Brüske-Hohlfeld and O.V. Salata. 2004. Nanoparticles—known and unknown health risks. J. Nanobiotechnol. 2: 12.

Hong, J. and P. Gong, D. Xu, L. Dong and S. Yao. 2007. Stabilization of α-chymotrypsin by covalent immobilization on amine-functionalized superparamagnetic nanogel. J. Biotechnol. 128: 597–605.

Hu, S. and Y. Zhang. 2010. Endostar-loaded PEG-PLGA nanoparticles: *in vitro* and *in vivo* evaluation. Int. J. Nanomedicine. 5: 1039–1048.

Hu, Y. and J. Xie, Y.W. Tong and C.H. Wang. 2007. Effect of PEG conformation and particle size on the cellular uptake efficiency of nanoparticles with the HepG2 cells. J. Control. Release. 118: 7–17.

Ishida, T. and H. Harashima and H. Kiwada. 2001. Interactions of liposomes with cells *in vitro* and *in vivo*: opsonins and receptors. Curr. Drug Metab. 2: 397–409.

Jain, R.A. 2000. The manufacturing techniques of various drug loaded biodegradable poly(lactide-co-glycolide) (PLGA) devices. Biomaterials. 21: 2475–2490.

Jani, P. and G.W. Halbert, J. Langridge and A.T. Florence. 1990. Nanoparticles uptake by the rat gastrointestinal mucosa: quantitation and particle size dependency. J. Pharm. Phamacol. 42: 821–826.

Jin, W. and P. Xu, Y. Zhan, Y. Shen, E.A. Van Kirk, B. Alexander, W.J. Murdoch, L. Liu and D.D. Isaak. 2007. Degradable cisplatin-releasing core-shell nanogels from zwitterionic poly(beta-aminoester)-graft-PEG for cancer chemotherapy. Drug Deliv. 14: 279–286.

Jo, Y.S. and M.C. Kim, D.K. Kim, C.J. Kim, Y.K. Jeong, K.J. Kim and M. Muhammed. 2004. Mathematical modelling on the controlled-release of indomethacin-encapsulated poly(lactic acid-co-ethylene oxide) nanospheres. Nanotechnology. 15: 1186–1194.

Ju, R.T. and P.R. Nixon, M.V. Patel and D.M. Tong. 1995. Drug release from hydrophilic matrices. 2. A mathematical model based on the polymer disentanglement concentration and the diffusion layer. J. Pharm. Sci. 84: 1464–1477.

Judefeind, A. and M.M. de Villiers. Drug loading into and *in vitro* release from nanosized drug delivery systems. pp. 129–162. *In*: M.M. de Villiers, P. Aramwit and G.S. Kwon [eds.]. 2009. Nanotechnology in Drug Delivery. Springer, New York, USA.

Kabanov, V.A. and V.B. Skobeleva, V.B. Rogacheva and A.B. Zezin. 2004. Sorption of proteins by slightly cross-linked polyelectrolyte hydrogels: kinetics and mechanism. J. Phys. Chem. B. 108: 1485–1490.

Kadam, R.S. and D.W. Bourne and U.B. Kompella. 2012. Nano-advantage in enhanced drug delivery with biodegradable nanoparticles: contribution of reduced clearance. Drug Metab. Dispos. 40: 1380–1388.

Kaewprapan, K. and P. Inprakhon, E. Marie and A. Durand. 2012. Enzymatically degradable nanoparticles of dextran esters as potential drug delivery systems. Carbohydr. Polym. 88: 875–881.

Kalam, M.A. and M. Humayun, N. Parvez, S. Yadav, A. Garg, S. Amin, Y. Sultana and A. Ali. 2007. Release kinetics of modified pharmaceutical dosage forms: a review. Cont. J. Pharm. Sci. 1: 30–35.

Kamruzzaman, S.K.M. and Y.S. Ha, S.J. Kim, Y. Chang, T.J. Kim, G.L. Ho and I.K. Kang. 2007. Surface modification of magnetite nanoparticles using lactobionic acid and their interaction with hepatocytes. Biomaterials. 28: 710–716.

Kang, E. and K. Vedantham, X. Long, M. Dadarlat, I.K. Kwon, M. Sturek and K. Park. 2009. Drug-eluting stent for delivery of signal pathway-specific 1,3-dipropyl-8-cyclopentyl xanthine. Mol. Pharm. 6: 1110–1117.

Karasulu, H.Y. and G. Ertan and T. Köse. 2000. Modeling of theophylline release from different geometrical erodible tablets. Eur. J. Pharm. Biopharm. 49: 177–182.

Kato, N. and U. Hasegawa, N. Morimoto, Y. Saita, K. Nakashima, Y. Ezura, H. Kurosawa, K. Akiyoshi and M. Noda. 2007. Nanogel-based delivery system enhances PGE2 effects on bone formation. J. Cell Biochem. 101: 1063–1070.

Katzhendler, I. and A. Hofmann, A. Goldberger and M. Friedman. 1997. Modeling of drug release from erodible tablets. J. Pharm. Sci. 86: 110–115.

Kezic, S. and J.B. Nielsen. 2009. Absorption of chemicals through compromised skin. Int. Arch. Occup. Environ. Health. 82: 677–688.

Khmelnitsky, Y.L. and I.N. Neverova, A.V. Gedrovich, V.A. Polyakov, A.V. Levashov and K. Martinek. 1992. Catalysis by alpha-chymotrypsin entrapped into surface-modified polymeric nanogranules in organic solvent. Eur. J. Biochem. 210: 751–757.

Kim, S.W. and Y.H. Bae and T. Okano. 1992. Hydrogels: swelling, drug loading, and release. Pharm. Res. 9: 283–290.

Kim, I.H. and J.H. Park, I.W. Cheong and J.H. Kim. 2003. Swelling and drug release behavior of tablets coated with aqueous hydroxypropyl methylcellulose phthalate (HPMCP) nanoparticles. J. Control. Release. 89: 225–233.

Kim, J. and W.J. Kim, S.J. Kim, C.W. Cho and S.C. Shin. 2006. Release characteristics of quinupramine from the ethylene-vinyl acetate matrix. Int. J. Pharm. 315: 134–139.

Kipen, H.M. and D.L. Laskin. 2005. Smaller is not always better: nanotechnology yields nanotoxicology. Am. J. Physiol. Lung Cell. Mol. Physiol. 289: L696–L697.

Knapp, L.F. 1922. The solubility of small particles and the stability of colloids. Trans. Faraday Soc. 17: 457–465.

Kohli, E. and H.Y. Han, A.D. Zeman and S.V. Vinogradov. 2007. Formulations of biodegradable nanogel carriers with 5′-triphosphates of nucleoside analogs that display a reduced cytotoxicity and enhanced drug activity. J. Control. Release. 121: 19–27.

Kojima, C. and K. Kono, K. Maruyama and T. Takagishi. 2000. Synthesis of polyamidoamine dendrimers having poly(ethylene glycol) grafts and their ability to encapsulate anticancer drugs. Bioconjug. Chem. 11: 910–917.

Kolhe, P. and E. Misra, R.M. Kannan, S. Kannan and M. Lieh-Lai. 2003. Drug complexation, *in vitro* release and cellular entry of dendrimers and hyperbranched polymers. Int. J. Pharm. 259: 143–160.

Kreuter, J. 2001. Nanoparticulate systems for brain delivery of drugs. Adv. Drug Deliv. Rev. 47: 65–81.

Kreyling, W.G. and M. Semmler-Behnke and W. Möller. 2006. Health implications of nanoparticles. J. Nanoparticle Res. 8: 543–562.

Kroll, A. and C. Dierker, C. Rommel, D. Hahn, W. Wohlleben, C. Schulze-Isfort, C. Göbbert, M. Voetz, F. Hardinghaus and J. Schnekenburger. 2011. Cytotoxicity screening of 23 engineered nanomaterials using a test matrix of ten cell lines and three different assays. Part. Fibre Toxicol. 8: 9–28.

Kulkarni, P.V. and C.A. Roney, P.P. Antich, F.J. Bonte, A.V. Raghu and T.M. Aminabhavi. 2010. Quinoline-n-butylcyanoacrylate-based nanoparticles for brain targeting for the diagnosis of Alzheimer's disease. Wiley Interdiscip. Rev. Nanomed. Nanobiotechnol. 2: 35–47.

Kulkarni, S.A. and S.S. Feng. 2011. Effects of surface modification on delivery efficiency of biodegradable nanoparticles across the blood-brain barrier. Nanomedicine (Lond.). 6: 377–394.

Kumari, A. and S.K. Yadav and S.C. Yadav. 2010. Biodegradable polymeric nanoparticles based drug delivery systems. Colloids Surf. B Biointerfaces. 75: 1–18.

Kuntsche, J. and H. Bunjes, A. Fahr, S. Pappinen, S. Rönkkö, M. Suhonen and A. Urtti. 2008. Interaction of lipid nanoparticles with human epidermis and an organotypic cell culture model. Int. J. Pharm. 354: 180–195.

Lambert, G. and E. Fattal, A. Brehier, J. Feger and P. Couvreur. 1998. Effect of polyisobutylcyanoacrylate nanoparticles and lipofectin loaded with oligonucleotides on cell viability and PKC alpha neosynthesis in HepG2 cells. Biochimie. 80: 969–976.

Lanone, S. and J. Boczkowski. 2006. Biomedical applications and potential health risks of nanomaterials: molecular mechanisms. Curr. Mol. Med. 6: 651–663.

Lao, L.L. and N.A. Peppas, F.Y. Boey and S.S. Venkatraman. 2011. Modeling of drug release from bulk-degrading polymers. Int. J. Pharm. 418: 28–41.

Lboutounne, H. and V. Faivre, F. Falson and F. Pirot. 2004. Characterization of transport of chlorhexidine-loaded nanocapsules through hairless and wistar rat skin. Skin Pharmacol. Physiol. 17: 176–182.

Le Bourlais, C.A. and F. Chevanne, B. Turlin, L. Acar, H. Zia, P.A. Sado, T.E. Needham and R. Leverge. 1997. Effect of cyclosporin A formulations on bovine corneal absorption: *ex-vivo* study. J. Microencapsul. 14: 457–467.

Lecaroz, C. and C. Gamazo, M.J. Renedo and M.J. Blanco-Prieto. 2006. Biodegradable micro- and nanoparticles as long-term delivery vehicles for gentamicin. J. Microencapsul. 23: 782–792.

Lee, B.R. and H.J. Baik, N.M. Oh and E.S. Lee. 2010. Intelligent polymeric nanocarriers responding to physical or biological signals: a new paradigm of cytosolic drug delivery for tumor treatment. Polymers 2: 86–101.

Leo, E. and A. Scatturin, E. Vighi and A. Dalpiaz. 2006. Polymeric nanoparticles as drug controlled release systems: a new formulation strategy for drugs with small or large molecular weight. J. Nanosci. Nanotechnol. 6: 3070–3079.

Li, H. and V.V. Tran, Y. Hu, W.M. Saltzman, C.J. Barnstable and J. Tombran-Tink. 2006. A PEDF N-terminal peptide protects the retina from ischemic injury when delivered in PLGA nanospheres. Exp. Eye Res. 83: 824–833.

Liu, Q. and R.T. Li, H.Q. Qian, M. Yang, Z.S. Zhu, W. Wu, X.P. Qian, L.X. Yu, X.Q. Jiang and B.R. Liu. 2012. Gelatinase-stimuli strategy enhances the tumor delivery and therapeutic efficacy of docetaxel-loaded poly(ethylene glycol)-poly(ε-caprolactone) nanoparticles. Int. J. Nanomedicine. 7: 281–295.

Lopes, E. and A.R. Pohlmann, V. Bassani and S.S. Guterres. 2000. Polymeric colloidal systems containing ethionamide: preparation and physico-chemical characterization. Pharmazie. 55: 527–530.

Lowe, P.J. and C.S. Temple. 1994. Calcitonin and insulin in isobutylcyanoacrylate nanocapsules: protection against proteases and effect on intestinal absorption in rats. J. Pharm. Pharmacol. 46: 547–552.

Lu, Z. and J. Bei and S. Wang. 1999. A method for the preparation of polymeric nanocapsules without stabilizer. J. Control. Release. 61: 107–112.

Luengo, J. and B. Weiss, M. Schneider, A. Ehlers, F. Stracke, K. König, K.H. Kostka, C.M. Lehr and U.F. Schaefer. 2006. Influence of nanoencapsulation on human skin transport of flufenamic acid. Skin Pharmacol. Physiol. 19: 190–197.

Lynch, I. and K.A. Dawson. 2008. Protein-nanoparticle interactions. Nano Today. 3: 40–47.

Ma, Z. and T.M. Lim and L.Y. Lim. 2005. Pharmacological activity of peroral chitosan-insulin nanoparticles in diabetic rats. Int. J. Pharm. 293: 271–280.

Maderuelo, C. and A. Zarzuelo and J.M. Lanao. 2011. Critical factors in the release of drugs from sustained release hydrophilic matrices. J. Control. Release. 154: 2–19.

Maeda, H. and M. Brandon and A. Sano. 2003. Design of controlled-release formulation for ivermectin using silicone. Int. J. Pharm. 261: 9–19.

Magenheim, B. and S. Benita. 1991. Nanoparticle characterization: a comprehensive physicochemical approach. S.T.P. Pharm. Sci. 1: 221–224.

Mahapatro, A. and D.K. Singh. 2011. Biodegradable nanoparticles are excellent vehicle for site directed *in vivo* delivery of drugs and vaccines. J. Nanobiotechnol. 9: 55–65.

Mainardes, R.M. and L.P. Silva. 2004. Drug delivery systems: past, present, and future. Curr. Drug Targets. 5: 449–455.

Malcolm, R.K. and S.D. McCullagh, A.D. Woolfson, S.P. Gorman, D.S. Jones and J. Cuddy. 2004. Controlled release of a model antibacterial drug from a novel self-lubricating silicone biomaterial. J. Control. Release. 97: 313–320.

Malcolm, R.K. and A.D. Woolfson, C.F. Toner, R.J. Morrow and S.D. McCullagh. 2005. Long-term, controlled release of the HIV microbicide TMC120 from silicone elastomer vaginal rings. J. Antimicrob. Chemother. 56: 954–956.

McAllister, K. and P. Sazani, M. Adam, M.J. Cho, M. Rubinstein, R.J. Samulski and J.M. DeSimone. 2002. Polymeric nanogels produced via inverse microemulsion polymerization as potential gene and antisense delivery agents. J. Am. Chem. Soc. 124: 15198–15207.

McClean, S. and E. Prosser, E. Meehan, D. O'Malley, N. Clarke, Z. Ramtoola and D. Brayden. 1998. Binding and uptake of biodegradable poly-DL-lactide micro- and nanoparticles in intestinal epithelia. Eur. J. Pharm. Sci. 6: 153–163.

Mihranyan, A. and M. Strømme. 2007. Solubility of fractal nanoparticles. Surf. Sci. 601: 315–319.

Missirlis, D. and N. Tirelli and J.A. Hubbell. 2005. Amphiphilic hydrogel nanoparticles. Preparation, characterization and preliminary assessment as new colloidal drug carriers. Langmuir. 21: 2605–2613.

Missirlis, D. and R. Kawamura, N. Tirelli and J.A. Hubbell. 2006. Doxorubicin encapsulation and diffusional release from stable, polymeric, hydrogel nanoparticles. Eur. J. Pharm. Sci. 29: 120–129.

Miyazaki, S. and A. Takahashi, W. Kubo, J. Bachynsky and R. Löebenberg. 2003. Poly n-butylcyanoacrylate (PNBCA) nanocapsules as a carrier for NSAIDs: *in vitro* release and *in vivo* skin penetration. J. Pharm. Pharm. Sci. 6: 238–245.

Modesti, G. and B. Zimmermann, M. Börsch, A. Herrmann and K. Saalwächter. 2009. Diffusion in model networks as studied by NMR and fluorescence correlation spectroscopy. Macromolecules. 42: 4681–4689.

Moghimi, S.M. and A.C. Hunter and J.C. Murray. 2001. Long-circulating and target-specific nanoparticles: theory to practice. Pharmacol. Rev. 53: 283–318.

Monteiro-Riviere, N.A. and A.O. Inman and L.W. Zhang. 2009. Limitations and relative utility of screening assays to assess engineered nanoparticle toxicity in a human cell line. Toxicol. Appl. Pharmacol. 234: 222–235.

Moore, J.W. and H.H. Flanner. 1996. Mathematical comparison of dissolution profiles. Pharm. Technol. 20: 64–74.

Morais, T. and M.E. Soares, J.A. Duarte, L. Soares, S. Maia, P. Gomes, E. Pereira, S. Fraga, H. Carmo and M.L. Bastos. 2012. Effect of surface coating on the biodistribution profile of gold nanoparticles in the rat. Eur. J. Pharm. Biopharm. 80: 185–193.

Münster, U. and C. Nakamura, A. Haberland, K. Jores, W. Mehnert, S. Rummel, M. Schaller, H.C. Korting, Ch. Zouboulis, U. Blume-Peytavi and M. Schafer-Korting. 2005. RU 58841-myristate-prodrug development for topical treatment of acne and androgenetic alopecia. Pharmazie. 60: 8–12.

Nagarwal, R.C. and D.N. Ridhurkar and J.K. Pandit. 2010. *In vitro* release kinetics and bioavailability of gastroretentive cinnarizine hydrochloride tablet. AAPS Pharm. Sci. Tech. 11: 294–303.

Niwa, T. and H. Takeuchi, T. Hino, N. Kunou and Y. Kawashima. 1993. Preparations of biodegradable nanospheres of water-soluble and insoluble drugs with D,L-lactide/glycolide copolymer by a novel spontaneous emulsification solvent diffusion method, and the drug release behavior. J. Control. Release. 25: 89–98.

Noyes, A.A. and W.R. Whitney. 1897. The rate of solution of solid substances in their own solutions. J. Am. Chem. Soc. 19: 930–934.

Oberdörster, G. 2010. Safety assessment for nanotechnology and nanomedicine: concepts of nanotoxicology. J. Intern. Med. 267: 89–105.

Oh, J.K. and D.J. Siegwart, H.I. Lee, G. Sherwood, L. Peteanu, J.O. Hollinger, K. Kataoka and K. Matyjaszewski. 2007. Biodegradable nanogels prepared by atom transfer radical polymerization as potential drug delivery carriers: synthesis, biodegradation, *in vitro* release, and bioconjugation. J. Am. Chem. Soc. 129: 5939–5945.

Oishi, M. and S. Sumitani and Y. Nagasaki. 2007. On-off regulation of 19F magnetic resonance signals based on pH-sensitive PEGylated nanogels for potential tumor-specific smart 19F MRI probes. Bioconjug. Chem. 18: 1379–1382.

Opanasopit, P. and T. Ngawhirunpat, A. Chaidedgumjorn, T. Rojanarata, A. Apirakaramwong, S. Phongying, C. Choochottiros and S. Chirachanchai. 2006. Incorporation of camptothecin into N-phthaloyl chitosan-g-mPEG self-assembly micellar system. Eur. J. Pharm. Biopharm. 64: 269–276.

Owens 3rd, D.E. and N.A. Peppas. 2006. Opsonization, biodistribution, and pharmacokinetics of polymeric nanoparticles. Int. J. Pharm. 307: 93–102.

Ozcan, I. and F. Segura-Sánchez, K. Bouchemal, M. Sezak, O. Ozer, T. Güneri and G. Ponchel. 2010. Pegylation of poly(γ-benzyl-L-glutamate) nanoparticles is efficient for avoiding mononuclear phagocyte system capture in rats. Int. J. Nanomedicine. 5: 1103–1111.

Ozturk, S.S. and B.O. Palsson, B. Donohoe and J.B. Dressman. 1988. Kinetics of release from enteric-coated tablets. Pharm. Res. 5: 550–565.

Page-Clisson, M.E. and H. Pinto-Alphandary, E. Chachaty, P. Couvreur and A. Andremont. 1998. Drug targeting by polyalkylcyanoacrylate nanoparticles is not efficient against persistent Salmonella. Pharm. Res. 15: 544–549.

Pan, Y. and Y.J. Li, H.Y. Zhao, J.M. Zheng, H. Xu, G. Wei, J.S. Hao and F.D. Cui. 2002. Bioadhesive polysaccharide in protein delivery systems: chitosan nanoparticles improve the intestinal absorption of insulin *in vivo*. Int. J. Pharm. 249: 139–147.

Pandey, R. and A. Sharma, A. Zahoor, S. Sharma, G.K. Khuller and B. Prasad. 2003. Poly(DL-lactide-co-glycolide) nanoparticle based inhalable sustained drug delivery system for experimental tuberculosis. J. Antimicrob. Chemother. 52: 981–986.

Pandey, R. and G.K. Khuller. 2004. Subcutaneous nanoparticle-based antitubercular chemotherapy in an experimental model. J. Antimicrob. Chemother. 54: 266–268.

Pandey, R. and Z. Ahmad, S. Sharma and G.K. Khuller. 2005. Nano-encapsulation of azole antifungals: potential applications to improve oral drug delivery. Int. J. Pharm. 301: 268–276.

Panyam, J. and M.M. Dali, S.K. Sahoo, W. Ma, S.S. Chakravarthi, G.L. Amidon, R.J. Levy and V. Labhasetwar. 2003. Polymer degradation and *in vitro* release of a model protein from poly(D,L-lactide-co-glycolide) nano- and microparticles. J. Control. Release. 92: 173–187.

Paraskar, A. and S. Soni, S. Basu, C.J. Amarasiriwardena, N. Lupoli, S. Srivats, R.S. Roy and S. Sengupta. 2011. Rationally engineered polymeric cisplatin nanoparticles for improved antitumor efficacy. Nanotechnology. 22: 265101.

Park, E.S. and M. Maniar and J.C. Shah. 1998. Biodegradable polyanhydride devices of cefazolin sodium, bupivacaine, and taxol for local drug delivery: preparation, and kinetics and mechanism of *in vitro* release. J. Control. Release. 52: 179–189.

Patel, D. and S. Naik and A. Misra. 2012. Improved transnasal transport and brain uptake of tizanidine HCl-loaded thiolated chitosan nanoparticles for alleviation of pain. J. Pharm. Sci. 101: 690–706.

Patri, A.K. and J.F. Kukowska-Latallo and J.R. Baker, Jr. 2005. Targeted drug delivery with dendrimers: comparison of the release kinetics of covalently conjugated drug and non-covalent drug inclusion complex. Adv. Drug Deliv. Rev. 57: 2203–2214.

Peer, D. and M.J. Karp, S. Hong, O.C. Farokhzad, R. Margalit and R. Langer. 2007. Nanocarriers as an emerging platform for cancer therapy. Nat. Nanotechnol. 2: 751–760.

Peppas, N.A. and J.J. Sahlin. 1989. A simple equation for the description of solute release. III. Coupling of diffusion and relaxation. Int. J. Pharm. 57: 169–172.

Pfeifer, B.A. and J.A. Burdick, S.R. Little and R. Langer. 2005. Poly(ester-anhydride): poly(beta-amino ester) micro- and nanospheres: DNA encapsulation and cellular transfection. Int. J. Pharm. 304: 210–219.

Pignatello, R. and C. Bucolo, P. Ferrara, A. Maltese, A. Puleo and G. Puglisi. 2002. Eudragit RS100 nanosuspensions for the ophthalmic controlled delivery of ibuprofen. Eur. J. Pharm. Sci. 16: 53–61.

Pinto-Alphandary, H. and M. Aboudakar, D. Jaillard, P. Couvreur and C. Vauthier. 2003. Visualization of insulin-loaded nanocapsules: *in vitro* and *in vivo* studies after oral administration to rats. Pharm. Res. 20: 1071–1084.

Pirollo, K.F. and E.H. Chang. 2008. Does a targeting ligand influence nanoparticle tumor localization or uptake? Trends Biotechnol. 26: 552–558.

Polakovic, M. and T. Görner, R. Gref and E. Dellacherie. 1999. Lidocaine loaded biodegradable nanospheres. II. Modelling of drug release. J. Control. Release. 60: 169–177.

Polli, J.E. and G.S. Rekhi, L.L. Augsburger and V.P. Shah. 1997. Methods to compare dissolution profiles and a rationale for wide dissolution specifications for metoprolol tartrate tablets. J. Pharm. Sci. 86: 690–700.

Ponchel, G. and M.J. Montisci, A. Dembri, C. Durrer and D. Duchêne. 1997. Mucoadhesion of colloidal particulate systems in the gastro-intestinal tract. Eur. J. Pharm. Biopharm. 44: 25–31.

Powell, C. and N. Fenwick, F. Bresme and N. Quirke. 2002. Wetting of nanoparticles and nanoparticle arrays. Colloids Surf. A Physicochem. Eng. Aspects. 206: 241–251.

Quaglia, F. and L. Ostacolo, G. De Rosa, M.I. La Rotonda, M. Ammendola, G. Nese, G. Maglio, R. Palumbo and C. Vauthier. 2006. Nanoscopic core-shell drug carriers made of amphiphilic triblock and star-diblock copolymers. Int. J. Pharm. 324: 56–66.

Radwan, M.A. 1995. *In vitro* evaluation of polyisobutylcyanoacrylate nanoparticles as a controlled drug carrier for theophylline. Drug Develop. Ind. Pharm. 21: 2371–2375.

Reddy, L.H. and R.S. Murthy. 2004. Pharmacokinetics and biodistribution studies of doxorubicin loaded poly(butyl cyanoacrylate) nanoparticles synthesized by two different techniques. Biomed. Papers. 148: 161–166.

Redhead, H.M. and S.S. Davis and L. Illum. 2001. Drug delivery in poly(lactide-co-glycolide) nanoparticles surface modified with Poloxamer 407 and Poloxamine 908: *in vitro* characterization and *in vivo* evaluation. J. Control. Release. 70: 353–363.

Riggs, P.D. and A.S. Clough, P.M. Jenneson, D.W. Drew, M. Braden and M.P. Patel. 1999. 3He ion-beam analysis of water uptake and drug delivery. J. Control. Release. 61: 165–174.

Ritger, P.L. and N.A. Peppas. 1987a. A simple equation for description of solute release. I. Fickian and non-Fickian release from non-swellable devices in the form of slabs, spheres, cylinders or discs. J. Control. Release. 5: 23–36.

Ritger, P.L. and N.A. Peppas. 1987b. A simple equation for description of solute release. II. Fickian and anomalous release from swellable devices. J. Control. Release. 5: 37–42.

Rothen-Rutishauser, B.M. and S.G. Kiama and P. Gehr. 2005. A three-dimensional cellular model of the human respiratory tract to study the interaction with particles. Am. J. Respir. Cell Mol. Biol. 32: 281–289.

Rothen-Rutishauser, B.M. and L. Mueller, F. Blank, C. Brandenberger, C. Muehlfeld and P. Gehr. 2008. A newly developed *in vitro* model of the human epithelial airway barrier to study the toxic potential of nanoparticles. ALTEX. 25: 191–196.

Rothstein, S.N. and W.J. Federspiel and S.R. Little. 2009. A unified mathematical model for the prediction of controlled release from surface and bulk eroding polymer matrices. Biomaterials. 30: 1657–1664.

Rouse, J.G. and J. Yang, J.P. Ryman-Rasmussen, A.R. Barron and N.A. Monteiro-Riviere. 2007. Effects of mechanical flexion on the penetration of fullerene amino acid-derivatized peptide nanoparticles through skin. Nano Lett. 7: 155–160.

Sadauskas, E. and H. Wallin, M. Stoltenberg, U. Vogel, P. Doering, A. Larsen and G. Danscher. 2007. Kupffer cells are central in the removal of nanoparticles from the organism. Part. Fibre Toxicol. 4: 10.

Sahana, D.K. and G. Mittal, V. Bhardwaj and M.N. Kumar. 2008. PLGA nanoparticles for oral delivery of hydrophobic drugs: influence of organic solvent on nanoparticle formation and release behavior *in vitro* and *in vivo* using estradiol as a model drug. J. Pharm. Sci. 97: 1530–1542.

Santos, M.C. and W. Mehnert, M. Schaller, H.C. Korting, A. Gysler, A. Haberland and M. Schäfer-Korting. 2002. Drug targeting by solid lipid nanoparticles for dermal use. J. Drug Target. 10: 489–495.

Sanvicens, N. and M.P. Marco. 2008. Multifunctional nanoparticles—properties and prospects for their use in human medicine. Trends Biotechnol. 26: 425–433.

Schierholz, J.M. and H. Steinhauser, and A.F. Rump, R. Berkels and G. Pulverer. 1997. Controlled release of antibiotics from biomedical polyurethanes: morphological and structural features. Biomaterials. 18: 839–844.

Schwab, G. and C. Chavany, I. Duroux, G. Goubin, J. Lebeau, C. Hélène and T. Saison-Behmoaras. 1994. Antisense oligonucleotides adsorbed to polyalkylcyanoacrylate nanoparticles specifically inhibit mutated Ha-ras-mediated cell proliferation and tumorigenicity in nude mice. Proc. Natl. Acad. Sci. U.S.A. 91: 10460–10464.

Sdobnyakov, N.Y. and V.M. Samsonov. 2005. On the size dependence of surface tension in the temperature range from melting point to critical point. Cent. Eur. J. Phys. 3: 247–257.

Serra, L. and J. Doménech and N.A. Peppas. 2006. Drug transport mechanisms and release kinetics from molecularly designed poly(acrylic acid-g-ethylene glycol) hydrogels. Biomaterials. 27: 5440–5451.

Service, R.F. 2004. Nanotoxicology. Nanotechnology grows up. Science. 304: 1732–1734.

Shah, V.P. and L.J. Lesko, J. Fan, N. Fleischer, J. Handerson, H. Malinowski, M. Makary, L. Ouderkirk, S. Roy, P. Sathe, G.J.P. Singh, L. Tillman, Y. Tsong and R.L. Williams. 1997. FDA guidance for industry: dissolution testing of immediate release solid oral dosage forms. Dissolution Technol. 4: 15–22.

Sharma, A. and S. Sharma and G.K. Khuller. 2004. Lectin-functionalized poly(lactide-co-glycolide) nanoparticles as oral/aerosolized antitubercular drug carriers for treatment of tuberculosis. J. Antimicrob. Chemother. 54: 761–766.

Sharma, G. and C.F. van der Walle and M.N. Ravi Kumar. 2013. Antacid co-encapsulated polyester nanoparticles for peroral delivery of insulin: development, pharmacokinetics, biodistribution and pharmacodynamics. Int. J. Pharm. 440: 99–110.

Shekunov, B.Y. and P. Chattopadhyay, J. Seitzinger and R. Huff. 2006. Nanoparticles of poorly water-soluble drugs prepared by supercritical fluid extraction of emulsions. Pharm. Res. 23: 196–204.

Sheng, Y. and C. Liu, Y. Yuan, X. Tao, F. Yang, X.Q. Shan, H. Zhou and F. Xu. 2009. Long-circulating polymeric nanoparticles bearing a combinatorial coating of PEG and water-soluble chitosan. Biomaterials. 30: 2340–2348.

Shim, J. and H.S. Kang, W.S. Park, S.H. Han, J. Kim and I.S. Chang. 2004. Transdermal delivery of minoxidil with block copolymer nanoparticles. J. Control. Release. 97: 477–484.

Siepmann, J. and A. Göpferich. 2001. Mathematical modeling of bioerodible, polymeric drug delivery systems. Adv. Drug Deliv. Rev. 48: 229–247.

Simmons, A. and A.D. Padsalgikar, L.M. Ferris and L.A. Poole-Warren. 2008. Biostability and biological performance of a PDMS-based polyurethane for controlled drug release. Biomaterials. 29: 2987–2995.

Soppimath, K.S. and T.M. Aminabhavi, A.R. Kulkarni and W.E. Rudzinski. 2001. Biodegradable polymeric nanoparticles as drug delivery devices. J. Control. Release. 70: 1–20.

Su, F.Y. and K.J. Lin, K. Sonaje, S.P. Wey, T.C. Yen, Y.C. Ho, N. Panda, E.Y. Chuang, B. Maiti and H.W. Sung. 2012. Protease inhibition and absorption enhancement by functional nanoparticles for effective oral insulin delivery. Biomaterials. 33: 2801–2811.

Takeuchi, H. and H. Yamamoto and Y. Kawashima. 2001. Mucoadhesive nanoparticulate systems for peptide drug delivery. Adv. Drug Deliv. Rev. 47: 39–54.

Tallury, P. and N. Alimohammadi and S. Kalachandra. 2007. Poly(ethylene-co-vinyl acetate) copolymer matrix for delivery of chlorhexidine and acyclovir drugs for use in the oral environment: effect of drug combination, copolymer composition and coating on the drug release rate. Dent. Mater. 23: 404–409.

Tan, J.P. and A.Q. Zeng, C.C. Chang and K.C. Tam. 2008. Release kinetics of procaine hydrochloride (PrHy) from pH-responsive nanogels: theory and experiments. Int. J. Pharm. 357: 305–313.

Tang, R. and R.N. Palumbo, W. Ji and C. Wang. 2009. Poly(ortho ester amides): acid-labile temperature-responsive copolymers for potential biomedical applications. Biomacromolecules. 10: 722–727.

Tinke, A.P. and K. Vanhoutte, R. De Maesschalck, S. Verheyen and H. De Winter. 2005. A new approach in the prediction of the dissolution behavior of suspended particles by means of their particle size distribution. J. Pharm. Biomed. Anal. 39: 900–907.

Tosi, G. and R.A. Fano, L. Bondioli, L. Badiali, R. Benassi, F. Rivasi, B. Ruozi, F. Forni and M.A. Vandelli. 2011. Investigation on mechanisms of glycopeptide nanoparticles for drug delivery across the blood-brain barrier. Nanomedicine (Lond.). 6: 423–436.

Tripathi, P.K. and A.J. Khopade, S. Nagaich, S. Shrivastava, S. Jain and N.K. Jain. 2002. Dendrimer grafts for delivery of 5-fluorouracil. Pharmazie. 57: 261–264.

Ungaro, F. and I. d'Angelo, C. Coletta, B.R. d'Emmanuele di Villa, R. Sorrentino, B. Perfetto, M.A. Tufano, A. Miro, M.I. La Rotonda and F. Quaglia. 2012. Dry powders based on PLGA nanoparticles for pulmonary delivery of antibiotics: Modulation of encapsulation efficiency, release rate and lung deposition pattern by hydrophilic polymers. J. Control. Release. 157: 149–159.

Varga, I. and I. Szalai, R. Mészaros and T. Gilanyi. 2006. Pulsating pH-responsive nanogels. J. Phys. Chem. B. 110: 20297–20301.

Vega, E. and M.A. Egea, O. Valls, M. Espina and M.L. García. 2006. Flurbiprofen loaded biodegradable nanoparticles for ophtalmic administration. J. Pharm. Sci. 95: 2393–2405.

Vega-Villa, K.R. and J.K. Takemoto, J.A. Yáñez, C.M. Remsberg, M.L. Forrest and N.M. Davies. 2008. Clinical toxicities of nanocarrier systems. Adv. Drug Deliv. Rev. 60: 929–938.

Veiseh, O. and C. Sun, C. Fang, N. Bhattarai, J. Gunn, F. Kievit, K. Du, B. Pullar, D. Lee, R.G. Ellenbogen, J. Olson and M. Zhang. 2009. Specific targeting of brain tumors with an optical/magnetic resonance imaging nanoprobe across the blood-brain barrier. Cancer Res. 69: 6200–6207.

Vinogradov, S.V. 2007. Polymeric nanogel formulations of nucleoside analogs. Expert Opin. Drug Deliv. 4: 5–17.

Vinogradov, S.V. and T.K. Bronich and A.V. Kabanov. 1998. Self-assembly of polyamine-poly(ethylene) with phosphorothioate oligonucleotides. Bioconjug. Chem. 9: 805–812.

Vinogradov, S.V. and E.V. Batrakova and A.V. Kabanov. 1999. Poly(ethylene glycol)-polyethyleneimine Nanogel particles: novel drug delivery systems for antisense oligonucleotides. Colloids Surf. B Biointerfaces. 16: 291–304.

Vinogradov, S.V. and E.V. Batrakova and A.V. Kabanov. 2004. Nanogels for oligonucleotide delivery to the brain. Bioconjug. Chem. 15: 50–60.

Vinogradov, S.V. and A.D. Zeman, E.V. Batrakova and A.V. Kabanov. 2005. Polyplex nanogel formulations for drug delivery of cytotoxic nucleoside analogs. J. Control. Release. 107: 143–157.

Vinogradov, S.V. and E. Kohli, A. Zeman and A.V. Kabanov. 2006. Chemical engineering of nanogel drug carriers: increased bioavailability and decreased cytotoxicity. Polymer Prepr. 47: 27–28.

Von Burkersroda, F. and L. Schedl and A. Göpferich. 2002. Why degradable polymers undergo surface erosion or bulk erosion. Biomaterials. 23: 4221–4231.

Wagner, J.G. 1969. Interpretation of percent dissolved-time plots derived from *in vitro* testing of conventional tablets and capsules. J. Pharm. Sci. 58: 1253–1257.

Wang, J. and G. Zhou, C. Chen, H. Yu, T. Wang, Y. Ma, G. Jia, Y. Gao, B. Li, J. Sun, Y. Li, F. Jiao, Y. Zhao and Z. Chai. 2007. Acute toxicity and biodistribution of different sized titanium dioxide in mice after oral administration. Toxicol. Lett. 168: 176–185.

Wang, X. and S.S. Venkatraman, F.Y. Boey, J.S. Loo and L.P. Tan. 2006. Controlled release of sirolimus from a multilayered PLGA stent matrix. Biomaterials. 27: 5588–5595.

Wiwattanapatapee, R. and L. Lomlim and K.Saramunee. 2003. Dendrimers conjugates for colonic delivery of 5-aminosalicylic acid. J. Control. Release. 88: 1–9.

Wohlfart, S. and S. Gelperina and J. Kreuter. 2012. Transport of drugs across the blood-brain barrier by nanoparticles. J. Control. Release. 161: 264–273.

Wood, R.W. and V.H.K. Li, J. Kreuter and J.R. Robinson. 1985. Ocular disposition of poly-hexyl-2-cyano 3-[^{14}C] acrylate nanoparticles in the albino rabbit. Int. J. Pharm. 23: 175–184.

Woolfson, A.D. and R.K. Malcolm, R.J. Morrow, C.F. Toner and S.D. McCullagh. 2006. Intravaginal ring delivery of the reverse transcriptase inhibitor TMC 120 as an HIV microbicide. Int. J. Pharm. 325: 82–89.

Xiao, K. and Y. Li, J. Luo, J.S. Lee, W. Xiao, A.M. Gonik, R.G. Agarwal and K.S. Lam. 2011. The effect of surface charge on *in vivo* biodistribution of PEG-oligocholic acid based micellar nanoparticles. Biomaterials. 32: 3435–3446.

Yadav, K.S. and S. Jacob, G. Sachdeva, K. Chuttani, A.K. Mishra and K.K. Sawant. 2011a. Long circulating PEGylated PLGA nanoparticles of cytarabine for targeting leukemia. J. Microencapsul. 28: 729–742.

Yadav, K.S. and K. Chuttani, A.K. Mishra and K.K. Sawant. 2011b. Effect of size on the biodistribution and blood clearance of etoposide-loaded PLGA nanoparticles. PDA J. Pharm. Sci. Technol. 65: 131–139.

Yan, M. and J. Ge, Z. Liu and P. Ouyang. 2006. Encapsulation of single enzyme in nanogel with enhanced biocatalytic activity and stability. J. Am. Chem. Soc. 128: 11008–11009.

Yan, M. and Z. Liu, D. Lu and Z. Liu. 2007. Fabrication of single carbonic anhydrase nanogel against denaturation and aggregation at high temperature. Biomacromolecules. 8: 560–565.

Yang, R.S. and L.W. Chang, C.S. Yang and P. Lin. 2010. Pharmacokinetics and physiologically-based pharmacokinetic modeling of nanoparticles. J. Nanosci. Nanotechnol. 10: 8482–8490.

Yemişci, M. and Y. Gürsoy-Özdemir, S. Caban, E. Bodur, Y. Capan and T. Dalkara. 2012. Transport of a caspase inhibitor across the blood-brain barrier by chitosan nanoparticles. Methods Enzymol. 508: 253–269.

Yoo, H.S. and J.E. Oh, K.H. Lee and T.G. Park. 1999. Biodegradable nanoparticles containing doxorubicin-PLGA conjugate for sustained release. Pharm. Res. 16: 1114–1118.

Youssef, M. and E. Fattal, M.J. Alonso, L. Roblot-Treupel, J. Sauzières, C. Tancrède, A. Omnès, P. Couvreur and A. Andremont. 1988. Effectiveness of nanoparticle-bound ampicillin in the treatment of Listeria monocytogenes infections in athymic nude mice. Antimicrob. Agents Chemother. 32: 1204–1207.

Yu, S. and J. Hu, X. Pan, P. Yao and M. Jiang. 2006. Stable and pH-sensitive nanogels prepared by self-assembly of chitosan and ovalbumin. Langmuir. 22: 2754–2759.

Zhang, J.X. and X.J. Li, L.Y. Qiu, X.H. Li, M.Q. Yan, Y. Jin and K.J. Zhu. 2006. Indomethacin-loaded polymeric nanocarriers based on amphiphilic polyphosphazenes with poly (N-isopropylacrylamide) and ethyl tryptophan as side groups: preparation, *in vitro* and *in vivo* evaluation. J. Control. Release. 116: 322–329.

Zhang, Y. and Y. Guan and S. Zhou. 2007. Permeability control of glucose-sensitive nanoshells. Biomacromolecules. 8: 3842–3847.

Zhang, C. and W. Wang, T. Liu, Y. Wu, H. Guo, P. Wang, Q. Tian, Y. Wang and Z. Yuan. 2012. Doxorubicin-loaded glycyrrhetinic acid-modified alginate nanoparticles for liver tumor chemotherapy. Biomaterials. 33: 2187–2196.

Zhou, J. and C. Leuschner, C. Kumar, J.F. Hormes and W.O. Soboyejo. 2006. Sub-cellular accumulation of magnetic nanoparticles in breast tumors and metastases. Biomaterials. 27: 2001–2008.

Zhu, Z. and C. Xie, Q. Liu, X. Zhen, X. Zheng, W. Wu, R. Li, Y. Ding, X. Jiang and B. Liu. 2011. The effect of hydrophilic chain length and iRGD on drug delivery from poly(ε-caprolactone)-poly(N-vinylpyrrolidone) nanoparticles. Biomaterials. 32: 9525–9535.

Zimmer, A. and J. Kreuter and J.R. Robinson. 1991. Studies on the transport pathway of PBCA nanoparticles in ocular tissues. J. Microencapsul. 8: 497–504.

CHAPTER 3

Nano-Sized Polymeric Drug Carrier Systems

Cornelia Vasile,[a,*] *Manuela Tatiana Nistor*[b] and *Anca-Maria Cojocariu*[c]

ABSTRACT

The development of polymeric nanocarriers for therapeutic agents requires compatibility with the human body, as well as close supervision in time of their effect on the human organism and their subsequent effect on human health. The important technological advantages of polymeric nanoparticles used as drug carriers are the suitable and high stability, high carrier capacity, feasibility of incorporation of hydrophilic and hydrophobic substances, variable routes of administration, controlled (sustained) drug release from the matrix, to cite just a few. These properties of the nanoparticles enable improvement of drug bioavailability triggering a reduction of the dosing frequency. In this chapter, the main types of polymeric nano-sized drug delivery systems, and their preparation and applications are described.

Introduction

The objectives of drug delivery by polymeric nano-sized systems are to: *i*) design nanoparticulate drug carriers that can incorporate different types of

"Petru Poni" Institute of Macromolecular Chemistry, Department of Physical Chemistry of Polymers, 41A Grigore Ghica Voda Alley, R0 700487, Iasi, Romania.
[a] Email: cvasile@icmpp.ro
[b] Email: manuela.pintilie@icmpp.ro
[c] Email: ancuta_cojocariu@yahoo.com
* Corresponding author

List of abbreviations after the text.

therapeutic agents in sufficient doses; *ii*) identify disease-specific ligands that can be conjugated to the drug nanocarrier to achieve targeted drug therapy; *iii*) protect drug molecules from degradation in the body prior to reaching the target; *iv*) develop carriers that can release the drug at the target site and at a desired or controllable rate, and for the duration necessary to elicit the desired pharmacological response; *v*) reduce the quantity of drug needed to attain a particular concentration in the target; *vi*) achieve effective intracellular drug delivery for those therapeutic agents whose receptor or site of action is intracellular; *vii*) develop nano-sized drug carriers biocompatible and biodegradable, so that they can be used safely in humans; and, *viii*) reduce the drug concentration at non-target sites, thus minimizing severe side effects (Sahoo et al. 2008). Nanoplatforms have many advantages over the microplatforms, such as circulation in blood stream for longer periods without being recognized by macrophages, ease of penetration into tissues through capillaries and biological membranes, ability to be taken up by target cells easily, and sustaining the effect at the desired area over a period of days or even weeks. Nanoscale manipulation of drug delivery vehicles can substantially improve pharmacokinetics, pharmacodynamics, non-specific toxicity, immunogenicity and biorecognition properties (Kopeček 2003).

The ideal drug delivery system protects drugs from degradation (via enzymatic, mechanical or chemical pathways), enhances diffusion through the epithelium, targets tissue distribution or increases penetration into its target cell, depending on the application (Couvreur et al. 2006). In their design and formulation, key parameters are size, drug entrapment method, drug stability, degradation parameters of the matrix and release kinetics of drugs. The control of the amount of drug delivered over time and the spatial localization of that delivery are paramount in overcoming the challenges of providing optimal therapy (Mainardes and Silva 2004). All these elements ultimately lead to a more effective delivery of the active agent to a desired physiological or pathophysiological location.

Nano-sized drug carriers can address some specific situations and enhance therapeutic efficacy, so that drugs will be less toxic and more effective, especially in the case of new generation of therapeutics which are either unstable in the biological environment, have poor transport properties across biological membranes, are insoluble in water or have very low bioavailability. Drug nanocarriers allow for the delivery of not only small-molecule drugs, but also nucleic acids and proteins as new biological drugs (Hughes 2005).

Nanoscale Drug Delivery Devices

Nano-sized controlled release systems for drug delivery are divided in several categories including: polymeric nanoparticles (NPs), nanowires,

nanocages, nanoemulsions, nanosuspensions, carbon nanotubes, polymeric micelles, metallic nanorods, liposomes, niosomes, dendrimers, supramolecular complexes and stimuli-responsive systems (with several examples in Fig. 3.1, Table 3.1) (Sahoo et al. 2008, Vasile and Dumitriu 2008, Vasile 2009). Most of these are generally classified as colloidal drug delivery systems, by virtue of their size and physico-chemical properties. Modification of the nanocarrier composition largely controls the release of the active agent. This can be accomplished by using various types of polymers or lipids, changing the molecular weight of those components, or changing the surface characteristics, such as by cross-linking or adding a separate component like Poly(Ethylene Glycol) (PEG). Polymeric carriers for genetic materials, such as plasmid deoxyribonucleic acid (DNA), small interfering ribonucleic acid (*si*RNA) and oligonucleotides are not covered here.

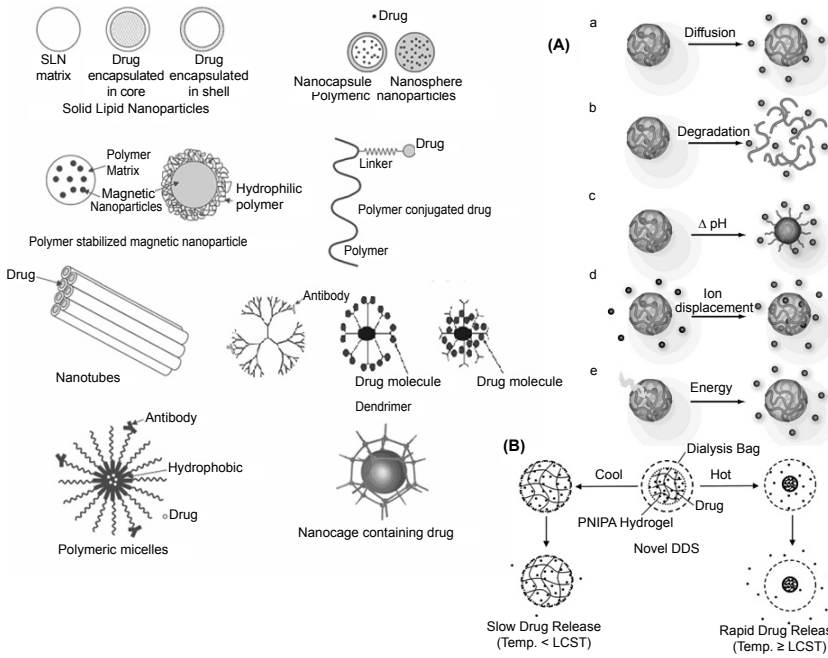

Figure 3.1. Schematic drawing of different types of nano-sized carriers for drug delivery, including schemes of incorporation of the drug within various nanostructures. (A) Responsive drug release profiles: (a) Diffusion of the drug from nanogels. (b) Drug release due to degradation of biodegradable polymer chains or cross-links. (c) Change in pH results in deionization of polymer network and release of electrostatically bound drug. (d) Multivalent low-molecular cations or polyions of either charge can displace drugs having the same charge sign from electrostatic complexes with ionic nanogel. (e) Drug release can be induced by external energy applied to nanogels that induces degradation or structural transition of the nanogel polymer chains. (B) Drug release from a temperature-responsive poly(*N*-isopropylacrylamide) hydrogel exhibiting a low critical solution temperature (LCST).

Table 3.1. Nanoparticle types as drug delivery systems.

Material	Shape	Therapeutic agent	Targeted therapeutic application	Reference
Synthetic polymer				
PBCA coated with polysorbate 80	NP		Drug target to the brain	Kreuter et al. 2003
PGuA	Conjugate	PTX	Cancer	Boock et al. 2011
PLGA, PLGA-PEI, and PLA	NP, micelle	DOC	Cancer	Agrawal et al. 2012
PLGA	NP, micelle	Insulin, nifedipine, pilocarpine	Intestinal tract, oral drug delivery, or ocular drug delivery	Wu et al. 2012, Park et al. 2011, Nair et al. 2012
PLA	NP	5-FU, dexamethasone	Cancer	Bourges et al. 2006
PLGA, and CS	NP	Spantide, ketoprofen, proteins, and peptides	Skin permeating nanogel. Oral drug delivery	Shah et al. 2012a, Zhang et al. 2012a
PLA-PEG	NP, micelle	Rifampin	Cancer	Chen et al. 2007
Copolymer of poly(3,4-dihydroxycinnamic acid)-*co*-poly(4-hydroxycinnamic acid) -*g*-dithiothreitiol	Biodegradable and photo-responsive NP	BSA	Drug delivery	Shi et al. 2011
Block copolymer	Micelle	Hydrophobic drug	Cancer	Kakizawa and Kataoka 2002
PEG-b-hydrophobic polymethacrylate block (PEYM) bearing acid-labile ortho ester side chains	Micelle	DOX	pH-responsive nanocarrier	Tang et al. 2011
N-vinylpyrrolidone PEG diacrylate, and chitosan		Theophylline, 5-FU		Shantha and Harding 2000
PEG-poly(α,β-aspartic acid) block copolymer	Micelle	DOX	Cancer	Kataoka et al. 2000
PEO-*b*-PCL	Micelle	Cyclosporine A	Efficient solubilization and controlled delivery	Aliabadi et al. 2005
PEG-*b*-poly (aspartic acid-statphenylalanine)	Micelle	Diminazene aceturate	Cancer	Prompruk et al. 2005

PEG, gelatin	NP	Hypocrellin B	Photodynamic cancer therapy	Babu et al. 2012
PEG, PCL	NP	4′-dimethylepipodophyllotoxin	Cancer	Zhang and Zhuo 2005
PEG-distearoyl phosphoethanolamine conjugate	Micelle	Vitamin K3	Cancer	Wang et al. 2004
Poly(*N*-(2-hydroxypropyl) methacrylamide)-*b*-PLA-*b*-poly(*N*-(2-hydroxy propyl) methacrylamide), poly(*N*-vinyl-2-pyrrolidone)-*b*-PLA-*b*-poly(*N*-vinyl-2-pyrrolidone), star-PLA-*b*-poly(*N*-(2-hydroxypropyl) methacrylamide), and star-PLA-*b*-poly(*N*-vinylpyrrolidone)	Micelle	Indomethacin, PTX	Cancer	Kang et al. 2004
Poly(2-hydroxyethyl methacrylate-*co*-3,9-divinyl-2,4,8,10-tetraoxaspiro(5.5) undecane)	NP	Indomethacin	pH-sensitive drug delivery	Chiriac et al. 2011
methylmethacrylate / glycidylmethacrylate copolymer	NP	Indomethacin	Controlled drug delivery	Nita et al. 2010
Grafted PLA to both ends of Pluronic® F-87 block copolymer (PEO-PPO-PEO)	Amphiphilic block copolymer	Procain hydrochloride		Xiong et al. 2005
N,*N*-diethylnicotinamide, *N*,*N*-dimethylbenzamide	Micelle	Griseofulvin, probucol, nifedipine, progesterone, PTX	Drug solubilization, controlled delivery, cancer therapy	Kim et al. 2011
N-isopropylacrylamide bearing pH-responsive polymer	Micelle, liposome	Photosensitizer aluminium chloride phthalocyanine	Photodynamic therapy, pH-responsive micelle	Leroux et al. 2001
PEO-PPO-PEO - Pluronic®-PCL block copolymer	Nanosphere	Indomethacin	Temperature dependence, sustained release	Kim et al. 2000

Table 3.1. contd....

Table 3.1. contd.

Material	Shape	Therapeutic agent	Targeted therapeutic application	Reference
Pluronic® F-127 block copolymer and methacrylate monomer	Amphiphilic pentablock copolymer	Anticancer drugs	Temperature and pH responsiveness, non-viral gene therapy	Determan et al. 2005
PEI with copper		5-FU	Cancer	Thomas et al. 2011
Natural polymer				
Ethylcellulose, methylcellulose	Sphere	Curcumin	Gastro-intestinal tract	Suwannatet al. 2011
N,*N*,*N*-trimethyl CS	NP	Vitamin B_9, B_{12}, and C	Pharmaceutical industry	de Britto et al. 2012
CS	NP	Human parathyroid hormone 1-34	Osteoporosis	Deepa et al. 2012
N,*O*-carboxymethyl CS	NP	5-FU	Breast cancer	Anitha et al. 2012
Glycol CS	NP	Retinoic acid	Cholangiocarcinoma	Chung et al. 2012
Folate-PEG-CS-cholesterol liposome	Liposome		Tumor-targeted delivery	Wang et al. 2010
CS coated with PBCA	NP	DOX	Cancer	Duan et al. 2012
CS ionic cross-linked with hydroxypropyl methylcellulose phthalate	pH-sensitive polymer	Insulin	Therapeutic peptide, oral delivery	Makhlof et al. 2011
CS-conjugated Pluronic®-based nanocarrier	NP	Anticancer drug	Cancer	Kim et al. 2010
BSA, *β*-cyclodextrin	NP	Tacrine	Alzheimer's disease	Luppi et al. 2011
Liposome	PEGylated liposome	Horse radish peroxidase protein, peptides	Brain delivery	Visser et al. 2005
Soya phosphatidylcholine	Unilamellar liposome	Diclofenac		Lopes et al. 2004
Liposome	Liposome	Cisplatin	Cancer	Arcon et al. 2004

Liposome	Thermosensitive liposome	DOX, carboxyfluorescein dye, gadodiamide	Cancer therapy, locally heated tumor	Tagami et al. 2011, Hossann et al. 2010
Elastin-like polypeptide		Radionuclide	Thermally responsive, chemotherapeutic and biomolecular therapeutic	Chilkoti et al. 2002
Neoglycoprotein-based	NP	Sodium ferulate	Liver cancer	Li et al. 2009
Inorganic natural clay				
Montmorillonite with polyurethane	Nanocomposite	Dexamethasone, triamcinolone acetonide	Local application, chronic inflammatory disease	Pinto et al. 2011
Bentonite	Nanocomposite hydrogel		Mucoadhesive	Lee et al. 2004
Dendrimer				
Dendrimer	Sphere	5-FU	Cancer	Tripathi et al. 2002
Generation 5 PEGylated poly(L-lysine) dendrimer	Conjugate	DOX	Metastatic tumor, HIV, lymphoma, and metastitial tuberculosis	Kaminskas et al. 2011
PAMAM dendrimer	Conjugate with ester-linked glycine and β-alanine spacers	Anticancer drug	Selectively treatment to mother or fetus	Goldberg et al. 2011, Menjoge et al. 2011
Nanoemulsion				
Silica	Hollow, mesoporous NP	DOX, insulin	Cancer, diabetes	Yang et al. 2008, Zhao et al. 2009
Ceramic	Porous	2-devinyl-2-(1-hexyloxyethyl) pyropheophorbide	Denaturation induced by changes in the external pH and temperature	Roy et al. 2003
Metallic				
Gold	Sphere	DOX	Cancer	Dhar et al. 2008
Silver	Nanosphere	9-aminoacridine	Cancer	Yang et al. 2009

Polymeric structures

Polymeric structures used to obtain nanocarriers can be synthetic and/or natural polymers (non-degradable and degradable, respectively). Through functionalization and structural manipulation of polymeric materials, drug molecules can be incorporated within the polymer.

An ideal polymer should be biocompatible, biodegradable with minimum toxicity, sterile and non-pyrogenic, and must have a high capacity to accommodate drugs and protect them from degradation. Generally, biodegradable and bioabsorbable matrices are preferred, so that they would degrade inside the body by hydrolysis or by enzymatic reactions, and do not require a surgical operation for removal after being placed into the body.

Non-degradable polymers used in drug delivery are characterized by tissue/blood compatibility, durability, robust structure and mechanical strength during *in vivo* application (Fig. 3.2). Sureskin® II Silver is a Food and Drug Administration (FDA)-approved wound dressing consisting of polyurethane foam that delivers silver-containing agents for treating dermal ulcers, post-operative wounds, superficial wounds and abrasions. However, the "non-degradability" also seems to limit the application of

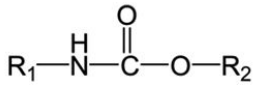

Urethane links

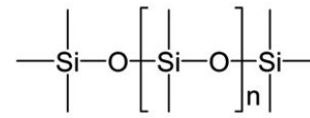

Polydimethylsiloxane

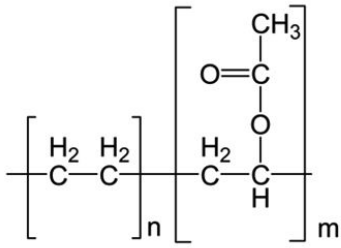

Ethylene vinylacetate

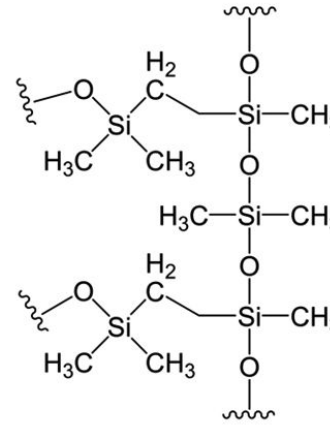

Crosslinked polydimethylsiloxane

Figure 3.2. Chemical structure of representative non-degradable pharmaceutically-related polymers.

polyurethanes in controlled drug delivery, because second interventions are sometimes necessary to remove the device after treatment.

Hydrophobic drugs are commonly loaded in polydimethylsiloxane-based delivery devices to achieve prolonged release profiles. Poly(ethylene vinyl acetate) based devices are designed to slowly release drug compounds over a relatively long period of time. The permeability of these copolymeric films changes substantially with varying vinyl acetate content (0–40%), and thus it is possible to tailor the release rate to a desired value by slightly changing the membrane compositions.

Biodegradable synthetic non-immunogenic polymers (Fig. 3.3), typically consisting of poly(D,L-lactic acid) (PLA) and its copolymers with poly(glycolic acid), are investigated for the delivery of proteins and genes, vaccines, anticancer drugs, ocular drugs and cytokines. Other polymers being investigated for the formulation of nanoscale drug carriers include poly(esters), poly(ortho esters), poly(anhydrides), poly(amides), PEG, poly(ethylene oxide) (PEO), phosphorus-containing polymers, poly(alkylcyanoacrylate) (PACA), poly(3-hydroxybutanoic acid), poly(organophosphazene), poly(ε-caprolactone) (PCL), poly(styrene-*co*-maleic anhydride), poly(divinylether-*co*-maleic anhydride), poly(vinylalcohol) (PVA).

In general, biodegradable polymers contain labile bonds such as ester-, amide- and anhydride-bonds that are prone to hydrolysis or enzymatic

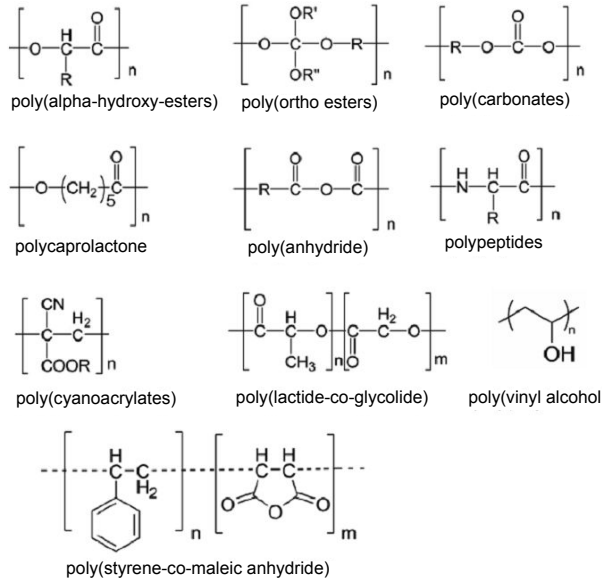

Figure 3.3. Chemical structure of the most important synthetic degradable polymers used as nano-sized carriers for drug delivery.

degradation. Two typical modes of degradation are surface degradation and bulk degradation. Water intrusion into the device is of significant importance for the study of degradation kinetics as well as release kinetics. The degradation of such polymers occurs in two stages: *i*) water infusion into the amorphous regions with random hydrolytic scission of labile bonds, such as ester bonds; and, *ii*) second stage starts when most of the amorphous regions are degraded. Polymer degradation can occur as the chain scission process by which polymer chains are cleaved into oligomers and monomers, while bioerosion refers to the loss of material from bulk or surface in contact with a biological system.

Poly(esters)

PLA and Poly(D,L-Lactic-*co*-Glycolic Acid) (PLGA) are the most extensively investigated for achieving controlled release of drug molecules, peptides and proteins. PLGA is the most common choice in pharmaceutical formulations probably because of its good biocompatibility and biodegradability, and of its approval by the FDA for human use (Jain 2000). These polyesters undergo hydrolysis of backbone ester linkages upon implantation in body tissues, through bulk erosion to biologically compatible and metabolizable moieties (e.g., lactic acid and glycolic acid), that are eventually removed from the body by the citric acid cycle. In addition, since biodegradation products are formed at a very slow rate, they appear not to interfere with normal cell functions to a significant extent. The degradation process is self-catalyzed as the number of terminal carboxylic acid groups rises with increasing chain scission and the acids catalyze the hydrolysis.

Poly(ortho esters)

Release rates from devices composed of poly(ortho esters) can be controlled by including acidic or basic excipients into the matrix, as its hydrolysis is acid catalyzed (Mainardes and Silva 2004).

Poly(anhydrides)

Poly(anhydrides) degrade by hydrolysis and, thus, surface erosion yet the polymer itself is hydrophobic in nature. The hydrolytic bond cleavage of poly(anhydrides) produces water-soluble products that in many cases are considered biocompatible. The most common polymers in this class are based on sebacic acid, *p*-(carboxyphenoxy)propane and *p*-(carboxyphenoxy) hexane. Variations in monomer composition, such as hydrophobicity, influence the degradation rate of the polymeric device. The degradation can last from days to years depending on the composition (Uhrich et al.

1999). The photosensitizer phthalocyanine was chemically incorporated into NPs based on biodegradable poly(sebacic anhydride) for cancer treatment through photodynamic therapy (Fu et al. 2002). Many other types of poly(anhydrides) have been used for drug delivery applications in the nano-sized range.

One advantage of synthetic polymers over natural ones is that they can yield NPs with the ability to sustain the release of the encapsulated therapeutic agent over longer periods of times (days to several weeks). However, the use of synthetic polymers in nanoparticulate technology is limited by the need to often use toxic organic solvents and relatively harsh formulation conditions. Synthetic polymers, such as PEG, can be used to encapsulate biological materials to create a more stable drug carrier. One example of a hybrid drug carrier is a liposome coated with PEG, called a stealth liposome. The striking advantage of synthetic polymers is the possibility of synthesizing them reproducibly with well-defined physico-chemical properties.

Biological structures

The "biologic world" is full of nanostructures, polymeric ones being discussed here.

Natural polymers, such as poly(amino acids), hyaluronic acid, albumin, gelatin, collagen, dextran, chitosan (CS), alginate (ALG), to cite just a few, due to their natural origin, are preferred considering non-toxicity and biodegradability. While each polymer has its own advantages, NPs can be synthesized with a high degree of reproducibility from most of them.

Biological materials existing as building blocks and nanostructures are polypeptides, nanowire and protein NPs, nucleic acids (DNA double nanowire), micelles, vesicles and multilayer films. Building blocks of proteins are 20 amino acids, each about 0.6 nm in size, which is slightly below the official lower limit of a NP.

Polypeptides contain hundreds, and in some cases thousands, of amino acids, thus they correspond to nanowires. Polypeptide nanowires undergo twisting and turning to compact themselves into a relatively small volume corresponding to a polypeptide NP with a diameter that is typically in the range of 4–50 nm. Thus, a protein is a NP consisting of a compacted polypeptide nanowire. The gelatin-like protein called collagen (1 nm) coils into a triple helix (2 nm). DNA also has the structure of a long double-stranded nanowire which undergoes systematic twisting and turning to become compacted into a chromosome about 6 μm long. Peptides possess many advantages, such as smallness, ease of synthesis and modification and good biocompatibility. Their functions in cancer nanomedicine, include serving as drug carriers, as targeting ligands and as protease-responsive substrates for drug delivery (Zhang et al. 2012b).

Gelatin is a naturally occurring biopolymer that is biocompatible and biodegradable. The polymer is obtained through heat-dissolution and partial hydrolysis of collagen obtained from animal connective tissues. It has been used for many years in pharmaceutical applications, such as capsules and ointments, as well as early nanoformulations (Zwiorek et al. 2004, Verma et al. 2005).

Albumin is a versatile protein carrier for drug delivery and has been shown to be non-toxic, non-immunogenic, biocompatible and biodegradable, thus being an ideal material to fabricate NPs for drug delivery. Market approved products include fatty acid derivatives of human insulin or the glucagon-like-1 peptide (Levemir® and Victoza®) for treating diabetes, the taxol albumin NP (Abraxane®) for treating metastatic breast cancer (also under clinical investigation in further tumor indications), and Tc-aggregated albumin (Nanocoll® and Albures®) for diagnosing cancer and rheumatoid arthritis (as well as for lymphoscintigraphy). An albumin-binding prodrug of doxorubicin (DOX) (INNO-206) is currently under use against sarcoma and gastric cancer. Novel approaches include attaching peptides with high-affinity for albumin to antibody fragments, and physical or covalent attachment of antiviral, antibacterial and anticancer drugs to HSA (Kratz 2008, Elsadek and Kratz 2012). In fact, in the last 30 years, both Bovine Serum Albumin (BSA) and Human Serum Albumin (HSA) have been widely employed to formulate microparticles and NPs. Site-specific drug targeting, the use of various ligands modifying the surface of albumin NPs, with special insights to the field of oncology, has been also investigated. (Elzoghby et al. 2012).

CS is a naturally derived polysaccharide created by the deacetylation of chitin. The advantageous properties of CS include its biocompatibility, positive charge, abundance of amine groups available for cross-linking, ease of processing, mucoadhesiveness and its degradation into amino sugars, which are all attractive for drug delivery applications (Agnihotri et al. 2004, Mainardes and Silva 2004). The release of the therapeutic agent from the particles depends on the molecular weight of the CS, its degree of deacetylation, the extent of cross-linking, its interactions with the encapsulated molecule, and the pH of the release media. Drug release from surface layers of the matrix involves a large burst effect, but increasing the cross-linking density can reduce this effect.

Dextran, a polysaccharide composed of a 1,6-polyglucose units has also been used in the preparation of polymer-drug conjugates.

Polymeric micelles

Block copolymeric micelles are generally formed by self-assembly of either amphiphilic or oppositely charged copolymers in aqueous medium. The

hydrophilic and hydrophobic blocks form the corona and the core of the micelles, respectively. A polymeric micelle usually consists of several hundred block copolymers and has a diameter ranging from 20 to 50 nm (Sahoo and Labhasetwar 2003, Gaucher et al. 2005). PEO is often used as the hydrophilic block. Hydrophobic blocks include poly(α-hydroxy acids) and poly(L-amino acids) (Kwon and Okano 1999, Lavasanifar et al. 2002). Polymeric micelles have a low critical micelle concentration, and have higher stability than low molecular weight surfactants and many liposomes. Micelles have a small size and small polydispersity due to their molecular organization. The hydrophilic shell has been shown to prevent immune recognition and increase circulation time *in vivo*, so they have been investigated for drug and gene delivery (Mainardes and Silva 2004). Incorporating the cross-linking into the preparation scheme increases the stability, and also affects the release of the active agent from the carrier. Hydrophobic drugs can be entrapped into the core during micelle formation. Polymer micelles have been used widely for delivery of poorly water-soluble drugs. If site-specific ligands or antibodies are conjugated onto their surface, the drug targeted delivery potential of polymeric micelles can be enhanced. In addition, the drug release rate can be modulated by the variation of the copolymer composition.

One polymer class popular for use as the dense core in polymeric micelles is poly(ortho esters), thanks to their hydrophobic nature and favorable interactions with poorly soluble hydrophobic drugs (Heller et al. 2002). The value for the critical micelle concentration for these types of polymers is in the range of 10^{-4} g/L, which is low enough to insure stability upon injection *in vivo*.

Polymer-drug conjugates

Polymer-drug conjugates are a class of polymeric therapeutics that consists of a water-soluble polymer chemically conjugated to a drug, through a biodegradable linker forming a new chemical entity. The rationale for this strategy was primarily based upon the fact that small molecule drugs, especially hydrophobic compounds, commonly have a low aqueous solubility and a broad tissue distribution profile. Therefore, administration of the free drug can result in serious side effects. The conjugation of these compounds to hydrophilic and biocompatible polymers can significantly increase their aqueous solubility, modify their tissue distribution profile and enhance their plasma circulation half life.

Polymers that can be used for this purpose must be non-toxic and non-immunogenic in terms of both the intact polymers and their metabolites. The molecular weight of the polymer (typically 10–100 kDa) needs to reach a specific cut-off if a prolonged circulation lifetime is required. If

the polymer is non-biodegradable, then the molecular weight should be less than 40 kDa to ensure elimination by renal excretion (Duncan et al. 2006). In addition, these systems need high drug content to polymer ratio in order to deliver sufficient drug within the allowed total polymer dose. *N*-(2-hydroxypropyl) methacrylamide, PEG, poly(glycolic acid) and dextran have been explored most extensively in the preparation of polymer-drug conjugates for anticancer therapy (Satchi-Fainaro et al. 2006). The bioconjugation of protein and peptide to PEG improve the efficacy of these macromolecular drugs by increasing their stability in the presence of proteases, by decreasing their immunogenicity and the fast renal clearance, and by preventing or delaying mononuclear phagocytic system uptake, thus leading to prolonged plasma half life.

Successful applications have led to several FDA-approved products (e.g., Zinostatin Stimalmer®, Oncaspar®, PEGIntron™, PEGasys®, Neulasta™) and other products in clinical trials [e.g., ADI-PEG20, PEG-poly(glycolic acid), Prothecan™]. The first practical use of polymer therapeutics that resulted in an FDA-approved anticancer treatment was the introduction of PEG-L-asparaginase (Oncaspar®) in 1994 (Graham 2003). This conjugate is composed of PEG polymer (molecular weight ≈ 5 kDa) attached to L-asparaginase. It is advantageously used for the treatment of acute lymphoblastic leukaemia, given the significant increase in the plasma half life of L-asparaginase that has been observed. Specifically, Oncaspar® has a plasma half life of 357 hours following intravenous administration (i.e., dose 500–8000 units/m^2 infused over 1 hour), compared to the unconjugated enzyme (half-life ≈ 20 hours). In addition, the conjugate required less frequent administration (i.e., once every two weeks *vs*. 2–3 times per week for four weeks), and vastly reduced the degree of hypersensitivity reactions.

Polymeric nanoparticles

NPs made from synthetic or natural polymers can entrap an active agent within the polymeric matrix, or the active agent can be adsorbed or conjugated to the outside of the particle. They enjoy tremendous popularity due to ease of preparation, ease of tuning physico-chemical properties (through an array of polymeric materials), possibility of surface modification, excellent stability and scalability to industrial production. Drug-loaded NPs have been developed for almost every route of administration (mainly, nasal, ocular, mucosal, inhalation, oral, transdermal and parenteral). The term NP encompasses both nanospheres and nanocapsules. Nanospheres are essentially monolithic systems having a solid matrix. Nanospheres have a matrix-like structure, where active compounds can be firmly adsorbed at their surface, entrapped or dissolved in the matrix. Ciardelli and Cioni (2004) studied the formation of poly(methylmethacrylate-*co*-methacrylic

acid) nanospheres which were imprinted with theophylline through template radical polymerization. Chen and Subirade (2005) prepared CS/β-lactoglobulin core-shell NPs highly sensitive to medium pH, by ionic gelation with sodium tripolyphosphate (TPP) to develop a biocompatible carrier for the oral administration of nutraceuticals.

NPs have been prepared by a temperature-induced phase transition in a mixture of Pluronic® F-68 and liquid PEG (molecular weight 400 Da) containing paclitaxel (PTX) with a fast, simple, continuous and solvent-free process. These PTX-loaded NPs exhibited a high antitumor efficacy (Oh et al. 2010). Tyrosine-derived nanospheres dispersed in Carbopol® and hydroxypropyl methylcellulose hydrophilic gels have been prepared, and successfully tested for topical delivery of lipophilic drugs and personal care agents to skin for treatment of cancers, psoriasis, eczema and microbial infections (Batheja et al. 2011).

Nanocapsules have core-shell morphology with the active agent trapped within the core by the polymeric shell. The matrix structure of a nanosphere serves to entrap drug molecules, or alternatively, the drug is conjugated at the surface of the particle. By decreasing particle sizes, nanosuspensions can enhance the dissolution rate and bioavailability of the active pharmaceutical ingredient. Micro-osmotic pumps are widely used in experimental pharmacology, and offer a tool of interest for the sustained release of nanosuspensions via the intraperitoneal or subcutaneous application site (Hill et al. 2012).

Polymeric nanofibers have shown good compatibility with other tissues when used as scaffolds and matrices. They often need to be functionalized to yield increased bioactivity and fiber-cell interaction.

Dendrimers are a cutting-edge of the drug delivery systems. They consist of a core and a series of branches symmetrically formed around it, leading to a monodisperse and symmetrical macromolecule. Dendrimers can be synthesized either starting from the core molecules, or going out to the periphery by connecting the branch groups or by forming the branches first and then collecting all around the core. Functionality of the branching units is generally two or three, which makes the layer of branching unit doubles or triples. The well-defined structure, monodispersity of size, surface functionalization capability and stability are properties of dendrimers that make them attractive drug carrier candidates. Since their discovery in the early 1980s, dendrimers are the best examples of controlled hierarchical synthesis, allowing the generation of complex systems (Morgan and Cloninger 2012, Popescu and Simionescu 2012). Drug molecules can be incorporated into dendrimers via either complexation or encapsulation (Fig. 3.1). The higher generation dendrimers occupy a smaller hydrodynamic volume compared to the corresponding linear polymers, as a result of their globular structure (Nierengarten et al. 2001).

Interaction of dendrimer macromolecules with the molecular environment is predominantly controlled by their terminal groups. By modifying their termini, the interior of a dendrimer may be made hydrophilic, while its exterior surface is hydrophobic or vice versa. Drug molecules can be loaded both in the interior of the dendrimers, as well as attached to the surface groups. Water-soluble dendrimers are capable of binding and solubilizing small molecules, and can be used as coating agents to protect or deliver drugs to specific sites in the body, or as time-release vehicles for transporting biologically active agents. The most commonly synthesized and studied dendrimers are the ones prepared from polyamidoamine (PAMAM). In early studies, DNA was complexed with PAMAM dendrimers for gene delivery applications (Jansen et al. 1995). Therefore, the nanometer size range, ease of preparation and functionalization, high degree of branching, multivalency, globular architecture, well-defined molecular weight, and their ability to display many surface groups for biological reorganization processes, make dendrimers promising new carriers for drug delivery (Padilla De Jesus et al. 2002, Quintana et al. 2002).

Finally, liposomes can be covered with polymers, such as PEG (in which case they are called PEGylated or stealth liposomes), and exhibit prolonged plasma half life. For instance, PEGylated liposomes via maleimide chemistry showed an improved targeting for the activated endothelium targeting peptide (Lehtinen et al. 2012). Hepatocellular carcinoma targeting lactoferrin modified PEGylated liposomes were developed for improving drug efficacies against hepatic cancer cells (Wei et al. 2012).

Stimuli-responsive drug delivery systems

Responsive drug delivery systems are able to act in response to an external signal or changes in the surrounding environment (Sawant et al. 2006, Tirelli 2006, Ganta et al. 2008, Vasile and Dumitriu 2008). The most important stimuli-sensitive polymers (He et al. 2012) can be natural polymers, modified polymers, copolymers or conjugated polymers: poly(L-histidine), PEG-*b*-poly(L-histidine), PEG-*b*-poly(L-histidine-*co*-L-phenylalanine), PLA-*b*-PEG-*b*-poly(L-histidine), PEG-*b*-poly(aspartic acid), PEG-*b*-poly(L-lysine), PEG-*b*-poly(3-morpholinopropyl aspartamide)-*b*-poly(L-lysine), PEG-*b*-poly(*N*-(2-aminoethyl)-2-aminoethyl aspartamide), PEG-poly(2-aminopentyl-*α,β*-aspartamide), methylamine functionalized poly(L-glutamate), diethylamine functionalized poly(L-glutamate), diisopropylamine functionalized poly(L-glutamate), poly(L-glutamate)-*g*-oligo(2-aminoethyl methacrylate), methoxyPEG-poly(L-histidine)-PLA triblock copolymer which self-assemble into NPs by sterocomplexation (Liu et al. 2012a).

Responsive nano-sized drug carriers gained great importance in 1990's and have been extensively evaluated for spatial site-specific drug

delivery. The triggered response could include dissolution, precipitation, degradation, swelling, collapsing, change in hydrophilic/hydrophobic balance, phase separation and shape alteration, among other conformational changes (Schmaljohann 2006). Two categories of responsive systems for drug delivery are known: externally regulated or pulsatile systems (also known as "open-loop" systems) and self-regulated systems (also known as "closed-loop") (Traitel et al. 2008). Externally regulated systems take advantage of external triggers for pulsatile delivery, such as, ultrasonic, magnetic, electric, light, chemical or biochemical agents. The release rate is controlled by feedback information, without any external intervention. Self-regulated systems utilize thermal, pH-sensitive polymers, enzyme-substrate reactions, pH-sensitive drug solubility, competitive binding, antibody interactions or metal-concentration-dependent hydrolysis. Responsive polymeric drug delivery systems are able to recognize and modulate drug delivery based on localized changes in temperature, pH or concentration of oxidizing molecules. They minimize the rates of drug release into the extracellular space, while maximizing drug concentration in their target site under a particular signal. One example includes the thermosensitive polymer is poly(*N*-isopropylacrylamide) (PNIPAAm). When PNIPAAm is copolymerized with acrylamide and polyvinyl ether, a hydrogel is formed which exhibits a LCST slightly above body temperature (Hirsch et al. 2006). Once this LCST is reached, the polymer matrix exhibits a drastic phase change and collapses. During the collapse, water and much of the encapsulated drug are expelled to enable effective cytosolic drug delivery (Lee et al. 2010). Sershen et al. (2000) proved that these hydrogel systems with entrapped gold nanoshells can in fact be used for pulsatile protein release in response to a pulsed near-infrared laser light. Owens and Peppas (2006) created temperature-sensitive inter-penetrating polymeric networks using acrylamides and acrylic acids formed as hydrogels which exhibited an Upper Critical Solution Temperature (UCST). Alternatively, the acidic pH in endosomes and specific enzymes can constitute internal signals to facilitate drug transport from endosomes or lysosomes to the cytoplasm. Temperature may also be manipulated as an external signal for the modulation of drug release kinetics for the cytoplasm. One interesting method to obtain a pulsatile drug release involves incorporation of metal nanoshells via entrapment into a temperature-sensitive polymeric drug matrix.

Temperature-sensitive nanoparticles

A thermoresponsive polymer exhibits a LCST (Schmaljohann 2006). Below the LCST the polymer is water-soluble, while above LCST it becomes insoluble. This behavior allows to control the delivery of active agents from

core-shell micelles of copolymers containing PNIPAAm and a hydrophobic polymer. If the LCST of a given temperature-sensitive polymer is higher than the physiological temperature (37ºC), micelles of this polymer will remain stable until the local temperature of the target pathological tissue is raised above the LCST by external heating.

For materials that have a LCST lower than normal body temperature, their thermoresponsive behavior can also be exploited for delivery of drugs to regions of low temperature such as hypoxic tissue (Patton and Palmer 2005). The LCST of polymers, such as PNIPAAm, can be increased or decreased upon conjugation to a hydrophobic or hydrophilic copolymer, respectively (Vasile et al. 2005, Schmaljohann 2006) or by grafting onto a hydrophylic polymer backbone as carboxymethylcellulose (Bokias et al. 2001). For example, PNIPAAm self-assembled with poly(undecylenic acid) in *Y*-shaped amphiphilic micelles exhibiting a very low critical micelle concentration of 20 mg/mL, and a LCST of 31ºC (Li et al. 2006). Above this temperature the PNIPAAm shell of the micelles becomes hydrophobic and deforms, thus leading to the rapid release of the antiinflammatory drug prednisone acetate. Nakayama et al. (2006) reported on the biodegradable polymeric micelles of the hydrophilic copolymer of PNIPAAm-poly(dimethylacrylamide) conjugated to the hydrophobic polymers PLA, PCL, or PLA-PCL, thus exhibiting a LCST ≈ 40ºC. The clinical applicability of temperature-responsive carriers is limited to the treatment of superficial malignancies, due to low penetration of common heating sources.

pH-responsive nanoparticles

Some polymers and corresponding drug delivery systems are able to undergo conformation changes depending on the acidity of the surrounding environment. Nanocarriers can selectively deliver chemotherapeutic agents into the tumor site as a result of the lower pH found in the tumor interstitium (Wike-Hooley et al. 1984, Vaupel et al. 1989, Schmaljohann 2006). pH-responsive systems have also been extensively studied for applications in oral drug delivery (Schmaljohann 2006). Responsive nanocarriers can protect labile drugs from the acid environment of the stomach while promoting their absorption in the more neutral small intestine.

NPs of poly(*β*-amino ester) modified with poloxamers, triblock copolymers of poly(ethylene oxide-*co*-propylene oxide-*co*-ethylene oxide) (PEO-PPO-PEO), were designed for the delivery of hydrophobic drugs to the acidic tumor environment and intracellular acidic organelles (Potineni et al. 2003, Shenoy et al. 2005a,b). Such pH responsive NPs were tested for delivery of PTX to ovarian cancer cells *in vitro* (Shenoy et al. 2005a,b), showing a greater therapeutic efficacy than the free drug (Devalapally et al. 2007). Block copolymers of poly((*N*,*N*-diethylamino)ethyl methacrylate)

(PDEA) and PEG formed ≈ 80 nm-sized core-shell NPs with a pH-responsive core and a PEG-dense shell. It was shown that PDEA–PEG NPs become soluble in the aqueous biological environment when the pH drops below ≈ 6 (Xu et al. 2006).

Block ionic complexes

Block ionic complexes, e.g., Pluronic® grafted with poly(acrylic acid) (PAA), formed by ionic interactions between hydrophilic block copolymers containing ionic and non-ionic regions with an oppositely charged molecule, have been proposed as responsive drug delivery systems because of their ability to undergo changes in response to environmental conditions (Oh et al. 2006). These complexes can respond to changes in salt concentration, pH and temperature. For example, an increase in salt concentration resulted in up to an eight-fold increase in particle size, up to a ceiling salt concentration above which the complexes completely dissociated.

Sawant et al. (2006) formulated nanocarriers by linking PEG and phosphatidylethanolamine via a hydrazone bond for targeting antibody to the diseased tissue. pH-responsive NPs for oral delivery of proteins were prepared by ionic complexation of poly(methacrylic acid)-CS-PEG (PMMA-CS-PEG) by free radical polymerization in an aqueous environment (Sajeesh and Sharma 2005). Release of BSA and insulin was significantly delayed at pH 1.2, representative of the stomach, compared to pH 7.4. The pH-dependent release behavior was attributed to the ability of the PMAA polymer to swell and shrink as the pH increases or decreases, because of the protonation and deprotonation of carboxylic acid groups, respectively.

Pulsatile release nanoparticles

The long-term constant drug concentrations in blood and tissue can cause problems, such as, resistance, tolerability and drug side effects. People vary considerably in their physiological and biochemical conditions during any day period, due to the circadian rhythm, and thus, the constant delivery of a drug into the body seems both unnecessary and undesirable. If the drug release profile mimics a living system's pulsatile hormone secretion, then it may improve drug efficacy, and reduce the toxicity of a specific drug administration schedule. This may be provided by a chronopharmaceutical dosage regimen with pulsatile release that matches the circadian rhythm resulting from a disease state, so optimizing the therapeutic effect while minimizing associated toxicity (Fig. 3.4) (Mandal et al. 2010, Lin and Kawashima 2012).

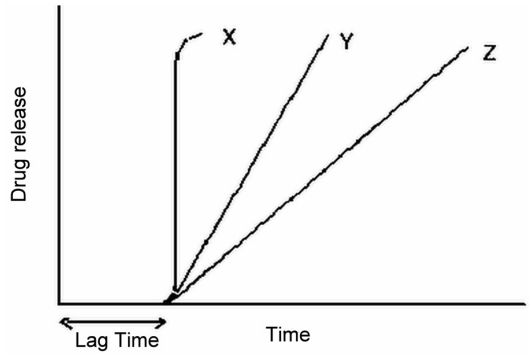

Figure 3.4. Pulsatile drug release pattern. *X*: complete drug release after lag time. *Y*: delayed drug release after lag time. *Z*: sustained drug release after lag time.

Dual responsive nanoparticles

Drug delivery systems incorporating both pH and temperature sensitivity moieties have been investigated, such as, core-shell NPs of PNIPAAm-*co*-*N*,*N*-dimethylacrylamide-*co*-10-undecenoic acid) (PNIPAAm-*co*-DMAAm-*co*-UA) (Soppimath et al. 2005) and collagen-PNIPAAm hydrogels (Nistor et al. 2013a,b). In the first system, UA made up the hydrophobic and pH-sensitive core, while PNIPAAm was present at the surface in contact with the aqueous environment. NPs from this copolymer could easily deliver drugs selectively to the acidic tumor interstitium, while remaining stable and preventing toxicity to non-diseased tissues. This system demonstrated significantly increased release rate of DOX, deformation and precipitation at acidic pH and physiological temperature.

Wei et al. (2006) prepared micelles from an amphiphilic copolymer poly(10-UA-*b*-NIPAAm), in which UA represented the hydrophilic block, while PNIPAAm represented the hydrophobic pH- and temperature-sensitive block which presented a critical micelle concentration of 174 mg/mL, an a LCST of 31°C. These micelles remained stable below the LCST despite changes in pH, but become unstable and release the loaded drug (prednisone acetate) in a pH-dependent manner above the LCST.

Enzyme-activating systems

Labile linkers, such as, disulfide bonds, ester bonds or certain peptide spacers, in drug carriers are readily cleaved via certain enzymatic reactions. These linkers cleaved by specific enzymes in the target sites, e.g., lysosome, endosome or cytoplasm, activated drug release by employing the strategy of destabilizing the drug nanocarrier.

Oxidation-responsive systems

Nanocarriers based on oxidation-sensitive materials have application in drug delivery to inflamed tissues rich in oxidizing substances (Tirelli 2006). These drug delivery systems have poly(propylene sulfide) as the main component, which by exposure to oxidizing conditions transforms from hydrophobic to hydrophilic poly(sulfoxide) (Napoli et al. 2004, Rehor et al. 2005).

Magnetic nanoparticles

Remote control of drug release through polymeric systems can also be achieved using magnetically responsive metal particles (Kost et al. 1987, Nita et al. 2006a,b). For instance, cylindrical magnets (1.4 mm) were placed inside polymeric matrices with encapsulated BSA. Upon induction of an oscillating magnetic field, BSA release rate significantly increased. Upon removal of the field, the release rate returned to baseline (diffusion-controlled release) (Kost et al. 1987). It has been proposed that the motion of magnets induced a mechanical deformation of the matrix, which in turn allowed for the increased drug release (Edelman et al. 1992).

Nanogels

The term "nanogels" usually defines aqueous dispersions of hydrogel particles formed by physically or chemically cross-linked polymeric networks of nano-scale size (Hamidi et al. 2008, Kabanov and Vinogradov 2009). Nanohydrogels are hydrogels prepared in water by self-aggregation of natural polymers, e.g., dextran, pullulan or cholesterol-containing polysaccharides. They are composed of hydrophilic or amphiphilic polymeric chains, which can be non-ionic or ionic. Nanogels are very promising as drug delivery carriers due to their high loading capacity, high stability and responsiveness to environmental factors, such as, ionic strength, pH or temperature (Vinogradov et al. 2002, Nayak and Lyon 2005). They can be designed to spontaneously absorb biologically active molecules through formation of salt bonds, hydrogen bonds or hydrophobic interactions.

Advantages of these systems include simplicity of formulation with the drug, high loading capacity and stability of the resulting formulation in dispersion. The swelling and collapse properties of nanogels are unique for the nanoscale pharmaceutical carriers, and provide multiple benefits for engineering an optimal drug loading and drug release. Nanogel networks are responsive to external environmental factors, can undergo rapid volume changes, and allow for stimuli-controlled release of encapsulated

biologically active compounds, including charged or hydrophobic drugs and biopolymers. Furthermore, nanogels can be chemically modified to incorporate various ligands for targeted drug delivery, triggered drug release or preparation of composite materials. Preclinical studies suggest that nanogels can be used for efficient delivery of biopharmaceuticals in cells, as well as for increasing drug delivery across cellular barriers.

Polyelectrolyte nanogels can readily incorporate oppositely charged low molecular mass drugs or biomacromolecules, such as, oligonucleotides, *si*RNA, DNA and proteins, which bind with nanogel ionic chains and phase separate within the finite nanogel volume. Such nanogels exhibit high stability and protect biological agents from degradation by cells metabolic systems.

Overall nanogels demonstrate excellent potential for systemic drug delivery, and enhancing oral and brain bioavailability of low molecular drugs and biomacromolecules. Multiple chemical functionalities of nanogels can be used for introduction of imaging labels, targeting molecules and triggered drug release capabilities, such as, stimuli-responsive and degradable cross-links. Recent studies suggested several promising biomedical applications of nanogels, including drug delivery of phosphorylated nucleoside analogues, oligonucleotides or *si*RNA for anticancer or antiviral treatment, encapsulation of bioactive proteins, fabrication of nanometallic or nanoceramic composites, imaging agents and oral and central nervous system drug delivery.

Preparation Methods for Polymeric Nanoparticles

Numerous techniques now exist for synthesizing different set of NPs based on the type of drugs used, and the targeted organ and delivery mechanism selected. Several methods to prepare polymeric NPs have been developed during the last two decades, classified according to whether the particle formation involves a polymerization reaction or arises from a macromolecule or preformed polymer (Pinto Reis et al. 2006). Mahapatro and Singh (2011) classified the preparation methods of polymeric NPs as: *i*) dispersion of preformed polymers; *ii*) polymerization; and, *iii*) ionic gelation method for hydrophilic polymers. Other classifications were also done as solvent-based methods including interfacial polymerization, evaporation of emulsions, nanoprecipitation and salting-out. However, in most cases these approaches lack precise control at the macro-level, so they yield particles with a broad size distribution. Consequently, extra steps such as filtration or centrifugation are required to isolate the population with the desired size.

Biodegradable NPs can be prepared from a variety of materials such as proteins, polysaccharides and synthetic degradable polymers. The selection of the base polymer depends on many factors, such as: *i*) size of the desired NP; *ii*) properties of the drug (aqueous solubility, stability, etc.) to be encapsulated; *iii*) surface characteristics and functionality; *iv*) degree of biodegradability and biocompatibility; and, *v*) drug release profile of the final product. Dispersion of preformed polymers is the most commonly used technique to prepare biodegradable NPs from PLA, PLGA and PACA, among other polymers (Mahapatro and Singh 2011).

Solvent elimination method

In this technique the polymer is dissolved in an organic solvent, such as, dichloromethane, chloroform or ethyl acetate. The drug is dissolved or dispersed in the preformed polymeric solution followed by emulsification of the mixture to form an oil-in-water (o/w) emulsion using an appropriate surfactant/emulsifying agent (i.e., gelatin, PVA). After formation of a stable emulsion the organic solvent is evaporated by increasing the temperature or pressure along with continuous stirring of the solution. Process parameters, such as, stabilizer and polymer concentration and stirring speed have a great influence on particle size. For instance, modified solvent evaporation technique was used for the production of poly(3-hydroxybutyrate-*co*-3-hydroxyhexanoate) NPs with an average size between 180 nm and 1.5 µm. By the increase in the homogenization rate and surfactant concentration, NP size was decreased, while the size was augmented by an increase in the polymer/solvent ratio (Kılıçay et al. 2011).

Emulsion technique

PCL and PLGA 50:50 NPs have been prepared by the multiple emulsion technique. The method was based on the use of a homogenizer in a two-step emulsification process. Briefly, 1 mL of an aqueous heparin solution (5000 IU) was first emulsified in methylene chloride (10 mL) containing the polymer(s) (0.25 g) by sonication for one minute at 60 W. The resulting water-in-oil (w/o) emulsion was thereafter poured into 200 mL of a PVA aqueous solution (0.1%, w/v) and homogenized at high shear for three minutes, involving the formation of the second water-in-oil-in-water (w/o/w) emulsion. After evaporation of methylene chloride, the polymer precipitated, and the NPs were isolated by centrifugation. The NPs were washed three times with deionized water before freeze-drying (Kim et al. 2001, Jiao et al. 2002, Choi et al. 2006, Kumari et al. 2010). For instance, the method has been applied in the formulation of tacrine-loaded CS NPs coated with polysorbate 80 (Wilson et al. 2010).

Emulsion/solvent elimination method

Docetaxel (DOC)-loaded PLGA NPs were prepared by a single emulsion technique and solvent evaporation. To obtain a smaller particle, Keum et al. (2011) used 0.2% PVA, 0.03% D-*α*-tocopheryl PEG 1000 succinate, 2% poloxamer 188, a five-minute sonication time, 130 W sonication power, evaporation with magnetic stirring and centrifugation at 8000 rpm.

PLGA NPs can be prepared by using the double-emulsion/solvent evaporation technique (Dinarvand et al. 2011, Van de Ven et al. 2011, Yang et al. 2012). PTX-loaded PLGA NPs incorporated with galactose-carrying polymer poly(vinyl benzyllactonamide) (PVLA) were also prepared by the emulsion/solvent evaporation method with PVA as co-emulsifier. The presence of PVLA led to the increase of zeta potential, reduction of the particle surface hydrophobic character, and more homogeneous particle size, but excessive PVLA accelerated burst drug release (Wang et al. 2012a).

In the spontaneous emulsification/solvent diffusion method, a water-miscible solvent (acetone or methanol) along with a water-insoluble organic solvent (dichloromethane or chloroform) are used as an oil phase. Due to the spontaneous diffusion of solvents, an interfacial turbulence is created between the two phases leading to the formation of smaller particles. As the concentration of water-soluble solvent increases, smaller NPs can be obtained. PLGA NPs containing estrogen were prepared by employing the emulsification/diffusion method, which consists of emulsifying a solution of polymer and drug in the aqueous phase containing the stabilizer didodecyl dimethyl ammonium bromide (Kwon et al. 2001). Poly(ethylenimine) (PEI) enhanced HSA NPs were prepared at room temperature by using an ethanol desolvation technique. After total dissolution, the solution was titrated to pH 8.5 with 1 N NaOH, and stirred for five minutes. This aqueous phase was desolvated by dropwise addition of ethanol to the aqueous HSA solution under constant stirring. Cross-linking agent, 8% glutaraldehyde, was added to form stable HSA NPs. PEI dissolved in deuterated water was added to the NP preparation to form an outer coating due to electrostatic binding (Abbasi et al. 2012).

Nanoprecipitation method

Typically, this method is used for hydrophobic drug entrapment, but it has been adapted for hydrophilic drugs as well. Polymers and drugs are dissolved in a polar, water-miscible solvent, such as, acetone, acetonitrile, ethanol or methanol. The solution is then poured in a controlled manner (i.e., drop-by-drop addition) into an aqueous solution with surfactant. NPs are formed instantaneously by rapid solvent diffusion. Finally, the solvent is removed under reduced pressure.

Recently, cationically modified PLGA NPs have been proposed as novel carriers for oral delivery (Zhang et al. 2012a). NPs made of tri-block PLA-PEG-PLA with controlled size were obtained by nanoprecipitation. It was described that polymer concentration was the most affecting parameter on NP size distribution (Asadi et al. 2011). Recently, Relton et al. (2012) developed nanocapsules and nanospheres based on PLGA containing magnetic NPs and rapamycin. Magnetic NPs were prepared by the co-precipitation of Fe^{2+} and Fe^{3+} salts by addition of NH_4OH.

PCL NPs decorated with the mucoadhesive polysaccharide CS, and containing curcumin were developed aiming buccal drug delivery. These NPs were prepared by nanoprecipitation using different molar masses and concentrations of CS and PEO-PPO-PEO to optimize the preparation conditions. CS-coated NPs showed positive surface charge and a mean particle radius between 114 and 125 nm, confirming the decoration of the NP with CS through hydrogen bonds between ether and amino groups from PEO and CS, respectively. These NPs showed a great ability to interact with mucin, thus indicating their suitability for mucoadhesive applications (Choi et al. 2006, Kumari et al. 2010, Mazzarino et al. 2012).

Combined methods

PLGA NPs have been mostly prepared by emulsion-diffusion, solvent evaporation and nanoprecipitation methods (Bala et al. 2004, Kumari et al. 2010, Yadav et al. 2010, Dinarvand et al. 2011). However, their negative surface charge decreases the bioavailability under oral administration.

Fluidic nanoprecipitation system

Xie and Smith (2010) developed a novel fluidic nanoprecipitation system (FNPS) which provide extremely precise control over most aspects of mixing and precipitation processes. With this approach highly uniform PLGA NPs with diameters < 50 nm can be fabricated. The device was used to enact the interfacial polymerization during flow in order to produce hollow polyamide shells with diameters ranging from 300 to 800 µm, depending on polymer concentration and flow rates. Particles fabricated were characterized by diameter of 148 ± 14 nm; on the other hand, particles fabricated by the conventional nanoprecipitation method and using the same solvents and polymer concentrations were characterized by a size of 211 ± 70 nm. Thus, to obtain NPs with smaller size distributions from conventional nanoprecipitation, a filtration step is usually necessary, but 95% of the particles could be lost during filtration. Because of the small size distribution of NPs generated by FNPS, filtration is not required prior to use (Xie and Smith 2010).

Salting out method

In this method, the polymer is dissolved in the organic phase, which should be water-miscible, like acetone or tetrahydrofuran. The organic phase is emulsified in an aqueous phase, under strong mechanical shear stress. The aqueous phase contains the emulsifier and a high concentration of salts which are not soluble in the organic phase. Typically, the salts used are 60% w/w of magnesium chloride hexahydrate, or calcium chloride or magnesium acetate tetrahydrate in 1:3 polymer to salt ratio (Eley et al. 2004). Contrary to the emulsion diffusion method, there is no diffusion of the solvent due to the presence of salts. The fast addition of pure water to the o/w emulsion under mild stirring reduces the ionic strength and leads to the migration of the water-soluble organic solvent to the aqueous phase, thus inducing nanosphere formation. The final step is purification of NPs by cross flow filtration or centrifugation to remove the salting out agent (Eley et al. 2004, Zweers et al. 2004). The main advantage of the salting out procedure is that it minimizes stress to protein encapsulants (Kumari et al. 2010). PLA and PLGA NPs have been mostly prepared by solvent evaporation, solvent displacement, salting out and solvent diffusion methods (Pinto Reis et al. 2006, Dinarvand et al. 2011).

Polymerization methods

PMMA-CS-PEG NPs have been prepared by dispersion polymerization of methacrylic acid, PEG and different CS grades in the presence of cross-linking agent ethylene dimethacrylate and polymer initiator potassium persulfate. Method development was carried out by varying formulation parameters such as type of CS, ratio of PEG to CS, quantity of solvent and polymer initiator. NPs were spherical with smooth surfaces ranging in size from 190 to 450 nm (Pawar et al. 2012). PACA NPs are prepared mostly by emulsion polymerization, interfacial polymerization and nanoprecipitation (Pinto Reis et al. 2006, Kumari et al. 2010).

Vaccines or drugs/therapeutic agents are also incorporated in NPs by dissolving the drug in the polymerization medium. Synthesis of NPs through emulsion polymerization involves presence of water, monomer and surfactant. The common known emulsion polymerization is the o/w emulsion. Experimentally, droplets of monomer (the oil) are emulsified (with surfactants) in a continuous phase of water. NP suspension is then purified by removing stabilizers, which may be recycled for subsequent polymerizations. This technique has been reported for making poly(butylcyanoacrylate) (PBCA) or PACA NPs (Boudad et al. 2001, Zhang et al. 2001). Polyacrylate-based NPs can be easily prepared by emulsion polymerization using a 7:3 mixture of butyl acrylate:styrene in water

containing sodium dodecylsulfate (surfactant) and potassium persulfate (water-soluble radical initiator). The resulting emulsion contains NPs (40–50 nm in diameter) with uniform morphology, which can be purified by centrifugation and dialysis. These purified emulsions can be lyophilized in the presence of maltose (a non-toxic cryoprotectant) to provide a homogeneous dried powder, which can be reconstituted as an emulsion by addition of an aqueous diluent. (Garay-Jimenez and Turos 2011). In NP synthesis, the surfactant plays an important role in dictate particle size. Depending on the polymer electrical charge in water, a series of surfactants can be used, e.g., anionic (sodium dodecylsulfate), cationic (cetylpyridinium bromide), zwitterionic (dipalmitoyl phosphatidyl choline) or non-ionic (polyoxyethylene lauryl ether, Brij® 30).

PACA NPs can be prepared by emulsion or interfacial polymerization (Kumari et al. 2010). For instance, NPs have been synthesized by mechanically polymerizing the dispersed methyl- or ethyl-cyanoacrylate in an aqueous acidic medium containing polysorbate 20 as a surfactant, without irradiation or an initiator. The drug was dissolved in the polymerization medium either before the addition of the monomer or at the end of the polymerization reaction. The NP suspension is then usually purified by ultracentrifugation. Polymerization follows an anionic mechanism, since it is initiated in the presence of nucleophilic initiators like OH, CHO and CH-COO, thus leading to the formation of NPs of low molecular mass due to a rapid polymerization. During polymerization, various stabilizers like, dextran-70, -40, or -10, and poloxamer-188, -184 or -237, to cite just a few, are added. Particle size and molecular mass of NPs depend upon the type and concentration of the stabilizer, the pH of the polymerization medium, the monomer concentration and the speed of stirring. PACA NPs have gained wide popularity in recent years despite some major drawbacks, e.g., cytotoxicity.

Poly(methylidenemalonate) (PDEMM) NPs have been found to be non-biodegradable both *in vitro* and *in vivo*. To overcome the problem, new derivatives of PDEMM have been proposed, i.e., ethyl-2-ethoxycarbonylme thylenoxycarbonyl acrylate. NPs from such monomers have been prepared by the same methods as those adopted for the preparation of PACA NPs (anionic polymerization). The pH of the polymerization medium critically influenced the physicochemical properties of NPs, but minimum-sized NPs were produced in the pH range of 5.5–6.0 (Kumaresh et al. 2001).

Novel biodegradable polyesters, consisting of short poly(lactone) chains grafted onto PVA or charge-modified sulfobutyl-PVA were prepared by bulk melt polymerization of lactide and glycolide in the presence of different core polyols. Modified backbones were obtained by reacting the activated PVA with the sulfobutyl groups. These polymers underwent spontaneous self-assembling to produce NPs, which form stable complexes with a number

of proteins (HSA, tetanus toxoid or cytocrome C). The development of NPs from such polymers does not require the use of solvents or surfactants (Kumaresh et al. 2001).

Ionic gelation method for hydrophilic polymers

Natural macromolecules used to prepare biodegradable NPs in this method include gelatin, ALG, CS and agarose. The procedure involves the transition from liquid to gel due to ionic interaction at room temperature. Gelatin emulsion droplets are cooled below the gelation point in an ice bath leading to gelation of the droplets into gelatin NPs (Mahapatro and Singh 2011).

ALG NPs can be produced by drop-by-drop extrusion of a sodium ALG solution into a calcium chloride solution. Sodium ALG gels in presence of multivalent cations, such as calcium. Calcium ALG NPs have been prepared in the aqueous phase of a w/o nanoemulsion from mixtures of the non-ionic surfactant tetraethylene glycol monododecyl ether, decane, and aqueous solutions of up to 2 wt % sodium ALG by the phase inversion temperature emulsification method (Aslani et al. 1996). This method allowed the preparation of finely dispersed emulsions without a large input of mechanical energy. With ALG concentrations of 1–2 wt % in the aqueous phase, emulsions showed good stability against Ostwald ripening and narrow, and monomodal distributions of droplets. The particles were essentially spherical with a homogeneous interior, and their size was similar to that of the initial emulsion droplets (< 100 nm) (Machado et al. 2012).

PEGylated-CS NPs were prepared using this method, and they had the capacity to carry genes and provide adequate transfection efficacy, with no toxicity when tested in neuronal cells. After the deprotection of PEGylated-phthaloyl CS, the polymer was dissolved in an acetic acid solution and the pH was adjusted to 5, and then TPP was added. NPs were formed after TPP drop-wise addition to the CS solution under constant magnetic stirring for 1 hour at room temperature (Malhotra et al. 2011).

Ionic cross-linking

As a widely used method for preparing CS NPs, ionic cross-linking is generated by auto-aggregation between CS (or its derivatives) and macromolecules of the opposite charge or when ionic cross-linking agent exists. The most commonly used cross-linking agent is sodium TPP (Danesh-Bahreini et al. 2011, Pourshahab et al. 2011). It was found that the particle size distribution of low molecular weight CS NPs could be significantly narrowed by decreasing the concentration of acetic acid and reducing the ambient temperature during the cross-linking process. Optimized NPs exhibited a mean hydrodynamic diameter of 138 nm (polydispersity index:

0.026), and a positive zeta potential (+ 35 mV). Good storage stability at room temperature was also found up to 20 days (Fan et al. 2012). In other cases, one phase contains the CS and a diblock copolymer of PEO-PPO and the other, contains the polyanion TPP. These NPs have a great protein loading capacity (entrapment efficiency up to 80% of BSA), and provide a continuous release of the entrapped protein for up to one week (Calvo et al. 1997, Agnihotri et al. 2004, Wang et al. 2012a). Chondroitin sulfate (ChS)-CS NPs have been prepared by ionic cross-linking of CS solution with ChS. These NPs showed a higher degree of ionic cross-linking and formation yield than TPP-CS NPs (Yeh et al. 2011).

Self-assembling method

Self-assembly reaction uses non-covalent interactions to organize atoms, ions or molecules into structured aggregates. In the spontaneous and reversible association into stable and structurally well-defined entities, molecules are held together by weak bonds. In the case of self-assembly of amphiphiles, the aggregation in water is entreated by hydrophobic interactions between hydrocarbons, van der Waals attraction between chains or hydrogen bonds and electrostatic attraction between polar groups. Amphiphilic compounds dispersed in water can form NPs with a core-shell structure by self-assembly. With a hydrophobic core and a hydrophilic shell, amphiphilic NPs can be simultaneously used as carriers for hydrophobic and hydrophilic drugs (250–300 nm in size), and the hydrophilic shell greatly reduced macrophage phagocytosis. Amphiphilic derivatives of *N*-octyl-*O*,*N*-carboxymethyl CS enhanced nearly 500-fold the solubility of the PTX, with a drug loading of 34.6% and an encapsulation rate of 89.9% (Danesh-Bahreini et al. 2011).

Oleoyl-carboxymethyl CS NPs based on CS with different molecular weights (50, 170 and 820 kDa) were prepared by a self-assembled method. NPs were characterized by a spherical shape, positive surface charge and mean diameters were 157.4, 274.1 and 396.7 nm, respectively (Liu et al. 2012b). Finally, gelatin NPs can be prepared by desolvation/coacervation or emulsion methods (Zillies et al. 2004, Kumari et al. 2010).

Complexation of polymers

Sarmento et al. (2006) obtained NPs based on complexation of dextran sulfate and CS, with promising properties towards the development of an oral delivery system for insulin.

Complexation between inorganic and organic NPs has been also proposed. By this method, inorganic NPs are covered with a polymeric sheet. Inorganic-organic NPs can be formulated as polyelectrolyte complexes made from mineral NPs and polyelectrolyte-neutral block copolymers in aqueous

solutions. Positively charged yttrium hydroxyacetate NPs (100 nm in size) and poly(acrylic acid)-*b*-poly(acrylamide) block copolymers were used to this aim. Around the inorganic NPs (2 nm-sized), a diffuse and protective polymeric corona was created to promote purely steric repulsions between the colloids, and to reduce the range and strength of electrostatic and van der Waals interactions (Berret et al. 2006). The hybrid aggregates had typical sizes in the range of 100 nm, and presented a remarkable colloidal stability even against ionic strength variations.

Aerosol flow reactor method

Aerosol reaction engineering refers to the design of ultra fine particles by liquid-to-particle conversion. The method consists in a two steps process, the atomization of the solution containing the drug and the polymer which lead to formation of drug-polymer droplets and drying the droplets by solvent evaporation and collection of the solid particles. Particles are dried in a heated tubular laminar flow reactor. The atomization of the solution is performed using a collision-type air jet atomizer as the aerosol generator. Usually, the solvent is ethanol, because it is a good solvent for polymers and drugs, it is non-toxic and pharmaceutically acceptable. The method is applied to prepare spherical, amorphous and homogeneous matrix-type drug-polymer NPs. Particle size depends on the vapor pressure of solvent, droplet size and polymer concentration. Controlling the droplet size distribution produced by the atomizer may result in formation of NPs in different morphology (solid, hollow or collapsed particles).

PCL NPs for transporting insulin were obtained by ultrasonic atomization method to form aerosol sprays. The droplet size depends on the ultrasonic frequency, limited by a maximum frequency of the piezoelectric material (Friend et al. 2008). Spherical monodispersed PCL NPs aggregate with diameter between 150 and 200 nm, and diameters were between 5 to 10 nm, depending on the conditions set during synthesis.

Eerikäinen et al. (2004) tested three types of copolymers (Eudragit® L, Eudragit® RS, and Eudragit® E), using the aerosol flow reactor method to obtain NPs as carriers for ketoprofen. These copolymers are based on methyl methacrylate monomers with repeating units in a different ratio with methyl methacrylic acid (Eudragit® L), dimethylaminoethyl methacrylate and butyl methacrylate monomers (Eudragit® E), and with ethyl acrylate and trimethylammonioethyl methacrylate chloride (Eudragit® RS). The stability of NPs during collection in the aerosol flow reactor method is affected by two factors: drug solubility and the thermal properties of the drug-polymer composite. Thus, drug crystallization was observed if the amount of drug in the polymeric matrix was higher than the solubility limit of the drug in the polymer. Thermal properties were affected if the

polymer glass transition temperature was above the ambient temperature. In this case, the polymeric component was in a glassy state which provides mechanical strength to particles, and the drug acted as a plasticizer to the polymers (Eerikäinen et al. 2004).

Dendrimers

Dendrimers are synthesized through covalent bonds by divergent or convergent methods, or by self-assembly of mutually complementary molecular building blocks. Starting from a reactive core, the dendrimer grows outwards from the core, diverging into space in the divergent method, while when using the convergent approach the dendrimer growth controlled to induce a selective functionalization by gradually linking surface units together with more monomers.

The convergent synthesis is frequently used for block copolymers. The divergent synthesis method is limited by the difficulty in purification and the potential for more defects due to stoichiometry. Diels-Alder reactions, thiol-yne reactions and azide-alkyne reactions are concerned in the synthesis method via click chemistry. The effect of dendrimer generation and charge ratio on physicochemical and biological properties of self-assembled antisense/poly(amidoamine) dendrimer NPs was discussed by the Nomani et al. (2010).

Dendrimers have also been used as templates to form dendrimer-metal NPs in aqueous and non-aqueous media (Esumi 2003). Methods of nanocomposite synthesis include the following approaches: encapsulation of inorganic NPs in one dendrimer template (dependent by the inert terminal or charged groups and inert tails), formation of NPs between dendrimers as surfactants or NP coating with dendrons with/without ligands, and synthesis of NPs in the presence of dendrons or by a growing dendrimer structure on a nanocore (Bronstein and Shifrina 2011). Niu et al. (2003) and Myers et al. (2011) presented several synthesis methods for dendrimer-encapsulated NP materials. The dendrimer-encapsulated metal NPs were synthesized using a template approach in which the metal ions were extracted into the interior of dendrimers, and then subsequently chemically reduced to yield nearly size-monodisperse particles having diameters in the 1–2 nm range. The dendrimer assembly approach includes physical or chemical interactions, by covalent, ionic, hydrogen-bonded assembly, and through coordination on a NP-core or cluster-core.

Polyelectrolyte nanoparticles

Polyelectrolytes can be used to mediate synthesis of NPs from precursors, or as media for film assembly of NPs. Polyelectrolyte NPs were synthesized

by dissolving the drug in the organic solvent, and then the drug nucleation was initiated by gradual worsening of the solution with addition of aqueous polyelectrolyte assisted by ultrasonication (Zheng et al. 2010). Curcumin NPs, polymeric tannins with a variety of biological activities (high antioxidant, antiviral properties and anticancer activities) were prepared by polycation adsorption onto particles followed by a polyelectrolyte layer-by-layer nanoshell formation. Shujun et al. (2011) prepared polysaccharide-based NPs of quaternized CS and dextran sulfate with diameter of 165–266 nm, dependent by the *N*-(2-hydroxyl) propyl-3-trimethyl ammonium CS chloride content through simple ionic-gelation self-assembled method. The sensitive character of polyelectrolyte NPs was controlled by the quaternized groups of CS to increase water solubility of CS, and inducing stability at physiological pHs, thus decreasing the loss of protein drugs caused by the gastric cavity.

Synthesis of polymeric nanoparticle—drug systems

Common types of polymer-drug conjugates are prepared by PEGylation, conjugation of the drug on the polymer chain via degradable pendant links, complexation of the pendant drug with polymer matrices, degradable polymer with drug repeatable units and polymeric micelles with degradable block copolymers backbone, and attaching the drug on the polymeric chain by complexation or conjugation.

The most common pathways to obtain a drug-NP system are by incorporating the drug inside already synthesized particles, by synthesis of NPs in a solution when the drug is solubilized, or by chemical binding of the drug to the NP surface (to release it under enzymatic attack). A wide range of such systems were obtained and presented in the literature with real potential to be included in clinical trials.

Poly(ethylene sebacate) (PES)-DOX NPs were prepared by modified nanoprecipitation using PES and Gantrez® AN 119 (complexing agent in the organic phase), while DOX was dissolved in the aqueous phase. Pullulan acted as asialoglycoprotein receptor ligand for hepatic targeting the system in hepatic cancer therapy (Guhagarkar et al. 2010). Another antitumor system was made of cisplatin-loaded gelatin-poly(acrylic acid) NPs (Ding et al. 2011). The NPs with a spherical shape and a mean size of ≈ 100 nm showed a high drug loading, as well as stability.

The covalent conjugation of synthetic polymers to therapeutic agents increases the plasma residence, reduces both drugs immunogenicity and toxicity, and increases the therapeutic index. The polymer conjugation alters the biodistribution of low molecular weight drugs, which limits the tumor-specific targeting and reduces the access to sites of toxicity. Drug molecules remain inactive when attached to the polymer, and are released at the

specific site under the enzyme action. Promising results were obtained for the polymeric system sensitive to metalloproteinases (enzymes presented in the skin). Several polymer-drug conjugates presented in clinical trials as anticancer agents are *N*-(2-hydroxypropyl) methacrylamide-conjugate with DOX, galactosamine, and PTX, polyglutamate conjugates with PTX and camptothecin and PEG conjugates with camptothecin. Conjugation with therapeutic agents was performed by using amide, ester or malonate linkers.

In another study, drug-loaded polymeric NPs were performed in two synthesis steps. Initially, the drug and PEG monomethyl ether were conjugated onto polyasparihyazide. The PEG monomethyl ether was grafted via hydrazone bonds to supply hydrophilic segments. Increasing the hydrophilic character ensured a longer plasma half life. The *in vitro* drug release profile showed a much faster release rate at pH 5.0 than that at pH 7.4 (Wang et al. 2012b).

Responsive polymeric systems

Poly(NIPAAm-*co*-methacrylic acid) NPs were obtained with sensitivity to acid pHs and temperature NPs, thus being of potential interest in targeted drug delivery (Moselhy et al. 2000).

Several polymeric structures based on 2-hydroxyethyl methacrylate and 3,9-divinyl-2,4,8,10-tetraoxaspiro(5.5)undecane with responsiveness at pH and temperature changes have been synthesized through radical polymerization, in the presence of different radical initiators, as well as surfactants and protective colloids (Fig. 3.5). The particle size and particle size distribution increased with the co-monomer amount from 193 nm for PHEMA, to 253 nm for the copolymer with maximum undecane content (10%), because of the modification of the spiroacetal moiety axial conformation. The pH sensitivity was attributed to the presence of spiroacetal moiety, while the temperature sensibility was principally attributed to undecane (Chiriac et al. 2011).

The utilization of enzyme-responsive NPs may facilitate the drug targeting to a specific tissue, and release of the therapeutic agent via enzymatic degradation of the polymeric support. Moreover, selective delivery may be achieved by incorporating to the NP structure sites for selective cleavage by enzymes. Products resulting from enzymatic degradation must not induce any toxicity, and also must be non-immunogenic. NPs based on *N*-(2-hydroxypropyl) methacrylamide were used for drug release triggered by a protease on a peptide sequence. De la Rica et al. (2012) classified enzyme-responsive NPs by the type of effector biomolecule in two classes: hydrolases and oxidoreductases. When using enzymes from the hydrolase class, including proteases, lipases and glycosidases, the therapeutic agent

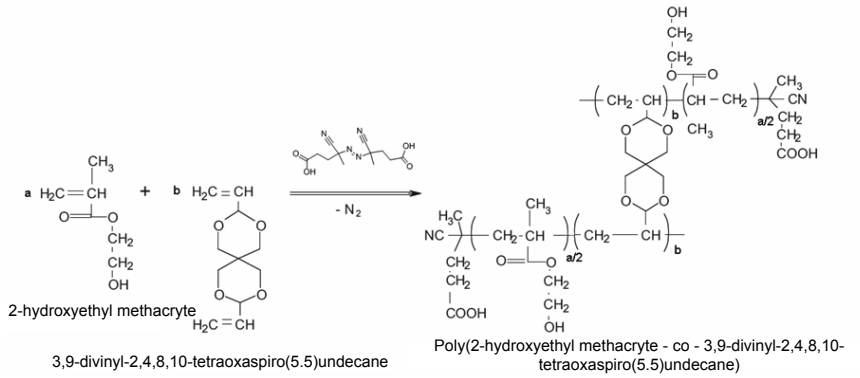

Figure 3.5. Reaction scheme for the synthesis of poly (2-hydroxyethyl methacrylate-*co*-3,9-divinyl-2,4,8,10-tetraoxaspiro(5.5)undecane).

is attached to the carrier through enzyme cleavable units. Oxidoreductase-responsive NPs are indicated in Alzheimer's disease and cancer, due to the therapeutic part of the oxidoreductases in oxidative stress. Synthesis of an oxidoreductase-responsive nanomaterial started from a copolymer, poly (propylene sulfide)-*co*-PEG that encapsulates glucose oxidase. Arruebo et al. (2009) reviewed antibody-conjugated NPs. Monoclonal antibodies already on the market, are either attached to drugs or radioisotopes used in cancer therapy. Antibody-conjugated NPs have been proposed for diagnosis, phototherapy, tissue engineering, radiotherapy and drug/gene delivery. Several PEGylated enzymes (such as asparaginase) and cytokines (including interferon-α and granulocyte colony-stimulating factor) have shown potential applications in drug release studies from polymeric carriers. Other polymers used in the preparation of antibody-conjugated NPs are PLGA/montmorillonite NPs conjugated with human epidermal growth factor receptor-2 antibodies for transporting PTX in breast cancer therapy.

In another study, a biodegradable thermo-responsive CS-*g*-poly(*N*-vinylcaprolactam) nanocomposite was developed as 5-fluorouracil (5-FU) carrier (Rejinold et al. 2011). The nanoformulation was prepared by ionic cross-linking, showing a LCST at 38ºC. Cell uptake of these NPs was confirmed by green fluorescence inside cells (rhodamine-123 conjugation). The nanoformulation increased apoptosis of cancer cells, compared to normal cells.

Hybrid nanoparticulate system synthesis

A wide range of nanocomposites obtained after incorporation of NPs in a polymeric matrix are known (Table 3.2). Metal, semiconductor and magnetic

Table 3.2. Polymeric nanocomposites.

Classification	**Type of composite structure**
Localization of particles in the composite	Core-shell
	Dispersion through the polymeric matrix
	Hollow
	Porous
Formation of the composite	Core-shell
	Dispersion through the polymeric matrix
	Agglomeration
	Coating
	Hollow
	Porous
Composite morphology	Compact material
	Nanoporous material
	Nanofilm

NPs can be encapsulated to provide enhanced stability and functional properties. Hybrid NPs usually contain organic and inorganic components. This category includes nanocomposites and core-shell structures, which are obtained by classical chemical reactions.

Castaneda et al. (2008) prepared collagen cross-linking with tiopronin (*N*-(2-mercaptopropionyl)glycine)-protected gold NPs using 1-ethyl-3-(3-dimethyl aminopropyl) carbodiimide as cross-linker agent. The reaction involved the lysine moieties of the collagen, and formed eight amide bonds with each gold particle unit. In another investigation, mixed particles of magnetic *N*-benzyl-*O*-carboxy methyl CS loaded with indomethacin were prepared (Debrassi et al. 2011). Zhu et al. (2009) prepared a thermo sensitive polymeric-magnetic nanosystem.

NP dispersion can be achieved by mild thermal annealing (which lead to free-standing as well as supported thin films of NP-embedded polymer), mechanical mixing (milling), sol-gel techniques (by introducing the filler before polymerization) or *in situ* generation of the filler or the latex route on colloidal mixtures. The thermal annealing method was used on gold NPs, which were passivated with thiol-terminated polystyrene (PS)-*b*-PEG copolymeric ligand joined via a Diels-Alder linkage (Costanzo et al. 2007). The study revealed that the NP location was dictated by the compatibility of the external shell with the block copolymeric matrix. The thermal treatment caused the Diels-Alder linkages between the polymer blocks to dissociate, leaving gold NPs functionalized by PS ligands, and the immiscibility within the PMMA matrix caused the migration of NPs to the PS domains, as a consequence of the reducing interfacial energy.

Synthetic strategies to improve the properties of polymers by incorporation of clay NPs have been recently proposed, especially to obtain

layered inorganic NPs or direct dispersion of clay NPs into a polymer mass. Nanocomposites preclinically tested are those based CS/montmorillonite hybrids (Cojocariu et al. 2012a,b). A promising system was obtained by dispersing montmorillonite NPs in a biodegradable polyurethane system having PCL and PEG as soft segments (Pinto et al. 2011). The clay NP-polymeric system was tested for transporting of a corticoid drug. It was concluded that the presence of montmorillonite particles in the nanocomposite influenced the drug release rate. In addition, it was proved that the disruption of the regular layered structure of montmorillonite was due to the delamination of the clay incorporated into the copolymeric structure, which induced a complete exfoliation due to the hydrophilic character of PEG chains, and the interaction with the polar clay surface. The presence of PEG segments within the polyurethane macromolecular architecture was useful in promoting complete exfoliation of the clay structure, because the polymeric chain restricted the clay NPs to pack again during drying of the aqueous dispersion.

Integrated nanoparticle-biomolecule system

Selective classes of NPs are integrated NP-biomolecule structures which are designed for bioanalytical applications, and for the fabrication of bioelectronic devices. Nanomaterials with similar dimensions to biomolecules, such as, proteins (enzymes, antigens, antibodies) or DNA represent an interest for NP-biomolecule assembly. NP-biomolecule systems have found interesting possibilities in separation and purification of bio-samples and in cancer therapy. The integrated NP-biomolecule structure can be prepared by NP functionalization and assembly of biomolecules, by NP complexation, chemical conjugation or co-precipitation. The synthesis of biomolecule-protein conjugated NPs opens the way for the fabrication of a wide range of biological probes, which can specifically target a wide range of cells.

Applications in Drug Delivery

Cancer

The nanotechnology for cancer therapy is proceeding on two main fronts, design "intelligent" injectable nanosystems, targeted contrast agents that improve the localization and resolution of cancer to the single cell level, and the design of selective drug-loaded nanoparticulate devices.

The innovative running to replace the conventional chemo-treatment with NP administration is the goal for many actual researches. The utilization of NPs in medical applications for cancer treatment is principally

focused on the inhibition of cancer cell growth, pain relief, and in the delivery of antitumor drugs. In this way, polymeric products can be formulated as gels, NPs, polymeric films, rods and wafers. With application on liver cancer treatment, a neoglycoprotein-based nanoparticulate system for targeted drug delivery to hepatic stellate cells has also been tested. The neoglycoprotein of BSA modified with mannose 6-phosphate was synthesized from mannose, and represented the matrix for the natural antifibrotic substance sodium ferulate (Li et al. 2009). Several NPs as matrix for chemotherapeutic agents are summarized in Table 3.3.

A different class of NPs used in cancer therapy is the enzyme-responsive NPs, which have shown potential application as biosensors and drug delivery systems. These polymeric NPs are covalently modified with drugs using an enzyme-cleavable linker so that the enzyme activity triggers drug delivery in the tissue of interest. Proteases or glycosidases can trigger drug delivery when the drug is linked to the carrier by a peptide or a polysaccharide. For instance, the targeted delivery of PEG monomethacrylate-PLA NPs functionalized with an analogue of the physiological ligand of E-selectin sialyl Lewis X has also been reported (Jubeli et al. 2012). The selection of ligand imposed specifically recognition, and internalized of drug-loaded NPs into the tumor, thereby increasing effectiveness of therapy and patient confidence in therapy. NPs were prepared by nanoprecipitation and ligand-functionalization placed the PEG monomethacrylate spacer at the end of the chain to improve accessibility.

A range of CS NPs were prepared and analyzed to be produced on an industrial scale. For example, CS NPs were loaded with a polysaccharide of *Ganoderma lucidum* using the ion-revulsion method. The entrapment efficiency of the polysaccharide and drug loading capacity were examined by the diethylaminoethanol weak anion exchange method. The authors showed the significant antitumor efficacy of CS-based NPs on HepG2, HeLa and A549 cancer cell lines (Li et al. 2010).

The science on advanced cancer treatment in terms of combining dual strategies by passive tumor targeting and cancer-selective efficacy is becoming more attractive. For instance, transferrin-mediated NPs as carrier for photodegradable and low bioavailability therapeutic agent as curcumin, will increase the photostability and enhance its anticancer activity. The curcumin manifests anticancer activity against MCF-7 breast cancer cells (Mulik et al. 2010). Another example are loaded with curcumin have demonstrated potential application against medulloblastoma and glioblastoma cells (Lim et al. 2011). NPs were prepared by polymerization starting with *N*-isopropylacrylamide (NIPAAm), vinylpyrrolidone and acrylic acid, using *N*,*N*′-methylene-bis-acrylamide and ammonium persulfate/ferrous sulfate as initiator/activator system.

Table 3. 3. Drug-loaded nanoparticles in cancer therapy.

Drug	Polymeric support	Cancer type	Mechanism of drug action	Reference
DOX	PLGA millirods, PBCA NPs coated with polysorbate 80, poly(benzylmalate), PEG-*b*-poly(benzylmalate), biotin-PEG-*b*-poly(benzylmalate)	Leukaemia, Hodgkin's lymphoma, bladder, breast, stomach, lung, ovaries, thyroid, soft tissue sarcoma	Interaction with DNA by intercalation and inhibition of macromolecular biosynthesis. Stopping the replication process	Wolinsky et al. 2012, Wohlfart et al. 2011, Huang et al. 2012
Cytarabine	PLGA, phospholipid gels	Leukaemia, lymphoma, brain	Antimetabolic agent	Yadav et al. 2010, Qi et al. 2012
Asparaginase	PLGA	Acute lymphoblastic leukaemia	Block the proliferation of tumor cell, depriving tumor cell of a required amino acid	Gasper et al. 1998, Vasudev et al. 2011
5-FU	*N*,*O*-carboxymethyl CS NP, PLA NP	Skin, colorectal, pancreatic, breast	Prevent the formation of RNA which will inhibit the formation of DNA, and thus cell multiplication	Anitha et al. 2012, Bourges et al. 2006
Capecitabine	Palmityl prodrug analogue of capecitabine, CS NP	Metastatic colorectal, breast	Capecitabine is a prodrug of 5-FU, and it is converted to 5-FU in the cancer cell by enzymatic degradation	Anitha et al. 2012
Gefitinib		Lung, breast	Selective inhibition of epidermal growth factor receptor's tyrosine kinase	Meco et al. 2009
Tamoxifen	PLGA NP, tamoxifen cross-linked to guar gum NP, poly(amidoamine) dendrimer conjugated with transferrin	Metastatic breast	Antagonist of the estrogen receptor in breast tissue, brain	Jain et al. 2011, Sarmah et al. 2011, Li et al. 2012
Cyclophosphamide	Albumin NP	In association with other drugs. Breast, ovarian, leukaemia	Induce the cross-linking of DNA at the interaction of the drug by creating of an alkyl group to the quinine base of DNA, and thus inhibits the DNA replication	Yardley et al. 2010
Leuprolide	Thiolated CS-thioglycolic acid, CS/reduced glutathione NPs	Prostate, breast, ovarian, endometrial	Agonist of pituitary GnRH receptors, leading to a dramatic reduction in estradiol and testosterone levels	Shahnaz et al. 2012, Iqbal et al. 2012

Ifosfamide	PEGylated liposomal doxorubicin, Caelyx®, in combination with ifosfamide, solid lipid NP based on glyceryl monooleate and CS	Testicular, breast, lymphoma, soft tissue sarcoma, osteogenic sarcoma, lung, cervical	Antineoplastic agent by interfering in DNA replication	Tascilar et al. 2007, Pandit et al. 2011
Cisplatin	PLGA NP, gelatin-poly(acrylic acid) NP, folate-conjugated HSA magnetic NP	Metastatic testicular, ovarian, bladder	Interfere with growth of cancer cell	Moreno-Jiménez et al. 2010, Ding et al. 2011
Mitomycin	Gelatin NPs, clusters coated with hyaluronan	Bladder, pancreatic, stomach	Cross-linking and inhibition of DNA synthesis and function	Erdoğar et al. 2010, Bachar et al. 2011
Vincristine	PLGA NPs	Rhabdomyosarcoma, neuroblastoma, Wilm's tumor, brain	Mitotic inhibitor by binding to tubulin dimmers and inhibiting microtubule assembly	Song et al. 2008
Bleomycin	Magnetic CS NP, gold NP	Palliative treatment for cell carcinoma, head and neck, lymphomas, testicular carcinoma	Glycopeptide antibiotic involved in modification of DNA replication by binding to quanosine-cytosin portions of DNA	Kavaz et al. 2010
PTX	PLGA-PEG-PLGA, ethylene glycol/propylene glycol triblock copolymer, gelatin NP, aldehyde PEG-PLA NP, polyampholyte NP	Brain, lung, bronchus, breast, prostate, colon, urinary bladder, uterine corpus or cervix	PTX is a cytoskeletal drugs that targets tubulin by stabilizing the microtubule. Thus, chromosomes are unable to achieve a metaphase spindle configuration, and in this condition the mitosis is blocked, which results in apoptosis or reversion to the G-phase of the cell cycle, without cell division	Wolinsky et al. 2012, Lu et al. 2009
Etoposide	Cholesterol-modified carboxymethyl konjac glucomannan conjugate, nanostructured lipid carrier with PEG	Ewing's sarcoma, lung, testicular, lymphoma, glioblastoma multiforme	Prevent relegation of DNA strands by interaction with DNA and topoisomerase II	Ha et al. 2011, Zhang et al. 2011

Degradable functional polyesters belonging to the poly(malic acid) family of poly(benzyl malate), i.e., PEG-*b*-poly(benzyl malate), showed promising antitumor activity when DOX was loaded in the polymeric NPs surface functionalized with biotin (Huang et al. 2012). This first line chemotherapeutic agent has been formulated in a wide range of polymeric nanoparticulate systems, e.g., CS NPs coated with PBCA (Duan et al. 2012). Drug release tests exhibited *in vitro* for folate-decorated CS/DOX PBCA NPs a selective targeting behavior against folate-positive cancer cells. The polymeric matrix improved the poor tumor targeting and attenuated the high toxic side effects that the DOX in single form can display (Duan et al. 2012). Folate-PEG coated polymeric liposome prepared from octadecyl-quaternized lysine modified CS and cholesterol has been presented as drug delivery system by Wang et al. (2010). Gelatin NPs loaded with tizanidine hydrochloride, gatifloxacin and fluconazole were prepared by nanoprecipitation using water and ethanol as solvent and non-solvent, respectively (Lee et al. 2012). PEG modified gelatin NPs were also investigated for their potential to enable efficient delivery and enhanced efficacy of the photodynamic agent hypocrellin B. Gelatin NPs possessed characteristic optical properties for photodynamic therapy and participated to photogeneration of reactive oxygen species (Babu et al. 2012). Headed with the similar goal, Allemann et al. (1995) have examined PLA NPs, PEG-coated NPs and a Cremophor® EL o/w emulsion to carry a second generation of sensitizer (hexadecafluoro zinc phthalocyanine, $ZnPcF_{16}$) for photodynamic therapy of mammary cancer (Allemann et al. 1995).

Brain cancer therapy

Requirements of NPs for treatment of brain cancer are imposed by the condition of non-aggregated, non-toxic, non-immunogenic, neutrally charged, biocompatibility, stability (in blood, lymph fluid and cytoplasm, without fouling coating), ability to permeate the Brain-Blood-Barrier (BBB) (receptor-mediated transcytosis across brain capillary endothelial cells) and avoidance of the monuclear phagocyte system (prolonged blood circulation time) (Sun et al. 2008, Veiseh et al. 2010).

Wohlfart et al. (2011) have investigated the kinetics of DOX transport across the BBB. No DOX uptake into the brain was recorded after administration of a drug solution, but clinically effective DOX concentrations were detected in rats which were injected with surfactant-coated NPs, promoting a significant transcytosis across the BBB.

A real potential in brain cancer therapy is to use NPs for the demarcation of malignant cells by injecting fluorescent NPs into the bloodstream. The therapeutic role of chlorotoxin is inhibiting tumor invasion. It was used CS as a linker and stabilizer, more precisely the amino and hydroxyl groups

of the CS glucosamine group. PEG was grafted onto CS by alkylation of depolymerized CS followed by Schiff base formation (Veiseh et al. 2009). The antitumor activity of all-trans retinoic acid incorporated into glycol CS NPs was debated by Chung et al. (2012). It was observed that retinoic acid incorporated into glycol CS NPs inhibited the proliferation of cholangiocarcinoma cells, while non-loaded glycol CS NPs did not affect the viability of tumor cells.

Delivering a drug to the brain intranasally is another approach in brain cancer therapy. The intranasal route may allow the therapeutic agents to pass the BBB via two ways. Drug transport can be performed through the olfactory epithelium and the perineural sheet, or via retrograde axonal transport along olfactory and trigeminal nerves. Mucoadhesive systems can be use to immediately deliver a drug as nasal spray via olfactory bulb. Medical observations have reported a better biodisponibility of the drug in the central nervous system. A particular part of the intranasal route is the high absorption rate of the drug into olfactory epithelium.

Breast cancer therapy

N,O-carboxymethyl CS NPs loaded with 5-FU have been developed with potential application for breast cancer therapy. The non-toxic, biocompatible and biodegradable properties of the polymeric support of the NPs along with the anticancer activity tested via tetrazolium reduction assay, indicated the possibility of using these NPs in breast cancer therapy (Anitha et al. 2012). In another investigation, folic acid-conjugated *O*-carboxymethyl CS NPs reduced the neurotoxicity of methotrexate and improved the targeted effect. Methotrexate is a widely used drug for the treatment of various neoplastic diseases, including leukemias, osteosarcoma, lymphomas, and breast cancer but with non-specific biodistribution and numerous side effects, i.e., neurotoxicity. Using a polymeric shell to obtain a long time release and to improve the specificity and selectivity of methotrexate is one of the promising ways. These drug-loaded NPs were prepared via a cross-linking reaction between the carboxyl groups of *O*-carboxymethyl carboxymethylcellulose and Ca^{2+} ions (Ji et al. 2012).

The coating method with polyelectrolyte is another effective way to improve and control DOC release from NPs. Agrawal et al. (2012) prepared three types of biodegradable drug delivery carriers, respectively PLGA, PLGA-PEI and PLA NPs. These polymeric NPs were coated with thin polyelectrolyte films using the layer by layer self assembly technique. By this methodology, an identical amount of the drug was found to be released for up to 7 days from PLGA, and up to 6 days from both PLGA-PEI and PLA NPs. The system was designed for application in breast cancer therapy to improve the therapeutic efficiency of DOC.

An efficient anticancer therapy has been described by using transferrin-mediated NPs as a carrier for the photodegradable and low bioavailability curcumin molecule. The nanoformulation increased the photostability and enhanced the antitumor activity against MCF-7 breast cancer cells (Mulik et al. 2010). Stimuli-sensitive NPs loaded with curcumin present potential application in the treatment of medulloblastoma and glioblastoma cells (Lim et al. 2011). The NPs were prepared by polymerization starting with N-isopropylacrylamide, vinylpyrrolidone, and acrylic acid, using N,N'-methylene-bis-acrylamide and ammonium persulfate/ferrous sulfate as initiator/activator system.

Lung cancer therapy

Formulations of NPs in aerosols, intravenous injections or oral delivery systems represent the most challenging research areas in therapy of asthma, cystic fibrosis, infectious diseases (in particular tuberculosis), some non-respiratory diseases (such as, type-I diabetes) and lung cancer. In this way, lung cancer therapy aims to the use of nanocarriers for drug/gene delivery, being suggested the displacement of antibodies conjugated onto the NP surface for a more efficient treatment (Azarmi et al. 2008).

Drug-NP systems are generally formulated as aerosolized drugs incorporated into a polymeric shell. In order to assure the long term deposition of the drug in lung regions, NPs based on aerosol are formulated with an appropriate aerodynamic diameter (and size distribution), porosity, density and surface chemistry for optimal dispersibility. In this respect, characteristics such as corrugated surfaces, reduced surface energy and adjustable hydrophobic/hydrophilic character should be conferred to the final product (Jiang et al. 2011). Thiolated CS NPs have been prepared in a two step reaction: CS NPs were synthesized using the ionotropic gelation method, and then NPs were thiolated by a carbodiimide method and loaded with tizanidine HCl. For a proper nasal administration, NP transport across a monolayer of RPMI 2650 cells (a human nasal septum carcinoma cell line) was evaluated. It was demonstrated that the viscosity properties of the CS solution provided high mucoadhesion of the system, improvement of transnasal permeation of hydrophilic drugs and low toxicity to nasal epithelial cells (Patel et al. 2012). Thus, the possibility of transporting antitumor drugs in brain cancer therapy by nasal administration was highlighted.

Gene therapy and vaccine delivery

NP capacity to transport without altering the agent has also been explored in gene therapy. The transfection capacity of new vectors in cancer therapy

is reflected on the transfer capacity of genetic material into second cells isolated from an individual cell or virus type, and it is expected to be responsible for bacterial transformation, and changes in cells caused by tumor viruses.

The transfection capacity of a new multicomponent system based on dextran, protamine and solid lipid NPs containing a plasmid was evaluated on four cell lines. A higher transfection capacity in cells with a high ratio of clathrin/caveolae-mediated endocytosis activity was described. The nanoplatform showed interesting potential in gene delivery for the treatment of genetic and non-genetic diseases (Delgado et al. 2012). Remarkable results were also obtained using CS NPs for transporting non-viral gene delivery vectors. NPs were used as adjuvant and carrier for vaccines (Köping-Höggård et al. 2005). In addition, sulfobutylated PVA-*g*-PLGA, PCL, and PLGA polymeric systems were developed for vaccine delivery (Wendorf et al. 2006).

Insulin delivery

Two-stage delivery systems composed of an enteric capsule and cationic NPs for oral insulin delivery was synthesized using PLGA as the matrix, and Eudragit® RS was introduced to enhance the penetration of insulin across the mucosal surface in the intestine. The system presented sensitivity to modification of environment parameters, and selectively release of insulin from NPs in the intestinal tract. The sensitivity was created upon coating the enteric capsule with pH-sensitive hydroxypropyl methylcellulose phthalate. NP synthesis was processed with the multiple emulsion/solvent evaporation method via ultrasonic emulsification (Wu et al. 2012).

The gastrointestinal barrier is a highly branched barrier consisting of glycoproteins and macromolecules, where the diffusion of a therapeutic agent can be restricted by the high adhesivity and viscoelasticity of the mucus. Several barriers encountered in oral delivery are linked to drug characteristics, such as, poor solubility, stability and bioavailability in the gastrointestinal tract, the acidic gastric environment and the continuous secretion of mucus (Ensign et al. 2012). To improve the quercetin solubility, this therapeutic agent was incorporated into amphiphilic PLA-hyperbranched polyglycerol NPs (Gao et al. 2011). It was demonstrated that the drug crystalline state was converted into an amorphous state, due to the intermolecular interaction with the polymeric support. Drug encapsulation efficiency and drug loading was 91.8 and 21%, respectively.

Intracellular delivery of anti-HIV drugs

The Human Immunodeficiency Virus (HIV) therapy is limited due to the lack of HIV infection markers or indication of infection onto the surface

of infected cells. However, several receptors are known, the HIV receptor CD_4, the CCR_5 and $CXCR_4$ co-receptors, and receptors relatively specific for macrophages which are used as targets for drug delivery studies in patients infected by HIV (Gunaseelan et al. 2010). For this purpose, several nanoparticulate systems have been proposed, e.g., PBCA, PCL, PEG, PEO, poly(hexylcyanoacrylate), PLA, poly(propyleneimine), peptide-based NPs, etc.

PLGA NPs has been tested to enhance tissue uptake, permeation and targeting for chemokine with anti-HIV-1 activity, *N*-*α*-(nonanoyl)-des-Ser-1 [L-thioproline-2, L-*α*-cyclohexyl-glycine-3] RANTES, into vaginal epithelial tissue. The system was clinical tested and represented a real potential in HIV therapy using NPs (Ham et al. 2009).

Malaria

In malaria therapy considerable progress has been made using gelatin NPs. For instance, gelatine NPs loaded with cryptolepine hydrochloride have been designed, and the haemolytic was tested *in vitro* (Kuntworbe et al. 2012). The NPs were prepared by a combined emulsification and congealing procedure, showing eligible properties to transport therapeutic drugs in malaria treatment.

Lymphatic drug delivery

The delivery of active agents to the lymphatic system has been extensively explored, given the manifested benefits for the immune system in recognition and response to disease. Such type of drug release is of interest in cancer therapy, because almost all solid cancers initially spread through lymphatics surrounding the primary tumor, and the lymph nodes play a key role in cancer prognosis and metastasis (Cai et al. 2011). Traditional administration routes (e.g., intravenous route) in lymphatic drug delivery are limited due to the poor lymph node uptake, and lymphatic absorption. Nanoproducts formulated as liposomes, lipid NPs and polymeric NPs have the potential to integrate and to transfer across channels from the injection site into the lymph node (Cohen and Forrest 2011, McAllaster and Cohen 2011). Copolymers of maleimide-PEG-PLGA obtained by conjugation of maleimide-PEG-NH to PLGA-COOH are the most representative NPs tested for drug delivery to the lymphatic system.

Intraocular drug delivery

Intraocular drug nanocarriers are principally formulated as solutions or gels. The immunological test is critical for such systems, and depends on

the base-polymers used in NP synthesis, and on the purification method. PLA NPs loaded with 5-FU and dexamethasone were tested *in vivo* as intraocular drug delivery systems (Bourges et al. 2006). These transscleral or intrasscleral implants were designed to be used as slow release devices, delivering the drug locally for an extended period of time. These nanoformulations represented a promising alternative to target specifically certain cells related to ocular diseases which affect the choroid and outer retina. In another publication, the influence of type of PLA (prepared from L-lactide and D-lactide) formulated as block copolymer with PEG by ring-opening polymerization in the presence of monomethoxy PEG on the release of rifampin has been recently investigated (Chen et al. 2007). Rifampin loading capacity and encapsulation efficiency by these micelles were higher than those values obtained by single polymer micelles. *In vitro*, the drug release profile depended on the composition of the block copolymer. Good thermodynamic stability in physiological conditions, and a low critical micelle concentration was also described.

Nanotechnology has shown the potential to overcome the poor bioavailability of drugs in the posterior chamber of the eye, compared to conventional ophthalmic dosage forms. Recently, an electrokinetically stable, and pharmacologically active NPs based on albumin and xanthan gum, prepared by coacervation, and loaded with acetylsalicylic acid has been developed. Drug release results indicated a sustained rate (90% at 72 hours), and 11% drug release in the posterior chamber over a period of 72 hours. Thus, it was suggested that these NPs have potential application in diabetic retinopathy (Das et al. 2012). In another investigation, the poor corneal residence time of pilocarpine was modified by its incorporation into PLGA NPs for ocular drug delivery. These NPs were prepared by double-emulsion (Nair et al. 2012).

Skin drug delivery

Nanoparticulate drug delivery is based on the specificity of the skin, and the openings of hair follicles or the open wounds. NPs based on PCL-*b*-PEG designed to deliver minoxidil have been recently tested (Prow et al. 2011). Highly branched biodegradable macromolecular systems, resulting from the grafting of carboxymethyl CS onto low generation poly(amidoamine) dendrimers, have been described to organize into sphere-like NPs. Dexamethasone was incorporated into such NPs to promote *in vitro* the osteogenic differentiation of rat bone marrow stromal cells, which is highly recommended as potential application in tissue engineering and regenerative medicine. The screen for cytotoxicity was performed by a MTT and luminescent cell viability assay (based on the adenosine triphosphate quantification) in L929 fibroblast cells, and rat bone marrow stromal cells

(Oliveira et al. 2008). In another study, a biodegradable polyurethane with PCL and PEG delivery device was prepared and characterized (Pinto et al. 2011). The composite was then loaded with montmorillonite particles and triamcinolone acetonide, followed by a drying step to produce an implantable drug delivery system.

Nanogels consisting of PLGA and CS polymeric bilayered particles surface-modified with oleic acid, and loaded with spantide and ketoprofen have been recently developed (Shah et al. 2012a,b). The formulation showed promising applications in the treatment of skin inflammatory disorders. The synthesis strategy required high efficiency dispersing agents with desired viscosity, i.e., hydroxypropyl methyl cellulose and Carbopol®. The nanogel demonstrated interesting possibilities in the promotion of keratinocyte proliferation and differentiation.

Oridonin-loaded micelles have shown great potential as transdermal drug delivery system in cancer chemotherapy. The polymeric support as a core-shell structure was represented by the monomethoxy PEG-PCL, and was efficient for the improvement of poor water-solubility of therapeutic agents (Bingxin et al. 2012). The formulation of the nanocarrier was based on a thin film hydration method, with final lyophilization into powder form. Drug permeation profiles through excised mouse skins showed much a better transdermal penetration (and sustained anticancer activity) compared to the drug solubilized in water.

Natural and synthetic polymers typically form the base of hydrogel NPs prepared by chemical- or physical-induced cross-linking (Hamidi et al. 2008). PVA, PEO, PEI, poly(vinyl pyrrolidone) and poly-*N*-isopropylacrylamide are frequently used to this aim. Hydrogel powders can ensure a close contact and high moisture rate, and can create a low pressure at the surface of the wound bed that will stimulate the formation of healthy granulation tissue. Hydrogel NPs are effective carriers in transdermal delivery, which can be obtained via a cross-linking reaction between hyaluronic acid and PEG. It has been described that such hydrogel NPs dispersed in an oil composition were less effective in skin penetration than those dispersed in an o/w emulsion (Lim et al. 2012). The possibility to use CS NPs loaded with human parathyroid hormone in the treatment of osteoporosis has been recently proposes (Deepa et al. 2012). The ionic gelation technique was used in the formulation of the NPs. The bioavailability and plasma half-life of the peptide was optimized.

Conclusions

Polymeric systems are very promising for drug delivery offering versatility, reproducibility, biocompatibility and biodegradability. Reformulating old drugs can reduce side effects and increase patient compliance, thus saving

money on health care. Researchers are continually investigating new ways to deliver macromolecules that will facilitate the development of new biological products, such as bioblood proteins and biovaccines. Similarly, the success of DNA and RNA therapies will depend on innovative drug delivery techniques.

New strategies in preparation of nanopolymers loaded with therapeutic agents include conjugation with molecular targets, combination of polymer conjugates with low molecular weight drugs and radiotherapy or tailor-made prodrugs.

Acknowledgement

This Chapter is dedicated to the 65th anniversary of the "Petru Poni" Institute of Macromolecular Chemistry of the Romanian Academy (Iasi, Romania).

Abbreviations

ALG	:	alginate
BBB	:	brain-blood-barrier
BSA	:	bovine serum albumin
ChS	:	chondroitin sulfate
CS	:	chitosan
DNA	:	deoxyribonucleic acid
DOC	:	docetaxel
DOX	:	doxorubicin
EDA	:	ethylene diamine
FDA	:	Food and Drug Administration
FNPS	:	fluidic nanoprecipitation system
5-FU	:	5-fluorouracil
HSA	:	human serum albumin
HIV	:	human immunodeficiency virus
LCST	:	low critical solution temperature
NIPAAm	:	*N*-isopropylacrylamide
NPs	:	nanoparticles
o/w	:	oil-in-water
PAMAM	:	polyamidoamine
PACA	:	poly(alkylcyanoacrylate)
PBCA	:	poly(butylcyanoacrylate)
PCL	:	poly(ε-caprolactone)
PDEA	:	poly((*N*,*N*-diethylamino)ethyl methacrylate)
PDEMM	:	poly(methylidenemalonate)
PEG	:	poly(ethylene glycol)

PEI	:	poly(ethylenimine)
PEO	:	poly(ethylene oxide)
PES	:	poly(ethylene sebacate)
PEO-PPO-PEO	:	poly(ethylene oxide-*co*-propylene oxide-*co*-ethylene oxide)
PGuA	:	poly(glutamic acid)
PLA	:	poly(D,L-lactic acid)
PLGA	:	poly(D,L-lactic-*co*-glycolic acid)
PMMA	:	poly(methacrylic acid)
PMMA-CS-PEG	:	poly(methacrylic acid)-*co*-chitosan-*co*-poly(ethylene glycol)
PNIPAAm	:	poly(*N*-isopropylacrylamide)
PNIPAAm-*co*-10-DMAAm-*co*-UA	:	PNIPAAm-*co*-*N*,*N*-dimethylacrylamide-*co*-10-undecenoic acid)
PPO	:	propylene oxide
PS	:	polystyrene
PTX	:	paclitaxel
PVA	:	poly(vinylalcohol)
PVLA	:	poly(vinyl benzyllactonamide)
RNA	:	ribonucleic acid
*si*RNA	:	small interfering ribonucleic acid
TPP	:	tripolyphosphate
UA	:	undecenoic acid
UCST	:	upper critical solution temperature
w/o	:	water-in-oil
w/o/w	:	water-in-oil-water

References

Abbasi, S. and A. Paul, W. Shao and S. Prakash. 2012. Cationic albumin nanoparticles for enhanced drug delivery to treat breast cancer: preparation and *in vitro* assessment. J. Drug Deliv. 2012: 686108 (8 pages).

Agnihotri, S.A. and N.N. Mallikarjuna and T.M. Aminabhavi. 2004. Recent advances on chitosan-based micro- and nanoparticles in drug delivery. J. Control. Release. 100: 5–28.

Agrawal, R. and A. Shanavas, S. Yadav, M. Aslam, D. Bahadur and R. Srivastava. 2012. Polyelectrolyte coated polymeric nanoparticles for controlled release of Docetaxel. J. Biomed. Nanotech. 8: 19–28.

Aliabadi, H.M. and A. Mahmud, D.A. Sharifabadi and A. Lavasanifar. 2005. Micelles of methoxy poly(ethylene oxide)-b-poly(ε-caprolactone) as vehicles for the solubilization and controlled delivery of cyclosporine A. J. Control. Release. 104: 301–311.

Allémann, E. and N. Brasseur, O. Benrezzak, J. Rousseau, S.V. Kudrevich, R.W. Boyle, J.C. Leroux, R. Gurny and J.E. van Lier. 1995. PEG-coated poly(lactic acid) nanoparticles for the delivery of hexadecafluoro zinc phthalocyanine to EMT-6 mouse mammary tumours. J. Pharm. Pharmacol. 47: 382–387.

Anitha, A. and K.P. Chennazhi, S.V. Nair and R. Jayakumar. 2012. 5-Flourouracil loaded N,O-carboxymethyl chitosan nanoparticles as an anticancer nanomedicine for breast cancer. J. Biomed. Nanotech. 8: 29–42.

Arčon, I. and A. Kodre, R.M. Abra, A. Huang, J.J. Vallner and D.D. Lasič. 2004. EXAFS study of liposome-encapsulated Cisplatin. Colloids Surf. B Biointerfaces. 33: 199–204.

Arruebo, M. and M. Valladares and Á. González-Fernández. 2009. Antibody-conjugated nanoparticles for biomedical applications. J. Nanomater. 2009: 439389 (24 pages).

Asadi, H. and K. Rostamizadeh, D. Salari and M. Hamidi. 2011. Preparation of biodegradable nanoparticles of tri-block PLA-PEG-PLA copolymer and determination of factors controlling the particle size using artificial neural network. J. Microencapsul. 28: 406–416.

Aslani, P. and R.A. Kennedy. 1996. Studies on diffusion in alginate gels. I. Effect of cross-linking with calcium or zinc ions on diffusion of acetaminophen. J. Control. Release. 42: 75–82.

Azarmi, S. and W.H. Roa and R. Löbenberg. 2008. Targeted delivery of nanoparticles for the treatment of lung diseases. Adv. Drug Deliv. Rev. 60: 863–875.

Babu, A. and K. Jeyasubramanian, P. Gunasekaran and R. Murugesan. 2012. Gelatin nanocarrier enables efficient delivery and phototoxicity of Hypocrellin B against a mice tumour model. J. Biomed. Nanotech. 8: 43–56.

Bachar, G. and K. Cohen, R. Hod, R. Feinmesser, A. Mizrachi, T. Shpitzer, O. Katz and D. Peer. 2011. Hyaluronan-grafted particle clusters loaded with Mitomycin C as selective nanovectors for primary head and neck cancers. Biomaterials. 32: 4840–4848.

Bala, I. and S. Hariharan and M.N. Kumar. 2004. PLGA nanoparticles in drug delivery: the state of the art. Crit. Rev. Ther. Drug Carrier Syst. 21: 387–422.

Batheja, P. and L. Sheihet, J. Kohn, A.J. Singer and B. Michniak-Kohn. 2011. Topical drug delivery by a polymeric nanosphere gel: formulation optimization and *in vitro* and *in vivo* skin distribution studies. J. Control. Release. 149: 159–167.

Berret, J.F. and K. Yokota, M. Morvan and R. Schweins. 2006. Polymer-nanoparticle complexes: from dilute solution to solid state. J. Phys. Chem. B. 110: 19140–19146.

Bingxin, X. and W. Yingjing, T. Xiaohai, X. Ping, W. Yujun, L. Feng, W. Chunjie and Q. Zhiyong. 2012. Biodegradable self-assembled MPEG-PCL micelles for hydrophobic Oridonin delivery *in vitro*. J. Biomed. Nanotech. 8: 80–89.

Boock-Eldar, A. and K. Miller, J. Sanchis, R. Lupu, M.J. Vicent and R. Satchi-Fainaro. 2011. Integrin-assisted drug delivery of nano-scaled polymer therapeutics bearing paclitaxel. Biomaterials. 32: 3862–3874.

Bokias, G. and Y. Mylonas, G. Staikos, G.G. Bumbu and C. Vasile. 2001. Synthesis and aqueous solution properties of novel thermoresponsive graft copolymers based on a carboxymethylcellulose backbone. Macromolecules. 34: 4958–4964.

Boudad, H. and P. Legrand, G. Lebas, M. Cheron, D. Duchêne and G. Ponchel. 2001. Combined hydroxypropyl-beta-cyclodextrin and poly(alkylcyanoacrylate) nanoparticles intended for oral administration of saquinavir. Int. J. Pharm. 218: 113–124.

Bourges, J.L. and C. Bloquel, A. Thomas, F. Froussart, A. Bochot, F. Azan, R. Gurny, D. BenEzra and F. Behar-Cohen. 2006. Intraocular implants for extended drug delivery: therapeutic applications. Adv. Drug Deliv. Rev. 58: 1182–1202.

Bronstein, L.M. and Z.B. Shifrina. 2011. Dendrimers as encapsulating, stabilizing, or directing agents for inorganic nanoparticles. Chem. Rev. 111: 5301–5344.

Cai, S. and Q. Yang, T.R. Bagby and M.L. Forrest. 2011. Lymphatic drug delivery using engineered liposomes and solid lipid nanoparticles. Adv. Drug Deliv. Rev. 63: 901–908.

Calvo, P. and J.L. Vila-Jato and M.J. Alonso. 1997. Evaluation of cationic polymer-coated nanocapsules as ocular drug carriers. Int. J. Pharm. 153: 41–50.

Castaneda, L. and J. Valle, N. Yang, S. Pluskat and K. Slowinska. 2008. Collagen crosslinking with Au nanoparticles. Biomacromolecules. 9: 3383–3388.

Ciardelli, G. and B. Cioni, C. Cristallini, N. Barbani, D. Silvestri and P. Giusti. 2004. Acrylic polymeric nanospheres for the release and recognition of molecules of clinical interest. Biosens. Bioelectron. 20: 1083–1090.

Chen, L. and M. Subirade. 2005. Chitosan/beta-lactoglobulin core-shell nanoparticles as nutraceutical carriers. Biomaterials. 26: 6041–6053.

Chen, L. and Z. Xie, J. Hu, X. Chen and X. Jing. 2007. Enantiomeric PLA-PEG block copolymers and their stereocomplex micelles used as rifampin delivery. J. Nanopart. Res. 9: 777–785.

Chilkoti, A. and M.R. Dreher and D.E. Meyer. 2002. Design of thermally responsive, recombinant polypeptide carriers for targeted drug delivery. Adv. Drug Deliv. Rev. 54: 1093–1111.

Chiriac, A.P. and L.E. Nita and M.T. Nistor. 2011. Nano-network with dual temperature and pH responsiveness based on copolymers of 2-hydroxyethyl methacrylate with 3,9-divinyl-2,4,8,10-tetraoxaspiro[5.5]-undecane. J. Nanopart. Res. 13: 6953–6962.

Choi, C. and S.Y. Chae and J.W. Nah. 2006. Thermosensitive poly(N-isopropylacrylamide)-b-poly(ε-caprolactone) nanoparticles for efficient drug delivery system. Polymer. 47: 4571–4580.

Chung, K.D. and Y.I. Jeong, C.W. Chung, H. do Kim and D.H. Kang. 2012. Anti-tumor activity of all-trans retinoic acid-incorporated glycol chitosan nanoparticles against HuCC-T1 human cholangiocarcinoma cells. Int. J. Pharm. 422: 454–461.

Cohen, M.S. and M.L. Forrest. 2011. Lymphatic drug delivery: therapy, imaging and nanotechnology. Adv. Drug Deliv. Rev. 63: 865–866.

Cojocariu, A. and L. Profire, M. Aflori and C. Vasile. 2012a. *In vitro* drug release from chitosan/cloisite 15A hydrogels. Appl. Clay Sci. 57: 1–9.

Cojocariu, A. and L. Profire, C. Cheaburu and C. Vasile. 2012b. Chitosan/montmorillonite composites as matrices for prolonged delivery of some novel nitric oxide donor compounds based on Theophylline and Paracetamol. Cellulose Chem. Technol. 46: 35–43.

Costanzo, P.J. and F.L. Beyer. 2007. Thermally driven assembly of nanoparticles in polymer matrices. Macromolecules. 40: 3996–4001.

Couvreur, P. and C. Vauthier. 2006. Nanotechnology: intelligent design to treat complex disease. Pharm. Res. 23: 1417–1450.

Danesh-Bahreini, M.A. and J. Shokri, A. Samiei, E. Kamali-Sarvestani, M. Barzegar-Jalali and S. Mohammadi-Samani. 2011. Nanovaccine for leishmaniasis: preparation of chitosan nanoparticles containing Leishmania superoxide dismutase and evaluation of its immunogenicity in BALB/c mice. Int. J. Nanomedicine. 6: 835–842.

Das, S. and J.R. Bellare and R. Banerjee. 2012. Protein based nanoparticles as platforms for aspirin delivery for ophthalmologic applications. Colloids Surf. B Biointerfaces. 93: 161–168.

de Britto, D. and M.R. de Moura, F.A. Aouada, L.H.C. Mattoso and O.B.G. Assis. 2012. N,N,N-trimethyl chitosan nanoparticles as a vitamin carrier system. Food Hydrocolloids. 27: 487–493.

De la Rica, R. and D. Aili and M.M. Stevens. 2012. Enzyme-responsive nanoparticles for drug release and diagnostics. Adv. Drug Deliv. Rev. 64: 967–978.

Debrassi, A. and C. Bürger, C.A. Rodrigues, N. Nedelko, A. Ślawska-Waniewska, P. Dłużewski, K. Sobczak and J.M. Greneche. 2011. Synthesis, characterization and *in vitro* drug release of magnetic N-benzyl-O-carboxymethylchitosan nanoparticles loaded with indomethacin. Acta Biomater. 7: 3078–3085.

Deepa, N. and A. Anitha, R. Jayakumar, S.V. Nair and K.P. Chennazhi. 2012. Synthesis, characterization and preliminary *in vitro* evaluation of PTH 1–34 loaded chitosan nanoparticles for osteoporosis. J. Biomed. Nanotech. 8: 98–106.

Delgado, D. and A.R. Gascón, A. del Pozo-Rodríguez, E. Echevarría, A.P.R. de Garibay, J.M. Rodríguez and M.Á. Solinís. 2012. Dextran-protamine-solid lipid nanoparticles as a non-viral vector for gene therapy: *in vitro* characterization and *in vivo* transfection after intravenous administration to mice. Int. J. Pharm. 425: 35–43.

Determan, M.D. and J.P. Cox, S. Seifert, P. Thiyagarajan and S.K. Mallapragada. 2005. Synthesis and characterization of temperature and pH-responsive pentablock copolymers. Polymer. 46: 6933–6946.

Devalapally, H. and D. Shenoy, S. Little, R. Langer and M. Amiji. 2007. Poly(ethylene oxide)-modified poly (β-amino ester) nanoparticles as a pH-sensitive system for tumor-targeted delivery of hydrophobic drugs: part 3. Therapeutic efficacy and safety studies in ovarian cancer xenograft model. Cancer Chemother. Pharmacol. 59: 477–484.

Dhar, S. and E.M. Reddy, A. Shiras, V. Pokharkar and B.L. Prasad. 2008. Natural gum reduced/stabilized gold nanoparticles for drug delivery formulations. Chemistry. 14: 10244–10250.

Dinarvand, R. and N. Sepehri, S. Manoochehri, H. Rouhani and F. Atyabi. 2011. Polylactide-co-glycolide nanoparticles for controlled delivery of anticancer agents. Int. J. Nanomedicine. 6: 877–895.

Ding, D. and Z. Zhu, Q. Liu, J. Wang, Y. Hu, X. Jiang and B. Liu. 2011. Cisplatin-loaded gelatin-poly(acrylic acid) nanoparticles: synthesis, antitumor efficiency *in vivo* and penetration in tumors. Eur. J. Pharm. Biopharm. 79: 142–149.

Duan, J. and M. Liu, Y. Zhang, J. Zhao, Y. Pan and X. Yang. 2012. Folate-decorated chitosan/doxorubicin poly(butyl)cyanoacrylate nanoparticles for tumor-targeted drug delivery. J. Nanopart. Res. 14: 761–769.

Duncan, R. and H. Ringsdorf and R. Satchi-Fainaro. 2006. Polymer therapeutics: polymers as drugs, drug and protein conjugates and gene delivery systems: past, present and future opportunities. J. Drug Target. 14: 337–341.

Edelman, E.R. and A. Fiorino, A. Grodzinsky and R. Langer. 1992. Mechanical deformation of polymer matrix controlled release devices modulates drug release. J. Biomed. Mater. Res. 26: 1619–1631.

Eerikäinen, H. and L. Peltonen, J. Raula, J. Hirvonen and E.I. Kauppinen. 2004. Nanoparticles containing ketoprofen and acrylic polymers prepared by an aerosol flow reactor method. AAPS Pharm. Sci. Tech. 5: e68.

Eley, J.G. and V.D. Pujari and J. McLane. 2004. Poly(lactide-co-glycolide) nanoparticles containing coumarin-6 for suppository delivery: *in vitro* releasee profile and *in vivo* tissue distribution. Drug Deliv. 11: 255–261.

Elsadek, B. and F. Kratz. 2012. Impact of albumin on drug delivery-new applications on the horizon. J. Control. Release. 157: 4–28.

Elzoghby, A.O. and W.M. Samy and N.A. Elgindy. 2012. Albumin-based nanoparticles as potential controlled release drug delivery systems. J. Control. Release. 157: 168–182.

Ensign, L.M. and R. Cone and J. Hanes. 2012. Oral drug delivery with polymeric nanoparticles: the gastrointestinal mucus barriers. Adv. Drug Deliv. Rev. 64: 557–570.

Erdoğar, N. and A. Mungan and E. Bilensoy. 2010. Preparation and characterization of cationic nanoparticles loaded with Mitomycin C by double emulsion and ionotropic gelation techniques. J. Control. Release. 148: e78–e79.

Esumi, K. 2003. Dendrimers for nanoparticle synthesis and dispersion stabilization. Top. Curr. Chem. 227: 31–52.

Fan, W. and W. Yan, Z. Xu and H. Ni. 2012. Formation mechanism of monodisperse, low molecular weight chitosan nanoparticles by ionic gelation technique. Colloids Surf. B Biointerfaces. 90: 21–27.

Friend, J.R. and L.Y. Yeo, D.R. Arifin and A. Mechler. 2008. Evaporative self-assembly assisted synthesis of polymeric nanoparticles by surface acoustic wave atomization. Nanotechnology. 19: 145301.

Fu, J. and X.Y. Li, K.P.N. Dennis and W. Chi. 2002. Encapsulation of phthalocyanines in biodegradable poly(sebacic anhydride) nanoparticles. Langmuir. 18: 3843–3847.

Ganta, S. and H. Devalapally, A. Shahiwala and M. Amiji. 2008. A review of stimuli-responsive nanocarriers for drug and gene delivery. J. Control. Release. 126: 187–204.

Gao, X. and X. Zhang, X. Zhang, Y. Wang, L. Sun and C. Li. 2011. Amphiphilic polylactic acid-hyperbranched polyglycerol nanoparticles as a controlled release system for poorly water-soluble drugs: physicochemical characterization. J. Pharm. Pharmacol. 63: 757–764.

Garay-Jimenez, J.C. and E. Turos. 2011. A convenient method to prepare emulsified polyacrylate nanoparticles from powders for drug delivery applications. Bioorg. Med. Chem. Lett. 21: 4589–4591.

Gasper, M.M. and D. Blanco, M.E. Cruz and M.J. Alonso. 1998. Formulation of L-asparaginase-loaded poly(lactide-co-glycolide) nanoparticles: influence of polymer properties on enzyme loading, activity and *in vitro* release. J. Control. Release. 52: 53–62.

Gaucher, G. and M.-H. Dufresne, V.P. Sant, N. Kang, D. Maysinger and J.C. Leroux. 2005. Block copolymer micelles: preparation, characterization and application in drug delivery. J. Control. Release. 109: 169–188.

Goldberg, D.S. and N. Vijayalakshmi, P.W. Swaan and H. Ghandehari. 2011. G3.5 PAMAM dendrimers enhance transepithelial transport of SN38 while minimizing gastrointestinal toxicity. J. Control. Release. 150: 318–325.

Graham, M.L. 2003. Pegaspargase: a review of clinical studies. Adv. Drug Deliv. Rev. 55: 1293–1302.

Guhagarkar, S.A. and R.V. Gaikwad, A. Samad, V.C. Malshe and P.V. Devarajan. 2010. Polyethylene sebacate-doxorubicin nanoparticles for hepatic targeting. Int. J. Pharm. 401: 113–122.

Gunaseelan, S. and K. Gunaseelan, M. Deshmukh, X. Zhang and P.J. Sinko. 2010. Surface modifications of nanocarriers for effective intracellular delivery of anti-HIV drugs. Adv. Drug Deliv. Rev. 62: 518–531.

Ha, W. and W. Hao, W. Xiao-Ling, P. Shu-Lin, D. Li-Sheng, S. Zhang and B.J. Li. 2011. Self-aggregates of cholesterol-modified carboxymethyl konjac glucomannan conjugate: preparation, characterization, and preliminary assessment as a carrier of etoposide. Carbohydr. Polym. 86: 513–519.

Ham, A.S. and M.R. Cost, A.B. Sassi, C.S. Dezzutti and L.C. Rohan. 2009. Targeted delivery of PSC-RANTES for HIV-1 prevention using biodegradable nanoparticles. Pharm. Res. 26: 502–511.

Hamidi, M. and A. Azadi and P. Rafiei. 2008. Hydrogel nanoparticles in drug delivery. Adv. Drug Deliv. Rev. 60: 1638–1649.

He, C. and X. Zhuang, Z. Tang, H. Tian and X. Chen. 2012. Stimuli-sensitive synthetic polypeptide-based materials for drug and gene delivery. Adv. Healthc. Mater. 1: 48–78.

Heller, J. and J. Barr, S.Y. Ng, K.S. Abdellauoi and R. Gurny. 2002. Poly(ortho esters): synthesis, characterization, properties and uses. Adv. Drug Deliv. Rev. 54: 1015–1039.

Hill, A. and S. Geißler, M. Weigandt and K. Mäder. 2012. Controlled delivery of nanosuspensions from osmotic pumps: zero order and non-zero order kinetics. J. Control. Release. 158: 403–412.

Hirsch, L.R. and A.M. Gobin, A.R. Lowery, F. Tam, R.A. Drezek, N.J. Halas and J.L. West. 2006. Metal nanoshells. Ann. Biomed. Eng. 34: 15–22.

Hossann, M. and T. Wang, M. Wiggenhorn, R. Schmidt, A. Zengerle, G. Winter, H. Eibl, M. Peller, M. Reiser, R.D. Issels and L.H. Lindner. 2010. Size of thermosensitive liposomes influences content release. J. Control. Release. 147: 436–443.

Huang, Z.W. and V. Laurent, G. Chetouani, J.Y. Ljubimova, E. Holler, T. Benvegnu, P. Loyer and S. Cammas-Marion. 2012. New functional degradable and bio-compatible nanoparticles based on poly(malic acid) derivatives for site-specific anti-cancer drug delivery. Int. J. Pharm. 423: 84–92.

Hughes, G.A. 2005. Nanostructure-mediated drug delivery. Nanomedicine. 1: 22–30.

Iqbal, J. and G. Shahnaz, G. Perera, F. Hintzen, F. Sarti and A. Bernkop-Schnürch. 2012. Thiolated chitosan: development and *in vivo* evaluation of an oral delivery system for leuprolide. Eur. J. Pharm. Biopharm. 80: 95–102.

Jain, R.A. 2000. The manufacturing techniques of various drug loaded biodegradable poly(lactide-co-glycolide) (PLGA) devices. Biomaterials. 21: 2475–2490.

Jain, R. and Vikas and K. Radhapyari. 2011. Voltammetric quantification of tamoxifen. Drug Test Anal. 3: 743–747.

Jansen, J.F.G.A and E.W. Meijer and E.M.M. de Brabander-van den Berg. 1995. The dendritic box: shape-selective liberation of encapsulated guests. J. Am. Chem. Soc. 117: 4417–4418.
Ji, J. and D. Wu, L. Liu, J. Chen and Y. Xu. 2012. Preparation, evaluation, and *in vitro* release of folic acid conjugated O-carboxymethyl chitosan nanoparticles loaded with Methotrexate. J. Appl. Polym. Sci. 125: E208–E215.
Jiang, X. and Y.S. Cheng and H.D.C. Smyth. 2011. Nanostructured aerosol particles: fabrication, pulmonary drug delivery, and controlled release. J. Nanomater. 2011: 198792 (2 pages).
Jiao, Y. and N. Ubrich, M. Marchand-Arvier, C. Vigneron, M. Hoffman, T. Lecompte and P. Maincent. 2002. *In vitro* and *in vivo* evaluation of oral heparin-loaded polymeric nanoparticles in rabbits. Circulation. 105: 230–235.
Jubeli, E. and L. Moine, V. Nicolas and G. Barratt. 2012. Preparation of E-selectin-targeting nanoparticles and preliminary *in vitro* evaluation. Int. J. Pharm. 426: 291–301.
Kabanov, A.V. and S.V. Vinogradov. 2009. Nanogels as pharmaceutical carriers: finite networks of infinite capabilities. Angew. Chem. Int. Ed. Engl. 48: 5418–5429.
Kakizawa, Y. and K. Kataoka. 2002. Block copolymer micelles for delivery of gene and related compounds. Adv. Drug Deliv. Rev. 54: 203–222.
Kaminskas, L.M. and B.D. Kelly, V.M. McLeod, G. Sberna, D.J. Owen, B.J. Boyd and C.J. Porter. 2011. Characterisation and tumour targeting of PEGylated polylysine dendrimers bearing doxorubicin via a pH labile linker. J. Control. Release. 152: 241–248.
Kang, N. and J.C. Leroux. 2004. Triblock and star-block copolymers of N-(2-hydroxypropyl) methacrylamide or N-vinyl-2-pyrrolidone and D,L-lactide: synthesis and self-assembling properties in water. Polymer. 45: 8967–8980.
Kataoka, K. and T. Matsumoto, M. Yokoyama, T. Okano, Y. Sakurai, S. Fukushima, K. Okamoto and G.S. Kwon. 2000. Doxorubicin-loaded poly(ethylene glycol)-poly(beta-benzyl-L-aspartate) copolymer micelles: their pharmaceutical characteristics and biological significance. J. Control. Release. 64: 143–153.
Kavaz, D. and S. Odabaş, E. Güven, M. Demirbilek and E.B. Denkbaş. 2010. Bleomycin loaded magnetic chitosan nanoparticles as multifunctional nanocarriers. J. Bioact. Compat. Polym. 25: 305–318.
Keum, C.G. and Y.W. Noh, J.S. Baek, J.H. Lim, C.J. Hwang, Y.G. Na, S.C. Shin and C.W. Cho. 2011. Practical preparation procedures for docetaxel-loaded nanoparticles using polylactic acid-co-glycolic acid. Int. J. Nanomedicine. 6: 2225–2234.
Kılıçay, E. and M. Demirbilek, M. Türk, E. Güven, B. Hazer and E.B. Denkbas. 2011. Preparation and characterization of poly(3-hydroxybutyrate-co-3-hydroxyhexanoate) (PHBHHX) based nanoparticles for targeted cancer therapy. Eur. J. Pharm. Sci. 44: 310–320.
Kim, S.Y. and J.C. Ha and Y.M. Lee. 2000. Poly(ethylene oxide)-poly(propylene oxide)-poly(ethylene oxide)/poly(ε-caprolactone) (PCL) amphiphilic block copolymeric nanospheres II. Thermo-responsive drug release behaviors. J. Control. Release. 65: 345–358.
Kim, S.Y. and Y.M. Lee. 2001. Taxol-loaded block copolymer nanospheres composed of methoxy poly(ethylene glycol) and poly(epsilon-caprolactone) as novel anticancer drug carriers. Biomaterials. 22: 1697–1704.
Kim, J.Y. and W.I. Choi, Y.H. Kim, G. Tae, S.Y. Lee, K. Kim and I.C. Kwon. 2010. *In vivo* tumor targeting of pluronic-based nano-carriers. J. Control. Release. 147: 109–117.
Kim, J.Y. and S. Kim, R. Pinal and K. Park. 2011. Hydrotropic polymer micelles as versatile vehicles for delivery of poorly water-soluble drugs. J. Control. Release. 152: 13–20.
Kost, J. and J. Wolfrum and R. Langer. 1987. Magnetically enhanced insulin release in diabetic rats. J. Biomed. Mater. Res. 21: 1367–1373.
Kratz, F. 2008. Albumin as a drug carrier: design of prodrugs, drug conjugates and nanoparticles. J. Control. Release. 132: 171–183.
Kopeček, J. 2003. Smart and genetically engineered biomaterials and drug delivery systems. Eur. J. Pharm. Sci. 20: 1–16.
Köping-Höggård, M. and A. Sánchez and M.J. Alonso. 2005. Nanoparticles as carriers for nasal vaccine delivery. Expert Rev. Vaccines. 4: 185–196.

Kreuter, J. and P. Ramge, V. Petrov, S. Hamm, S.E. Gelperina, B. Engelhardt, R. Alyautdin, H. von Briesen and D.J. Begley. 2003. Direct evidence that polysorbate-80-coated poly(butylcyanoacrylate) nanoparticles deliver drugs to the CNS via specific mechanisms requiring prior binding of drug to the nanoparticles. Pharm. Res. 20: 409–416.

Kumaresh, S.S. and M.A. Tejraj, A.R. Kulkarnia and W.E. Rudzinski. 2001. Biodegradable polymeric nanoparticles as drug delivery devices. J. Control. Release. 70: 1–20.

Kumari, A. and S.K. Yadav and S.C. Yadav. 2010. Biodegradable polymeric nanoparticles based drug delivery systems. Colloids Surf. B Biointerfaces. 75: 1–18.

Kuntworbe, N. and R. Al-Kassas. 2012. Design and *in vitro* haemolytic evaluation of cryptolepine hydrochloride-loaded gelatine nanoparticles as a novel approach for the treatment of malaria. AAPS Pharm. Sci. Tech. 13: 568–581.

Kwon, G.S. and T. Okano 1999. Soluble self-assembled block copolymers for drug delivery. Pharm. Res. 16: 597–600.

Kwon, H.Y. and J.Y. Lee, S.W. Choi, Y. Jang and J.H. Kim. 2001. Preparation of PLGA nanoparticles containing estrogen by emulsification–diffusion method. Colloids Surf. A Physicochem. Eng. Aspects. 182: 123–130.

Lavasanifar, A. and J. Samuel and G.S. Kwon. 2002. Poly(ethylene oxide)-block-poly(L-amino acid) micelles for drug delivery. Adv. Drug Deliv. Rev. 54: 169–190.

Lee, W.F. and Y.C. Chen. 2004. Effect of bentonite on the physical properties and drug-release behavior of poly (AA-co-PEGMEA)/bentonite nanocomposite hydrogels for mucoadhesive. J. Appl. Polym. Sci. 91: 2934–2941.

Lee, B.R. and H.J. Baik, N.M. Oh and E.S. Lee. 2010. Intelligent polymeric nanocarriers responding to physical or biological signals: a new paradigm of cytosolic drug delivery for tumor treatment. Polymers. 2: 86–101.

Lee, Y.R. and Y.H. Lee, S.A. Im, K. Kim and C.K. Lee. 2011. Formulation and characterization of antigen-loaded PLGA nanoparticles for efficient cross-priming of the antigen. Immune Netw. 11: 163–168.

Lee, E.J. and S.A. Khan, J.K. Park and K.H. Lim. 2012. Studies on the characteristics of drug-loaded gelatin nanoparticles prepared by nanoprecipitation. Bioprocess Biosyst. Eng. 35: 297–307.

Lehtinen, J. and A. Magarkar, M. Stepniewski, S. Hakola, M. Bergman, T. Róg, M. Yliperttula, A. Urtti and A. Bunker. 2012. Analysis of cause of failure of new targeting peptide in PEGylated liposome: molecular modeling as rational design tool for nanomedicine. Eur. J. Pharm. Sci. 46: 121–130.

Leroux, J. and E. Roux, D. Le Garrec, K. Hong and D.C. Drummond. 2001. N-isopropylacrylamide copolymers for the preparation of pH-sensitive liposomes and polymeric micelles. J. Control. Release. 72: 71–84.

Li, Y.Y. and X.Z. Zhang, H. Cheng, G.C. Kim, S.X. Cheng and R.X. Zhuo. 2006. Novel stimuli-responsive micelle self-assembled from Y-shaped P(UA-Y-NIPAAm) copolymer for drug delivery. Biomacromolecules. 7: 2956–2960.

Li, F.Q. and H. Su, X. Chen, X.J. Qin, J.Y. Liu, Q.G. Zhu and J.H. Hu. 2009. Mannose 6-phosphate-modified bovine serum albumin nanoparticles for controlled and targeted delivery of sodium ferulate for treatment of hepatic fibrosis. J. Pharm. Pharmacol. 61: 1155–1161.

Li, N. and Y.L. Hu, C.X. He, C.J. Hu, J. Zhou, G.P. Tang and J.Q. Gao. 2010. Preparation, characterisation and anti-tumour activity of Ganoderma lucidum polysaccharide nanoparticles. J. Pharm. Pharmacol. 62: 139–144.

Lim, K.J. and S. Bisht, E.E. Bar, A. Maitra and C.G. Eberhart. 2011. A polymeric nanoparticle formulation of curcumin inhibits growth, clonogenicity and stem-like fraction in malignant brain tumors. Cancer Biol. Ther. 11: 464–473.

Lim, H.J. and E.C. Cho, J.A. Lee and J. Kim. 2012. A novel approach for the use of hyaluronic acid-based hydrogel nanoparticles as effective carriers for transdermal delivery systems. Colloids Surf. A Physicochem. Eng. Aspects. 402: 80–87.

Lin, S.Y and Y. Kawashima. 2012. Current status and approaches to developing press-coated chronodelivery drug systems. J. Control. Release. 157: 331–353.

Liu, R. and B. He, D. Li, Y. Lai, J.Z. Tang and Z. Gu. 2012a. Stabilization of pH-sensitive mPEG-PH-PLA nanoparticles by stereocomplexation between enantiomeric polylactides. Macromol. Rapid Commun. 33: 1061–1066.

Liu, Y. and X.J. Cheng, Q.F. Dang, F.K. Ma, X.G. Chen, H.J. Park and B.K. Kim. 2012b. Preparation and evaluation of oleoyl-carboxymethy-chitosan (OCMCS) nanoparticles as oral protein carriers. J. Mater. Sci. Mater. Med. 23: 375–384.

Lopes, L.B. and M.V. Scarpa, G.V. Silva, D.C. Rodrigues, C.V. Santilli and A.G. Oliveira. 2004. Studies on the encapsulation of diclofenac in small unilamellar liposomes of soya phosphatidylcholine. Colloids Surf. B Biointerfaces. 39: 151–158.

Luppi, B. and F. Bigucci, G. Corace, A. Delucca, T. Cerchiara, M. Sorrenti, L. Catenacci, A.M. Di Pietra and V. Zecchi. 2011. Albumin nanoparticles carrying cyclodextrins for nasal delivery of the anti-Alzheimer drug tacrine. Eur. J. Pharm. Sci. 44: 559–565.

Machado, A.H. and D. Lundberg, A.J. Ribeiro, F.J. Veiga, B. Lindman, M.G. Miguel and U. Olsson. 2012. Preparation of calcium alginate nanoparticles using water-in-oil (w/o) nanoemulsions. Langmuir. 28: 4131–4141.

Malhotra, M. and C. Lane, C. Tomaro-Duchesneau, S. Saha and S. Prakash. 2011. A novel method for synthesizing PEGylated chitosan nanoparticles: strategy, preparation, and *in vitro* analysis. Int. J. Nanomedicine. 6: 485–494.

Mahapatro, A. and D.K. Singh. 2011. Biodegradable nanoparticles are excellent vehicle for site directed *in vivo* delivery of drugs and vaccines. J. Nanobiotechnology. 9: 55–65.

Mainardes, R.M. and L.P. Silva. 2004. Drug delivery systems: past, present, and future. Curr. Drug Targets. 5: 449–455.

Makhlof, A. and Y. Tozuka and H. Takeuchi. 2011. Design and evaluation of novel pH-sensitive chitosan nanoparticles for oral insulin delivery. Eur. J. Pharm. Sci. 42: 445–451.

Mandal, A.S. and N. Biswas, K.M. Karim, A. Guha, S. Chatterjee, M. Behera and K. Kuotsu. 2010. Drug delivery system based on chronobiology—a review. J. Control. Release. 147: 314–325.

Mazzarino, L. and C. Travelet, S. Ortega-Murillo, I. Otsuka, I. Pignot-Paintrand, E. Lemos-Senna and R. Borsali. 2012. Elaboration of chitosan-coated nanoparticles loaded with curcumin for mucoadhesive applications. J. Colloids Interface Sci. 370: 58–66.

McAllaster, J.D. and M.S. Cohen. 2011. Role of the lymphatics in cancer metastasis and chemotherapy applications. Adv. Drug Deliv. Rev. 63: 867–875.

Meco, D. and T. Servidei, A. Riccardi, C. Ferlini, G. Cusano, G.F. Zannoni, F. Giangaspero and R. Riccardi. 2009. Antitumor effect in medulloblastoma cells by gefitinib: ectopic HER2 overexpression enhances gefitinib effects *in vivo*. Neuro Oncol. 11: 250–259.

Menjoge, A.R. and A.L. Rinderknecht, R.S. Navath, M. Faridnia, C.J. Kim, R. Romero, R.K. Miller and R.M. Kannan. 2011. Transfer of PAMAM dendrimers across human placenta: prospects of its use as drug carrier during pregnancy. J. Control. Release. 150: 326–338.

Moreno-Jiménez, M. and J. Valero, J.M. López-Picazo, L. Arbea, J. Aristu, M. Cambeiro, J. Alcalde and R. Martínez-Monge. 2010. Concomitant cisplatin, paclitaxel, and hyperfractionated radiotherapy in locally advanced head and neck cancer: comparison of two different schedules. Am. J. Clin. Oncol. 33: 137–143.

Morgan, J.R. and M.J. Cloninger. 2002. Heterogeneously functionalized dendrimers. Curr. Opin. Drug Discov. Devel. 5: 966–997.

Moselhy, J. and X.Y. Wu, R. Nicholov and K. Kodaria. 2000. *In vitro* studies of the interaction of poly(NIPAm/MAA) nanoparticles with proteins and cells. J. Biomater. Sci. Polym. Ed. 11: 123–147.

Mulik, R.S. and J. Mönkkönen, R.O. Juvonen, K.R. Mahadik and A.R. Paradkar. 2010. Transferrin mediated solid lipid nanoparticles containing curcumin: enhanced *in vitro* anticancer activity by induction of apoptosis. Int. J. Pharm. 398: 190–203.

Myers, V.S. and M.G. Weir, E.V. Carino, D.F. Yancey, S. Pande and R.M. Crooks. 2011. Dendrimer-encapsulated nanoparticles: new synthetic and characterization methods and catalytic applications. Chem. Sci. 2: 1632–1646.

Nainwal, N. 2012. Chronotherapeutics—a chronopharmaceutical approach to drug delivery in the treatment of asthma. J. Control. Release. 163: 353–360.
Nair, K.L. and S. Vidyanand, J. James and G.S.V. Kumar. 2012. Pilocarpine-loaded poly(DL-lactic-co-glycolic acid) nanoparticles as potential candidates for controlled drug delivery with enhanced ocular pharmacological response. J. Appl. Polym. Sci. 124: 2030–2036.
Nakayama, M. and T. Okano, T. Miyazaki, F. Kohori, K. Sakai and M. Yokoyama. 2006. Molecular design of biodegradable polymeric micelles for temperature-responsive drug release. J. Control. Release. 115: 46–56.
Napoli, A. and M. Valentini, N. Tirelli, M. Müller and J.A. Hubbell. 2004. Oxidation-responsive polymeric vesicles. Nat. Mater. 3: 183–189.
Nayak, S. and L.A. Lyon. 2005. Soft nanotechnology with soft nanoparticles. Angew. Chem. Int. Ed. Engl. 44: 7686–7708.
Nierengarten, J.F. and J.F. Eckert, Y. Rio, M.P. Carreon, J.L. Gallani and D. Guillon. 2001. Amphiphilic diblock dendrimers: synthesis and incorporation in Langmuir and Langmuir-Blodgett films. J. Am. Chem. Soc. 123: 9743–9748.
Nistor, M.T. and A.P. Chiriac, L.E. Nita and C. Vasile. 2013a. Characterization of the semi-interpenetrated network based on collagen and poly(N-isopropyl acrylamide-co-diethylene glycol diacrylate). Int. J. Pharm. 452: 92–101.
Nistor, M.T. and C. Vasile, A.P. Chiriac and L. Tartau. 2013b. Biocompatibility, biodegradability, and drug carrier ability of hybrid collagen-based hydrogel nanocomposites. J. Bioact. Compat. Polym. 28: 540–556.
Nita, L.E. and A.P. Chiriac and C. Vasile. 2006a. Possibilities of collagen adsorption on some polymeric matrices based on styrene copolymers. J. Appl. Polym. Sci. 100: 3554–3561.
Nita, L.E. and A.P. Chiriac, I. Neamtu and C. Vasile. 2006b. Magnetic composites obtainment based on styrene polymers. J. Appl. Polym. Sci. 100: 4133–4141.
Nita, L.E. and A.P. Chiriac and M.T. Nistor. 2010. An *in vitro* release study of indomethacin from nanoparticles based on methyl methacrylate/glycidyl methacrylate copolymers. J. Mater. Sci. Mater. Med. 21: 3129–3140.
Niu, Y. and R.M. Crooks. 2003. Dendrimer-encapsulated metal nanoparticles and their applications to catalysis. C.R. Chimie. 6: 1049–1059.
Nomani, A. and I. Haririan, R. Rahimnia, S. Fouladdel, T. Gazori, R. Dinarvand, Y. Omidi and E. Azizi. 2010. Physicochemical and biological properties of self-assembled antisense/poly(amidoamine) dendrimer nanoparticles: the effect of dendrimer generation and charge ratio. Int. J. Nanomedicine. 5: 359–369.
Oh, K.T. and T.K. Bronich, L. Bromberg, T.A. Hatton and A.V. Kabanov. 2006. Block ionomer complexes as prospective nanocontainers for drug delivery. J. Control. Release. 115: 9–17.
Oh, K.S. and J.Y. Song, S.H. Cho, B.S. Lee, S.Y. Kim, K. Kim, H. Jeon, I.C. Kwon and S.H. Yuk. 2010. Paclitaxel-loaded Pluronic nanoparticles formed by a temperature-induced phase transition for cancer therapy. J. Control. Release. 148: 344–350.
Oliveira, J.M. and N. Kotobuki, A.P. Marques, R.P. Pirraco, J. Benesch, M. Hirose, S.A. Costa, J.F. Mano, H. Ohgushi and R.L. Reis. 2008. Surface engineered carboxymethylchitosan/poly(amidoamine) dendrimer nanoparticles for intracellular targeting. Adv. Funct. Mater. 18: 1840–1853.
Owens III, D. and N. Peppas. 2006. Integration of thermally responsive nanosphere hydrogels with gold nanoparticles for intelligent therapeutic applications. Trans. Soc. Biomater. 31: 150–151.
Padilla De Jesús, O.L. and H.R. Ihre, L. Gagne, J.M. Fréchet and F.C. Szoka, Jr. 2002. Polyester dendritic systems for drug delivery applications: *in vitro* and *in vivo* evaluation. Bioconjug. Chem. 13: 453–461.
Pandit, A.A. and A.K. Dash. 2011. Surface-modified solid lipid nanoparticulate formulation for ifosfamide: development and characterization. Nanomedicine (Lond.). 6: 1397–1412.

Park, Y.H. and S.H. Jeong, S.M. Yi, B.H. Choi, Y.R. Kim, I.K. Kim, M.K. Kim and S.W. Son. 2011. Analysis for the potential of polystyrene and TiO2 nanoparticles to induce skin irritation, phototoxicity and sensitization. Toxicol. *In Vitro*. 25: 1863–1869.

Patel, D. and S. Naik and A. Misra. 2012. Improved transnasal transport and brain uptake of tizanidine HCl-loaded thiolated chitosan nanoparticles for alleviation of pain. J. Pharm. Sci. 101: 690–706.

Patton, J.N. and A.F. Palmer. 2005. Engineering temperature-sensitive hydrogel nanoparticles entrapping hemoglobin as a novel type of oxygen carrier. Biomacromolecules. 6: 2204–2212.

Pawar, H. and D. Douroumis and J.S. Boateng. 2012. Preparation and optimization of PMAA-chitosan-PEG nanoparticles for oral drug delivery. Colloids Surf. B Biointerfaces. 90: 102–108.

Pinto, F.C.H. and A. Silva-Cunha, G.A. Pianetti, E. Ayres, R.L. Oréfice and G.R. Da Silva. Montmorillonite clay-based polyurethane nanocomposite as local triamcinolone acetonide delivery system. J. Nanomater. 2011: 528628 (11 pages).

Pinto Reis, C. and R.J. Neufeld, A.J. Ribeiro and F. Veiga. 2006. Nanoencapsulation I. Methods for preparation of drug-loaded polymeric nanoparticles. Nanomedicine. 2: 8–21.

Popescu, M.C. and B.C. Simionescu. 2012. Multivariate statistical analysis of mid-infrared spectra for a G1 allyl-terminated carbosilane dendrimer. Spectrochim. Acta A Mol. Biomol. Spectrosc. 92: 398–405.

Pourshahab, P.S. and K. Gilani, E. Moazeni, H. Eslahi, M.R. Fazeli and H. Jamalifar. 2011. Preparation and characterization of spray dried inhalable powders containing chitosan nanoparticles for pulmonary delivery of isoniazid. J. Microencapsul. 28: 605–613.

Potineni, A. and D.M. Lynn, R. Langer and M.M. Amiji. 2003. Poly(ethylene oxide)-modified poly(β-amino ester) nanoparticles as a pH-sensitive biodegradable system for paclitaxel delivery. J. Control. Release. 86: 223–234.

Prompruk, K. and T. Govender, S. Zhang, C.D. Xiong and S. Stolnik. 2005. Synthesis of a novel PEG-block-poly(aspartic acid-stat-phenylalanine) copolymer shows potential for formation of a micellar drug carrier. Int. J. Pharm. 297: 242–253.

Prow, T.W. and J.E. Grice, L.L. Lin, R. Faye, M. Butler, W. Becker, E.M. Wurm, C. Yoong, T.A. Robertson, H.P. Soyer and M.S. Roberts. 2011. Nanoparticles and microparticles for skin drug delivery. Adv. Drug Deliv. Rev. 63: 470–491.

Qi, N. and X. Tang, X. Lin, P. Gu, C. Cai, H. Xu, H. He and Y. Zhang. 2012. Sterilization stability of vesicular phospholipid gels loaded with cytarabine for brain implant. Int. J. Pharm. 427: 234–241.

Quintana, A. and E. Raczka, L. Piehler, I. Lee, A. Myc, I. Majoros, A.K. Patri, T. Thomas, J. Mulé and J.R. Baker, Jr. 2002. Design and function of a dendrimer based therapeutic nanodevice targeted to tumor cells through the folate receptor. Pharm. Res. 19: 1310–1316.

Rejinold, N.S. and K.P. Chennazhi, S.V. Nair, H. Tamura and R. Jayakumar. 2011. Biodegradable and thermo-sensitive chitosan-g-poly(N-vinylcaprolactam) nanoparticles as a 5-fluorouracil carrier. Carbohydr. Polym. 83: 776–786.

Rehor, A. and J.A. Hubbell and N. Tirelli. 2005. Oxidation-sensitive polymeric nanoparticles. Langmuir. 21: 411–417.

Relton, O.R. and F.S. Ferreira, E.R. Cintra, L.C. Branquinho, A.F. Bakuzis and E.M. Lima. 2012. Magnetic nanoparticles and rapamycin encapsulated into polymeric nanocarriers. J. Biomed. Nanotech. 8: 193–201.

Roy, I. and T.Y. Ohulchanskyy, H.E. Pudavar, E.J. Bergey, A.R. Oseroff, J. Morgan, T.J. Dougherty and P.N. Prasad. 2003. Ceramic-based nanoparticles entrapping water-insoluble photosensitizing anticancer drugs: a novel drug carrier system for photodynamic therapy. J. Am. Chem. Soc. 125: 7860–7865.

Sahoo, S.K. and V. Labhasetwar. 2003. Nanotech approaches to drug delivery and imaging. Drug Discov. Today. 8: 1112–1120.

Sahoo, S.K. and T.K. Jain, M.K. Reddy and V. Labhasetwar. 2008. Nano-sized carriers for drug delivery. pp. 329–349. *In*: O. Shoseyov and I. Levy [eds.]. 2008. NanoBioTechnology—BioInspired Devices and Materials of the Future. Humana Press Inc., New Jersey, USA.

Sajeesh, S. and C.P. Sharma. 2005. Novel pH responsive polymethacrylic acid-chitosan-polyethylene glycol nanoparticles for oral peptide delivery. J. Biomed. Mater. Res. B Appl. Biomat. 76: 298–305.

Sarmah, J.K. and R. Mahanta, S.K. Bhattacharjee, R. Mahanta and A. Biswas. 2011. Controlled release of tamoxifen citrate encapsulated in cross-linked guar gum nanoparticles. Int. J. Biol. Macromol. 49: 390–396.

Sarmento, B. and A. Ribeiro, F. Veiga and D. Ferreira. 2006. Development and characterization of new insulin containing polysaccharide nanoparticles. Colloids Surf. B Biointerfaces. 53: 193–202.

Satchi-Fainaro, R. and R. Duncan and C.M. Barnes. 2006. Polymer therapeutics for cancer: current status and future challenges. Adv. Polym. Sci. 193: 1–65.

Sawant, R.M. and J.P. Hurley, S. Salmaso, A. Kale, E. Tolcheva, T.S. Levchenko and V.P. Torchilin. 2006. "SMART" drug delivery systems: double-targeted ph-responsive pharmaceutical nanocarriers. Bioconjug. Chem. 17: 943–949.

Schmaljohann, D. 2006. Thermo- and pH-responsive polymers in drug delivery. Adv. Drug Deliv. Rev. 58: 1655–1670.

Sershen, S.R. and S.L. Westcott, N.J. Halas and J.L. West. 2000. Temperature-sensitive polymer nanoshell composites for photothermally modulated drug delivery. J. Biomed. Mater. Res. 51: 293–298.

Shah, P.P. and P.R. Desai, A.R. Patel and M.S. Singh. 2012a. Skin permeating nanogel for the cutaneous co-delivery of two anti-inflammatory drugs. Biomaterials. 33: 1607–1617.

Shah, P.P. and P.R. Desai and M. Singh. 2012b. Effect of oleic acid modified polymeric bilayered nanoparticles on percutaneous delivery of spantide II and ketoprofen. J. Control. Release. 158: 336–345.

Shahnaz, G. and A. Vetter, J. Barthelmes, D. Rahmat, F. Laffleur, J. Iqbal, G. Perera, W. Schlocker, S. Dünnhaput, P. Augustijns and A. Bernkop-Schnürch. 2012. Thiolated chitosan nanoparticles for the nasal administration of leuprolide: bioavailability and pharmacokinetic characterization. Int. J. Pharm. 428: 164–170.

Shantha, K.L. and D.R. Harding. 2000. Preparation and *in vitro* evaluation of poly[N-vinyl-2-pyrrolidone-polyethylene glycol diacrylate]-chitosan interpolymeric pH-responsive hydrogels for oral drug delivery. Int. J. Pharm. 207: 65–70.

Shenoy, D. and S. Little, R. Langer and M. Amiji. 2005a. Poly(ethylene oxide)-modified poly(β-amino ester) nanoparticles as a pH-sensitive system for tumor-targeted delivery of hydrophobic drugs. 1. *In vitro* evaluations. Mol. Pharm. 2: 357–366.

Shenoy, D. and S. Little, R. Langer and M. Amiji. 2005b. Poly(ethylene oxide)-modified poly(β-amino ester) nanoparticles as a pH-sensitive system for tumor-targeted delivery of hydrophobic drugs: part 2. *In vivo* distribution and tumor localization studies. Pharm. Res. 22: 2107–2114.

Shi, D. and M. Matsusaki and M. Akashi. 2011. Photo-tunable protein release from biodegradable nanoparticles composed of cinnamic acid derivatives. J. Control. Release. 149: 182–189.

Shujun, S. and S. Lei, Z. Xinge, W. Zhongming, W. Zhen and L. Chaoxing. 2011. Polysaccharides-based polyelectrolyte nanoparticles as protein drugs delivery system. J. Nanopart. Res. 13: 3657–3670.

Song, X. and Y. Zhao, S. Hou, F. Xu, R. Zhao, J. He, Z. Cai, Y. Li and Q. Chen. 2008. Dual agents loaded PLGA nanoparticles: systematic study of particle size and drug entrapment efficiency. Eur. J. Pharm. Biopharm. 69: 445–453.

Soppimath, K.S. and D.C.W. Tan and Y.Y. Yang. 2005. pH-Triggered thermally responsive polymer core-shell nanoparticles for drug delivery. Adv. Mater. 17: 318–323.

Sun, C. and J.S. Lee and M. Zhang. 2008. Magnetic nanoparticles in MR imaging and drug delivery. Adv. Drug Deliv. Rev. 60: 1252–1265.

Suwannateep, N. and W. Banlunara, S.P. Wanichwecharungruang, K. Chiablaem, K. Lirdprapamongkol and J. Svasti. 2011. Mucoadhesive curcumin nanospheres: biological activity, adhesion to stomach mucosa and release of curcumin into the circulation. J. Control. Release. 151: 176–182.

Tagami, T. and M.J. Ernsting and S.D. Li. 2011. Efficient tumor regression by a single and low dose treatment with a novel and enhanced formulation of thermosensitive liposomal doxorubicin. J. Control. Release. 152: 303–309.

Tang, R. and W. Ji, D. Panus, R.N. Palumbo and C. Wang. 2011. Block copolymer micelles with acid-labile ortho ester side-chains: synthesis, characterization, and enhanced drug delivery to human glioma cells. J. Control. Release. 151: 18–27.

Tascilar, M. and W.J. Loos, C. Seynaeve, J. Verweij and S. Sleijfer. 2007. The pharmacologic basis of ifosfamide use in adult patients with advanced soft tissue sarcomas. Oncologist. 12: 1351–1360.

Thomas, A.M. and A.I. Kapanen, J.I. Hare, E. Ramsay, K. Edwards, G. Karlsson and M.B. Bally. 2011. Development of a liposomal nanoparticle formulation of 5-Fluorouracil for parenteral administration: formulation design, pharmacokinetics and efficacy. J. Control. Release. 150: 212–219.

Tirelli, N. 2006. (Bio)responsive nanoparticles. Curr. Opin. Colloid. Interface Sci. 11: 210–216.

Traitel, T. and R. Goldbart and J. Kost. 2008. Smart polymers for responsive drug-delivery systems. J. Biomater. Sci. Polym. Ed. 19: 755–767.

Tripathi, P.K. and A.J. Khopade, S. Nagaich, S. Shrivastava, S. Jain and N.K. Jain. 2002. Dendrimer grafts for delivery of 5-fluorouracil. Pharmazie. 57: 261–264.

Uhrich, K.E. and S.M. Cannizzaro, R.S. Langer and K.M. Shakesheff. 1999. Polymeric systems for controlled drug release. Chem. Rev. 99: 3181–3198.

Van de Ven, H. and M. Vermeersch, A. Matheeussen, J. Vandervoort, W. Weyenberg, S. Apers, P. Cos, L. Maes and A. Ludwig. 2011. PLGA nanoparticles loaded with the antileishmanial saponin β-aescin: factor influence study and *in vitro* efficacy evaluation. Int. J. Pharm. 420: 122–132.

Vasile, C. and G.G. Bumbu, G. Bokias, G. Staikos and Y. Milanos. 2005. Synthesis and aqueous solution properties of novel thermoresponsive graft copolymers based on maleic acid vinyl-acetate copolymer backbone. Chin. J. Light Scat. 17: 228–232.

Vasile, C. [ed.]. 2009. Environmentally Degradable Polymer Materials based on Multicomponent Polymeric System. Koninklijke Brill NV, Leiden, The Netherlands.

Vasile, C. and R.P. Dumitriu. 2008. Stimuli Responsive Polymeric Materials. P.I.M., Iași, Romania.

Vasudev, S.S. and S. Ahmad, R. Parveen, F.J. Ahmad, C.K. Anish, M. Ali and A.K. Panda. 2011. Formulation of PEG-ylated L-asparaginase loaded poly(lactide-co-glycolide) nanoparticles: influence of Pegylation on enzyme loading, activity and *in vitro* release. Pharmazie. 66: 956–960.

Vaupel, P. and F. Kallinowski and P. Okunieff. 1989. Blood flow, oxygen and nutrient supply and metabolic microenvironment of human tumors: a review. Cancer Res. 49: 6449–6465.

Veiseh, O. and C. Sun, C. Fang, N. Bhattarai, J. Gunn, F. Kievit, K. Du, B. Pullar, D. Lee, R.G. Ellenbogen, J. Olson and M. Zhang. 2009. Specific targeting of brain tumors with an optical/magnetic resonance imaging nanoprobe across the blood-brain barrier. Cancer Res. 69: 6200–6207.

Veiseh, O. and J.W. Gunn and M. Zhang. 2010. Design and fabrication of magnetic nanoparticles for targeted drug delivery and imaging. Adv. Drug Deliv. Rev. 62: 284–304.

Verma, A.K. and K. Sachin, A. Saxena and H.B. Bohidar. 2005. Release kinetics from bio-polymeric nanoparticles encapsulating protein synthesis inhibitor-cycloheximide, for possible therapeutic applications. Curr. Pharm. Biotechnol. 6: 121–130.

Vinogradov, S.V. and T.K. Bronich and A.V. Kabanov. 2002. Nanosized cationic hydrogens for drug delivery: preparation, properties and interactions with cells. Adv. Drug Deliv. Rev. 54: 135–147.

Visser, C.C. and S. Stevanović, L.H. Voorwinden, L. van Bloois, P.J. Gaillard, M. Danhof, D.J. Crommelin and A.G. de Boer. 2005. Targeting liposomes with protein drugs to the blood-brain barrier *in vitro*. Eur. J. Pharm. Sci. 25: 299–305.

Wang, J. and D.A. Mongayt, A.N. Lukyanov, T.S. Levchenko and V.P. Torchilin. 2004. Preparation and *in vitro* synergistic anticancer effect of Vitamin K3 and 1,8-diazabicyclo[5,4,0]undec-7-ene in poly(ethyleneglycol)-diacyllipid micelles. Int. J. Pharm. 272: 129–135.

Wang, H. and P. Zhao, X. Liang, X. Gong, T. Song, R. Niu and J. Chang. 2010. Folate-PEG coated cationic modified chitosan-cholesterol liposomes for tumor-targeted drug delivery. Biomaterials. 31: 4129–4138.

Wang, Y. and G. Jiang, T. Qiu and F. Ding. 2012a. Preparation and evaluation of paclitaxel-loaded nanoparticle incorporated with galactose-carrying polymer for hepatocyte targeted delivery. Drug Dev. Ind. Pharm. 38: 1039–1046.

Wang, X. and G. Wu, C. Lu, W. Zhao, Y. Wang, Y. Fan, H. Gao and J. Ma. 2012b. A novel delivery system of doxorubicin with high load and pH-responsive release from the nanoparticles of poly(α,β-aspartic acid) derivative. Eur. J. Pharm. Sci. 47: 256–264.

Wei, H. and X.Z. Zhang, H. Cheng, W.Q. Chen, S.X. Cheng and R.X. Zhuo. 2006. Self-assembled thermo- and pH-responsive micelles of poly(10-undecenoic acid-b-N-isopropylacrylamide) for drug delivery. J. Control. Release. 116: 266–274.

Wei, M. and Y. Xu, Q. Zou, L. Tu, C. Tang, T. Xu, L. Deng and C. Wu. 2012. Hepatocellular carcinoma targeting effect of PEGylated liposomes modified with lactoferrin. Eur. J. Pharm. Sci. 46: 131–141.

Wendorf, J. and M. Singh, J. Chesko, J. Kazzaz, E. Soewanan, M. Ugozzoli and D. O'Hagan. 2006. A practical approach to the use of nanoparticles for vaccine delivery. J. Pharm. Sci. 95: 2738–2750.

Wike-Hooley, J.A. and J. Haveman and H.S. Reinhold. 1984. The relevance of tumor pH to the treatment of malignant disease. Radiother. Oncol. 2: 343–366.

Wilson, B. and M.K. Samanta, K. Santhi, K.P. Kumar, M. Ramasamy and B. Suresh. 2010. Chitosan nanoparticles as a new delivery system for the anti-Alzheimer drug tacrine. Nanomedicine. 6: 144–152.

Wohlfart, S. and A.S. Khalansky, S. Gelperina, D. Begley and J. Kreuter. 2011. Kinetics of transport of doxorubicin bound to nanoparticles across the blood-brain barrier. J. Control. Release. 154: 103–107.

Wolinsky, J.B. and Y.L. Colson and M.W. Grinstaff. 2012. Local drug delivery strategies for cancer treatment: gels, nanoparticles, polymeric films, rods, and wafers. J. Control. Release. 159: 14–26.

Wu, Z.M. and L. Zhou, X.D. Guo, W. Jiang, L. Ling, Y. Qian, K.Q. Luo and L.J. Zhang. 2012. HP55-coated capsule containing PLGA/RS nanoparticles for oral delivery of insulin. Int. J. Pharm. 425: 1–8.

Xie, H. and J.W. Smith. 2010. Fabrication of PLGA nanoparticles with a fluidic nanoprecipitation system. J. Nanobiotechnology. 8: 18.

Xiong, X.Y. and K.C. Tam and L.H. Gan. 2005. Synthesis and thermal responsive properties of P(LA-b-EO-b-POb-EO-b-LA) block copolymers with short hydrophobic poly(lactic acid) (PLA) segments. Polymer. 46: 1841–1850.

Xu, P. and E.A. Van Kirk, W.J. Murdoch, Y. Zhan, D.D. Isaak, M. Radosz and Y. Shen. 2006. Anticancer efficacies of cisplatin-releasing pH-responsive nanoparticles. Biomacromolecules. 7: 829–835.

Yadav, A.K. and A. Agarwal, G. Rai, P. Mishra, S. Jain, A.K. Mishra, H. Agrawal and G.P. Agrawal. 2010. Development and characterization of hyaluronic acid decorated PLGA nanoparticles for delivery of 5-fluorouracil. Drug Deliv. 17: 561–572.

Yang, J. and J. Lee, J. Kang, K. Lee, J.S. Suh, H.G. Yoon, Y.M. Huh and S. Haam. 2008. Hollow silica nanocontainers as drug delivery vehicles. Langmuir. 24: 3417–3421.

Yang, J. and H. Wang, Z. Wang, X. Tan, C. Song, R. Zhang, J. Li and Y. Cui. 2009. Interaction between antitumor drug and silver nanoparticles: combined fluorescence and surface enhanced Raman scattering study. Chin. Opt. Lett. 7: 894–897.

Yang, J. and H. Sun and C. Song. 2012. Preparation, characterization and *in vivo* evaluation of pH-sensitive oral insulin-loaded poly(lactic-co-glycolicacid) nanoparticles. Diabetes Obes. Metab. 14: 358–364.

Yardley, D. and H. Burris 3rd, N. Peacock, E. Raefsky, M. Melnik, R. Inhorn, D. Shipley and J. Hainsworth. 2010. A pilot study of adjuvant nanoparticle albumin-bound (nab) paclitaxel and cyclophosphamide, with trastuzumab in HER2-positive patients, in the treatment of early-stage breast cancer. Breast Cancer Res. Treat. 123: 471–475.

Yeh, M.K. and K.M. Cheng, C.S. Hu, Y.C. Huang and J.J. Young. 2011. Novel protein-loaded chondroitin sulfate-chitosan nanoparticles: preparation and characterization. Acta Biomater. 7: 3804–3812.

Zhang, C. and W. Wang, T. Liu, Y. Wu, H. Guo, P. Wang, Q. Tian, Y. Wang and Z. Yuan. 2012. Doxorubicin-loaded glycyrrhetinic acid-modified alginate nanoparticles for liver tumor chemotherapy. Biomaterials. 33: 2187–2196.

Zhang, Q. and Z. Shen and T. Nagai. 2001. Prolonged hypoglycemic effect of insulin-loaded polybutylcyanoacrylate nanoparticles after pulmonary administration to normal rats. Int. J. Pharm. 218: 75–80.

Zhang, Y. and R.X. Zhuo. 2005. Synthesis and *in vitro* drug release behavior of amphiphilic triblock copolymer nanoparticles based on poly (ethylene glycol) and polycaprolactone. Biomaterials. 26: 6736–6742.

Zhang, C.Z. and H.T. Zhang, G.C. Chen and P.B. Lai. 2011. Trichostatin A sensitizes HBx-expressing liver cancer cells to etoposide treatment. Apoptosis. 16: 683–695.

Zhang, X. and M. Sun, A. Zheng, D. Cao, Y. Bi and J. Sun. 2012a. Preparation and characterization of insulin-loaded bioadhesive PLGA nanoparticles for oral administration. Eur. J. Pharm. Sci. 45: 632–638.

Zhang, X.X. and H.S. Eden and X. Chen. 2012b. Peptides in cancer nanomedicine: drug carriers, targeting ligands and protease substrates. J. Control. Release. 159: 2–13.

Zhao, Y. and B.G. Trewyn, I.I. Slowing and V.S. Lin. 2009. Mesoporous silica nanoparticle-based double drug delivery system for glucose-responsive controlled release of insulin and cyclic AMP. J. Am. Chem. Soc. 131: 8398–8400.

Zheng, Z. and X. Zhang, D. Carbo, C. Clark, C. Nathan and Y. Lvov. 2010. Sonication-assisted synthesis of polyelectrolyte-coated curcumin nanoparticles. Langmuir. 26: 7679–7681.

Zhu, Y. and S. Kaskel, T. Ikoma and N. Hanagata. 2009. Magnetic SBA-15/poly(N-isopropylacrylamide) composite: preparation, characterization and temperature-responsive drug release property. Micropor. Mesopor. Mater. 123: 107–112.

Zillies, J.C. and K. Zwiorek, F. Hoffmann, A. Vollmar, T.J. Anchordoquy, G. Winter and C. Coester. 2008. Formulation development of freeze-dried oligonucleotide-loaded gelatin nanoparticles. Eur. J. Pharm. Biopharm. 70: 514–521.

Zweers, M.L. and G.H. Engbers, D.W. Grijpma and J. Feijen. 2004. *In vitro* degradation of nanoparticles prepared from polymers based on D,L-lactide, glycolide and poly(ethylene oxide). J. Control. Release. 100: 347–356.

Zwiorek, K. and J. Kloeckner, E. Wagner and C. Coester. 2004. Gelatin nanoparticles as a new and simple gene delivery system. J. Pharm. Pharm. Sci. 7: 22–28.

CHAPTER 4

Reversible Cross-Linked Polymeric Nanoplatform in Drug Delivery

Yuanpei Li,[1,a] *Kai Xiao*[2] and *Kit S. Lam*[1,b,*]

ABSTRACT

In the past decade, polymeric micelles self-assembled from amphiphilic block copolymers have emerged as a major class of nanocarriers for drug delivery. There has been an increasing interest in using the cross-linking approach to improve the stability of conventional thermodynamic polymeric micelles. Recently, much effort has been directed to the development of reversibly cross-linked micelles that respond to endogenous and/or exogenous stimuli, in particular, pH, temperature or redox potential. Reversibly cross-linked micelles represent an ideal nanocarrier system for targeted drug delivery. These micelles exhibit superior structural stability compared to non-cross-linked counterparts. Therefore, these nanocarriers are able to minimize the premature drug release during blood circulation. The introduction of environmentally sensitive pendants to the block copolymers or the utilization of environmentally sensitive cross-linkers makes these micelles responsive to the endogenous or exogenous stimuli. The release of encapsulated drugs can be readily modulated by

[1] Department of Biochemistry & Molecular Medicine, UC Davis Cancer Center, University of California Davis, 2700 Stockton Blvd, Sacramento, CA 95817, USA.
[a] Email: lypli@ucdavis.edu; liyuanpei@gmail.com
[b] Email: kit.lam@ucdmc.ucdavis.edu
[2] National Chengdu Center for Safety Evaluation of Drugs, West China Hospital, Sichuan University, Chengdu 610041, China.
Email: iamxiaokai@hotmail.com
* Corresponding author

List of abbreviations after the text.

these stimuli. The stimuli-responsive release may result in significantly enhanced therapeutic efficacy and minimized possible side effects. This chapter focuses on the various strategies used for the design, preparation, stimuli-responsiveness and potential medical applications of reversibly cross-linked micelles for drug delivery. *In vivo* evidence demonstrating the effectiveness of reversibly cross-linked micelles will be presented. Lastly, future perspectives for the development of reversibly cross-linked micelle systems for drug delivery will also be explored.

Introduction

Polymeric micelles have emerged as a major class of nanocarriers for drug delivery (Liu et al. 2006, Li et al. 2009a). For effective cancer therapy, desired characteristics of micellar nanocarriers include the following: *i*) negligible to no toxicity of the nanocarrier; *ii*) high stability of the nanocarrier in the blood stream, with minimal premature drug release; *iii*) low uptake of the nanoparticle's drug payload into all healthy organs and the reticuloendothelial system; *iv*) high tumor uptake and prolonged retention of nanoparticle's drug inside the tumor; *v*) ability of the nanoparticle's drug to be taken up by tumor cells; *vi*) inherent mechanisms of drug release from the nanocarrier at the tumor site or inside tumor cells; and, *vii*) ability to release the loaded drug from the nanocarrier on-demand. Criteria *ii*, *vi*, and *vii* will be addressed in this chapter.

Polymeric micelles are generally formed by the spontaneous solution phase self-assembly of amphiphilic block copolymers comprised of hydrophobic and hydrophilic segments. This process can produce well-defined aggregates, known as polymer micelles, which in aqueous solution consist of a hydrophobic core and a surrounding hydrophilic shell layer or corona. The major driving force is the minimization of the free energy of the system by segregating the hydrophobic segments from the aqueous environment, resulting in the formation of a relatively solid hydrophobic core encased by the hydrophilic segments. This is often called the hydrophobic effect. Lipophilic drugs can be encapsulated in the hydrophobic cores during the self-assembly, significantly increasing the drug concentration in an aqueous environment. Polymeric micelle drug delivery systems offer several distinct advantages, such as improved solubility, controlled drug release, prolonged circulation time, passive and active tumor targeting and overcoming Multidrug Resistance (MDR) of cancer cells (Li et al. 2009a, Cabral et al. 2011). In the field of cancer drug delivery, polymeric micelles in the size range of 10–100 nm can passively accumulate at the tumor site through leaky vasculatures via the Enhanced Permeability and Retention (EPR) effect (Davis et al. 2008).

Although promising, several problems associated with self-assembled polymeric micelles may limit their applications in the clinic. Polymeric

micelles are thermodynamic self-assemble systems, and there is a well-known equilibrium that exhibits between micelles and unimers (single polymer unit) in aqueous conditions. Conventional self-assembled polymeric micelles are susceptible to dilution below the Critical Micelle Concentration (CMC) after injection into the blood stream. This may lead to the dissociation of micelles into unimers. Furthermore, after entering into blood circulation, polymeric micelles immediately confront blood proteins and lipoprotein particles such as High Density Lipoprotein (HDL), Low Density Lipoprotein (LDL), Very Low Density Lipoprotein (VLDL) and chylomicron. These particles may interact with micelles which often lead to the early disintegration or aggregation of polymeric micelles and premature drug release before reaching target sites (Rijcken et al. 2007). To resolve these problems, cross-linking strategies have been introduced to improve the stability of polymeric micelles suitable for drug delivery. The formation of covalent cross-links between specific domains of the micelles offers stability to the nanosized assemblies by providing reinforcement to the weak non-covalent intermolecular interactions that facilitate polymer micelle assembly and integrity. Furthermore, cross-linking not only can improve the structural stability of micelles, but can also control the release rate of the trapped drugs (Qi et al. 2004, Liu et al. 2007, Rijcken et al. 2007, Chan et al. 2008, Jiang et al. 2009). However, to be effective, drugs encapsulated inside micelles need to be released inside the target cells or within the target organs or tumors. Excessively stabilized micelles may prevent the drug from releasing to target sites, thus reducing the therapeutic efficacy (Li et al. 2009b).

Among the reported polymeric micelles, reversibly cross-linked micelles represent an ideal nanocarrier system for targeted drug delivery (Rijcken et al. 2007, Hennink et al. 2010, Li et al. 2009b, 2011) (Fig. 4.1). Due to the intra-micellar cross-link, reversibly cross-linked micelles exhibit superior structural stability under physiological conditions when compared to their non-cross-linked counterparts. As a result, these nanocarriers are able to better retain the encapsulated drug and minimize premature release during blood circulation (Rijcken et al. 2007, Hennink et al. 2010, Li et al. 2011). The introduction of environmentally sensitive pendants to the assembly units or the utilization of environmentally sensitive cross-linkers make these micelles responsive to the endogenous stimuli in the local microenvironment of the target sites (Koo et al. 2008, Li et al. 2009b, 2011) or via application of exogenous stimuli. In these instances, the payload drug is released almost exclusively in the target tissue (Rijcken et al. 2007, Hennink et al. 2010, Li et al. 2011). A large variety of amphiphilic block copolymers has been used to prepare cross-linked micelles that are responsive to physical and chemical stimuli. Stimuli-responsive polymers undergo dramatic and abrupt physical and chemical changes in response to external stimuli. They are also called

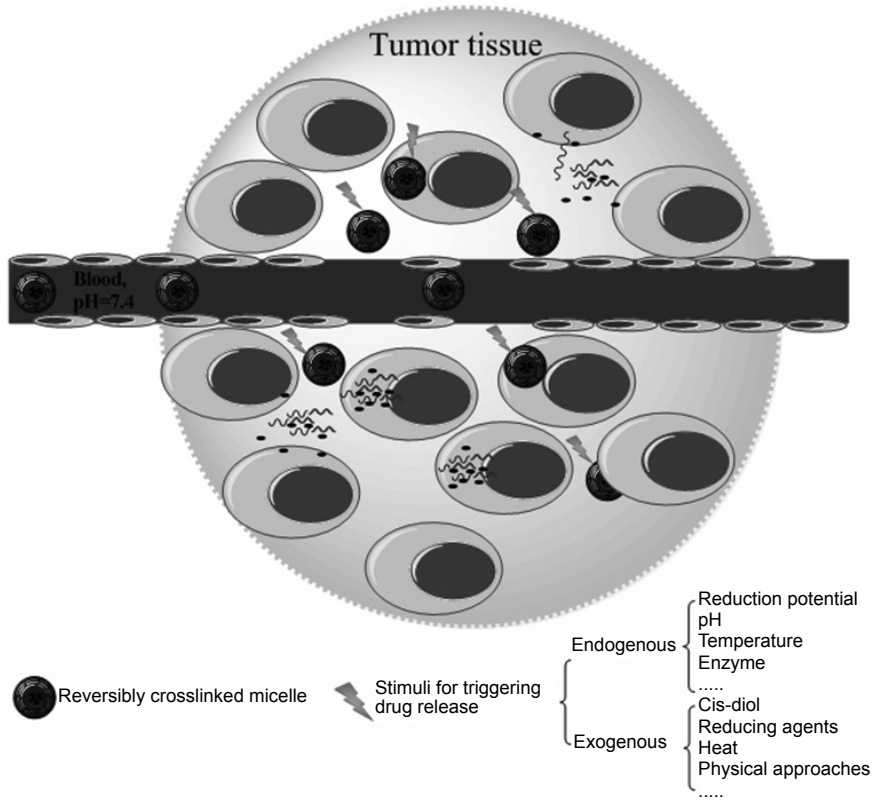

Figure 4.1. Schematic illustration of reversibly cross-linked micelles for cancer therapy.

"smart" or "environmentally sensitive" polymers. One important feature of this type of polymeric material is reversibility, i.e., the ability of the polymer to return to its initial state upon application of a counter-trigger (Cabane et al. 2012). Various hydrolysable or cleavable cross-linkers have also been employed to control the drug release from the micelles (Rijcken et al. 2007, Li et al. 2011, Xing et al. 2011). Remarkable progress has been achieved in the development of reversibly cross-linked polymeric micelles in recent years (Hennink et al. 2010, Li et al. 2011). This chapter presents particular focus on novel design, preparation, cross-linking strategy, triggering release mechanism and *in vitro* and *in vivo* applications.

Reversibly Cross-linked Polymeric Nanoplatforms

Cross-linking is an excellent approach to increase the stability of the micelles and prevent the premature drug release during blood circulation. There are several potential sites for cross-linking within block copolymer

micelles, these include shell cross-linking (Qi et al. 2004, Liu et al. 2007), core-cross-linking (Rijcken et al. 2007, Chan et al. 2008, Jiang et al. 2009), and cross-linking at the core-shell interface (Harada and Kataoka 2006, Koo et al. 2008). The location of this cross-linked domain can dramatically affect the physical and chemical properties of the resulting micelles. In addition to the method used, the extent of the cross-linking can also impact the stability, structure and thus applications of the resulting micelles. Primary chemistries that have been used for core-cross-linking and stabilization of micellar particles include the introduction of cross-linking reagents, and the incorporation of polymerizable or photo/UV cross-linkable groups. Many groups have reported the utilization of bi-functional cross-linking reagents, which allow for the selective covalent stabilization of the core domain. In addition, various cleavable cross-linkages, such as reducible disulfide bonds (Li et al. 2011), pH cleavable (Xing et al. 2011) or hydrolysable ester bonds (Rijcken et al. 2007), have also been utilized to create cross-linked micelles. Recently, *in situ* cross-linking has been reported, where cross-linkable groups are introduced for spontaneous cross-linking of micelles during the micelle formation via self-assembly in aqueous media (Li et al. 2011, 2012a).

The responsiveness or "smartness" of a nanocarrier system refers to its ability to receive, transmit a stimulus and respond with a desirable effect. Typical stimuli are redox, various "signaling" molecules (enzymes), pH, temperature, light, magnetic field and concentrations of electrolytes. The consequent responses to the above mentioned signals include bond cleavage, degradation dissolution/precipitation, swelling/collapsing, hydrophilic/hydrophobic transition, drug release, and so on. The use of light or magnetic field to trigger drug release is theoretically feasible, but in practice not applicable in many clinical situations. For example, metastatic lesions inside internal organs are not easily reached by light. Polymeric nanocarrier systems responsive to changes in temperature and pH, and internal redox have been the focus of many studies (Meng et al. 2009a). Generally, polymers and cross-linkers used as drug carrier systems are designed in such a way that their structures can be disrupted, thus triggering the release of encapsulated molecules, under the following conditions: *i*) acidic conditions, with a pH below the physiological pH; *ii*) high reductive conditions; and, *iii*) at temperatures higher than normal body temperature (37°C). Very recently, a few studies have succeeded in systemically applying external stimuli, such as exogenous reducing agents and cis-diols to trigger the drug release from the nanocarriers. An overview of the reversibly cross-linked micelle systems including the assembly units, preparation methods, cross-linking strategy, stimuli response and their applications are given in Table 4.1.

Table 4.1. An overview of the reported reversible cross-linked micelle systems.

Polymers	Preparation method	Cross-link	Stimulus	Application	Reference
PEG-oligocholic acids	Solvent evaporation	Disulfide	Reduction	PTX delivery	Li et al. 2011
PEG-oligocholic acids	Solvent evaporation	Disulfide	Reduction	VCR delivery	Kato et al. 2012
Polyethyleneimine	Aqueous media	Disulfide	Reduction	DNA delivery	Gosselin et al. 2001
PEG-*b*-poly(L-lysine)/PEG-*b*-poly(L-aspartic acid)	Aqueous media	Disulfide	Reduction	*si*RNA delivery	Kakizawa et al. 1999
PEG-*b*-poly(L-lysine)	Aqueous media	Disulfide	Reduction	Plasmid DNA delivery	Miyata et al. 2004
Iminothiolane-modified PEG-*b*-poly(L-lysine)	Aqueous media	Disulfide	Reduction	*si*RNA delivery	Matsumoto et al. 2009
Poly(PEG methyl ether methacrylate)-*b*-poly(5′-O-methacryloyluridine)	Aqueous/dimethyl sulfoxide solution	Disulfide	Reduction	Riboflavin delivery	Zhang et al. 2008b
Poly(amidoamine)-cholesterol conjugates	Water/chloroform emulsion	Disulfide	Reduction	Azobenzene and estradiol	Ranucci et al. 2008
PCL-*b*-poly(mercaptoethyl ethylene phosphate)-*b*-PEG	Dialysis	Disulfide	Reduction	DOX delivery	Wang et al. 2010
PEG-*b*-PLys-*b*-PPhe	Dialysis	Disulfide	Reduction	MTX delivery	Koo et al. 2008
Disulfide cross-linked polyethylenimine	NaCl solution	Disulfide	Reduction	Gene delivery (plasmid pGL3)	Peng et al. 2009
PEG-PCL diblock copolymer containing two lipoyl groups at the middle	Dialysis	Disulfide	Reduction	DOX delivery	Xu et al. 2009b
Lipoic acid containing dextran derivatives	Dialysis	Disulfide	Reduction	DOX delivery	Li et al. 2009b
mPEG-cysteine-PCL	Dialysis	Disulfide	Reduction	DOX delivery	Kim et al. 2010b
Thiolated c(RGDfK)-PEG-*b*-poly(L-lysine)	Dialysis	Disulfide	Reduction	Plasmid DNA delivery	Oba et al. 2008

Table 4.1. contd....

Table 4.1. contd.

Polymers	Preparation method	Cross-link	Stimulus	Application	Reference
Poly(L-cysteine)-*b*-poly(L-lactide)	Aqueous/dimethyl sulfoxide solution	Disulfide	Reduction	Drug delivery	Sun et al. 2008
PEG-*b*-P(DEA-*s*-TMSPMA)	Aqueous/tetrahydrofuran solution	Siloxane	pH		Du and Armes 2005
PEO-*b*-poly(*N*- isopropylacrylamide-*co*-*N*-acryloxysuccinimide)	Aqueous solution upon heating	Cystamine	Temperature and reduction	Drug delivery	Jiang et al. 2009
Poly(*N*-isopropylacrylamide-*co*-3-(trimethoxysilyl)propyl methacrylate)-*b*-poly(2-(diethylamino)ethyl methacrylate)	Aqueous/tetrahydrofuran solution	Silica-based cross-linking	Temperature and pH	Prednisone delivery	Chang et al. 2009
Poly(acryloyl glucosamine)-*b*- poly(*N*-isopropylacryamide)	Aqueous solution	Covalent	Temperature and pH	Drug delivery	Zhang et al. 2008a
PHEA-*b*-PBA	Ethanol/phosphate buffer solution	Divinyl acid labile cross-linker	pH	DOX delivery	Chan et al. 2008
PEG-oligocholic acids	Evaporation	Boronate	pH, cis-diol	PTX delivery	Li et al. 2012a
PEO-*b*-PMA/Ca^{2+}	Aqueous solution	Disulfide	Reduction	DOX delivery	Kim et al. 2010a
mPEO-PAPMA-PDPAEMA	Aqueous solution	Disulfide	pH, reduction	Drug delivery	Xu et al. 2009a
mPEG-*b*-poly[*N*-(2-hydroxyethyl) methacrylamide)-lactate]	"rapid heating"	Hydrazone linker	Hydrolysable	DOX delivery	Rijcken et al. 2007, Talelli et al. 2010a,b
PEG-PAsp-PPhe	Dialysis	Ketal-containing cross-linkers	Hydrolysable	DOX delivery	Lee et al. 2011
Poly(sodium 2-acrylamido-2-methyl-1-propanesulfonate-*b*-*N*-acryloyl-L-alanine)	1 M HCl/water	Inter-polyelectrolyte	pH/salt		Kellum et al. 2010
mPEO-PAPMA-PDPAEMA	Water with heat	Imine	Temperature and pH	Prednisolone 21-acetate delivery	Xu et al. 2011

Redox-sensitive cross-linked micelle system

Among all applied stimuli, redox potential is one that is most promising and clinically applicable. It is well-known that the redox potential in blood and extracellular space is low and inside the cells is high. The intracellular concentration of glutathione (GSH), a thiol-containing tripeptide generated in the cell cytoplasm, is known to be ≈ 100–1000 fold higher than that in the extracellular space (Koo et al. 2008). Furthermore, the cytosolic GSH concentration in some tumor cells has been found to be about seven times higher than that in normal cells (Black and Wolf 1991, Takae et al. 2008). Disulfide bond, which is stable at a normal physiological condition but respond to the reductive condition via reversible cleavage into free thiols, has been exploited by many groups for intracellular drug release (Kakizawa et al. 1999, Koo et al. 2008, Meng et al. 2009b). Following the pioneer work by Kataoka's group (Kakizawa et al. 1999), others have applied Disulfide Cross-linked Micelles (DCMs) in the delivery of doxorubicin (DOX) (Wang et al. 2010), paclitaxel (PTX) (Li et al. 2011), methotrexate (MTX) (Koo et al. 2008), vincristine (VCR) (Kato et al. 2011), deoxyribonucleic acid (DNA) (Gosselin et al. 2001), and small interfering ribonucleic acid (*si*RNA) (Koo et al. 2008, Li et al. 2009b).

Zhong et al. reported the development of several DCMs by introducing Lipoic Acids (LAs) as cross-linkable groups to several block copolymers and dextran followed by catalytic amount of dithiothreitol (DTT) to initiate the cross-link reaction between different LA molecules (Li et al. 2009b). For example, reduction-sensitive reversibly core-cross-linked micelles were developed based on poly(ethylene glycol)-*b*-poly(*N*-2-hydroxypropyl methacrylamide)-lipoic acid (PEG-*b*-PHPMA-LA) conjugates for triggered DOX release. PEG-*b*-PHPMA block copolymers were synthesized by reversible addition-fragmentation chain transfer (RAFT) polymerization. The hydroxyl groups in the PEG-*b*-PHPMA copolymers were esterified with LA resulting in amphiphilic PEG-*b*-PHPMA-LA conjugates. Monodispersed micelles with average sizes ranging from 85.3 to 142.5 nm were formed by PEG-*b*-PHPMA-LA conjugates and were readily cross-linked with a catalytic amount of DTT. It was demonstrated that DOX can be loaded in the micelles with superior loading content and loading efficiency. *In vitro* release studies showed that only a small percentage of DOX was released in 12 hours from cross-linked micelles at 37°C, whereas most of DOX was released in the presence of excess amount of DTT (10 mM) under the same conditions.

To minimize premature release of drugs from the nanocarriers during circulation, our group has recently developed reversible DCMs that can be triggered to release drug at the tumor site and inside cancer cells with high reductive potential (Fig. 4.2). In this novel nanoplatform, four cysteines

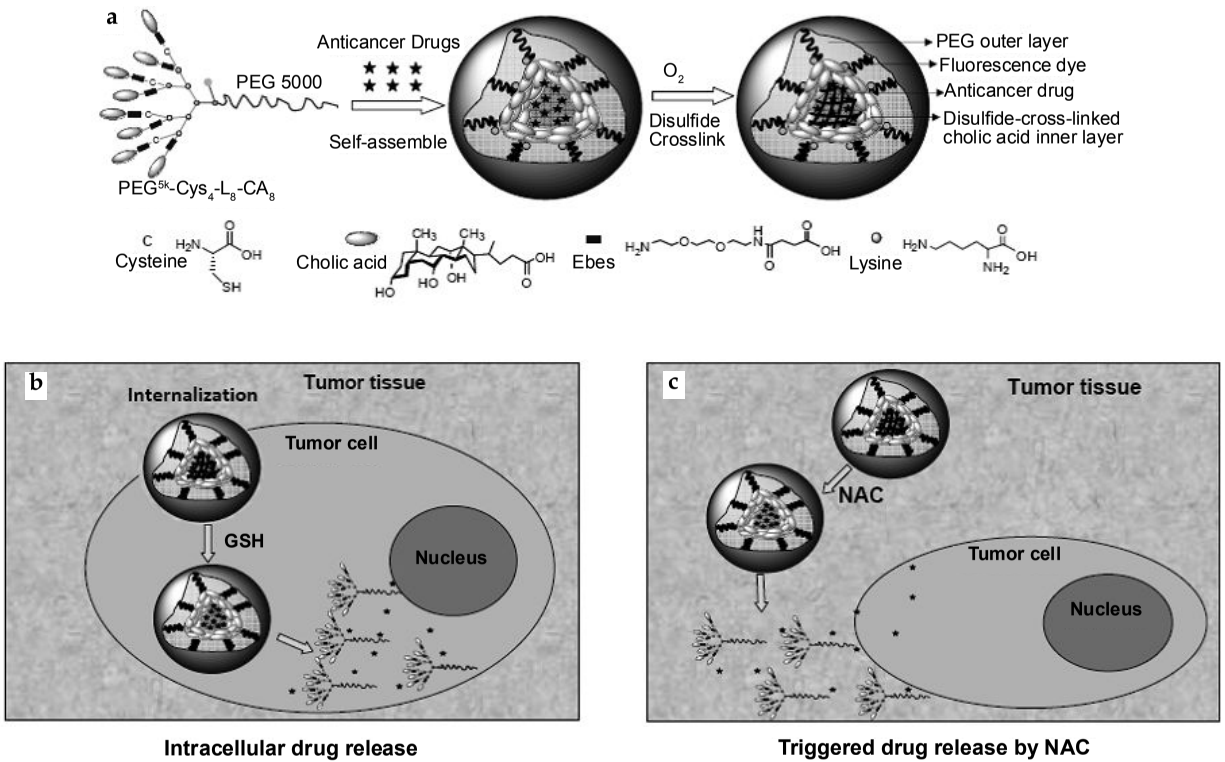

Figure 4.2. Schematic representation of DCMs formed by oxidization of thiolated telodendrimer PEG^{5k}-Cys_4-L_8-CA_8 after self-assemble (a). Schematic illustration of the hypothesized mechanisms for reducing agents (b: glutathione, GSH; c: N-acetylcysteine, NAC) mediated drug release once the PTX-DCMs is accumulated into the tumor site. Adapted with permission from Matsumoto et al. (2009). Copyright Elsevier (2009).

were first introduced onto the poly(L-lysine) backbone of the well-defined amphiphilic telodendrimer PEG^{5k}-CA_8. The resulting micelles were then cross-linked by disulfide bond through air oxidation (Matsumoto et al. 2009). The stability of the micelles was studied by monitoring the change in particle size by Dynamic Light Scattering (DLS) after the addition of Sodium Dodecyl Sulfate (SDS), an ionic-detergent, which has been reported to be able to efficiently break down polymeric micelles (Koo et al. 2008). The immediate disappearance of particle signal (light scattering signal) of the parent PEG^{5k}-CA_8 micelles reflects the distinct dynamic association-dissociation property of non-cross-linked micelles (NCMs) (Fig. 4.3a). The maintenance of constant particle size of the DCMs under similar condition over days indicated that such cross-linked nanoparticles remained intact. However, in the presence of SDS and the reducing agent (10 mM GSH), the particle signal of DCMs remained unchanged for 30 minutes until it disappeared suddenly (within 10 seconds), indicating that rapid dissociation of the micelle occurred when a critical number of disulfide bonds are reduced. As shown in Fig. 4.3b, the release of the encapsulated PTX from cross-linked micelles was much slower than from the non-cross-linked ones. However, in the presence of 10 mM GSH, the release rate increased to approximately the same as that of the NCMs, indicating the cleavage of the disulfide cross-links. *N*-acetylcysteine (NAC), a Food and Drug Administration (FDA) approved reducing agent, was also found to have the same effect as GSH in triggering the PTX release from DCMs. Therefore, NAC can be applied *in vivo* as an on-demand cleavage agent to trigger drug release from DCMs when they are accumulated into the tumor sites.

Some functional polymeric micelles with ionic cores containing disulfide cross-links have been developed for the delivery of genes (Kakizawa et al. 1999, Matsumoto et al. 2009), and chemotherapeutic agents (Kim et al.

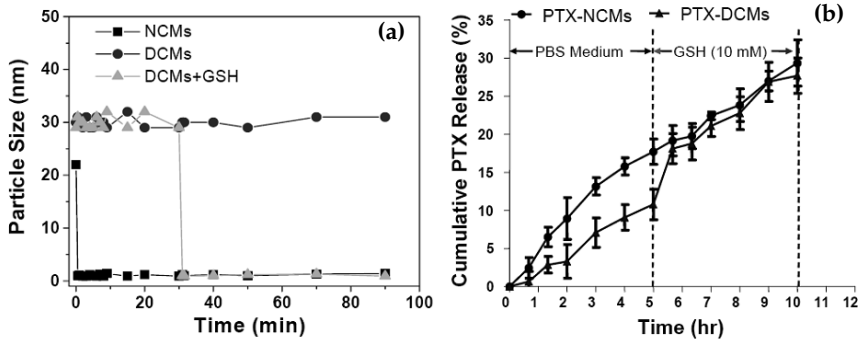

Figure 4.3. (a) Stability in particle size of NCMs and DCMs in the presence of 2.5 mg/mL SDS measured by DLS. (b) GSH-responsive PTX release profiles of PTX-DCMs by adding GSH (10 mM) at a specific release time (5 hours) comparing with PTX-NCMs. Adapted with permission from Koo et al. (2008). Copyright RSC Publishing (2008).

2010a). The reversible cross-linking of a PEG-*b*-poly(L-lysine) micelle was demonstrated by the Kataoka's group (Kakizawa et al. 1999), by the selective introduction of thiol groups to a fraction of the lysine repeat units and then assembly to form a PIC micelle with a poly(aspartic acid) polymer. Upon assembly into spherical structures, thiol residues in the lysine core domain were oxidized to form disulfide linkages between polymer chains and afforded a stabilized and robust core-cross-linked micelle. These cross-links throughout the core domain are reversible as they contain disulfide bonds, which can be readily cleaved upon addition of a reducing agent such as DTT or GSH. Kim et al. (2010a) have reported the use of Block Ionomer Complexes (BICs) of poly(ethylene oxide)-*b*-poly (methacylic acid) (PEO-*b*-PMA) and divalent metal cations (Ca^{2+}) as templates. Disulfide bonds were introduced into the ionic cores by using cystamine as a biodegradable cross-linker. The resulting DCMs demonstrated time-dependent degradation in the conditions mimicking the intracellular reducing environment by using DTT. The ionic character of the cores allowed a very high level of DOX loading (50%, w/w) into the cross-linked micelles. These DOX-loaded cross-linked micelles exhibited higher cytotoxicity against ovarian carcinoma cells as compared to micellar formulations without disulfide linkages.

pH-sensitive cross-linked micelle system

The pH-responsive cross-linked micelle system has attracted great attention because of the pH variations within the body. For instance, the pH changes from very acidic in stomach (pH 1–2) to more basic in the intestine (pH 5–8) along the gastrointestinal tract, which has to be considered for oral drug delivery. pH differences within different tissues and cellular compartments are more subtle. For example, the pH value in extracellular environment of cancerous tissue is slightly acidic (pH 6.5–7.2). The pH is ≈ 7.4 in cytosol of normal tissue and blood. In endosome, the pH is ≈ 5.0–6.5, and lysosome has an even lower pH of 4.5–5.0. This intrinsic characteristic of the body in terms of pH values has been used to direct the response to a certain tissue (e.g., tumor tissue) or cellular compartment.

Jiang and his colleagues have reported the development of pH-responsive polymeric hollow spheres formed by self-assembly of graft copolymers based on hydroxyethyl cellulose-*g*-poly(acrylic acid) (HEC-*g*-PAA) in aqueous media (Dou et al. 2003). HEC-*g*-PAA was readily dissolved in solutions with pH range of 4 to 13.5. As the pH was decreased to less than 4, 250–330 nm core-shell micelles were formed because of the transition from individual molecules to aggregates. PAA chains of micelles were then cross-linked. Upon increasing the pH (pH > 3), the micelles reversibly changed into hollow spheres with a particle size ≈ 600 nm. Both the micellization and the transition from micelles to hollow spheres were reversible. However,

the hollow spheres showed "on-off" character at a pH of 2–4, which is not in a biologically relevant pH range.

A type of acid-labile, core-cross-linked amphiphilic block copolymer micelles for pH-triggered release of DOX was reported by Chan et al. (2008). Micelles of a model amphiphilic block copolymer, poly(hydroxyethyl acrylate)-*b*-poly(*n*-butyl acrylate) (PHEA-*b*-PBA), were cross-linked by copolymerization of a degradable cross-linker from the living RAFT-end groups of PBA chains, yielding a cross-linked core. The cross-linked micelles possessed a similar size as the original NCM. High DOX loading capacities (60 wt %) were achieved by this type of cross-linked micelles. Hydrolysis of less than half of the cross-links in the core was found to be sufficient to release DOX faster at acidic pH compared to neutral pH.

Du and Armes (2005) reported pH-responsive self-cross-linked polymersomes from poly(ethylene glycol)-*b*-poly((2-(diethylamino)ethyl methacrylate)-*s*-(3-(trimethoxysilyl) propyl methacrylate)) (PEG-*b*-P(DEA-*s*-TMSPMA)). The 200–400 nm-sized vesicles formed spontaneously in aqueous/THF solution, with the pH-sensitive P(DEA-*s*-TMSPMA) blocks located in the membrane. The $-Si(OCH_3)_3$ groups in the hydrophobic block hydrolyzed *in situ* to $-Si(OH)_3$, which subsequently reacted to produce siloxane cross-links. The swelling of the membrane and therefore the permeability of the vesicle walls can be tuned in different pHs due to the pH dependent ionization state of the PDEA block.

Hydrolyzable cross-linked micelle system

Several biodegradable polymers, such as polylactate (PLA) or poly(ε-caprolactone) (PCL), have been utilized to design hydrolyzable cross-linked micelles. For example, core-cross-linked biodegradable polymeric micelles composed of methoxy poly(ethylene glycol)-*b*-poly[*N*-(2-hydroxypropyl) methacrylamide-lactate] (mPEG-*b*-p($HPMA_m$-Lac_n)) diblock copolymers have been reported by Talelli et al. (2010a). These micelles have shown prolonged circulation in the blood stream upon intravenous administration and enhanced tumor accumulation through EPR effect. The DOX-methacrylamide (DOX-MA) derivative was incorporated and covalently linked into the micellar core by using free radical polymerization. The structure of the DOX derivative exhibited pH dependence, enabling controlled release of the drug in acidic conditions. Thirty to forty percent w/w of the DOX-MA was covalently trapped in the core of the micelles, and the drug-loaded micelles had an average diameter of 80 nm. Most of the drug contents were released from the micelles within 24 hours incubation at pH 5 and 37°C, whereas only about 5% of drug release was observed at pH 7.4 at the same temperature. DOX-loaded micelles showed higher cytotoxicity against B16F10 melanoma and OVCAR-3 ovarian cancer cells compared

to small molecule DOX-MA, likely due to enhanced cellular uptake of the micelles via endocytosis and triggered intracellular drug release by the acidic endosome pH. The micelles showed better therapeutic efficacy than the free DOX in mice bearing B16F10 melanoma carcinoma.

Lee et al. (2011) reported a biocompatible, robust polymer micelle bearing pH-hydrolyzable shell cross-links for intracellular delivery of DOX. The triblock copolymer of poly(ethylene glycol)-poly(L-aspartic acid)-poly(L-phenylalanine) (PEG-PAsp-PPhe) self-assembled to form polymer micelles with three distinct domains, namely, the PEG outer corona, the PAsp middle shell and the PPhe inner core. The shell of the micelles was cross-linked by the reaction of ketal-containing cross-linkers with Asp moieties in the middle shells. The shell cross-linking of the micelles did not affect the size of the micelles and their spherical morphology. The formation of shell cross-linked diffusion barrier was confirmed by fluorescence quenching experiments, as judged by the reduced Stern-Volmer quenching constant (KSV). DLS and fluorescence spectroscopy experiments showed that shell cross-linking improved the micellar physical stability even in the presence of strong detergent. The hydrolysis kinetics study showed that the hydrolysis half-life of ketal cross-links was 74-fold faster at pH 5.0 than that at pH 7.4. The ketal cross-linked micelles also showed the rapid DOX release at endosomal pH (pH 5.0), compared to physiological blood pH (pH 7.4).

Multi-responsive cross-linked micelle system

Currently, second generation reversibly cross-linked micelles able to respond to multiple stimuli are being actively pursued as tools for achieving the multistage delivery of drugs to the complex *in vivo* microenvironment (Ma et al. 2010, Dai et al. 2011, Wei et al. 2011). These stimuli include: pH/reduction, temperature/reduction, temperature/pH and pH/cis-diol. This section presents the recent advance in the development of reversibly cross-linked micelle systems responsive to multiple stimuli.

pH/reduction responsive cross-linked micelle system

Shuai and co-workers described a Highly Packed Interlayer-Cross-linked Micelle (HP-ICM) with reduction and pH dual sensitivity, which comprises a PEG corona to stabilize the particles, a highly compressed pH-sensitive partially hydrated core to load anticancer drugs and a disulfide cross-linked interlayer to tie up the core against expansion at neutral pH (Dai et al. 2011). The HP-ICM was stable and no obvious drug leakage from the micelles was observed in a neutral pH environment without a reducing agent. However, the pH-sensitive core of the micelles was unpacked and the encapsulated

anticancer drug was released extensively when the HP-ICM was internalized into cells with a low pH (≈ 5) and reducing environment.

Disassembly of polymeric nanoparticles into their component polymer chains triggered by the simultaneous application of two different stimuli (pH/reduction) has been described by Dai et al. (2011). RAFT polymerization was utilized to prepare acrylamide-based linear copolymers displaying pyridyl disulfide appendages and either aldehyde or amine functional groups. These copolymer chains were intermolecularly cross-linked through imine bond formation at pH 8.0 followed by disulfide bond formation to afford multiple polymer chain cross-linked polymeric nanoparticles. A cargo of small hydrophobic molecules, such as nile red, could be encapsulated into these polymeric nanoparticles during the cross-linking reactions. The dissociation of the polymeric nanoparticles was achieved by the hydrolysis of the imine cross-links and cleavage of the disulfide cross-links at acidic pH (≈ 5.5) and in the presence of a reducing agent tris(2-carboxyethyl) phosphine (TCEP). They were able to demonstrate that application of either low pH alone or TCEP alone does not trigger the disassembly of the polymeric nanoparticle as there is sufficient density of the remaining imine or disulfide cross-links which are able to maintain the structural integrity of the polymeric nanoparticle.

Xu et al. (2009a) reported the synthesis of a pH-responsive triblock copolymer, methoxy poly(ethylene oxide)-*b*-poly(*N*-(3-aminopropyl) methacrylamide)-poly(2-(diisopropylamino)ethyl methacrylate) (mPEO-PAPMA-PDPAEMA) via aqueous RAFT polymerization. This triblock copolymer dissolves in aqueous solution at acidic pH (< 5.0) due to protonation of primary amine residues on the PAPMA block and tertiary amine residues on the PDPAEMA block. At higher pH (pH 6.0), the block copolymers self-assembled into micelles consisting of mPEO coronas, PAPMA shells and PDPAEMA cores. The micelles exhibited a hydrodynamic diameter ≈ 100 nm at pH 9.0 as demonstrated by DLS studies. A bi-functional, reversible cross-linker, dimethyl 3,3-dithiobispropionimidate (DTBP), was used to cross-link the micelles. The "one-pot" formation of shell-cross-linked micelles (SCMs) was accomplished at room temperature in water by mixing the triblock copolymers and DTBP at acidic pH (pH 3.0) followed by slowly increasing the solution pH to ≈ 9.0, leading to the simultaneous formation of micelles and cross-linking. These SCMs were found to be readily cleaved by the addition of the reducing agent DTT and can be re-cross-linked simply by exposure to air.

Temperature/reductive responsive cross-linked micelle system

The fabrication of dual temperature- and reductive-responsive core-cross-linked micelles co-functionalized with carbohydrate and biotin

moieties was reported by Jiang et al. (2009). Well-defined poly (2-aminoethylmethacrylamide) (PAEMA) homopolymer was first synthesized in a controlled fashion via RAFT polymerization. Core-cross-linked micelles comprising of PAEMA coronas and thermo-responsive cores were then obtained in a one-pot manner via RAFT copolymerization of *N*-isopropylacrylamide (NIPAM) and bis(2-methacryloyloxyethyl) disulfide (DSDMA) difunctional monomers by employing PAEMA as the macromolecular RAFT agent. The resulting cross-linked micelles can be disassembled into unimers due to the cleavage of disulfide cross-linkers in the presence of DTT, whereas deswelling of micellar cores can be achieved via heating above the phase transition temperature of PNIPAM. Therefore, drug release profiles for these nanocarriers can be triggered by temperature and reducing agents, or a combination of both.

Temperature/pH responsive cross-linked micelle system

Babin et al. (2008) reported the use of Atom Transfer Radical Polymerization (ATRP) to graft polymers onto preformed shell-cross-linked reverse micelles (SCRMs). Reverse polymer micelles were first prepared in organic solvents. The micellar shells were then cross-linked by photoinduced dimerization of coumarin groups. The SCRMs then served as micellar macroinitiators for further polymerization from their surface of monomers such as styrene and dimethylaminoethyl methacrylate (DMAEMA) via ATRP. The resulting nanocarriers were soluble in water and sensitive to changes in pH and temperature. These reversibly cross-linked micelles were also found to be sensitive to light. The micellar aggregates could be disintegrated by photo-induced cleavage of the cyclobutane bridges leading to the de-cross-linking of the shell and release of the payload.

Synthesis of pH- and thermosensitive core-cross-linked micelles via simultaneous self-assembling and cross-linking of thermoresponsive block copolymer such as poly(acryloyl glucosamine)-block-poly(*N*-isopropylacryamide) ($PAGA_{180}$-*b*-$PNIPAAM_{350}$) has been documented by Zhang et al. (2008a). An acid-labile cross-linking agent, 3,9-divinyl-2,4,8,10-tetraoxaspiro[5.5]-undecane, was used to generate thermosensitive and acid-degradable core-shell nanoparticles. These dual sensitive core-cross-linked micelles were stable against degradation at pH ≈ 6 and ≈ 8.2, but could be broken down to free block copolymers at lower pH (30 minutes and 12 hours, respectively at pH ≈ 2 and ≈ 4).

pH/cis-diol responsive cross-linked micelle system

Boronic acids are able to bind cis-diols forming reversible boronate esters that exhibit fast dual responsiveness to external pH and competing diols

(Springsteen and Wang 2002, Qin et al. 2005, Zhu et al. 2006, Sumerlin et al. 2008). Among diols, catechols are excellent reactants for the formation of complexes with boronic acids, because of the favorable syn-peri-planar arrangement of the aromatic hydroxyl groups combined with their electron-donating character (Springsteen and Wang 2002, Marken et al. 2010). On the basis of previously reported telodendrimers systems for efficient anticancer drug delivery, we have developed another novel class of dual-responsive Boronate Cross-linked Micelles (BCMs) for drug delivery based on the self-assembly and *in situ* complexation of boronic acid containing polymers and catechol containing polymers (Li et al. 2012a). Our hypothesis was that the micelles cross-linked by the well-known reversible boronic acid/catechol complexation, should be able to maintain their stability and minimize the premature drug release under physiological conditions, while selectively releasing the payload drugs at the targeted sites when triggered by low pH values or exogenous competing diols (Fig. 4.4). A series of BCMs, formed by using equal molar ratios of the boronic acid- and catechol-containing telodendrimers, were synthesized, and their physical properties including CMCs, particle size and stability were determined. BCM4, self-assembled from the telodendrimer pair of PEG_{5k}-NBA_4-CA_8 and PEG_{5k}-$catechol_4$-CA_8, stood out as one of the best candidates for additional drug delivery evaluation. BCM4 had no significant particle size change when exposed to 50% (v/v) human plasma for 24 hours, and even after being exposed to a 2.5 mg/mL SDS solution for two days. However, particle size of BCM4 decreased shortly in presence of SDS along with lower pH (pH 5.0) or excess of mannitol (100 mM, a safe FDA approved drug for diuresis), indicating that the micelle rapidly dissociated when a critical percentage of boronate bonds were hydrolyzed (Fig. 4.5a). PTX was used as a model drug to study the release kinetics of the reversible BCMs in comparison with the NCMs (Li et al. 2012a). The catechol-boronate bond weakens under acidic environment (pH 5). Therefore, it was expected that the drug will be released inside endosomes of tumor cells. Nanoparticles not taken up by the tumor cells but present at the tumor sites can be readily triggered to release drug with exogenously administered mannitol. Figure 4.5b shows the cumulative PTX release properties of the standard non-cross-linked and the BCMs, and the result of the triggered drug release by at pH 5, 100 mM mannitol or a combination of both triggering agents. PTX release from BCM4 was significantly slower than that from NCMs at the initial 5 hours. When 100 mM mannitol was added or the pH of the medium was adjusted to 5.0 at the 5 hours time point, there was a burst of drug release from the BCM4. It should be noted that PTX release can be further accelerated via the combination of 100 mM of mannitol and pH 5.0. This two-stage release strategy can be exploited so that premature drug release can be minimized

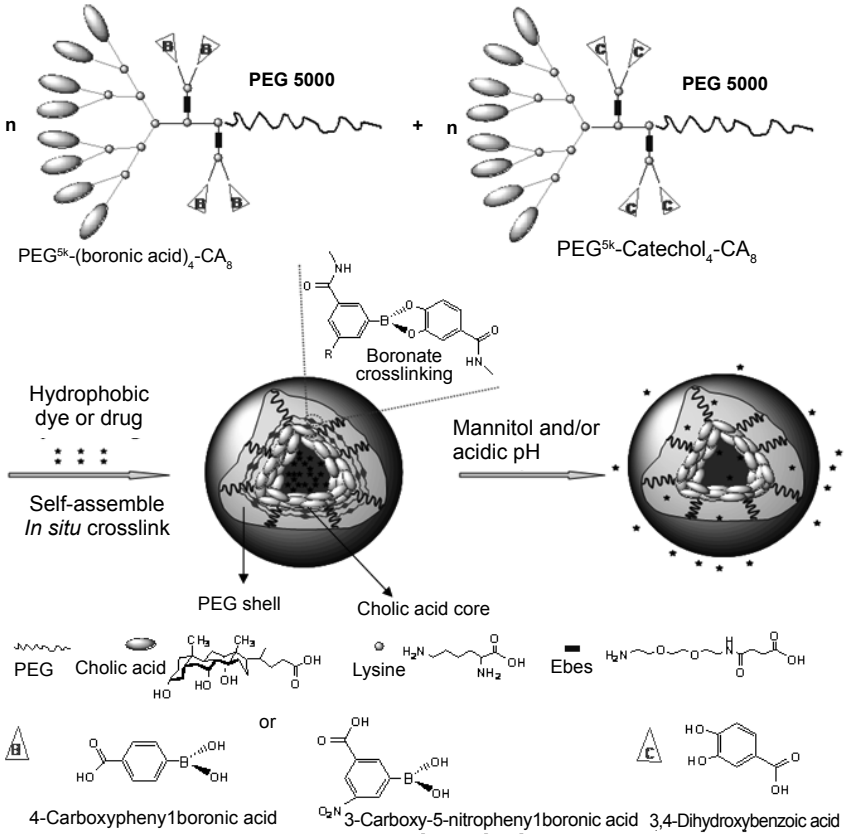

Figure 4.4. Schematic representation of the telodendrimer pair [PEG^{5k}-(boronic acid/catechol)$_4$-CA$_8$] and the resulting BCMs in response to mannitol and/or acidic pH. Adapted with permission from Li et al. (2012a). Copyright John Wiley & Sons, Inc. (2012).

during circulation *in vivo* followed by rapid drug release triggered by the acidic tumor microenvironment, or upon micelle exposure to the acidic compartments of cancer cells or by the administration of mannitol.

Applications of Reversibly Cross-linked Micelles for Drug Delivery

The various strategies to prepare reversibly cross-linked micelles have been discussed in the last section. In this section, we will focus on the preclinical application of reversibly cross-linked micelles for drug delivery, both *in vitro* and *in vivo*. This is summarized in Table 4.2.

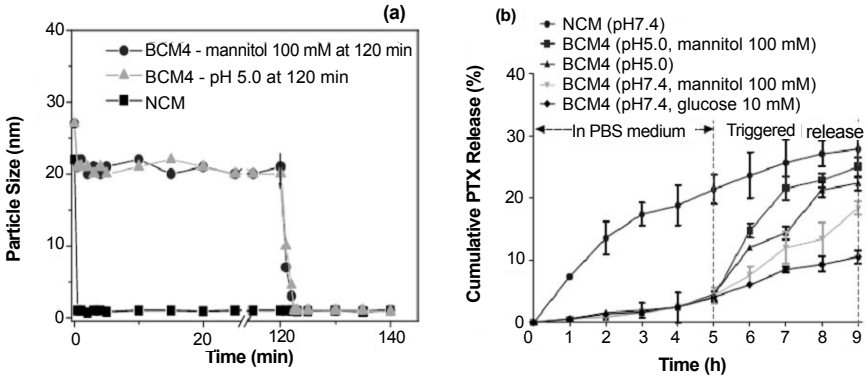

Figure 4.5. (a) Continuous DLS measurements of NCMs in SDS and BCM4 in SDS for 120 minutes, at which time mannitol was added or pH of the solution was adjusted to 5.0 (time: 120 minutes). (b) pH- and diol- responsive PTX release profiles of BCM4 by treating with diols (mannitiol and glucose) and/or pH 5.0 at 5 hours compared with that of NCMs. Adapted with permission from Li et al. (2012a). Copyright John Wiley & Sons, Inc. (2012).

In vitro drug delivery

Kataoka et al. reported an environment-responsive disulfide cross-linked polyion complex (PIC) through the assembly of iminothiolane-modified PEG-*b*-poly(L-lysine) for enhanced *si*RNA delivery (Matsumoto et al. 2009). The micellar structure was maintained at physiological ionic strength but was disrupted under reductive conditions because of the cleavage of disulfide cross-links, which is desirable for *si*RNA release in the intracellular reductive environment. They demonstrated that PIC DCMs achieved ≈ 100-fold higher *si*RNA (*si*RNA against Pp-Luc gene) transfection efficacy compared with non-cross-linked PIC assemblies of PEG-*b*-poly(L-lysine), which were not stable at physiological ionic strength. This indicates a significant improvement in *si*RNA transfection efficacy by the introduction of disulfide cross-links to the PIC DCM structure. Confocal laser scanning microscopic analysis further demonstrated that the incorporation of Cy5-labeled *si*RNA in cross-linked PIC DCMs significantly improved the cellular uptake, when compared to naked Cy5-*si*RNA or Cy5-*si*RNA transfected with non-cross-linked PEG-*b*-poly(L-lysine). These results suggested that the highly efficient knockdown of the Pp-Luc gene by PIC DCMs was achieved by an effective uptake of *si*RNA in the cell, presumably due to the formation of a stable micellar structure.

Lee and co-workers reported biocompatible, cell-permeable disulfide cross-linked PEG-poly(amino acids) copolymer micelles based on the self-assembling ABC triblock copolymer of poly(ethylene glycol)-*b*-poly(L-lysine)-*b*-poly(L-phenylalanine) (PEG-*b*-PLys-*b*-PPhe) (Koo et al. 2008).

Table 4.2. Illustrative examples of the *in vitro* and/or *in vivo* applications of the reversibly cross-linked micelles.

Reversible cross-linking type	Polymer	Delivered drug	Properties	*In vitro* and/or *in vivo* therapeutic outcome	Reference
Disulfide cross-linking	Pluronic® F-127	PTX	The core-cross-linked micelles were stable, and showed minimal drug release under a non-reductive environment. The micelles also released drugs rapidly and quantitatively in response to the intracellular level of the reducing potential	PTX-loaded micelles (1.5 mg/mL) displayed ≈ 39% cell viability in A549 cells	Abdullah-Al-Nahain et al. 2011
	Telodendrimers comprised of linear PEG and a dendritic cluster of cholic acids	PTX, VCR	The release of PTX/VCR from the DCMs was significantly slower than that from NCMs, but can be gradually facilitated by increasing the concentration of reducing agent (glutathione) to an intracellular reductive level	DCMs demonstrated a longer blood circulation time, less hemolytic activities, and superior toxicity profiles in nude mice, when compared to NCMs. The *in vivo* anti-tumor efficacy of drug-loaded DCMs was better than both free drug and the NCMs formulation, and can be further enhanced by triggering drug release on-demand by the administration of the FDA approved reducing agent *N*-acetylcysteine	Li et al. 2011, Kato et al. 2012
	Poly(PEG methyl ether methacrylate)-*b*-poly(5′-O-methacryloyluridine)	Vitamin B_2	The loading capacity increased with increasing cross-linking degree. Drug release reached 60–70% after 7 hr in the presence of DTT, while the cross-linked micelle in the absence of DTT exhibited a delayed drug release	Cytotoxicity tests confirmed the biocompatibility of the polymers and the residues after reduction	Zhang et al. 2007

	Thiolated c(RGDfK)-PEG-*b*-poly(L-lysine)	Plasmid DNA	The physicochemical characteristics of the polyplex micelles are quite similar regardless of the thiolation degree or the introduction of RGD ligands	Polyplex micelles achieved remarkably enhanced transfection efficiency against cultured HeLa cells	Oba et al. 2008
	Iminothiolane-modified PEG-*b*-poly(L-lysine)	*si*RNA	The micelles showed a spherical shape of ≈ 60 nm in diameter with a narrow distribution. The micellar structure was maintained at physiological ionic strength but was disrupted under reductive conditions because of the cleavage of disulfide cross-links	This environment-responsive micelles achieved 100-fold higher *si*RNA transfection efficacy compared with non-cross-linked micelles prepared from PEG-*b*-poly(L-lysine)	Matsumoto et al. 2009
	PEG-*b*-PLys-*b*-PPhe	MTX	The release of trapped MTX was greatly retarded for SCMs compared to NCMs. At a cellular GSH level, the cleavage of disulfide linkages is more pronounced to accelerate MTX release	MTX-loaded SCMs showed GSH dose-dependent cellular toxicity against A549 lung carcinoma cells	Koo et al. 2008
	PEG-*b*-PCL	DOX	DOX was quantitatively released within 12 hr under a reductive environment, whereas minimal drug release (< 20%) was observed under non-reductive conditions	The shell-sheddable micelles accomplished a much faster DOX release inside cells and greater anticancer efficacy, compared to the reduction insensitive control	Sun et al. 2009
Boronate-catechol cross-linking	Boronic acid- or catechol- containing telodendrimers (PEG^{5k}-NBA_4-CA_8 or PEG^{5k}-$catechol_4$-CA_8)	PTX	PTX release from BCMs was significantly slower than that from NCMs, but can be accelerated by acidic pH values and/or mannitol	PTX-BCM4 was found to be considerably less cytotoxic than Taxol and PTX-loaded NCMs, but its cytotoxicity can be significantly enhanced at pH 5.0 in the presence of mannitol (100 mM)	Li et al. 2012a
Polyelectrolyte cross-linking	Poly(2-(dimethylaminoethyl methacrylate)-*b*-poly(PEG methacrylate)		The CMC was absent in the cross-linked system which exhibited a better stability against disintegration, and a slightly superior tendency to bind oligonucleotides	Cytotoxicity tests confirmed a significant improvement of the biocompatibility of the micelle compared to that of the highly toxic poly(2-(dimethylaminoethyl methacrylate)	Zhang et al. 2007

Cross-linking of PLys middle shells was performed by adding 3,3′-dithiobis (sulfosuccinimidylpropionate) (DTSSP) to an aqueous solution of PEG-*b*-PLys-*b*-PPhe. MTX was able to be efficiently encapsulated into the polymer SCMs. Interestingly, MTX release from SCMs was much slower than that from NCMs, which would minimize the loss of the trapped drug before reaching the target tissue. MTX release profiles from SCMs at different GSH concentrations were further investigated. At the extracellular GSH level (2 mM), the MTX release pattern from SCM was similar to that of SCM in the release media without GSH. However, the MTX release from SCMs was gradually facilitated as the GSH concentration increases up to the cytoplasm level. Fluorescence microscopy images showed that fluorescein isothiocyanate (FITC)-labeled SCMs were internalized into A549 lung carcinoma cells and localized mainly in the cytoplasm. The GSH-mediated MTX release was further evaluated in living cells by manipulating the intracellular GSH concentration through adding glutathione monoester (GSH-OEt) into the culture media. As the GSH-OEt concentration increases, the inhibition activity for cell proliferation was enhanced, which indicates that GSH is responsible for modulating the MTX release from the SCM with GSH-reducible shell cross-links.

As mentioned in the last section, we have recently developed a novel class of reversible DCMs based on thiolated linear-dendritic polymers (telodendrimers) comprised of linear poly(ethylene glycol) (PEG) and a dendritic cluster of cholic acids (Li et al. 2011). The DCMs were able to easily encapsulate PTX in the core with superior loading capacity up to 35.5% (w/w, drug/micelle). The release of PTX from the DCMs was significantly slower than that from NCMs, but can be gradually facilitated by increasing the concentration of reducing agent (GSH) to an intracellular reductive level or by the administration of exogenous NAC. This two-stage drug release strategy can be exploited to ensure prevention of premature drug release during circulation *in vivo*, and fast drug release upon the internalization of DCMs into cancer cells. It is essential to investigate internalization, since the GSH-mediated drug release from DCMs should occur inside the cells. Confocal microscopy images demonstrated that fluorescence dye DiD-labeled DCMs were efficiently internalized into SKOV-3 ovarian cancer cells, and were mainly localized in the cytoplasmic region (Fig. 4.6a). To demonstrate whether the blank DCMs are biocompatible and non-toxic, 3-[4,5-dimethylthiazol-2-yl]-2,5-diphenyl tetrazolium bromide (MTT) colorimetric cell viability assays were performed and the results showed no observable *in vitro* cytotoxicity for blank DCMs up to 1.0 mg/mL (Fig. 4.6b). In addition, PTX-DCMs were found to be less cytotoxic than equivalent dose of Taxol® and PTX-NCMs, which was probably due to the slower release of PTX from DCMs in the cell culture media and inside the cells after their cellular uptake. To investigate whether the enriched

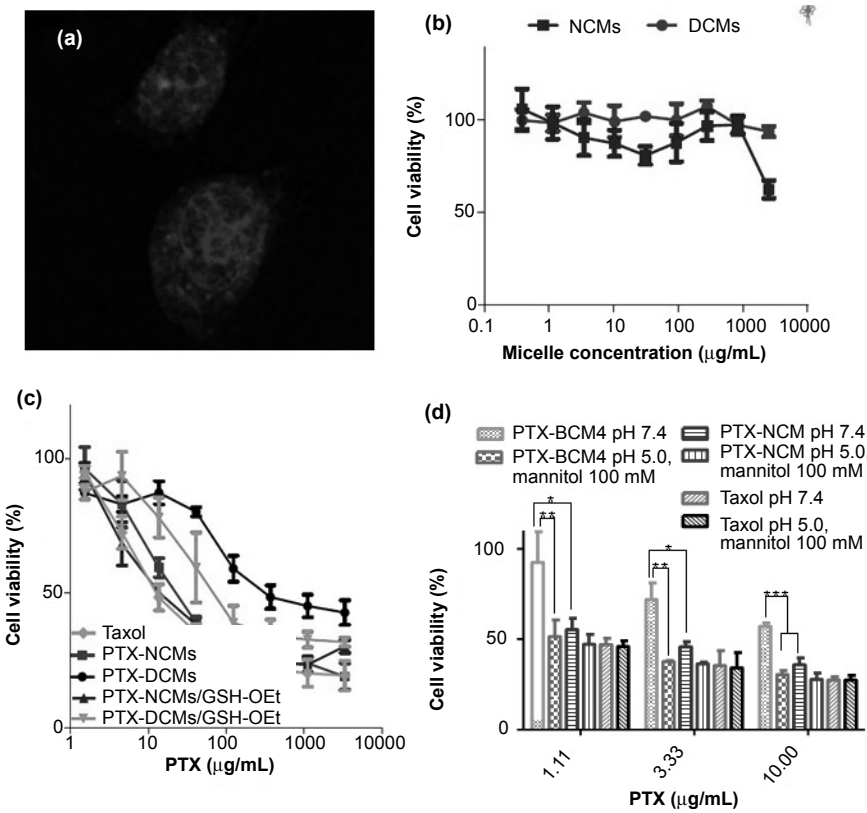

Figure 4.6. (a) Cellular uptake of DiD-labeled DCMs in SKOV-3 ovarian cancer cells after 3 hours incubation time, observed by confocal microscopy, and cell viability of SKOV-3 cells treated with (b) different concentrations of blank NCMs and DCMs, (c) Taxol®, PTX-NCMs and PTX-DCMs with and without pre-treatment of 20 mM GSH-OEt, and (d) Taxol®, PTX-NCMs and PTX-BCM4 with or without treatment with 100 mM mannitol at pH 5.0. Adapted with permission from Li et al. (2011). Copyright Elsevier (2011).

Color image of this figure appears in the color plate section at the end of the book.

GSH level in the cytoplasm could enhance the intracellular drug release of PTX-DCMs, SKOV-3 cells were pre-treated with 20 mM GSH-OEt for 2 hours, followed by the treatment with PTX nanoformulations. The results demonstrated that pre-incubation of cells with GSH-OEt enhanced the *in vitro* cytotoxicity of PTX-DCMs (Fig. 4.6c).

We also evaluated the *in vitro* anticancer activity of PTX-loaded reversible BCMs (PTX-BCM4) in comparison with PTX-loaded NCMs (PTX-NCMs) and Taxol® on SKOV-3 ovarian cancer cells for 1 hour incubation followed by PBS wash and 23 hours further incubation. PTX-NCMs showed comparable *in vitro* antitumor effects against SKOV-3 cells as Taxol®

(Fig. 4.6d). PTX-BCM4 was found to be considerably less cytotoxic than Taxol® and PTX-NCMs at equal dose levels, probably given the slower PTX release from BCM4 within the cell culture media (pH 7.4, 5.5 mM glucose) (Fig. 4.6d). There were minimal changes in the toxicity profile of PTX-NCMs and free drug triggered with acidic pH and mannitol. In contrast, PTX-BCM4 showed significantly enhanced cancer cell kill at pH 5.0 in the presence of mannitol (100 mM) (Fig. 4.6d). As described above, the combination of acidic pH and mannitol facilitated drug release because of cleavage of the cross-linking boronates of BCM4 resulting in enhanced cytotoxicity. Due to the enhanced stability, BCM4 is expected to be able to deliver higher concentrations of PTX to the tumor site than NCMs for *in vivo* applications. Thus, subsequent drug release on-demand should result in better antitumor effects.

Pharmacokinetics and biodistribution

It is generally believed that the cross-linking could stabilize the micelles against premature dissociation upon dilution and interaction with plasma proteins and lipoproteins (i.e., HDL, LDL, VLDL, and chylomicron), prolong the blood circulation time of micelles, and eventually allow drug accumulation into the tumor tissue via the so-called EPR effect (Matsumura and Maeda 1986). Since micelle nanoformulation could greatly affect the pharmacokinetic profiles of encapsulated drugs, it is very important to monitor the pharmacokinetics and biodistribution of cross-linked micelles to understand and predict their efficacy and side effects. Currently, it is still challenging to find a method to directly observe and quantify micelles under *in vivo* conditions, although some indirect methods such as radio-labeling or fluorescent-labeling of polymer carriers and/or drug payloads are the most efficient way so far to determine the *in vivo* fate of polymeric micelles. However, it should be kept in mind that these indirect methods are not able to differentiate micelles from unimers, once the micelles are disintegrated.

The pharmacokinetics and biodistribution of ^{3}H-labeled core-cross-linked micelles based on $mPEG_{5000}$ and *N*-(2-hydroxyethyl) methacrylamide-oligolactates were investigated in 14C (head and neck squamous cell carcinoma line)-tumor bearing mice, when compared with those of the corresponding NCMs with similar particle size (50–60 nm) (Rijcken et al. 2007). The NCMs were rapidly eliminated from circulation and only 6% of the Injected Dose (ID) was present in blood after 4 hours. At 4 hours post-injection, low amounts (1% of the ID) resided in the spleen while liver uptake was high (28% of the ID). NCMs showed some initial tumor localization at early time points (2.5% ID at 4 hours post-injection), however only 1.1% ID/g was recovered in the tumors after 24 hours, thus indicating

the absence of significant extravasation and retention of the NCMs in the tumors. The blood polymer concentration directly after the administration of NCMs was approximately 1 mg/mL, which is far above the CMC (0.08 mg/mL). The rapid blood clearance of the NCMs is likely due to the premature dissociation of the micelles after the interactions with plasma proteins and lipoproteins, or the opsonization of micelles, which leads to macrophage recognition. In contrast, core-cross-linked micelles exhibited significantly prolonged circulation times and the Area Under the Curve (AUC) was substantially higher than that of NCMs (990 *vs*. 136% ID × hour/mL blood). After 24 hours, tumor accumulation of core-cross-linked micelles was almost 6 times higher than that of NCMs, while liver accumulation was more than 2-fold lower than that of NCMs (10 *vs*. 24% ID). More importantly, a considerable tumor accumulation was observed after 48 hours (5.8% ID/g) although blood levels of ^{3}H-labeled core-cross-linked micelles were negligible by then. This clearly indicates that these core-cross-linked micelles were able to extravasate from the circulation and were retained into the tumor tissue, which is likely due to their prolonged blood retention and efficient tumor permeability as a result of their small size.

Sill et al. reported the *in vivo* pharmacokinetics of daunorubicin-loaded pH-reversibly cross-linked micelles based on triblock copolymer consisting of PEG-*b*-poly (aspartic acid)-*b*-poly(D-leucine-*co*-tyrosine) (Rios-Doria et al. 2012). The poly(aspartic acid) middle block is the cross-linking block that stabilizes the micelle based on the metal acetate chemistry. In contrast to cross-linking in the core or shell of the micelle, this pH-reversible cross-linking in the middle block is advantageous since it does not interfere with the core region (where the drug resides). Rats were intravenously injected with 10 mg/Kg of free daunorubicin, non-cross-linked daunorubicin micelles, or cross-linked daunorubicin micelles and the concentration of daunorubicin in plasma was determined over 24 hours. The results demonstrated that AUC of cross-linked daunorubicin micelles was 90-fold higher than that of free daunorubicin, and 78-fold higher than that of non-cross-linked daunorubicin micelles (Fig. 4.7a). Cross-linked daunorubicin micelles also exhibited a 46-fold higher maximum plasma concentration (C_{max}) than free daunorubicin and a 59-fold higher C_{max} than NCMs. These data demonstrated that the pH-reversible cross-linking significantly increase the *in vivo* stability of the drug-loaded micelles.

We have used the fluorescent-labeling method to investigate the kinetics of *in vivo* blood elimination and biodistribution of our previously developed DCMs. BODIPY 650/665, an organic near infrared dye, was conjugated to telodendrimers to track the *in vivo* fate of the carrier. A hydrophobic near infrared dye, DiD, was physically encapsulated into the core of the micelles as a drug surrogate to monitor the *in vivo* distribution of payloads. After the intravenous injection in mice, BODIPY signals of NCMs was rapidly

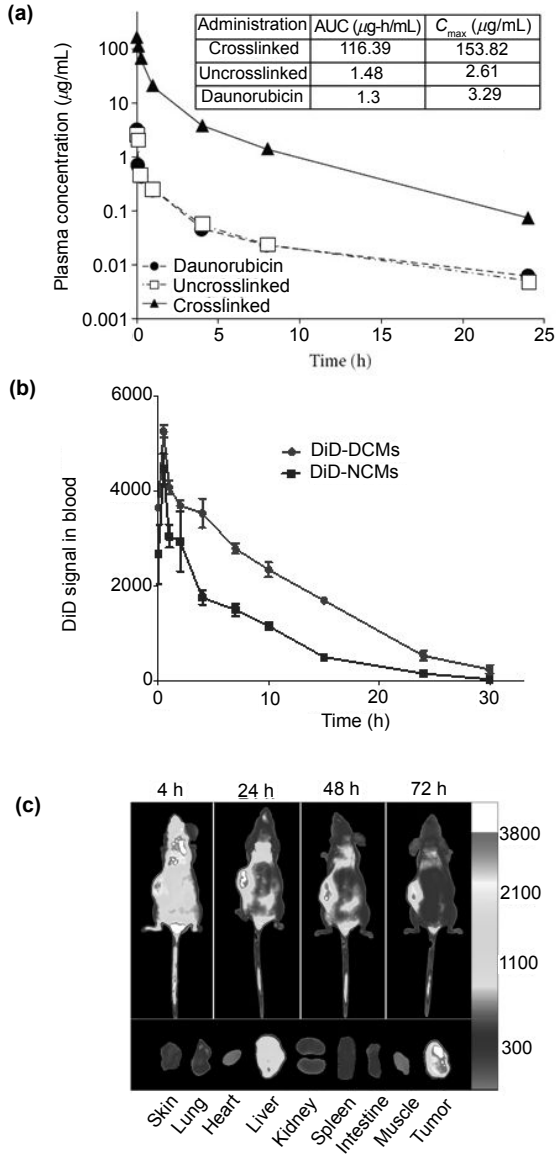

Figure 4.7. (a) Pharmacokinetics of daunorubicin-loaded micelles in Sprague-Dawley rats. The rats were given a single intravenous administration of cross-linked daunorubicin micelle, uncross-linked daunorubicin daunorubicin micelle or free daunorubicin at a 10 mg/Kg drug dose. *In vivo* pharmacokinetics (b) and biodistribution (c) of DiD-loaded DCMs and NCMs in nude mice bearing SKOV-3 ovarian cancer xenograft. Adapted with permission from Rios-Doria et al. (2012). Copyright Hindawi Publishing Corporation (2012).

Color image of this figure appears in the color plate section at the end of the book.

eliminated from circulation and fell into a background level within 8 hours post-injection. At 8 hours post-injection, BODIPY signal of DCMs in blood was 8 times higher than that of NCMs. A similar trend of circulation kinetics was observed for the DiD-loaded NCMs and DCMs. DiD payload from NCMs was eliminated much faster than that from DCMs during the entire period of time (Fig. 4.7b). The above profiles of elimination kinetics for both vehicle and payload indicated that the cross-linked micelles have longer blood circulation times than the NCMs. Non-invasive near infrared fluorescence optical imaging approach was utilized to monitor the biodistribution and tumor targeting ability of DiD-labeled micelles in SKOV-3 ovarian cancer xenograft bearing mice. We demonstrated that DiD and PTX co-loaded DCMs were preferentially accumulated into SKOV-3 tumors. A significant contrast of fluorescence signal was observed between tumor and background 4 hours after administration, which sustained up to 72 hours. *Ex vivo* imaging at 72 hours post-injection further confirmed the preferential uptake of DCMs in the tumor compared to normal organs (Fig. 4.7c).

We have also studied the kinetics of *in vivo* blood elimination of reversible BCMs compared with NCMs using rhodamine B-labeled micelles (Li et al. 2012a). After an intravenous injection into mice, the rhodamine B signal of NCMs was rapidly eliminated from blood circulation and fell into background levels within 10 hours post-injection. Rhodamine B signaling of BCM4 in blood was 6 times higher than that of NCMs at 10 hours post-injection and sustained for more than 24 hours. These kinetic profiles indicated that the cross-linked micelles have longer blood circulation times than the NCMs, and therefore may significantly improve the pharmacokinetic profile of many hydrophobic anticancer drugs that are difficult to formulate or have very poor pharmacokinetic profile.

To summarize, the few studies published so far on pharmacokinetics and biodistribution suggest that the cross-linking of micelles is able to prolong the circulation time, reduce the non-specific uptake by macrophages in spleen and liver and enhance tumor accumulation.

In vivo therapeutic efficacy

Although numerous studies of reversibly cross-linked micelles have been published in the last couples of years, most of these studies are still at a proof-of-concept stage. Despite some promising investigations which have demonstrated that reversibly cross-linked micelles exhibit controlled and on-demand drug release *in vitro* and *in vivo*, and favorable pharmacokinetics and biodistribution properties *in vivo*, only a few have so far further explored the actual therapeutic effects of drug-loaded cross-linked micelles in tumor bearing animals.

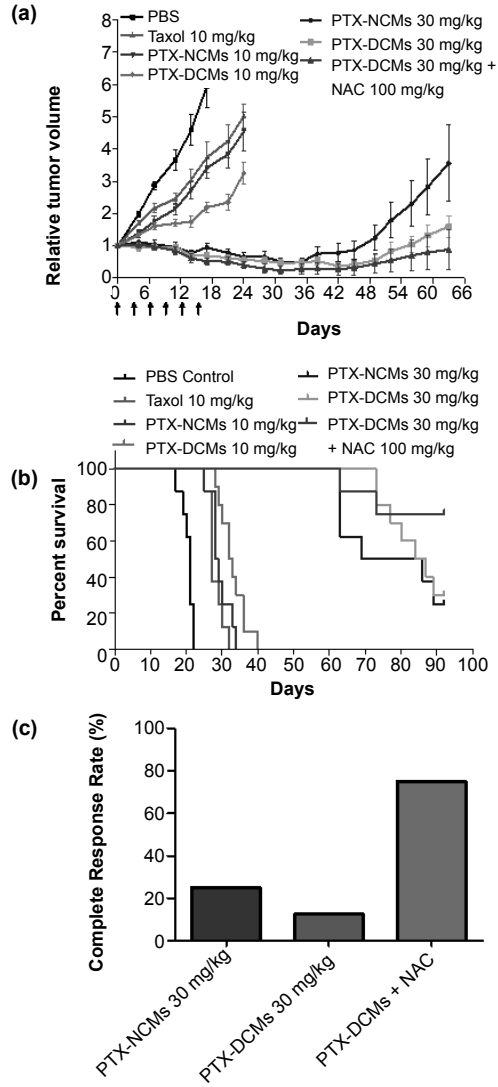

Figure 4.8. (a) *In vivo* antitumor efficacy after intravenous treatment of different PTX formulations in the subcutaneous mouse model of SKOV-3 ovarian cancer. Tumor bearing mice were administered intravenously with PBS (control) and PTX formulations (PTX-loaded NCMs: PTX-NCMs; and PTX-loaded DCMs: PTX-DCMs; equivalent dose of PTX: 10 mg/Kg) on days 0, 3, 6, 9, 12, 15 when tumor volume reached ≈ 100–200 mm^3 ($n = 8$). (b) Survival of mice in the treatment groups. (c) Complete tumor response rate (%) of mice treated with PTX-loaded NCMs, and PTX-loaded DCMs (equivalent dose of PTX: 30 mg/Kg) with or without the trigger release by NAC. Adapted with permission from Li et al. (2011). Copyright Elsevier (2011).

Color image of this figure appears in the color plate section at the end of the book.

We have recently evaluated the *in vivo* anticancer therapeutic efficacy and toxicity profiles of our newly developed DCMs for the targeted delivery of PTX and VCR in the treatment of ovarian cancer and B-cell lymphoma, respectively (Li et al. 2011, Kato et al. 2012). The results of our studies will be summarized in this section. The antitumor effect of PTX-loaded DCMs was evaluated in subcutaneous SKOV-3 ovarian cancer xenograft bearing mice, when compared with those of PTX-loaded NCMs and the clinical formulation of PTX (Taxol®) (Li et al. 2011). SKOV-3 tumor bearing mice ($n = 8$) were injected intravenously (tail vein) with different PTX formulations every 3 days (6 doses). Compared with the control group (injected with PBS), mice in all the other groups showed significant inhibition of tumor growth ($p < 0.05$). However, both nanoformulations of PTX (PTX-loaded NCMs and PTX-loaded DCMs) exhibited superior tumor growth inhibition (Fig. 4.8a), and longer survival time (Fig. 4.8b) compared to Taxol® at the equivalent dose of PTX (10 mg/Kg). These results can be attributed to the higher amount of PTX that reached the tumor site, thanks to the EPR effect associated to the micellar formulations. More importantly, tumor growth rate of mice treated with PTX-loaded DCMs was significantly lower than those treated with PTX-loaded NCMs at the equivalent PTX doses (10 and 30 mg/Kg). The enhanced *in vivo* therapeutic efficacy of PTX-loaded DCMs compared to PTX-loaded NCMs was probably because DCMs significantly prevented premature drug release, prolonged their circulation time, and facilitated a greater PTX delivery to the tumor site. It is expected that the high GSH level at the tumor site and particularly inside tumor cells, breaks up the disulfide cross-linking and facilitates drug release from the micelles. To accelerate PTX release from micelles after reaching the tumor site, we further tested the *in vivo* trigger release on demand by NAC (a reducing agent approved by the FDA for mucolytic therapy, Mucomyst®, and the treatment of acetoaminophen overdose). NAC was intravenously injected at a dose of 100 mg/Kg at 24 hours after the administration of every dose of PTX-loaded DCMs (equivalent dose of PTX: 30 mg/Kg). Results demonstrated that the combined use of PTX-loaded DCMs and NAC determined a greater antitumor effect (better tumor inhibition, prolonged survival time and higher complete tumor response rate) than the treatment without NAC (Fig. 4.8c). Thus, it can be said that NAC mainly played the role of a reducing agent to cleave the intramicellar disulfide bridges, and release the drug on-demand when DCMs accumulated into tumor site at 24 hours post-injection. This important *in vivo* observation has great translational potential and could be easily tested in clinical trials in the near future.

We have also investigated the therapeutic efficacy of VCR-loaded DCMs in a xenograft model of non-Hodgkin's lymphoma, compared to conventional VCR (Kato et al. 2012). All VCR treatments caused a

significant ($p < 0.05$) reduction in tumor growth as compared to the PBS control. Interestingly, mice receiving VCR-loaded DCMs (equivalent dose of VCR: 1 mg/Kg) did not exhibit a superior antitumor effect compared with conventional VCR at the same dose. However, in combination with on-demand addition of NAC, VCR-loaded DCMs exhibited a superior antitumor effect compared to conventional VCR. The enhanced efficacy might be attributed to the on-demand drug release from DCMs by NAC, once they accumulated at the tumor site, as discussed earlier. Although conventional VCR and VCR-loaded DCMs without NAC exhibited equivalent efficacy, the group of mice receiving VCR-loaded DCMs (with and without NAC) had significantly less body weight loss than the group of mice receiving conventional VCR. In terms of a clinical benefit, VCR-loaded DCMs may offer a less toxic treatment option that does not sacrifice efficacy. The greatest reduction in tumor volume was observed in the group receiving VCR-loaded DCMs (equivalent dose of VCR: 2.5 mg/Kg) ($p < 0.005$), with the equivalent amount of body weight loss as the 1 mg/Kg conventional VCR group. The toxicity profiles of different VCR formulations were further evaluated. It was found that VCR-loaded DCMs were well tolerated with no significant changes in complete blood count, serum chemistry and histology of the sciatic nerve.

Conclusions

Blood is a hostile environment for the micellar nanocarrier. After intravenous administration, the micelles encounter many different blood components leading to micellar dissociation and premature drug release. Electron paramagnetic resonance studies with spin-labeled telodendrimers have shown that the culprit blood components accelerating the dissociation of NCMs are the lipoprotein particles ubiquitously present in blood: HDL, LDL, VLDL and chylomicron (Li et al. 2012b). Covalent cross-linking of the micellar components avoids dissociation of the nanocarrier and premature drug release. It is clear from the few *in vivo* studies reported in the literature that reversibly cross-linked micelle can obviate this problem and achieve desirable therapeutic effects that nanomedicine has promised.

Most of the published work on reversibly cross-linked nanocarriers relies on the reductive microenvironment inside the cytoplasm or the acidic pH inside the endosomes of target cells. Therefore, to be fully effective, drug-loaded nanoparticles need to be delivered intracellularly. This can be achieved with nanocarriers decorated with cell surface targeting ligands that facilitate endocytic uptake (von Maltzahn et al. 2008, Song et al. 2009, Xiao et al. 2012). The introduction of on-demand cleavable linkers to the

drug nanocarrier allows to administer exogenous cleavage agents at the desirable moment to trigger drug release: *i*) at the target tissue for enhancing the therapeutic effects (Li et al. 2011, 2012a); or, *ii*) in blood circulation to release the therapeutic payload for rapid excretion, thus minimizing the side effects to the healthy organs. In a murine ovarian cancer xenograft model, it was demonstrated that the administration of NAC 24 hours after each dose of micellar PTX was superior to micellar PTX alone (Li et al. 2011). Although the result was promising, more work is needed to define the optimal delay time before giving the on-demand cleavage agent in mouse. Undoubtedly, the optimal delay time for murine model and human patient will be very different.

Addition of reversible cross-linkers to the nanocarrier will certainly add complexity and cost to their formulation. For successful clinical translation, scale-up production of the drug nanocarrier needs to be economical, reproducible and robust. In addition, shelf-life of the nanoformulation needs to be measured in months, particle size distribution needs to be narrow, and formulation procedures by the pharmacist at the clinic need to be simple and reproducible.

Unlike *hard* nanoparticles comprised of gold, silver or silica, which are not easily biodegradable, polymer-based micelles and their components are generally biodegradable or can be excreted by the kidneys. Nonetheless, it is important to understand the biodistribution of the cross-linked nanocarriers and their components to ensure that they are biodegradable and not toxic.

Although most drug-loaded nanoparticles will be administered intravenously, there will be clinical situations where other routes of administration are preferable. For instance, stage III ovarian cancer in which cancer cells are confined to the abdominal cavity, the best treatment approach may be to administer the drug nanocarrier both intravenously and intraperitoneally, a current practice for the administration of PTX in this disease. For pulmonary diseases, inhalation of aerosolized drug-loaded nanoparticles may be an excellent route. Intraocular injection may be the preferred route for drug delivery to the orbit. Depending on the disease indication, drug(s) to be delivered, and desired release kinetics and dynamics, different cross-links may be desirable.

In spite of the numerous challenges, we believe the future of nanotherapeutics is bright, especially for reversibly cross-linked and disease tissue specific targeting nanocarriers. Many drugs that had failed previously because of formulation or toxicity issues may possibly be resurrected by incorporating and adopting the reversibly cross-linked smart nanocarriers technology in the appropriate nanotherapeutic formulations.

Acknowledgements

Dr. Ivy kekessie and Mr. Joel Kugelmass for editorial help. NIH/NCI (R01CA115483 to K.S.L.), NIH/NIBIB (R01EB012569 to K.S.L.), Prostate Cancer Foundation Creative Award (to K.S.L.), US Department of Defense (DoD) PCRP Postdoctoral Training Award (W81XWH-12-1-0087 to Y.L.), and DoD BCRP Postdoctoral Fellowship Award (W81XWH-10-1-0817 to K.X.) for financial support.

Abbreviations

ATRP	:	atom transfer radical polymerization
AUC	:	area under the curve
BCMs	:	boronate cross-linked micelles
BICs	:	block ionomer complexes
C_{max}	:	maximum plasma concentration
CMC	:	critical micelle concentration
DCMs	:	disulfide cross-linked micelles
DLS	:	dynamic light scattering
DMAEMA	:	dimethylaminoethyl methacrylate
DNA	:	deoxyribonucleic acid
DOX	:	doxorubicin
DOX-MA	:	DOX-methacrylamide
DSDMA	:	bis(2-methacryloyloxyethyl) disulfide
DTBP	:	dimethyl 3,3-dithiobispropionimidate
DTSSP	:	3,3′-dithiobis(sulfosuccinimidylpropionate)
DTT	:	dithiothreitol
EPR	:	enhanced permeability and retention
FDA	:	Food and Drug Administration
FITC	:	fluorescein isothiocyanate
GSH	:	glutathione
GSH-OEt	:	glutathione monoester
HDL	:	high density lipoprotein
HEC-*g*-PAA	:	cellulose-*g*-poly(acrylic acid)
HP-ICM	:	highly packed interlayer-cross-linked micelle
ID	:	injected dose
KSV	:	Stern-Volmer quenching constant
LAs	:	lipoic acids
LDL	:	low density lipoprotein
MDR	:	multidrug resistance
mPEG-*b*-p ($HPMA_m$-Lac_n)	:	methoxy poly(ethylene glycol)-*b*-poly[*N*-(2-hydroxypropyl) methacrylamide-lactate]

mPEO-PAPMA -PDPAEMA	:	methoxy poly(ethylene oxide)-*b*-poly(*N*-(3-aminopropyl) methacrylamide)-poly(2-(diisopropylamino)ethyl methacrylate)
MTT	:	3-[4,5-dimethylthiazol-2-yl]-2,5-diphenyl tetrazolium bromide
MTX	:	methotrexate
NAC	:	*N*-acetylcysteine
NCMs	:	non-cross-linked micelles
NIPAM	:	*N*-isopropylacrylamide
PAEMA	:	poly(2-aminoethylmethacrylamide)
$PAGA_{180}$-*b*-$PNIPAAM_{350}$	:	poly(acryloyl glucosamine)-block-poly(*N*-isopropylacryamide)
PCL	:	poly(*ε*-caprolactone)
PEG	:	poly(ethylene glycol)
PEG-*b*-P(DEA -*s*-TMSPMA)	:	poly(ethylene glycol)-*b*-poly((2-(diethylamino) ethyl methacrylate)-*s*-(3-(trimethoxysilyl)propyl methacrylate))
PEG-*b*-PHPMA -LA	:	poly(ethylene glycol)-*b*-poly(*N*-2-hydroxypropyl methacrylamide)-lipoic acid
PEG-PAsp-PPhe	:	poly(ethylene glycol)-poly(L-aspartic acid)-poly(L-phenylalanine)
PEG-*b*-PLys-*b* -PPhe	:	poly(ethylene glycol)-*b*-poly(L-lysine)-*b*-poly(L-phenylalanine)
PEO	:	poly(ethylene oxide)
PEO-*b*-PMA	:	poly(ethylene oxide)-*b*-poly(methacylic acid)
PHEA-*b*-PBA	:	poly(hydroxyethyl acrylate)-*b*-poly(*n*-butyl acrylate)
PIC	:	polyion complex
PLA	:	polylactate
PTX	:	paclitaxel
RAFT	:	reversible addition-fragmentation chain transfer
SCMs	:	shell-cross-linked micelles
SCRMs	:	shell-cross-linked reverse micelles
SDS	:	sodium dodecyl sulfate
*si*RNA	:	small interfering ribonucleic acid
TCEP	:	tris(2-carboxyethyl)phosphine
VCR	:	vincristine
VLDL	:	very low density lipoprotein

References

Abdullah-Al-Nahain and H. Lee, Y.S. Lee, K.D. Lee and S.Y. Park. 2011. Development of disulfide core-cross-linked pluronic nanoparticles as an effective anticancer-drug-delivery system. Macromol. Biosci. 11: 1264–1271.

Babin, J. and M. Lepage and Y. Zhao. 2008. "Decoration" of shell cross-linked reverse polymer micelles using ATRP: a new route to stimuli-responsive nanoparticles. Macromolecules. 41: 1246–1253.

Black, S.M. and C.R. Wolf. 1991. The role of glutathione-dependent enzymes in drug resistance. Pharmacol. Ther. 51: 139–154.

Cabane, E. and X. Zhang, K. Langowska, C.G. Palivan and W. Meier. 2012. Stimuli-responsive polymers and their applications in nanomedicine. Biointerphases. 7: 9.

Cabral, H. and Y. Matsumoto, K. Mizuno, Q. Chen, M. Murakami, M. Kimura, Y. Terada, M.R. Kano, K. Miyazono, M. Uesaka, N. Nishiyama and K. Kataoka. 2011. Accumulation of sub-100 nm polymeric micelles in poorly permeable tumours depends on size. Nat. Nanotechnol. 6: 815–823.

Chan, Y. and T. Wong, F. Byrne, M. Kavallaris and V. Bulmus. 2008. Acid-labile core cross-linked micelles for pH-triggered release of antitumor drugs. Biomacromolecules. 9: 1826–1836.

Chang, C. and H. Wei, J. Feng, Z.C. Wang, X.J. Wu, D.Q. Wu, S.X. Cheng, X.Z. Zhang and R.X. Zhuo. 2009. Temperature and pH double responsive hybrid cross-linked micelles based on P(NIPAAm-co-MPMA)-b-P(DEA): RAFT synthesis and "schizophrenic" micellization. Macromolecules. 42: 4838–4844.

Dai, J. and S. Lin, D. Cheng, S. Zou and X. Shuai. 2011. Interlayer-cross-linked micelle with partially hydrated core showing reduction and pH dual sensitivity for pinpointed intracellular drug release. Angew Chem. Int. Ed. Engl. 50: 9404–9408.

Davis, M.E. and Z.G. Chen and D.M. Shin. 2008. Nanoparticle therapeutics: an emerging treatment modality for cancer. Nat. Rev. Drug Discov. 7: 771–782.

Dou, H. and M. Jiang, H. Peng, D. Chen and Y. Hong. 2003. pH-dependent self-assembly: micellization and micelle-hollow-sphere transition of cellulose-based copolymers. Angew Chem. Int. Ed. Engl. 42: 1516–1519.

Du, J. and S.P. Armes. 2005. pH-responsive vesicles based on a hydrolytically self-cross-linkable copolymer. J. Am. Chem. Soc. 127: 12800–12801.

Gosselin, M.A. and W. Guo and R.J. Lee. 2001. Efficient gene transfer using reversibly cross-linked low molecular weight polyethylenimine. Bioconjug. Chem. 12: 989–994.

Harada, A. and K. Kataoka. 2006. Supramolecular assemblies of block copolymers in aqueous media as nanocontainers relevant to biological applications. Prog. Polym. Sci. 31: 949–982.

Hennink, W.E. and M. Talelli, M. Iman, A.K. Varkouhi, C.J.F. Rijcken, R.M. Schiffelers, T. Etrych, K. Ulbrich, C.F. van Nostrum, T. Lammers and G. Storm. 2010. Core-cross-linked polymeric micelles with controlled release of covalently trapped doxorubicin. Biomaterials. 31: 7797–7804.

Jiang, X.Z. and S.Y. Liu and R. Narain. 2009. Degradable thermoresponsive core cross-linked micelles: fabrication, surface functionalization, and biorecognition. Langmuir. 25: 13344–13350.

Kakizawa, Y. and A. Harada and K. Kataoka. 1999. Environment-sensitive stabilization of core-shell structured polyion complex micelle by reversible cross-linking of the core through disulfide bond. J. Am. Chem. Soc. 121: 11247–11248.

Kato, J. and Y. Li, K. Xiao, J.S. Lee, J. Luo, J.M. Tuscano, R.T. O'Donnell and K.S. Lam. 2012. Disulfide cross-linked micelles for the targeted delivery of vincristine to B-cell lymphoma. Mol. Pharm. 9: 1727–1735.

Kellum, M.G. and A.E. Smith, S.K. York and C.L. McCormick. 2010. Reversible interpolyelectrolyte shell cross-linked micelles from pH/salt-responsive diblock copolymers synthesized via RAFT in aqueous solution. Macromolecules. 43: 7033–7040.

Kim, J.O. and G. Sahay, A.V. Kabanov and T.K. Bronich. 2010a. Polymeric micelles with ionic cores containing biodegradable cross-links for delivery of chemotherapeutic agents. Biomacromolecules. 11: 919–926.

Kim, J.E. and E.J. Cha and C.H. Ahn. 2010b. Reduction-sensitive self-aggregates as a novel delivery system. Macromol. Chem. Phys. 211: 956–961.

Koo, A.N. and H.J. Lee, S.E. Kim, J.H. Chang, C. Park, C. Kim, J.H. Park and S.C. Lee. 2008. Disulfide-cross-linked PEG-poly(amino acid)s copolymer micelles for glutathione-mediated intracellular drug delivery. Chem. Commun. (Camb.). 48: 6570–6572.

Lee, S.J. and K.H. Min, H.J. Lee, A.N. Koo, H.P. Rim, B.J. Jeon, S.Y. Jeong, J.S. Heo and S.C. Lee. 2011. Ketal cross-linked poly(ethylene glycol)-poly(amino acid)s copolymer micelles for efficient intracellular delivery of doxorubicin. Biomacromolecules. 12: 1224–1233.

Li, Y. and S. Pan, W. Zhang and Z. Du. 2009a. Novel thermo-sensitive core-shell nanoparticles for targeted paclitaxel delivery. Nanotechnology. 20: 065104.

Li, Y. and L. Zhu, Z. Liu, R. Cheng, F. Meng, J. Cui, S. Ji and Z. Zhong. 2009b. Reversibly stabilized multifunctional dextran nanoparticles efficiently deliver doxorubicin into the nuclei of cancer cells. Angew. Chem. Int. Ed. Engl. 48: 9914–9918.

Li, Y. and K. Xiao, J. Luo, W. Xiao, J.S. Lee, A.M. Gonik, J. Kato, T.A. Dong and K.S. Lam. 2011. Well-defined, reversible disulfide cross-linked micelles for on-demand paclitaxel delivery. Biomaterials. 32: 6633–6645.

Li, Y. and W. Xiao, K. Xiao, L. Berti, J. Luo, H.P. Tseng, G. Fung and K.S. Lam. 2012a. Well-defined, reversible boronate cross-linked nanocarriers for targeted drug delivery in response to acidic pH values and cis-diols. Angew. Chem. Int. Ed. Engl. 51: 2864–2869.

Li, Y. and M. Budamagunta, J. Luo, W. Xiao, J.C. Voss and K.S. Lam. 2012b. Probing of the assembly structure and dynamics within nanoparticles during interaction with blood proteins. ACS Nano. 6: 9485–9495.

Liu, J. and H. Lee and C. Allen. 2006. Formulation of drugs in block copolymer micelles: drug loading and release. Curr. Pharm. Des. 12: 4685–4701.

Liu, H. and X.Z. Jiang, J. Fan, G.H. Wang and S.Y. Liu. 2007. Aldehyde surface-functionalized shell cross-linked micelles with pH-tunable core swellability and their bioconjugation with lysozyme. Macromolecules. 40: 9074–9083.

Ma, N. and Y. Li, H. Xu, Z. Wang and X. Zhang. 2010. Dual redox responsive assemblies formed from diselenide block copolymers. J. Am. Chem. Soc. 132: 442–443.

Marken, F. and Y.J. Huang, Y.B. Jiang, J.S. Fossey and T.D. James. 2010. Assembly of N-hexadecyl-pyridinium-4-boronic acid hexafluorophosphate monolayer films with catechol sensing selectivity. J. Mater. Chem. 20: 8305–8310.

Matsumoto, S. and R.J. Christie, N. Nishiyama, K. Miyata, A. Ishii, M. Oba, H. Koyama, Y. Yamasaki and K. Kataoka. 2009. Environment-responsive block copolymer micelles with a disulfide cross-linked core for enhanced siRNA delivery. Biomacromolecules. 10: 119–127.

Matsumura, Y. and H. Maeda. 1986. A new concept for macromolecular therapeutics in cancer chemotherapy: mechanism of tumoritropic accumulation of proteins and the antitumor agent smancs. Cancer Res. 46: 6387–6392.

Meng, F. and Z. Zhong and J. Feijen. 2009a. Stimuli-responsive polymersomes for programmed drug delivery. Biomacromolecules. 10: 197–209.

Meng, F. and W.E. Hennink and Z. Zhong. 2009b. Reduction-sensitive polymers and bioconjugates for biomedical applications. Biomaterials. 30: 2180–2198.

Miyata, K. and Y. Kakizawa, N. Nishiyama, A. Harada, Y. Yamasaki, H. Koyama and K. Kataoka. 2004. Block catiomer polyplexes with regulated densities of charge and disulfide cross-linking directed to enhance gene expression. J. Am. Chem. Soc. 126: 2355–2361.

Oba, M. and K. Aoyagi, K. Miyata, Y. Matsumoto, K. Itaka, N. Nishiyama, Y. Yamasaki, H. Koyama and K. Kataoka. 2008. Polyplex micelles with cyclic RGD peptide ligands and

disulfide cross-links directing to the enhanced transfection via controlled intracellular trafficking. Mol. Pharm. 5: 1080–1092.

Peng, Q. and C. Hu, J. Cheng, Z.L. Zhong and R.X. Zhuo. 2009. Influence of disulfide density and molecular weight on disulfide cross-linked polyethylenimine as gene vectors. Bioconjug. Chem. 20: 340–346.

Qi, K. and Q.G. Ma, E.E. Remsen, C.G. Clark and K.L. Wooley. 2004. Determination of the bioavailability of biotin conjugated onto shell cross-linked (SCK) nanoparticles. J. Am. Chem. Soc. 126: 6599–6607.

Qin, Y. and V. Sukul, D. Pagakos, C.Z. Cui and F. Jakle. 2005. Preparation of organoboron block copolymers via ATRP of silicon and boron-functionalized monomers. Macromolecules. 38: 8987–8990.

Ranucci, E. and M.A. Suardi, R. Annunziata, P. Ferruti, F. Chiellini and C. Bartoli. 2008. Poly(amidoamine) conjugates with disulfide-linked cholesterol pendants self-assembling into redox-sensitive nanoparticles. Biomacromolecules. 9: 2693–2704.

Rijcken, C.J. and C.J. Snel, R.M. Schiffelers, C.F. van Nostrum and W.E. Hennink. 2007. Hydrolysable core-cross-linked thermosensitive polymeric micelles: synthesis, characterisation and *in vivo* studies. Biomaterials. 28: 5581–5593.

Rios-Doria, J. and A. Carie, T. Costich, B. Burke, H. Skaff, R. Panicucci and K. Sill. 2012. A versatile polymer micelle drug delivery system for encapsulation and *in vivo* stabilization of hydrophobic anticancer drugs. J. Drug Deliv. 2012: 951741.

Song, S. and D. Liu, J. Peng, H. Deng, Y. Guo, L.X. Xu, A.D. Miller and Y. Xu. 2009. Novel peptide ligand directs liposomes toward EGF-R high-expressing cancer cells *in vitro* and *in vivo*. FASEB J. 23: 1396–1404.

Springsteen, G. and B.H. Wang. 2002. A detailed examination of boronic acid-diol complexation. Tetrahedron. 58: 5291–5300.

Sumerlin, B.S. and D. Roy and J.N. Cambre. 2008. Sugar-responsive block copolymers by direct RAFT polymerization of unprotected boronic acid monomers. Chem. Commun. (Camb.). 21: 2477–2479.

Sun, J. and X. Chen, T. Lu, S. Liu, H. Tian, Z. Guo and X. Jing. 2008. Formation of reversible shell cross-linked micelles from the biodegradable amphiphilic diblock copolymer poly(L-cysteine)-block-poly(L-lactide). Langmuir. 24: 10099–10106.

Sun, H. and B. Guo, R. Cheng, F. Meng, H. Liu and Z. Zhong. 2009. Biodegradable micelles with sheddable poly(ethylene glycol) shells for triggered intracellular release of doxorubicin. Biomaterials. 30: 6358–6366.

Takae, S. and K. Miyata, M. Oba, T. Ishii, N. Nishiyama, K. Itaka, Y. Yamasaki, H. Koyama and K. Kataoka. 2008. PEG-detachable polyplex micelles based on disulfide-linked block catiomers as bioresponsive nonviral gene vectors. J. Am. Chem. Soc. 130: 6001–6009.

Talelli, M. and M. Iman, C.J. Rijcken, C.F. van Nostrum and W.E. Hennink. 2010a. Targeted core-cross-linked polymeric micelles with controlled release of covalently trapped doxorubicin. J. Control. Release. 148: e121–e122.

Talelli, M. and M. Iman, A.K. Varkouhi, C.J. Rijcken, R.M. Schiffelers, T. Etrych, K. Ulbrich, C.F. van Nostrum, T. Lammers, G. Storm and W.E. Hennink. 2010b. Core-cross-linked polymeric micelles with controlled release of covalently trapped doxorubicin. Biomaterials. 31: 7797–7804.

von Maltzahn, G. and Y. Ren, J.H. Park, D.H. Min, V.R. Kotamraju, J. Jayakumar, V. Fogal, M.J. Sailor, E. Ruoslahti and S.N. Bhatia. 2008. *In vivo* tumor cell targeting with "click" nanoparticles. Bioconjug. Chem. 19: 1570–1578.

Wang, Y.C. and Y. Li, T.M. Sun, M.H. Xiong, J. Wu, Y.Y. Yang and J. Wang. 2010. Core-shell-corona micelle stabilized by reversible cross-linkage for intracellular drug delivery. Macromol. Rapid Commun. 31: 1201–1206.

Wei, C. and J. Guo and C. Wang. 2011. Dual stimuli-responsive polymeric micelles exhibiting "AND" logic gate for controlled release of adriamycin. Macromol. Rapid Commun. 32: 451–455.

Xiao, K. and Y. Li, J.S. Lee, A.M. Gonik, T. Dong, G. Fung, E. Sanchez, L. Xing, H.R. Cheng, J. Luo and K.S. Lam. 2012. "OA02" peptide facilitates the precise targeting of paclitaxel-loaded micellar nanoparticles to ovarian cancer *in vivo*. Cancer Res. 72: 2100–2110.

Xing, M.M.Q. and C.H. Lu and W. Zhong. 2011. Shell cross-linked and hepatocyte-targeting nanoparticles containing doxorubicin via acid-cleavable linkage. Nanomedicine. 7: 80–87.

Xu, X.W. and A.E. Smith and C.L. McCormick. 2009a. Facile "one-pot" preparation of reversible, disulfide-containing shell cross-linked micelles from a RAFT-synthesized, pH-responsive triblock copolymer in water at room temperature. Aust. J. Chem. 62: 1520–1527.

Xu, Y. and F. Meng, R. Cheng and Z. Zhong. 2009b. Reduction-sensitive reversibly cross-linked biodegradable micelles for triggered release of doxorubicin. Macromol. Biosci. 9: 1254–1261.

Xu, X.W. and J.D. Flores and C.L. McCormick. 2011. Reversible imine shell cross-linked micelles from aqueous RAFT-synthesized thermoresponsive triblock copolymers as potential nanocarriers for "pH-triggered" drug release. Macromolecules. 44: 1327–1334.

Zhang, L. and T.L. Nguyen, J. Bernard, T.P. Davis, C. Barner-Kowollik and M.H. Stenzel. 2007. Shell-cross-linked micelles containing cationic polymers synthesized via the RAFT process: toward a more biocompatible gene delivery system. Biomacromolecules. 8: 2890–2901.

Zhang, L. and J. Bernard, T.P. Davis, C. Barner-Kowollik and M.H. Stenzel. 2008a. Acid-degradable core-cross-linked micelles prepared from thermosensitive glycopolymers synthesized via RAFT polymerization. Macromol. Rapid Commun. 29: 123–129.

Zhang, L. and W.G. Liu, L. Lin, D.Y. Chen and M.H. Stenze. 2008b. Degradable disulfide core-cross-linked micelles as a drug delivery system prepared from vinyl functionalized nucleosides via the RAFT process. Biomacromolecules. 9: 3321–3331.

Zhu, L. and S.H. Shabbir, M. Gray, V.M. Lynch, S. Sorey and E.V. Anslyn. 2006. A structural investigation of the N-B interaction in an o-(N,N-dialkylaminomethyl)arylboronate system. J. Am. Chem. Soc. 128: 1222–1232.

CHAPTER 5

Cyclodextrins in Drug Delivery

Nazlı Erdoğar[a] and *Erem Bilensoy*[b,*]

ABSTRACT

Cyclodextrins have been widely applied to the pharmaceutical field due to their ability to include hydrophobic molecules in their cavity and to mask certain physicochemical characteristics of the included molecule, such as, low water solubility, stability problems, unwanted side effects, taste, odor, irritation and incompatibility of drugs and excipients. Currently, a large number of cyclodextrin derivatives are produced industrially and used in many fields, such as, drug delivery, cosmetics, food, textile and agricultural industries. Cyclodextrins were first discovered in 1891 by Villiers. They are produced by an intramolecular trans-glycosylation reaction from the degradation of starch by the Cyclodextrin Glucosyltransferase (CGTase) enzyme. The molecular structure and shape render the unique ability to entrap guest molecules in their cavity as a molecular reservoir. Given the continuous finding of novel applications in drug delivery, it is expected that cyclodextrins will solve many problems associated with the delivery of active molecules through different delivery routes.

This chapter will deal with the general overview concerning the properties, toxicity and different application routes of cyclodextrins and their derivatives in the design of advanced drug delivery systems, i.e., liposomes, microspheres, microcapsules and nanoparticles. In addition to their well-known effects on drug solubility and dissolution, bioavailability, safety and stability, their use as excipients in drug formulation will be also

Department of Pharmaceutical Technology, Faculty of Pharmacy, Hacettepe University, 06100 Sıhhiye-Ankara, Turkey.

[a] Email: nerdogar@hacettepe.edu.tr

[b] Email: eremino@hacettepe.edu.tr

* Corresponding author

List of abbreviations after the text.

discussed. Various administration routes influencing the toxicity profiles, and on amphiphilic cyclodextrins as new excipients in drug delivery are also focused.

Introduction

Cyclodextrins (CDs) have been known for over 100 years. They were first discovered as "cellulosine" in 1891 by Villiers (1891). A few years later, Schardinger suggested that "crystalline dextrin" would be a better name for these molecules. During the period 1930s–1970s, the structures of α-, β-, γ-CDs, and some inclusion complexes were first determined by X-ray diffraction analysis. This was followed by the first patent and first fundamental review on CDs and derivatives published in 1953 and 1957, respectively (Freundenberg et al. 1953). At the end of 1960s, CDs were considered to be promising molecules, despite large scale commercial production was prevented due to their high cost and safety. Nowadays, CDs are used as potent, non-toxic, and multifunctional new pharmaceutical excipients. A large number of CD derivatives are produced industrially and used in many fields, such as, drug carriers, cosmetics, food, textile, and agricultural industries (Laza-Knoerr et al. 2010).

In this chapter, the more than promising applicability of CDs and derivatives in the development of advanced drug delivery systems and in drug formulation are updated. In this line, special emphasis is given to the analysis of their physical chemistry which determines their use as excipients to these aims.

General Overview of Cyclodextrins

Chemistry and properties

CDs are natural products resulting from the enzymatic degradation of starch with specialized bacteria using cyclodextrin glucosyltransferase (CGTase) enzyme (Szetjli 1998). They are cyclic oligosaccharides composed of six to more than 100 glucose units linked together covalently by oxygen atoms, and held in shape via hydrogen bonding between the secondary hydroxyl groups on adjacent units at the wider rim of the cavity. CDs are not cylindrical molecules, but are toroidal or cone shaped due to the lack of free rotation around the bonds between glucopyranose units. Consequently, the molecular structure and shape acquire the unique ability to entrap guest molecules in their cavity as molecular reservoirs. Broken covalent bonds are not observed during the formation of CD-drug complexes. Also such complexes readily dissociate and release drug molecules remaining in equilibrium with the molecules that are bound with the CD cavity. Finally,

CDs do not permeate across lipophilic membranes given their large structure with a number of hydrogen donors and acceptors (Tiwari et al. 2010).

Natural cyclodextrins and cyclodextrin derivatives

Natural CDs result from starch degradation by CGTases produced by various bacilli, principally *Bacillus macerans* and *Bacillus circulans*. CDs are cyclic oligosaccharides that can be comprised of six, seven or eight α(1,4)-linked D(+)-glucopyranose units as α-, β-, and γ-CD, so-called "parent CDs", respectively (Loftsson and Brewster 2012). The central cavity of CDs, which is composed of glucose residues, is relatively hydrophobic, while the outer surface shows a hydrophilic behavior because of the presence of hydroxyl groups. The primary hydroxyl groups are located on the narrow side, and the secondary groups can be found on the wider side (Fig. 5.1). In aqueous solution, water molecules inside the CD cavity can easily be replaced by apolar molecules or apolar parts of molecules, leading to an inclusion host-guest complex which can be isolated (Zia et al. 2001).

Some of the most relevant properties of α-, β-, γ-, and δ-CDs are summarized in Table 5.1. The inner diameter of the cavity in unmodified CDs ranges from ≈ 4.7 to 8.3 Å, depending on the size of the ring (Table 5.1), and is ≈ 8 Å in depth. These dimensions allow for the inclusion of several guest molecule types (bearing appropriate size) to form inclusion complexes. Some of the properties of guest molecules change through the formation of inclusion complexes, e.g., the solubility and reactivity. This phenomenon constitutes the basis of most of the pharmaceutical applications of CDs (Zhou and Ritter 2010).

The aqueous solubility of CDs is somewhat limited. This is the consequence of strong binding of CD molecules inside the crystal lattice with hydrogen bonds between hydroxyl groups. In the case of β-CD, poor

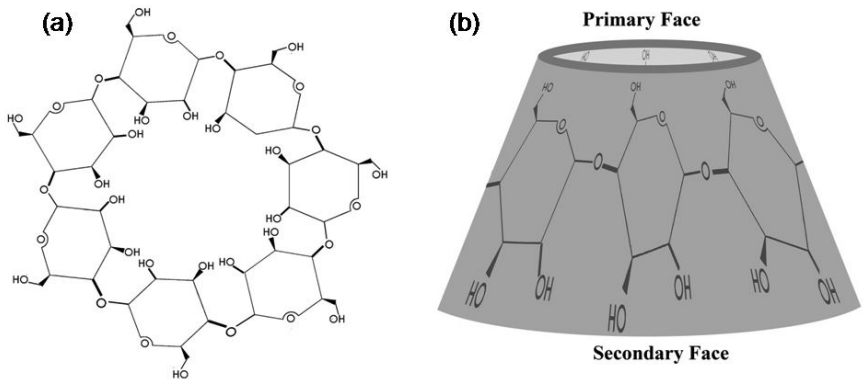

Figure 5.1. Chemical (a), and 3D (b) structure of β-CD.

Table 5.1. Characteristics of α-, β-, γ-, and δ-CDs.

Type of CD	Diameter of cavity (Å)	Molecular weight (Da)	Solubility (g/100 mL)
α-CD	4.7–5.3	972	14.2
β-CD	6.0–6.5	1135	1.85
γ-CD	7.5–8.3	1297	23.2
δ-CD	10.3–11.2	1459	8.19

water solubility is the consequence of glucopyranose units determining the formation of intramolecular hydrogen bonds between hydroxyl groups, thus preventing hydrogen bond formation with surrounding water molecules. This is believed to be due to the relatively strong binding of CD molecules in the crystal state (Loftsson and Brewster 2010). Low water solubility of β-CD limits its applications, since complex formation with lipophilic compounds frequently results in the precipitation of solid CD complexes. Any substitution on the hydroxyl groups, even by hydrophobic moieties, leads to a dramatic increase in water solubility. The different CD derivatives are still able to include molecules inside their cavity, but with a different affinity than that of the parent CD. Thus, lot of water soluble CD derivatives has been synthesized (Loftsson and Brewster 2012).

Parent CDs such as α-, β-, and γ-CDs have been widely used in pharmaceutical research and development studies. However, it has been observed that the diameter of the cavity of α-CD is not enough to encapsulate many drugs, and γ-CD is expensive. β-CD is the most widely used type of CD thanks to its availability and adequate diameter of cavity for many drugs.

Table 5.2 collects the most significant physical characteristics of CDs. In general, δ-CD has a weaker complex-forming ability than that of conventional CDs. Manufacturing of the three most common natural CDs (i.e., α-CD, β-CD and γ-CD) is a three step process: *i*) bacterial fermentation and extraction of CGTase; *ii*) enzymatic CD production from starch and precipitation of CD through complexation; and, *iii*) removal of the complexing agent and product purification. CDs with more than eight glucopyranose units (i.e., the large-ring CDs) are usually produced through chromatographic separation of the enzymatic product without precipitation.

Compared with α-CDs and β-CDs, γ-CD (characterized by a large internal cavity and high solubility) exhibits more favorable properties. Thus, many attempts have been made to modify the properties of CGTase to increase the production of γ-CD. The C-2-OH group of one glucopyranoside unit can form a hydrogen bond with the C-3-OH group of the adjacent glucopyranose unit. In the CD molecule, a complete secondary belt is formed by these hydrogen bonds. Therefore, β-CD has a rather rigid structure (Fig. 5.1). In the α-CD molecule, the hydrogen bond belt is incomplete, because one

Table 5.2. Physical properties of α-, β-, and γ-CDs.

Characteristic	**α-CD**	**β-CD**	**γ-CD**
Diameter of cavity (Å)	4.7–5.3	6.0–6.5	7.5–8.3
Height of torus (Å)	7.9	7.9	7.9
Diameter of periphery	14.6	15.4	17.5
Approximate volume of cavity	174	262	472
Per mole of CD (mL)	104	157	256
Per gram of CD (mL)	0.1	0.14	0.2

glucopyranose unit is in a distorted position. As a result, of the six possible bonds only four can be established. The γ-CD molecule is a non-coplanar and flexible structure, being the most soluble of three natural CDs.

Chemically modified CDs are synthesized to increase the inclusion capacity and extend the physicochemical properties of parent CDs. In addition to this, CD derivatives have been used to optimize the bioavailability, aqueous solubility, stability and biological activity of therapeutic agents. In addition, they can prevent drug-drug and drug-excipient interactions, reduce ocular and gastrointestinal irritation and diminish bad taste and odor (Laza-Knoerr et al. 2010).

The most widely used β-CD derivatives in drug development studies contain methyl, dimethyl, diethyl, hydroxyethyl, hydroxypropyl, carboxymethyl, carboxymethyl ethyl, sulfobutyl ether, glucosyl or maltosyl derivative groups (Table 5.3).

Table 5.4 summarizes the potential use of CD derivatives in solid dosage forms with different release profiles. Hydrophilic CDs can undertake a role in drug delivery in immediate release formulations, modify the release rate of the active ingredient and increase drug absorption through biological barriers. On the other hand, hydrophobic CDs can undertake a role in the sustained release of water soluble drugs. With the combined use of two different types of CDs, prolonged release products can be prepared to enhance oral bioavailability (Rasheed et al. 2008).

Hydroxypropyl-β-cyclodextrin (HP-β-CD) and branched β-CD have received special attention because their extremely low toxicity and their very high aqueous solubility, thus suggesting a favorable parenteral use. Notably, CD derivatives having a targeting ability for cell specific drug delivery have been developed. For example, heterobranched CDs having a galactose, fucose or mannose moiety to target CDs toward lectin on cell surfaces have been reported as well as folate-conjugated CD derivatives to deliver drugs to tumor cells that overexpress folate receptors on cell surfaces. Furthermore, ionizable CDs include sulfobutyl ether-β-cyclodextrin (SBE-β-CD), having a degree of substitution of sulfobutyl ether groups of ≈ 7 (SBE-7-β-CD, Captisol®), can improve the inclusion capacity, modify the dissolution rate and alleviate local irritation induced by drugs. Thus, these

Table 5.3. Most significant derivatives of *β*-CD.

Derivatives	**Properties**
Hydrophilic derivatives	
Methylated Methyl-*β*-cyclodextrin (M-*β*-CD) Dimethyl-*β*-cyclodextrin (DM-*β*-CD) Trimethyl-*β*-cyclodextrin (TM-*β*-CD) 2,6-di-O-methyl-3-O-acetyl-*β*-cyclodextrin (DMA-*β*-CD)	 Soluble in cold water and in inorganic solvents Surface active, hemolytic Soluble in water, low hemolytic
Hydroxyalkylated 2-hydroxyethyl-*β*-cyclodextrin (2-HE-*β*-CD) 2-hydroxypropyl-*β*-cyclodextrin (2-HP-*β*-CD) 3-hydroxypropyl-*β*-cyclodextrin (3-HP-*β*-CD)	 Amorphous mixture with different derivatives (Encapsin®) Highly water soluble (> 50%), low toxicity
Branched Glucosyl-*β*-cyclodextrin (G1-*β*-CD) Maltosyl-*β*-cyclodextrin (G2-*β*-CD)	 Highly water soluble (> 50%) Low toxicity
Hydrophobic derivatives	
Alkylated Diethyl-*β*-cyclodextrin (DE-*β*-CD) Triethyl-*β*-cyclodextrin (TE-*β*-CD)	 Water insoluble, soluble in organic solvents, surface active
Acylated Triacetyl-*β*-cyclodextrin (TA-*β*-CD) Tributyryl-*β*-cyclodextrin (TB-*β*-CD) Trivaleryl-*β*-cyclodextrin (TV-*β*-CD)	 Water insoluble, soluble in organic solvents, surface active Mucoadhesive Film formation
Ionizable derivatives	
Anionic Carboxymethyl-O-ethyl-*β*-cyclodextrin (CME-*β*-CD) *β*-CD sulfate Sulfobutyl ether-4-*β*-cyclodextrin (SBE-4-*β*-CD) Sulfobutyl ether-7-*β*-cyclodextrin (SBE-7-*β*-CD)	 pKa: 3–4, soluble at pH > 4 pKa > 1, water soluble Water soluble Water soluble (Captisol®)

Table 5.4. Use of CDs in solid dosage forms with different release profiles.

CD	**Aim/use**	**Release pattern**
HP-*β*-CD, SBE-*β*-CD, methylated *β*-CD, branched *β*-CD	Enhanced dissolution and absorption of poorly water soluble drugs	Immediate
Ethylated *β*-CD, per-O-acylated *β*-CD	Sustained release of water soluble drugs	Prolonged
CME-*β*-CD	pH-dependent (enteric) release of unstable drugs or drugs that can irritate the stomach	Delayed
CDs in combination with pharmaceutical excipients	More balanced bioavailability with prolonged therapeutic effect	Modified
Drug-CD conjugate	Colonic delivery	Site specific
Dendrimer-CD conjugate	Gene delivery	

CDs can modify various properties of drugs, pharmaceutical formulations and biomembranes, leading to the enhancement and/or modulation of the bioavailability in various routes of administration (Arima et al. 2011).

Complexation and effects of cyclodextrins on important drug properties in formulation

In aqueous solutions, CDs form inclusion complexes with poorly water soluble drugs by taking up a lipophilic moiety of the drug molecule into its somewhat hydrophobic central cavity. However, CDs are also known to form drug-CD complexes that are not inclusion complex.

Non-covalent bonds are formed or broken during formation of the drug-CD complexes and in aqueous solutions, drug molecules located within the CD cavity are in dynamic equilibrium with free drug molecules. The affinity of a drug for a given CD is determined by the stability constant of the drug-CD complex (K). Most methods for determination of the K values are based on titrating changes in the physicochemical properties of the guest molecule (i.e., the drug molecule) with CD, and then analyzing the concentration dependencies. In this way, properties that can be titrated include aqueous solubility, chemical stability, molar absorptivity, Nuclear Magnetic Resonance (NMR) chemical shifts, pKa values and High Performance Liquid Chromatography (HPLC) retention times (Brewster and Loftsson 2007). CD inclusion complexation has many advantages, as listed below:

- As a result of forming inclusion complexes with apolar molecules and functional groups, CDs can increase the solubility of lipophilic drugs. The complex masks hydrophobic functionalities into the CD cavity, meanwhile hydroxyl groups on the external surface are exposed to the environment.
- Due to low solubility, poor bioavailability can sometimes be observed. However, when a drug is complexed with CD, the dissolution rate and absorption are increased resulting in accelerated and significantly improved bioavailability (Fig. 5.2). In addition, CDs prevent the crystallization of active substances by complexing drug molecules, thus they can no longer self-assemble into a crystal network. In the case of hydrophobic drugs, CDs can increase the permeability by increasing drug solubility, dissolution, and thus making the drug available at the surface of the biological barrier, from where it partitions into the membrane without disrupting the lipid layers.
- When an inclusion complex is formed, it gradually dissociates and reduces the local concentration of free drug. As a result, the concentration remains below the levels that may be irritating to the stomach, skin or eye.

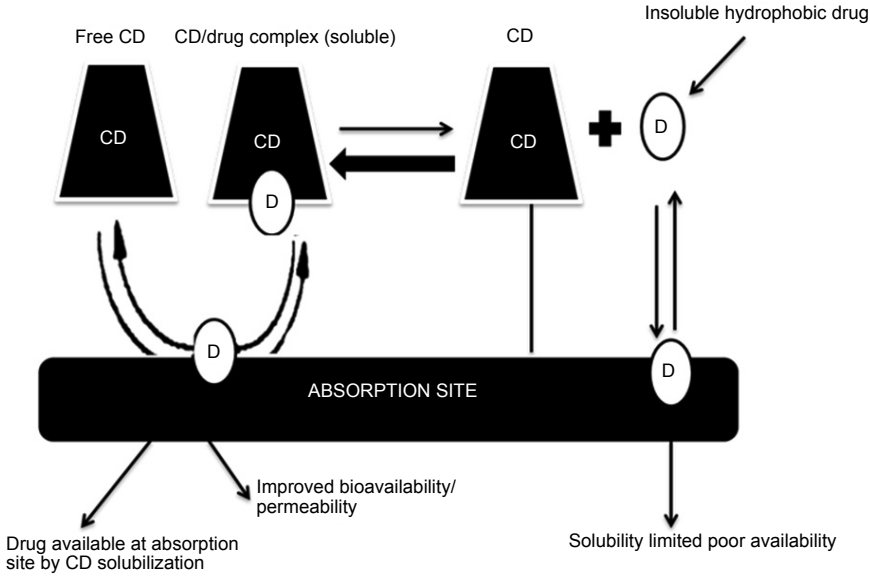

Figure 5.2. Mechanism of enhanced drug penetration by CDs.

- Functional groups or molecules that cause undesired odor or taste of drugs are encapsulated into the CD cavity. As a consequence, no taste or odor is perceived, and they are more acceptable to patients.
- Complexation with CDs transforms liquid substances into microcrystalline or amorphous powders that can be handled and formulated into solid dosage forms by conventional production techniques.
- Drugs or excipients which are incompatible with each other can be encapsulated by CD. The formulation is then stabilized and components are separated to prevent drug-drug or drug-excipient interactions.
- CD complexation can improve the chemical, thermal and physical stability. When an active molecule is entrapped into the CD cavity, it is protected from degradation by oxygen, water, radiation or heat (Tiwari et al. 2010).
- Rate-controlled and time-controlled drug release via oral delivery can also be achieved through CD complexation. Hydrophobic CDs, such as ethylated and acylated CDs, with low aqueous solubility are known to work as prolonged release carriers of water soluble drugs. HP-β-CD is a derivative which has gel forming properties that can be useful to assure prolonged release properties of water soluble drugs. SBE-7-β-CDs can serve as either a solubility modulating or an osmotic agent in the formulation of controlled porosity osmotic pump

tablets, from which the release rate of both highly and poorly water soluble drugs can be precisely controlled (Okimoto et al. 1999). The combined use of CDs complex and CDs conjugates will be useful for the preparation of time-controlled oral drug delivery formulations. Drug release from drug-CD conjugates after oral administration shows a typical delayed release behavior. Therefore, when CD conjugates are used in the formulation of drug release preparations, a more advanced and optimized drug release system is obtained with balanced oral bioavailability and prominent therapeutic efficacy.

Amphiphilic cyclodextrins

Amphiphilic CDs were synthesized to solve the limitations of natural CDs, such as (Bilensoy and Hıncal 2009): *i*) increase of the contact of CDs with biological membranes, thanks to a high external hydrophilic character; *ii*) improvement of the interaction CD-hydrophobic drug; and, *iii*) allow the spontaneous self-assembly of CDs into nano-sized drug carriers, i.e., nanospheres or nanocapsules, depending on the preparation technique. The major advantage of amphiphilic CDs is their self-alignment properties at interfaces, which is sufficient to form nanoparticles spontaneously without the presence of a surfactant, along with their ability of forming inclusion complexes with drugs (into their cavity or within their long aliphatic chains).

Amphiphilic CDs are generally classified according to their surface charge as follows: non-ionic amphiphilic CDs, cationic amphiphilic CDs and anionic amphiphilic CDs.

Non-ionic amphiphilic cyclodextrins

Non-ionic amphiphilic CDs have been developed by incorporating hydrocarbon chains into the hydroxyl groups of the primary and/or secondary face of the α-, β-, or γ-CD as seen in Fig. 5.3. Depending on their structure, amphiphilic CDs have been named as follows:

- Skirt-shaped CDs. They are obtained by adding aliphatic esters (C2–C14) into the secondary face of β- and γ-CDs.
- Lollipop CDs. They are obtained by adding aliphatic esters into 6-amino-β-CDs.
- Bouquet-shaped CDs. They are synthesized by grafting of 14 polymethylene chains to 3-monomethylated β-CD, meaning 7 chains on each side of the CD ring molecule.

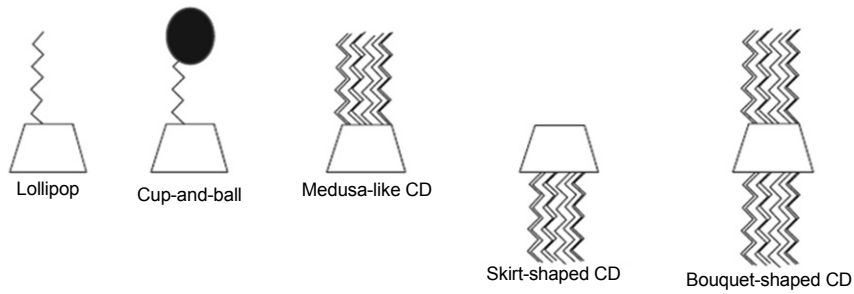

Figure 5.3. Some non-ionic amphiphilic CDs reported in the literature.

- Cup-and-ball CDs. They are obtained by adding a big group (i.e., tert-butyl) to the end of the aliphatic chain.
- Medusa-like CDs. They are obtained by incorporating hydrophobic aliphatic chains (10C–16C) into all primary hydroxyl groups of CD.

Cationic amphiphilic cyclodextrins

Recently, cationic amphiphilic CDs were synthesized carrying an amino group as ionic group. Structural properties of cationic amphiphilic CDs were believed to arise from the balance between hydrophobic tails (thioalkyl chains) and the hydrophilic moieties (ethylene glycol oligomers). Ethylene glycol chains increase the colloidal stability of nanoaggregates of cationic amphiphilic CDs. Amphiphilic alkylamino α- and β-CDs have also been reported regarding their synthesis, characterization and film-forming properties with water soluble molecules (Matsumoto et al. 2004).

Neutral CDs can interact with nucleotides and nucleic acids, and enhance the transfection efficiency *in vivo*. On the other hand, cationic CDs have shown greater ability to bind nucleotides, and enhance the delivery by viral vectors. The main advantage of polycationic CDs and their nanoparticles is their enhanced ability to interact with nucleic acids, combined with their self-organization properties (Cryan et al. 2004).

Anionic amphiphilic cyclodextrins

Anionic amphiphilic CDs carry a sulfate group that gives the anionic property to their structure. An efficient synthetic route to obtain acyl-sulfated β-CDs has been introduced in which the upper rim is functionalized with sulfates and the lower rim with fatty acid esters. These derivatives are able to form supramolecular aggregates in aqueous media (Dubes et al. 2001).

Sulfated amphiphilic *α*-, *β*-, and *γ*-CDs can form 1:1 inclusion complexes with the antiviral drug acyclovir. This condition was explained by the fact that non-covalent interactions between acyclovir and non-sulfated amphiphilic CDs (non-ionic amphiphilic CDs) took place, both in the cavity of the CD and inside the hydrophobic zone generated by the alkanoyl chains. On the contrary, in the case of sulfated anionic amphiphilic CDs, the interactions occurred exclusively in the hydrophobic region of the alkanoyl chains (Dubes et al. 2003).

Fluorine-containing anionic *β*-CDs functionalized at the 6-position by trifluoromethylthio groups have been developed (Granger et al. 2000). These molecules show amphiphilic behavior at the air-water interface, and were demonstrated to be good candidates for a new class of amphiphilic carriers. The synthesis of new amphiphilic perfluorohexyl- and perfluorooctyl-thio-*β*-CDs, and their alkyl analogue, nonanethio-*β*-CD has been described (Peroche et al. 2005). The ability of these products to form nanoparticles was also investigated by particle size measurement (Photon Correlation Spectroscopy, PCS) and imaging techniques, such as, Scanning Electron Microscopy (SEM) and Transmission Electron Microscopy (TEM) following freeze-fracture.

Fluorophilic CD derivatives have been obtained as combination of CDs and a linear perfluorocarbon. 2,3-di-*O*-decafluorooctanoyl-*γ*-CD was obtained by following a protection-deprotection-based synthetic method, and characterized further by sophisticated techniques, including Thin Layer Chromatography (TLC), Fourier transform infrared spectroscopy (FTIR), Differential Scanning Calorimetry (DSC), and elemental analysis and Time-of-Flight Mass Spectrometry (TOF-MS) (Skiba et al. 2002).

Toxicity

CDs have shown ideally favorable toxicological profiles in comparison to other pharmaceutical excipients, such as, organic solvents, surfactants and water soluble polymers. Most CDs are obtained due to bacterial digestion of starch. Their hydrophilic character (log $K_{octanol/water}$: –8 to –12), their high molecular weight (M_W), and the large number of hydrogen donors and acceptors result in a very low oral bioavailability (< 4%), meaning that they act as true drug carriers. At first, the toxicity profiles of CDs depend on the route of administration. Toxicological studies have shown that orally administered CDs are practically non-toxic because of their low absorption into the blood circulation (Loftsson and Brewster 2012). After oral administration, a partial or complete hydrolysis of CDs occurs by amylases from digestive tract, similar to that of starch. CDs can form inclusion complexes with other compounds present in the digestive tract (such as, biliary salts) in a reversible manner. Whether the hydrolysis is

partial or total, CDs are non-toxic when administered through the oral route. γ-CD with a large internal cavity is more easily hydrolyzed than α-CD, which exhibits a small internal cavity, whereas β-CD lies in between (Laza-Knoerr et al. 2010).

50 to 65% of the oral CD dose is excreted intact in the feces and the remaining is mainly metabolized by bacteria in the colon. The CD which is absorbed intact is then rapidly excreted in the urine, except randomly methylated-β-cyclodextrins (RM-β-CDs) which are more lipophilic (log $K_{octanol/water}$: –2.4) and have fewer hydrogen bond donors than other CDs. Consequently, its oral bioavailability is slightly higher (up to 12% in rats). Oral administration of RM-β-CDs is limited by their potential toxicity. Oral administration of α-CD, β-CD, γ-CD, HP-β-CD, and SBE-β-CD is well tolerated and is not associated with adverse effects. The main side effects coming from the oral administration of high doses of these CDs are flatulence and soft stools. These effects are similar to those related to poorly digestible carbohydrates. α-CD, β-CD and HP-β-CD can be found in various oral drug products, while α-CD, β-CD, and γ-CD are being used in dietary products.

When CDs are given via parenteral administration, hydrophilic CDs are primarily eliminated unchanged from the body via renal excretion, with a total plasma clearance close to glomerular filtration rates. In patients with normal kidney function, ≈ 90% of the CD will be excreted within 6 hours and ≈ 99% within 12 hours after intravenous administration. Thus, the administration of CD containing drug formulations will result in negligible accumulation of CD in individuals with normal kidney function (Loftsson and Brewster 2010). However, parenteral administration of CDs can be slightly limited due to the additional complexation of some blood components, such as, cholesterol. Upon intravenous administration, β-CDs can destabilize the red blood cell membrane by forming inclusion complexes with some of their constituents, thus leading to hemolysis (Duchene et al. 2009). At the same time, when administered in high doses to animals by the subcutaneous route, β-CD might cause nephrotoxicity, decrease in body weight and decrease in liver weight. The hemolytic effect of CDs on human erythrocytes in phosphate buffered saline is in the order: RM-β-CD > β-CD > HP-β-CD > α-CD > γ-CD > HP-γ-CD > SBE-β-CD. There appears to be a correlation between the hemolytic activity and the ability of the CDs to bind or extract cholesterol from the membranes. β-CD cannot be given by parenteral administration due to its low aqueous solubility and related adverse effects, e.g., nephrotoxicity. *In vivo* studies have shown that RM-β-CDs and β-CD cannot be used in parenteral formulations, while some derivatives of CDs can be used as alternatives to α-, β-, and γ-CDs because of their lower toxicity. HP-β-CD has a small volume of distribution (V_d: 0.2 L/Kg) and a short plasma half-life ($t_{1/2}$: 1.7 hour), and is mainly excreted

unchanged in the urine after parenteral administration to humans. In humans, there is a linear relationship between the dose of HP-*β*-CD given by parenteral administration and the area under the plasma concentration-time curve (AUC). No side effects were observed after the daily parenteral administration of up to 24 g of HP-*β*-CD (12 g twice daily) for 15 days (Loftsson and Brewster 2010). Human experience with CD derivatives, especially SBE-*β*-CD (Captisol®), indicates that these two CDs are well tolerated with negligible toxicity, following either oral or intravenous administration (Stella and He 2008). The pharmacokinetics of SBE-*β*-CD is very similar to that of HP-*β*-CD. The total plasma clearance of both HP-*β*-CD and SBE-*β*-CD is similar to the glomerular filtration rate, and they are predominately eliminated unchanged in urine with a $t_{1/2}$ that will increase with impaired or reduced kidney function (Loftsson and Brewster 2010). Following both oral and intravenous administration, no adverse effects on the kidney or other organs was observed with HP-*β*-CD and SBE-*β*-CD.

HP-*β*-CD, *α*-CD, *γ*-CD, HP-*γ*-CD and SBE-*β*-CD can be found in marketed parenteral formulations, i.e., with an intravenous dose of up to 16 g of HP-*β*-CD daily (Sporanox®, Janssen Pharmaceutica, Belgium) and 14 g of SBE-*β*-CD daily (Vfend®, Pfizer, USA). Because of its polyanionic structure, SBE-*β*-CD interacts very well with neutral and cationic drugs to facilitate their solubility and stability (Stella and He 2008). *γ*-CD can be found in one parenteral diagnostic product (CardioTec® kit for the preparation of technetium (^{99m}Tc) teboroxime, Squibb Diagnostics, USA), but it has been replaced by HP-*γ*-CD in this product (CardioTec®, Bracco, USA). The main reason depends on aqueous *γ*-CD solutions that tend to turn opalescent due to aggregation, while HP-*γ*-CD solutions remain clear. The parenteral dose of *γ*-CD and HP-*γ*-CD in CardioTec® is ≈ 50 mg (Loftsson and Brewster 2010).

Cyclodextrins in the Development of Conventional and Novel Drug Delivery Systems

Conventional drug delivery systems

Given their interesting multifunctional properties, CDs are used in the development of diverse drug delivery systems. Currently, more than 35 pharmaceutical products are marketed worldwide containing drug-CD complexes, e.g., tablets, eye drops, ointments, parenteral solutions and suppositories (Table 5.5). Recent work which has been carried out in different drug delivery fields is presented below.

Table 5.5. Marketed pharmaceutical products containing CD as excipient.

Drug-CD complex		Trade name	Formulation	Company (Country)
α-CD	Alprostadil	Caverject®	Intravenous solution	Pfizer (Europe)
	Cefotiam hexetil hydrochloride	Pansporin® T	Tablet	Takeda (Japan)
	Limaprost	Opalmon®	Tablet	Ono (Japan)
	Prostaglandin E1	Prostavastin®	Parenteral solution	Ono (Japan), Schwarz (Europe)
β-CD	Benexate hydrochloride	Ulgut®	Capsule	Teikoku (Japan), Shionogi (Japan)
	Cephalosporin B	Meiact®	Tablet	Meiji Seika (Japan)
	Cetirizine	Cetrizin®	Chewable tablet	Losan Pharma (Germany)
	Chlordiazepoxide	Transillium®	Tablet	Gador (Argentina)
	Dexamethasone	Glymesason®	Ointment, tablet	Fujinaga (Japan)
	Dextromethorphan	Rynathisol®	Tablet	Synthelabo (Europe)
	Diphenhydramine and chlortheophylline	Stada-Travel®	Chewable tablet	Stada (Europe)
	Ethinylestradiol and drospirenone	Yaz®	Tablet	Bayer (Europe, USA)
	Iodine	Mena-Gargle®	Solution	Kyushin (Japan)
	Meloxicam	Mobitil®	Tablet, suppository	Medical Union (Egypt)
	Nicotine	Nicorette®	Sublingual tablet	Pfizer (Europe)
	Nimesulide	Nimodex®	Tablet	Novartis (Europe)
	Nitroglycerin	Nitropen®	Sublingual tablet	Nihon Kayaku (Japan)
	Omeprazole	Omebeta®	Tablet	Betafarm (Europe)
	Prostaglandin E2	Prostarmon® E	Sublingual tablet	Ono (Japan)
	Piroxicam	Brexin®, Flogene®, Cicladon®	Tablet, suppository	Chiesi (Europe), Aché (Brazil)
	Tiaprofenic acid	Surgamyl®	Tablet	Roussel-Maestrelli (Europe)

Table 5.5. contd....

Table 5.5. contd.

Drug-CD complex		Trade name	Formulation	Company (Country)
2-HP-*β*-CD	Cisapride	Propulsid®	Suppository	Janssen (Europe)
	Indometacin	Indocid®	Eye drop solution	Chauvin (Europe)
	Itraconazole	Sporanox®	Oral and intravenous solution	Janssen (Europe, USA)
	Mitomycin	MitoExtra®, Mitozytrex®	Intravenous infusion	Novartis (Europe)
SBE-*β*-CD sodium salt	Aripiprazole	Abilify®	Intramuscular solution	BMS (USA), Otsuka Pharm. (USA)
	Maropitant	Cerenia®	Parenteral solution	Pfizer Animal Health (USA)
	Voriconazole	Vfend®	Intravenous solution	Pfizer (USA, Europe, Japan)
	Ziprasidone mesylate	Geodon®, Zeldox®	Intramuscular solution	Pfizer (USA, Europe)
RM-*β*-CD	17-*β*-estradiol	Aerodiol®	Nasal spray	Servier (Europe)
	Chloramphenicol	Clorocil®	Eye drop solution	Oftalder (Europe)
γ-CD	Technetium (^{99m}Tc) teboroxime	CardioTec®	Intravenous solution	Squibb Diagnostics (USA)
2-HP-*γ*-CD	Diclofenac sodium salt	Voltaren® Ophtha	Eye drop solution	Novartis (Europe)
	Technetium (^{99m}Tc) teboroxime	CardioTec®	Intravenous solution	Bracco (USA)

Oral drug delivery systems

The oral route has been the most popular route for designing a drug delivery system. CDs and derivatives have been used as excipients to transport drugs through an aqueous medium to the lipophilic absorption surface in the gastrointestinal tract. Complexation with CDs has been used to enhance the duration of drug release and the dissolution rate of poorly soluble drugs and, in consequence, to improve the drug bioavailability (Tiwari et al. 2010). In this topic, many recent reviews deal with the use of CDs as excipients for oral drug delivery. Thus, the usefulness of CDs has been demonstrated in the case of various drugs, such as, cilostazol, flurbiprofen, paclitaxel (PTX), andragrapholide, gefitinib, efavirenz, triclosan and many others.

At the same time, CDs (especially hydrophilic CDs) may decrease local gastrointestinal tract irritation or bitter taste induced by drugs. Rapid dissolving complexes with CDs have also been formulated for buccal and sublingual administration. In this type of drug delivery system, a rapid increase in the systemic drug concentration takes place along with the avoidance of systemic and hepatic first-pass metabolism (Bayomi et al. 2002).

At present, oral administration of inclusion complexes of CDs with many poorly water soluble drugs is possible because of natural α- and β-CDs, unlike γ-CD (with a very large cavity), are not hydrolyzed by human saliva. α-CD, β-CD, γ-CD and their derivatives [sulfated-α-CD, sulfated-β-CD, carboxymethyl-β-cyclodextrin (CM-β-CD) and 2-HP-β-CD] have been utilized in oral hygiene products to bind large-sized compounds with undesirable odor residing in the mouth (organic acids, amines, amino acids). In addition, CDs can form complexes with polyphenols and chlorogenic acid, thus preventing a bad sensation in mouth. An important tool in this regard is the use of CDs and their derivatives via dynamic complex formation, so that the complexes overcome undesirable physicochemical properties of drugs, including low aqueous solubility, poor dissolution rate and limited stability (Laza-Knoerr et al. 2010).

Nasal drug delivery systems

Transporting drugs through the nasal mucosa is a novel approach for the systemic delivery of high potency drugs with low oral bioavailability. Given the fact that CDs can enhance drug delivery through biological barriers (without affecting the barrier function), it is believed that they are ideal penetration enhancers for intranasal drug delivery. CDs are used as excipients in the development of nasal drug delivery systems, provided that they should be non-irritating and non-allergenic excipients with absence of local (even on nasal mucociliary functions) or systemic effect.

Application of CD solution directly onto the nasal mucosa is regarded as safe for hydrophilic and natural CDs in a wide range of concentrations, but the exposure time and concentration should be carefully controlled in the case of RM-*β*-CDs. For example, Boulmedarat et al. indicated that the application of a 10% solution of RM-*β*-CD on epithelial cells presented toxic and inflammatory effects, depending on the exposure time (Boulmedarat et al. 2005). Recently, a novel inclusion complex of ibuprofen with natural CDs and 2-HP-*β*-CD has been described. The free drug exhibited an irritant effect on the oral cavity, throat and pharynx so that its administration was unpleasant. However, its complexation with these CDs helped preventing these unwanted side effects (Al Omaria et al. 2009).

Ocular drug delivery systems

Drug formulations are generally applied to the surface of the eye to provide intraocular treatment throughout the cornea like glaucoma, and to treat the outside of the eye for infections, such as conjunctivitis. The most preferred dosage form is the eye drop, due to the easy instillation in the eye but its major disadvantage is its inability to sustain high local drug concentrations. On the other hand, a major problem in ophthalmic drug delivery is the rapid drug loss caused by drainage and high tear fluid. The drug has to penetrate into the eye through conjunctiva, cornea and/or sclera membranes (which are lipophilic). These membranes are surrounded by an aqueous tear fluid and by a mucin layer. Thus, ophthalmic drugs must be water soluble (hydrophilic) to penetrate the exterior surface of the eye (tear fluid and mucin layer) but, at the same time, they have to display enough lipophilic character to penetrate the ocular barrier. As a result, upon ophthalmic application of drug formulations, only < 5% can penetrate the cornea and the intraocular tissues.

In this line, CDs have been used to increase the solubility and/or stability of drugs, resulting in improved corneal permeability and negligible side effects (such as, irritation and discomfort). To be used as excipients in ocular drug delivery system, CDs should be non-toxic, well tolerated, inert, non-irritating, and should enhance the drug permeability through the corneal mucosa.

Inclusion complexes of ophthalmic hydrophobic drugs with CDs were found to be capable of delivering the entrapped drug directly to the ocular surface, without affecting their chemical structure and/or activity after penetration through the mucin layer. For example, the increase in water solubility and efficacy of acetazolamide was observed in aqueous solutions of 2-HP-*β*-CD by the formation of a drug-CD complex. This CD derivative was found to be non-toxic toward the ocular tissue, because it was unable

to penetrate the eye cornea, and its aqueous formulation was well tolerated (Palma et al. 2009).

CD derivatives (2-HP-β-CD or SBE-β-CD) were successfully used to increase the aqueous stability of dipivefrin (dipivalyl epinephrine, DPE). These drug-CD complexes were studied in an isolated rabbit cornea. It was shown that the formation of such strong inclusion complexes significantly increased the aqueous stability of DPE (at room temperature, and at pH values of 5 and 7.4) (Jarho et al. 1997).

Rectal drug delivery systems

Rectal mucosa can be preferred as a potential site for delivering drugs which have a bad taste, a high first-pass metabolism, and significant degradation in the gastrointestinal pH. In addition, it is an ideal route to deliver drugs to children, infants, patients with nausea, swallowing problems or vomiting.

However, rectal mucosa offers limited absorbing surface area, inefficient dissolution due to insufficient fluid in the rectum and drug metabolism. To overcome these disadvantages, CDs have been found to be more useful among a number of excipients like surfactants, absorption enhancers, etc. When CDs are used as excipients in the development of rectal drug delivery systems, they should be non-irritating to the rectal mucosa, inhibit the reverse drug diffusion into the vehicle, and have a low affinity for the suppository base.

Complexation of drugs with CDs (parents and derivatives) is believed to inhibit drug bioconversion in the rectum, and to make drugs insoluble in oleaginous suppository base. For example, it has been reported that the combination of α-CD and xanthan gum reduced the bioconversion of morphine in the rectal mucosa. Hence, it appeared that xanthan gum combined with α-CD increased drug stability and facilitated the transport of morphine through the rectal mucosa (Kondo et al. 1996).

Finally, numerous reports have demonstrated that the effects of CDs in rectal drug delivery depend on the type of vehicle and physicochemical properties of the inclusion complexes.

Topical (transdermal) delivery

CDs are able to increase dermal and transdermal drug delivery with minimal effect on the barrier function (skin). These systems are thought to enhance topical drug delivery by increasing drug availability at the lipophilic (skin) barrier surface. Due to their relatively high M_W, they are considered to be safe, because only insignificant amounts of CDs are able to penetrate into the lipophilic biological barrier (intact skin), and will most likely be eliminated

when the skin naturally renews itself. Also, they enhance drug release and stability, and can minimize local irritation (Loftsson and Masson 2001).

Betadex, which is β-CD, is the only CD that appears in the list of inactive ingredients for topical indications approved by the Food and Drug Administration (FDA). It is approved as an excipient for topical drugs up to 1% concentration, and therefore can only be used as part of the vehicle.

Isotretinoin-loaded HP-β-CD has been formulated into elastic liposomes upon an encapsulation process (Kaur et al. 2010). Then, the effect of this dual carrier approach on isotretinoin targeting to the skin was investigated. The dual carrier was found to dramatically improve the photostability of the drug and to increase skin targeting, while decreasing the skin irritation and toxicity in comparison with the drug solution.

Peptide and protein delivery

Various problems are observed with the practical use of therapeutic peptides and proteins, such as, poor absorption through biological membranes, chemical and enzymatic instability, rapid plasma clearance, individual dose-response curves and immunogenicity. CD complexation seems to be an attractive approach to solve all these problems.

For instance, the formulation of an oral insulin delivery system has reported significant advantages when combining CD complexation and nanoparticulate mucoadhesive delivery systems. While mucoadhesive Poly(Methacrylic Acid) (PMA) nanoparticles were intended to provide higher residence time and reduce proteolytic degradation, HP-β-CD complexation was expected to improve the stability and absorption of insulin formulations. The formation of the HP-β-CD-insulin complex was demonstrated by FTIR and fluorescence spectroscopy. Very stable PMA nanoparticles (size: 500–800 nm) were prepared by a novel inter-ionic gelation technique. These nanoparticles showed good insulin Entrapment Efficiency (EE) and a pH-dependent release profile. Thus, such PMA mucoadhesive nanoparticles loaded with insulin-HP-β-CD complexes are useful candidates for oral insulin delivery (Sajeesh and Sharma 2006).

Gene delivery

Generally, CD polymers are used to form "polyplexes" that are self-aggregated carrier systems for genes and oligonucleotides.

The efficiency of gene delivery systems can be improved by the incorporation of CD derivatives as excipients. Cholesterol-containing gene delivery formulations have also been investigated with the addition of CDs. Cholesterol can regulate the membrane fluidity and, therefore, the cellular uptake. However, conventional lipid-based formulations are not

sufficient to enhance gene uptake due to the low solubility resulting from cholesterol. To overcome the problem, cholesterol-containing gene delivery formulations were prepared in the form of complexes with β-CD (Ortiz Mellet et al. 2011).

Possibilities in the design of novel drug delivery systems

CDs have been used as base materials to prepare colloidal drug carriers, or they can be incorporated into new drug delivery systems to improve the physicochemical properties, and to enhance their efficacy and safety. These novel delivery systems include liposomes, nanoparticles, CD polymers, hydrogels, implants, osmotic systems, microspheres and microcapsules and sugammadex.

Liposomes

Liposomes are microscopic vesicles obtained from membranous lipid bilayer(s) mainly composed of natural or synthetic phospholipids surrounding an aqueous phase.

Liposomes can entrap hydrophilic drugs into the aqueous phase and hydrophobic drugs into the lipid bilayers, and retain drugs in targeted organs. The major problems of these vesicular systems arise from their structure or preparation, and result in low drug loading values, both rapid and early drug release in contact with plasma, or even slow and incomplete drug release. These problems can be overcome by using CDs. When CD-drug complexes are entrapped into liposomes, advantages of both CDs (such as, increased drug solubility) and liposomes (e.g., drug targeting) can be combined into a single delivery system. By forming water soluble complexes, CDs may allow insoluble drugs to accommodate in the aqueous phase of vesicles and, thus, potentially increase drug-to-lipid mass ratio levels, enlarge the range of insoluble drugs amenable for encapsulation, allow drug targeting and reduce drug toxicity (Vyas et al. 2008).

Novel nanoparticulate systems

Nanoparticles are stable systems suitable to provide targeted drug delivery, and their high surface area can lead to intimate contact with biological membranes, giving way to enhance the bioavailability of poorly soluble drugs. However, the safety and efficacy of nanoparticles are limited by their low drug loading (and EE) that may lead to excessive administration of polymeric material. Many efforts have been directed to use CD-based materials for the design of nanoparticles. Two applications of CDs have been found very promising in the design of nanoparticles: *i*) they can

increase the drug loading capacity of nanoparticles; and, *ii*) they can lead to the spontaneous formation of either nanocapsules or nanospheres by nanoprecipitation of amphiphilic CDs diesters. CD-based nanoparticulate systems have been reported to be useful in oral and parenteral drug administration (Bilensoy et al. 2007, 2008).

In a recent study, the influence of the type of CD on the physicochemical characteristics and bioadhesive properties of the resulting nanoparticles have been described (Agueros et al. 2009). Different oligosaccharides were assayed including *β*-CD, HP-*β*-CD and 6-monodeoxy-6-monoamino-*β*-cyclodextrin (NH-*β*-CD). The resulting particles showed an average size of ≈ 150 nm. It was found that *β*-CD was incorporated in a more effective way to the poly(anhydride) nanoparticles than other oligosaccharides, because of the relatively lower aqueous solubility of *β*-CD compared with the hydroxypropyl and amino derivatives. In addition, the bioadhesive properties of the nanoparticles were evaluated by quantifying the adhered fraction in different segments of the gastrointestinal tract of rats. It was shown that all the CD-poly(anhydride) nanoparticles displayed a higher ability to develop bioadhesive interactions with the gut mucosa than control ones. From fluorescence microscopy visualization studies, it was determined that CD-poly(anhydride) nanoparticles were homogeneously distributed along the ileum mucosa, whereas conventional nanoparticles were found mainly in the outer layer (mucus) of the ileum. On the other hand, after radiolabeling of the nanoparticles with technetium, it was observed that the nanoparticles remained in the stomach during the first hour after oral administration. Then, they were slowly discharged in the small intestine and continued to move along the gut during the time of the experiment.

In another study, CD-poly(anhydride) nanoparticles have been evaluated for the oral delivery of the anticancer agent PTX (Agueros et al. 2010). However, the oral bioavailability of PTX with conventional formulations is very low due to its low aqueous solubility, *P*-glycoprotein (*P*-gp) efflux and first-pass metabolism by cytochrome P_{450} located in the gut and the liver. To solve all these problems, the combination between bioadhesive nanoparticles and CDs, as "soft" inhibitors of biological transporters and cytochrome P_{450}, can be a promising strategy to increase the oral PTX bioavailability. The first step in this investigation was the preparation of an inclusion complex between the CDs and PTX which was characterized by a globular morphology and an average size of ≈ 30 nm. Then, the inclusion complex was mixed with the polymer, and nanoparticles were obtained by a desolvation process (average size ≈ 300 nm). Drug loading was found to be dependent on the type of CD used. For instance, PTX-NH-*β*-CD nanoparticles and PTX-*β*-CD nanoparticles were characterized by a drug loading of ≈ 90 and 40 μg/mg, respectively; and the greatest drug loading was obtained when HP-*β*-CD was used (≈ 160

μg/mg). On the other hand, when nanoparticles were prepared without CD, PTX loading was found to be very low. In pharmacokinetic studies, it was found that the maximum plasma concentration (C_{max}) value was similar for PTX-HP-*β*-CD and PTX-*β*-CD nanoparticles, and five times greater for PTX-NH-*β*-CD nanoparticles. Similar plasmatic curves were observed when the nanoparticulate formulations were evaluated in mice. Nevertheless, very low plasma levels of PTX were found when it was administered as complex with HP-*β*-CD alone or physically mixed with empty nanoparticles. In all cases, such levels were always above the therapeutic threshold (85.3 ng/mL). Similar results were obtained when animals were treated with PTX nanoparticles or with the free drug (Taxol®). Concerning the relative oral PTX bioavailability in rats, it was calculated to be ≈ 80% for both PTX-*β*-CD and PTX-HP-*β*-CD nanoparticles. On the other hand, oral PTX bioavailability for PTX-NH-*β*-CD nanoparticles was found to be ≈ 18%, which would be related to a rapid release in the stomach of an important fraction of the loaded drug. Finally, it was hypothesized that nanoparticles would transport the drug-CD complexes to the surface of the mucosa where these carriers would remain immobilized in intimate contact with the absorptive membrane. Then, nanoparticles would progressively release their contents to the environment, and PTX would be rapidly absorbed (upon dissociation from CD), whereas the CDs would interact with the lipophilic components of the membrane, thus disturbing the activity of *P*-gp efflux and cytochrome P_{450} (Fig. 5.4).

PTX has also been encapsulated in amphiphilic CD nanoparticles (Bilensoy et al. 2008). Safety of blank nanoparticles was compared against commercial vehicle Cremophor®:ethanol (50:50, v/v) by hemolysis and cytotoxicity experiments. Data revealed that nanoparticles caused

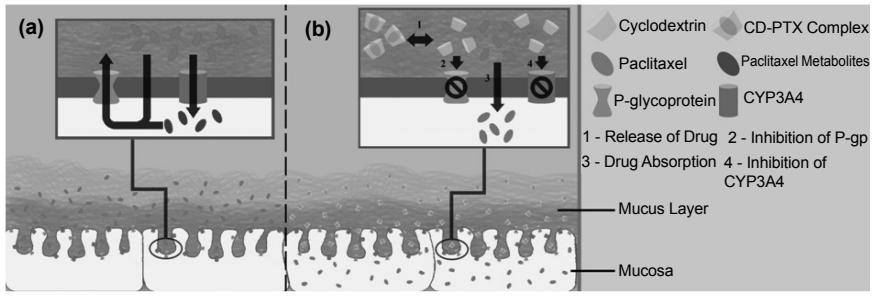

Figure 5.4. (a) Limited oral bioavailability of PTX conventional formulations due to *P*-gp efflux, and first-pass metabolism by cytochrome P_{450} 3A4 isoenzyme. (b) Mechanism by which the combination between CDs and poly(anhydride) nanoparticles would improve PTX absorption: (1) PTX release; (2 and 4) inhibition of *P*-gp and cytochrome P_{450} 3A4 by free CD, respectively; and, (3) PTX absorption.

Color image of this figure appears in the color plate section at the end of the book.

significantly less hemolysis compared to the control. These results were confirmed by SEM imaging of erythrocytes (Fig. 5.5). In addition, a huge difference between the cytotoxicity of nanoparticles and Cremophor®:ethanol mixture was observed in L929 cells. Physical stability of PTX in nanoparticles was assessed for one month with repeated particle size and zeta potential measurements, and Atomic Force Microscopy (AFM) imaging determinations. It was shown that PTX recrystallization, very typical in diluted aqueous solutions, did not take place when the drug was bound to CD nanoparticles. Finally, the anticancer efficacy against MCF-7 cells of PTX-loaded nanoparticles was evaluated in comparison to PTX in the Cremophor®:ethanol vehicle. It was found that CD nanoparticles induced a slightly greater anticancer effect than the Cremophor®:ethanol vehicle. Thus, amphiphilic CD nanoparticles emerged as a promising alternative formulation for PTX administration with low toxicity and similar efficacy.

Cyclodextrin polymers

Recently, great attention has been focused on the synthesis and use of CD polymers. The synthesis of water soluble CD polymers involves the use of cross-linking agents like epichlorohydrin, diisocyanates, polycarboxylic acids or anhydrides. Epichlorohydrin is the most popular cross-linking agent used in the synthesis of β-CD polymers. Because the reaction between β-CD and epichlorohydrin requires a high concentration of sodium hydroxide (to activate the hydroxyl groups of CD and to accelerate the hydrolyzation of epichlorohydrin), a large quantity of epichlorohydrin might be wasted in the reaction. Nevertheless, most of these cross-linking agents used in the synthesis of CD polymers have a potential toxic effect for human health and environment. Comparatively, citric acid features a lower toxicity and is environment friendly. The condensation between β-CD and citric acid has been done at a temperature not higher than 170°C, and without using any organic solvent. However, the drawback of this method lies in the weak reactivity of citric acid compared with epichlorohydrin or diisocyanates (Martel et al. 2005, Laza-Knoerr et al. 2010).

CD polymers in association with other polymers constitute another area of current interest. For example, promising results have been obtained by mixing hydrophobic dextrans (bearing dodecyl moieties) with β-CD polymer. Owing to the inclusion of hydrophobic side chains of dextran into CD cavities, spontaneous association occurs in solution (Daoud-Mahammed et al. 2007). Encapsulation of lipophilic drugs, such as benzophenone and tamoxifen, in this system was achieved by their complexation in the remaining free cavities of CDs.

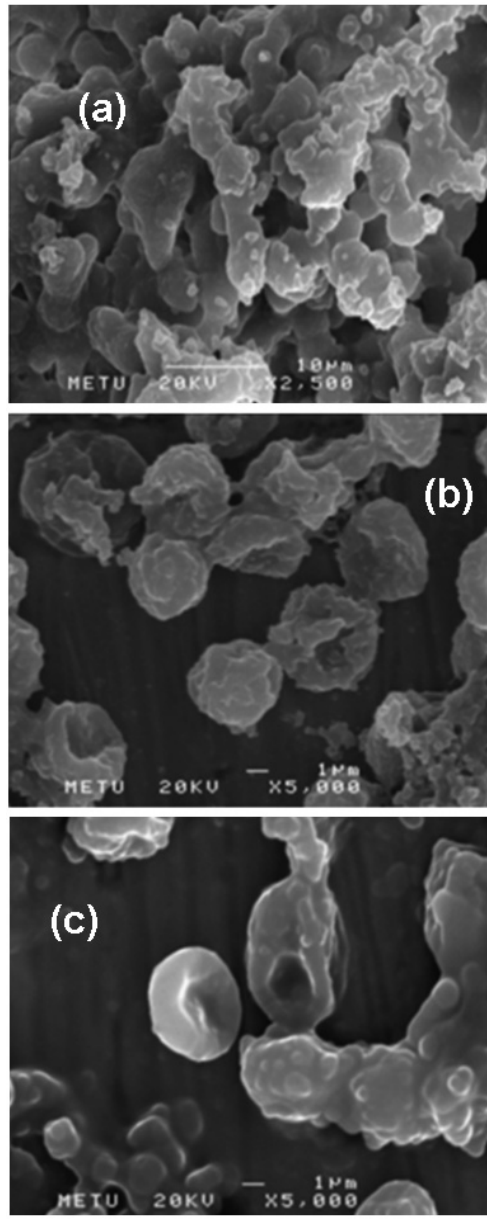

Figure 5.5. SEM microphotograph of erythrocyte suspensions treated with: (a) Cremophor®:ethanol 50:50 (v/v) mixture (magnification: 2500×), (b) amphiphilic CD nanospheres (magnification: 5000×), and (c) amphiphilic CD nanocapsules (magnification: 5000×). Adapted with permission from Bilensoy et al. (2008). Copyright Elsevier (2008).

CD polymers provide unique capabilities as vehicles for delivery of nucleic acids into cells. Such complexes have demonstrated lower toxicities than polymers lacking CD. The CDs endow the nucleic acid delivery vehicles with the ability to be modified by compounds that form inclusion complexes with them, and these modifications can be performed without disruption of the polymer-nucleic acid interactions. The development of polyplexes (cationic polymer + nucleic acid) as gene carriers is based on the hypothesis that it may be possible to prepare low toxicity polycations from CDs, given the fact that numerous CDs exhibit low toxicity and do not elicit immune responses in animals.

Polyplex formulations optimized for *in vitro* delivery are typically not appropriate for *in vivo* use, because successful systemic delivery requires different particle properties. After an intravenous injection, cationic polyplexes interact with serum proteins, and are quickly eliminated from the bloodstream by phagocytic cells. However, the use of CD-containing polycations in polyplex formulation provides significant advantages. In fact, it can be modified the surface of polyplexes formed with CD polymers to obtain modified polyplexes appropriate for systemic gene delivery (Davis and Bellocq 2002).

Hydrogels

Of growing interest in the pharmaceutical world is the use of hydrogels for the controlled release of therapeutics. Hydrogels are cross-linked structures of hydrophilic homopolymers or copolymers. Hydrogels are highly biocompatible and well tolerated when implanted *in vivo*, due to their high water content. These systems can be used for the controlled delivery of low M_W drugs, as well as peptides and proteins.

When solutions of drug-CD complexes are diluted in physiological fluids, drug release rapidly occurs. However, in the case of the CD hydrogels, the CD units are covalently attached to each other, and the volume of water which can enter the hydrogel is limited by its own network. This provides a microenvironment rich in cavities available to interact with the surrounding drug molecules. As a result, sustained drug release is obtained with such delivery systems comprising chemically linked CDs (Kanjickal et al. 2005).

A recent investigation reported the formulation of pH-dependent hydrogels made of CM-β-CD and the crosslinker epichlorohydrin (Yang and Kim 2010). The reason why CM-β-CD was used in the preparation of these pH-sensitive hydrogels, was that the hydrogel could load not only water soluble compounds, but also oil-soluble compounds due to the hydrophobic cavity. The degree of release of blue dextran from the hydrogel was studied by varying the pH of the release medium. It was determined

that this degree of release from the hydrogel increased with increasing pH values, given the fact that the swelling ratio, a measure of hydrogel capacity to imbibe water, increased with the pH value. At higher pHs, the electrostatic repulsion developed in the hydrogel would be responsible for the higher swelling ratio and the higher degree of release.

Implants

Implants are emerging systems allowing for optimized therapeutic effects. Importantly, implants are designed to release drugs into their vicinity (tissues with very slowly moving extracellular fluids).

A recent investigation described the development of a polypropylene (PP) artificial abdominal wall implant for prolonged ciprofloxacin (CFX) release (Laurent et al. 2011). HP-γ-CD- and maltodextrin (MD)-modified supports were immersed in a CFX solution, and then assessed in batch release tests. It was observed that HP-γ-CD-finished supports loaded a greater CFX amount, and released it over a sustained period, compared with MD-finished supports. By an indirect method, CFX was adsorbed onto the HP-γ-CD-finished textile either through ionic and hydrogen bonding, or through inclusion in the cavity. Moreover, the advantage of HP-γ-CD with regard to MD was confirmed by microbiological tests, which demonstrated a sustained antimicrobial activity for the HP-γ-CD-finished meshes.

Osmotic systems

Osmotically controlled oral drug delivery systems are used in various designs to control drug release based on the principle of osmosis. Osmotic tablets offer many advantages, such as, zero-order drug release rate, high degree of *in vitro-in vivo* correlation and patient compliance. Oral osmotic pump tablets generally consist of a core including the active agent, an osmotic agent and other common excipients, coated with a semipermeable membrane. The drug release rate from the osmotic pump depends on the drug solubility and the osmotic pressure of the core. Hence, these systems are suitable for the delivery of drugs with moderate water solubility. CDs have been playing a very important role in the formulation of poorly water soluble drugs by improving the apparent drug solubility and/or dissolution, through inclusion complexation or solid dispersion by acting.

For instance Mehramizi et al. (2007) developed controlled release formulations of lovastatin based on an oral osmotic pump technology. Solubility studies clearly indicate that the solubility of lovastatin increased by complexation with β-CD. It was found that the ratio of β-CD has a profound positive effect on controlled drug release.

Microspheres and microcapsules

CDs are also incorporated into micron-sized drug delivery systems like microspheres and microcapsules. According to the biopharmaceutical classification system, celecoxib (CXB) is a class II drug which has very poor water solubility and a low and highly variable bioavailability that give rise to formulation problems. Mennini et al. (2012) developed a multiparticulate system to improve CXB solubility which was based on a CXB-HP-β-CD complex combined the hydrophilic polymer polyvinylpyrrolidone (PVP). The microsystem was intended for colon-specific CXB delivery for both systemic and local therapy.

In another study, new allicin microcapsules were developed via a spray drying technology using β-CD with porous starch (Wang et al. 2012). Allicin (a diallyl thiosulfinate, derived from garlic) is known to possess numerous biological functions, such as, antiparasitic, antihypertensive, cardioprotective, anti-inflammatory and anticancer properties, and can be also used in the food industry as a food preservative. However, its low stability and water solubility limit its use as a food preservative. This novel microsystem can be efficiently obtained by using β-CD and porous starch as wall materials that improve their properties (i.e., increased water solubility). Furthermore, the stability of allicin microcapsules against heat, pH, light and oxygen are also improved.

Sugammadex

Sugammadex, originally known as Org 25969 (Bridion®), is a modified γ-CD to be used as a therapeutic agent that is a selective inhibitor of steroidal neuromuscular blocking agents (NMBAs). Sugammadex is the first drug to be introduced as a Selective Relaxant Binding Agent (SRBA). The generic name of this modified γ-CD comes from: *Su* (sugar molecule), *gamma* (γ core of 8 glucose units) and *dex* (CD).

Sugammadex specifically encapsulates and binds aminosteroid NMBAs, i.e., rocuronium, vecuronium and pancuronium. Sugammadex has 2.5 times the affinity for rocuronium *vs*. vecuronium, and little affinity for pancuronium. Sugammadex forms a 1:1 tight non-covalent complex with steroid-based NMBAs, and develops the role of a chelating agent. The stability of the rocuronium-sugammadex complex is the result of intermolecular (van der Waals) forces, hydrogen bonds and hydrophobic interactions. The vecuronium-sugammadex complex exists in equilibrium with a high association rate and a low dissociation rate, which favors a stable tight complex.

Numerous studies have shown its high safety profile. In fact, it is well tolerated during maintenance of anesthesia with sevoflurane or propofol,

although safety profile is somewhat more favorable under propofol anesthesia. The high binding affinity and specificity of sugammadex for rocuronium (and other aminosteroid NMBAs) led to its use in anesthesia as an innovative and useful agent for rapid reversal of rocuronium-induced neuromuscular block, by sequestering the drug as an inclusion complex (Akha et al. 2010, Baldo et al. 2011).

Conclusions

In view of several studies and patents dealing with CDs as multifunctional excipients, it is clear that CDs are promising materials for drug delivery. Their regulatory status is established for the most frequently used derivatives, i.e., *β*-CD, HP-*β*-CD or SBE-*β*-CD. They are listed in pharmacopoeial monographs and are considered as "Generally Recognized As Safe (GRAS)", a FDA designation to chemicals or substances added to food being considered safe by experts.

CDs have been discovered more than 100 years ago and have received increasing attention and applications since then. This interest has increased with the reduction of cost for CD large-scale production. Several pharmaceutical or cosmetic products are present in the market in regulated countries and regions, e.g., Japan, European Union or the United States of America. On the other hand, new CD derivatives provide novel qualities to CDs in nano- or micro-sized drug delivery systems, such as, drug targeting or enhanced drug penetration through mucosa. New modifications improve the multifunctionality of this pharmaceutical excipient, and will receive further attention in the field of pharmaceutical research and development.

Abbreviations

AFM	:	atomic force microscopy
AUC	:	area under the plasma concentration-time curve
CD	:	cyclodextrin
CDP	:	cyclodextrin-containing polymers
CFX	:	ciprofloxacin
CGTase	:	cyclodextrin glucosyltransferase
CM-*β*-CD	:	carboxymethyl-*β*-cyclodextrin
C_{max}	:	maximum plasma concentration
CME-*β*-CD	:	carboxymethyl-O-ethyl-*β*-cyclodextrin
CXB	:	celecoxib
DE-*β*-CD	:	diethyl-*β*-cyclodextrin
DM-*β*-CD	:	dimethyl-*β*-cyclodextrin
DMA-*β*-CD	:	2,6-di-O-methyl-3-O-acetyl-*β*-cyclodextrin

DPE	:	dipivalyl epinephrine
DSC	:	differential scanning calorimetry
EE	:	entrapment efficiency
FDA	:	Food and Drug Administration
FTIR	:	Fourier transform infrared spectroscopy
G1-*β*-CD	:	glucosyl-*β*-cyclodextrin
G2-*β*-CD	:	maltosyl-*β*-cyclodextrin
GRAS	:	generally recognized as safe
HE-*β*-CD	:	hydroxyethyl-*β*-cyclodextrin
HP-*β*-CD	:	hydroxypropyl-*β*-cyclodextrin
HPLC	:	high performance liquid chromatography
M-*β*-CD	:	methyl-*β*-cyclodextrin
MD	:	maltodextrin
M_W	:	molecular weight
NH-*β*-CD	:	6-monodeoxy-6-monoamino-*β*-cyclodextrin
NMBA	:	neuromuscular blocking agent
NMR	:	nuclear magnetic resonance
PCS	:	photon correlation spectroscopy
PMA	:	poly(methacrylic acid)
PP	:	polypropylene
PVP	:	polyvinylpyrrolidone
P-gp	:	*P*-glycoprotein
PTX	:	paclitaxel
RM-*β*-CD	:	randomly methylated-*β*-cyclodextrin
SBE-*β*-CD	:	sulfobutyl ether-*β*-cyclodextrin
SEM	:	scanning electron microscopy
SRBA	:	selective relaxant binding agent
$t_{1/2}$	:	plasma half-life
TA-*β*-CD	:	triacetyl-*β*-cyclodextrin
TB-*β*-CD	:	tributyryl-*β*-cyclodextrin
^{99m}Tc	:	technetium
TE-*β*-CD	:	triethyl-*β*-cyclodextrin
TEM	:	transmission electron microscopy
TLC	:	thin layer chromatography
TM-*β*-CD	:	trimethyl-*β*-cyclodextrin
TOF-MS	:	time-of-flight mass spectrometry
TV-*β*-CD	:	trivaleryl-*β*-cyclodextrin
V_d	:	volume of distribution

References

Agueros, M. and V. Zabaleta, S. Espuelas, M.A. Campanero and J.M. Irache. 2010. Increased oral bioavailability of paclitaxel by its encapsulation through complex formation with cyclodextrins in poly(anhydride) nanoparticles. J. Control. Release. 145: 2–8.

Agueros, M. and P. Areses, M.A. Campanero, H. Salman, G. Quincoces, I. Peñuelas and J.M. Irache. 2009. Bioadhesive properties and biodistribution of cyclodextrin-poly(anhydride) nanoparticles. Eur. J. Pharm. Sci. 37: 231–240.

Akha, A.S. and J. Rosa, J.S. Jahr, A. Li and K. Kiai. 2010. Sugammadex: cyclodextrins, development of selective binding agents, pharmacology, clinical development, and future directions. Anesthesiol. Clin. 28: 691–708.

Al Omaria, M.M. and N.H. Daraghmeha, M.I. El-Barghouthib, M.B. Zughul, B.Z. Chowdhry, S.A. Leharne and A.A. Badwan. 2009. Novel inclusion complex of ibuprofen tromethamine with cyclodextrins: physico-chemical characterization. J. Pharm. Biomed. Anal. 50: 449–458.

Arima, H. and K. Motoyama and T. Irie. Recent findings on safety profiles of cyclodextrins, cyclodextrin conjugates, and polypseudorotaxanes. pp. 91–122. *In*: E. Bilensoy [ed.]. 2011. Cyclodextrins in Pharmaceutics, Cosmetics and Biomedicine: Current and Future Industrial Applications. John Wiley & Sons, New York, USA.

Baldo, B.A. and N.J. McDonnell and N.H. Pham. 2011. Drug-specific cyclodextrins with emphasis on sugammadex, the neuromuscular blocker rocuronium and perioperative anaphylaxis: implications for drug allergy. Clin. Exp. Allergy. 41: 1663–1678.

Bayomi, M. and K. Abanumay and A. Ai-Angary. 2002. Effect of inclusion complexation with cyclodextrins on photostability of nifedipine in solid state. Int. J. Pharm. 243: 107–117.

Bilensoy, E. and O. Gürkaynak, M. Ertan and A.A. Hıncal. 2007. Development of nonsurfactant cyclodextrin nanoparticles loaded with anticancer drug paclitaxel. J. Pharm. Sci. 97: 1519–1529.

Bilensoy, E. and O. Gürkaynak, A.L. Doğan and A.A. Hıncal. 2008. Safety and efficacy of amphiphilic β-cyclodextrin nanoparticles for paclitaxel delivery. Int. J. Pharm. 347: 163–170.

Bilensoy, E. and A.A. Hıncal. 2009. Recent advances and future directions in amphiphilic cyclodextrin nanoparticles. Expert Opin. Drug Deliv. 6: 1161–1173.

Boulmedarat, L. and A. Bochot, S. Lesieur and E. Fattal. 2005. Evaluation of buccal methyl-beta-cyclodextrin toxicity on human oral epithelial cell culture model. J. Pharm. Sci. 94: 1300–1309.

Brewster, M.E. and T. Loftsson. 2007. Cyclodextrins as pharmaceutical solubilizers. Adv. Drug Deliv. Rev. 59: 645–666.

Chowdhary, K.P.R. and B.N. Nalluri. 2000. Nimesulide and b-cyclodextrin inclusion complexes: physico-chemical characterization and dissolution rate studies. Drug Dev. Ind. Pharm. 26: 1217–1219.

Cryan, S.A. and A. Holohan, R. Donohue, R. Darcy and C.M. O'Driscoll. 2004. Cell transfection with polycationic cyclodextrin vectors. Eur. J. Pharm. Sci. 21: 625–633.

Daoud-Mahammed, S. and C. Ringard-Lefebvre, N. Razzouq, V. Rosilio, B. Gillet, P. Couvreur, C. Amiel and R. Gref. 2007. Spontaneous association of hydrophobized dextran and poly-beta-cyclodextrin into nanoassemblies. Formation and interaction with a hydrophobic drug. J. Colloid Interface Sci. 307: 83–93.

Davis, M.E. and N.C. Bellocq. 2002. Cyclodextrin-containing polymers for gene delivery. J. Incl. Phenom. Macrocycl. Chem. 44: 17–22.

Dubes, A. and D. Bouchu, R. Lamartine and H. Parrot-Lopez. 2001. An efficient regiospecific synthetic route to multiply substituted acyl-sulphated β-cyclodextrins. Tetrahedron Lett. 42: 9147–9151.

Dubes, A. and G. Degobert, H. Fessi and H. Parrot-Lopez. 2003. Synthesis and characterisation of sulfated amphiphilic alpha-, beta- and gamma-cyclodextrins: application to the complexation of acyclovir. Carbohydr. Res. 338: 2185–2193.

Duchene, D. and A. Bochot and T. Loftsson. 2009. Les cyclodextrines et leurs utilisations en pharmacie et cosmétologie. STP Pharma Pratiques. 19: 15–27.

Freundenberg, K. and F. Cramer and H. Plieninger. 1953. Inclusion compounds of physiologically active organic compounds. German patent DE895769C.

Granger, C.E. and C.P. Feliz, H. Parrot-Lopez and B.R. Langlois. 2000. Fluroine containing β-cyclodextrin: a new class of amphiphilic carriers. Tetrahedron Lett. 41: 9257–9260.

Jarho, P. and K. Jarvinen, A. Urtti, V.J. Stella and T. Jarvinen. 1997. The use of cyclodextrins in ophthalmic formulations of dipivefrin. Int. J. Pharm. 153: 225–233.

Kanjickal, D. and S. Lopina, M.M. Evancho-Chapman, S. Schmidt and D. Donovan. 2005. Improving delivery of hydrophobic drugs from hydrogels through cyclodextrins. J. Biomed. Mater. Res. A. 74: 454–460.

Kaur, N. and R. Puri and S.K. Jain. 2010. Drug-cyclodextrin-vesicles dual carrier approach for skin targeting of anti-acne agent. AAPS Pharm. Sci. Tech. 11: 528–537.

Kondo, T. and T. Irie and K. Uekama. 1996. Combination effects of α-cyclodextrin and xanthan gum on rectal absorption and metabolism of morphine from hollow-type suppositories in rabbits. Biol. Pharm. Bull. 19: 280–286.

Laurent, T. and I. Kacem, N. Blanchemain, F. Cazaux, C. Neut, H.F. Hildebrand and B. Martel. 2011. Cyclodextrin and maltodextrin finishing of a polypropylene abdominal wall implant for the prolonged delivery of ciprofloxacin. Acta Biomater. 7: 3141–3149.

Laza-Knoerr, A.L. and R. Gref and P. Couvreur. 2010. Cyclodextrins for drug delivery. J. Drug Target. 18: 645–656.

Loftsson, T. and M. Masson. 2001. Cyclodextrins in topical drug formulations: theory and practice. Int. J. Pharm. 225: 15–30.

Loftsson, T. and M.E. Brewster. 2010. Pharmaceutical applications of cyclodextrins: basic science and product development. J. Pharm. Pharmacol. 62: 1607–1621.

Loftsson, T. and M.E. Brewster. 2012. Cyclodextrins as functional excipients: methods to enhance complexation efficiency. J. Pharm. Sci. 101: 3019–3032.

Martel, B. and D. Ruffin, M. Weltrowski, Y. Lekchiri and M. Morcellet. 2005. Water-soluble polymers and gels from the polycondensation between cyclodextrins and poly(carboxylic acid)s: a study of the preparation parameters. J. Appl. Polym. Sci. 97: 433–442.

Matsumoto, M. and Y. Matsuzawa, S. Noguchi, H. Sakai and M. Abe. 2004. Structure of Langmuir-Blodgett films of amphiphilic cyclodextrin and water-soluble benzophenone. Mol. Cryst. Liq. Cryst. 425: 197–204.

Mehramizi, A. and E. Asgari Monfared, M. Pourfarzib, Kh. Bayati, F.A. Dorkoosh and M. Rafiee-Tehrani. 2007. Influence of β-cyclodextrin complexation on lovastatin release from osmotic pump tablets. DARU J. Pharm. Sci. 15: 71–78.

Mennini, N. and S. Furlanetto, M. Cirri and P. Mura. 2012. Quality by design approach for developing chitosan-Ca-alginate microspheres for colon delivery of celecoxib-hydroxypropyl-β-cyclodextrin-PVP complex. Eur. J. Pharm. Biopharm. 80: 67–75.

Okimoto, K. and A. Ohike, R. Ibuki, N. Ohnishi, R.A. Rajewski, V.J. Stella, T. Irie and K. Uekama. 1999. Design and evaluation of an osmotic pump tablet (OPT) for chlorpromazine using (SBE)7m-beta-CD. Pharm. Res. 16: 549–554.

Ortiz Mellet, C. and J.M. García Fernández and J.M. Benito. 2011. Cyclodextrin-based gene delivery systems. Chem. Soc. Rev. 40: 1586–1608.

Palma, S.D. and L.I. Tartara, D. Quinteros, D.A. Allemandi, M.R. Longhi and G.E. Granero. 2009. An efficient ternary complex of acetazolamide with HP-ss-CD and TEA for topical ocular administration. J. Control. Release. 138: 24–31.

Péroche, S. and G. Degobert, J.L. Putaux, M.G. Blanchin, H. Fessi and H. Parrot-Lopez. 2005. Synthesis and characterization of novel nanospheres made from amphiphilic perfluoroalkylthio-β-cyclodextrins. Eur. J. Pharm. Biopharm. 60: 123–131.

Rasheed, A. and A. Kumar and V. Sravanthi. 2008. Cyclodextrins as drug carrier molecule: a review. Sci. Pharm. 76: 567–598.
Sajeesh, S. and C.P. Sharma. 2006. Cyclodextrin-insulin complex encapsulated polymethacrylic acid based nanoparticles for oral insulin delivery. Int. J. Pharm. 325: 147–154.
Skiba, M. and M. Skiba-Lahiani and P. Arnaud. 2002. Design of nanocapsules based on novel fluorophilic cyclodextrin derivatives and their potential role in oxygen delivery. J. Incl. Phenom. Macrocycl. Chem. 44: 151–154.
Stella, V.J. and Q. He. 2008. Cyclodextrins. Toxicol. Pathol. 36: 30–42.
Szejtli, J. 1998. Introduction and general overview of cyclodextrin chemistry. Chem. Rev. 98: 1743–1754.
Tiwari, G. and R. Tiwari and K.A. Rai. 2010. Cyclodextrins in delivery systems: applications. J. Pharm. Bioallied Sci. 2: 72–79.
Wang, Y. and J. Shao, Z. Wang and Z. Lu. 2012. Study of allicin microcapsules in β-cyclodextrin and porous starch mixture. Food Res. Int. 49: 641–647.
Villiers, A. 1891. Sur la transformation de la fécule en dextrine par le ferment butyrique. Compt. Rend. Fr. Acad. Sci. 112: 435–438.
Vyas, A. and S. Saraf and S. Saraf. 2008. Cyclodextrin based novel drug delivery systems. J. Incl. Phenom. Macrocycl. Chem. 62: 23–42.
Yang, X. and J. Kim. 2010. pH-dependent release of blue dextran from carboxymethyl-β-cyclodextrin hydrogels. J. Ind. Eng. Chem. 16: 763–766.
Zia, V. and R.A. Rajewski and V.J. Stella. 2001. Effect of cyclodextrin charge on complexation of neutral and charged substrates: comparison of (SBE)7M-beta-CD to HP-beta-CD. Pharm. Res. 18: 667–673.
Zhou, J. and H. Ritter. 2010. Cyclodextrin functionalized polymers as drug delivery systems. Polym. Chem. 1: 1552–1559.

CHAPTER 6

Drug Delivery Systems Based on Tyrosine-derived Nanospheres (TyroSpheres™)

Zheng Zhang,[1] *Tannaz Ramezanli,*[2,3,a] *Pei-Chin Tsai*[2,3,b] and *Bozena B. Michniak-Kohn*[2,3,c,*]

ABSTRACT

Polymeric nanoparticles are nano-sized drug carriers that provide controlled and improved loading, protection, tunable release and targeted delivery of drugs. Amphiphilic block copolymers composed of poly(ethylene glycol) as the hydrophilic segments and degradable synthetic polyesters as the hydrophobic segments are widely used to build the nanospheres, and the core-shell structure enables dramatically increased blood circulation time and significantly suppressed protein adsorption and uptake of the nanoparticles by the reticuloendothelial system. In this chapter, we describe a novel platform of nanospheres from biodegradable, tyrosine-derived

[1] New Jersey Center for Biomaterials, Rutgers-The State University of New Jersey, 145 Bevier Road, Piscataway, NJ 08854, USA.
Email: zhang@biology.rutgers.edu
[2] Center for Dermal Research, Rutgers-The State University of New Jersey, 145 Bevier Road, Life Sciences Bldg. Room 109, Piscataway, NJ 08854, USA.
[a] Email: tr243@eden.rutgers.edu
[b] Email: tsai.p1027@gmail.com
[c] Email: michniak@biology.rutgers.edu
[3] Department of Pharmaceutics, Ernest Mario School of Pharmacy, Rutgers-The State University of New Jersey, Piscataway, NJ 08854, USA.
* Corresponding author

List of abbreviations after the text.

amphiphilic block copolymers composed of tyrosine dipeptide derivatives, naturally occurring diacid and poly(ethylene glycol); the hydrophobic segments of the polymers are based on naturally occurring metabolites. These nanospheres are trademarked TyroSpheres™ and are vehicles for lipophilic drugs. By changing the molecular weight of poly(ethylene glycol) and the pendent group of the dipeptide derivatives, the size of the TyroSpheres™ can be regulated within a range of 36 to 122 nm. The size distribution is narrow as the polydispersity index is less than 0.25. For the leading polymer, poly(ethylene glycol)$_{5k}$-oligo(desaminotyrosyltyrosine octyl-suberic acid)-poly(ethylene glycol)$_{5k}$, more than 10 lipophilic drugs and fluorescent model compounds have been successfully loaded into TyroSpheres™, without changing their size and size distribution. Significant efforts have been devoted to paclitaxel-loaded TyroSpheres™. Up to 8 wt% of paclitaxel can be loaded into TyroSpheres™ with the encapsulation efficiency higher than 70 wt%. Sustained release pattern of paclitaxel from paclitaxel-TyroSpheres™ dispersions was recorded under sink conditions, and the release rates were regulated by the initial loading of the paclitaxel. The potential of TyroSpheres™-based delivery systems in medical applications was explored for the treatment of skin diseases and breast cancer, respectively. In the former case, a high viscous formulation was developed, showing enhanced skin penetration of the loaded fluorescent compounds as well as paclitaxel, which were delivered predominantly into the deeper layers of epidermis, less into dermis and with negligible systemic exposure. In the latter case, paclitaxel-loaded TyroSpheres™ showed equivalent efficacy in the antitumor activity as compared to the paclitaxel containing, clinically used Cremophor® EL in an *in vivo* study using two clinically relevant breast cancer murine models: MDA-MB-435 estrogen independent and ZR-75-1 estrogen dependent. Remarkably, in a parallel *in vivo* study using NCr nu/nu mice, it was found that treatment with TyroSpheres™ provided superior safety and significantly improved tolerability to higher doses of paclitaxel as compared to Cremophor® EL. In conclusion, TyroSpheres™ are excellent nano-sized carrier systems for lipophilic drugs.

Introduction

Tyrosine-derived nanospheres (TyroSpheres™), proven as a versatile drug carrier for lipophilic compounds and offering a controlled drug release pattern, were developed and patented by the group at the New Jersey Center for Biomaterials (Rutgers-The State University of New Jersey). The medical applications of this new technology have been explored, focusing on topical and intravenous (i.v.) routes of administration. The broad scope and the depth in detail of the research conducted over the past decade demonstrated the potential of TyroSpheres™ for the pharmaceutical, personal care and cosmetic industries.

Background: polymeric nanoparticles as nano-sized drug carriers

The era of modern drug discovery began more than a century ago, when the "magic bullet" concept was made popular by Paul Ehrlich (1854–1915, Nobel Prize winner in 1908 in Physiology/Medicine). The key idea of the "magic bullet" concept is to deliver a toxin for disease-causing organism selectively to the target (Ehrlich 1906). Penicillin, one of the greatest discoveries, was generally considered as the first great "magic bullet" due to its safety, efficacy and in particular, its specificity at killing gram positive bacteria that caused lethal infections, and this changed the course of history in and beyond the battlefields of World War II.

In the second half of the 20th century, the focus of the pharmaceutical industry was shifted from the search for drugs that treat and prevent bacterial infections to advancing new drugs that treat specific diseases. Over 690 New Chemical Entities (NCEs) were approved by the Food and Drug Administration (FDA) in the United States from 1963 to 1999, since the 1962 amendments to the Federal Food, Drug and Cosmetic Act of 1938 (Dimasi 2000). However, the advance in drug discovery has been limited by the toxicity, side effects and poor stability and bioavailability of the various drugs. The complex nature of diseases, such as cancer, has also weakened the efficacy of the conventional drug delivery approaches. To overcome these hurdles, a new concept of targeted and controlled drug delivery approaches using polymeric matrix systems to load and deliver drugs to the targeted sites has been proposed and developed (for review, see Uhrich et al. 1999).

Among the different vehicles of delivery approaches, nano-sized drug carriers are one of the most extensively studied systems. Nano-sized carriers have many unique features as the "magic bullet", including: *i*) sustained and controlled release of drugs; *ii*) stabilization of compounds by providing both chemical and physical protection; *iii*) provision of higher drug concentrations in tumors due to the Enhanced Permeation and Retention (EPR) effect (Matsumura and Maeda 1986); *iv*) cell and tissue specific targeting via conjugating antibodies and peptides to carrier surfaces; and, *v*) gene delivery via preparing drug-vehicle complexes that can be internalized (Zhang et al. 2013).

Depending on the composition and structure, nano-sized carriers can be categorized into several classes including polymeric nanoparticles, solid lipid nanoparticles, inorganic nanoparticles, liposomes, nanoemulsions, etc. Among these nano-sized carriers, polymeric nanoparticles with readily tunable chemical and physical features can effectively protect unstable drugs from degradation/denaturation, and decrease the side effects of toxic drugs by controlled release.

The development of polymeric nanoparticle systems for the controlled delivery started in the 1970s (Birrenback and Speiser 1976, Couvreur et al. 1979, Kreuter 1991, Couvreur et al. 1995). Since then, significant efforts have been devoted to the research and development (R&D) of polymeric nanoparticles (Farokhzad and Langer 2009). Several nanoparticle-based treatments have already been approved by FDA, such as, micellar nanoparticles (Estrasorb®) for menopause and albumin-bounded paclitaxel (PTX) nanoparticles (Abraxane®) for breast cancer treatment.

In general, polymeric nanoparticles can be divided into three different categories: *i*) nanocapsules, the vesicular systems in which a liquid core is surrounded by a polymeric membrane (Couvreur et al. 2002); *ii*) polymeric micelles, dispersions of amphiphilic block copolymers that self-assemble into core-shell structures (hydrophobic cores stabilized by the hydrophilic shells), being spherical and fairly monodisperse in size (Couvreur et al. 1995, Kwon 1998, Torchilin 1998); and, *iii*) nanospheres, a dispersion of polymeric matrices that are spherical in shape, but in general larger and more polydisperse than polymeric micelles (Torchilin 1998). In the published literature, the colloidal dispersions of amphiphilic block copolymers are often referred to as polymeric micelles or nanospheres; the distinction being rather ambiguous.

The polymers used to prepare nanoparticles are preferably biodegradable so that after the release of the encapsulated drugs, no original polymer remains permanently in the body. According to the source of the polymer, two classes can be identified: natural and synthetic polymers (for a recent review, see Zhang et al. 2013). Natural polymeric nanoparticles are composed of polymers occurring in nature, such as, chitosan, alginate, gelatin and albumin. An advantage of the natural polymers is their functional carboxylic and amine groups, allowing for cross-linking, hydrogen bond formation and surface modification. In addition, the tendency of these natural polymers to form hydrogels makes them ideal carriers for oligonucleotides, peptides, proteins and hydrophilic drugs. On the other hand, there are a number of disadvantages of the use of natural polymers: *i*) these natural polymers are usually obtained from extraction followed by various purification procedures and, therefore, large batch-to-batch variations in physical and chemical properties can be expected; *ii*) it is difficult to load them with lipophilic drugs; *iii*) the rate of degradation is less easily tunable for various applications; and, *iv*) potential antigenic materials may be associated with the natural polymers.

Nanoparticles based on synthetic polymers offer advantages including: *i*) defined and reproducible physical and chemical properties; *ii*) possibilities to regulate the rate of degradation and mechanical properties; *iii*) capability of loading both lipophilic and hydrophilic compounds; and, *iv*) readily tunable release profiles. Much research has been conducted to prepare

nanoparticles based on aliphatic degradable polyester (co)polymers of lactic acid and/or glycolic acid, as well as their block copolymers with poly(ethylene glycol) (PEG) (Brannon-Peppas 1995, Uhrich et al. 1999, Dailey et al. 2005). However, the degradation products resulting from polyester hydrolysis can lead to an increase in the local acidity that could be deleterious to the loaded active components (Fu et al. 1987). Also the autocatalytic bulk degradation behavior of polyesters may result in an accelerated release of the drug at the late stages of the degradation process (Pitt and Gu 1987). A strategy to alleviate these concerns is to use polymers possessing benign degradation properties with neither autocatalytic degradation nor acidic end degradation products. Examples of such polymers are trimethylene carbonate-based aliphatic polycarbonate, i.e., poly(trimethylene carbonate) (PTMC) and amphiphilic diblock copolymers monomethoxy-terminated poly(ethylene glycol) (mPEG)-PTMC (Zhang et al. 2006a,b). The rationale of using PTMC-based (co)polymers is that they degrade *in vivo* by enzymatic surface erosion without forming acidic by-products (Zhang et al. 2006c).

A new concept is to prepare nanoparticles from polymers based on naturally occurring metabolites. Tyrosine-derived polymers, as the representing example, have been developed and explored for medical applications by Kohn et al. at the New Jersey Center for Biomaterials (Rutgers-The State University of New Jersey). Tyrosine, the only major, natural nutrient containing an aromatic hydroxyl group was used as the starting moiety; modification of its amino and carboxylic groups offers the strategy to create a platform of non-toxic polymers whose main degradation products are naturally occurring metabolites (Kohn and Langer 1987, Pulapura and Kohn 1992, Hooper et al. 1998, Bourke and Kohn 2003, Kohn 2004). Within this framework, a family of degradable polymers composed of tyrosine dipeptide derivative, naturally occurring diacid and PEG are created and used to prepare nanoparticles for drug delivery. A detailed discussion is given below.

Development of Tyrosine-Derived NanoSpheres (TyroSpheres™)

Tyrosine-derived amphiphilic block copolymers PEG-*b*-oligo(DTR-XA)-*b*-PEG

TyroSpheres™ are based on amphiphilic block copolymers composed of hydrophilic outer segments (PEG) and a hydrophobic inner segment (polyarylate oligomer). The inner segment is made of a tyrosine-derived diphenol and a diacid (Fig. 6.1).

The synthesis of this family of tyrosine-derived polymers was reported previously (Nardin et al. 2004, Sheihet et al. 2005). In brief, it is a step-

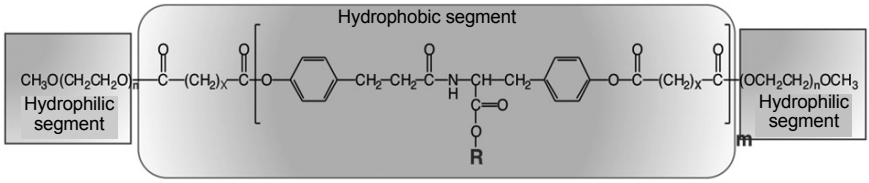

Figure 6.1. Chemical structure of a tyrosine-derived amphiphilic block copolymer. Hydrophilic segments: PEG; hydrophobic segment: polyarylate oligomer composed of a tyrosine dipeptide derivative and a diacid. Nomenclature: The polymers are named PEG-*b*-oligo(DTR-XA)-*b*-PEG triblock copolymers.

wise reaction in which the oligo(DTR-XA) inner block is first prepared by polycondensation, and then the oligo(DTR-XA) is coupled with mPEG. Here the alkyl pendent group (R) in desaminotyrosyltyrosine alkyl (DTR) ester provides a convenient way to modify the polyarylate structure and properties, while the number of methylene groups (X) in the diacid (XA) provides a convenient way to regulate the hydrophobic character of the polymer backbone. By changing the ratio of molecular weights between the hydrophilic and the hydrophobic segments, the length of the diacid (XA), and the pendent group of the dipeptide (R), a large number of interrelated polymers with different physicochemical properties can be obtained. The wide range of the polymer properties provides freedom in design of TyroSpheres™ and drug-loaded TyroSpheres™ complexes suitable for versatile applications.

The amphiphilic structure presented in Fig. 6.1 addresses a number of features that enable the formation of nanoparticles as lipophilic drug carriers:

- In general, the nanoparticle dispersion is stabilized by the PEG segments of the block copolymers positioned at the periphery of the nanoparticles, while the lipophilic drug molecules are incorporated in the hydrophobic domains inside the nanoparticles.
- PEG is the most widely applied hydrophilic building block of polymeric biomaterials. It is non-toxic and biocompatible (Greenwald et al. 2003). Nanoparticles made of amphiphilic copolymers containing PEG exhibited dramatically increased blood circulation time (Gref et al. 1994) and significantly suppressed protein adsorption and uptake of the nanoparticles by the reticuloendothelial system (Xu et al. 2005).
- The inner block of the copolymer is a low weight average molecular weight (M_w) version of a family of tyrosine-based polyarylates developed at New Jersey Center for Biomaterials (Rutgers-The State University of New Jersey) (Hooper et al. 1998). Such polyarylates are biodegradable and the final degradation products are naturally occurring metabolites (Bourke and Kohn 2003). FDA clearance of the

polyarylates was obtained in 2006 and the polymers are marketed by TyRx Pharma, Inc. (New Jersey, USA) in a medical device for hernia repair. These results reflect the benign biocompatibility of the tyrosine-derived copolymers.

- The oligo(DTR-XA) inner blocks are in general amorphous having low glass transition temperature (T_g). For example, the T_g values of desaminotyrosyltyrosine *n*-butyl (DTB)-suberic acid (SA) and desaminotyrosyltyrosine octyl (DTO)-SA are 42 and 21ºC, respectively. The amphiphilic block copolymer PEG-*b*-oligo(DTR-XA)-*b*-PEG showed a T_g at –32 to –34ºC, and a melting transition between 47 and 54ºC. In the wet status, both the hydrophilic PEG segments and the amorphous oligo(DTR-XA) segment are flexible, ensuring the self-assembly of the polymers into a dynamic and non-frozen structure in aqueous media (Nardin et al. 2004, Sheihet et al. 2005).

Fabrication of TyroSpheres™

In general, nanoparticles based on synthetic polymers can be prepared by four methods: emulsification-evaporation, solvent displacement, salting-out and emulsification-diffusion (Quintanar-Guerrero et al. 1998). In the emulsification-evaporation method, the organic phase (polymer solution in a water immiscible, volatile solvent, e.g., dichloromethane) is emulsified in the aqueous phase into liquid droplets. The subsequent evaporation of the organic solvent leads to nanoparticle formation. In the solvent displacement method, the polymer is dissolved in a semi-polar water miscible solvent, e.g., ethanol or acetone. Adding the organic phase into the aqueous phase, results in the formation of nanoparticles. The organic solvent is then removed by dialysis, ultracentrifugation or evaporation. In the salting-out method, the organic phase is a polymer solution in water miscible solvent, and the aqueous phase is a highly concentrated salt solution that is not miscible with the organic phase. After emulsification of the organic phase in the highly salted aqueous phase, the addition of an excess amount of water results in the extraction of the organic solvent from the emulsified droplets into the much diluted aqueous phase. The salt and solvent are removed by ultracentrifugation or cross-flow filtration. In the emulsification-diffusion method, the organic phase of polymer in water miscible organic solvent is emulsified in an aqueous phase saturated with partially water soluble solvent, e.g., benzyl alcohol or ethyl acetate. Similar to the salting-out method, now adding an excess amount of water leads to the formation of the nanoparticles. The partially water soluble solvent can be removed by evaporation or cross-flow filtration. All the above mentioned methods are suitable for loading hydrophobic drugs by co-dissolving the drug with the polymer in the organic phase. On the other hand, hydrophilic drugs

can be loaded by introducing a water-in-oil emulsification before adding the oil phase into the second aqueous phase. For example, by water/oil/water double emulsion. Alternatively for nanoparticles based on natural polymers, hydrophilic drugs can self-assemble with the natural polymer via static electric interactions, *in situ* cross-linking, etc.

Scientists in New Jersey Center for Biomaterials (Rutgers-The State University of New Jersey) have developed a technique for TyroSpheres™ preparation (Nardin et al. 2004, Sheihet et al. 2005). Briefly, tyrosine-derived amphiphilic copolymer is dissolved in a water miscible solvent, e.g., tetrahydrofuran (THF) or *N*,*N*-dimethylformamide (DMF), and added dropwise into an aqueous phase; gentle magnetic stirring is applied. Typically, a bluish dispersion of nanospheres is then formed. The preparation is purified by filtration (using 0.22 μm polytetrafluoroethylene filters), ultracentrifugation, re-dispersion and a second filtration. Co-dissolving the drug in the organic phase allows drug loading (Fig. 6.2). This process has a number of advantages: *i*) the involvement of chlorinated solvent and high temperature is avoided; therefore, the procedure can be readily scaled up; and, *ii*) it is a simple method without sophisticated laboratory skills. In the past five years much effort has been directed toward TyroSpheres™ preparation and characterization, as well as validation of techniques and reproducibility of batches, e.g., size and size distribution of the nanospheres, drug Loading Efficiency (LE), drug Binding Efficiency (BE), etc.

In the preparation of TyroSpheres™, the use of external surfactant/stabilizers is avoided. This is attributed to the amphiphilic nature of the PEG-*b*-oligo(DTR-XA)-*b*-PEG: the PEG segments of the block copolymers (positioned at the periphery of the nanoparticles) can stabilize the nanosphere dispersion.

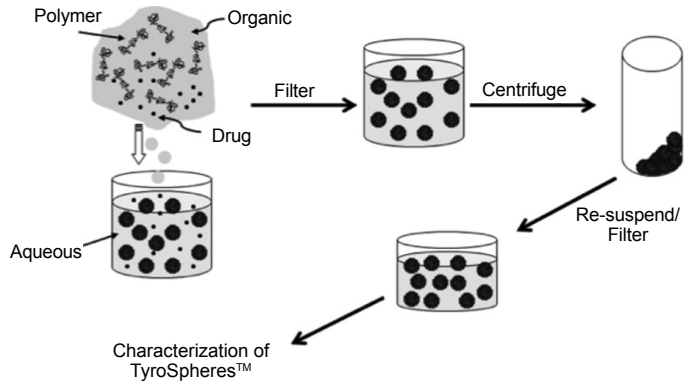

Figure 6.2. Preparation and purification of (drug-loaded) TyroSpheres™.

A number of tyrosine-derived amphiphilic block copolymers, as illustrated in Fig. 6.1, were applied for TyroSpheres™ preparation. Variations in polymer structure are created by: *i*) pendent group [DTE (R = ethyl), DTO (R = octyl) and DTD (R = dodecyl)]; *ii*) diacid length [SA (X = suberic acid or suberate) and DA (X = dodecanoate)]; and, *iii*) PEG length (number average molecular weight, M_N = 2.0–5.0 Kg/mol) (Sheihet et al. 2007). For all the polymers applied, nanoparticles were successfully prepared and the sizes (hydrodynamic diameter measured via dynamic light scattering, DLS) ranged from 36 to 122 nm, depending on the structure of the polymer.

It was found that the hydrodynamic diameter of the triblock copolymer nanospheres is strongly dependent on the length of PEG blocks and pendent R groups, but less dependent on the diacid length (Sheihet et al. 2007). With respect to the length of the PEG blocks, the shorter the PEG block, the smaller the diameter of the nanospheres. This may be explained by the chain package of the amphiphilic block copolymers in the relatively hydrophobic core of the nanospheres (block copolymers with shorter PEG chains can be packed in a relatively tighter manner than the ones with longer PEG chains). Regarding the pendent R groups, DTO-based copolymers resulted in the smallest nanospheres in size. This may be related to the nature of the hydrophobic chain package within the hydrophobic core of the nanospheres.

From preliminary drug encapsulation experiments in which various lipophilic drugs were loaded into nanospheres based on different copolymers, we selected PEG_{5k}-*b*-oligo(DTO-SA)-*b*-PEG_{5k} copolymer as the leading polymer with a PEG length of 5 Kg/mol. A standard operating procedure for the preparation of 100 g scale PEG_{5k}-*b*-oligo(DTO-SA)-*b*-PEG_{5k} was developed in the New Jersey Center for Biomaterials (Rutgers-The State University of New Jersey). The characteristics of the block copolymers were found to be reproducible: the typical M_N of the block copolymer was in the range of 20–24 Kg/mol, and the molecular weight distribution was narrow (M_w/M_N = 1.3). In the following section, we describe the results of PEG_{5k}-*b*-oligo(DTO-SA)-*b*-PEG_{5k}-based nanospheres unless mentioned otherwise.

The nature of PEG_{5k}-*b*-oligo(DTO-SA)-*b*-PEG_{5k}-based TyroSpheres™ has been characterized by light scattering techniques. The size (hydrodynamic diameter measured by DLS) was in the range of 60–80 nm with polydispersity index (PDI) less than 0.25 (Sheihet et al. 2005, 2007). The Critical Aggregation Concentration (CAC) measured by Static Light Scattering (SLS) was 2.6×10^{-7} g/mL (Nardin et al. 2004). Such a low CAC value ensures the integrity of TyroSpheres™ after any reasonable dilution: taking i.v. injection as an example, the minimal amount of administered TyroSpheres™ would be

approximately as low as 2 mg to avoid the dissociation of the TyroSpheres™ due to dilution in the systemic circulation.

Independently, the morphology and the size of the TyroSpheres™ were investigated by Transmission Electron Microscopy (TEM) analysis. It was illustrated that the TyroSpheres™ were spherical (Fig. 6.3). Compared to the size measured via DLS, the diameters of the spherical features in the TEM images are smaller. This can be explained by the different sample preparation conditions using the two techniques: DLS measures the hydrodynamic diameter in the dispersion, while TEM analyzes the nanospheres after drying in vacuum.

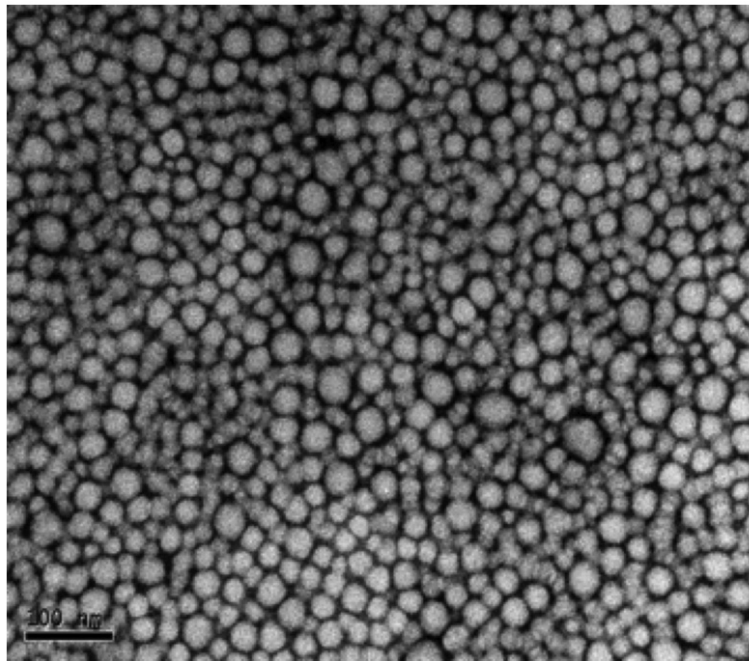

Figure 6.3. TEM image of TyroSpheres™ dispersed in phosphate buffered saline (PBS) and dried on gold grids. Negative staining (uranyl acetate) was applied. Scale bar: 100 nm. Reprinted with permission from Sheihet et al. (2012). Copyright Elsevier (2012).

TyroSpheres™ as Drug Carriers

TyroSpheres™ have been developed as a widely applicable, nano-sized carrier for the highly hydrophobic drugs PTX and curcumin and the vitamin D_3 analogue (Sheihet et al. 2005, 2007, 2012). Table 6.1 lists some of the drugs and the fluorescent model compounds that have been encapsulated in TyroSpheres™.

Table 6.1. Drugs and fluorescent model compounds that have been encapsulated into TyroSpheres™.

Drugs	**Fluorescent model compounds**
Cytarabine	Nile red
Camptothecin	5-dodecanoylaminofluorescein (DAF)
Colchicine	
Curcumin	
Diclofenac sodium	
Nocodazole	
PTX	
Rapamycin	
Vitamin D_3 analogue	

Incorporation of these drugs into TyroSpheres™ had negligible impact on the size (60–80 nm in diameter) and size distribution (PDI < 0.25) of the TyroSpheres™ (Sheihet et al. 2005, 2007, 2012). This size range of the drug-loaded TyroSpheres™ has significant advantages for medical applications: *i*) for safety, the TyroSpheres™ are small enough for i.v. injection without risks of the blockage of the capillary blood vessels, while large enough to prevent risks of penetrating biological barriers, e.g., stratum corneum in skin, mucosal barrier in the gastrointestinal tract and alveolar-capillary barrier in the lungs; *ii*) PEGylated particles with diameters less than 200 nm avoid the entrapment by the reticuloendothelial system, thus the rate of clearance is decreased and the circulation time is extended; and, *iii*) the nano-ranged size and the prolonged circulation time would result in the accumulation of the nanoparticles in tissues with increased vascular permeability, such as, tumors. Therefore, the drug efficacy would increase and the toxicity to healthy tissues would be minimized (Matsumura and Maeda 1986).

To investigate the drug-polymer interactions in TyroSpheres™, a computational modeling study combining molecular dynamics simulations and docking calculations was carried out using three model compounds: the nutraceutical compound curcumin, the anticancer drug PTX and an analogue of the prehormone vitamin D_3 (Costache et al. 2009). It was found that the binding affinity of drugs to polymers depended not only on their hydrophobic compatibility (meaning the more hydrophobic the drug is, the higher that can be expected the binding affinity), but also on other physical interactions, such as, hydrogen binding and π-π stacking. The computation study and the experimental data fit well for the three model drugs: the most hydrophobic drug, vitamin D_3, showed the highest affinity to the particular PEG_{5k}-*b*-oligo(DTO-SA)-*b*-PEG_{5k}-based TyroSpheres™ assembly (experimental maximum drug loading 36%, w/w). For curcumin and PTX, the hydrophobic values were found to be similar. However, the maximum

amount of curcumin encapsulated was more than double of that for PTX (29 and 12%, w/w, respectively). This was related to the data obtained via docking calculations on the drug-polymer assembly following the lowest energy confirmation: curcumin has more hydrogen bonds and π-π interactions with the polymer as compared to PTX (Costache et al. 2009).

Significant effort has also been made at the New Jersey Center for Biomaterials (Rutgers-The State University of New Jersey) to develop clinically relevant paclitaxel-loaded tyrosine-derived nanospheres (PTX-TyroSpheres™) formulations. PTX is a mitotic inhibitor promoting the assembly and stabilization of microtubules and eventually leading to cell death (Koziara et al. 2004). It is clinically used for cancer treatment, the available marketed formulations being Taxol™ (PTX in Cremophor® EL) and Abraxane® (PTX-loaded albumin nanoparticles). Due to its ability to prevent cellular overproliferation, PTX can potentially be used to treat psoriasis as well. It was reported that the systemic administration of PTX-loaded nanoparticles composed of poly(D,L-lactide) and methoxypolyethylene copolymers resulted in the reduction of psoriasis severity and reduced epidermal thickness (Ehrlich et al. 2004).

However, the poor solubility of PTX and its toxicity limits the medical applications of this drug. An efficient and reproducible loading of PTX into TyroSpheres™ is the prerequisite for the development of PTX-TyroSpheres™ formulations. Therefore, the encapsulation behavior of PTX in TyroSpheres™ was studied in detail. After preparation and purification of PTX-TyroSpheres™ following the steps as illustrated in Fig. 6.2, the PTX concentration in final formulations was determined using extraction and high performance liquid chromatography (HPLC) techniques (Sheihet et al. 2007). The encapsulation behavior of PTX was characterized by BE (%) [(mass of PTX in TyroSpheres™/mass of PTX in the feed) × 100], and LE (%) [(mass of PTX in TyroSpheres™/mass of TyroSpheres™) × 100] (Sheihet et al. 2007, Kilfoyle et al. 2012).

Figure 6.4 shows the BE and LE values of PTX by TyroSpheres™, in which the initial input (in feed) of PTX to polymer ratio was gradually increased from 4 to 10% (w/w). Clearly, PTX was effectively encapsulated by TyroSpheres™ up to an initial drug input of 8% (w/w) to polymer; up to this level, the LE was proportional to the initial drug input, and the BE was greater than 70%. For cases where the initial drug inputs were respectively 9 and 10% (w/w), both the LE and BE values dropped markedly. In addition, the small standard error (SE) of the data suggests that the encapsulation of PTX into TyroSpheres™ was reproducible (Kilfoyle et al. 2012).

At the maximum LE (8.4%, w/w) tested, TyroSpheres™ provided significant enhancement of PTX solubility (1160 µg/mL). This is much higher than the solubility of PTX in PBS and in PBS supplemented with

0.1% (w/v) and 1.0% (w/v) of Tween® 80, respectively being 0.3, 2.7, and 13.8 µg/mL) (Kilfoyle et al. 2012).

Under sink conditions, sustained release patterns of PTX were recorded for a series of PTX-TyroSpheres™ dispersions with PTX LE ranging between 1.2 and 8.4% (w/w). PTX release was performed for up to 72 hours. Interestingly, at the end of the study, approximately 8, 44, and 58% of the drug was released from the 1.2, 5.0, and 8.4% (w/w) PTX-TyroSpheres™, respectively (Fig. 6.5) (Kilfoyle et al. 2012). Results suggested that the

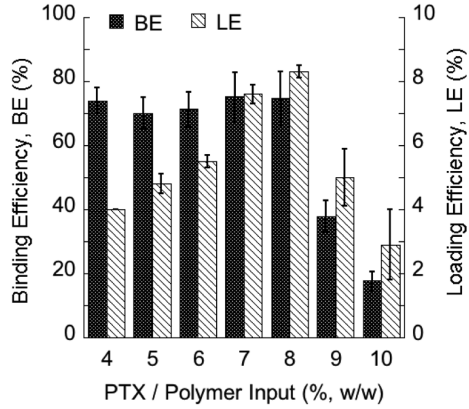

Figure 6.4. BE (%) and LE (%) values of PTX by TyroSpheres™ as a function of the initial input of PTX to polymer ratio (%, w/w). The results are presented as mean ± SE. *n* values for each tested PTX/polymer input were: 16 (4%), 6 (5%), 8 (6%), 12 (7%), 16 (8%), 12 (9%), and 7 (10%). Reprinted with permission from Kilfoyle et al. (2012). Copyright Elsevier (2012).

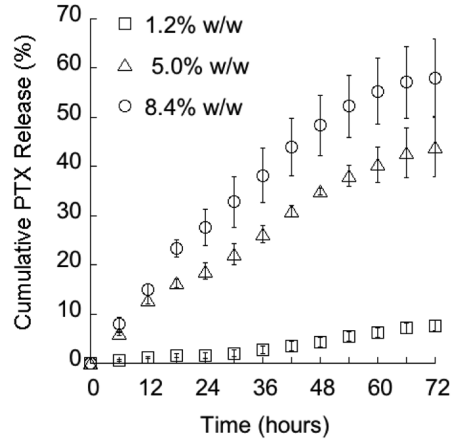

Figure 6.5. The effect of PTX content on drug release from PTX-TyroSpheres™. Cumulative PTX release (%) measured using the Franz cell method from: 1.2% (w/w, □), 5.0% (w/w, Δ), and 8.4% (w/w, ○) PTX-TyroSpheres™. The results are presented as mean ± SE ($n = 3$). Reprinted with permission from Kilfoyle et al. (2012). Copyright Elsevier (2012).

lower the PTX loading, the slower the drug release. This phenomenon can be potentially explained by the different binding affinities of PTX in the TyroSpheres™ where the available "hot spots" are occupied first, followed by the binding sites with weaker affinities (Costache et al. 2009). Therefore, the higher LE can be linked to a quicker release of the loosely bound PTX molecules. This provides an easy way to control PTX release by simply tuning the amount of the loaded drug.

One advantage of the release patterns is that the burst release, which often occurs for the nanoparticle-based system, was not observed. This may be attributed to the low T_g values of the inner block (Nardin et al. 2004, Sheihet et al. 2005), resulting in the dynamic chain arrangement of the PTX-polymer complexes (see above). The aggregation of highly hydrophobic PTX molecules at the periphery of the nanospheres, which can directly lead to burst release, is then avoided.

It was further found that the polymer, PEG_{5k}-*b*-oligo(DTO-SA)-*b*-PEG_{5k}, was stable when the aqueous nanospheres dispersion was kept at room temperature as well as 37ºC for one week. In these conditions, the TyroSpheres™ are found to be stable as well, without any change in size and size distribution. Therefore, it is reasonable to assume that the diffusion mechanism plays a significant role for the release of loaded drugs. The burst release of drugs in the later time post-administration, which is caused by the polymer degradation and nanospheres dissociation, can be thus prevented.

Bio-response of TyroSpheres™ and paclitaxel-TyroSpheres™

The controlled release may enhance the efficacy of PTX in preventing unwanted cellular overproliferation, while still decreasing the side effects from, e.g., pulsatile drug administration or burst release. To test this hypothesis, and also to evaluate the biocompatibility/toxicity of TyroSpheres™ as a vehicle, a number of *in vitro* experiments were carried out.

The biocompatibility of non-loaded TyroSpheres™ was evaluated in a series of studies in which a wide range of cells were used. The maximum tested concentrations of TyroSpheres™ varied between 2.0 and 11.5 mg/mL, and negligible cytotoxicity was recorded in all the cases. These results are summarized in Table 6.2. Clearly, TyroSpheres™ showed excellent biocompatibility.

Then, the cytotoxicity assay was conducted in which the antiproliferation effect of PTX on KB human cervical carcinoma cells, breast cancer cell lines and HaCaTs (a human keratinocyte cell line) was evaluated. For some of the cells, the cytotoxicity of free PTX [applied via dissolving the drug in dimethyl sulfoxide, DMSO and then adding the DMSO-containing drug

stock solutions into the cell culture media (DMSO:cell culture media = 1:1000, v/v)] was evaluated as the reference. The half maximum inhibitory concentrations (IC_{50}) of PTX, in the loaded form in TyroSpheres™ and as free drug, are summarized in Table 6.3. Results confirmed the potency of PTX-TyroSpheres™ to all the cells tested, with IC_{50} < 5 nM. To KB human cervical carcinoma cells and HaCaTs, PTX-TyroSpheres™ showed much lower IC_{50} as compared to PTX applied as free drug. Especially for KB human cervical carcinoma cells, the IC_{50} of PTX-TyroSpheres™ was only ≈ 17% of that of free PTX. Clearly, TyroSpheres™, as a non-toxic vehicle, enhanced the antiproliferative effect of PTX and such enhancement was shown to be cell type dependent.

Table 6.2. Maximum concentrations (mg/mL) of TyroSpheres™ tested in cytotoxicity studies using different cells. No cytotoxicity was found in all the studies.

Cell line	TyroSpheres™ concentration (mg/mL)	Reference
UMR-106 osteosarcoma	2.0	Nardin et al. 2004
KB human cervical carcinoma	4.0	Sheihet et al. 2005
Human dermal fibroblast	11.5	Batheja et al. 2011
Human neonatal keratinocyte	11.5	
MDA-MB-435 breast cancer	6.0	Sheihet et al. 2012
ZR-75-1 breast cancer	2.5	

Table 6.3. IC_{50} (nM) of free PTX and PTX-TyroSpheres™ on various types of cells.

Cell line	IC_{50} free PTX (nM)	IC_{50} PTX-TyroSpheres™ (nM)	Reference
KB human cervical carcinoma	28.9 ± 5.4	4.9 ± 0.1	Sheihet et al. 2007
HaCaTs	3.3 ± 0.5	1.7 ± 0.3	Kilfoyle et al. 2012
MDA-MB-435 breast cancer	Not defined	≈ 0.1	Sheihet et al. 2012

Exploration of the Therapeutic Applications of TyroSpheres™

TyroSpheres™-based topical drug delivery system for the treatment of skin diseases

Topically applied, polymeric nanoparticulate-based drug delivery systems for the treatment of skin diseases have many benefits including: *i*) the skin permeation of therapeutics, especially poorly water soluble drugs (such as, PTX), can be effectively enhanced due to the increased concentration gradient across the skin; *ii*) the carrier systems can protect the drugs from degradation/denaturation and improve the drug stability for non-stable

compounds; *iii*) when relatively toxic drugs are applied, controlled and sustained release patterns have the potential to decrease side effects, such as, skin irritation; and, *iv*) the systemic exposure is minimized and the drugs are delivered effectively to the target site associated with the skin disease (Zhang et al. 2013).

In order to evaluate the feasibility of TyroSpheres™ as a topically applied drug delivery system, the percutaneous penetration of lipophilic fluorescent dyes, i.e., nile red (log *D*: 3.10) and DAF (log *D*: 7.54) that were applied topically, either in TyroSpheres™ dispersions or in propylene glycol (PG, as control), respectively were investigated. Nile red and DAF were chosen as lipophilic model compounds since their skin penetration can be visualized via fluorescent imaging and the relative dye content can be quantified by fluorescent yield. Franz diffusion cell modules (receptor volume 5 mL and donor area of 0.64 cm^2) were used to mimic *in vivo* topical application conditions, and human cadaver skin specimens were used (Sheihet et al. 2008). It was found that TyroSpheres™ delivered respectively 9.0 times the amount of nile red and 2.5 times the amount of DAF into skin strata as those obtained from the control experiments using PG formulations. Convincingly, TyroSpheres™ facilitated the skin delivery of these lipophilic compounds (Sheihet et al. 2008).

The aqueous dispersion of TyroSpheres™ is not ideal for topical applications since the formulation tends to run off the skin application area. This decreases the contact time between formulation and site of application. To address this issue, we tested a series of high viscosity formulations based on hydroxypropyl methylcellulose (HPMC) and PG. In an *ex vivo* skin permeation study using Franz diffusion cells (the "run off" issue is prevented for the TyroSpheres™ dispersion since it is a static cell design), the equivalent penetration of nile red into stratum corneum and viable epidermis was recorded for the nile red-loaded TyroSpheres™ dispersion and the nile red-loaded TyroSpheres™-HPMC-PG formulation. Both cases resulted in significantly increased skin penetration as compared to that obtained using nile red in aqueous PG as control (Batheja et al. 2011). Remarkably, in an *in vivo* study using pigs, the nile red skin penetration from topically applied nile red-loaded TyroSpheres™-HPMC-PG formulation was ≈ 40% higher than that obtained from nile red-TyroSpheres™ dispersion applied via Hill Top Chambers® (occlusive patch test systems) (Batheja et al. 2011). These results suggest the efficiency and advantage of using highly viscous formulations for topical application.

TyroSpheres™-based topical delivery systems using compounds exemplified by PTX were further developed, aiming at treating skin conditions, such as, psoriasis. In the leading formulation (1%, w/v HPMC), the use of PG was excluded to avoid possible skin irritation (Kilfoyle et

al. 2012). Homogeneity of the PTX-TyroSphere™-HPMC formulation stored at 4ºC was evaluated by determining PTX content from different areas within the formulation. The similar amounts of PTX in one gram of formulation were recorded at times 0 (141.9 ± 0.9 µg) and eight weeks (143.0 ± 6.6 µg), respectively (n = 10). The small Standard Deviations (SDs) were an indication of formulation homogeneity while no significant change in PTX concentration over the eight-week time period was an indication of formulation stability during storage at 4ºC (Kilfoyle et al. 2012).

Release of PTX from the PTX-TyroSpheres™-HPMC viscous (gel-like) formulation was similar to the release of PTX from TyroSpheres™ without HPMC at the same concentration of PTX and TyroSpheres™ (Fig. 6.6). In an *ex vivo* skin permeation study using Franz diffusion cells, it was found that the PTX-TyroSpheres™-HPMC formulation delivered slightly less amount of PTX into skin strata as compared to TyroSpheres™ aqueous dispersion. For both TyroSpheres™-based viscous and aqueous dispersion formulations, significant amounts of PTX were delivered into the epidermis, followed by dermal penetration which was ≈ 8–10 times lower, while the amount of PTX in the receptor chamber (representing systemic exposure) was minimal (Fig. 6.7).

The skin distribution results demonstrated that both TyroSpheres™ formulations can address the requirements of an efficient topical drug delivery system for the treatment of skin conditions, such as, psoriasis.

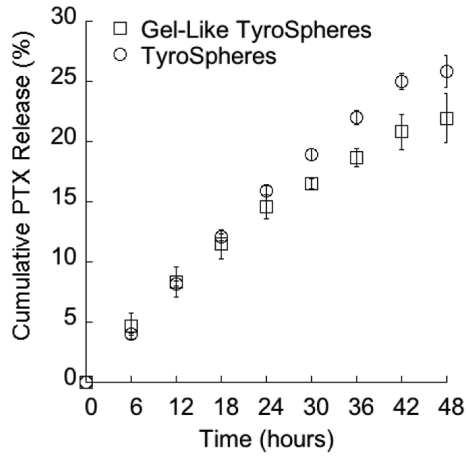

Figure 6.6. Cumulative drug release (%) from 5% w/w PTX-TyroSphere™ formulations with (□, gel-like PTX-TyroSpheres™) and without (○, PTX-TyroSpheres™) HPMC as a thickening agent. Results are presented as mean ± SE (n = 3). Reprinted with permission from Kilfoyle et al. (2012). Copyright Elsevier (2012).

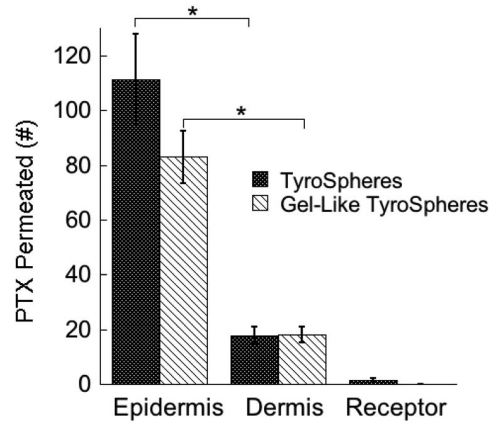

Figure 6.7. Skin distribution of PTX delivered via TyroSpheres™ (0% HPMC) and gel-like TyroSpheres™ (1% HPMC). Liquid chromatography-mass spectrometry (LC-MS) was used as a detection method to quantify PTX deposited into different skin strata and receptor fluid. On the *Y* axis, the units of PTX permeation (#) are: ng/cm^2 of tissue surface area for PTX in the epidermis and dermis, and ng/mL for PTX measured in the receptor compartment. The statistical data is expressed as mean ± SE (n = 8). The statistical test was significant *$p < 0.001$ between the amount of PTX present in the epidermis and dermis for both PTX-TyroSpheres™ and gel-like PTX-TyroSpheres™. Reprinted with permission from Kilfoyle et al. (2012). Copyright Elsevier (2012).

TyroSpheres™-based injectable drug delivery system for the treatment of breast cancer

The clinical applicability of TyroSpheres™-based injectable system has been evaluated as well. Initially, the *in vivo* toxicity profiles of TyroSpheres™, as well as Cremophor® EL, loaded with 0–50 mg of PTX per Kg were compared in NCr nu/nu mice. Treatment with PTX-TyroSpheres™ provided superior safety and significantly improved tolerability to higher doses of PTX as compared to Cremophor® EL (Sheihet et al. 2012).

Further, to assess the clinical potential of PTX-TyroSpheres™ for breast cancer treatment, the *in vivo* antitumor efficacy of PTX-TyroSpheres™ was evaluated in two clinically relevant breast cancer murine models: MDA-MB-435 estrogen independent (estrogen receptor negative, ER–) and ZR-75-1 estrogen dependent (estrogen receptor positive, ER+) (Sheihet et al. 2012). The i.v. administration of PTX-TyroSpheres™ showed comparable antitumor effects as the clinically used PTX formulation in Cremophor® EL in both mouse models (Fig. 6.8).

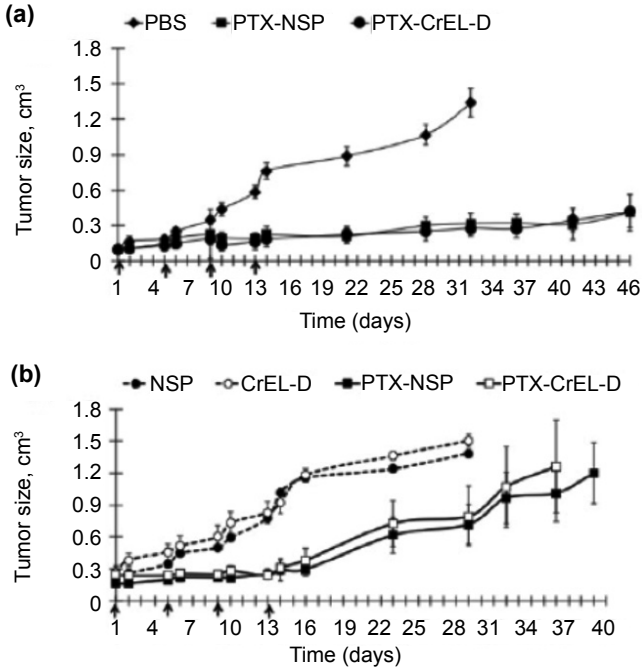

Figure 6.8. Antitumor activity (tumor size evolution, mean ± SE, cm^3) of PTX via TyroSpheres™ or clinically used Cremophor® EL in two murine models: (a) estrogen receptor negative (ER–), and (b) estrogen receptor positive (ER+). Mice (n = 6) were treated (0.2 mL) on days 1, 5, 9, and 13 with 20 mg/Kg of PTX in TyroSpheres™ (13 mg) or Cremophor® EL (52 mg) in both studies. PBS: control group; NSP: PTX-unloaded TyroSpheres™; CrEL-D = Cremophor® EL; PTX-NSP = PTX-TyroSpheres™; PTX-CrEL-D = PTX in Cremophor® EL. Reprinted with permission from Sheihet et al. (2012). Copyright Elsevier (2012).

Conclusions

TyroSpheres™ provide a platform technology of nano-sized carriers for the loading and delivery of various lipophilic compounds topically and intravenously. The application of PTX as the leading drug was explored for both psoriasis and breast cancer treatments. We believe that the TyroSpheres™ topical system can be used to prepare formulations containing various lipophilic pharmaceutical/personal care and cosmetic ingredients, and may have potential use in areas, such as, hair removal, hair loss treatment, sunscreen applications, the treatment of melanoma, contact dermatitis, etc. TyroSpheres™-based injectable systems may be a promising drug delivery vehicle for the treatment of solid mammary tumors.

Acknowledgements

The authors wish to thank our colleagues Drs. Joachim Kohn, Larisa Sheihet and Brian E. Kilfoyle (New Jersey Center for Biomaterials, Rutgers-The State University of New Jersey) for their contributions on the development of tyrosine-derived nanospheres. The work described in this chapter was supported by the New Jersey Center for Biomaterials (Rutgers-The State University of New Jersey), Grant No. EB00286 from NIH, Grant No. W81XWH-04-2-0031 from the breast cancer research program by the office of the Congressionally Directed Medical Research Programs and Grant No. 5R01AR056079 from the National Institute of Arthritis and Musculoskeletal and Skin Diseases (NIAMS-NIH).

Abbreviations

BE	:	binding efficiency
CAC	:	critical aggregation concentration
DAF	:	5-dodecanoylaminofluorescein
DLS	:	dynamic light scattering
DMF	:	*N*,*N*-dimethylformamide
DMSO	:	dimethyl sulfoxide
DTB	:	desaminotyrosyltyrosine *n*-butyl
DTO	:	desaminotyrosyltyrosine octyl
DTR	:	desaminotyrosyltyrosine alkyl
EPR	:	enhanced permeation and retention
ER–	:	estrogen receptor negative
ER+	:	estrogen receptor positive
FDA	:	Food and Drug Administration
HPLC	:	high performance liquid chromatography
HPMC	:	hydroxypropyl methylcellulose
IC_{50}	:	half maximum inhibitory concentration
i.v.	:	intravenous
LC-MS	:	liquid chromatography-mass spectrometry
LE	:	loading efficiency
mPEG	:	monomethoxy-terminated poly(ethylene glycol)
M_N	:	number average molecular weight
M_w	:	weight average molecular weight
NCE	:	new chemical entity
PBS	:	phosphate buffered saline
PDI	:	polydispersity index
PEG	:	poly(ethylene glycol)
PG	:	propylene glycol
PTMC	:	poly(trimethylene carbonate)

PTX	:	paclitaxel
PTX-TyroSpheres™	:	paclitaxel-loaded tyrosine-derived nanospheres
R&D	:	research and development
SA	:	suberic acid
SD	:	standard deviation
SE	:	standard error
SLS	:	static light scattering
TEM	:	transmission electron microscopy
T_g	:	glass transition temperature
THF	:	tetrahydrofuran
TyroSpheres™	:	tyrosine-derived nanospheres

References

Batheja, P. and L. Sheihet, J. Kohn, A.J. Singer and B. Michniak-Kohn. 2011. Topical drug delivery by a polymeric nanosphere gel: formulation optimization and *in vitro* and *in vivo* skin distribution studies. J. Control. Release. 149: 159–167.

Birrenbach, G. and P. Speiser. 1976. Polymerized micelles and their use as adjuvants in immunology. J. Pharm. Sci. 65: 1763–1766.

Bourke, S.L. and J. Kohn. 2003. Polymers derived from the amino acid L-tyrosine: polycarbonates, polyarylates and copolymers with poly(ethylene glycol). Adv. Drug Deliv. Rev. 55: 447–466.

Brannon-Peppas, L. 1995. Recent advances on the use of biodegradable microparticles and nanoparticles in controlled drug delivery. Int. J. Pharm. 116: 1–9.

Costache, A.D. and L. Sheihet, K. Zaveri, D.D. Knight and J. Kohn. 2009. Polymer-drug interactions in tyrosine-derived triblock copolymer nanospheres: a computational modeling approach. Mol. Pharm. 6: 1620–1627.

Couvreur, P. and B. Kante, M. Roland, P. Guiot, P. Baudhuin and P. Speiser. 1979. Polycyanoacrylate nanocapsules as potential lysosomotropic carriers: preparation, morphological and sorptive properties. J. Pharm. Pharmacol. 31: 331–332.

Couvreur, P. and C. Dubernet and F. Puisieux. 1995. Controlled drug delivery with nanoparticles: current possibilities and future trends. J. Pharm. Biopharm. 41: 2–13.

Couvreur, P. and G. Barratt, E. Fattal, P. Legrand and C. Vauthier. 2002. Nanocapsule technology: a review. Crit. Rev. Ther. Drug Carrier Syst. 19: 99–134.

Dailey, L.A. and W. Wittmar and T. Kissel. 2005. The role of branched polyesters and their modifications in the development of modern drug delivery vehicles. J. Control. Release. 101: 137–149.

Dimasi, J.A. 2000. New drug innovation and pharmaceutical industry structure: trends in the output of pharmaceutical firms. Drug Inf. J. 34: 1169–1194.

Ehrlich, P. 1906. Collected Studies on Immunity. John Wiley & Sons, New York, USA.

Ehrlich, A. and S. Booher, Y. Becerra, D.L. Borris, W.D. Figg, M.L. Turner and A. Blauvelt. 2004. Micellar paclitaxel improves severe psoriasis in a prospective phase II pilot study. J. Am. Acad. Dermatol. 50: 533–540.

Farokhzad, O.C. and R. Langer. 2009. Impact of nanotechnology on drug delivery. ACS Nano. 3: 16–20.

Fu, K. and D.W. Pack, A.M. Klibanov and R. Langer. 2000. Visual evidence of acidic environment within degrading poly(lactic-co-glycolic acid) (PLGA) microspheres. Pharm. Res. 17: 100–106.

Greenwald, R.B. and Y.H. Choe, J. McGuire and C.D. Conover. 2003. Effective drug delivery by PEGylated drug conjugates. Adv. Drug Deliv. Rev. 55: 217–250.

Gref, R. and Y. Minamitake, M.T. Peracchia, V. Trubetskoy, V. Torchilin and R. Langer. 1994. Biodegradable long-circulating polymeric nanospheres. Science. 263: 1600–1603.

Hooper, K.A. and N.D. Macon and J. Kohn. 1998. Comparative histological evaluation of new tyrosine-derived polymers and poly(L-lactic acid) as a function of polymer degradation. J. Biomed. Mater. Res. 41: 443–454.

Kilfoyle, B.E. and L. Sheihet, Z. Zhang, M. Laohoo, J. Kohn and B. Michniak-Kohn. 2012. Development of paclitaxel-TyroSpheres for topical skin treatment. J. Control. Release. 163: 18–24.

Kohn, J. 2004. New approaches to biomaterials design. Nat. Mater. 3: 745–747.

Kohn, J. and R. Langer. 1987. Polymerization reactions involving the side chains of α-L-amino acids. J. Am. Chem. Soc. 109: 817–820.

Koziara, J.M. and P.R. Lockman, D.D. Allen and R.J. Mumper. 2004. Paclitaxel nanoparticles for the potential treatment of brain tumors. J. Control. Release. 99: 259–269.

Kreuter, J. 1991. Nanoparticle-based drug delivery systems. J. Control. Release. 16: 169–176.

Kwon, G.S. 1998. Diblock copolymer nanoparticles for drug delivery. Crit. Rev. Ther. Drug Carrier Syst. 15: 481–512.

Matsumura, Y. and H. Maeda. 1986. A new concept for macromolecular therapeutics in cancer chemotherapy: mechanism of tumoritropic accumulation of proteins and the antitumor agent smancs. Cancer Res. 46: 6387–6392.

Nardin, C. and D. Bolikal and J. Kohn. 2004. Nontoxic block copolymer nanospheres: design and characterization. Langmuir. 20: 11721–11725.

Pitt, C.G. and Z.W. Gu. 1987. Modification of the rates of chain cleavage of poly(ε-caprolactone) and related polyesters in the solid state. J. Control. Release. 4: 283–292.

Pulapura, S. and J. Kohn. 1992. Tyrosine derived polycarbonates: backbone modified, "pseudo"-poly(amino acids) designed for biomedical applications. Biopolymers. 32: 411–417.

Quintanar-Guerrero, D. and E. Allémann, H. Fessi and E. Doelker. 1998. Preparation techniques and mechanisms of formation of biodegradable nanoparticles from preformed polymers. Drug Dev. Ind. Pharm. 24: 1113–1128.

Sheihet, L. and P. Chandra, P. Batheja, D. Devore, J. Kohn and B. Michniak. 2008. Tyrosine-derived nanospheres for enhanced topical skin penetration. Int. J. Pharm. 350: 312–319.

Sheihet, L. and R. Dubin, D. Devore and J. Kohn. 2005. Hydrophobic drug delivery by self-assembling triblock copolymer-derived nanospheres. Biomacromolecules. 6: 2726–2731.

Sheihet, L. and K. Piotrowska, R.A. Dubin, J. Kohn and D. Devore. 2007. Effect of tyrosine-derived triblock copolymer compositions on nanosphere self-assembly and drug delivery. Biomacromolecules. 8: 998–1003.

Sheihet, L. and O. Garbuzenko, J. Bushman, M.K. Gounder, T. Minko and J. Kohn. 2012. Paclitaxel in tyrosine-derived nanospheres as a potential anti-cancer agent: *in vivo* evaluation of toxicity and efficacy in comparison with paclitaxel in Cremophor. Eur. J. Pharm. Sci. 45: 320–329.

Torchilin, V.P. 1998. Polymer-coated long-circulating microparticulate pharmaceuticals. J. Microencapsul. 15: 1–20.

Uhrich, A.E. and S.M. Cannizzaro, R.S. Langer and K.M. Shakesheff. 1999. Polymeric systems for controlled drug release. Chem. Rev. 99: 3181–3198.

Xu, Z.K. and F.Q. Nie, C. Qu, L.S. Wan, J. Wu and K. Yao. 2005. Tethering poly(ethylene glycol)s to improve the surface biocompatibility of poly(acrylonitrile-co-maleic acid) asymmetric membranes. Biomaterials. 26: 589–598.

Zhang, Z. and D.W. Grijpma and J. Feijen. 2006a. Poly(trimethylene carbonate) and monomethoxy poly(ethylene glycol)-block-poly(trimethylene carbonate) nanoparticles for the controlled release of dexamethasone. J. Control. Release. 111: 263–270.

Zhang, Z. and D.W. Grijpma and J. Feijen. 2006b. Thermo-sensitive transition of monomethoxy poly(ethylene glycol)-block-poly(trimethylene carbonate) films to micellar like nanoparticles. J. Control. Release. 112: 57–63.

Zhang, Z. and R. Kuijer, S.K. Bulstra, D.W. Grijpma and J. Feijen. 2006c. The *in vivo* and *in vitro* degradation behavior of poly(trimethylene carbonate). Biomaterials. 27: 1741–1748.

Zhang, Z. and P.C. Tsai, T. Ramezanli and B.B. Michniak-Kohn. 2013. Polymeric nanoparticles-based topical delivery systems for the treatment of dermatological diseases. Wiley Interdiscip. Rev. Nanomed. Nanobiotechnol. 5: 205–218.

CHAPTER 7

Carbon Nanotubes for Drug Delivery Applications

Yitzhak Rosen[1,*] and *Pablo Gurman*[2]

ABSTRACT

During the last years, pharmaceutical companies have been facing the challenge of developing new molecules to replace the existing ones in order to sustain their core business. This became a very expensive, time-consuming and frustrating task. It is now being realized that an alternative to drug development is to reuse the existing drugs by changing their pharmacokinetic or pharmacodynamic properties thanks to their incorporation to drug carriers. The so-called drug delivery systems hold promise to optimize drug absorption, distribution, metabolism and excretion (pharmacokinetics), and ultimately to improve the clinical efficacy of pharmacotherapies.

In the last 20 years with the advent of micro- and nano-technologies, a variety of micro- and nano-devices including nanostructures have been developed for their application as drug delivery systems. Among them, carbon nanotubes, carbon fibers with a few nanometers in diameter and several microns length, have called the attention of the scientific community due to their large surface area, high aspect ratio and their extraordinary mechanical and electrical properties. Carbon nanotubes are produced by different methods, including chemical vapor deposition,

[1] CEO Superior NanoBioSystems LLC, 1725 T Street, Suite 31, Washington DC, 20009, USA. Email: yitzhakrosen@yahoo.com

[2] Argonne National Laboratory, Material Science Division, 9700 S. Cass Avenue, Argonne, IL 60439, USA. Email: pablogurman@gmail.com

* Corresponding author

List of abbreviations after the text.

laser ablation and arc discharge. Carbon nanotubes have been investigated for applications ranging from cancer therapy to gene therapy and small interfering ribonucleic acid delivery. However, a serious concern is the potential toxicity of carbon nanotubes as has been shown *in vitro* and *in vivo*. Ultimately, a balance between benefits and risks will dictate whether carbon nanotube-based drug delivery systems will reach the market in the years to come.

Introduction

Much research for the advancement of Drug Delivery Systems (DDSs) has been taking place at a fast rate as a consequence of the need to optimize clinical efficacy, pharmacokinetics, pharmacodynamics, bioavailability and toxic profiles of pharmacotherapies. Drug absorption, distribution, metabolism, mechanism of action and excretion, along with additional individual clinical parameters, impact these afore mentioned pharmacological parameters. Toxic profiles play a critical role when juxtaposed with clinical efficacy, thereby creating a benefit *versus* risk management role (Ladeira et al. 2010).

In order to address these issues, pharmaceutical companies face the challenge of developing new molecules to replace the existing ones. This can be a very expensive and time-consuming process. It is now being realized that an alternative to drug development is to use the existing drugs and encapsulate them into carriers. These carriers have been termed as DDS. From a pharmacological standpoint, the aim of DDS is to transport the drug dose throughout the organism, from the site of administration to the biophase, where the drug exerts its action. In this manner, the DDS protects the drug from unwanted degradation or undesirable distribution sites. There are many classes of DDSs ranging from simple capsules (mainly made of polymers) to complex microchips (where the drug is stored in silicon microreservoirs and released on demand by an electronic signal). Most of these complex carriers are now being considered as medical devices that can incorporate different geometries and materials (Elman et al. 2009).

In the last 20 years with the advent of micro- and nano-technologies, including micro- and nano-devices, carbon structures have called the attention of the scientific and medical device communities for their application in drug delivery. Carbon Nanotubes (CNTs) have attracted much attention since they exhibit unique mechanical (the strongest material known with high flexibility), chemical (amenable to functionalization), and electrical (semimetallic or metallic) properties. However, it must be emphasized that they do carry a toxicity capability that has yet to be fully elucidated (Iijima 1991, Lanone and Boczkowski 2006, Singh et al. 2006, Liu et al. 2008, Takagi et al. 2008, Elman et al. 2009, Rosen and Elman 2009, Rosen et al. 2011, Rümmelli et al. 2011, Wang et al. 2011).

Basic Aspects of Carbon Nanotubes

CNTs are graphene sheets made of carbon atoms forming hexagons that roll into tubes, where the edge of the tube is formed by pentagons in order to close the tube. CNTs are carbon structures that can be a few nanometers in width (0.4 to 100 nm), and ranging from one to several microns in length up to the millimeter range (Fig. 7.1). Their width varies accordingly if the CNT are Single-Walled Carbon Nanotubes (SWCNTs) or Multi-Walled Carbon Nanotubes (MWCNTs). Moreover, the manner in which graphene sheets roll into a CNT define the type of CNT, each having distinct physical properties (Krajcik et al. 2008, Kostarelos et al. 2009, Liu et al. 2009, Rosen and Elman 2009, Rosen et al. 2011).

The term helicity is used to define the way CNTs folds. Different helicities can give rise to CNTs with radically different electronic structures, changing their behavior from semimetallic- to metallic-based entities with such properties (Baughman et al. 2002). The structures of CNTs, along with their biological activity (such as, biofunctionalization and toxicity), could be affected by the synthetic methodology followed in their preparation (Iijima 1991, Geng et al. 2007, Guo et al. 2007, Foldvari and Bagonluri 2008, Rosen et al. 2011, Rümmelli et al. 2011).

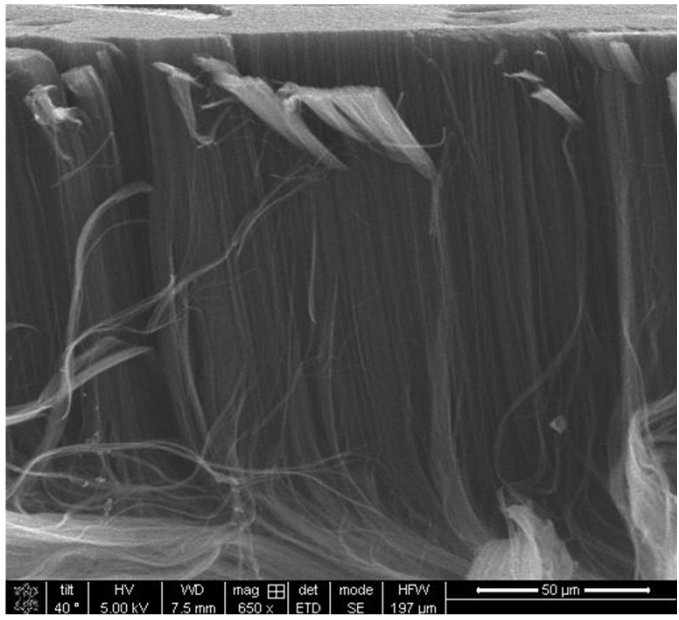

Figure 7.1. Scanning electron microscopy image of vertically aligned CNTs grown on silicon substrate using an iron catalyst. Bar length: 50 µm. Credit: A.V. Sumant (Argonne National Laboratory, IL, USA).

Synthesis

While it is beyond the scope of this chapter to review thoroughly all the synthesis methods, a number of synthesis routes have been explored to produce CNTs.

Arc discharge

CNTs are produced by vaporization of a graphite anode that interacts with a cathode creating an electrical discharge between them. The energy created in the arc is enough to volatilize the carbon atoms present in the graphite anode. As a result, carbon atoms in the vapor phase will reorganize and deposit as CNTs. The yield of this method is not too high, and impurities, such as, fullerenes and incomplete forms of CNT, might also be obtained. More important is the concern of the presence of a catalyst, i.e., nickel or iron nanoparticles, in the end product. Some of the issues related to CNT toxicity have been attributed to the presence of such catalysts (Journet et al. 1997, Bachilo et al. 2003, Hata et al. 2004, Rosen et al. 2011).

Laser ablation

In this method a chamber heated at 1200ºC containing a carbon source is bombarded with a laser beam, resulting in the evaporation of the carbon source (phase transition of the material from the solid to the vapor phase). An inert gas, such as argon, is flooded through the tube carrying the carbon atoms to a colder place where they sublimate and condense to form the CNTs (Rosen et al. 2011).

Chemical Vapor Deposition

This is considered the more scalable method among all the existent techniques. In fact, this is the current technique to grow CNTs in bulk quantities. Chemical Vapor Deposition (CVD) consists of carbon precursors that can chemically react in the presence of plasma to produce carbon atoms that are deposited on a substrate in the form of CNTs (Nessim 2010, Rosen et al. 2011).

Properties and application in drug delivery

CNTs have an extraordinary surface area rendering them attractive for high drug payloads. It has been demonstrated that physical or chemical adsorption of biomolecules to CNTs could take place on the outer surface of the nanotube. However, several studies of molecular dynamics have

also demonstrated the plausibility of encapsulating drugs inside CNTs. This may have a profound impact in the drug delivery strategy, since the manner in which a drug is released depends on its location in the CNT. However, it must be taken into account that CNT are usually found in the form of bundles, where the specific surface area (and thus the drug amount that can be loaded) could differ from that of a single CNT (Andrews et al. 1999, Hilder and Hill 2008, Al-Jamal et al. 2010, Ilbasmiş-Tamer et al. 2010, Rosen et al. 2011, Elhissi et al. 2012).

In addition to their high surface area, CNTs have unique electrical properties that emerge as a consequence of quantum mechanical phenomena at the nanoscale range. Their tubular shape and helicity also explain some of these properties. In addition to changes in the electronic structure of a single CNT, electron-electron interactions (from different geometries, such as, SWCNT bundles, or between shells in MWCNT) have been shown to influence the electronic conductance of the CNT. The unique electrical conductivity of CNT could be harnessed to develop novel mechanisms of drug release and desorption. For example, iontophoretic devices based on CNT (which rely on the electrically induced opening of pores through cell membranes) could be developed to enhance drug penetration through biological barriers (Degim et al. 2010, Im et al. 2010).

Chemical properties of CNTs are a very important feature that must be considered in drug loading and for preparing a biocompatible vehicle to be administered into the human body. CNTs have been considered hydrophobic in nature and tend to agglomerate. Therefore, they are not dispersed in water solutions, this representing an issue for developing any therapeutic system that will contact the systemic circulation. An approach to overcome this problem is to modify the CNT surface with polar molecules (such as, polymers), biomolecules (e.g., proteins) or genetic material [i.e., deoxyribonucleic acid (DNA) or ribonucleic acid (RNA)]. This can be accomplished through covalent or non-covalent bonding. Covalent bonding uses chemical reactions to modify the CNT surface. Some of these reactions utilize strong bases (such as, KOH and NaOH) that can attack the CNT surface, thus oxidizing their surface and creating radical groups, such as –COOH, that could be further linked via amide bonding with $–NH_2$ radicals existing in biomolecules (e.g., monoclonal antibodies, receptors, and DNA). Another chemical reaction to achieve the bioconjugation of CNT is based on 1,3-dipolar cycloaddition. Non-covalent modification of CNTs includes interactions between biomolecules and the surface of the CNT, through van der Vaal forces, charge transfer interactions and π-π interactions. Lastly, it is important to confirm that functionalization of CNTs has occurred. To this aim, a number of surface characterization techniques are used, including infrared and Raman spectroscopy, near-infrared light absorption or transmission electron microscopy (Mandani et al. 2012).

Pharmacokinetics and pharmacodynamics

Pharmacokinetics has a very close relationship with the chemical composition of a drug and its hydrophilic/hydrophobic nature. In fact, biodistribution of drugs or any material highly depends upon whether they are hydrophobic or hydrophilic. Since the blood compartment is a highly hydrophilic environment, hydrophobic compounds tend to accumulate outside the bloodstream in more hydrophobic sites, such as, the fat tissue. Renal excretion of drugs depends also strongly in their hydrophilic nature. CNTs are hydrophobic structures, although they could be modified and become hydrophilic by changing their surface with hydrophilic molecules, such as, Poly(Ethylene Glycol) (PEG). This is necessary to allow the circulation of the CNT in the bloodstream, thus reaching the site of action (Lacerda et al. 2008a,b, Liu et al. 2008, Rosen et al. 2011).

The pharmacodynamic concept of target selectivity has to be considered in order to allow CNTs with their cargo to bind only to specific targets. This can be done by a proper surface functionalization of the CNTs with targeting molecules. This means that a targeting molecule is attached to the outside surface of the CNT, while the delivered entity is encapsulated inside. In this way, many biomolecules including DNA, RNA and proteins (i.e., receptor ligands like folate molecules) could be attached to CNT surface. The concept of selectivity has tremendous importance to assure the therapeutic effect and to minimize the toxic side effects (Lanone and Boczkowski 2006, Hong et al. 2010, Ladeira et al. 2010, Rosen et al. 2011, Mandani et al. 2012).

Toxicity

The toxicity of CNT remains a subject of debate. However, recent *in vitro* and *in vivo* studies had shed some light in this issue. First, it has been observed that the surface chemistry and length are important parameters determining CNT toxicity. Second, some toxicity issues on CNTs could be related to their biopersistence, as happen with to several kinds of fibers including asbestos. In a recent investigation, CNT biopersistence was studied systematically by measuring the degradability of CNT on a simulated biological fluid (Gambles solution) that resembles the intracellular phagolysosome environment, the harshest environment to which a nanoparticle can be exposed inside a cell (Osmond-McLeod et al. 2011). This study was carried out with existing fibers that have shown to be pathogenic, e.g., asbestos, to compare the degradability rates of CNTs with the ones of them. It was found that the amount of CNT present in the sample exposed to the Gambles

solution did not change over time. This result favors the hypothesis of non-degradability, and thus biopersistence and pathogenicity of CNT.

Biopersistence of CNT inside cells may occur because there is no enzymatic pathway to degrade CNT intracellularly. As a consequence, a process known as "frustrated" phagocytosis occurs, leading to choric inflammation with the release of inflammatory mediators (e.g., cytokines) that attract more inflammatory cells to the site, thus resulting in an endless circle of inflammation and chemotaxis of immune cells that leads to more inflammation and tissue damage (Murphy et al. 2012). Several animal studies have corroborated the pro-inflammatory effect of CNTs. Most of these studies were performed using tracheal instillation or inhalation of CNTs, since one of the main concerns of CNTs is their pulmonary toxicity. Acute, subacute and chronic toxicity has been demonstrated using different approaches. Bronchoalveolar lavage was performed to study the presence of inflammatory cells immediately after CNT administration. Inflammatory cells were shown to be present 24 hours after CNT administration. Another study demonstrated the presence of inflammatory cells in bronchoalveolar lavage after 30 days of exposure (Wang et al. 2011). Histopathology analyses have shown the presence of fibrotic response (subacute response) and granulomas (chronic response) to CNTs. Fibrotic response has been described in animal models as a consequence of fibroblast proliferation and collagen production induced by CNTs that entered into the alveolar interstitium after being inhaled or instilled triggering fibroblast proliferation in the septa of the alveolar walls. Of concern is the finding of erythrocyte toxicity to CNTs both *in vivo* and *in vitro*. Although the mechanism of toxicity has not yet been elucidated, an acute decrease in the number of erythrocytes has been observed after intravenous administration and intratraqueal instillation (but not by the oral or intraperitoneal route) of CNTs. The effect was found to be time- and dose-dependent (Sachar and Saxena 2011). Finally, potential toxicity to CNTs in the testis of male mice upon their intravenous administration was found (Im et al. 2010). In this study, two different protocols were followed: injecting a group of mice with a single dose and, to assess cumulative effects, the intravenous administration of five doses to another group. Mice were evaluated by histopathology on day 15 after the beginning of the study. Histopathology showed damage in the seminiferous tubules with alterations in Sertoli cells, but no damage was found in spermatids. Tissue damaged was attributed to the production of free radicals that caused lipid peroxidation and cell death. The histopathological changes reverted at days 60 and 90. No alterations were found in hormone levels, and fertility was not affected.

Carbon Nanotubes for Gene and Small Interfering Ribonucleic Acid Delivery

Gene delivery, also known as gene therapy, aims at delivering a gene to a cell, to integrate the gene in the cell genome, and finally to express a protein that will replace or substitute a defective protein from the cell. Since the beginnings of gene therapy, the need was soon realized to reach the nucleus of the cell and inserting the gene in the host DNA, without hindering cell homeostasis or gene expression or inducing any undesirable side effect, such as, expressing oncogenic genes. The search for a viable gene delivery system has focused on viral and non-viral vectors. It was soon discovered that viral vectors had many disadvantages, including immunogenic and inflammatory reactions that may cause transient transgene expression, and potential oncogenic effects that may occur later. As a result, non-viral vectors have been developed, providing several advantages over viral vectors, i.e., the assembly in cell-free systems from well-defined components. These components may provide them key advantages over viral vectors in terms of safety and manufacturing (Kam et al. 2005a, Bianco et al. 2008, Rosen and Elman 2009). However, many non-viral vector technologies where developed (including liposomes and dendrimers) wherein the poor efficiency in gene transfer has demanded new approaches. In this line, CNTs have gained attention as gene delivery systems, since they are amenable to be functionalized with DNA by electrostatic interaction or by encapsulation. They are also excellent vectors because of their small diameter that allows them to penetrate cell membranes. In this regard, CNT nanoinjectors have been developed (Wallace and Sansom 2008). The mechanism of entry is still under study but the evidence suggests that CNTs could enter cells either by active (endocytic pathways) or passive mechanisms (non-endocytic pathways, such as, diffusion across the cell membrane). Once in the cytoplasm, CNTs can release their cargo (i.e., DNA) that diffuses into the nucleus. Another feature that was used to enhance cell penetration was to harness the magnetic properties of the nickel nanoparticles located inside the CNT as a residue of its synthesis in order to magnetically assist the CNT internalization. The use of a rotating magnetic field followed by the application of a static magnetic field allows the CNTs to reach and penetrate the cell membrane, thus significantly enhancing gene transfection.

The p53 tumor suppressor gene is activated to either repair DNA damage or induce apoptosis in cells that have failed to repair their DNA before entering the mitotic phase. Failure in the p53 gene activity has been correlated with numerous malignancies (Takagi et al. 2008). It has been shown that ethylenediamine-functionalized SWCNTs can be used to deliver the p53 gene to MCF-7 breast cancer cells, thus suppressing their growth (Karmakar et al. 2011).

Small interfering ribonucleic acid (*si*RNA) can be also delivered to cells by using CNTs (Davis et al. 2010, Rosen et al. 2011). *si*RNA are small strands of RNA that bind to the complementary RNA, inhibiting RNA transcription and protein expression. For example, persistent viral infections (e.g., hepatitis C virus, hepatitis B virus and human immunodeficiency virus) may benefit from *si*RNA therapy with an effective delivery system (Kam et al. 2005a, Krajcik et al. 2008, Podesta et al. 2009, Al-Jamal et al. 2010, Ladeira et al. 2010, Rosen et al. 2011). Cancer therapy can also take advantage from the use of *si*RNA. For instance, CNTs have been functionalized with *si*RNA codifying for the Telomerase Reverse Transcriptase (TERT), an enzyme involved in the stabilization of chromosomes during the mitotic phase of the cell cycle, which has been related with several types of cancer. TERT *si*RNA was delivered to ovarian carcinoma, lung carcinoma and cervical carcinoma tumor cell lines in complex with positively charged SWCNTs. Suppression of tumor growth was possible thanks to the inhibition of TERT transcription and TERT protein expression. *In vivo* xenograft models using the HeLa cell line and the LLC cell line demonstrated the efficient reduction of tumor growth by this nanomedicine (Zhang et al. 2006).

Carbon Nanotubes as Delivery Systems for Infectious Diseases

A clinically effective antimicrobial agent has several important requirements and characteristics. First, it must target the microbial infection leading to concentrations that can eradicate or even prevent the proliferation. Second, the agent must stand the microbial drug resistance. Third, its toxicity must be kept to a very minimum (Agerberth and Gudmundsson 2006, Kang et al. 2007, 2008a,b, Arias and Murray 2008, Banerjee et al. 2008, Pitout 2008, Toupet et al. 2008, Mandell et al. 2010, Trivedi and Kompella 2010, Prajapati et al. 2011, Rosen et al. 2011).

A key medication that has significant toxicity yet is very effective for lethal infections, particularly fungal, is amphotericin B (AmB) (Mandell et al. 2010). It has been shown that CNTs can deliver AmB against Leishmaniasis with greater efficacy when compared to AmB in both *in vitro* and *in vivo* trials. In this study, a wider therapeutic window and negligible cytotoxicity were described for the AmB-loaded CNTs (Prajapati et al. 2011).

Drug resistance may occur in many different ways. One common possibility involves β-lactamases, which can disrupt the β-lactamase ring of penicillin, thereby causing resistance to penicillin molecules. Another resistance mechanism involves the modification of the antibiotic binding site, i.e., in lethal methicillin-resistant *Staphylococcus aureus* strains. Finally, the use of alternative metabolic pathways by bacteria is another common method of resistance that requires clinical cognizance (Cohen 1992, Arias and Murray 2008, Banerjee et al. 2008, Pitout 2008, Rosen and Elman 2009,

Mandell et al. 2010). In order to overcome drug resistance, the combined use of therapeutic agents has been proposed. This is the case of active tuberculosis infections wherein resistance (leading to severe clinical consequences) can be developed very rapidly. Unfortunately, drug resistance can even occur in such complex combined treatment schedules (Mandell et al. 2010).

In this line, CNTs could be engineered as DDSs capable of delivering multiple payloads (Krajcik et al. 2008, Rosen and Elman 2009). Interestingly, CNTs themselves may have antibacterial effects due to cell membrane damage by direct contact with them (Schiffman and Elimelech 2011). Therefore, such DDS may actively participate in such combined treatment schedule (Pastorin et al. 2006, Kang et al. 2007, 2008a,b, Dhar et al. 2008, Doshi and Mitragotri 2009, Schiffman and Elimelech 2011).

Carbon Nanotubes as Drug Delivery for Cancer Treatment

Many of the frequent side effects described in chemotherapy, e.g., cardiac toxicity by doxorubicin and renal toxicity by cisplatin, are the consequence of an unspecific drug interaction with healthy cells. DDSs provide, in addition to an improvement in drug transport, the opportunity to target cancer cells selectively by incorporating a molecular recognition moiety to the DDS surface. In this regard, folate molecules have been surface incorporated to the DDS in order to assure its selective binding to cells overexpressing folate receptors, i.e., some cancer cell lines (Kam et al. 2005b).

CNTs can load a number of antitumor agents either onto their surface (that has to be modified to allow the grafting of the chemotherapy agent), or entrapped into the interior of the CNT (Lanone and Boczkowski 2006, Hong et al. 2010, Rosen et al. 2011, Mandani et al. 2012). Once the drug-loaded CNT has been formulated, it has to reach (and generally enter) the cancer cells without entering into healthy cells (Lanone and Boczkowski 2006, Mandani et al. 2012). As previously described, this can be accomplished by incorporating a binding ligand (such as, a monoclonal antibody) onto the CNT surface. The mechanism determining the entrance of the drug-loaded CNT into the cancer cell remains unclear but two routes of internalization have been described: *i*) passive diffusion across the lipid bilayer; and/or, *ii*) active internalization via endocytosis (Mu et al. 2009).

Carbon Nanotubes for Enhanced Vaccine Delivery

A clinically effective vaccine should be able to elicit a specific and lasting immune response without inducing adverse effects. In cancer, wherein antigens from cancer cells are used to elicit an immune response against the tumor, as well as in many infectious diseases, an adjuvant (a substance that

improves the antigen immune response) is needed to provide a synergistic effect when used with the antigen. Nanoparticulate-based drug delivery systems have been shown to elicit a more specific immune response acting as adjuvants for the antigen being presented (Pantarotto et al. 2003, Rosen and Elman 2009).

In this way, CNTs may have the potential for enhancing the immune response to vaccines. CNTs have shown to deliver intracellularly the antigen, thereby affecting the intracellular trafficking of the antigen and reaching cellular compartments rich in human leukocyte antigen class II (HLA II, a biomacromolecule needed for antigen presentation to T cells and activation of a specific immune response) (Villa et al. 2011). Such advanced vaccines are necessary for targets having the ability to evade the immune system, or for weakly immunogenic targets, such as, some tumors and infectious agents (e.g., helminthes, protozoa with malaria among them, etc.). Ideal drug delivery systems should be capable of preserving the antigen in its correct conformation in order to maintain the specificity on T cell activation. In addition, the immunogenic response to the nanocarrier needs to be minimized in order to be clinically effective. In this regard, CNTs have shown to be non-immunogenic and, thus, attractive as antigen delivery systems (Pantarotto et al. 2003, Rosen and Elman 2009). There has been evidence that CNTs can optimize vaccine delivery by enhancing the antibody response (Pantarotto et al. 2003, Rosen et al. 2011). For example, immunization with peptide-functionalized CNTs can enhance virus-specific neutralizing antibody responses. In this way, CNTs have been covalently linked to neutralizing *B* epitopes on foot-and-mouth disease virus (Pantarotto et al. 2003).

Conclusions

CNTs represent a novel carrier suitable to transport different kinds of biomolecules including, but not limited to, drugs, proteins, peptides, DNA or *si*RNA, for a wide range of clinical applications (cancer, infectious diseases, etc.). Their unique properties include:

- A very large surface area which translates into delivering more drug payload or number of receptors per vector unit. The latter allowing a greater interaction CNT-target (Kam et al. 2005a,b, Cherukuri et al. 2006, Ladeira et al. 2010, Rosen et al. 2011, Mandani et al. 2012).
- Functionalization capabilities. CNTs can be surface modified with carboxyl radicals that can interact with functional groups (i.e., amines) existing in the chemical structure of antibodies and receptors. CNTs can be also surface functionalized by electrostatic modification in order to allow the electrostatic binding to DNA and RNA molecules (Kam et

al. 2005b, Cherukuri et al. 2006, Ladeira et al. 2010, Rosen et al. 2011, Mandani et al. 2012).
- Cell penetration (due to their small size) by passive diffusion or by endocytosis (Krajcik et al. 2008, Kostarelos et al. 2009, Ladeira et al. 2010, Rosen et al. 2011).
- Excellent mechanical properties and chemical resistance, thus protecting the cargo inside while they are being transported extracellularly and intracellularly (Kostarelos et al. 2009, Mu et al. 2009, Rosen et al. 2011).

There still much concern and controversy about the potential toxicity of CNTs (Lacerda et al. 2008a,b, Schipper et al. 2008, Kostarelos et al. 2009, Rosen et al. 2011, Sachar and Saxena 2011, Murphy et al. 2012). Further studies are required to demonstrate that the risk *versus* the benefit ratio of using CNTs. Furthermore, a comparative analysis of other drug delivery systems is required to assess for possible alternatives (Bottini et al. 2006, Liu et al. 2007, 2008, 2009, Takagi et al. 2008, Rosen et al. 2011). In any case, much can be learned about nanoparticulate DDS based on CNTs as research model for clinical applications.

Abbreviations

AmB	:	amphotericin B
CNT	:	carbon nanotube
CVD	:	chemical vapor deposition
DDS	:	drug delivery system
DNA	:	deoxyribonucleic acid
HLA II	:	human leukocyte antigen class II
MWCNT	:	multi-walled carbon nanotube
PEG	:	poly(ethylene glycol)
RNA	:	ribonucleic acid
*si*RNA	:	small interfering ribonucleic acid
SWCNT	:	single-walled carbon nanotube
TERT	:	telomerase reverse transcriptase

References

Agerberth, B. and G.H. Gudmundsson. 2006. Host antimicrobial defence peptides in human disease. Curr. Top Microbiol. Immunol. 306: 67–90.

Al-Jamal, K.T. and F.M. Toma, A. Yilmazer, H. Ali-Boucetta, A. Nunes, M.A. Herrero, B. Tian, A. Eddaoudi, W.T. Al-Jamal, A. Bianco, M. Prato and K. Kostarelo. 2010. Enhanced cellular internalization and gene silencing with a series of cationic dendron-multiwalled carbon nanotube: siRNA complexes. FASEB J. 24: 4354–4365.

Andrews, R. and D. Jacques, A.M. Rao, F. Derbyshire, D. Qian, X. Fan, E.C. Dickey and J. Chen. 1999. Continuous production of aligned carbon nanotubes: a step closer to commercial realization. Chem. Phys. Lett. 303: 467–474.

Arias, C.A. and B.E. Murray. 2008. Emergence and management of drug-resistant enterococcal infections. Expert Rev. Anti Infect. Ther. 6: 637–655.

Bachilo, S.M. and L. Balzano, J.E. Herrera, F. Pompeo, D.E. Resasco and R.B. Weisman. 2003. Narrow (n,m)-distribution of single-walled carbon nanotubes grown using a solid supported catalyst. J. Am. Chem. Soc. 125: 11186–11187.

Banerjee, R. and G.F. Schecter, J. Flood and T.C. Porco. 2008. Extensively drug-resistant tuberculosis: new strains, new challenges. Expert Rev. Anti Infect. Ther. 6: 713–724.

Baughman, R.H. and A.A. Zakhidov and W.A. de Heer. 2002. Carbon nanotubes—the route toward applications. Science. 297: 787–792.

Bianco, A. and R. Sainz, S. Li, H. Dumortier, L. Lacerda, K. Kostarelos, S. Giordani and M. Prato. Biomedical applications of functionalised carbon nanotubes. pp. 23–50. *In*: F. Cataldo and T. da Ros [eds.]. 2008. Medicinal Chemistry and Pharmacological Potential of Fullerenes and Carbon Nanotubes. Springer, Netherlands.

Bottini, M. and S. Bruckner, K. Nika, N. Bottini, S. Bellucci, A. Magrini, A. Bergamaschi and T. Mustelin. 2006. Multi-walled carbon nanotubes induce T lymphocyte apoptosis. Toxicol. Lett. 160: 121–126.

Cherukuri, P. and C.J. Gannon, T.K. Leeuw, H.K. Schmidt, R.E. Smalley, S.A. Curley and R.B. Weisman. 2006. Mammalian pharmacokinetics of carbon nanotubes using intrinsic near-infrared fluorescence. Proc. Natl. Acad. Sci. USA. 103: 18882–18886.

Cohen, M.L. 1992. Epidemiology of drug resistance: implications for a post-antimicrobial era. Science. 257: 1050–1055.

Davis, M.E. and J.E. Zuckerman, C.H. Choi, D. Seligson, A. Tolcher, C.A. Alabi, Y. Yen, J.D. Heidel and A. Ribas. 2010. Evidence of RNAi in humans from systemically administered siRNA via targeted nanoparticles. Nature. 464: 1067–1070.

Degim, I.T. and D.J. Burgess and F. Papadimitrakopoulos. 2010. Carbon nanotubes for transdermal drug delivery. J. Microencapsul. 27: 669–681.

Dhar, S. and Z. Liu, J. Thomale, H. Dai and S.J. Lippard. 2008. Targeted single-wall carbon nanotube-mediated Pt(IV) prodrug delivery using folate as a homing device. J. Am. Chem. Soc. 130: 11467–11476.

Doshi, N. and S. Mitragotri. 2009. Designer biomaterials for nanomedicine. Adv. Funct. Mater. 19: 3843–3854.

Elhissi, A.M. and W. Ahmed, I.U. Hassan, V.R. Dhanak and A. D'Emanuele. 2012. Carbon nanotubes in cancer therapy and drug delivery. J. Drug Deliv. 2012: 837327.

Elman, N.M. and Y. Patta, A.W. Scott, B. Masi, H.L. Ho Duc and M.J. Cima. 2009. The next generation of drug-delivery microdevices. Clin. Pharmacol. Ther. 85: 544–547.

Foldvari, M. and M. Bagonluri. 2008. Carbon nanotubes as functional excipients for nanomedicines: I. Pharmaceutical properties. Nanomedicine. 4: 173–182.

Geng, Y. and P. Dalhaimer, S. Cai, R. Tsai, M. Tewari, T. Minko and D.E. Discher. 2007. Shape effects of filaments versus spherical particles in flow and drug delivery. Nat. Nanotechnol. 2: 249–255.

Guo, J. and X. Zhang, Q. Li and W. Li. 2007. Biodistribution of functionalized multiwall carbon nanotubes in mice. Nucl. Med. Biol. 34: 579–583.

Hata, K. and D.N. Futaba, K. Mizuno, T. Namai, M. Yumura and S. Iijima. 2004. Water-assisted highly efficient synthesis of impurity-free single-walled carbon nanotubes. Science. 306: 1362–1364.

Hilder, T.A. and J.M. Hill. 2008. Probability of encapsulation of paclitaxel and doxorubicin into carbon nanotubes. Micro Nano Lett. 3: 41–49.

Hong, S.Y. and G. Tobias, K.T. Al-Jamal, B. Ballesteros, H. Ali-Boucetta, S. Lozano-Perez, P.D. Nellist, R.B. Sim, C. Finucane, S.J. Mather, M.L. Green, K. Kostarelos and B.G. Davis. 2010. Filled and glycosylated carbon nanotubes for *in vivo* radioemitter localization and imaging. Nat. Mater. 9: 485–490.

Iijima, S. 1991. Helical microtubules of graphitic carbon. Nature. 354: 56–58.
Ilbasmiş-Tamer, S. and S. Yilmaz, E. Banoğlu and I.T. Değim. 2010. Carbon nanotubes to deliver drug molecules. J. Biomed. Nanotechnol. 6: 20–27.
Im, J.S. and B.Ch. Bai and Y.S. Lee. 2010. The effect of carbon nanotubes on drug delivery in an electro-sensitive transdermal drug delivery system. Biomaterials. 31: 1414–1419.
Journet, C. and W.K. Maser, P. Bernier, A. Loiseau, M. Lamy de la Chapelle, S. Lefrant, P. Deniard, R. Lee and J.E. Fischer. 1997. Large-scale production of single-walled carbon nanotubes by the electric-arc technique. Nature. 388: 756–758.
Kam, N.W. and Z. Liu and H. Dai. 2005a. Functionalization of carbon nanotubes via cleavable disulfide bonds for efficient intracellular delivery of siRNA and potent gene silencing. J. Am. Chem. Soc. 127: 12492–12493.
Kam, N.W. and M. O'Connell, J.A. Wisdom and H. Dai. 2005b. Carbon nanotubes as multifunctional biological transporters and near-infrared agents for selective cancer cell destruction. Proc. Natl. Acad. Sci. USA. 102: 11600–11605.
Kang, S. and M. Pinault, L.B. Pfefferle and M. Elimelech. 2007. Single-walled carbon nanotubes exhibit strong antimicrobial activity. Langmuir. 23: 8670–8673.
Kang, S. and M.S. Mauter and M. Elimelech. 2008a. Physicochemical determinants of multiwalled carbon nanotube bacterial cytotoxicity. Environ. Sci. Technol. 42: 7528–7534.
Kang, S. and M. Herzberg, D.F. Rodrigues and M. Elimelech. 2008b. Antibacterial effects of carbon nanotubes: size does matter. Langmuir. 24: 6409–6413.
Karmakar, A. and S.M. Bratton, E. Dervishi, A. Ghosh, M. Mahmood, Y. Xu, L.M. Saeed, T. Mustafa, D. Casciano, A. Radominska-Pandya and A.S. Biris. 2011. Ethylenediamine functionalized-single-walled nanotube (f-SWNT)-assisted *in vitro* delivery of the oncogene suppressor p53 gene to breast cancer MCF-7 cells. Int. J. Nanomedicine. 6: 1045–1055.
Kostarelos, K. and A. Bianco and M. Prato. 2009. Promises, facts and challenges for carbon nanotubes in imaging and therapeutics. Nat. Nanotechnol. 4: 627–633.
Krajcik, R. and A. Jung, A. Hirsch, W. Neuhuber and O. Zolk. 2008. Functionalization of carbon nanotubes enables non-covalent binding and intracellular delivery of small interfering RNA for efficient knock-down of genes. Biochem. Biophys. Res. Commun. 369: 595–602.
Lacerda, L. and H. Ali-Boucetta, M.A. Herrero, G. Pastorin, A. Bianco, M. Prato and K. Kostarelos. 2008a. Tissue histology and physiology following intravenous administration of different types of functionalized multiwalled carbon nanotubes. Nanomedicine (Lond.). 3: 149–161.
Lacerda, L. and M.A. Herrero, K. Venner, A. Bianco, M. Prato and K. Kostarelos. 2008b. Carbon nanotube shape and individualization critical for renal excretion. Small. 4: 1130–1132.
Ladeira, M.S. and V.A. Andrade, E.R. Gomes, C.J. Aguiar, E.R. Moraes, J.S. Soares, E.E. Silva, R.G. Lacerda, L.O. Ladeira, A. Jorio, P. Lima, M.F. Leite, R.R. Resende and S. Guatimosim. 2010. Highly efficient siRNA delivery system into human and murine cells using single-wall carbon nanotubes. Nanotechnology. 21: 385101.
Lanone, S. and J. Boczkowski. 2006. Biomedical applications and potential health risks of nanomaterials: molecular mechanisms. Curr. Mol. Med. 6: 651–663.
Liu, Z. and W. Cai, L. He, N. Nakayama, K. Chen, X. Sun, X. Chen and H. Dai. 2007. *In vivo* biodistribution and highly efficient tumour targeting of carbon nanotubes in mice. Nat. Nanotechnol. 2: 47–52.
Liu, Z. and C. Davis, W. Cai, L. He, X. Chen and H. Dai. 2008. Circulation and long-term fate of functionalized, biocompatible single-walled carbon nanotubes in mice probed by Raman spectroscopy. Proc. Natl. Acad. Sci. USA. 105: 1410–1415.
Liu, Z. and S. Tabakman, K. Welsher and H. Dai. 2009. Carbon nanotubes in biology and medicine: *in vitro* and *in vivo* detection, imaging and drug delivery. Nano Res. 2: 85–120.
Madani, S.Y. and A. Tan, M. Dwek and A.M. Seifalian. 2012. Functionalization of single-walled carbon nanotubes and their binding to cancer cells. Int. J. Nanomedicine. 7: 905–914.

Mandell, G.L. and J.E. Bennett and R. Dolin. 2010. Principles and Practice of Infectious Diseases, 7th ed. Churchill Livingstone Elsevier, Philadelphia, USA.

Mu, Q. and D.I. Broughton and B. Yan. 2009. Endosomal leakage and nuclear translocation of multiwalled carbon nanotubes: developing a model for cell uptake. Nano Lett. 9: 4370–4375.

Murphy, F.A. and A. Schinwald, C.A. Poland and K. Donaldson. 2012. The mechanism of pleural inflammation by long carbon nanotubes: interaction of long fibres with macrophages stimulates them to amplify pro-inflammatory responses in mesothelial cells. Part. Fibre Toxicol. 9: 8.

Nessim, G.D. 2010. Properties, synthesis, and growth mechanisms of carbon nanotubes with special focus on thermal chemical vapor deposition. Nanoscale. 2: 1306–1323.

Osmond-McLeod, M.J. and C.A. Poland, F. Murphy, L. Waddington, H. Morris, S.C. Hawkins, S. Clark, R. Aitken, M.J. McCall and K. Donaldson. 2011. Durability and inflammogenic impact of carbon nanotubes compared with asbestos fibres. Part. Fibre Toxicol. 8: 15.

Pantarotto, D. and C.D. Partidos, J. Hoebeke, F. Brown, E. Kramer, J.P. Briand, S. Muller, M. Prato and A. Bianco. 2003. Immunization with peptide-functionalized carbon nanotubes enhances virus-specific neutralizing antibody responses. Chem. Biol. 10: 961–966.

Pastorin, G. and W. Wu, S. Wieckowski, J.P. Briand, K. Kostarelos, M. Prato and A. Bianco. 2006. Double functionalization of carbon nanotubes for multimodal drug delivery. Chem. Commun. (Camb.). 11: 1182–1184.

Prajapati, V.K. and K. Awasthi, S. Gautam, T.P. Yadav, M. Rai, O.N. Srivastava and S. Sundar. 2011. Targeted killing of Leishmania donovani *in vivo* and *in vitro* with amphotericin B attached to functionalized carbon nanotubes. J. Antimicrob. Chemother. 66: 874–879.

Pitout, J.D. 2008. Multiresistant Enterobacteriaceae: new threat of an old problem. Expert Rev. Anti Infect. Ther. 6: 657–669.

Podesta, J.E. and K.T. Al-Jamal, M.A. Herrero, B. Tian, H. Ali-Boucetta, V. Hegde, A. Bianco, M. Prato and K. Kostarelos. 2009. Antitumor activity and prolonged survival by carbon-nanotube-mediated therapeutic siRNA silencing in a human lung xenograft model. Small. 5: 1176–1185.

Rosen, Y. and N.M. Elman. 2009. Carbon nanotubes in drug delivery: focus on infectious diseases. Expert Opin. Drug Deliv. 6: 517–530.

Rosen, Y. and B. Mattix, A. Ra and F. Alexis. Carbon nanotubes in infectious diseases. pp. 249–268. *In*: R.J. Hunter and V.R. Preedy [eds.]. 2011. Nanomedicine in Health and Disease. Science Publishers, New Hampshire, USA.

Rümmeli, M.H. and A. Bachmatiuk, F. Börrnert, F. Schäffel, I. Ibrahim, K. Cendrowski, G. Simha-Martynkova, D. Plachá, E. Borowiak-Palen, G. Cuniberti and B. Büchner. 2011. Synthesis of carbon nanotubes with and without catalyst particles. Nanoscale Res. Lett. 6: 303.

Sachar, S. and R.K. Saxena. 2011. Cytotoxic effect of poly-dispersed single walled carbon nanotubes on erythrocytes *in vitro* and *in vivo*. PLoS One. 6: e22032.

Schiffman, J.D. and M. Elimelech. 2011. Antibacterial activity of electrospun polymer mats with incorporated narrow diameter single-walled carbon nanotubes. ACS Appl. Mater. Interfaces. 3: 462–468.

Schipper, M.L. and N. Nakayama-Ratchford, C.R. Davis, N.W. Kam, P. Chu, Z. Liu, X. Sun, H. Dai and S.S. Gambhir. 2008. A pilot toxicology study of single-walled carbon nanotubes in a small sample of mice. Nat. Nanotechnol. 3: 216–221.

Singh, R. and D. Pantarotto, L. Lacerda, G. Pastorin, C. Klumpp, M. Prato, A. Bianco and K. Kostarelos. 2006. Tissue biodistribution and blood clearance rates of intravenously administered carbon nanotube radiotracers. Proc. Natl. Acad. Sci. USA. 103: 3357–3362.

Takagi, A. and A. Hirose, T. Nishimura, N. Fukumori, A. Ogata, N. Ohashi, S. Kitajima and J. Kanno. 2008. Induction of mesothelioma in p53+/– mouse by intraperitoneal application of multi-wall carbon nanotube. J. Toxicol. Sci. 33: 105–116.

Toupet, K. and V. Compan, C. Crozet, C. Mourton-Gilles, N. Mestre-Francés, F. Ibos, P. Corbeau, J.M. Verdier and V. Perrier. 2008. Effective gene therapy in a mouse model of prion diseases. PLoS One. 3: e2773.

Trivedi, R. and U.B. Kompella. 2010. Nanomicellar formulations for sustained drug delivery: strategies and underlying principles. Nanomedicine (Lond.). 5: 485–505.

Villa, C.H. and T. Dao, I. Ahearn, N. Fehrenbacher, E. Casey, D.A. Rey, T. Korontsvit, V. Zakhaleva, C.A. Batt, M.R. Philips and D.A. Scheinberg. 2011. Single-walled carbon nanotubes deliver peptide antigen into dendritic cells and enhance IgG responses to tumor-associated antigens. ACS Nano. 5: 5300–5311.

Wallace, E.J. and M.S. Sansom. 2008. Blocking of carbon nanotube based nanoinjectors by lipids: a simulation study. Nano Lett. 8: 2751–2756.

Wang, X. and P. Katwa, R. Podila, P. Chen, P.C. Ke, A.M. Rao, D.M. Walters, C.J. Wingard and J.M. Brown. 2011. Multi-walled carbon nanotube instillation impairs pulmonary function in C57BL/6 mice. Part. Fibre Toxicol. 8: 24.

Zhang, Z. and X. Yang, Y. Zhang, B. Zeng, S. Wang, T. Zhu, R.B. Roden, Y. Chen and R. Yang. 2006. Delivery of telomerase reverse transcriptase small interfering RNA in complex with positively charged single-walled carbon nanotubes suppresses tumor growth. Clin. Cancer Res. 12: 4933–4939.

CHAPTER 8

Metallic Nanoparticulate Drug Delivery Systems

Varsha B. Pokharkar,[1,a,*] *Vividha V. Dhapte*[1,b] and *Shivajirao S. Kadam*[2,c]

ABSTRACT

Currently, metal- and metal oxide-based nanoparticles are burgeoning avenues in the field of targeted novel drug delivery systems with incredible prospects for improvement in prevention, diagnosis and treatment of existing human ailments. Biocompatible gold nanoparticles are exhaustively harnessed in tumor alleviation, gene therapy, and imaging procedures. Known for first-rate antimicrobial and anti-inflammatory effects, nanocrystalline silver appears as an excellent wound healing agent, surgical dressing and filter device. Titanium dioxide and zinc oxide nanoparticles are commercially branded as authentic sunscreen agents for their overall UV attenuation efficacy. Distinctive paramagnetic properties of iron oxide nanoparticles craft them as tailored contrast agents for imaging, and as cargos for targeted drug delivery in concert. Metallic nanoparticles gifted with unique size and shape dependent optoelectronic properties carry the potential as future self-therapeutics. Conventional

[1] Department of Pharmaceutics, Poona College of Pharmacy, Bharati Vidyapeeth University, Erandwane, Pune 411038. Maharashtra State, India.
[a] Email: vbpokharkar@yahoo.co.in
[b] Email: vividhadhapte@gmail.com
[2] Bharati Vidyapeeth University, Bharati Vidyapeeth Bhavan, Lal Bahadur Shastri Marg, Pune 411030. Maharashtra State, India.
[c] Email: sskadam.vc@gmail.com
* Corresponding author

List of abbreviations after the text.

methods of chemical reduction, physical processes and green synthesis are employed in preparation of metal nanoparticles. Bottom-up methods facilitate size controlled fabrication of nanoparticles compared to top-down approaches. For targeted drug delivery, surface engineering of bare metal nanoparticles with different ligands, peptides, polymers, markers, and antibodies augment their stability, pharmacokinetics and efficacy. In principal, the nanoparticulate-cellular interactions largely define the therapeutic effects and toxicity of metallic nanoparticles. Disparity amid toxicity and functional profiles of promising nanoparticles backfire their commercial prospects. Harmonized regulations and apt risk assessment would venture out safe nanoparticles in the market. This chapter is an effort to review various aspects of metallic nanoparticulate system right from their inception to commercialization.

Introduction

Nanoparticulate-based drug delivery has brought a renaissance in the global health arena. Akin to their organic counterparts, metallic colloidal particles have a long established potential in the areas of biology, catalysis, diagnostics and therapeutics. As early as 2500 BC, metallic particles were recognized as indigenous part of the traditional system of medicine in Chinese and Indian cultures. These familiar "Bhasmas" are metal-based compounds known for their vital medicinal value (Perks 2010). During the 17th century, gold (Au) was popularly used in the coloring of glass to produce intense shades of yellow, red or brown depending on the concentration used. An exemplary case in point are the Lycurgus cup (Perks 2010) and the Fabergé's Imperial Easter eggs. In 1857, Michael Faraday reported the preparation of a deep red colored solution of Au colloids by the reduction of aqueous chloroaurate ions ($AuCl_4^-$). In modern medicine, the initial use of Au was discovered by Robert Koch (1890) against the tubercle bacillus (Daniel and Astruc 2004). Commercially Ridauro™, Myochrysine™, and Solgonal™ like Au-based compounds are still used today for various therapeutic applications (Shaw 1999).

Another noble metal, silver (Ag) contained medicinal properties and could cure multiple maladies as proclaimed by Hippocrates. As Ag was plugged to have antiseptic properties, Phoenicians used Ag vessels for food storage to prevent spoilage. Prior to evolution of antibiotics, Ag compounds were widely used against various maladies (Atiyeh et al. 2007). In the early 20th century, scores of medicinal nano-Ag colloids, Collargol™, Argyrol™, and Protargol™ were prescribed over a 50 year period to treat various diseases, such as, syphilis and other bacterial infections (Fung and Bowen 1996). The United States (US) Environmental Protection Agency (EPA) has registered multiple Ag-impregnated water filters since the 1970s for safe

domestic water applications, such as, drinking water and swimming pool filters.

Recent newcomers to this field of inorganic materials are the metal oxide nanoparticles (NPs). Zinc oxide (ZnO) NPs have received considerable attention for their exclusive antimicrobial as well as ultraviolet (UV) filtering properties, and high catalytic and photochemical activities (Meruvu et al. 2011). Superparamagnetic iron oxide (SPIO) NPs find ample biomedical applications, such as, Magnetic Resonance Imaging (MRI) contrast agents, tissue repair, immunoassay, detoxification of biological fluids, hyperthermia, drug delivery and cell separation owing to the high magnetization values at nanoscale (Sun et al. 2008). Titanium dioxide (TiO_2) NPs have proved effective as tumor cell killing agents, disinfectants, antibiotics, biosensors and sunscreen agents (Fadeel and Garcia-Bennett 2010).

This chapter makes an attempt to cover various aspects related to Metallic Nanoparticles (MNPs) such as the synthesis, properties, characterization, biological and engineering aspects, regulatory perspectives and promising applications.

Types of Metallic Nanoparticles

Anatomy of a MNP (including metal NPs and metal oxide NPs) consists of two main parts: the inside core and a stabilizing/functional layer. Structure of noble MNPs defines their optical and electronic properties, stability, utility and cellular internalization. MNPs exist in various geometries, being spherical NPs, nanorods, nanocubes, triangles, nanopolyhedrons, nanoshells or nanocages (Drezek et al. 2008) (Fig. 8.1).

Nanorods and other anisometric NPs draw considerable attention due to the possible rational control over the aspect ratio which is primarily responsible for the change in their optical properties and the Enhanced Permeability and Retention (EPR) effect. The higher the aspect ratio of NPs, the more the probability of their cellular internalization (Petros and DeSimone 2010). Dimensions of nanorods can be precisely controlled by

Figure 8.1. Characteristic geometries of MNPs.

varying the applied energy to the system compared to conventional NPs. Snipping edges of triangular NPs, symmetry and thickness of nanodisks influence their optical properties and biological fate. According to Chen et al. (2011), size and morphology of MNPs can be tailored by opting relevant fabrication techniques. Based on their make-up, MNPs can be classified as homofunctional, heterofunctional, multimodal and bimetallic NPs. Shore et al. (2011) have reported Au/Ag (core/shell) MNPs and alloy bimetallic NPs of Au-Ag alloy with highly tunable optical and catalytic properties. In 2011, Edrissi and Norouzbeigi have synthesized deer-horn shape ZnO NPs by microwave synthesis (Edrissi and Norouzbeigi 2011). For targeted drug delivery and programmed cellular uptake, MNPs are coupled using ligands, stabilizers, antibodies or polyelectrolytes. Etame et al. (2011) designed Poly(Ethylene Glycol) (PEG)-functionalized Au NPs to realize an EPR effect within permissive tumor microvasculature in malignant brain tumors.

Properties of Metallic Nanoparticles

Optoelectronic properties based on shape- and size-dependent characteristics underline the exclusivity of MNPs for various biomedical applications. MNPs of Au, Ag and copper (Cu) possess brilliant colors due to the presence of the Surface Plasmon Resonance (SPR) band (Mukherjee et al. 2011). Ag NPs of spherical, pentagonal and triangular shape appear blue, green and red, respectively under a dark field microscope (Mock et al. 2002). The SPR band is the outcome of the collective oscillations of the electron gas at the surface of MNPs allied with the electromagnetic field of the incoming light, explicitly, the excitation of the coherent oscillation of the conduction band (Daniel and Astruc 2004). As per Mie's theory, the SPR band is influenced by the particle shape and size of MNPs, the medium dielectric constant and the temperature. Concentration/attachment of ligands like thiols (–SH), polymers, stabilizers or the presence of impurities/aggregation in MNPs accounts for either a red or blue shift in the fundamental SPR. MNPs are capable of resonantly scattering visible and Near-Infrared (NIR) light upon the excitation of their surface plasmon oscillation indicative of their size and aggregation. Au NPs (size: 58 nm) scatter green light while 78 nm-sized Au NPs scatter yellow light. Au nanorods scatter red light under illumination of a beam of white light (Sönnichsen et al. 2002). The core charge of MNPs is another essential factor; surplus electronic charge causes shifts to higher energy, whereas electron deficiency causes shifts to lower energy. The ratio of scattering to absorption increases with increasing particle size. Twenty nm-sized nanospheres show merely SPR-generated absorption without any significant scattering (Jain et al. 2006). Deep red color of 20 nm-sized Au nanoshells displayed a strong UV-visible extinction band at a wavelength of 520 nm, which undergo bathochromic shift with increase in NP diameter.

Metal oxides, such as, IO and ZnO NPs, possess strong and stable photoluminescence. ZnO NPs usually emit strong UV light at 378 nm without any emission spectrum in the visible wavelength range. Incorporation of organic surface modifiers improves this emission for harnessing ZnO NPs in various biological applications (Wu et al. 2007). Out of the various crystalline structures of ZnO and TiO_2, wurtzite and rutile, respectively are the most stable forms and birefringent crystals with higher refractive indices in UV-visible range. Nano-sizing helps to eliminate the natural opaqueness (due to high refractive indices) of ZnO and TiO_2 NPs without reducing their UV blocking efficacy (Smijs and Pavel 2011).

When Iron Oxide (IO) is reduced to NPs, their ferromagnetism tunes to a single magnetic domain and, therefore, maintains one large magnetic moment. Yet, at high blocking temperatures, energy is sufficient to induce free rotation of the NP causing loss of net magnetization in the absence of an external magnetic field. This superparamagnetic property indicated lack of remnant magnetization after removal of external magnetic fields. This attribute assists IO [SPIO and ultrasmall superparamagnetic iron oxide (USPIO)] NPs to maintain their colloidal stability for diagnostic and biomedical applications. Also, the coupling interactions within these single magnetic domains result in much higher magnetic susceptibilities than the paramagnetic materials (Sun et al. 2008).

MNPs below 100 nm size have low melting points than in its bulk state. Nano-sizing increases the number of surface atoms, decreases the coordination number of atoms for ease of atomic rearrangement, thereby lowering the melting point temperature (Castro et al. 1990).

Synthesis of Metallic Nanoparticles

Different fabrication methods and processing conditions outline the final characteristics of MNPs (Table 8.1). Choice of an appropriate synthetic method is based on the criteria of size, shape, surface functionalities, desirable properties, applications and biological fate of MNPs. Several conventional and advanced strategies for MNP synthesis are reported. In general, two approaches, "bottom-up" and "top-down" techniques are used for the synthesis of MNPs. "Top-down" methods employ sizing down of a suitable starting material by milling, attrition, and other mechanical and energy addition processes, but results into imperfections of the surface structure. Major limitation of "top-down" methods lies in the difficulty of size control. On other hand, the "bottom-up" approach refers to the self-assembly of nuclei into nanostructures with comparatively lesser defects, more control over the size of NPs and, hence, more homogeneous chemical composition (Nguyen et al. 2011).

Table 8.1. Summary of various synthetic techniques for MNPs.

MNPs	Method of synthesis	Applications	Reference
Au NPs	Porphyran-mediated biosynthesis	Enhanced delivery of doxorubicin to human glioma LN-229 cell line	Pokharkar et al. 2011
Au NPs	Biosynthesis using plant chloroplasts	Ultrasensitive detection of biomarkers	Zhang et al. 2011a
Au(core)/Ag(shell) alloy NPs	Digestive ripening followed by annealing	Tunable bimetallic NPs for catalysis, and as taggants for security applications	Shore et al. 2011
Au NPs	Cefaclor-mediated reduction	As potent antimicrobial coatings	Perry et al. 2010
Au NPs	Biosynthesis via the enzyme serratiopeptidase	Improved anti-inflammatory activity	Venkatpurwar and Pokharkar 2010
Au NPs	Biomicrowave synthesis using the *Psidium guajava* leaf extract	Biodetection and other biomedical applications	Raghunandan et al. 2009
Au NPs	Chemical synthesis using natural and biocompatible gellan gum	Improved delivery of the cationic drug (doxorubicin hydrochloride)	Pokharkar et al. 2008
Amino acid-protected Au NPs	Spontaneous, sequential synthesis by borohydride reduction, followed by capping with tryptophan	Catalysis, sensors, molecular markers and other biological applications	Selvakannan et al. 2004
Ag NPs	Green synthesis using a marine polysaccharide	Enhanced antibacterial activity	Venkatpurwar and Pokharkar 2011
Ag NPs	Microwave-assisted template synthesis using starch	Medical and biological applications	Sreeram et al. 2008
Ag nanoplates and Au nanorings	Ultrasonic-assisted synthesis	Catalysis, optics, surface-enhanced Raman scattering (SERS)	Jiang et al. 2004a
Ag NPs	Pulsed sono-electrochemical technique	Photographic process, SERS and catalysis	Jiang et al. 2004b
ZnO NPs	Microwave heating of a bis(2-pyridinethiol *N*-oxide) Zn (II) complex	Removal of sulfur-containing gases in petrochemical industries	Edrissi and Norouzbeigi 2011
TiO_2 NPs	Low-temperature alkaline hydrolysis	Next generation antibiotics, biosensors, tumor cell-killing agent and gene targeting	Thurn et al. 2011

TiO_2 NPs	CVD and supercritical fluid (SCF) process	Enhanced photoactivity for industrial applications	Wu et al. 2010
Amorphous IO NPs	Sonolysis in the presence of sodium dodecyl sulfate (SDS)	Molecular imaging, magnetic separation of proteins, and hyperthermia therapy	Muller et al. 2008
SPIO NPs	*Actinobacter* sp. bacteria-mediated precursor-dependent biosynthesis	Magnetic recording and magnetic storage devices, ferrofluids and contrast enhancers in MRI	Bharde et al. 2008
IO NPs	Facile organic-phase synthesis through high-temperature reductive decomposition	Gas sensors, biosensors and catalysis	Sun et al. 2007

Physical methods

In 2004, Wostek-Wojciechowska et al. discussed the thermal decomposition of organometallic precursors for the preparation of Au NPs in solid state. Commonly used techniques for physical synthesis of MNPs basically include attrition, thermal quenching and pyrolysis like mechanical methods (Fig. 8.2, Table 8.1). In attrition, starting materials are reduced to submicron-sized particles by means of planetary ball mill, media mill, etc. (Thakkar et al. 2010). In pyrolysis, an organic precursor (liquid/gas) is forced through an orifice at higher pressure and burned into ash from which oxidized MNPs are recovered. In Physical Vapor Deposition (PVD), metal films of nanometer thickness are produced by electrical heating of metal under high vacuum. In Chemical Vapor Deposition (CVD), carrier gasses containing the elements of desired compounds are passed over heated surfaces resulting in decomposition of atoms/molecules on the surface (Burda et al. 2005). The Solvated Metal Atom Deposition (SMAD) technique involves heating of bulk metal for evaporation under vacuum followed by cocondensation of its vapors with solvents to form MNPs in solution. Singh et al. (2008) synthesized nano-sized Ag particles through inert gas condensation techniques: evaporation of bulk metal in an inert atmosphere with the subsequent cooling for nucleation and growth of Ag NPs. In the laser ablation technique, intense laser pulses are focused on metal targets immersed in a solvent containing surfactant. Due to the high temperature resulting from intense laser pulses, metal atoms are vaporized and solvated by surfactant molecules to form NPs. Ultrasonic irradiation was applied to synthesize mesoporous solids with Au NPs inside its pores (Chen et al. 2001). Sonication employs ultrasonic waves in the presence of an acoustic field which results into continuous bubbling at high temperature conditions, thus leading to the generation of reactive radicals which catalyze the formation of MNPs (Fig. 8.2).

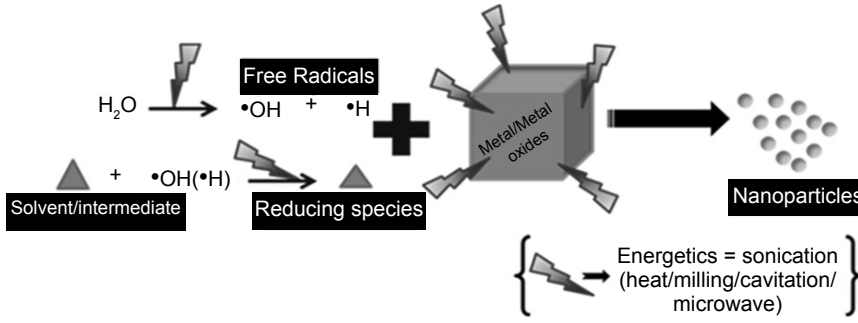

Figure 8.2. Physical techniques like sonication and other energy adding mechanisms employed in synthesis of MNPs.

At higher temperature conditions, ferrous salts are converted into magnetite (Fe_3O_4) NPs owing to the rapid collapse of sonically generated cavities. At 20 kHz sonication, 20 nm-sized bimetallic, crystalline, Au-Ag NPs were obtained from a mixture of $AuCl_4^-$ and silver nitrate ($AgNO_3$) under room temperature and argon (Ar) atmosphere (Shchukin et al. 2010). Also, solvated electrons or free radicals produced by radiolysis induce the reduction of metal salts into MNPs. Low production rate, higher expenses, enormous energy consumption and high pressure/temperature requirements limit the applications of physical methods for NP synthesis.

Chemical methods

Wet-chemical procedures are the most widely used methods for controlled synthesis of MNPs (Table 8.1). Generally speaking, the chemical reduction method is used for the synthesis of MNPs with a dual step mechanism of nucleation and successive growth (Nguyen et al. 2011). Initially, MNPs are nucleated by the reduction reaction and collision between ions and atoms. Subsequent controlled growth controls the size and shape of MNPs under the specific conditions of chemical concentration, mixing ratios, surfactant nature, pH, temperature, etc. Size-controlled growth of MNPs requires an isotropic growth on the surface of the metal nuclei which results in increasing particle size to eventually become spherical. Anisotropic growth of particles stimulates the formation of MNPs with varied aspect ratios and morphologies (Nguyen et al. 2011). A typical procedure involves growing MNPs in a liquid medium containing metal precursors and reducing agents, e.g., sodium borohydride, sodium citrate, hydrazine and gellan gum. Stabilizers, such as, sodium dodecyl benzyl sulfate, poly(*N*-vinyl-2-pyrrolidone) (PVP), and a variety of biomolecules like proteins, peptides, and gums are added to the reaction mixture to prevent the agglomeration of MNPs (Park et al. 2012). In 2008, Dhar et al. employed natural gums (anionic gellan gum) for the synthesis of biocompatible Au NPs which were further conjugated with doxorubicin via ionic interactions (Fig. 8.3). In 2006, Chen et al. synthesized single crystalline, slightly truncated shape, Ag nanocubes through reduction of $AgNO_3$ in the presence of PVP. Temperature, concentration, and the nature of precursors, reducing agents and stabilizers can affect the size, morphology and properties of MNPs.

The Turkevich method, the most conventional procedure for the synthesis of spherical Au NPs, involves the reduction of $AuCl_4^-$ in a boiling sodium citrate solution (Turkevich et al. 1951). Later, the very same method was used by Frens et al. (1973) with modification in the ratio of citrate/$AuCl_4^-$ to produce Au NPs with desirable morphology. Particle size decreases as the ratio citrate/$AuCl_4^-$ increases because of the stabilizing process of the citrate. Under mild conditions of reducing agent and Au

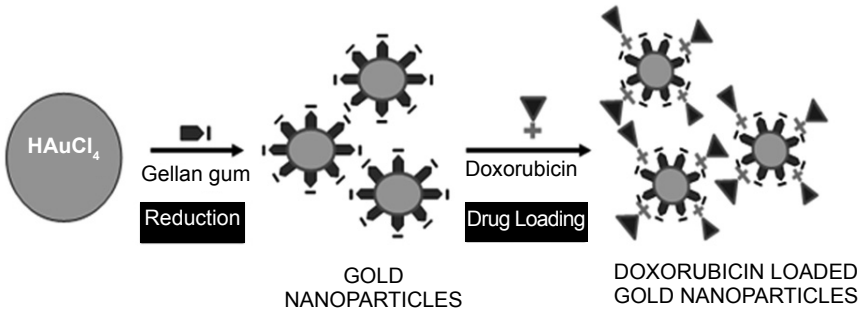

Figure 8.3. Chemical reduction synthesis of Au NPs using gellan gum with subsequent loading of doxorubicin.

precursor, particle size can be controlled by the "seed-mediated growth of Au NPs". Initially, small Au particles are prepared and used as the seed particles for the subsequent growth. In these tailor-made Au NPs, all new metal atoms generated by a reduction reaction were deposited on the surface of the seed particles without further nucleation (Daniel and Astruc 2004).

Conventionally, chemical co-precipitation of ferrous salts yields Fe_3O_4 NPs from an aging stoichiometric mixture of ferrous and ferric salts in aqueous medium (Laurent et al. 2008). Sol-gel reactions are the most apt synthetic routes for nanostructured metal oxides. In these reactions, a "sol" of MNPs originates from the hydroxylation and condensation of molecular precursors; subsequent condensation and inorganic polymerization leads to a three dimensional (3D) metal oxide network denominated "wet gel". Non-agglomerated Fe_3O_4 particles with uniform shape and narrow size distribution can be synthesized when triethylene glycol is directly reacted with the 2,4-pentanedione iron(III) derivative [$Fe_{(acac)3}$] at elevated temperatures. A non-aqueous sol-gel approach involving titanium isopropoxide ($Ti(O^iPr)_4$) and benzyl alcohol has been proposed for the fabrication of crystalline 15 nm-sized TiO_2 NPs (Koziej et al. 2009).

Also, combined physicochemical approaches are valuable in the preparation of MNPs. In 2008, Shen et al. exercised a solution free, mechanochemical approach for the direct synthesis of ZnO NPs. In the initial step, grinding a powder mixture of zinc acetate [$Zn(CH_3COO)_2$] and oxalic acid dihydrate ($H_2C_2O_4{\cdot}2H_2O$) at room temperature formed zinc oxalate dihydrate ($ZnC_2O_4{\cdot}2H_2O$) NPs. This was followed by thermal decomposition of $ZnC_2O_4{\cdot}2H_2O$ NPs at 450ºC to form highly crystalline ZnO NPs (size: 24–40 nm).

Modification in the chemical state of reactants, choice of different solvent media (aqueous, organic, or supercritical fluids), freedom of assembly at various interfaces (air-water or liquid-liquid interfaces), monitoring of shape and size of MNPs, and ease of surface functionalization are the most

attractive features of the chemical synthesis routes of MNPs. Generally, chemical methods are low-cost for high volume synthesis. However, their drawbacks include contamination from precursor chemicals, use of toxic solvents and generation of hazardous by-products.

Biosynthesis

To overcome the limitations of physical and chemical methods, biological routes for synthesis of zero-valent MNPs are explored as they offer simple, high-yielding, low-cost, non-toxic and ecofriendly procedures. Different biological resources including plants, algae, fungi, yeast, bacteria, and their products are available for green synthesis of MNPs (Fig. 8.4, Table 8.1). Biodegradable, highly soluble and less toxic components from plant extracts contain flavonoids, caffeine, polyphenols, antioxidants, anthocyanins, carotenoids, catechins, quercitins, rutins and their derivatives, which act as reducing as well as stabilizing agents for the production of Ag, Au, iron (Fe) and platinum (Pt) NPs. Many unicellular and multicellular organisms are known to produce inorganic materials either intracellularly or extracellularly. For instance, microorganisms synthesizing inorganic materials include magnetotactic bacteria (synthesize Fe_3O_4 NPs), diatoms (synthesize siliceous materials) and *S*-layer bacteria (synthesize calcium carbonate layers) (Ankamwar 2010). Many researchers have reported the use of bacteria like *Bacillus koriensis*, *Bacillus subtilis*, and fungi, such as, *Aspergillus fumigatus* and *Fusarium oxysporum* for the biosynthesis of Ag NPs

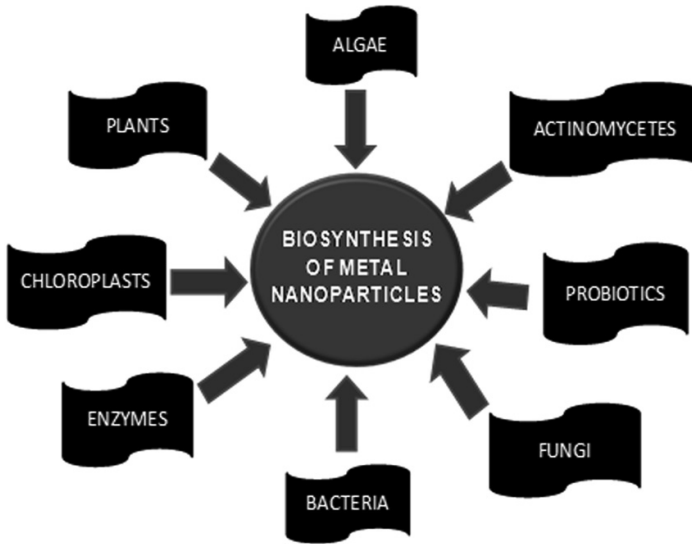

Figure 8.4. Various routes for the biosynthesis of MNPs.

(Venkatpurwar and Pokharkar 2011). In a similar experiment, it was shown that the bacteria *Rhodopseudomonas capsulata* produces Au NPs of different sizes and shapes. At neutral pH, spherical Au NPs were formed, whereas Au nanoplates were produced at slightly acidic pH. Physicochemical conditions of solution pH, temperature and incubation time control the morphology of biogenic MNPs. Au NPs and Pt NPs can be prepared using the marine algae *Sargassum wightii*. In the synthesis of intracellular Ag NPs using the fungus *Verticillium*, additional downstream processing was essential when the site of MNPs synthesis is intracellular, thus adding to the complexity and cost of the process. Comparatively, extracellular synthesis offers simple and cost-effective technique as illustrated from the extracellular biosynthesis of Au NPs by the actinomycete *Thermomonosporas*, and of Ag NPs using the filamentous fungus *Aspergillus fumigatus* (Thakkar et al. 2010). Recently, Pokharkar et al. (2011) isolated and applied a marine polysaccharide for the synthesis of Au NPs as well as Ag NPs. Zhang et al. (2011a) have reported the use of chloroplasts as reductants and stabilizers for the one-pot biosynthesis of Au NPs. Jha and Prasad et al. (2010) reported an economical and reproducible green synthesis of Ag NPs and TiO_2 NPs mediated via the probiotic microbe *Lactobacillus sporogens*. From a commercial and environment safety point of view, it would be advantageous to have non-pathogenic and biomimetic approaches for MNP production and advances in nanomaterials.

Microwave-assisted synthesis

Currently, microwaves are applied as an alternative methodology for the rapid and controlled synthesis of MNPs. When the microwave radiation interacts with the reaction system, reducing species are formed *in situ* for conventional synthesis of MNPs (Fig. 8.2). Absence of external reducing agents, such as, hydrides or citrates, eliminates additional contamination sources. During microwave synthesis, both thermal and non-thermal effects occur. As microwave radiation is a function of the dielectric properties of the irradiated molecules, their absorption increases the thermal energy of the reaction system. The most remarkable part of this synthetic method is the formation of 3D nanostructures by assembling NPs in a specific geometry so as to tune their physical, optical and electrical properties (Gutiérrez-Wing et al. 2012). The resulting structure would lead the developments in modern-day photonics, diagnostics, nanodevices and multifunctional nanomedicine. Au NPs (1.8 nm-sized) can be synthesized via microwave-assisted process in a two-phase system that self-assembled into 1 mm-diameter self-supported superstructures, spontaneously producing an off-white powder. The *n*-alkanethiol molecules from 1-dodecanethiol interacted to form the cubic arrangement between the Au NPs leading to the formation

of the superstructure, with a mean interparticulate distance of 3.56 nm. In a microwave-assisted synthesis of deer horn-like and spherical ZnO NPs, the influence of the pyrolysis time on the average particle size distribution was studied (Edrissi and Norouzbeigi 2011). In 2011, Blosi et al. adopted the microwave-assisted polyol synthesis of stable Cu NPs for scale-up at the industrial large-scale production level.

Surface Functionalization

Nascent MNPs are unstable and prone to instant aggregation and rapid clearance in the physiological milieu. Engineering the surface of MNPs thus becomes indispensable for systemic applications. In fact, long-circulating MNPs are desirable for passive targeting. Surface functionalization directs MNPs to specific disease areas and allows them to selectively and competitively interact with cellular components. Surface conjugation of MNPs with antibodies, peptides, deoxyribonucleic acid (DNA), ribonucleic acid (RNA), ligands, markers and other targeting moieties is usually achieved by their reversible association-dissociation interactions with the metal surface (Fig. 8.5).

Such transactions may denature proteins and thermolabile molecules, or limit the ligand-cellular interactions due to a steric hindrance. When MNPs are tethered with functionalities, quantification of functional groups at the MNPs surface, their binding strength, bioavailability and toxicity turns out to be essential (Lindfors et al. 2004).

Diverse surface modification strategies have been adopted, i.e., partial chemical (precipitation, esterification, coupling), mechanochemical (adsorption, grafting, UV rays), external membrane and high-energy surface modification reactions. Numerous functional groups, such as, polyelectrolytes, –SH, hydroxyl (–OH), phosphine ($–PH_2$) and amino ($–NH_2$) have been reported (Daniel and Astruc 2004). Monofunctional,

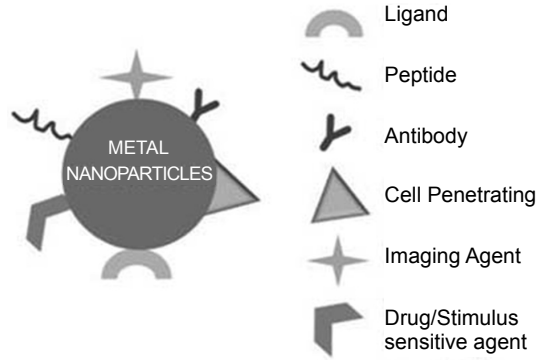

Figure 8.5. Multiple functionalities for the surface engineering of MNPs.

homofunctional or heterofunctional PEGs are commonly used spacers for the modification of MNPs in order to evade the macrophage-mediated uptake (Shenoy et al. 2006). As weighed against other functionalities, sulfur-based ligands offer stronger conjugation via covalent bonding (bond energy 47 Kcal/mol) for higher stability of MNPs. Another rationale for opting –SH functionality is the higher intracellular glutathione levels which are known partially to displace the SH-monolayer particle surface for releasing the therapeutic cargo which is covalently bound to the monolayer. Usually, the sulfur-containing ligands, such as, alkanethiols, xanthates, disulphides and trithiols, are used for the engineering of Au NPs (Daniel and Astruc 2004). A cyclical disulfide binds in a multidentate fashion with the metal surface to provide multiple binding points and enhanced stability. However, sometimes a weaker binding may be required as part of a drug release mechanism. This can be achieved via non-covalent interactions based on electrostatics, van der Waals forces and hydrogen bonding between ligands and MNPs. In the realm of pseudo-covalent interactions amid MNPs and amines (lower bond energy ≈ 6 Kcal/mol), drug release could be substantially easier than in the case of SH-bound ligands.

In 2012, Park et al. decorated Au/nickel (Ni) segmented nanorods with Pluronic® on Au segment to facilitate doxorubicin loading, and with folic acid on Ni segment for targeting human nasopharynx KB carcinoma cells. Typically inert coatings of silica, dextran, alginate, chitosan and PEG on the surface of Fe_3O_4 NPs prevent their aggregation in liquid, improve their chemical stability and offer a better protection against toxicity (Laurent et al. 2008). Of late, herceptin- and cisplatin-conjugated Au-Fe_3O_4 nanocarriers delivered the drug into human epidermal growth factor receptor 2 (Her2)-positive Sk-Br3 human breast cancer cells with strong therapeutic results (Bhattacharyya et al. 2012). In 2008, Thevenot et al. revealed the higher antitumor potential of –NH_2 and –OH functionalized TiO_2 NPs than –COOH functionalized TiO_2 NPs in B16F10 melanoma, Lewis Lung Carcinoma (LLC), JHU prostate cancer cells, and 3T3 fibroblasts to underline the significance of surface engineering for targeted cancer therapy. Surface chemistry of Ag NPs has a predominant effect on the efficacy owing to their interactions with viruses. Differences observed in Ag NPs induced Human Immunodeficiency Virus type 1 (HIV-1) inhibition were justified as PVP and Bovine Serum Albumin (BSA) remained directly bound and totally encapsulated to the NP surface, while the uncoated Ag NPs exhibited fundamentally a free surface area for stronger interactions, superior inhibition and cytotoxicity (Elechiguerra et al. 2005). By linking organic chains onto the surfaces, the size of ZnO NPs can be controlled. Bare ZnO NPs emit strong UV light at 378 nm which could damage cells. In 2011, Premanathan et al. developed ZnO NPs capped with organic chains composed of hydrophilic amide and urethane linkages along with terminal –NH_2 groups on the surfaces as

binding sites for biomolecules. With photoluminescent spectrum at higher wavelength (515 nm), capped ZnO NPs proved to be non-cytotoxic.

Biological Fate of Metallic Nanoparticles

In the last decade, nanotechnology invigorated miscellaneous novel solutions for loads of human ailments. Lack of fundamental understanding of the nanoparticulate-cellular interactions defers their end applications pertaining to tailored drug delivery. Cellular internalization mechanisms of MNPs need to be defined so as to ascertain their benefit-to-risk ratio. Elevated surface area and surface free energy, nature of ligand, propensity of aggregation, charge, size and morphology of MNPs play decisive roles in framing their biological fate.

Cellular interactions

There are diverse uptake mechanisms of MNPs, either in the form of endocytosis or phagocytosis. Non-phagocytic cells may undergo clathrin- or caveolin-mediated endocytosis and even macropinocytosis. Besides, secondary endocytic mechanisms like dynamin- and clathrin-dependent or dynamin- and clathrin-independent endocytosis exist. Intracellular localization and trafficking of MNPs depends on the form of endocytosis. Rationally modified MNPs target malignant cells which are known to undergo frequent alterations in the endocytic pathways. In 2011, Thurn et al. demonstrated that temperature-, concentration-, and time-dependent internalization of TiO_2 NPs followed clathrin-mediated endocytosis, caveolin-mediated endocytosis, as well as macropinocytosis in prostate cancer PC3M cells.

There is a difference of opinion concerning the reliability of *in vitro* cellular assays in mapping out the biological activity and safety of MNPs. As reported by Villiers et al. (2010), 10 nm-sized citrate capped Au NPs showed no cytotoxicity even after their significant internalization in endocytic compartments, but the cytokine profile was considerably altered, thus indicating an alteration in the immune response.

Many *in vivo* studies showed that MNPs are localized in various cell organelles like mitochondria, lipid vesicles, fibroblasts, nucleus or macrophages. MNP-cellular interactions may result into: *i*) formation of Reactive Oxygen Species (ROS) leading to oxidative stress and inflammation; *ii*) genetic manipulation encoding the proteins involved in cellular abnormalities; and/or, *iii*) lipid peroxidation of cellular membranes, resulting in cell injury.

It is reported that smaller, 1.4 nm-sized Au NPs trigger cellular necrosis via mitochondrial disruption and ROS generation (Pan et al. 2009). Addition

of reducing compounds, such as, glutathione and *N*-acetyl cysteine, improved their cytotoxicity. In a parallel investigation, Li et al. (2010a) found 20 nm-sized Au NPs triggered oxidative stress and autophagy in human lung fibroblasts, along with elevated lipid peroxidation levels and up-regulation of autophagy related ATG-7 gene and inflammatory enzyme cyclooxygenase-2 gene production. Surface properties of MNPs influence their efficacy: charged Au NPs induce apoptosis, and neutral Au NPs promote necrosis. The higher the hydrophobic character and cationic nature of MNPs, the greater is their acute toxicity and decrease in DNA damage. As reviewed by Mukherjee et al. (2012), biological responses mediated by Ag NPs are selective and specifically associated with their size and concentration. Yu et al. (2011) found cellular internalization of 20 nm-sized cationic ZnO NPs easier than 70 nm-sized anionic ZnO NPs. Surface masking of MNPs with ligands, PEG-SH, antibodies or markers is known to circumvent the body's defenses, especially against macrophage recognition and clearance, thereby improving their half-lives. Also the functional groups prevent the aggregation and destabilization of MNPs, once inside the physiological environment. Blank Au NPs are taken up by macropinocytosis, clathrin- and caveolin-mediated endocytosis, whereas PEG-coated Au NPs uptake occurs via caveolin- and/or clathrin-mediated endocytosis, but not by macropinocytosis (Brandenberger et al. 2010a). This might be due to interactions of MNPs with different proteins or lipids, related to one of the uptake mechanisms and their increased aggregation ability.

Recently, Comfort et al. (2011) studied the effect of Au NPs, Ag NPs and IO NPs (of similar size and morphology) on Epidermal Growth Factor (EGF) signal transduction in the A-431 human epithelial cell line. A comparative study revealed various effects of these 3 MNPs over each other: Ag NPs increased ROS levels considerably, Au NPs reduced EGF-dependent phosphorylation levels and IO NPs brought about minimum modifications in EGF-dependent gene transcription. Thus, MNPs are capable of destroying cellular functionality irrespective of their make and mechanism.

Particle geometry significantly affects cellular internalization of MNPs. Anisotropic and high-aspect-ratio MNPs internalizes more readily and efficiently than isotropic low-aspect-ratio MNPs, sharing equal volumes. Identical dimensions of low-aspect-ratio MNPs result into equal rates of internalization, as well as drainage from the cells. Asymmetrical morphology of high-aspect-ratio MNPs maintains higher uptake rates with less clearance rates so as to retain them in the cellular environment to cause the desired EPR effect (Fig. 8.6). In 2006, Chithrani et al. observed significant uptake of Au nanorods with larger aspect ratios compared to spherical particles that have equivalent size characteristics.

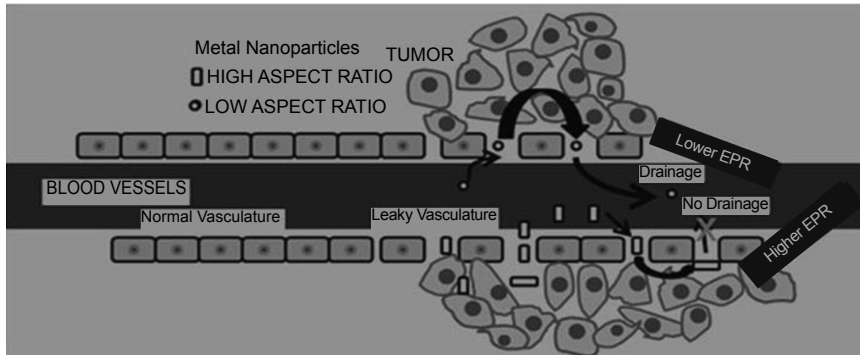

Figure 8.6. Passive targeting and EPR effect of MNPs with high-aspect- and low-aspect-ratios.

Pharmacokinetics

Pharmacokinetic profiling helps to study the amount absorbed into systemic circulation and the clearance following exposure in order to trace out the efficacy and safety of MNPs. Further, it aids in identifying the potential and latent tissues for accumulation of MNPs that reflect the toxicity (and *in vivo* mechanism). The surface characteristics of MNPs outline the opsonization and the Mononuclear Phagocyte System (MPS) uptake to deeply influence their pharmacokinetics. MNPs in the size range of 100 nm with a neutral and hydrophilic polymer-coated surface exhibit prolonged blood circulation and an increased accumulation in tumor cells. Surface functionalization through various strategies (PEGylation, mechanochemical modification, etc.) reduces the rate of MPS uptake and increases the circulation half-life by minimizing opsonization and preventing protein binding. Mukherjee et al. (2012) investigated the role of surface charge and route of administration in determining the pharmacokinetics of engineered Au NPs. Neutral and zwitterionic PEGylated Au NPs imparted the highest concentrations and intraperitoneal bioavailability, thus maximizing the circulation time. In another study, Baek et al. (2012) studied the pharmacokinetics, biodistribution and clearance of MNPs by considering 20 nm-sized and 70 nm-sized ZnO NPs as prototypes. Irrespective of the size, dose and gender, the capacity of body to absorb ZnO NPs was limited since the uptake of metals is controlled by metal-binding proteins and other specific receptors. Metallothionein, a cysteine rich metal binding protein, is assigned a role in absorption, distribution and clearance of MNPs. In fact, MNPs are known to ionize and interact with the sulfur-containing ligands in proteins.

Various reports on biodistribution studies revealed the customary distribution pattern of MNPs in the liver and spleen. Macrophages aid

phagocytosis across these organs, and thus assist in the uptake of these NPs. After an intravenous injection, 20 nm-sized Ag NPs occurred predominantly in the liver, kidney and spleen, while 80 nm-sized and 110 nm-sized Ag NPs were distributed in the spleen, liver and lung. Similarly, 5 nm-sized and 10 nm-sized PEGylated Au NPs accumulated in the liver as against the 30 nm-sized Au NPs in the spleen after the intraperitoneal injection (Zhang et al. 2011b). IO NPs were distributed to the liver and spleen after intragastric administration. Equally, 20 nm-sized TiO_2 NPs would deposit mainly in the liver and spleen after intravenous injection (Baek et al. 2012).

Several researchers have reported the size-dependent elimination kinetic for MNPs which is influenced by high dissolution, large surface area, protein binding and high reactivity. The overall size of a typical MNP must be sufficiently small to evade rapid splenic filtration but large enough to avoid renal clearance. Baek et al. (2012) showed the easy clearance of 20 nm-sized ZnO NPs as compared to 70 nm-sized ZnO NPs, suggesting that the small ZnO NPs tend to be more rapidly cleared than the larger ones. The primary mechanism of excretion for the majority of MNPs is fecal excretion. Also, urine and biliary excretions play a role in their elimination. For 20 nm-sized TiO_2 NPs, kidneys form the main excretion pathway compared to fecal excretion (Xie et al. 2011). Larger MNPs (sized above 200 nm) are generally filtered and sequestered by the spleen, and eventually taken away by phagocytes dropping off their bioavailability. On oral administration, blank MNPs are absorbed scarcely and the greater part is cleared off. Uncoated Ag NPs have shown incomplete absorption in the gastrointestinal tract and are mostly excreted directly via the feces (Baek et al. 2012). On the other hand, masking MNPs with PEGs, block polymers and ligands precludes opsonization and MPS uptake to improve blood circulation and reduce clearance rates. At the same time, surface engineering facilitates the rapid renal clearance of non-targeted conjugates in order to minimize their toxic effects toward healthy cells. Adversely, addition of excess targeting ligands also facilitates the MPS clearance because more proteins are "visible" on the NP surface. Additionally, surface charge defines the absorption and elimination behavior of MNPs. On one side, cationic MNPs quit out rapidly from the blood and cause several complications, such as, hemolysis and platelet aggregation. On other hand, anionic MNPs present moderate systemic exposure and clearance. However, neutral and zwitterionic particles provide high systemic exposure and low clearance for a sustainable effect (Arvizo et al. 2011). Unlike therapeutic moieties, MNPs as imaging and contrast agents must have a rapid clearance from the blood so as to obtain low background signals and better images.

Toxicity

While dealing with novel therapeutics for perks in the kinetics, toxicity issues need to be addressed. Higher uptake and accumulation of MNPs in the target tissue indeed results in an enhanced therapeutic effect. Contrarily, a large amount of MNPs distributed to non-target organs may instigate unwanted toxicity. The primary mechanism proven to contribute for nanotoxicity is the size of MNPs (Table 8.2). MNPs offer greater surface area prone to higher reactivity than larger particles to produce ROS and free radicals which may result in oxidative stress, inflammation, mutations and protein and membrane denaturation. Inflammation is a possible adverse effect of MNP exposure attributed to the release of proinflammatory cytokines including interleukins (IL, e.g., IL-1β, IL-6, and IL-8) and Tumor Necrosis Factor-α (TNF-α). At greater exposure levels, ZnO NPs can stimulate the production of proinflammatory cytokines, TNF-α, interferon-γ (IFN-γ) and IL-12, during *in vitro* and *in vivo* pulmonary inhalation studies (Hanley et al. 2009). Oxidative stress effects induced by TiO_2 NPs on the mitochondrial membrane potential of PC12 cells represented a dose-dependent decrease in the membrane potential (Wu et al. 2010). In Ag NPs, free Ag^+ liberation induced an oxidative stress-mediated toxicity due to pro-apoptotic signals in liver. Among other sizes, 30 nm-sized amorphous TiO_2 NPs and 15 nm-sized Ag NPs have provoked the highest generation of ROS. Due to induction of ROS and autophagy by 20 nm-sized Au NPs in human lung fibroblasts, lipid peroxidation is triggered followed by oxidative damage (Yildirimer et al. 2011).

In 2010, Lacerda et al. described another mechanism for toxicity: conformational changes in biomolecules (e.g., lipids and serum proteins) caused by MNPs show profound effects on the immune system, thus stimulating hypersensitivity. Yen et al. (2009) correlated the differences in uptake mechanism and toxicity between Au NPs and Ag NPs to variations in serum protein binding of the MNPs by affecting endocytic pathways. MNPs are known to create imbalance in cellular homeostasis, and hence can alter the intracellular signaling routes responsible for several toxic effects, such as: *i*) altered transcription-translation functions as a result of perinuclear localization of MNPs; *ii*) modified gene expression in response to leaching of free metal ions; *iii*) impeded activation status of proteins; or, *iv*) perturbed genetic expression due to the cellular stress encumbered by MNPs (Soenen et al. 2011).

Next to stability and uptake profile, surface chemistry of MNPs is the foremost issue governing their toxic potential. Ligands like PEG, chitosan, dextran and PLGA can functionalize MNPs to camouflage them against the

Table 8.2. Toxicity assessment of various MNPs.

MNPs	Toxicity study	Consequences	Reference
Au NPs	Triple cell co-culture model simulating the alveolar lung epithelium	Au NPs ≤ 2 nm in size were toxic, while those with a diameter of 13–20 nm were non-toxic due to catalytic activity and DNA interactions	Brandenberger et al. 2010b
Au NPs	*Mytilus edulis* animal model for environmental toxicity studies	≈ 5 nm-sized Au NPs caused significantly greater oxidative stress than large Au NPs	Tedesco et al. 2010
Chitosan reduced Au NPs	Acute and subacute toxicity studies in Wistar rats	NP concentration up to 300 ppm were found non-toxic	Pokharkar et al. 2009
13 nm-sized PEGylated Au NPs	Terminal deoxynucleotidyl transferase (TDT)-mediated biotin-2′-deoxyuridine-5′-triphosphate (dUTP) nick end labeling (TUNEL) assay, immunohistochemistry	Acute inflammation and apoptosis in the mouse liver	Cho et al. 2009
Au NPs	Toxicity in BALB/C mice	3, 5, 50, and 100 nm-sized Au NPs showed no harmful effects, but 8 to 37 nm-sized Au NPs induced severe sickness in mice. Modifying the NP surface with immunogenic peptides ameliorated their toxicity	Chen et al. 2009a
Ag NPs	Subchronic inhalational toxicity in Sprague-Dawley rats	Dose-dependent increase in lesions	Yu et al. 2009
Ag NPs	Zebrafish model	Dose-dependent toxicity in embryos	Asharani et al. 2008
TiO_2 NPs	Acute toxicity in mice after intraperitioneal injection	Acute toxicity with passive behavior	Chen et al. 2009b
TiO_2 NPs	Ecotoxicity to aquatic life using rainbow trout (*Oncorhynchus mykiss*)	TiO_2 NPs were not major ionoregulatory toxicant or hemolytic. Respiratory distress and sublethal toxicity occurred due to oxidative stress	Handy et al. 2007
ZnO NPs	3-(4,5-dimethylthiazol-2-yl)-2,5 diphenyl tetrazolium bromide (MTT) assay, water soluble tetrazolium (WST) assay, and flow cytometry	Selective cytotoxicity on rapidly proliferating cells	Taccola et al. 2011

ZnO NPs	Comet assay, genotoxicity in human epidermal A431 cells	Low concentrations were genotoxic in human epidermal cells due to lipid peroxidation	Dhawan et al. 2009
IO NPs, Ag NPs, and Au NPs	Impact on pulmonary macrophages	Internalized NPs cause death and destruction of the phagocytizing cell via membranolysis	Katsnelson et al. 2012
SPIO NPs	MTT assay, and 2′,7′-dichlorofluorescein diacetate (H_2DCFDA) assay in murine macrophage J774 cells	Low optimum concentration helps in avoidance of oxidative stress-induced cell injury and death	Dinda et al. 2010
Metal oxide NPs	Lactate dehydrogenase (LDH) activity assay, MTT assay in BRL 3A cells	Ag NPs were highly toxic due to oxidative stress whereas IO NPs showed less toxicity	Hussain et al. 2005

unfavorable opsonization and non-targeted tissue uptake in an attempt to avert the adverse effects and improve the efficacy (Table 8.2). Contrary to this, surface modification may exaggerate the existing toxicity potential of MNPs. The poly(acrylic acid) coating of Au NPs is known to interact and denature fibrinogen to bind with the macrophage 1 antigen (Mac-1) integrin receptor and lead to inflammation (Deng et al. 2010). Cationic (ammonium-functionalized) NPs were undoubtedly more cytotoxic than the anionic (carboxylate-functionalized) ones. Recently, Niidome et al. (2006) confirmed that the chemicals employed in the synthesis of Au nanorods are critical in defining their potential toxicity. As against PEGylated Au nanorods, cetyltrimethylammonium bromide (CTAB)-stabilized Au nanorods showed strong cytotoxicity on HeLa cells compared to free CTAB in solution. This was substantiated with the removal of surplus CTAB from the PEGylated Au nanorods solution which yielded 90% cell viability. There is a high probability of argyria or argyrosis, a bluish-gray irreversible discoloration of the skin, due to the excess consumption of Ag NPs. Ag-based compounds are associated with chronic neurological, renal and hepatic complications on oral consumption. For this reason, the administration of Ag NPs is limited to topical applications and low exposure levels (Rai et al. 2009). Data on preclinical safety of USPIO NPs exhibited low to moderate toxicity at low concentrations, and significant toxic effects at high doses like neurobehavioral effects, reproductive toxicity, fetal malformations and teratogenicity (Mahmoudi et al. 2012).

As a word of caution, nanomaterials are also associated with ecological toxicity (Table 8.2). Environmental and occupational exposure to ultrafine particles (aerodynamic diameter ≈ 100 nm) is known to induce pulmonary inflammation, oxidative injury and fibrosis. The US EPA and the European Community (within the Registration, Evaluation, Authorization, and Restriction of Chemical Substances Law) are taking steps to tackle NP-associated health and ecological risks (Smijs and Pavel 2011).

Risk assessment and computational management

Standard cytotoxicity assays assist in evaluating toxicity mechanisms to some extent. On other hand, ethical regulations curb the *in vivo* testing of MNPs for weighing out the risks associated with them. When it comes to nanomaterials, the *in vitro-in vivo* correlation (IVIVC) is less significant. However, the use of advanced *ab initio* approaches based on quantum chemical calculations and molecular dynamic simulations may prove useful to address the potential risks associated with nanomaterials (Gajewicz et al. 2012). Computational studies comprise interactions of MNPs with physiological milieu by the way of algorithms plotted to determine the likelihood of toxicity in various natural environments. Comprehension

of interatomic interactions between MNPs and biological molecules will aid in safe production and utilization of nanomaterials. Unlike large molecules, MNPs deal the least with the convergence problems but remain associated with intensive computations. Toropov et al. (2005) proposed the Graph of Atomic Orbitals (GAO) theory to describe NP composition by applying a single Correlation Weights Descriptor (CWD) for computing the effects of metal oxide NPs. In 2011, Puzyn et al. designed a NP-toxicity model (nanoparticle quantitative structure-activity relationship, nano-QSAR, model), to link the computations with the experimental variables at mechanistic levels in order to calculate the risk of toxicity for untested MNPs. Standard toxicity assays, *in vitro* cell line studies, *in vivo* animal models along with *ab initio* simulations would certainly figure out the comprehensive health hazards and environmental risks of nanomaterials.

Applications

Metallic nanoparticulate drug delivery is a mushrooming field with massive potential for a plethora of therapeutic and diagnostic applications, ranging from delivery cargos to nanobiosensors (Table 8.3). A high degree of versatility, unique properties and ease of engineering, make MNPs indispensable for targeted drug delivery applications. Taken care of the safety assessment, MNPs would create a revolution in the health care system by imparting novel solutions to the existing chronic ailments.

As biosensors

IO NPs are commonly in use for MRI, magnetic resonance spectroscopy, and as sensors for various biomolecules. With the aid of peptides, antibodies and other ligands, targeted delivery of IO NPs has been accomplished especially in tumor therapy. SPIO and USPIO NPs are commonly used as contrasting agents to image the gastrointestinal tract, liver, spleen and lymph nodes. To perk up their bioavailability and stability, these NPs are functionalized with dextran, albumin or starch. Major differences between SPIO and USPIO NPs are associated with their morphology and circulatory half-life. Antibody-functionalized Fe_3O_4 NPs find uses for the immunoassay of Staphylococcal Enterotoxin B (SEB), wherein 100 pg/mL of the enterotoxin can be detected (Soelberg et al. 2009). IO NPs are the most prevalent and the only US Food and Drug Administration (FDA) approved biocompatible Fe_3O_4 NPs for MRI. Dextran-coated Fe_3O_4 NPs covalently attached to human holotransferrin are used for monitoring *in vivo* transgene expression in gene therapy via MRI.

Spherical Au NPs form brilliant scaffolds for drug attachment but fail to display a strong light absorbance in the visible range. Au NPs demonstrate

Table 8.3. Examples of biomedical applications of MNPs.

Applications	Description	Reference
Au NPs		
Detection of tumor biomarkers	Au NP-based immunosensors help to detect α-fetoprotein (AFP) by immobilizing AFP antibodies onto Au NP-decorated thionine/nafion membranes	Rotello et al. 2012
Drug targeting	Bimetallic Au/Ni nanorods. Pluronic® selectively attached to the Au segment facilitates doxorubicin loading, while the Ni segment decorated with folic acid aids targeting to KB cells	Yoo et al. 2012
Antimicrobial effect	Cefaclor-reduced Au NPs coated to a poly(ethyleneimine) (PEI) modified glass. Highly effective and robust antimicrobial coatings which might be useful for coating biomedical devices, implants, and textiles for the treatment of wounds or burns, and glass windows and other surfaces to maintain hygienic conditions in laboratories and hospital set-ups	Perry et al. 2010
Biobarcode assays	Functionalized Au NPs with a second recognition agent and "barcode" (marker) DNA strands used for measuring the concentration of amyloid-β-derived diffusible ligand (ADDL), a potential Alzheimer's disease marker present at extremely low concentrations (< 1 pmol/L) in the cerebrospinal fluid (CSF)	Franco et al. 2008
Delivery of biomolecules	Oligo(ethylenediamino)-modified Au NPs delivered plasmid DNA into breast MCF-7 cancer cells	Ghosh et al. 2008
Ag NPs		
Antibacterial activity	Ag NPs-impregnated chitosan films. Fast and long-lasting antibacterial activity due to the combined bactericidal effect of Ag NPs and cationic chitosan	Wei et al. 2009
Wound dressings, treatment of water, eco friendly nanopaints	Ag NPs composites	Rai et al. 2009
ZnO NPs		
Cancer chemotherapy	Selective generation of ROS and induction of apoptosis in human myeloblastic HL60 leukemia cells	Premanathan et al. 2011
Diagnosis	Non-cytotoxic and visible-light emitting ZnO non-core/shell NP loaded with fluorophores and with binding sites for biomolecules: novel diagnostic strategy for intractable diseases, including cancer	Sato et al. 2010

TiO_2 NPs		
Inorganic physical sun blockers	TiO_2 and ZnO NPs in sunscreens for broad-band UV protection	Smijs and Pavel 2011
Cancer treatment	Photocatalyzed TiO_2 NPs. Significant surface chemistry-dependent cytotoxicity on JHU and LLC cancer cells	Thevenot et al. 2008
IO NPs		
Liver imaging and cellular labeling	Ferumoxide® (AMI-25): 120 to 180 nm-sized dextran coated SPIO NPs	Muller et al. 2008
Theranosis	PEGylated amine functionalized polyacrylamide NPs containing IO NPs and the photosensitizer photofrin: light-activated theranostic nanoagents for selective imaging and targeted treatment of brain tumors	McCarthy and Weissleder 2008

large optical absorption due to SPR which makes them appealing as imaging and detection agents. Spherical Au NPs absorb light only in the visible range (520–550 nm) which limits their biological applications, given the fact that biological tissues are less transparent to visible light. On the contrary, Au nanorods, Au nanoshells and other Au NPs with high-aspect-ratio display strong SPR in the NIR region where the tissues have better transparency. Of course, covalent functionalization can also be the best alternative. Anti-EGFR functionalized Au NPs-based biosensors were developed for *in vitro* diagnosis of oral epithelial cancer cells [HOC313 clone 8, and HSC-3 (a human tongue squamous cell carcinoma cell line)]. An ultrasensitive Au NP-based biobarcode assay was designed to amplify and identify multiple DNA targets and bacterial genomic DNA. This biobarcode assay was used to detect ADDL, a soluble pathogenic Alzheimer's disease marker in the CSF at clinically relevant concentrations (< 1 pM) that were not detectable by conventional immunoassays (Fadeel and Garcia-Bennett 2010).

Au surface DNA arrays-Ag NPs multiplex probes have been proposed for detection of Herpes Simplex Virus (HSV), Epstein-Barr Virus (EBV) and Cytomegalovirus (CMV) sequences (Li et al. 2010b). Conjugation of Ag NPs allowed 103-fold amplification and detection of infinitesimal target DNA due to the excellent electroactive properties of Ag NPs. Many researchers have employed a MNP-optimized SERS technique for the detection of tumor markers and their modified analogues. TiO_2 NPs were conjugated with alizarin red S for quantitative analysis of the kinetics and endocytic pathways involved in the uptake of TiO_2 NPs into prostate PC-3M cancer cells (Thurn et al. 2011).

The development of NIR (630–900 nm) active MNPs as excellent contrast agents for photoacoustic imaging or photoacoustic tomography opens up one of the potential avenues for *in vivo* imaging with simultaneous therapeutic measures (theranosis). AuroLaser® Therapy (Nanospectra Biosciences, USA) that combines Au nanoshells with photothermal therapy for simultaneous *in vivo* imaging and therapy is in pipeline for clinical approval (Doria et al. 2012).

In tumor therapy

Treatment against tumors constitute the conventional surgeries, chemotherapies and radiation therapies which follow the "whole-body" approach causing major damage to healthy tissues. In order to overcome the collapse of non-cancerous tissues, tumor-targeted drug delivery is crucial. Passive drug targeting helps to localize the therapeutic agents at the tumor site, taking advantage of the highly leaky vasculature of cancer

cells (Fig. 8.6). Active drug targeting occurs at the cellular level where the active moiety is directly targeted for delivery only into the tumor cells. High-aspect-ratio MNPs aid in passive targeting of anticancer agents across tumor interstitium. Functionalized MNPs allows for the selective destruction of tumor cells by active drug targeting. Methotrexate-loaded PEGylated IO NPs showed higher cellular uptake by glioma cells than control NPs (Laurent et al. 2008). In 2010, Kang et al. developed PEGylated 30 nm-sized Au NPs bioconjugated with an arginine-glycine-aspartic acid peptide and a nuclear localization signal peptide for their selective transportation into human oral squamous carcinoma cell (HSC) nucleus.

As antiangiogenic agents

Angiogenesis is a key factor in a number of diseases, such as, cancer and rheumatoid arthritis. Blood vessels supply oxygen and other nutrients to tumor cells, allowing them to grow, migrate and metastasize to different organs. Vascular Endothelial Growth Factor (VEGF), basic Fibroblast Growth Factor (bFGF), Platelet-derived Growth Factor (PDGF), and transforming growth factor-β (TGF-β) trigger tumor angiogenesis (Paciotti and Tamarkin 2007). MNPs may prove to be more effective since they target multiple pathways and can overcome the unusual toxicities associated with conventional antiangiogenic agents. Blank Au NPs are known to inhibit VEGF induced angiogenesis and the activity of heparin binding proteins, such as, $VEGF_{165}$ and bFGF, while non-heparin binding proteins ($VEGF_{121}$ and EGF) retained their intrinsic activity. Ag NPs suppress the formation of new blood vessels to activate and target PI3K/Akt signaling pathway which in turn inhibits cell proliferation and migration in VEGF-induced angiogenesis in bovine retinal epithelial cells (Arvizo et al. 2012).

In multiple myeloma and leukemia

MNPs like Au NPs can inhibit the proliferation of multiple myeloma cells, a plasma cell disorder caused by growth factors [VEGF, insulin like growth factor-I (IGF-I), and TNF-α]. Au NPs arrests the G_1 phase of cell cycle, followed by the up-regulation of cyclin-dependent kinase inhibitors (p21 and p27 transcripts), thus inhibiting cell proliferation (Mahmoudi et al. 2012). Au NPs conjugated with anti-VEGF antibodies can provoke a dose-dependent apoptosis as compared to blank Au NP for the treatment of B type chronic lymphocytic leukemia (B-CLL). Guo et al. (2008) demonstrated synergistic cytotoxic effects on leukemic cancer cells on co-administration of ZnO NPs and daunorubicin, which were further enhanced by UV irradiation.

In rheumatoid arthritis

Rheumatoid arthritis is an inflammatory disease where angiogenesis plays a significant role. MNPs can treat a multitude of inflammatory diseases. In a recent study for collagen-induced arthritis, the intra-articular administration of Au NPs reduced TNF-α and IL-β levels for the attenuation of arthritic symptoms, such as, inflammation and reduced macrophage infiltration (Mukherjee et al. 2007).

In photoactivated chemotherapy/photodynamic therapy

By means of photoexcitation, metals are known to radiate excited energy via releasing electrons, losing ligands, and transferring energy to nearby species. Photoexcited states of metal complexes generate free radicals, highly reactive singlet oxygen ($^1O_2$) species, and a high amount of energy capable of DNA damage, thus leading to tumor destruction. This process is known as photoactivated chemotherapy (PACT)/photodynamic therapy (PDT) where the photoexcited energy is liberated in the form of heat instead of radioactive decay for destroying cancer cells. In PDT, the optimum wavelength of 620–850 nm helps to achieve the maximum tissue penetration. In case of TiO_2 NPs, UVA light irradiation of Ti^{4+} ions reduces to Ti^{3+} ions, thus generating free radicals that ultimately kill cancer cells (Bhattacharyya et al. 2011). Bartczak et al. (2012) found a 100-fold greater uptake for Au nanorods by Human Umbilical Vein Endothelial Cells (HUVECs) than Au NPs with varied morphology when irradiated with laser. However, all the Au NPs displayed an equal efficiency in tumor destruction. In cancer therapy, the magnetophoretic control by multifunctional IO NPs can assist in enhancing cellular uptake, imaging, and targeted delivery of nanocarriers with light activated PDT.

In radiotherapy

Ionizing radiations form useful and selective therapeutic approaches for terminating the proliferation of tumors. Exceptional optical properties and structural tuning coupled with the ease of functionalization make MNPs indispensable in radiotherapy. On X-ray irradiation, MNPs generate free radicals that induce cellular apoptosis. Low permeability, short plasma half-life, higher survival rates and other intrinsic radioactive properties, make radioactive isotopes like ^{198}Au (radiogold) ideal candidates for radiotherapy (Arvizo et al. 2012). Radioactive Au NPs conjugated with gum arabic glycoprotein (GA - ^{198}Au NPs) were used for the inhibition and treatment of human prostrate tumor without any obvious side effects. GA - ^{198}Au NPs got accumulated inside the tumor zone with minimal leakage of

radioactivity to normal tissues. In another report, Xu et al. (2009) assessed the cytotoxicity in glioma cells when treated with Au NPs and Ag NPs at low radiation doses. Due to the release of Ag^+ from Ag NPs, the sensitivity to irradiation was increased many folds compared to Au NPs, followed by electron capture that resulted into the production of intracellular ROS for tumor treatment.

In central nervous system drug delivery

Convection-Enhanced Delivery (CED) discharges the therapeutic or diagnostic MNPs straight into the brain to ensure high intratumoral concentrations with calculated risk of systemic toxicity (Biddlestone-Thorpe et al. 2012). CED maximizes the administration and uniformity of drug delivery to tumor cells for a longer period. Epidermal Growth Factor Receptor variant III (EGFRvIII) antibody conjugated IO NPs for CED enabled the targeted MRI of human glioblastoma multiforme cells. Also, IO NPs coupled with EGFRvIII antibody facilitated the MRI contrast enhancement along with improved survival rates in mice.

As anti-infective agents

MNPs are considered perfect carriers for large amounts of antimicrobials without compromising their activity. Antibiotics and MNPs act synergistically to overcome the probability of resistance development: if pathogens develop resistance against one of them, a further component could destroy them in a different mechanism. Enhanced antimicrobial activity was observed for vancomycin-loaded Au NPs on vancomycin-resistant enterococci. Cefaclor-reduced Au NPs have revealed a potent antimicrobial activity on both gram-positive and gram-negative bacteria compared to cefaclor and Au NPs alone (Perry et al. 2010). Even 8 nm-sized ZnO NPs depicted a prominent antimicrobial activity against *Staphylococcus aureus*.

Some MNPs, like Ag NPs, themselves are well-established broad spectrum antimicrobial agents. Biologically synthesized Ag NPs have proved useful in medical textiles for their efficient antimicrobial function. Aquacel Ag hydrofiber (ConvaTec, Skillman, USA) consists of Ag NPs impregnated carboxymethylcellulose dressings which functions by slowly releasing Ag ions upon hydration. Ag NPs have significant antiviral activity as they prevent plaque formation in Vero cells due to poxvirus infection. MNPs are portrayed as effective agents against HIV-1 infections. *In vitro* studies showed that Ag NPs can preclude the binding of virus to host cells. Besides, Ag as a virucidal agent is known to bind with the glycoprotein gp120 which in turn prevents the CD4-virion binding so as to reduce HIV-1

infection. Other MNPs are found effective as antiviral agents against HSV, influenza and respiratory viruses (Rai et al. 2009).

In cosmetics

For years together, ZnO and TiO_2 materials are commonly used in sunscreens to block UV exposure. Such NPs have become popular as they efficiently block UVA/UVB radiation, while eliminating the white chalky appearance of conventional sunscreens. ZnO or TiO_2 NPs-based products are known for their transparency which increase their aesthetic appeal, while overcomes issues related with odor, greasy nature and toxicity (Smijs and Pavel 2011). Unfortunately, uncoated ZnO and TiO_2 NPs can absorb photons of light and emit an excited electron that transfers into free radicals and absorbs in dermal layers, resulting into oxidative damage. To prevent the formation of ROS and agglomeration, ZnO and TiO_2 NPs are generally coated with aluminum oxide, silicon dioxide or silicon oils. Boots, Avon, The Body Shop, L'Oréal, Nivea, and Unilever have launched several sunscreens and moisturizers containing these metal oxide NPs.

As wound healing agents

In the wound stratum, nanocrystalline Ag^+ can inhibit diverse immunomodulatory factors in order to promote wound healing: low proinflammatory IL-6 and TGF-β1 levels in the wound area indicates scarless healing while higher IL-10, VEGF, and IFN-γ levels at the wound edge account for a rapid wound recovery (Rai et al. 2009). Additionally, Ag NPs possess an efficient broad spectrum of antimicrobial activity than other Ag salts due to their exceptionally large surface area which offer a better microbial contact. Ag NPs attached to the cell membrane of pathogens can interact and inactivate sulfur- as well as phosphorus-containing proteins. On further penetration into the bacterial cytoplasm, they can attack the respiratory chain, and cell division to bring about bacterial cell lysis. The loss of rubor in chronic wounds treated with colloidal Ag proves the anti-inflammatory activity of Ag NPs (Tian et al. 2007). With this multifunctionality, Ag NPs have evolved as novel wound healing agents. Ag NPs would be beneficial in chronic ailments like diabetes: in early healing of diabetic wounds with minimal scar.

As disinfectants

MNPs in general and Ag NPs in particular are the next generation of water disinfectants. De Gusseme et al. (2010) evaluated the antiviral efficacy of Ag NPs and their promising use for continuous water disinfection. Both

ionic Ag^{+} NPs and zero-valent silver nanoparticles (nAg^{0}) have affinity for –SH groups and glycoproteins exposed on the viral surface, and tend to interact with the phosphorus containing nucleic acids of pathogens. nAg^{0} carries a large specific surface area for rendering a better contact with phage viruses, thus leading to an enhanced disinfectant activity.

Miscellaneous applications

MNPs are also being explored for intracellular delivery of DNA, small interfering ribonucleic acid (*si*RNA), proteins, peptides, and as platforms for targeted gene delivery. Functional Au NPs can improve DNA transfection efficiency by forming a complex with charged DNA. Under NIR illumination, Au NPs displayed their capacity as optical switches for gene delivery when used in releasing gene interfering DNA oligonucleotides. Joshi et al. (2006) have exploited Au NPs as carriers for efficient transmucosal insulin delivery. Besides, metal oxide NPs saturated polyvinylidene difluoride (PVDF) membranes alleviated the biofouling problems of Reverse Osmosis (RO) membranes and membrane bioreactors systems (Xie et al. 2011). EPA-registered Ag NPs have been safely used as swimming pool algicides, drinking water filter systems, and in other high volume water-contact applications bringing benefit to millions of people over last five decades (Nowack et al. 2011). The far-reaching applications of MNPs are summarized in Table 8.3.

Regulatory Aspects

Novel materials blossomed out of nanotechnology like the MNPs have become indispensable for the future of human beings. Their inherent properties are likely to revolutionize the next generation of drug delivery systems. These very similar attributes proven to impart high reactivity and efficacy to NPs, make them harmful to the environment, and toxic to humans. Scale-up of MNPs from laboratory to commercial level is still in its infancy. Lack of uniform data and dearth of experimental protocols prevent the comprehensive risk assessment of MNPs. Toxicity, ecological damage and potential health risks associated with nanomaterials are studied, but are short of monitoring mechanisms. Work-place exposure/inhalation/oral ingestion/skin penetration of airborne NPs may lead to carcinogenic effects, impaired immune responses and asbestosis-like syndromes. Thus, establishing the potential impacts of MNPs on human health and environment is vital for balancing MNPs benefits and objectionable effects (Gajewicz et al. 2012). Tracking production and clinical effects of large MNP volumes poses a major challenge. Application of theoretical and computational methods would tally the risks of MNPs,

and assess their commercial potential. On the lines of the International Conference on Harmonization (ICH) guidelines for conventional products, there is a need for global harmonization of frameworks and standards for commercialization of nanoformulations and nanodevices. Even though FDA is familiar with nanotechnology, still it has not issued any relevant guidance which could supervise NP quality. Regardless of the regulatory challenges, numerous companies producing nanodrugs and nanodevices have taken initiative toward current Good Manufacturing Practices (cGMP) compliance. In discrete areas, organizations such as the Organization for Economic Cooperation and Development (OECD), the European Union NanoSafety Cluster, European Food Safety Authority (EFSA), and EPA are designing protocols for comprehensive hazard management of MNPs. Few entities have adopted regulations (Toxic Substances Control Act, TSCA, by US), International Organization for Standardization (ISO) standards (ISO/TS 27687:2008, ISO/TC 229) and bylaws (European Union Cosmetic Products Regulation 1223/2009, The Manufactured Nanoscale Health and Safety Ordinance, Berkeley Municipal Code Section 15.12.040) for risk assessment of NPs (Nowack et al. 2011). While framing regulatory guidelines, first and foremost necessity is to construct a universal terminology and classification for MNPs. As per the Woodrow Wilson International Centre for Scholars, standardization of NPs in connection with their efficacy and toxicity is usually done in accordance with their size or weight only. However, at the commercial and environmental level, surface area becomes the major parameter affecting the efficacy and toxicity of NPs than size and weight. Hence, the forthcoming regulations should emphasize more on the surface characteristics of MNPs. Moreover, the penetration potential and permeability of MNPs must be gauged and standardized in terms of benefit/risk ratio. Regulation of MNPs would be a complex and dynamic process which may revolve around their physical, chemical and biological traits that influence their toxicity and efficacy with social, economical, and ecological impact.

Conclusions

MNPs carry immense potential for forthcoming applications in imaging, diagnosis, prevention and therapeutics (drug delivery). Fundamental notions and mechanisms behind pharmacokinetics, cellular uptake, targeted delivery, trafficking and toxicity need to be completely understood prior to commercialization. Surface functionalization with biomolecules, ligands, peptides and antibodies bring up the next generation of multifunctional MNPs to offer flexibility in improvement of their efficacy without any intrinsic side effects. In fact, multifunctional MNPs would emerge as promising scaffolds to endorse the notion of individualized medicines.

Apparently, Au NPs have emerged as relatively safe and prospective candidates in cancer therapeutics and gene delivery. Fe and IO NPs have been explored in both diagnosis and therapeutics, exclusively as MRI contrasting agents and for magnetically targeted drug delivery. Ag NPs are massively applied as antimicrobials and anti-inflammatory agents, and show a positive effect on wound healing. TiO_2 and ZnO NPs are frequently used in sunscreens as they suffice rare UVB/UVA FDA protection obligation for sunscreens. In the near future, MNP-mediated gene therapy would be a major breakthrough in the contemporary avant-garde medical field considering the centrality on nucleic acids. Forthcoming Au and Fe_3O_4 NPs may tune up as "theranostics" for simultaneous detection and treatment of critical maladies. Surface modified MNPs possibly will open out new-fangled "leeways" to conjugate and inactivate the "disease inducing" functionalities, especially in angiogenesis-dependent cancer and arthritis.

In spite of functional applications and rapid advancements, MNPs may cause unintended effects on human health and environment. These concerns have aggravated due to inadequate understanding of the fate and behavior of MNPs in humans and the environment. Currently, nanotechnology risk assessment and management is an upcoming arena to carefully evaluate the total life cycle of MNPs, right from the production stage to the consumption phase with focus on the potential human health, occupational hazards and ecological impacts in an attempt to weigh benefits of MNPs against their toxic effects. There is an urgent need to frame and adopt harmonized regulations and guidelines for screening and tracing the production of massive volume of NPs along with their consequent impact. Thus, coherent MNP designs would tussle against fatal diseases, physiologically untreatable complexities, ultimately leading to safe human health care system for future generations.

Abbreviations

ADDL	:	amyloid-β-derived diffusible ligand
AFP	:	α-fetoprotein
Ag	:	silver
$AgNO_3$	:	silver nitrate
Au	:	gold
Ar	:	argon
$AuCl_4^-$	:	chloroaurate ion
B-CLL	:	B type chronic lymphocytic leukemia
bFGF	:	basic fibroblast growth factor
BSA	:	bovine serum albumin
CED	:	convection-enhanced delivery
cGMP	:	current good manufacturing practices

CMV	:	cytomegalovirus
CSF	:	cerebrospinal fluid
CTAB	:	cetyltrimethylammonium bromide
Cu	:	copper
CVD	:	chemical vapor deposition
CWD	:	correlation weights descriptor
DNA	:	deoxyribonucleic acid
dUTP	:	2′-deoxyuridine-5′-triphosphate
EBV	:	Epstein-Barr virus
EFSA	:	European Food Safety Authority
EGF	:	epidermal growth factor
EGFRvIII	:	epidermal growth factor receptor variant III
EPA	:	Environmental Protection Agency
EPR	:	enhanced permeability and retention
FDA	:	Food and Drug Administration
Fe	:	iron
$Fe_{(acac)3}$	:	2,4-pentanedione iron(III) derivative
Fe_3O_4	:	magnetite
GA -^{198}Au NP	:	gold nanoparticle conjugated with gum arabic
GAO	:	graph of atomic orbitals
$H_2C_2O_4{\cdot}2H_2O$	:	oxalic acid dehydrate
H_2DCFDA	:	2′,7′-dichlorofluorescein diacetate
Her2	:	human epidermal growth factor receptor 2
HIV-1	:	human immunodeficiency virus type 1
HSC	:	human oral squamous carcinoma cell
HSV	:	herpes simplex virus
HUVEC	:	human umbilical vein endothelial cell
ICH	:	International Conference on Harmonization
IFN-γ	:	interferon-γ
IGF-I	:	insulin like growth factor-I
IL	:	interleukin
IO	:	iron oxide
ISO	:	International Organization for Standardization
IVIVC	:	*in vitro-in vivo* correlation
LDH	:	lactate dehydrogenase
LLC	:	Lewis lung carcinoma
Mac-1	:	macrophage 1 antigen
MNP	:	metallic nanoparticle
MPS	:	mononuclear phagocyte system
MRI	:	magnetic resonance imaging
MTT	:	3-(4,5-dimethylthiazol-2-yl)-2,5 diphenyl tetrazolium bromide
nAg^0	:	zero-valent silver nanoparticles

nano-QSAR	:	nanoparticle quantitative structure-activity relationship
$–NH_2$	:	amino
Ni	:	nickel
NIR	:	near-infrared
NP	:	nanoparticle
$^1O_2$	:	singlet oxygen
OECD	:	Organization for Economic Cooperation and Development
–OH	:	hydroxyl
PACT	:	photoactivated chemotherapy
PDGF	:	platelet-derived growth factor
PDT	:	photodynamic therapy
PEG	:	poly(ethylene glycol)
$–PH_2$	:	phosphine
PEI	:	poly(ethyleneimine)
Pt	:	platinum
PVD	:	physical vapor deposition
PVDF	:	polyvinylidene difluoride
PVP	:	poly(*N*-vinyl-2-pyrrolidone)
RNA	:	ribonucleic acid
RO	:	reverse osmosis
ROS	:	reactive oxygen species
SDS	:	sodium dodecyl sulfate
SEB	:	Staphylococcal enterotoxin B
SERS	:	surface-enhanced Raman scattering
–SH	:	thiol
*si*RNA	:	small interfering ribonucleic acid
SMAD	:	solvated metal atom deposition
SPIO	:	superparamagnetic iron oxide
SPR	:	surface plasmon resonance
TDT	:	terminal deoxynucleotidyl transferase
TGF-β	:	transforming growth factor-β
TiO_2	:	titanium dioxide
$Ti(O^iPr)_4$	:	titanium isopropoxide
TNF-α	:	tumor necrosis factor-α
TSCA	:	Toxic Substances Control Act
US	:	United States
USPIO	:	ultrasmall superparamagnetic iron oxide
UV	:	ultraviolet
VEGF	:	vascular endothelial growth factor
WST	:	water soluble tetrazolium
$Zn(CH_3COO)_2$	:	zinc acetate

$ZnC_2O_4 \cdot 2H_2O$	:	zinc oxalate dihydrate
ZnO	:	zinc oxide
3D	:	three dimensional

References

Ankamwar, B. 2010. Biosynthesis of gold nanoparticles (green-gold) using leaf extract of *Terminalia catappa*. E-J. Chem. 7: 1334–1339.

Arvizo, R.R. and O.R. Miranda, D.F. Moyano, C.A. Walden and K. Giri. 2011. Modulating pharmacokinetics, tumor uptake and biodistribution by engineered nanoparticles. PLoS One. 6: e24374.

Arvizo, R.R. and S. Bhattacharyya, R.A. Kudgus, K. Giri, R. Bhattacharya and P. Mukherjee. 2012. Intrinsic therapeutic applications of noble metal nanoparticles: past, present and future. Chem. Soc. Rev. 41: 2943–2970.

Asharani, P.V. and Y. Wu, Z. Gong and S. Valiyaveettil. 2008. Toxicity of silver nanoparticles in zebrafish model. Nanotechnology. 19: 255102.

Atiyeh, B.S. and M. Costagliola, S.N. Hayek and S.A. Dibo. 2007. Effect of silver on burn wound infection control and healing: review of the literature. Burns. 33: 139–148.

Baek, M. and H.E. Chung, J. Yu, J.A. Lee, T.H. Kim, J.M. Oh, W.J. Lee, S.M. Paek, J.K. Lee, J. Jeong, J.H. Choy and S.J. Choi. 2012. Pharmacokinetics, tissue distribution, and excretion of zinc oxide nanoparticles. Int. J. Nanomedicine. 7: 3081–3097.

Baptista, P. and E. Pereira, P. Eaton, G. Doria, A. Miranda, I. Gomes, P. Quaresma and R. Franco. 2008. Gold nanoparticles for the development of clinical diagnosis methods. Anal. Bioanal. Chem. 391: 943–950.

Bartczak, D. and O.L. Muskens, S. Nitti, T. Sanchez-Elsner, T.M. Millar and A.G. Kanaras. 2012. Interactions of human endothelial cells with gold nanoparticles of different morphologies. Small. 8: 122–130.

Bharde, A.A. and R.Y. Parikh, M. Baidakova, S. Jouen and B. Hannoyer. 2008. Bacteria-mediated precursor-dependent biosynthesis of superparamagnetic iron oxide and iron sulfide nanoparticles. Langmuir. 24: 5787–5794.

Bhattacharyya, S. and R.A. Kudgus, R. Bhattacharya and P. Mukherjee. 2011. Inorganic nanoparticles in cancer therapy. Pharm. Res. 28: 237–259.

Biddlestone-Thorpe, L. and N. Marchi, K. Guo, C. Ghosh, D. Janigro, K. Valerie and H. Yang. 2012. Nanomaterial-mediated CNS delivery of diagnostic and therapeutic agents. Adv. Drug Deliv. Rev. 64: 605–613.

Blosi, M. and S. Albonetti, M. Dondi, C. Martelli and G. Baldi. 2011. Microwave-assisted polyol synthesis of Cu nanoparticles. J. Nanopart. Res. 13: 127–138.

Brandenberger, C. and C. Mühlfeld, Z. Ali, A.G. Lenz, O. Schmid, W.J. Parak, P. Gehr and B. Rothen-Rutishauser. 2010a. Quantitative evaluation of cellular uptake and trafficking of plain and polyethylene glycol-coated gold nanoparticles. Small. 6: 1669–1678.

Brandenberger, C. and B. Rothen-Rutishauser, C. Mühlfeld, O. Schmid, G.A. Ferron, K.L. Maier, P. Gehr and A.G. Lenz. 2010b. Effects and uptake of gold nanoparticles deposited at the air-liquid interface of a human epithelial airway model. Toxicol. Appl. Pharmacol. 242: 56–65.

Burda, C. and X. Chen, R. Narayanan and M.A. El-Sayed. 2005. Chemistry and properties of nanocrystals of different shapes. Chem. Rev. 105: 1025–1102.

Castro, T. and R. Reifenberger, E. Choi and R.P. Andres. 1990. Size dependent melting temperature of individual nanometer sized metallic clusters. Phys. Rev. B Condens. Matter. 13: 8548–8556.

Chen, W. and W. Cai, L. Zhang, G. Wang and L. Zhang. 2001. Sonochemical processes and formation of gold nanoparticles within pores of mesoporous silica. J. Colloid Interface Sci. 238: 291–295.

Chen, J. and J. McLellan, A. Siekkinen, Y. Xiong, Z.Y. Li and Y. Xia. 2006. Facile synthesis of gold-silver nanocages with controllable pores on the surface. J. Am. Chem. Soc. 128: 14776–14777.

Chen, Y. and Y. Hung, I. Liau and G.S. Huang. 2009a. Assessment of the *in vivo* toxicity of gold nanoparticles. Nanoscale Res. Lett. 4: 858–864.

Chen, J. and X. Dong, J. Zhao and G. Tang. 2009b. *In vivo* acute toxicity of titanium dioxide nanoparticles to mice after intraperitioneal injection. J. Appl. Toxicol. 29: 330–337.

Chen, D. and G. Zhu, X. Zhu, X. Qiao and J. Chen. 2011. Controlled synthesis of monodisperse silver nanocubes via a solvothermal method. J. Mater. Sci. Mater. Electron. 22: 1788–1795.

Chithrani, B.D. and A.A. Ghazani and W.C.W. Chan. 2006. Determining the size and shape dependence of gold nanoparticle uptake into mammalian cells. Nano Lett. 6: 662–668.

Cho, W.S. and M. Cho and J. Jeong. 2009. Acute toxicity and pharmacokinetics of 13 nm-sized PEG-coated gold nanoparticles. Toxicol. Appl. Pharmacol. 236: 16–24.

Comfort, K.K. and E.I. Maurer, L.K. Braydich-Stolle and S.M. Hussain. 2011. Interference of silver, gold, and iron oxide nanoparticles on epidermal growth factor signal transduction in epithelial cells. ACS Nano. 5: 10000–10008.

Daniel, M.C. and D. Astruc. 2004. Gold nanoparticles: assembly, supramolecular chemistry, quantum-size-related properties and applications toward biology, catalysis, and nanotechnology. Chem. Rev. 104: 293–346.

Dhar, S. and E.M. Reddy, A. Shiras, V. Pokharkar and B.L. Prasad. 2008. Natural gum reduced/stabilized gold nanoparticles for drug delivery formulations. Chemistry. 14: 10244–10250.

Dhar, S. and E.M. Reddy, A. Prabhune, V. Pokharkar, A. Shiras and B.L. Prasad. 2011. Cytotoxicity of sophorolipid-gellan gum-gold nanoparticle conjugates and their doxorubicin loaded derivatives towards human glioma and human glioma stem cell lines. Nanoscale. 3: 575–580.

De Gusseme, B. and L. Sintubin, L. Baert, E. Thibo, T. Hennebel, G. Vermeulen, M. Uyttendaele, W. Verstraete and N. Boon. 2010. Biogenic silver for disinfection of water contaminated with viruses. Appl. Environ. Microbiol. 76: 1082–1087.

Deng, Z.J. and M. Liang, M. Monteiro, I. Toth and R.F. Minchin. 2010. Nanoparticle-induced unfolding of fibrinogen promotes Mac-1 receptor activation and inflammation. Nat. Nanotechnol. 6: 39–44.

Doria, G. and J. Conde, B. Veigas, L. Giestas, C. Almeida, M. Assunção, J. Rosa and P.V. Baptista. 2012. Noble metal nanoparticles for biosensing applications. Sensors. 12: 1657–1687.

Edrissi, M. and R. Norouzbeigi. 2011. Synthesis of deer horn-like and spherical ZnO nanoparticles by microwave decomposition of bis(2-pyridinethiol N-oxide)zinc using factorial and Taguchi experimental designs. J. Mater. Sci. Mater. Electron. 22: 328–334.

Elechiguerra, J.L. and J.L. Burt, J.R. Morones, A. Camacho-Bragado, X. Gao, H.H. Lara and M.J. Yacaman. 2005. Interaction of silver nanoparticles with HIV-1. J. Nanobiotechnology. 3: 6.

Etame, A.B. and C.A. Smith, W.C. Chan and J.T. Rutka. 2011. Design and potential application of PEGylated gold nanoparticles with size-dependent permeation through brain microvasculature. Nanomedicine. 7: 992–1000.

Fadeel, B. and A.E. Garcia-Bennett. 2010. Better safe than sorry: understanding the toxicological properties of inorganic nanoparticles manufactured for biomedical applications. Adv. Drug Deliv. Rev. 62: 362–374.

Federici, G. and B.J. Shaw and R.D. Handy. 2007. Toxicity of titanium dioxide nanoparticles to rainbow trout (*Oncorhynchus mykiss*): gill injury, oxidative stress and other physiological effects. Aquat. Toxicol. 84: 415–430.

Frens, G. 1973. Controlled nucleation for the regulation of the particle size in monodisperse gold suspensions. Nature (London) Phys. Sci. 241: 20–22.

Fung, M.C. and D.L. Bowen. 1996. Silver products for medical indications: risk-benefit assessment. J. Toxicol. Clin. Toxicol. 34: 119–126.

Gajewicz, A. and B. Rasulev, T.C. Dinadayalane, P. Urbaszek, T. Puzyn, D. Leszczynska and J. Leszczynski. 2012. Advancing risk assessment of engineered nanomaterials: application of computational approaches. Adv. Drug Deliv. Rev. 64: 1663–1693.

Ghosh, P. and G. Han, M. De, C. Kim and V.M. Rotello. 2008. Gold nanoparticles in delivery applications. Adv. Drug Deliv. Rev. 60: 1307–1315.

Guo, D. and C. Wu and H. Jiang. 2008. Synergistic cytotoxic effect of different sized ZnO nanoparticles and daunorubicin against leukemia cancer cells under UV irradiation. J. Photochem. Photobiol. B. 93: 119–126.

Gutiérrez-Wing, C. and R. Esparza, C. Vargas-Hernández, M.E. Fernández García and M. José-Yacamán. 2012. Microwave-assisted synthesis of gold nanoparticles self-assembled into self-supported superstructures. Nanoscale. 4: 2281–2287.

Hanley, C. and A. Thurber, C. Hanna, A. Punnoose, J. Zhang and D.G. Wingett. 2009. The influences of cell type and ZnO nanoparticle size and immune cell cytotoxicity and cytokine induction. Nanoscale Res. Lett. 4: 1409–1420.

Hou, Y. and Z. Xu and S. Sun. 2007. Controlled synthesis and chemical conversions of FeO nanoparticles. Angew. Chem. Int. Ed. Engl. 46: 6329–6332.

Hussain, S.M. and K.L. Hess, J.M. Gearhart, K.T. Geiss and J.J. Schlager. 2005. *In vitro* toxicity of nanoparticles in BRL 3A rat liver cells. Toxicol. In Vitro. 19: 975–998.

Jain, P.K. and K.S. Lee, I.H. El-Sayed and M.A. El-Sayed. 2006. Calculated absorption and scattering properties of gold nanoparticles of different size, shape, and composition: applications in biological imaging and biomedicine. J. Phys. Chem. B. 110: 7238–7248.

Jha, A.K. and K. Prasad. 2010. Biosynthesis of metal and oxide nanoparticles using *Lactobacilli* from yoghurt and probiotic spore tablets. Biotechnol. J. 5: 285–291.

Jiang, L. and S. Xu, J. Zhu, J. Zhang, J. Zhu and H. Chen. 2004a. Ultrasonic-assisted synthesis of monodisperse single-crystalline silver nanoplates and gold nanorings. Inorg. Chem. 43: 5877–5833.

Jiang, L. and A. Wang, Y. Zhao, J. Zhang and J. Zhu. 2004b. A novel route for the preparation of monodisperse silver nanoparticles via a pulsed sonoelectrochemical technique. Inorg. Chem. Commun. 7: 506–509.

Joshi, H.M. and D.R. Bhumkar, K. Joshi, V. Pokharkar and M. Sastry. 2006. Gold nanoparticles as carriers for efficient transmucosal insulin delivery. Langmuir. 22: 300–305.

Kang, B. and M.A. Mackey and M.A. El-Sayed. 2010. Nuclear targeting of gold nanoparticles in cancer cells induces DNA damage, causing cytokinesis arrest and apoptosis. J. Am. Chem. Soc. 132: 1517–1519.

Katsnelson, B.A. and L.I. Privalova, M.P. Sutunkova, M.Y. Khodos, V.Y. Shur, E.V. Shishkina, L.G. Tulakina, S.V. Pichugova and J.B. Beikin. 2012. Uptake of some metallic nanoparticles by, and their impact on pulmonary macrophages *in vivo* as viewed by optical, atomic force and transmission electron microscopy. J. Nanomedic. Nanotechnol. 3: 129.

Koziej, D. and F. Fischer, N. Kränzlin, W.R. Caseri and M. Niederberger. 2009. Nonaqueous TiO_2 nanoparticle synthesis: a versatile basis for the fabrication of self-supporting, transparent, and UV-absorbing composite films. ACS Appl. Mater. Interfaces. 1: 1097–1104.

Lacerda, S.H. and J.J. Park, C. Meuse, D. Pristinski, M.L. Becker and A. Karim. 2010. Interaction of gold nanoparticles with common human blood proteins. ACS Nano. 4: 365–369.

Laurent, S. and D. Forge, M. Port, A. Roch, C. Robic, L.V. Elst and R.N. Muller. 2008. Magnetic iron oxide nanoparticles: synthesis, stabilization, vectorization, physicochemical characterizations, and biological applications. Chem. Rev. 108: 2064–2110.

Lewinski, N. and V. Colvin and R. Drezek. 2008. Cytotoxicity of nanoparticles. Small. 4: 26–49.

Li, J. and D. Hartono, C.N. Ong, B.H. Bay and L.Y.L. Yung. 2010a. Autophagy and oxidative stress associated with gold nanoparticles. Biomaterials. 31: 5996–6003.

Li, H. and Z. Sun, W. Zhong, N. Hao, D. Xu and H.Y. Chen. 2010b. Ultrasensitive electrochemical detection for DNA arrays based on silver nanoparticle aggregates. Anal. Chem. 82: 5477–5483.

Lindfors, K. and P.S. Kalkbrenner and V. Sandoghdar. 2004. Detection and spectroscopy of gold nanoparticles using supercontinuum white light confocal microscopy. Phys. Rev. Lett. 93: 037401.

Mahmoudi, M. and H. Hofmann, B. Rothen-Rutishauser and A. Petri-Fink. 2012. Assessing the *in vitro* and *in vivo* toxicity of superparamagnetic iron oxide nanoparticles. Chem. Rev. 112: 2323–2338.

McCarthy, J.R. and R. Weissleder. 2008. Multifunctional magnetic nanoparticles for targeted imaging and therapy. Adv. Drug Deliv. Rev. 60: 1241–1251.

Meruvu, H. and M. Vangalapati, S.C. Chippada and S.R. Bammidi. 2011. Synthesis and characterization of zinc oxide nanoparticles and its antimicrobial activity against *Bacillus subtilis* and *Escherichia coli*. Rasāyan J. Chem. 4: 217–222.

Mock, J.J. and M. Barbic, D.R. Smith, D.A. Schultz and S. Schultz. 2002. Shape effects in plasmon resonance of individual colloidal silver nanoparticles. J. Chem. Phys. 116: 6755–6760.

Mukherjee, P. and R. Bhattacharya, N. Bone, Y.K. Lee, C.R. Patra, S. Wang, L. Lu, C. Secreto, P.C. Banerjee, M.J. Yaszemski, N.E. Kay and D. Mukhopadhyay. 2007. Potential therapeutic application of gold nanoparticles in B-chronic lymphocytic leukemia (BCLL): enhancing apoptosis. J. Nanobiotechnology. 5: 4.

Naqvi, S. and M. Samim, M.Z. Abdin, F.J. Ahmed, A.N. Maitra, C.K. Prashant and A.K. Dinda. 2010. Concentration-dependent toxicity of iron oxide nanoparticles mediated by increased oxidative stress. Int. J. Nanomedicine. 5: 983–989.

Niidome, T. and M. Yamagata, Y. Okamoto, Y. Akiyama, H. Takahashi, T. Kawano, Y. Katayama and Y. Niidome. 2006. PEG-modified gold nanorods with a stealth character for *in vivo* applications. J. Control. Release. 114: 343–347.

Nguyen, D.T. and D.J. Kim and K.S. Kim. 2011. Controlled synthesis and biomolecular probe application of gold nanoparticles. Micron. 42: 207–227.

Nowack, B. and H.F. Krug and M. Height. 2011. 120 years of nanosilver history: implications for policy makers. Environ. Sci. Technol. 45: 1177–1183.

Paciotti, G.F. and L. Tamarkin. Biological and engineering considerations for developing tumor-targeting metallic nanoparticle drug-delivery systems. pp. 141–158. *In*: D. Thassu, M. Deleers and Y. Pathak [eds.]. 2007. Nanoparticulate Drug Delivery Systems. Informa Healthcare, New York, USA.

Pan, Y. and A. Leifert, D. Ruau, S. Neuss, J. Bornemann, G. Schmid, W. Brandau, U. Simon and W. Jahnen-Dechent. 2009. Gold nanoparticles of diameter 1.4 nm trigger necrosis by oxidative stress and mitochondrial damage. Small. 5: 2067–2076.

Park, S. and Y.J. Son, K.W. Leong and H.S. Yoo. 2012. Therapeutic nanorods with metallic multi-segments: thermally inducible encapsulation of doxorubicin for anti-cancer therapy. Nano Today. 7: 76–84.

Perks, B. 2010. Gold Fever. Chemistry World. 3: 48–50.

Petros, R.A. and J.M. DeSimone. 2010. Strategies in the design of nanoparticles for therapeutic applications. Nat. Rev. Drug Discov. 9: 615– 627.

Pokharkar, V. and S. Dhar, D. Bhumkar, V. Mali, S. Bodhankar and B. Prasad. 2009. Acute and subacute toxicity studies of chitosan reduced gold nanoparticles: a novel carrier for therapeutic agents. J. Biomed. Nanotechnol. 5: 1–7.

Premanathan, M. and K. Karthikeyan, K. Jeyasubramanian and G. Manivannan. 2011. Selective toxicity of ZnO nanoparticles toward Gram-positive bacteria and cancer cells by apoptosis through lipid peroxidation. Nanomedicine. 7: 184–192.

Puzyn, T. and B. Rasulev, A. Gajewicz, X. Hu, T.P. Dasari, A. Michalkova, H.M. Hwang, A. Toropov, D. Leszczynska and J. Leszczynski. 2011. Using nano-QSAR to predict the cytotoxicity of metal oxide nanoparticles. Nat. Nanotechnol. 6: 175–178.

Raghunandan, D. and S. Basavaraja, B. Mahesh, S. Balaji, S.Y. Manjunath and A. Venkataraman. 2009. Biosynthesis of stable polyshaped gold nanoparticles from microwave-exposed aqueous extracellular anti-malignant guava (*Psidium guajava*) leaf extract. Nanobiotechnol. 5: 34–41.

Rai, M. and A. Yadav and A. Gade. 2009. Silver nanoparticles as a new generation of antimicrobials. Biotechnol. Adv. 27: 76–83.

Rai, A. and A. Prabhune and C.C. Perry. 2010. Antibiotic mediated synthesis of gold nanoparticles with potent antimicrobial activity and their application in antimicrobial coatings. J. Mater. Chem. 20: 6789–6798.

Saha, K. and S.S. Agasti, C. Kim, X. Li and V.M. Rotello. 2012. Gold nanoparticles in chemical and biological sensing. Chem. Rev. 112: 2739–2779.

Sato, M. and H. Harada, S. Morito, Y. Fujita, S. Shimosaki, T. Urano and M. Nakamura. 2010. Preparation, characterization and properties of novel covalently surface-functionalized zinc oxide nanoparticles. Appl. Surf. Sci. 256: 4497–4501.

Selvakannan, P.R. and S. Mandal, S. Phadtare, A. Gole, R. Pasricha, S.D. Adyanthaya and M. Sastry. 2004. Water-dispersible tryptophan protected gold nanoparticles prepared by the spontaneous reduction of aqueous chloroaurate ions by the amino acid. J. Colloid Interface Sci. 269: 97–102.

Sharma, V. and R.K. Shukla, N. Saxena, D. Parmar, M. Das and A. Dhawan. 2009. DNA damaging potential of zinc oxide nanoparticles in human epidermal cells. Toxicol. Lett. 185: 211–218.

Shaw, C. 1999. Gold-based therapeutic agents. Chem. Rev. 99: 2589–2600.

Shchukin, D.G. and D. Radziuk and H. Möhwald. 2010. Ultrasonic fabrication of metallic nanomaterials and nanoalloys. Annu. Rev. Mater. Res. 40: 345–362.

Shen, W. and Z. Li, H. Wang, Y. Liu, Q. Guo and Y. Zhang. 2008. Photocatalytic degradation for methylene blue using zinc oxide prepared by codeposition and sol-gel methods. J. Hazard Mater. 152: 172–175.

Shenoy, D. and W. Fu, J. Li, C. Crasto, G. Jones, C. Dimarzio, S. Sridhar and M. Amiji. 2006. Surface functionalization of gold nanoparticles using hetero-bifunctional poly(ethylene glycol) spacer for intracellular tracking and delivery. Int. J. Nanomedicine. 1: 51–58.

Shiying, H. and Y. Zhang, Z. Guo and N. Gu. 2008. Biological synthesis of gold nanowires using extract of *Rhodopseudomonas capsulate*. Biotechnol. Prog. 24: 476–480.

Shore, M.S. and J. Wang, A.C. Johnston-Peck, A.L. Oldenburg and J.B. Tracy. 2011. Synthesis of Au(Core)/Ag(Shell) nanoparticles and their conversion to Au–Ag alloy nanoparticles. Small. 7: 230–234.

Singh, M. and S. Singh, S. Prasada and I.S. Gambhir. 2008. Nanotechnology in medicine and antibacterial effect of silver nanoparticles. Digest J. Nanomater. Biostructures. 3: 115–122.

Smijs, T.G. and S. Pavel. 2011. Titanium dioxide and zinc oxide nanoparticles in sunscreens: focus on their safety and effectiveness. Nanotechnol. Sci. Appl. 4: 95–112.

Soelberg, S.D. and R.C. Stevens, A.P. Limaye and C.E. Furlong. 2009. Surface plasmon resonance detection using antibody-linked magnetic nanoparticles for analyte capture, purification, concentration, and signal amplification. Anal. Chem. 81: 2357–2363.

Soenen, S.J. and P. Rivera-Gil, J. Montenegro, W.J. Parak, S.C. DeSmedt and K. Braeckmans. 2011. Cellular toxicity of inorganic nanoparticles: common aspects and guidelines for improved nanotoxicity evaluation. Nano Today. 6: 446–465.

Sönnichsen, C. and T. Franzl, T. Wilk, G. von Plessen, J. Feldmann, O. Wilson and P. Mulvaney. 2002. Drastic reduction of plasmon damping in gold nanorods. Phys. Rev. Lett. 88: 077402.

Sreeram, K.J. and M. Nidhin and B.U. Nair. 2008. Microwave assisted template synthesis of silver nanoparticles. Bull. Mater. Sci. 31: 937–942.

Sun, C. and J.S.H. Lee and M. Zhang. 2008. Magnetic nanoparticles in MR imaging and drug delivery. Adv. Drug Deliv. Rev. 60: 1252–1265.

Sung, J.H. and J.H. Ji, J.D. Park, J.U. Yoon, D.S. Kim, K.S. Jeon, M.Y. Song, J. Jeong, B.S. Han, J.H. Han, Y.H. Chung, H.K. Chang, J.H. Lee, M.H. Cho, B.J. Kelman and I.J. Yu. 2009. Subchronic inhalation toxicity of silver nanoparticles. Toxicol. Sci. 108: 452–461.

Taccola, L. and V. Raffa, C. Riggio, O. Vittorio, M.C. Lorio, R. Vanacore, A. Pietrabissa and A. Cuschieri. 2011. Zinc oxide nanoparticles as selective killers of proliferating cells. Int. J. Nanomedicine. 6: 1129–1140.

Tedesco, S. and H. Doyle, J. Blasco, G. Redmond and D. Sheehan. 2010. Oxidative stress and toxicity of gold nanoparticles in *Mytilus edulis*. Aquat. Toxicol. 100: 178–186.

Thakkar, K.N. and S.S. Mhatre and R.Y. Parikh. 2010. Biological synthesis of metallic nanoparticles. Nanomedicine. 6: 257–262.

Thevenot, P. and J. Cho, D. Wavhal, R.B. Timmons and L. Tang. 2008. Surface chemistry influences cancer killing effect of TiO_2 nanoparticles. Nanomedicine. 4: 226–236.

Thurn, K.T. and H. Arora, T. Paunesku, A. Wu, E.M. Brown, C. Doty, J. Kremer and G. Woloschak. 2011. Endocytosis of titanium dioxide nanoparticles in prostate cancer PC-3M cells. Nanomedicine. 7: 123–130.

Tian, J. and K.K. Wong, C.M. Ho, C.N. Lok, W.Y. Yu, C.M. Che, J.F. Chiu and P.K. Tam. 2007. Topical delivery of silver nanoparticles promotes wound healing. Chem. Med. Chem. 2: 129–136.

Toropov, A.A. and I. Gutman and B. Furtula. 2005. Graph of atomic orbitals and the molecular structure descriptors based on it. J. Serb. Chem. Soc. 70: 669–674.

Turkevich, J. and P.C. Stevenson and J. Hillier. 1951. A study of the nucleation and growth processes in the synthesis of colloidal gold. Discuss. Faraday. Soc. 11: 55–75.

Venkatpurwar, V.P. and V.B. Pokharkar. 2010. Biosynthesis of gold nanoparticles using therapeutic enzyme: *in vitro* and *in vivo* efficacy study. J. Biomed. Nanotechnol. 6: 667–674.

Venkatpurwar, V. and V. Pokharkar. 2011. Green synthesis of silver nanoparticles using marine polysaccharide: study of *in vitro* antibacterial activity. Mater. Lett. 65: 999–1002.

Villiers, C. and H. Freitas, R. Couderc, M.B. Villiers and P. Marche. 2010. Analysis of the toxicity of gold nanoparticles on the immune system: effect on dendritic cell functions. J. Nanopart. Res. 12: 55–60.

Wei, D. and W. Sun, W. Qian, Y. Ye and X. Ma. 2009. The synthesis of chitosan-based silver nanoparticles and their antibacterial activity. Carbohydr. Res. 344: 2375–2382.

Wostek-Wojciechowska, D. and J.K. Jeszka, P. Uznanski, C. Amiens, B. Chaudret and P. Lecante. 2004. Synthesis of gold nanoparticles in solid state by thermal decomposition of an organometallic precursor. Mater. Sci. Poland. 22: 407–413.

Wu, Y.L. and A.I.Y. Tok, F.Y.C. Boey, X.T. Zeng and X.H. Zhang. 2007. Surface modification of ZnO nanocrystals. Appl. Surf. Sci. 253: 5473–5479.

Wu, J. and J. Sun and Y. Xue. 2010. Involvement of JNK and P53 activation in G2/M cell cycle arrest and apoptosis induced by titanium dioxide nanoparticles in neuron cells. Toxicol. Lett. 199: 269–276.

Xie, G. and C. Wang, J. Sun and G. Zhong. 2011. Tissue distribution and excretion of intravenously administered titanium dioxide nanoparticles. Toxicol. Lett. 205: 55–61.

Xu, R. and J. Ma, X. Sun, Z. Chen, X. Jiang, Z. Guo, L. Huang, Y. Li, M. Wang, C. Wang, J. Liu, X. Fan, J. Gu, X. Chen, Y. Zhang and N. Gu. 2009. Ag nanoparticles sensitize IR-induced killing of cancer cells. Cell Res. 19: 1031–1034.

Yen, H.J. and S.H. Hsu and C.L. Tsai. 2009. Cytotoxicity and immunological response of gold and silver nanoparticles of different sizes. Small. 5: 1553–1561.

Yildirimer, L. and N.T.K. Thanh, M. Loizidoua and A.M. Seifalian. 2011. Toxicological considerations of clinically applicable nanoparticles. Nano Today. 6: 585–607.

Yu, J. and M. Baek, H.E. Chung and S.J. Choi. 2011. Effects of physicochemical properties of zinc oxide nanoparticles on cellular uptake. J. Phys. Conf. Ser. 304: 012007.

Zhang, Y.X. and J. Zheng, G. Gao, Y.F. Kong, X. Zhi, K. Wang, X.Q. Zhang and X. Cui. 2011a. Biosynthesis of gold nanoparticles using chloroplasts. Int. J. Nanomedicine. 6: 2899–2906.

Zhang, X.D. and D. Wu and X. Shen. 2011b. Size-dependent *in vivo* toxicity of PEG-coated gold nanoparticles. Int. J. Nanomedicine. 6: 2071–2081.

CHAPTER 9

Porous Silica Nanoparticles for Drug Delivery and Controlled Release

Xiaoxing Sun[1] and *Brian G. Trewyn*[2,*]

ABSTRACT

The advancement of porous silica nanoparticles with unique structural features as non-invasive and biocompatible carriers to deliver drug molecules into animal and plant cells has been well established in pharmaceutical research over the recent decade. Herein, we review synthetic approaches of porous silica nanoparticles and current progress on their functionalization with organic components and inorganic nanoparticles plus a short survey of characterization methods frequently discussed. Utilizing these flexible functionalization methods, versatile porous silica nanoparticle assemblies are fabricated and used as drug delivery devices via numerous mechanisms. We highlight the development of the design and synthesis of nanovalve and capping systems on porous silica nanoparticles, where drugs are encapsulated in the pores and released in a controlled fashion by physical, chemical or biological external or internal stimuli. Moreover, when functionalized with specific cell and antigen targeting moieties, porous silica nanoparticles can selectively deliver drugs to diseased cells, and hence enhance chemotherapy effectiveness and

[1] Department of Chemistry, Iowa State University, Ames, IA, 50011, USA.
Email: sunxiaoxing@gmail.com
[2] Department of Chemistry and Geochemistry, Colorado School of Mines, Golden, CO, 80403, USA.
Email: btrewyn@mines.edu
* Corresponding author

List of abbreviations after the text.

reduce side effects. Recent reports have also demonstrated paradigms of successful *in vivo* drug delivery systems using porous silica nanoparticles as a scaffold. We further discuss investigations on the biocompatibility and on the internalization efficiency of porous silica nanoparticles by animal and plant cells.

Introduction

During the past several decades, a steadily growing number of drugs have been discovered. However about 40% of newly designed drugs, especially those which are based on biomolecules [e.g., peptides, oligonucleotides, proteins and deoxyribonucleic acid (DNA)], often exhibit low bioavailability and are rejected by the pharmaceutical industry. Therefore, there is an increasing demand for the development of Drug Delivery Systems (DDSs) to minimize drug degradation, manipulate drug pharmacological profile, diversify drug administration routes, decrease detrimental drug side effects and target specific sites. To achieve these goals, numerous materials have been extensively investigated, such as, amphiphilic block copolymers (Gref et al. 1994, Jeong et al. 1997, Discher et al. 1999), liposomes (Torchilin 2005), dendrimers (Gao and Yan 2004, Lee et al. 2005), hydrogels (Peppas et al. 2000, 2006), as well as inorganic nanoparticles (NPs) (Lai et al. 2003, Vivero-Escoto et al. 2010).

Among all the DDSs tested, Porous Silica Nanoparticles (PSNPs) stand out to be a promising candidate, which have the potential to perform simultaneously all the above mentioned functions. Typically, PSNPs used as DDSs are featured by their ordered arrays of two dimensional (2D) hexagonal micro- or mesopore-structure, uniform particle sizes (mean value: 80–500 nm), large surface areas (> 1000 m^2/g), high pore volumes (0.5–2.5 cm^3/g), tunable pore diameters (1.3–30 nm), controllable particle morphologies, and both exterior and interior surfaces that could be independently modified with a variety of functional groups. In contrast to conventional polymer-based DDS which usually suffer from problems like low drug loading capacity and poor drug release control, PSNPs-based DDSs successfully avoid these issues. The high surface areas and pore volumes allow for a large drug payload. The pore environment and surface can be adjusted by functional groups favored by drug molecules in order to further enhance drug loading and releasing ability. The highly stable pore channels prevent encapsulated drug molecules from degradation in harsh environments during administration. The tunable morphology of PSNPs renders their excellent biocompatibility at concentrations adequate for pharmacological applications.

Furthermore, the most remarkable advantage of PSNPs as DDSs is their "zero premature controlled drug release" property. Namely, drugs are carried with precise control of location and time without leaching prior to reaching the targeted cells or tissues. This technique is realized by encapsulating drug molecules inside the PSNP pores followed by blocking the pore entrances with stimuli-responsive agents, or so called "caps". Hence, drug delivery takes place only when these caps leave the PSNP assembly, when triggered by external or internal stimuli that can be manipulated manually at a desired location and time. In addition, it is also possible to deliver guest molecules repeatedly in small portions by reversibly switching the PSNP-based DDSs between "on" and "off" status.

In this chapter we review recent endeavors on the development of PSNP-based controlled release DDS, as well as investigations on their *in vitro* and *in vivo* applications.

Synthesis of Porous Silica Nanoparticles

The family of porous silica materials was independently discovered by Kresge et al. (1992) at the Mobil Oil Company (USA) and the Kuroda research group (Inagaki et al. 1993) at the Waseda University (Japan) in the early 1990s. Since then, research in this field has tremendously expanded. Porous silica materials with different mesophases have been synthesized by varying experimental conditions, such as, pH, temperature, templates and molar ratios (Hoffmann et al. 2006, Wan and Zhao 2007). The earliest and most well-known porous silica representative is the mobile catalytic material number 41 (MCM-41), exhibiting a 2D hexagonal mesopore arrangement (Fig. 9.1). Another example is the Santa Barbara Amorphous material number 15 (SBA-15), sharing a 2D hexagonal structure, but it has wider tunable pore size range, and greater hydrothermal stability than MCM-41. Both types of PSNPs have found applications as drug delivery devices (Vallet-Regí et al. 2001, 2007, Lai et al. 2003, Song et al. 2005, Trewyn et al. 2007).

The key principle for synthesizing PSNPs is the condensation of silica precursors directed by self-assembled liquid crystal arrays of surfactants. In depth investigations have led to two proposed mechanisms involved in the formation of supramolecular aggregates of surfactants and subsequent generation of PSNPs (Vartuli et al. 1994). In the Liquid Crystal Templating (LCT) mechanism, surfactants form liquid crystal structures at concentrations above their Critical Micelle Concentration (CMC) and serve as templates, without requiring the addition of silica precursors. While an alternative mechanism was proposed that the final mesopore ordering is a process of cooperative interaction between surfactants and silica precursors.

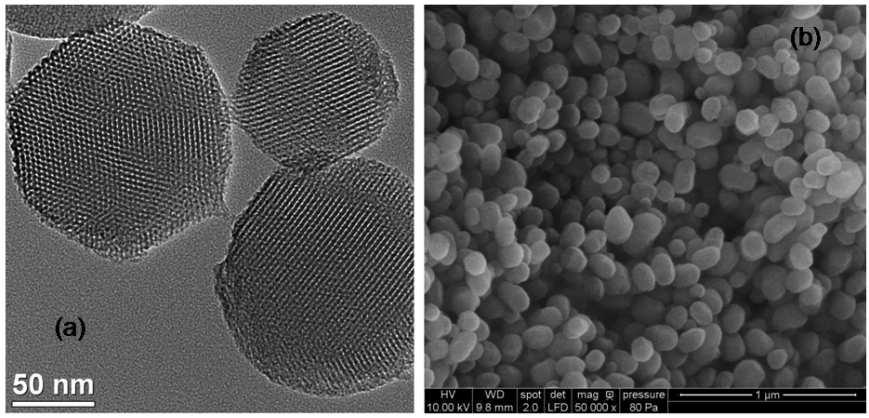

Figure 9.1. Transmission (a) and scanning (b) electron micrographs of MCM-41. Bar lengths: (a) 50 nm, and (b) 1 µm.

For example, PSNPs could be prepared even at surfactant concentrations far below the CMC, in which case an ordered liquid crystal structure could develop under the second mechanism (Cai et al. 1999).

In a typical surfactant-silica precursor interaction, tetramethyl orthosilicate (TMOS) or tetraethyl orthosilicate (TEOS) is normally added as silica precursor, and cationic alkyltrimethylammonium salts are used as templates under a basic reaction condition. Further exploration was conducted by the Stucky research group, where a series of block copolymer surfactants were used as structure directing agents to synthesize PSNPs in acidic environments (Huo et al. 1995, 1996, Zhao et al. 1998a,b). A variety of strategies have been proposed to attain tunable pore sizes from less than 2 nm up to 30 nm, including the adjustment of the hydrocarbon chain length of small surfactant templates (Beck et al. 1992, Widenmeyer and Anwander 2002), the use of pore swelling agents, such as, mesitylene (Beck et al. 1992) or hydrothermal treatments (Sayari et al. 1997). The control over the surfactant-silica interaction enables a versatile synthesis condition for PSNPs, and thus allows for the functionalization of other species into the silica framework.

Surface Functionalization of Porous Silica Nanoparticles

A notable advantage of using biocompatible PSNPs as DDS is the relative ease to incorporate enormous variation of organic species. The flexibility to modify PSNP surfaces leads to the generation of a considerable number of PSNP-based hybrid materials that possess specific functions for drug delivery. Illustrations of these PSNP-derivatized materials and their functions will be discussed in later sections. The commonly used organic precursors

are organotrialkoxysilanes [$(R'O)_3SiR$], and organotrichlorosilanes (Cl_3SiR). Two popular pathways are available for surface functionalization (Fig. 9.2). One is to introduce organosilanes simultaneously with silica precursors during the synthesis of PSNPs ("co-condensation") (Fig. 9.2a). The other pathway is to prepare non-functionalized PSNPs and subsequently modify their surfaces with organosilanes ("grafting") (Fig. 9.2b).

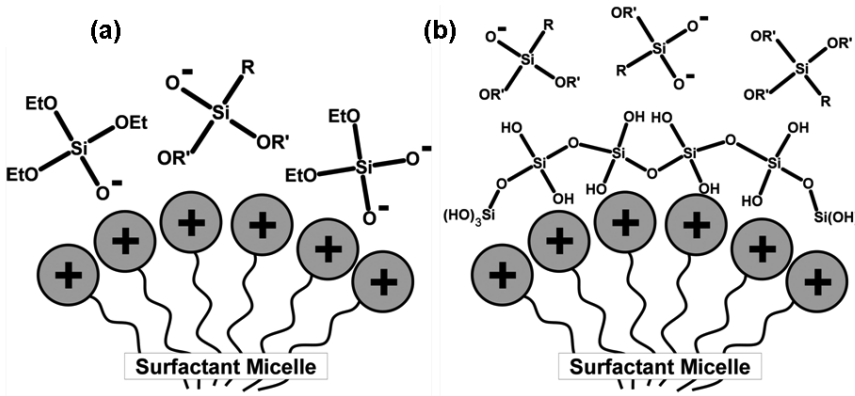

Figure 9.2. Surface functionalization of PSNPs by (a) the co-condensation method, and by (b) the post-synthesis grafting method.

Surface functionalization by the co-condensation method

Co-condensation is a direct synthesis method where organosilanes are condensed along with the silica precursors in the presence of surfactant templates. As a result, the organic groups are homogeneously distributed within the porous structure. Also, it is possible to control the mesoporous silica NP morphology by introducing different organosilanes (Fig. 9.3). Lin and co-workers proposed that interactions between organosilanes and surfactant molecules, such as, electrostatic interaction, hydrophobic interaction or hydrogen bonding could contribute to the variation in particle morphology (Huh et al. 2003a). They demonstrated that organosilanes with hydrophobic groups tend to intercalate such groups into the surfactant micelles and interact with the hydrophobic tails of surfactants, thus stabilizing the formation of long cylindrical micelles and giving rise to rod-shaped PSNPs. On the contrary, hydrophilic organosilanes would inhibit micelle growth and yield spherical particles with randomly oriented pore structures. As a result, by using two organosilanes with opposite head group properties and varying their ratios, the surface functionality and morphology of PSNPs can be tuned with the co-condensation method (Huh et al. 2003b).

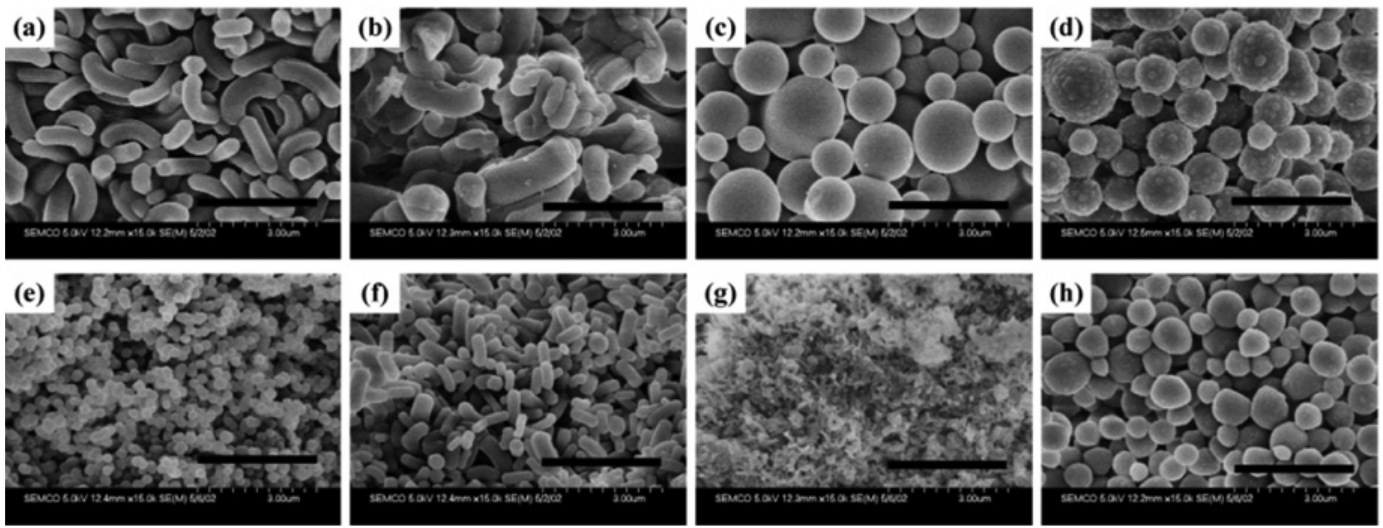

Figure 9.3. Field emission scanning electron microscopy (FeSEM) images of: (a) 3-aminopropyl-PSNPs, (b) *N*-(2-aminoethyl)-3-aminopropyl-PSNPs, (c) 3-[2-(2-aminoethylamino)ethylamino]propyl-PSNPs, (d) 3-ureidopropyl-PSNPs, (e) 3-isocyanatopropyl-PSNPs, (f) 3-cyanopropyl-PSNPs, (g) allyl-PSNPs, and (h) non-functionalized PSNPs. All images are presented using the same scale. Bar lengths: 3 μm. Reprinted with permission from Huh et al. (2003a). Copyright American Chemical Society (2003).

In order to preserve the pore structure and long range pore ordering of PSNPs, the amount of functional groups incorporated by the co-condensation method does not normally exceed 25% of surface coverage due to the difference in condensation rates between organosilanes and silica precursors. The efficiency of loading depends on the nature of the organic functional groups. A detailed study has been conducted by Lin and co-workers (Radu et al. 2005), where they summarized that the amount of chemically accessible functional groups is proportional to the interfacial electrostatic matching between the functional groups and the surfactant head groups. Functional groups possessing a stronger ability to compete with the silicate anions in binding with surfactant molecules would be more likely to appear at PSNP surfaces than those weakly binding functional groups which are usually embedded within the silica framework and are hence inaccessible. Based on their results, the degree of surface functionalization can be adjusted by choosing appropriate organic functional groups.

Surface functionalization by the post-synthesis grafting method

In this method, major functionalization reactions take place between organic precursors and free silanol groups at the exterior surface and at the opening of the pores of PSNPs. Compared to the co-condensed material, organosilane-grafted PSNPs have better retained pore structures and are more thermally stable. However, in most cases, the degree of functionalization by the grafting method is lower than that of co-condensation method, owing to the limited number of free surface silanol groups. As opposed to the homogeneous functional group coverage obtained by the co-condensation method, it has been reported that most functional groups are preferentially attached to the external surface or the pore openings, since the silanol groups are more easily accessible there than the interior pore surface which suffer from lower diffusion rates of organic precursors (Lim and Stein 1999). In certain situations, such as, when organic precursors are too big for the pores or they are unfavorable for the pore environment, their penetration to the inner sites of the pores is extremely impaired, leading to an unmodified internal surface. Taking advantage of this feature, it is feasible to selectively functionalize the external and internal surfaces of PSNPs with different functional groups.

Multiple functionalizations

To satisfy the need for constructing more complex PSNP-based DDSs, it is desirable to be able to incorporate more than one type of functional group with

the PSNP. Co-condensing two different organosilanes with silica precursors could be a simple solution, but as mentioned previously, different hydrolysis rates of silanes would undermine the ordering of PSNPs and restrict the loading quantity. Furthermore, locations of the functional groups cannot be regulated accurately. Therefore, a co-condensation and post-synthesis grafting combined approach for selectively incorporating functional groups onto external and internal surface of PSNPs was developed by Lin and co-workers (Radu et al. 2004a). Mercaptopropyl-functionalized PSNPs were first prepared by the co-condensation method, yielding 90% of total thiol groups inside the pore channels, followed by 5,6-epoxyhexyltriethoxysilane grafted onto the outer surface of the thiol-functionalized PSNPs with 43% surface coverage. The mercaptopropyl groups were converted to *o*-phthalic hemithioacetal groups and the 5,6-dihydroxyhexyl groups were used for a poly(lactic acid) coating. This assembly was reported as a detector for amino-containing neurotransmitters. In their study, both outer and inner surfaces of the PSNP were modified without interacting with each other. Another strategy of sequential grafting was designed by the Ruiz-Hitzky's research group where external grafting with alkyl groups was carried out before removing surfactant templates so that surfactant molecules would prevent the penetration of organic precursors into the pores (de Juan and Ruiz-Hitzky 2000). Templates were extracted afterward by refluxing the particles in an ammonium chloride containing *n*-heptane/ethanol mixture. This template-free material then received a second grafting with aryl groups. Since most of the external silanol groups were consumed in the first grafting, a majority of aryl groups reacted mainly with silanol groups inside the pore channels, thus generating PSNPs functionalized with organic groups topologically located as desired.

In a recent paper reported by Lo and co-workers (Cheng et al. 2010), tri-functionalized PSNPs were synthesized containing three distinct domains: the silica framework, the hexagonal pores and the outermost surfaces, which were independently functionalized with contrast agents for imaging, drug payloads for cancer therapy and biomolecular ligands for cancer cell targeting, respectively. A near-infrared fluorescent contrast agent was co-condensed with TEOS for the optical tracking of PSNPs. The surfactant templates were then removed, followed by the grafting of nanochannels with a palladium/porphyrin-based photosensitizer, which was exploited in photodynamic therapy. The third functionalization reaction occurred on the external surfaces with cyclic arginine-glycine-aspartic acid-D-tyrosine-lysine (*c*RGDyK) peptides that specifically bind to integrins overexpressed by cancer cells.

Biological Performance of Porous Silica Nanoparticles

Intracellular uptake of porous silica nanoparticles

To deliver encapsulated drug molecules into mammalian cells and perform therapeutic functions, PSNP-based DDSs have to overcome the cell membrane boundary and be internalized by cells. Many research groups have demonstrated that PSNPs can be efficiently internalized by a variety of mammalian cells, including cancer cells (HeLa, CHO, lung, PANC-1, MCF-7, RIN-5F) and non-cancer cells (liver, endothelial, skin fibroblast) (Radu et al. 2004b, Giri et al. 2005, Slowing et al. 2006, 2007, Vivero-Escoto et al. 2010). However, thorough understanding of cellular internalization mechanisms has not been fully unveiled. At the size domain of PSNPs, particles have found to enter cells through endocytosis pathways in the majority of cases (Prokop and Davidson 2008). Various factors have been outlined to influence the kinetics and efficiency of intracellular endocytosis of PSNPs.

One of the factors dictating particle endocytosis is the surface functional group, as reported by Slowing et al. (2006). The results showed that the surface functionalities not only regulate the uptake of PSNPs by HeLa cells, but also affect their ability to escape endosomal entrapment. Positively charged PSNPs exhibited better endocytosis efficiency than negatively charged PSNPs, owing to a greater electrostatic affinity to negatively charged cell membranes. On the other hand, the negatively charged particles possess superior endosomal escape ability, presumably due to a "proton sponge effect". In addition, folate groups on PSNPs could facilitate the HeLa cell uptake efficiency through a folate-receptor mediated endocytosis pathway. Therefore, as will be discussed, Folic Acid (FA) is widely used as a targeting ligand to regulate the drug delivery accuracy.

Particle size and morphology also plays a role on the endocytosis of PSNPs. The Lin research group observed a faster and higher intracellular uptake of smaller PSNPs compared with larger ones (Trewyn et al. 2008). This effect was further explored by Mou and co-workers (Lu et al. 2009), indicating an optimal particle size of 50 nm to reach the maximum PSNP uptake by HeLa cells. Also, distinct endocytosis efficiencies were found with spherical- and tubular-shaped PSNPs. Their investigations may allow researchers to control the rate of drug delivery more accurately.

Biocompatibility of porous silica nanoparticles

To evaluate the potential of PSNPs as drug delivery devices, issues regarding the biocompatibility, biodistribution, retention and clearance of PSNPs on cellular systems were examined by many research groups (Lai et al. 2003, Slowing et al. 2006, Chung et al. 2007, Vallhov et al. 2007, He

et al. 2008, 2011, Hudson et al. 2008, Jiang et al. 2008, Huang et al. 2011). No significant cytotoxicity was observed toward HeLa and CHO cells at dosages below 100 μg/mL, even after 6 days of incubation. A size- and concentration-dependent effect of PSNPs on human dendritic cell viability was reported by Vallhov et al. (2007). They found that smaller particles and lower concentrations affected human dendritic cells to a minor degree compared to larger particles and higher concentrations, in terms of viability, uptake and immune regulatory markers, which were consistent with the *in vitro* results.

Likewise, a size- and morphology-dependent cytotoxicity of PSNPs on human Red Blood Cells (RBCs) was recently shown (Lin and Haynes 2010, Zhao et al. 2011). It was determined that in contrast to severe hemolytic activity of amorphous silica, PSNPs showed high biocompatibility towards RBCs at concentrations up to 100 μg/mL, which is possibly attributed to restricted RBC access to silanol groups on the surface of the PSNP structures. Furthermore, PSNPs with size of 600 nm caused an echinocytic shape transformation of RBCs and a subsequent hemolytic effect. These findings suggest that careful control over particle size and surface functionalities can minimize the toxicity of PSNPs.

Recent investigations on the biodistribution determined that silica NPs accumulated mainly in the liver, kidney and urinary bladder after an intravenous injection, and then were partially excreted through the renal route (He et al. 2008, 2011, Kim et al. 2008, Wu et al. 2008, Huang et al. 2011). It is worth noting that Hyeon and co-workers observed an accumulation of PSNPs (size < 200 nm) in tumor masses 24 hours after administration, which was probably due to an Enhanced Permeability and Retention (EPR) effect at tumor sites (Kim et al. 2008). Interestingly, the blood circulation time can be regulated by different surface functional groups. It was also reported that no short term toxic effect of PSNPs was observed on mice at a dosage below 200 mg/Kg, which is already significantly higher than the necessary dosage for drug delivery applications (Hudson et al. 2008, Kim et al. 2008). In a long term study, the accumulation of PSNPs was observed in the liver for up to three months without apparent toxicity (Wu et al. 2008). Therefore, although detailed information on the biocompatibility of PSNPs still needs further investigations, there is little doubt that PSNPs will be a promising drug delivery device in clinical trials.

Porous Silica Nanoparticles for Controlled Drug Release

As mentioned previously in the first section, the large drug loading capability, the flexible surface modification, the rigid porous structures and the excellent biocompatibility of PSNPs are ideal for drug delivery applications. Initial research of using porous silica materials for drug

adsorption/desorption was conducted by Vallet-Regí et al. (2001) at the beginning of this century. They successfully demonstrated that 80% of previously loaded ibuprofen was released in three days. In order to achieve an accurate control of drug releasing rate, a stimuli-triggered release concept was brought forward simultaneously by Tanaka and co-workers and Lin and co-workers two years later (Lai et al. 2003, Mal et al. 2003). In Tanaka's approach, coumarin ligands were immobilized at the pore entrance and on the external surface by a grafting method. The uptake and release of guest molecules from pore voids were photoregulated. Coumarin molecules underwent a dimerization reaction to completely seal the pore entrances when this sample was exposed to ultraviolet (UV) light ($\lambda > 310$ nm). Release of guest molecules was triggered by the cleavage of the coumarin dimers with UV light irradiation ($\lambda = 250$ nm).

However, porous silica samples prepared in Tanaka's study have no defined morphology or monodispersed size, so that the biocompatibility of these materials was unsatisfactory for drug delivery applications. The first example of using biocompatible PSNPs as carriers and inorganic NPs as caps to effectively deliver drug molecules into animal cells with zero premature release was developed by the Lin research group (Lai et al. 2003). They prepared spherical PSNPs with a uniform particle diameter of 200 nm and pore size of 2.3 nm, and then functionalized the NPs with 2-(propyldisulfanyl)ethylamine groups. This PSNPs sample was soaked in a concentrated solution of vancomycin or adenosine triphosphate (ATP) to allow the diffusion of cargo molecules into the pores. Water soluble cadmium sulfide (CdS) nanocrystals with mercaptoacetic acid groups were then added to react with the terminal amino groups on the surface of the PSNPs. Thus, CdS nanocrystals were covalently bonded to PSNPs, and blocked the pore entrances. The resulting vancomycin- or ATP-loaded CdS-capped PSNPs were washed to remove physisorbed molecules. A quantitative analysis of the amount of each compound was monitored by HPLC and the mean loading efficiency of vancomycin and ATP was calculated to be 25 and 47 μmol/g, respectively. Regarding the controlled release performance of this DDS, it exhibited less than 1% drug release in buffer solution over a 12 hour period, suggesting a good pore blockage and minimal premature release. With the addition of disulfide reducing reagents, such as, dithiothreitol (DTT) or mercaptoethanol (ME) to cleave the CdS-PSNP linkage, a rapid release was triggered and 85% of entrapped molecules were released within 24 hours. To further demonstrate its *in vitro* control release behavior, ATP-loaded CdS-capped PSNPs were cultured with astrocytes loaded with a calcium-chelating fluorescent dye. Perfusion application of ME led to a pronounced increase of intracellular calcium concentration which was stimulated by the ATP molecules carried by this DDS.

Over the past decade, many research groups have made great endeavors in the development of PSNP-based DDSs with stimuli-responsive triggered release property (Fig. 9.4). A number of regulating mechanisms have been proposed and confirmed their feasibility for intracellular drug delivery with precise control of location and timing. The triggers or stimuli can be internal, meaning that they are already present in the living organism or external, which requires a simple and convenient pathway for application. Internal stimuli are often unique to the targeted pathology, which enables the DDS to respond specifically to the desired location and release drugs in a self-regulated fashion. External controls are mostly non-invasive and easy to manipulate, so that they could assist to localize the drug release and optimize the degree of the drug delivery process. Examples of these triggers include pH, light, redox potential, temperature and enzymes, to cite just a few.

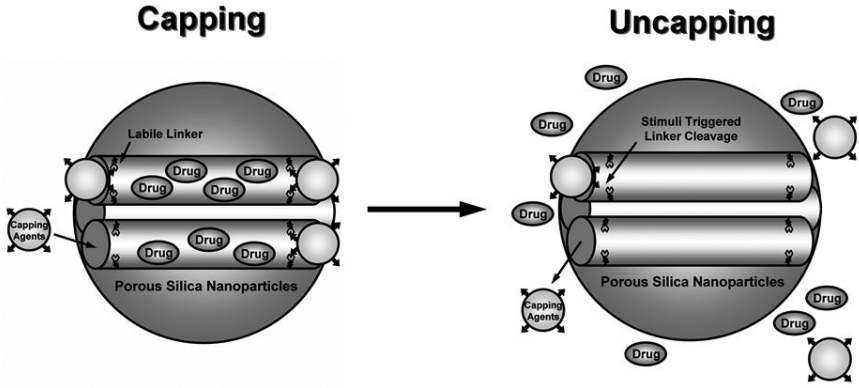

Figure 9.4. Design principle of PSNPs for controlled drug release. The capping agents block pore entrances and trap drug molecules by labile linkers which later respond to specific stimuli, thus triggering a drug release.

pH-triggered release

A series of pH-responsive linkers have been exploited for controlled release applications by taking advantage of the acidic environment at tumor or inflammatory sites (pH ≈ 6.8), endosomal or lysosomal compartments of cells (pH ≈ 5–6), as well as the stomach (pH ≈ 1.5–3.5). These pH-responsive linkers feature an inert responce to physiological pH and a robust release at low pH environment.

An early example of a pH-responsive release system was reported by Casasús et al. (2004), where they created a pH and anion controlled DDS. The PSNPs were prepared by the co-condensation of mercaptopropyltriethoxysilane with TEOS. A second grafting reaction was

carried out with *N*-(3-triethoxysilylpropyl-2-aminoethyl)ethylenediamine to get a preferential anchoring of amino groups on the external surfaces. At high pH values, the amines were deprotonated and were tightly packed through hydrogen bonding interactions so that the DDS was at its "open gate" state. However, when the amines were protonated at low pH conditions, they repelled each other and covered the pore openings due to the coulombic repulsion effect between positively charged amine groups, and the DDS was monitored to its "close gate" state. In addition, a significant synergic effect was observed in the presence of anions, which could intercalate into the open chain polyamines and seal the pore openings. This effect is clearly associated with the anion size and the strength of the polyamine-anion electrostatic interaction. Using this pH-responsive DDS, they have successfully demonstrated pH controlled release of squaraine and vitamin B_2 (Bernardos et al. 2008).

A pH-responsive DDS for protein drugs was designed by Kawi and co-workers (Song et al. 2007). In order to encapsulate bulky proteins without denaturing, PSNPs with pore diameters above 10.5 nm and pore volumes around 1 cm^3/g were synthesized in this study. These PSNPs were further modified with amine groups by co-condensation and were loaded with a model protein, Bovine Serum Albumin (BSA). The positively charged BSA-loaded PSNPs were then mixed with a solution of poly(acrylic acid) (PAA) at pH 5.35. The electrostatic assembly of PAA blocked the pore entrances and trapped the BSA proteins, the final loading amount of BSA was calculated to be 16.3%. In pH 1.2 acidic medium, no release of BSA from the PAA-encapsulated sample was measured within 5 hours, and it released only 10% after 36 hours. However, in pH 7.4 Phosphate Buffered Saline (PBS), carboxyl groups on the PAA chains started to dissociate and repel each other, causing PAA to swell and dissolve into the buffer solution. As a result, 40% of the entrapped BSA was released from the sample, suggesting a good pH-responsive capability. Additionally, PAA was found to be able to protect proteins from enzymatic degradation. By comparing the Ultraviolet Circular Dichroism (UV-CD) spectra of native and released BSA, they concluded that the BSA conformation has not been severely altered by the adsorption process, inferring a well preserved protein activity. They envisioned that this material has the potential for the oral delivery of protein drugs to the target sites with higher pH values, such as, small intestine or colon.

Covalently-immobilized PAA on PSNPs was studied as a pH-sensitive DDS by the Hong research group using a reversible addition-fragmentation chain transfer (RAFT) polymerization of acrylic acid (Hong et al. 2009) (Fig. 9.5). In this example, 5,6-epoxyhexyltriethoxysilane was grafted on the PSNPs, followed by the template removal. A RAFT agent, *S*-1-dodecyl-*S*-(α,α'-dimethyl-α''-acetic acid)trithiocarbonate, was attached to the PSNP exterior surface through an esterification reaction with the hydroxyl groups.

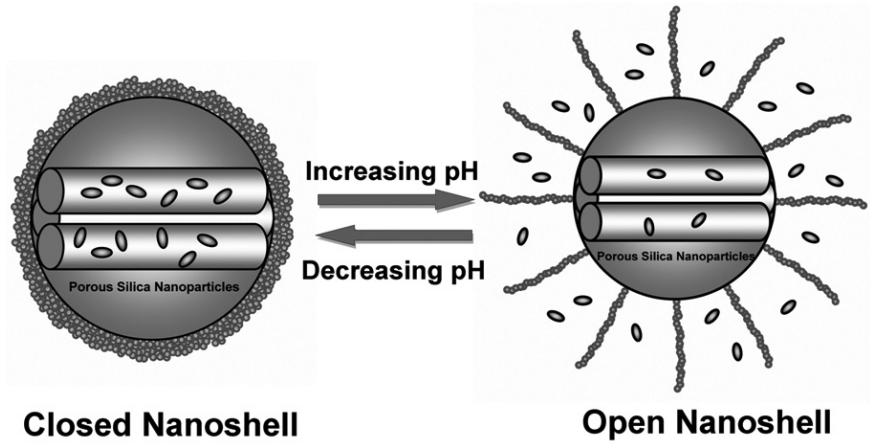

Figure 9.5. Schematic illustration of opening and closing of the core-shell structured NP triggered by pH.

Finally, acrylic acid was allowed to polymerize under vacuum to form a covalently-bonded PAA nanoshell coating on the PSNPs. The structure of the PAA nanoshell was highly dependent on the pH value of the medium. At pH 8.0, the PAA nanoshell is deprotonated and soluble in aqueous solutions, thus forming an open state with accessible pore entrances. However, when the pH drops below 4.0, the PAA nanoshell becomes insoluble and collapses onto the surface of PSNPs, rendering a compact layer. Fluorescein was used to evaluate the pH-regulated drug release performance of these PSNPs. They observed both fluorescein uptake and release by PAA-coated PSNPs at pH 8.0, but neither was detected with the same material at pH 4.0. Their results verified that the PAA-coated PSNPs can reversibly regulate the loading and releasing of guest molecules by adjusting pH values.

The unique structural and physiochemical properties of pseudorotaxanes have been exploited for the fabrication of a series of pH-responsive drug delivery devices. In a system reported by Kim and co-workers (Park et al. 2007), low molecular weight poly(ethyleneimine) (PEI, M_W = 1100 Da) and cyclodextrin (CD) were assembled onto the surface of PSNPs as the rod and the ring components, respectively. PEI was grafted by a 1,1′-carbonyldiimidazole catalyzed reaction with carboxylic group-functionalized PSNPs. Calcein was then loaded as a guest molecule to the PEI-PSNP hybrid material. Self-assembly of CDs (ring) with PEI (rod) was carried out under basic conditions, at which the CD was able to form hydrogen bonding with the deprotonated nitrogen atoms of PEI. Both α-CD and γ-CD showed effective blockage of the pores, whereas β-CD did not form a stable pseudorotaxane with PEI. The pH values of the suspensions of the calcein-loaded samples were adjusted from 11 to 5.5 to examine the

dethreading of CD and the consequent releasing of calcein. Only weak fluorescence intensity was observed at high pH values. But an immediate increase in the fluorescence intensity was measured upon acidification of the solution to pH 5.5. The system provided an example of pseudorotaxane-based PSNPs for pH-regulated drug delivery. However, the harsh working condition remains a concern for practical applications.

Similar constitution of pseudorotaxane has been created by Zink and co-workers (Angelos et al. 2008). The threading axis was a bisammonium stalk and cucurbit[6]uril (CB[6]) was used as the ring unit. Aminopropyl-functionalized PSNPs were suspended in a methanol solution of propargyl bromide to obtain alkyne-terminated silica NPs. After a loading with rhodamine B (RhB), the material was capped with CB[6]-disubstituted 1,2,3-triazole pseudorotaxanes by means of a CB[6]-catalyzed 1,3-dipolar cycloaddition of alkyne groups on PSNPs and 2-azidoethylamine. At neutral and acidic environments, the CB[6] encircles the bisammonium stalk tightly through ion-dipolar interactions. Raising the pH value results in deprotonation of the stalk and dethreading of CB[6], and subsequent unblocking of the pores. They also discovered that the use of a shorter stalk would bring the CB[6] ring closer to the surface of PSNPs and strengthen its ability of preventing leakage. They proposed that their system can be tuned to operate under gentler pH by switching to other bisammonium ion centers with favorable pK_a values.

The same research group later constructed a CB[6]-trisammonium pseudorotaxane-based PSNPs that could release guest molecules at either elevated or reduced pH values (Angelos et al. 2009a). The trisammonium stalk consists of a tetramethylenediammonium group and an anilinium group. The anilinium nitrogen atom is 10^6-fold less basic than the alkyl nitrogen atoms. Therefore, it stays unprotonated at neutral conditions, leaving the CB[6] ring residing on the tetramethylenediammonium unit to block the pore channels. When the pH increased, all of the nitrogen atoms become deprotonated, resulting in the dethreading of the CB[6] ring. Otherwise, at lower pH with all nitrogen atoms protonated, the CB[6] moiety shuttles to the distal hexamethylenediammonium unit because its ion-dipole complexation is order of magnitude greater for the six-carbon spacer than that of the four-carbon spacer. In both cases, the motion of CB[6] gives rise to pore opening and controlled drug release. Furthermore, they demonstrated that the release profiles were different for aniline and *p*-anisidine functionalities due to their distinct pK_a values. It is conceivable that the material sensitivity to specific pH values can be rationally tuned by selecting appropriately substituted anilines.

Light-triggered release

Light irradiation is a convenient remote control approach for site-specific drug delivery. The uptake and release of guest molecules can be rapidly induced upon exposure to light with certain wavelengths. After Tanaka and co-workers first demonstration of a coumarin-functionalized PSNP material to manipulate drug release as previously discussed, photochemical responsive linkers, such as, azobenzene (AB), *o*-nitrobenzyl ester and thymine bases, are incorporated onto the surface of PSNPs to render them photochemically susceptible for light controlled release.

By varying the stalk and ring components, the pseudorotaxanes approach was also applied to control drug release with light (Fig. 9.6). Zink and co-workers constituted a photosensitive pseudorotaxane of AB

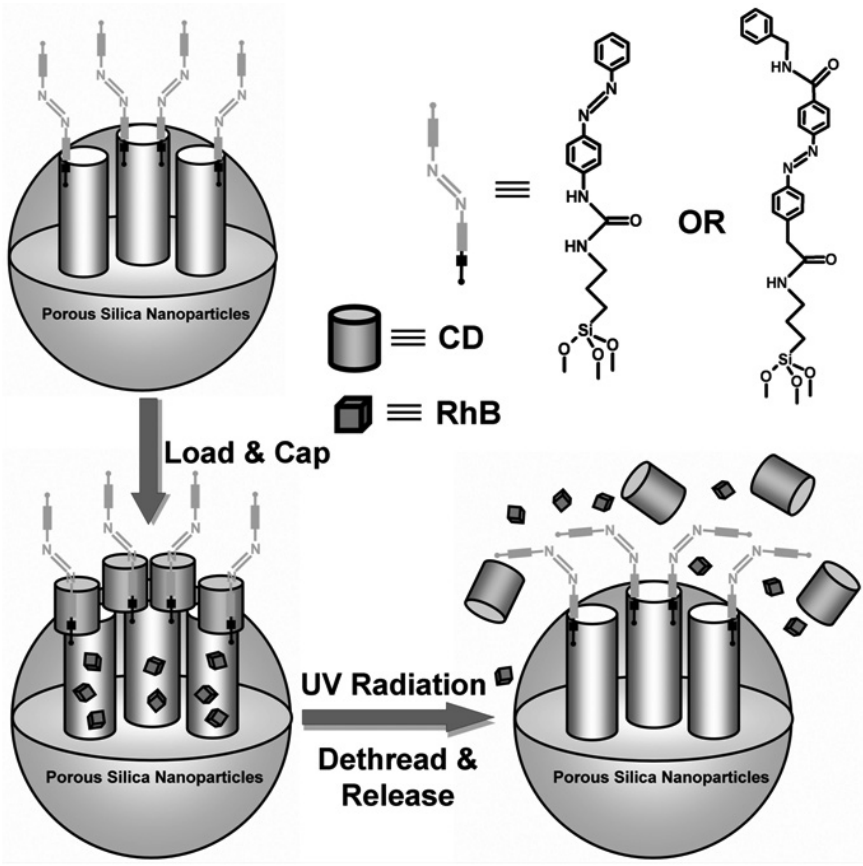

Figure 9.6. Schematic representation illustrating the capping of PSNPs by py-*β*-CD-based pseudorotaxane, and the dethreading of pseudorotaxane upon UV radiation.

derivative and *β*-CD (Ferris et al. 2009). Unfunctionalized PSNPs were grafted with 4-(3-triethoxylsilylpropylureido)azobenzene (TSUA) groups or more water soluble (E)-4-((4-(benzylcarbamoyl)phenyl)diazenyl)benzoic acid groups, as the pseudorotaxane stalks. Upon light irradiation (λ = 351 nm), both AB derivatives isomerized from the more stable *trans* form to a less stable *cis* configuration. *β*-CD or fluorescently-labeled pyrene-*β*-cyclodextrin (py-*β*-CD) were then introduced. The high binding affinity between *trans*-AB and *β*-CD locked the *β*-CD rings at the orifice. On the other hand, owing to the weak binding between *cis*-AB and *β*-CD, the isomerization of *tran*s-AB to *cis*-AB stalks led to the dissociation of pseudorotaxanes, thus permitting the release of cargo molecules. Experimental data confirmed that the AB stalks and py-*β*-CD assembly was stable without UV radiation (λ = 351 nm), whereas a complete py-*β*-CD dissociation was determined when the sample was exposed to this UV excitation beam for 400 minutes. Likewise, results from RhB-loaded samples revealed that more than 90% of RhB was released from the laser light exposed sample, while less than 30% was released from the unexposed one, over a period of 7 hours. They concluded that their material was applicable to light-operated intracellular DDSs.

CD was also employed by the Kim research group to cover the porous reservoirs (Park et al. 2009a). In their work, PSNPs were functionalized with aminopropyl groups, which were then treated with succinic anhydride in the presence of triethylamine to generate a carboxylic acid-terminated PSNP sample. The sample was further functionalized by alkyne end groups through a coupling reaction with 2-nitro-5-(2-propyn-1-yloxy)-benzenemethanol, producing a photosensitive *o*-nitrobenzyl ester moiety that would decompose upon UV light exposure (λ = 350 nm). Following a calcein dye loading, the pores were capped with the mono-6-azido-*β*-CD, by the Huigsen 1,3-dipolar cycloaddition reaction. In order to test the feasibility of their approach, the fluorescence intensity of a CD-capped calcein-loaded PSNP sample suspension was monitored over time. Only a very weak signal was detected in the dark, indicating that the calcein molecules were retained inside the pores. When the sample was irradiated with UV light, a remarkable increase in the fluorescence intensity was observed due to the photolysis of the *o*-nitrobenzyl ester linkage and the diffusion of CD and calcein molecules. Furthermore, they noted a periodic release behavior of their sample in response to successive UV irradiation over short periods of time.

Gold (Au) NPs, for the demonstrated excellent biocompatibility, were used as pore blocking caps in a research conducted by Lin and co-workers (Vivero-Escoto et al. 2009) (Fig. 9.7). A photoresponsive (PR) linker (thioundecyl-tetraethylenegly-colester-*o*-nitrobenzyl-ethyldimethyl ammonium bromide) was immobilized onto the surface of the Au NPs.

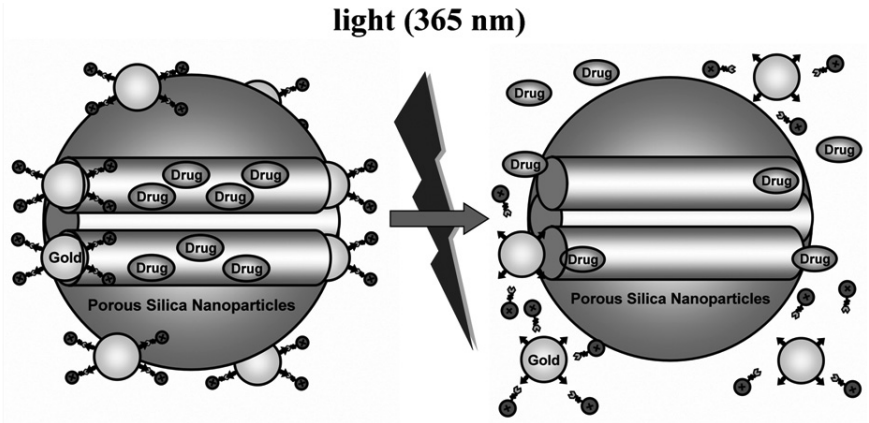

Figure 9.7. Schematic illustration of photoinduced drug release of PR-Au NPs-capped PSNPs.

These positively charged species then attached on the negatively charged PSNPs through the electrostatic interaction to produce a PR-Au NP-capped PSNP system, the structure of which was later confirmed by Transmission Electron Microscopy (TEM). Good capping efficiency was verified by the fact that no release of cargo was found even after 80 hours in the dark. Photoirradiation at 365 nm resulted in the cleavage of the *o*-nitrobenzyl ester containing linker, forming the negatively charged thioundecyltetraethyleneglycolcarboxylate-functionalized Au NPs. Hence, the charge repulsion between Au NPs and PSNPs uncovered the pores and allowed the diffusion of guest molecules. In addition, intracellular studies were executed using an anticancer drug as cargo for the controlled release in human liver and fibroblast cells. Both cell lines were incubated with either the drug-loaded sample or the drug-free sample and were either exposed to light or kept in the dark. Only cells exposed to UV light with internalized drug-loaded PSNPs caused significant cell death greater than 50%, suggesting that this system could indeed transport and release drug molecules inside human liver cells under the control of photoirradiation.

Thymine bases are a group of molecules that undergo photodimerization and revert back to monomeric thymines upon light irradiation above and below 270 nm, respectively. He et al. (2012) functionalized PSNPs with thymine and loaded the cavities with a $Ru(bipy)_3^{2+}$ dye. UV irradiation (λ = 365 nm) led to the formation of a cyclobutane ring and thus covered the pore outlets. A reversed photoreaction was triggered by exposure to light (λ = 240 nm), along with a release of 80% of loaded $Ru(bipy)_3^{2+}$. Their study provided another illustration for light-triggered drug delivery.

Redox potential-triggered release

The designs of redox responsive linkers are mainly based on the disulfide bond. It draws much interest in these systems because of its relative stability in plasma. Intracellular antioxidant species levels are 100 to 1000 fold higher than that in the extracellular space, resulting in a high redox potential difference between the oxidizing extracellular space and the reducing intracellular space (Saito et al. 2003). This difference is more significant in cancer cells than that in healthy cells, which renders the disulfide linkage more vulnerable in cancer cells leading to potentially higher drug concentrations at tumor sites. Thus, the demand for both outstanding delivery efficiency and minimized cytotoxicity can be realized by PSNP-based DDSs.

The feasibility of the redox-responsive linkage has been well established and reported in a number of recent publications. In addition to the original CdS-capped PSNPs, Lin and co-workers refined the system by replacing the CdS caps to more biocompatible superparamagnetic magnetite (Fe_3O_4) NPs (Giri et al. 2005). PSNPs were functionalized with 3-(propyldisulfanyl) propionic acid and incubated in a fluorescein solution. 3-aminopropylsiloxyl-coated Fe_3O_4 NPs were then allowed to react with the carboxyl groups of PSNPs to form a covalent amide bond. Less than 1% of fluorescein leaching was observed after 130 hours in a PBS suspension. A drastic release of 40% of loaded fluorescein was observed within two days upon the addition of DTT, or dihydrolipoic acid (an antioxidant naturally present in the cells). A series of cell biological studies further confirmed successful endocytosis and intracellular fluorescein cargo release. Additionally, when a magnet was placed on the side of a cuvette, HeLa cells with internalized magnetic Fe_3O_4-capped PSNPs were shown migrating across the cuvette. Confocal fluorescence microscopy images of the HeLa cells cultured with Fe_3O_4-capped PSNPs for 10 hours revealed green fluorescent cell bodies, proving that the disulfide bond cleavage and uncapping process took place after the PSNPs were internalization by the cells.

Not limiting to inorganic NPs, polymers, such as polyelectrolyte multilayers (PEMs), have also been used to inhibit premature drug release. Yang, Wang and co-workers synthesized PSNPs with disulfide bond cross-linked multilayers of poly(*N*-vinyl-2-pyrrolidone) and thiolated poly(methacrylic acid) through a layer-by-layer method (Zhu et al. 2005). No detectable release of loaded fluorescein isothiocyanate (FITC) was observed after 24 hours incubation. Treatment with DTT caused the deconstruction of polyelectrolytes and the subsequent release of the encapsulated FITC. The PEM-PSNPs were further conjugated with a cancer specific DNA aptamer for cell targeting. A cell viability study results showed that doxorubicin (DOX)-loaded PEM-PSNP-aptamer samples led to more pronounced cancer

cell death and non-cancer cell viability than the aptamer-free sample, thus demonstrating a redox-responsive controlled drug release system with targeted delivery ability.

A series of pseudorotaxanes have been developed by the Zink research group (Nguyen et al. 2007) (Fig. 9.8). In their first attempt, 1,5-dioxynaphthalene containing derivatives (DNPDs) were tethered to the surface of PSNPs, acting as the pseudorotaxane rod, followed by the assembly of cyclobis(paraquat-*p*-phenylene) ($CBPQT^{4+}$) which non-covalently complexed with DNPD. The bulky $CBPQT^{4+}$ tetracations thus obstruct the pore openings. The sample was loaded with a fluorescent dye [tris(2,2′-phenylpyridyl)iridium(III)] to investigate the release behavior of this complex system. Upon addition of reducing agent, the pseudorotaxanes on the PSNP surface immediately dethreaded and opened up the pores. A fast increase in luminescence intensity was observed, thus indicating a rapid release of entrapped molecules.

The system was improved by including a second recognition site derived from tetrathiafulvalene (TTF) (Nguyen et al. 2005). A much stronger binding affinity between $CBPQT^{4+}$ and TTF exists than between $CBPQT^{4+}$ and DNPD, which ensured that over 95% of the $CBPQT^{4+}$ rings encircled the TTF station. However, oxidization of the TTF component to TTF^{2+} destabilized this interaction and repel the $CBPQT^{4+}$ rings to shuttle along the axis to the DNPD recognition sites. This process is reversible upon the

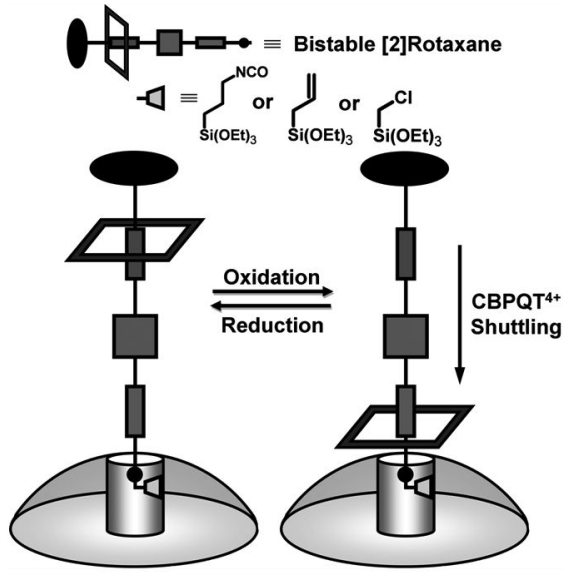

Figure 9.8. Graphical representation of the assembly of bistable [2]rotaxanes to form nanovalves and the possible positions (IN and OUT) regulated by the oxidation state. The cycle can be repeated several times.

addition of a reducing agent, such as, ascorbic acid, so that the $CBPQT^{4+}$ ring returns to the thermally favored TTF sites. They later established a general trend for the optimal design of their system: small guest molecules require short linkers and large guest molecules require long linkers.

Temperature-triggered release

The local temperature difference between tumor sites and non-tumor sites has been shown to be useful as an internal trigger for the controlled release of drugs. It is desirable to design a temperature-responsive drug carrier that only releases drugs at temperatures above 37°C, but keeps drugs encapsulated while in circulation. Poly(*N*-isopropylacrylamide) (PNiPAAm), a popular thermosensitive polymer, has been functionalized onto PSNPs to modulate the transport of guest molecules (Rama Rao et al. 2002, Fu et al. 2003, 2007, Yang et al. 2008, You et al. 2008). PNiPAAm has a Low Critical Solution Temperature (LCST) close to 37°C (Heskins and Guillet 1968), below which it is hydrated and swollen so that it covers the cavities of PSNPs. While at temperatures above LCST, PNiPAAm undergoes a conformation change to a hydrophobic, shrunken state in aqueous solution, thus opening up the pore entrance (Pelton 2000, Li et al. 2007).

Initial studies were conducted by Lopez and co-workers, where they demonstrated three different approaches to prepare hybrid PNiPAAm-functionalized PSNPs (Rama Rao et al. 2002, Fu et al. 2003, 2007). In their first method, PNiPAAm was mixed with silica precursors at the condensation stage, giving rise to a sample with random porosity (Rama Rao et al. 2002). The product was found not feasible as a drug carrier due to its limited mass transport property. Their second mechanism was to form a copolymer of *N*-isopropylacrylamide and 3-methacryloxypropyltrimethoxysilane through free radical polymerization (Fu et al. 2007). Then, the PNiPAAm-silane copolymer was allowed to co-condense with TEOS to obtain PNiPAAm-functionalized PSNPs. But the particles were too large to be applied for intracellular application. So a third approach was proposed by growing PNiPAAm on the external surface of pre-synthesized PSNPs (Fu et al. 2003). This method is widely used because particle size can be very well controlled (Yang et al. 2008, You et al. 2008). Typically, a polymerization initiator, 1-(trichlorosilyl)-2-(*m*/*p*-(chloromethyl)phenyl)ethane was grafted onto PSNPs, followed by an *in situ* atom-transfer radical polymerization of monomers at a slow and uniform rate to prevent clogging of the pores with free polymers. Additionally, the degree of polymerization could be tuned. It was further demonstrated that the PNiPAAm-coated PSNPs were able to uptake fluorescein molecules at low temperatures and release them at temperatures above LCST. Investigations in the cellular properties of PNiPAAm-coated PSNPs showed no acute cytotoxicity and

good endocytosis efficiency on human breast carcinoma cells. Successful intracellular release of a fluorescent dye at elevated temperature was observed by confocal fluorescence microscopy.

Another thermoresponsive uncapping mechanism was developed based on DNA oligomers. The Bein research group attached biotin-labeled DNA double strands onto the external surface of PSNPs by click chemistry (Schlossbauer et al. 2010). Avidin proteins were then coordinated with biotin and capped the pores of the NPs. Upon temperature increase, the DNA double strands would dehybridize and release the biotin-avidin moiety into suspension, reaching an "open state". By picking different lengths of DNA oligomers, they were able to control the temperature threshold for gate opening. This DNA dehybridization induced uncapping mechanism enables a precise adjustment for desired applications.

Enzyme-triggered release

The development of smart, controlled release delivery systems triggered by biomolecules, such as, enzymes, is a very promising research direction, owing to their excellent biocompatibilities and their rapid and specific biological activities.

An enzyme-responsive CD containing rotaxane was reported by Patel et al. (2008) (Fig. 9.9). PSNPs were functionalized with monoazide-terminated triethylene glycol (TEG) by a two-step grafting process. After soaking the PSNPs in a solution of RhB, α-CD was threaded onto the TEG chain and effectively blocked the pores. A bulky adamantyl ester-linked stopper group was tethered to the terminal azide groups by Huisgen cycloaddition, and hence interlocked α-CD to the rotaxane stalk. An enzyme-triggered release was verified by the addition of porcine liver esterase which broke the ester bonds on the stopper groups and enabled α-CD rings to escape from the TEG thread, therefore permitting the diffusion of cargo molecules. It is interesting to note that when the ester bond of the stopper group was replaced by an amide bond, it was no longer activated by esterase cleavage, thus demonstrating a high selectivity of the enzyme.

An extensively applied linker system is the biotin-avidin linker first prepared by Bein and co-workers, synthesizing biotinylated PSNPs by a reaction of thiol-functionalized PSNPs and biotin-maleimide (Schlossbauer et al. 2009). The avidin caps were then strongly complexed to the biotin terminals on the PSNPs, forming a tight closure of the pores. The avidin-biotin linked PSNPs exhibited zero release until the addition of protease trypsin, which digested avidin by the tryptic hydrolysis process and led to the release of guest molecules. Release reached completion after 140 minutes following the treatment of trypsin. The biotin-avidin linker was also useful for targeted drug delivery.

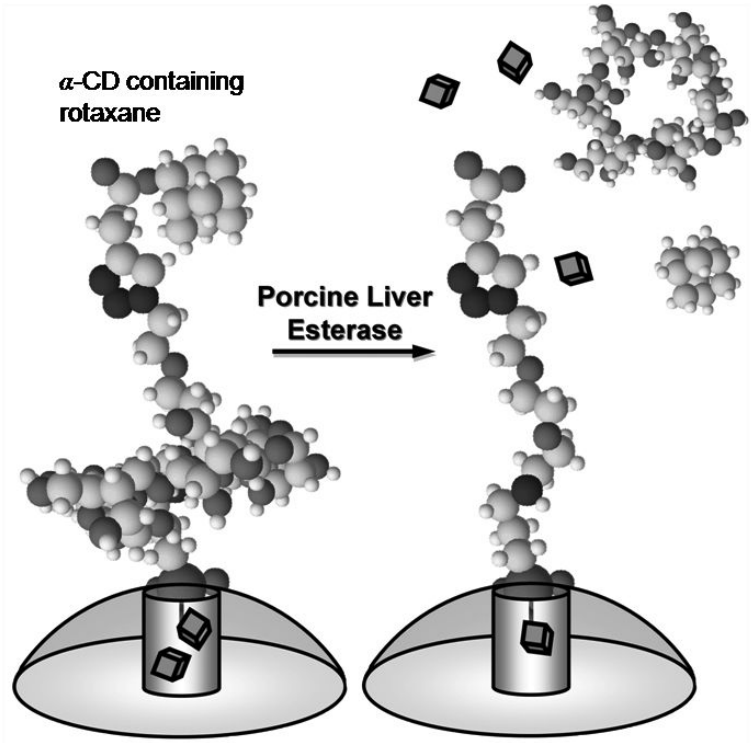

Figure 9.9. Esterase-activated pore opening of α-CD containing rotaxane-capped PSNPs.

Another approach to develop enzyme-sensitive linkers was reported by Bernardos et al. (2009). PSNP as a starting material was loaded with $[Ru(bipy)_3]Cl_2$ for monitoring the enzyme controlled release process. This sample was then capped with β-D-galactose and β-D-glucose disaccharides linked triethoxysilane. The capped sample was resuspended in a pH 7.5 buffer solution. Only a negligible release of cargo was observed after 5 hours. In contrast, the addition of β-D-galactosidase hydrolyzed the glycosidic bond, resulting in a decrease in the size of the capping agent, and induced $[Ru(bipy)_3]Cl_2$ cargo release. They also demonstrated that when the capped sample was treated with either digestive pepsin or denatured β-D-galactosidase, no release was observed, thus demonstrating that β-D-galactosidase was responsible for dye release in their experiments.

Other stimuli

A novel biocompatible surfactant-assisted controlled release system was proposed by Tsai et al. (2011). The high cytotoxicity has always been a defect

of the traditional cetyltrimethylammonium pore template, therefore the surfactant molecules have to be adequately removed before administration. To avoid this problem, a non-cytotoxic anionic surfactant, undec-1-en-11-yltetra(ethylene glycol) phosphate monoester (PMES), was developed to function as a structure directing agent. The presence of hydrophobic tails on the surfactant makes this material especially effective for the uptake of hydrophobic molecules. The PMES-modified PSNPs sample possesses a four-fold greater loading ability for hydrophobic molecules in comparison to the calcined sample. Release of guest molecules occurred in conjunction with the diffusion of PMES when the drug-loaded PMES-PSNPs were suspended in a PBS solution. The authors confirmed good biocompatibility and high cellular uptake efficiency for the PMES-modified PSNPs. In addition, an intracellular DOX release was exemplified with CHO cells.

A glucose-responsive delivery system was fabricated by Lin and co-workers consisting of phenylboronic acid (PBA)-modified PSNPs and gluconic acid-modified insulin (G-Ins) (Zhao et al. 2009) (Fig. 9.10). The G-Ins serving as caps were attached to PBA-PSNPs through reversible covalent bonding between the vicinal diols of G-Ins and the PBA groups on the NPs. Release of guest molecules can be triggered by introducing saccharides (i.e., glucose), which forms much more stable cyclic esters with PBA than the acyclic diols and hence substitutes G-Ins moieties. This system is especially promising for the treatment of diabetes because it responds only at diabetic glucose levels while remaining intact at normal

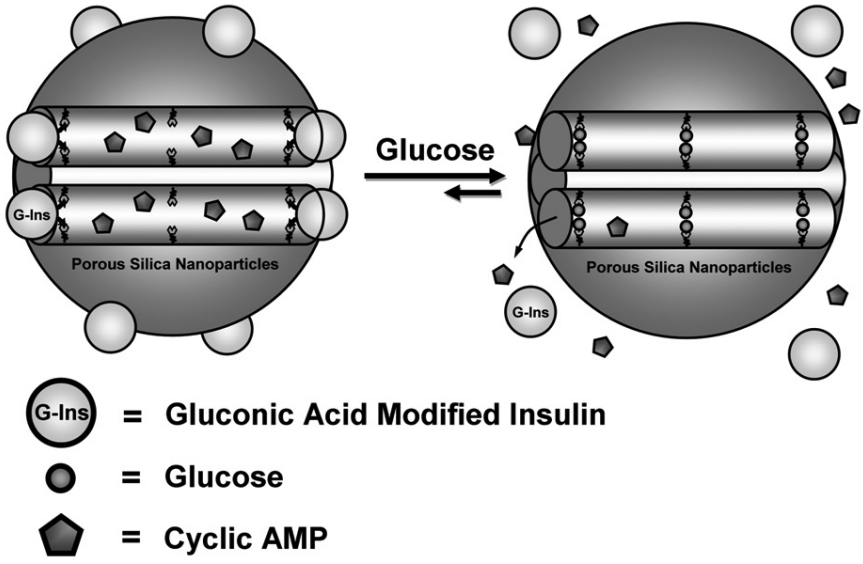

Figure 9.10. Glucose-responsive PSNP-based delivery system for controlled release of bioactive G-Ins and *c*AMP.

conditions. Moreover, cyclic adenosine monophosphate (*c*AMP), known as an insulin secretion stimulating agent, can be encapsulated inside the pores and released subsequent to G-Ins diffusion to achieve a synergic effect for the regulation of blood glucose levels.

The antigen-antibody pair is another strong and specific binding linker for controlled release. Climent et al. (2009) first anchored the outer surface of PSNPs with a derivative of the hapten 4-(4-aminobenzenesulfonylamino) benzoic acid and the orifices were blocked when a polyclonal antibody of sulfathiazole bound to the surface functional group. The delivery protocol of entrapped molecules occurred through a displacement reaction of the sulfathiazole-antibody pairs. Experimental results showed that release efficiency was closely associated with the concentration of sulfathiazole in the buffer solution. The delivery behavior was also determined to be antigen-specific which makes their approach appealing for customizing controlled delivery devices.

A biomolecule-sensitive controlled release system was also reported by Yang and co-workers (Zhu et al. 2011). This modulating scheme took advantage of specific aptamer-target interactions. Adenosine-functionalized PSNPs were synthesized through amide coupling of amine-modified PSNPs and adenosine-5′-carboxylic acid. ATP aptamer-immobilized Au NPs were used as capping agents since the aptamers recognized and attached to the adenosine moieties on the PSNPs. The Au NP caps sufficiently inhibited cargo release in the absence of ATP molecules. In contrast, in the presence of aptamer target molecules, a competitive displacement reaction destroyed the aptamer-adenosine interaction and, thus, cleaved the Au caps from the exterior surface of the PSNPs. Significant release of cargo was then observed. A high specificity of ATP-aptamer affinity was evaluated by comparing the release profiles triggered by ATP, cytidine triphosphate (CTP), guanosine triphosphate (GTP), and uridine triphosphate (UTP). It is noteworthy that other than ATP molecules, the complementary deoxyribonucleic acid (*c*DNA) is also able to selectively and efficiently bind to aptamers and trigger the cargo delivery.

Ultrasound can serve as a non-invasive external stimulus to achieve localized drug delivery. In the work by Honma and co-workers, PSNPs were coated with poly(dimethylsiloxane) which restricted the diffusion of drug molecules (Kim et al. 2006). On the other hand, ultrasound irradiation could enhance the permeability of water and drug molecules through the polymer layer which is explained by the cavitation effect. Diffusion coefficient was four times higher for the ultrasound treated sample than that of the sample under non-ultrasound conditions. Moreover, their material also revealed a regular pulsatile release pattern with repeated ultrasound irradiation.

The Martínez-Máñez and Stroeve research groups constructed a series of alkyl chain anchored PSNPs to control delivery modulation (Aznar et

al. 2012). Pore outlets were decorated with alkylsilanes of variant chain length as diffusion controllers. They demonstrated that longer alkyl chains led to a slower release rate. Therefore, mass transport can be regulated artificially.

Release rates can also be tuned by controlling pore sizes. In a recent study by Gao et al. (2011), PSNPs with pore sizes of 3.2 nm, 6.1 nm and 12.6 nm were prepared and all three materials were loaded with DOX. Through a series of investigations on *in vitro* cytotoxicity, cellular uptake efficiency, intracellular drug release behavior, permeability glycoprotein expression and ATP levels of the drug-resistant MCF-7/ADR cell line, they claimed that PSNPs with a larger pore size could suppress cancer cells more effectively, due to a faster DOX release and a better endocytosis efficiency compared to PSNPs with smaller pores.

Multiple stimuli-triggered release

Along with the extensive research conducted on single stimulus-triggered drug delivery, multi-responsive controlled release systems have been developed to achieve complex release behaviors in either an independent or a synergistic fashion.

A dual pH and light controlled release system based on the combination of pH-sensitive pseudorotaxane and photosensitive nanoimpeller AB was designed by Angelos et al. (2009b). A silylated AB derivative was co-condensed with TEOS to produce pore surface functionalized PSNPs and CB[6]/bisalkylammonium containing pseudorotaxane was anchored on the exterior surface of PSNPs. They determined that cargo delivery occurred only when it was triggered by both stimuli. They envisioned that it is possible to manually regulate the delivery dosage with this system.

Another pH and photo-switch release approach was demonstrated by Aznar et al. (2009). They used a boronate ester linker formed between saccharide-functionalized PSNPs and boronic acid-anchored Au NP caps. Two opening protocols were proposed to break the boronate ester linkage. One is to lower the pH value to 3. The other is to irradiate the material with a laser beam at 1064 nm which induces plasmon resonance excitation in Au NPs to produce a photothermal effect. Both triggers were shown to be able to generate a pulsatile release of guest molecules by administrating stimulus repeatedly.

In another pseudorotaxane-based PSNPs reported by Kim and co-workers, three independent stimuli were confirmed to be capable of sufficiently unblocking the pore voids (Park et al. 2009b). The pseudorotaxane unit consisted of an *o*-nitrobenzene ester containing stalk and a β-CD ring. The stalk can either be ruptured by UV light irradiation or be decomposed by lipase, and the β-CD ring can be digested by α-amylase. Therefore, the

release of guest molecules can be diversely triggered by enzymes or light individually, or by both to achieve a synergistic acceleration effect.

A tristimuli-responsive delivery system was developed by Feng and coworkers involving the construction of a pyridyldithio-containing polymer-functionalized PSNPs that were disulfide bond linked to thiol-modified β-CD (Liu et al. 2009) (Fig. 9.11). The β-CD moieties were further cross-linked by diazo-linkers to inhibit the release of entrapped molecules. Their assembly was expected to respond to UV light irradiation, as well as to the addition of DTT or α-CD. Under a 365 nm UV light, the *trans*- configured diazo-linkers would transform into a *cis*-AB and thus lose their high affinity to β-CD molecules. Addition of DTT would cleave the disulfide linkage between β-CD and PSNPs. The introduction of excess α-CD would result in the formation of a more stable α-CD-diazo cross-linkage and displace β-CD. In all three scenarios, the pore-blocking polymeric network was opened, thus leading to tristimuli-triggered release.

The fact that magnetic nanocrystals are able to generate heat energy under high frequency alternating magnetic fields was applied in the design of temperature-responsive delivery systems by the Vallet-Regí research group (Baeza et al. 2012). Magnetic iron oxide nanocrystals were embedded inside the silica matrix of PSNPs, and the PSNP surface was decorated with a thermosensitive copolymer of poly(ethyleneimine)-*b*-poly(*N*-isopropylacrylamide) (PEI-*b*-PNiPAAm). They demonstrated that this device could deliver proteins with preserved activity, triggered by a temperature increase, as well as an alternating magnetic field that heat up the local environment through encapsulated iron oxide nanocrystals.

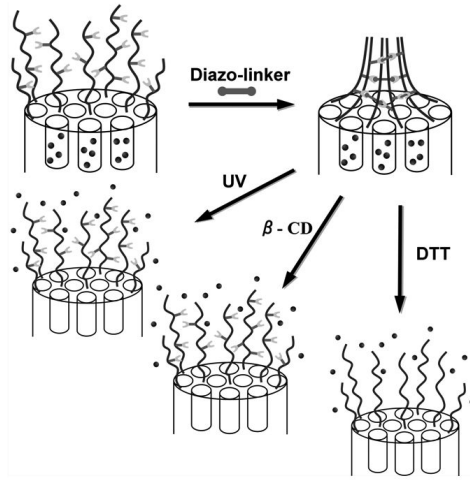

Figure 9.11. Multi-responsive nanogated ensemble based on supramolecular polymeric network-capped PSNPs.

Targeted Drug Delivery by Porous Silica Nanoparticles

Cell-specific targeting is highly attractive as an approach to spontaneously distinguish the site of disease diagnosis and, as a result, this technique reduces the drug dose and diminishes the toxic side effects of drugs during circulation. Both passive strategies and active surface decoration methods have been applied to the fabrication of novel PSNP-based DDS for targeted release.

Passive routes

Passive accumulation of PSNPs in tumor tissue can be realized by the EPR effect, a theory first postulated by Matsumura and Maeda (1986). They hypothesized that the differential localization of macromolecules as well as particles of certain sizes is attributed to the tumor microenvironment, the relative slow elimination rate and poor lymphatic drainage. Effectiveness of the EPR effect can be mediated by particle size, surface charge and/or hydrophobic character. Tamanoi and co-workers demonstrated a preferential accumulation of fluorescently-labeled PSNPs (100–130 nm in diameter) in tumors of mice within 4 hours of an intravenous injection. The fluorescent signal then gradually decreased to the same level as in the whole body after 48 hours (Lu et al. 2010). A similar phenomenon was also reported by the Hyeon research group that PSNPs less than 200 nm in diameter accumulated in tumor 24 hours after administration (Kim et al. 2008).

Surface decoration with targeting ligands

Efforts have been made to functionalize the PSNP surface with cancer-specific targeting ligands for an enhanced particle uptake by cancer cells compared to non-cancerous cells. One such ligand is FA (Rosenholm et al. 2009, Wang et al. 2010, Guo et al. 2012), as folate receptors are overexpressed in several types of human cancer, including ovarian, endometrial, colorectal, breast and lung (Sudimack and Lee 2000). Using FA-conjugated PSNPs, it was observed that the total number of particles internalized by HeLa cancer cells was about one order of magnitude higher than that of FA-modified PSNPs internalized by non-cancerous cells, although non-cancerous cells normally do express folate receptors (Rosenholm et al. 2009). Besides FA, other small cell nutrient molecules, such as, mannose, was also shown to selectively improve the uptake of PSNPs by breast cancer cells (Brevet et al. 2009).

Another group of targeting ligands is the arginine-glycine-aspartic acid (RGD) peptide which interacts with the highly overexpressed $\alpha_v\beta_3$ integrin receptor in metastatic cancers. Lo and co-workers verified an

integrin-dependent endocytosis process of cyclic arginine-glycine-aspartic acid (*c*RGD)-anchored PSNPs by U87-MG cells (Cheng et al. 2010). Furthermore, Zink and co-workers synthesized *c*RGD-modified PSNPs targeting metastatic cancer cells, as well as transferrin-modified PSNPs targeting transferrin receptor overexpressed primary cancer cells (Ferris et al. 2011). They observed a positive interaction between targeting ligands and upregulated receptors. They also envisaged that by altering the surface groups, the PSNP-based DDS can be manipulated to target different stages of cancers.

Further research on the RGD peptide-facilitated cancer cell delivery was conducted by Trewyn research group (Fang et al. 2012). It was found that RGD-modified PSNPs remained in the endosomes for a longer period of time compared to PSNPs without RGD ligand attached. Moreover, their results indicated that the conformation of the RGD peptide affects the uptake efficiency of RGD-modified PSNPs, where *c*RGD peptides possess greater affinity to the cell membrane integrins and facilitate the endocytosis process better, compare to linear RGD peptides. Other proteins or peptides, such as, monoclonal herceptin antibody (Tsai et al. 2009), or TAT peptide (Pan et al. 2012) have also been immobilized onto PSNPs and shown to increase the uptake efficiency by cancerous cells.

Aptamers are recognized as molecule-specific targeting agents, so it is feasible to furnish PSNPs with cell-specific aptamers for targeted delivery. In work by Zhu et al. (2009), a cancer cell-targeted DNA aptamer, sgc8, was selected as a recognition molecule. Significant enhancement of HeLa cell uptake of aptamer-conjugated PSNPs compared to aptamer-free PSNPs was monitored by flow cytometry.

In vivo and *in planta* delivery with Porous Silica Nanoparticles

In vivo delivery

Despite the numerous studies that have demonstrated the *in vitro* therapy efficacy of PSNP-based smart DDSs, the feasibility of using PSNPs for *in vivo* drug delivery has to be further evaluated. Recently, several groups have explored extended *in vivo* investigations. In the experiments on mice carried out by the Tamanoi research group, camptothecin (CPT)-loaded PSNPs showed to be effective in suppressing tumor growth (Lu et al. 2010). For nude mice injected with CPT-loaded PSNPs, the tumor significantly decreased in size or was completely eliminated by the end of treatment (52 days). Another important finding was that a targeting moiety functionalization dramatically increased tumor-suppressing effects of CPT-loaded PSNPs (Lu et al. 2012). FA-modified PSNPs induced an enhanced

tumor inhibition and faster tumor regression than unmodified PSNPs, thus suggesting a good targeting efficacy of FA.

In vivo therapeutic efficacy of PSNP-based DDSs was also assessed by Chen and co-workers (Li et al. 2010). Mice with tumors of ≈ 200 mm^3 were treated with docetaxel (Dtxl)-loaded PSNPs, Taxotere®, or physiological saline for 17 days. It was observed that Dtxl-PSNPs treatment decreased tumor weight to only 28% compared to the control group which was also significantly lower than the tumor weight of the Taxotere® group. The enhanced tumor suppression of Dtxl-PSNPs may be attributed to the sustained drug release as well as intratumor drug accumulation due to the EPR effect.

In planta delivery

PSNP-based systems have also been reported to overcome the rigid plant cell wall barrier and undergo plant cell internalization in a study by Wang and co-workers (Torney et al. 2007) (Fig. 9.12). First, they proved that PSNPs functionalized with TEG were successfully internalized by tobacco mesophyll protoplasts. Using confocal fluorescence microscopy, they demonstrated that TEG-PSNPs can function as DNA delivery agents to efficiently carry the Green Fluorescent Protein (GFP) plasmid into protoplast cells, leading to transgene expression. In depth applications for gene and guest molecules co-delivery with this system were inspected. A chemical trigger, β-estradiol, was loaded into inducible GFP-coated PSNPs and capped with Au NPs by a redox-responsive disulfide linkage. Non-transgenic plants bombarded with this material exhibited gene transcription only after DTT triggered the release of β-estradiol. Their findings indicated

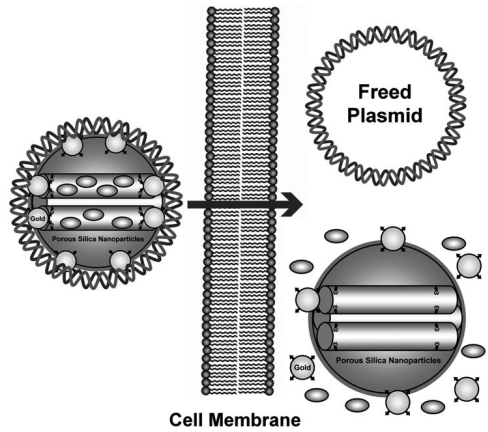

Figure 9.12. DNA plasmid-coated Au NP-capped PSNP for the simultaneous delivery of a gene and its promoter into plant cells.

that PSNP-based delivery systems can be applied to plant science research to aid further investigations of plant genomics and gene function.

Conclusions

The emergence of PSNPs has been appreciated by the biomedical and plant science field for the design of smart drug delivery devices. The unique characteristics of PSNPs have created a fast growing number of stimuli-responsive release systems. A high degree of specificity and control in drug delivery is achieved by versatile uncapping mechanisms and new approaches for PSNP synthesis. However, despite the encouraging progress, these systems are mostly investigated outside the biological system, and have not yet been proven for *in vivo* biomedical applications. Although ingenious work is required to conquer remaining challenges, it is reasonable to believe that these multifunctional PSNP-based DDSs will promote the development in clinical and other biotechnological fields.

Abbreviations

AB	:	azobenzene
ATP	:	adenosine triphosphate
Au	:	gold
BSA	:	bovine serum albumin
*c*AMP	:	cyclic adenosine monophosphate
CB[6]	:	cucurbit[6]uril
$CBPQT^{4+}$	:	cyclobis(paraquat-*p*-phenylene)
CD	:	cyclodextrin
*c*DNA	:	complementary deoxyribonucleic acid
CdS	:	cadmium sulfide
Cl_3SiR	:	organotrichlorosilanes
CMC	:	critical micelle concentration
CPT	:	camptothecin
*c*RGD	:	cyclic arginine-glycine-aspartic acid
*c*RGDyK	:	cyclic arginine-glycine-aspartic acid-D-tyrosine-lysine
CTP	:	cytidine triphosphate
DDS	:	drug delivery system
DNA	:	deoxyribonucleic acid
DNPD	:	1,5-dioxynaphthalene containing derivative
DOX	:	doxorubicin
DTT	:	dithiothreitol
Dtxl	:	docetaxel
EPR	:	enhanced permeability and retention

FA	:	folic acid
Fe_3O_4	:	magnetite
FeSEM	:	field emission scanning electron microscopy
FITC	:	fluorescein isothiocyanate
G-Ins	:	gluconic acid-modified insulin
GFP	:	green fluorescent protein
GTP	:	guanosine triphosphate
LCST	:	low critical solution temperature
LCT	:	liquid crystal templating
MCM-41	:	mobile catalytic material number 41
ME	:	mercaptoethanol
M_W	:	molecular weight
NP	:	nanoparticle
PAA	:	poly(acrylic acid)
PBA	:	phenylboronic acid
PBS	:	phosphate buffered saline
PEI	:	poly(ethyleneimine)
PEI-*b*-PNiPAAm	:	poly(ethyleneimine)-*b*-poly(*N*-isopropylacrylamide)
PEM	:	polyelectrolyte multilayer
PMES	:	undec-1-en-11-yltetra(ethylene glycol) phosphate monoester
PNiPAAm	:	poly(*N*-isopropylacrylamide)
PR	:	photoresponsive
PSNP	:	porous silica nanoparticle
py-*β*-CD	:	pyrene-*β*-cyclodextrin
$(R'O)_3SiR$	:	organotrialkoxysilanes
RAFT	:	reversible addition-fragmentation chain transfer
RBC	:	red blood cell
RGD	:	arginine-glycine-aspartic acid
RhB	:	rhodamine B
SBA-15	:	Santa Barbara Amorphous material number 15
TEG	:	triethylene glycol
TEM	:	transmission electron microscopy
TEOS	:	tetraethyl orthosilicate
TMOS	:	tetramethyl orthosilicate
TSUA	:	4-(3-triethoxylsilylpropylureido)azobenzene
TTF	:	tetrathiafulvalene
UTP	:	uridine triphosphate
UV	:	ultraviolet
UV-CD	:	ultraviolet circular dichroism
2D	:	two dimensional

References

Angelos, S. and Y.W. Yang, K. Patel, J.F. Stoddart and J.I. Zink. 2008. pH-responsive supramolecular nanovalves based on cucurbit[6]uril pseudorotaxanes. Angew. Chem. Int. Ed. 47: 2222–2226.

Angelos, S. and N.M. Khashab, Y.W. Yang, A. Trabolsi, H.A. Khatib, J.F. Stoddart and J.I. Zink. 2009a. pH clock-operated mechanized nanoparticles. J. Am. Chem. Soc. 131: 12912–12914.

Angelos, S. and Y.W. Yang, N.M. Khashab, J.F. Stoddart and J.I. Zink. 2009b. Dual-controlled nanoparticles exhibiting AND logic. J. Am. Chem. Soc. 131: 11344–11346.

Aznar, E. and M.D. Marcos, R. Martínez-Máñez, F. Sancenon, J. Soto, P. Amorós and C. Guillem. 2009. pH- and photo-switched release of guest molecules from mesoporous silica supports. J. Am. Chem. Soc. 131: 6833–6843.

Aznar, E. and F. Sancenon, M.D. Marcos, R. Martínez-Máñez, P. Stroeve, J. Cano and P. Amorós. 2012. Delivery modulation in silica mesoporous supports via alkyl chain pore outlet decoration. Langmuir. 28: 2986–2996.

Baeza, A. and E. Guisasola, E. Ruiz-Hernandez and M. Vallet-Regí. 2012. Magnetically triggered multidrug release by hybrid mesoporous silica nanoparticles. Chem. Mater. 24: 517–524.

Beck, J.S. and J.C. Vartuli, W.J. Roth, M.E. Leonowicz, C.T. Kresge, K.D. Schmitt, C.T.W. Chu, D.H. Olson, E.W. Sheppard, S.B. McCullen, J.B. Higgins and J.L. Schlenker. 1992. A new family of mesoporous molecular sieves prepared with liquid crystal templates. J. Am. Chem. Soc. 114: 10834–10843.

Bernardos, A. and E. Aznar, C. Coll, R. Martínez-Máñez, J. Barat, M.D. Marcos, F. Sancenón, A. Benito and J. Soto. 2008. Controlled release of vitamin B2 using mesoporous materials functionalized with amine-bearing gate-like scaffoldings. J. Control. Release. 131: 181–189.

Bernardos, A. and E. Aznar, M.D. Marcos, R. Martínez-Máñez, F. Sancenón, J. Soto, J.M. Barat and P. Amorós. 2009. Enzyme-responsive controlled release using mesoporous silica supports capped with lactose. Angew. Chem. Int. Ed. Engl. 48: 5884–5887.

Brevet, D. and M. Gary-Bobo, L. Raehm, S. Richeter, O. Hocine, K. Amro, B. Loock, P. Couleaud, C. Frochot, A. Morère, P. Maillard, M. Garcia and J.O. Durand. 2009. Mannose-targeted mesoporous silica nanoparticles for photodynamic therapy. Chem. Commun. (Camb.). 12: 1475–1477.

Cai, Q. and W.Y. Lin, F.S. Xiao, W.Q. Pang, X.H. Chen and B.S. Zou. 1999. The preparation of highly ordered MCM-41 with extremely low surfactant concentration. Micropor. Mesopor. Mater. 32: 1–15.

Casasús, R. and M.D. Marcos, R. Martínez-Máñez, J.V. Ros-Lis, J. Soto, L.A. Villaescusa, P. Amorós, D. Beltrán, C. Guillem and J. Latorre. 2004. Toward the development of ionically controlled nanoscopic molecular gates. J. Am. Chem. Soc. 126: 8612–8613.

Cheng, S.H. and C.H. Lee, M.C. Chen, J.S. Souris, F.G. Tseng, C.S. Yang, C.Y. Mou, C.T. Chen and L.W. Lo. 2010. Tri-functionalization of mesoporous silica nanoparticles for comprehensive cancer theranostics-the trio of imaging, targeting and therapy. J. Mater. Chem. 20: 6149–6157.

Chung, T.H. and S.H. Wu, M. Yao, C.W. Lu, Y.S. Lin, Y. Hung, C.Y. Mou, Y.C. Chen and D.M. Huang. 2007. The effect of surface charge on the uptake and biological function of mesoporous silica nanoparticles in 3T3-L1 cells and human mesenchymal stem cells. Biomaterials. 28: 2959–2966.

Climent, E. and A. Bernardos, R. Martínez-Máñez, A. Maquieira, M.D. Marcos, N. Pastor-Navarro, R. Puchades, F. Sancenón, J. Soto and P. Amorós. 2009. Controlled delivery systems using antibody-capped mesoporous nanocontainers. J. Am. Chem. Soc. 131: 14075–14080.

de Juan, F. and E. Ruiz-Hitzky. 2000. Selective functionalization of mesoporous silica. Adv. Mater. 12: 430–432.

Discher, B.M. and Y.Y. Won, D.S. Ege, J.C.M. Lee, F.S. Bates, D.E. Discher and D.A. Hammer. 1999. Polymersomes: tough vesicles made from diblock copolymers. Science. 284: 1143–1146.

Fang, I.J. and I.I. Slowing, K.C.W. Wu, V.S.Y. Lin and B.G. Trewyn. 2012. Ligand conformation dictates membrane and endosomal trafficking of arginine-glycine-aspartate (RGD)-functionalized mesoporous silica nanoparticles. Chem. Eur. J. 18: 7787–7792.

Ferris, D.P. and Y.L. Zhao, N.M. Khashab, A. Hussam, J.F. Stoddart and J.I. Zink. 2009. Light-operated mechanized nanoparticles. J. Am. Chem. Soc. 131: 1686–1688.

Ferris, D.P. and J. Lu, C. Gothard, R. Yanes, C.R. Thomas, J.C. Olsen, J.F. Stoddart, F. Tamanoi and J.I. Zink. 2011. Synthesis of biomolecule-modified mesoporous silica nanoparticles for targeted hydrophobic drug delivery to cancer cells. Small. 7: 1816–1826.

Fu, Q. and G.V. Rama Rao, L.K. Ista, Y. Wu, B.P. Andrzejewski, L.A. Sklar, T.L. Ward and G.P. Lopez. 2003. Control of molecular transport through stimuli-responsive ordered mesoporous materials. Adv. Mater. 15: 1262–1266.

Fu, Q. and G.V. Rama Rao, T.L. Ward, Y. Lu and G.P. Lopez. 2007. Thermoresponsive transport through ordered mesoporous silica/PNIPAAm copolymer membranes and microspheres. Langmuir. 23: 170–174.

Gao, C. and D. Yan. 2004. Hyperbranched polymers: from synthesis to applications. Prog. Polym. Sci. 29: 183–275.

Gao, Y. and Y. Chen, X. Ji, X. He, Q. Yin, Z. Zhang, J. Shi and Y. Li. 2011. Controlled intracellular release of doxorubicin in multidrug-resistant cancer cells by tuning the shell-pore sizes of mesoporous silica nanoparticles. ACS Nano. 5: 9788–9798.

Giri, S. and B.G. Trewyn, M.P. Stellmaker and V.S. Lin. 2005. Stimuli-responsive controlled-release delivery system based on mesoporous silica nanorods capped with magnetic nanoparticles. Angew. Chem. Int. Ed. Engl. 44: 5038–5044.

Gref, R. and Y. Minamitake, M.T. Peracchia, V. Trubetskoy, V. Torchilin and R. Langer. 1994. Biodegradable long-circulating polymer nanospheres. Science. 263: 1600–1603.

Guo, R. and L.L. Li, W.H. Zhao, Y.X. Chen, X.Z. Wang, C.J. Fang, W. Feng, T.L. Zhang, X. Ma, M. Lu, S.Q. Peng and C.H. Yan. 2012. The intracellular controlled release from bioresponsive mesoporous silica with folate as both targeting and capping agent. Nanoscale. 4: 3577–3583.

He, X. and H. Nie, K. Wang, W. Tan, X. Wu and P. Zhang. 2008. *In vivo* study of biodistribution and urinary excretion of surface-modified silica nanoparticles. Anal. Chem. 80: 9597–9603.

He, Q. and Z. Zhang, F. Gao, Y. Li and J. Shi. 2011. *In vivo* biodistribution and urinary excretion of mesoporous silica nanoparticles: effects of particle size and PEGylation. Small. 7: 271–280.

He, D. and X. He, K. Wang, J. Cao and Y. Zhao. 2012. A light-responsive reversible molecule-gated system using thymine-modified mesoporous silica nanoparticles. Langmuir. 28: 4003–4008.

Heskins, M. and J.E. Guillet. 1968. Solution properties of poly(N-isopropylacrylamide). J. Macromol. Sci. Chem. 2: 1441–1455.

Hoffmann, F. and M. Cornelius, J. Morell and M. Fröba. 2006. Silica-based mesoporous organic-inorganic hybrid materials. Angew. Chem. Int. Ed. Engl. 45: 3216–3251.

Hong, C.Y. and X. Li and C.Y. Pan. 2009. Fabrication of smart nanocontainers with a mesoporous core and a pH-responsive shell for controlled uptake and release. J. Mater. Chem. 19: 5155–5160.

Huang, X. and L. Li, T. Liu, N. Hao, H. Liu, D. Chen and F. Tang. 2011. The shape effect of mesoporous silica nanoparticles on biodistribution, clearance, and biocompatibility *in vivo*. ACS Nano. 5: 5390–5399.

Hudson, S.P. and R.F. Padera, R. Langer and D.S. Kohane. 2008. The biocompatibility of mesoporous silicates. Biomaterials. 29: 4045–4055.

Huh, S. and J.W. Wiench, B.G. Trewyn, S. Song, M. Pruski and V.S. Lin. 2003a. Tuning of particle morphology and pore properties in mesoporous silicas with multiple organic functional groups. Chem. Commun. (Camb.). 18: 2364–2365.

Huh, S. and J.W. Wiench, J.C. Yoo, M. Pruski and V.S. Lin. 2003b. Organic functionalization and morphology control of mesoporous silicas via a co-condensation synthesis method. Chem. Mater. 15: 4247–4256.

Huo, Q. and R. Leon, P.M. Petroff and G.D. Stucky. 1995. Mesostructure design with gemini surfactants: supercage formation in a three-dimensional hexagonal array. Science. 268: 1324–1327.

Huo, Q. and D.I. Margolese and G.D. Stucky. 1996. Surfactant control of phases in the synthesis of mesoporous silica-based materials. Chem. Mater. 8: 1147–1160.

Inagaki, S. and Y. Fukushima and K. Kuroda. 1993. Synthesis of highly ordered mesoporous materials from a layered polysilicate. J. Chem. Soc. Chem. Commun. 8: 680–682.

Jeong, B. and Y.H. Bae, D.S. Lee and S.W. Kim. 1997. Biodegradable block copolymers as injectable drug-delivery systems. Nature. 388: 860–862.

Jiang, W. and B.Y. Kim, J.T. Rutka and W.C. Chan. 2008. Nanoparticle-mediated cellular response is size-dependent. Nat. Nanotechnol. 3: 145–150.

Kim, H.J. and H. Matsuda, H. Zhou and I. Honma. 2006. Ultrasound-triggered smart drug release from a poly(dimethylsiloxane)-mesoporous silica composite. Adv. Mater. 18: 3083–3088.

Kim, J. and H.S. Kim, N. Lee, T. Kim, H. Kim, T. Yu, I.C. Song, W.K. Moon and T. Hyeon. 2008. Multifunctional uniform nanoparticles composed of a Fe_3O_4 nanocrystal core and a mesoporous silica shell for magnetic resonance and fluorescence imaging and for drug delivery. Angew. Chem. Int. Ed. Engl. 47: 8438–8441.

Kresge, C.T. and M.E. Leonowicz, W.J. Roth, J.C. Vartuli and J.S. Beck. 1992. Ordered mesoporous molecular sieves synthesized by a liquid-crystal template mechanism. Nature. 359: 710–712.

Lai, C.Y. and B.G. Trewyn, D.M. Jeftinija, K. Jeftinija, S. Xu, S. Jeftinija and V.S. Lin. 2003. A mesoporous silica nanosphere-based carrier system with chemically removable CdS nanoparticle caps for stimuli-responsive controlled release of neurotransmitters and drug molecules. J. Am. Soc. Chem. 125: 4451–4459.

Lee, C.C. and J.A. Mackay, J.M. Fréchet and F.C. Szoka. 2005. Designing dendrimers for biological applications. Nat. Biotechnol. 23: 1517–1526.

Li, D. and Y. Cui, K. Wang, Q. He, X. Yan and J. Li. 2007. Thermosensitive nanostructures comprising gold nanoparticles grafted with block copolymers. Adv. Funct. Mater. 17: 3134–3140.

Li, L. and F.Q. Tang, H.Y. Liu, T.L. Liu, N.J. Hao, D. Chen, X. Teng and J.Q. He. 2010. *In vivo* delivery of silica nanorattle encapsulated docetaxel for liver cancer therapy with low toxicity and high efficacy. ACS Nano. 4: 6874–6882.

Lim, M.H. and A. Stein. 1999. Comparative studies of grafting and direct syntheses of inorganic-organic hybrid mesoporous materials. Chem. Mater. 11: 3285–3295.

Lin, Y.S. and C.L. Haynes. 2010. Impacts of mesoporous silica nanoparticle size, pore ordering, and pore integrity on hemolytic activity. J. Am. Chem. Soc. 132: 4834–4842.

Liu, R. and Y. Zhang and P. Feng. 2009. Multiresponsive supramolecular nanogated ensembles. J. Am. Chem. Soc. 131: 15128–15129.

Lu, F. and S.H. Wu, Y. Hung and C.Y. Mou. 2009. Size effect on cell uptake in well-suspended, uniform mesoporous silica nanoparticles. Small. 5: 1408–1413.

Lu, J. and M. Liong, Z. Li, J.I. Zink and F. Tamanoi. 2010. Biocompatibility, biodistribution, and drug-delivery efficiency of mesoporous silica nanoparticles for cancer therapy in animals. Small. 6: 1794–1805.

Lu, J. and Z. Li, J.I. Zink and F. Tamanoi. 2012. *In vivo* tumor suppression efficacy of mesoporous silica nanoparticles-based drug-delivery system: enhanced efficacy by folate modification. Nanomedicine. 8: 212–220.

Mal, N.K. and M. Fujiwara and Y. Tanaka. 2003. Photocontrolled reversible release of guest molecules from coumarin-modified mesoporous silica. Nature. 421: 350–353.
Matsumura, Y. and H. Maeda. 1986. A new concept for macromolecular therapeutics in cancer chemotherapy: mechanism of tumoritropic accumulation of proteins and the antitumor agent smancs. Cancer Res. 46: 6387–6392.
Nguyen, T.D. and H.R. Tseng, P.C. Celestre, A.H. Flood, Y. Liu, J.F. Stoddart and J.I. Zink. 2005. A reversible molecular valve. Proc. Nat. Acad. Sci. USA. 102: 10029–10034.
Nguyen, T.D. and Y. Liu, S. Saha, K.C. Leung, J.F. Stoddart and J.I. Zink. 2007. Design and optimization of molecular nanovalves based on redox-switchable bistable rotaxanes. J. Am. Chem. Soc. 129: 626–634.
Pan, L. and Q. He, J. Liu, Y. Chen, M. Ma, L. Zhang and J. Shi. 2012. Nuclear-targeted drug delivery of TAT peptide-conjugated monodisperse mesoporous silica nanoparticles. J. Am. Chem. Soc. 134: 5722–5725.
Park, C. and K. Oh, S.C. Lee and C. Kim. 2007. Controlled release of guest molecules from mesoporous silica particles based on a pH-responsive polypseudorotaxane motif. Angew. Chem. Int. Ed. Engl. 46: 1455–1457.
Park, C. and K. Lee and C. Kim. 2009a. Photoresponsive cyclodextrin-covered nanocontainers and their sol-gel transition induced by molecular recognition. Angew. Chem. Int. Ed. Engl. 48: 1275–1278.
Park, C. and H. Kim, S. Kim and C. Kim. 2009b. Enzyme responsive nanocontainers with cyclodextrin gatekeepers and synergistic effects in release of guests. J. Am. Chem. Soc. 131: 16614–16615.
Patel, K. and S. Angelos, W.R. Dichtel, A. Coskun, Y.W. Yang, J.I. Zink and J.F. Stoddart. 2008. Enzyme-responsive snap-top covered silica nanocontainers. J. Am. Chem. Soc. 130: 2382–2383.
Pelton, R. 2000. Temperature-sensitive aqueous microgels. Adv. Colloid Interface Sci. 85: 1–33.
Peppas, N.A. and P. Bures, W. Leobandung and H. Ichikawa. 2000. Hydrogels in pharmaceutical formulations. Eur. J. Pharm. Biopharm. 50: 27–46.
Peppas, N.A. and J.Z. Hilt, A. Khademohosseini and R. Langer. 2006. Hydrogels in biology and medicine: from molecular principles to bionanotechnology. Adv. Mater. 18: 1345–1360.
Prokop, A. and J.M. Davidson. 2008. Nanovehicular intracellular delivery systems. J. Pharm. Sci. 97: 3518–3590.
Radu, D.R. and C.Y. Lai, J.W. Wiench, M. Pruski and V.S. Lin. 2004a. Gatekeeping layer effect: a poly(lactic acid)-coated mesoporous silica nanosphere-based fluorescence probe for detection of amino-containing neurotransmitters. J. Am. Chem. Soc. 126: 1640–1641.
Radu, D.R. and C.Y. Lai, K. Jeftinija, E.W. Rowe, S. Jeftinija and V.S. Lin. 2004b. A polyamidoamine dendrimer-capped mesoporous silica nanosphere-based gene transfection reagent. J. Am. Chem. Soc. 126: 13216–13217.
Radu, D.R. and C.Y. Lai, J. Huang, X. Shu and V.S. Lin. 2005. Fine-tuning the degree of organic functionalization of mesoporous silica nanosphere materials via an interfacially designed co-condensation method. Chem. Commun. (Camb.). 10: 1264–1266.
Rama Rao, G.V. and M.E. Krug, S. Balamurugan, H. Xu, Q. Xu and G.P. Lopez. 2002. Synthesis and characterization of silica-poly(N-isopropylacrylamide) hybrid membranes: switchable molecular filters. Chem. Mater. 14: 5075–5080.
Rosenholm, J.M. and A. Meinander, E. Peuhu, R. Niemi, J.E. Eriksson, C. Sahlgren and M. Linden. 2009. Targeting of porous hybrid silica nanoparticles to cancer cells. ACS Nano. 3: 197–206.
Saito, G. and J.A. Joel and K.D. Lee. 2003. Drug delivery strategy utilizing conjugation via reversible disulfide linkages: role and site of cellular reducing activities. Adv. Drug Deliv. Rev. 55: 199–215.
Sayari, A. and P. Liu, M. Kruk and M. Jaroniec. 1997. Characterization of large-pore MCM-41 molecular sieves obtained via hydrothermal restructuring. Chem. Mater. 9: 2499–2506.

Schlossbauer, A. and J. Kecht and T. Bein. 2009. Biotin-avidin as a protease-responsive cap system for controlled guest release from colloidal mesoporous silica. Angew. Chem. Int. Ed. Engl. 48: 3092–3095.

Schlossbauer, A. and S. Warncke, P.M. Gramlich, J. Kecht, A. Manetto, T. Carell and T. Bein. 2010. A programmable DNA-based molecular valve for colloidal mesoporous silica. Angew. Chem. Int. Ed. Engl. 49: 4734–4737.

Slowing, I. and B.G. Trewyn and V.S. Lin. 2006. Effect of surface functionalization of MCM-41-type mesoporous silica nanoparticles on the endocytosis by human cancer cells. J. Am. Chem. Soc. 128: 14792–14793.

Slowing, I.I. and B.G. Trewyn and V.S. Lin. 2007. Mesoporous silica nanoparticles for intracellular delivery of membrane-impermeable proteins. J. Am. Chem. Soc. 129: 8845–8849.

Song, S.W. and K. Hidajat and S. Kawi. 2005. Functionalized SBA-15 materials as carriers for controlled drug delivery: influence of surface properties on matrix-drug interactions. Langmuir. 21: 9568–9575.

Song, S.W. and K. Hidajat and S. Kawi. 2007. pH-Controllable drug release using hydrogel encapsulated mesoporous silica. Chem. Commun. (Camb.). 42: 4396–4398.

Sudimack, J. and R.J. Lee. 2000. Targeted drug delivery via the folate receptor. Adv. Drug Deliv. Rev. 41: 147–162.

Torchilin, V.P. 2005. Recent advances with liposomes as pharmaceutical carriers. Nat. Rev. Drug Discov. 4: 145–160.

Torney, F. and B.G. Trewyn, V.S. Lin and K. Wang. 2007. Mesoporous silica nanoparticles deliver DNA and chemicals into plants. Nat. Nanotechnol. 2: 295–300.

Trewyn, B.G. and S. Giri, I.I. Slowing and V.S. Lin. 2007. Mesoporous silica nanoparticle based controlled release, drug delivery, and biosensor systems. Chem. Commun. (Camb.). 31: 3236–3245.

Trewyn, B.G. and J.A. Nieweg, Y. Zhao and V.S. Lin. 2008. Biocompatible mesoporous silica nanoparticles with different morphologies for animal cell membrane penetration. Chem. Eng. J. 137: 23–29.

Tsai, C.P. and C.Y. Chen, Y. Hung, F.H. Chang and C.Y. Mou. 2009. Monoclonal antibody-functionalized mesoporous silica nanoparticles (MSN) for selective targeting breast cancer cells. J. Mater. Chem. 19: 5737–5743.

Tsai, C.H. and J.L. Vivero-Escoto, I.I. Slowing, I.J. Fang, B.G. Trewn and V.S. Lin. 2011. Surfactant-assisted controlled release of hydrophobic drugs using anionic surfactant templated mesoporous silica nanoparticles. Biomaterials. 32: 6234–6244.

Vallet-Regí, M. and A. Rámila, R.P. del Real and J. Pérez-Pariente. 2001. A new property of MCM-41: drug delivery system. Chem. Mater. 13: 308–311.

Vallet-Regí, M. and F. Balas and D. Arcos. 2007. Mesoporous materials for drug delivery. Angew. Chem. Int. Ed. Engl. 46: 7548–7558.

Vallhov, H. and S. Gabrielsson, M. Strømme, A. Scheynius and A.E. Garcia-Bennett. 2007. Mesoporous silica particles induce size dependent effects on human dendritic cells. Nano Lett. 7: 3576–3582.

Vartuli, J.C. and K.D. Schmitt, C.T. Kresge, W.J. Roth, M.E. Leonowicz, S.B. McCullen, S.D. Hellring, J.S. Beck, J.L. Schlenker, D.H. Olson and E.W. Sheppard. 1994. Effect of surfactant/silica molar ratios on the formation of mesoporous molecular sieves: inorganic mimicry of surfactant liquid-crystal phases and mechanistic implications. Chem. Mater. 6: 2117–2326.

Vivero-Escoto, J.L. and I.I. Slowing, C.W. Wu and V.S. Lin. 2009. Photoinduced intracellular controlled release drug delivery in human cells by gold-capped mesoporous silica nanosphere. J. Am. Chem. Soc. 131: 3462–3463.

Vivero-Escoto, J.L. and I.I. Slowing, B.G. Trewyn and V.S. Lin. 2010. Mesoporous silica nanoparticles for intracellular controlled drug delivery. Small. 6: 1952–1967.

Wan, Y. and D. Zhao. 2007. On the controllable soft-templating approach to mesoporous silicates. Chem. Rev. 107: 2821–2860.

Wang, L.S. and L.C. Wu, S.Y. Lu, L.L. Chang, I.T. Teng, C.M. Yang and J.A. Ho. 2010. Biofunctionalized phospholipid-capped mesoporous silica nanoshuttles for targeted drug delivery: improved water suspensibility and decreased nonspecific protein binding. ACS Nano. 4: 4371–4379.

Widenmeyer, M. and R. Anwander. 2002. Pore size control of highly ordered mesoporous silica MCM-48. Chem. Mater. 14: 1827–1831.

Wu, S.H. and Y.S. Lin, Y. Hung, Y.H. Chou, Y.H. Hsu, C. Chang and C.Y. Mou. 2008. Multifunctional mesoporous silica nanoparticles for intracellular labeling and animal magnetic resonance imaging studies. Chembiochem. 9: 53–57.

Yang, Y. and X. Yan, Y. Cui, Q. He, D. Li, A. Wang, J. Fei and J. Li. 2008. Preparation of polymer-coated mesoporous silica nanoparticles used for cellular imaging by a "graft-from" method. J. Mater. Chem. 18: 5731–5737.

You, Y.Z. and K.K. Kalebaila, S.L. Brock and D. Oupicky. 2008. Temperature-controlled uptake and release in PNIPAM-modified porous silica nanoparticles. Chem. Mater. 20: 3354–3359.

Zhao, D. and J. Feng, Q. Huo, N. Melosh, G.H. Frederickson, B.F. Chmelka and G.D. Stucky. 1998a. Triblock copolymer syntheses of mesoporous silica with periodic 50 to 300 angstrom pores. Science. 279: 548–552.

Zhao, D. and Q. Huo, J. Feng, B.F. Chmelka and G.D. Stucky. 1998b. Nonionic triblock and star diblock copolymer and oligomeric surfactant syntheses of highly ordered, hydrothermally stable, mesoporous silica structures. J. Am. Chem. Soc. 120: 6024–6036.

Zhao, Y. and B.G. Trewyn, I.I. Slowing and V.S. Lin. 2009. Mesoporous silica nanoparticle-based double drug delivery system for glucose-responsive controlled release of insulin and cyclic AMP. J. Am. Chem. Soc. 131: 8398–8400.

Zhao, Y. and X. Sun, G. Zhang, B.G. Trewyn, I.I. Slowing and V.S. Lin. 2011. Interaction of mesoporous silica nanoparticles with human red blood cell membranes: size and surface effects. ACS Nano. 5: 1366–1375.

Zhu, C.L. and X.Y. Song, W.H. Zhou, H.H. Yang, Y.H. Wen and X.R. Wang. 2009. An efficient cell-targeting and intracellular controlled-release drug delivery system based on mesoporous silica nanoparticle-polyelectrolyte multilayer-aptamer conjugates. J. Mater. Chem. 19: 7765–7770.

Zhu, C.L. and C.H. Lu, X.Y. Song, H.H. Yang and X.R. Wang. 2011. Bioresponsive controlled release using mesoporous silica nanoparticles capped with aptamer-based molecular gate. J. Am. Chem. Soc. 133: 1278–1281.

CHAPTER 10

Iron Oxides in Drug Delivery

Fahima Dilnawaz[a] and *Sanjeeb Kumar Sahoo*[b,*]

ABSTRACT

Iron oxide nanoparticles are extremely useful in biomedical applications especially in drug delivery due to their unique magnetic properties as well as the ability to function at the cellular and molecular level of biological interactions. The use of iron oxide nanoparticles in biomedicine mainly depends on the synthetic routes of preparation, and selection of appropriate agents for surface functionalization. With the incorporation of highly specific targeting ligands and functional moieties, the drug delivery efficacy of iron oxide nanoparticles can be optimized. In this chapter, we will discuss the drug delivery aspects of these magnetic nanoparticles and their huge potential in the field of biomedical sciences.

Introduction

Nanotechnology offers an incredible scope to fabricate, characterize, and especially tailor the functional properties of Nanoparticles (NPs) for biomedical applications (Moghimi et al. 2001, Gupta and Gupta 2005). Inorganic NPs are ideal elements for the construction of nanostructured materials and devices with adjustable physical and chemical properties (Babes et al. 1999). Iron oxide (IO) NPs, such as, maghemite (γ-Fe_2O_3)

Laboratory of Nanomedicine, Institute of Life Sciences, Nalco Square, Chandrasekharpur, Bhubaneswar 751023, Odisha, India.
[a] Email: fahimadilnawaz@gmail.com
[b] Email: sanjeebsahoo2005@gmail.com
* Corresponding author

List of abbreviations after the text.

and magnetite (Fe_3O_4), are used in biomedicine, out of which Fe_3O_4 is a very promising candidate mostly for drug delivery/imaging owing to its biocompatibility and biodegradability (Reddy et al. 2012). In fact, upon metabolism, iron (Fe) ions are added to the body's Fe stores, and are eventually incorporated by erythrocytes as hemoglobin, allowing their safe use *in vivo* (Weissleder et al. 1989).

IO NPs can be produced by a variety of synthesis processes, ranging from traditional wet chemistry solution-based methods to more exotic techniques, such as, laser pyrolysis or chemical vapor deposition. Successful application of Magnetic Nanoparticles (MNPs) are highly dependent on their stability under a range of different synthesis conditions. The performance of the particle is best when it is below the critical size (< 15 nm), subsequently each NP turned out to be single magnetic domain and shows superparamagnetic behavior. Such individual NP has a huge constant magnetic moment and acts like a giant paramagnetic atom with a fast response to applied magnetic fields, negligible remanence (residual magnetism) and coercivity (the field required to bring the magnetization to zero) (Coey 1971). These features make superparamagnetic NPs an attractive platform for a broad range of biomedical applications. The advantageous aspect of superparamagnetism is that the NP can retain its magnetism in the presence of a magnetic field, where as the magnetism disappears when the magnetic field is removed. Hence, it leads to a wide collection of biomedical applications, such as, cell labeling and sorting, targeting and tissue repair, drug delivery, Magnetic Resonance Imaging (MRI), hyperthermia, magnetofection, etc. (Moghimi et al. 2001, Gupta and Gupta 2005). These colloidal IO NPs have demonstrated some degree of success and have shown satisfactory toleration by patients in early clinical trials (Lübbe et al. 2001). In the following section, we will focus on different synthetic routes developed to formulate IO NPs, and on some aspects related to the drug delivery approach in biomedical sciences.

Synthesis Methods of Iron Oxide Nanoparticles

Various synthetic routes have been proposed to formulate IO NPs which controls the morphology, stability and their monodispersion nature. Different popular synthesis methods are exercised towards the synthesis of high quality MNPs, such as, co-precipitation, thermal decomposition and/or reduction, micelle synthesis, hydrothermal synthesis and laser pyrolysis techniques. We will briefly comment on the most significant ones.

Co-precipitation method

Co-precipitation is the simple and suitable way to synthesize IO NPs (either Fe_3O_4 or γ-Fe_2O_3) from aqueous Fe^{2+}/Fe^{3+} salt solutions, by the addition of

a base under inert atmosphere (by purging N_2 gas) at room temperature and at elevated temperature. The ratio of Fe^{2+} and Fe^{3+}, ionic strength of the media, pH, and salts used (e.g., chlorides, sulfates, nitrates, perchlorates, etc.) mostly control the size and shape, and composition of the NPs (Massart 1981). This synthetic route yields NPs with rich magnetic saturation values in the range of 30–70 emu/g. However, synthetic Fe_3O_4 NPs are not very stable under ambient conditions, thus being frequently subjected to oxidation. On the contrary, in the formation of γ-Fe_2O_3 NPs (ferrimagnets), oxidation is the less significant problem. In order to prevent the Fe_3O_4 NPs from oxidation as well as agglomeration, they are usually coated with organic or inorganic materials during the precipitation process. In addition, the adsorption of additives during the precipitation process inhibits the growth of the particles and favors the creation of smaller particles.

Microemulsion method

Microemulsions are colloidal systems thermodynamically stable. They are isotropic liquid mixtures of oil, water and surfactants often in combination with a cosurfactant. In this method, i.e., water-in-oil (w/o) fine microdroplets of the aqueous phase are trapped within assemblies of surfactant molecules dispersed in a continuous oil phase. The surfactant-stabilized microcavities (typically in the range of 10 nm) provide a confinement effect that limits particle nucleation, growth and agglomeration. MNPs $\approx$ 4 nm in diameter can be prepared by the controlled hydrolysis with reduction of ammonium hydroxide-based iron(II) chloride ($FeCl_2$) and iron(III) chloride ($FeCl_3$) aqueous solutions within the reverse micelle nanocavities generated by using dioctyl sodium sulfosuccinate (or docusate sodium) as surfactant and heptane as the continuous oil phase (López-Quintela and Rivas 1993). The reverse micelle reaction can also be carried out using cetyltrimethylammonium bromide (CTAB) as the surfactant, octane as the oil phase and aqueous reactants as the water phase. Therefore, the w/o microemulsion method has the versatility to prepare nano-sized particles, which makes this technique useful for both *in vivo* and *in vitro* biomedical applications.

Synthesis of polyol

This technique is very promising in the preparation of uniform NPs to be used in biomedicine (e.g., for drug delivery and MRI applications). The liquid polyol (compound with multiple hydroxyl functional groups) acts as the solvent for the synthesis of Fe-based alloys (Fievet et al. 1989). The reaction takes place between Fe_2Cl_3, sodium hydroxide (NaOH), and Ethylene Glycol (EG) or Poly(Ethylene Glycol) (PEG), and particle

precipitation occurs at a particular temperature range (80–100ºC) to form nanoparticulate clusters (≈ 300 nm-sized). When propylene glycol is used as the solvent, IO NPs rapidly self-assemble with many misarrangements into nanoparticulate clusters (≈ 50 nm-sized). As the reaction time extends, these clusters collapse and splits into porous NPs.

Size-controlled IO NPs (9–10 nm in size) can also be formulated by using chloroplatinic acid or hexachloroplatinic acid hexahydrate [$H_2PtCl_6 \cdot (H_2O)_6$] as the nucleating agent. However, the size of cubic Fe particles synthesized without the nucleating agent has been defined to be ≈ 150 nm. In fact, it has been postulated that gradual decrease in size can be possible with an increase in platinum (Pt) ion concentration (Joseyphus et al. 2007).

High-temperature decomposition of organic precursor's synthesis method

In this method, the Fe precursors are decomposed in the presence of hot organic surfactants yielding good size control, crystallinity, narrow size distribution and dispersible magnetic IO NPs. It has been reported that injecting solutions of iron cupferron complex ($FeCup_3$) (Cup: *N*-nitrosophenylhydroxylamine) in octylamine at 250–300ºC can yield γ-Fe_2O_3 nanocrystals (≈ 4 to 10 nm in size) which are dispersible in organic solvents (Rockenberger et al. 1999). Monodispersed Fe_3O_4 NPs (size: 3–20 nm) can be formed at high temperature (265ºC) by reacting Fe(III) acetylacetonate with phenyl ether in the presence of alcohol, oleic acid and oleylamine (Sun and Zeng 2002). MNPs prepared by this method can be used for drug delivery, MRI, magnetic cell separation and magneto-relaxometry.

Role of the polymeric coating on biomedical applications

NPs are more reactive than their bulk counterparts given their high surface to volume ratio. Therefore, to utilize IO NPs in biomedicine, consideration of stability and long term storage of the particulate system is of utmost important. However, bare IO NPs demonstrate instability during the synthesis process because of the existence of strong hydrophobic interactions between them. As a result, particles tend to agglomerate and form large clusters, thanks to strong magnetic dipole-dipole attractions between them. In this line, large aggregates are also formed because each NP comes into the magnetic field of the neighbor (Tepper et al. 2003).

Encapsulating IO NPs within either organic or inorganic polymers has become the most important approach to overcome such a challenge. This shell provides them with important properties that the naked (uncoated) NPs are deficient in. Moreover, polymer coating enhances compatibility

with organic ingredients, reduce susceptibility to leaching and protect the NP surface from oxidation. Polymeric encapsulation further improves NP dispersibility in an aqueous medium, chemical stability and reduces toxicity. All these characteristics are desirable when biomedical applications are intended. Both synthetic and natural polymers can be incorporated to the IO NP surface. Synthetic polymers, such as, poly(ethylene-*co*-vinyl acetate), poly(D,L-lactide-*co*-glycolide) (PLGA), PEG, poly(methylacrylic acid) (PMAA), polyvinyl alcohol (PVA) and poly(*N*-vinyl-2-pyrrolidone) (PVP), to cite just a few, have been proposed. In this line, natural polymers (e.g., dextran, chitosan, pullulan, and gelatin) (Gupta and Gupta 2005), and surfactants (i.e., sodium oleate, dodecylamine, sodium carboxymethylcellulose, glyceryl monooleate) (Jain et al. 2005, Dilnawaz et al. 2010) have also been investigated.

Longevity of the nanoparticulate system in the blood is a key property in drug delivery approaches based on both passive and active targeting strategies. Generally, when NPs are intravenously injected, they are subjected to opsonization processes. NPs with hydrophobic surfaces are more prone to opsonization due to hydrophobic-hydrophobic interactions with plasma proteins (opsonins). Subsequently, rapid removal of opsonized NPs by the Reticuloendothelial System (RES) takes place (Moghimi et al. 2001). Therefore, chemical modification of IO NPs with certain (synthetic) polymers is the most frequent way to add *in vivo* longevity to these drug delivery systems. In fact, NPs with hydrophilic surfaces (coatings) delay the opsonization process, thus being stabilized in biological suspensions and exhibiting longer circulation times (because of the minimization of RES uptake).

Iron Oxide for Drug Delivery

IO NPs have been widely investigated in the area of drug delivery due to their superior biocompatibility, lack of significant toxicity and non-immunogenic nature, in comparison to other magnetic materials. Several types of IOs exist in nature or can be prepared in the laboratory, but nowadays only Fe_3O_4 or its oxidized form (γ-Fe_2O_3) are able to fulfill such requirements. These small-sized IO particles with large surface area and a significant magnetic responsiveness (allowing to direct them with an external magnetic field), are ideal nanoplatforms for the delivery of therapeutic agents with sustained release activity.

Generally speaking, the MNPs surface can be functionalized using inert metals and/or biomolecules (Fig. 10.1), such as, antibodies, plasmid deoxyribonucleic acid (*p*DNA), and small interfering ribonucleic acid (*si*RNA) for effective *in vivo* therapeutic applications. IO-based drug nanocarriers are expected to exhibit prolonged circulation times and

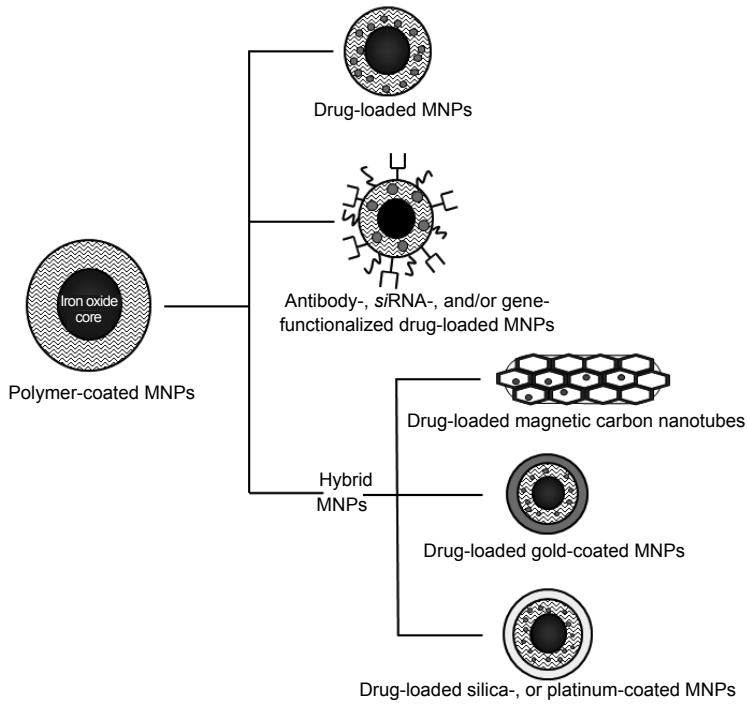

Figure 10.1. Representative functional structures of polymer-coated drug-loaded MNPs.

a selective accumulation in pathological sites with leaky vasculature (i.e., tumor, inflammation and infarcted area), thanks to the enhanced permeability and retention (EPR) effect. The nanoparticulate system can reach the non-healthy site by two ways: *i*) passive targeting (EPR effect-mediated), on the basis of the previously commented longevity of drug-loaded MNPs in blood (Fig. 10.2a); and/or, *ii*) active targeting (ligand-mediated), by attaching specific ligands to the NPs surface that can recognize and bind to specific receptors overexpressed by non-healthy tissues or cells (Fig. 10.2b). These drug targeting strategies are discussed below, by using tumor drug targeting as the illustrative example.

Passive mode of iron oxide-based drug delivery

Passive mode of drug delivery permits the drug to diffuse/penetrate through the vascular system (capillaries), leading to a local therapeutic effect. In this line, superparamagnetic IO NPs have been properly engineered to take advantage of the EPR effect. In the late 1970's, Widder et al. (1978) first attempted the application of IO NPs for drug delivery. It

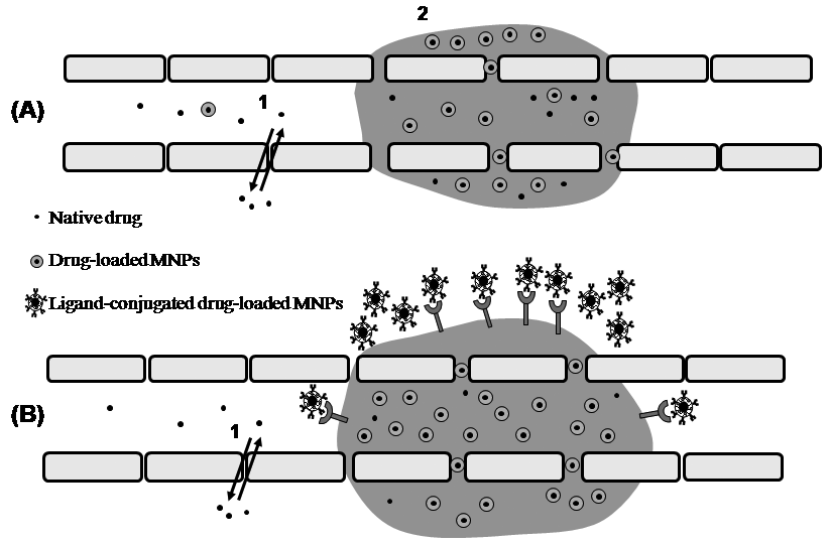

Figure 10.2. (a) Passive drug targeting approach illustrating the EPR effect (1: drug molecules can pass through the endothelium of healthy vessels in both directions; whereas, 2: drug-loaded MNPs cannot extravasate through the normal endothelium and only pass through the leaky vasculature of non-healthy tissues/organs, thus leading to significant drug concentration). (b) Active drug targeting approach where ligand-conjugated drug-loaded MNPs can selectively recognize specific receptors located in the non-healthy tissue/cell, thus leading to an intense internalization processes (drug accumulation).

was described that IO NPs can hold a large drug pay load on their surface, and were driven with the aid of an external magnet to the targeted organ or diseased site.

It has been hypothesized that after systemic administration, NPs larger than 200 nm in diameter are easily taken by the spleen (mechanical filtration), and/or are eventually removed by cells of the RES, thus resulting in decreased blood circulation times. In addition, smaller particles (< 10 nm in diameter) are also rapidly removed from blood by extravasation and renal clearance. On the other hand, particles ranging from ≈ 10 to 100 nm in size have exhibited the most prolonged circulation times, thus being very suitable for intravenous injection. In fact, particles in this size range are small enough to escape from RES, and can penetrate the extremely small capillaries within the body, thus leading to a more effective biodistribution (Stolnik et al. 1995).

In tumor therapy, MNPs targeted by an external magnet are a promising approach to overcome problems associated with conventional chemotherapy (Alexiou et al. 2000): an external magnetic field is used to localize the drug-loaded MNPs at the tumor site where the drug is released either via

enzymatic activity or due to changes in the physiological conditions, such as, pH, osmolality or temperature. Moreover, a phase I human clinical trial with 4-epidoxorubicin-loaded NPs showed encouraging results about the physiological tolerance of magnetic drug targeting by patients (Lübbe et al. 2001). *In vivo* experiments on animal models have also shown that IOs are suitable for drug delivery applications (Alexiou et al. 2000, Lübbe et al. 2001). Antitumor drugs, such as, etoposide, doxorubicin and methotrexate (MTX), have been loaded (attached or encapsulated) to MNPs in order to treat diseases ranging from rheumatoid arthritis to highly malignant prostate and breast cancer (Kohler et al. 2006). In a recent investigation, the controlled delivery and release of MTX in breast and brain tumor cells when loaded to IO NPs was described (Kohler et al. 2006). It was shown that the controlled release of MTX into the cellular cytosol, subsequently improved the cytotoxicity to these cancer cells. In another study conducted by Zhu et al. (2009), camptothecin (CPT) was loaded to polysaccharide-modified IO NPs, which displayed a greater cytotoxic activity on hepatocarcinoma cells.

Active mode of iron oxide-based drug delivery

The active mode of drug delivery by IO NPs is basically based on ligand-receptor recognition processes. In this way, the specific knowledge about the receptors present in the diseased site helps in achieving an effective treatment (with minimized toxicity). IO NPs can be surface functionalized with monoclonal antibodies (MAbs), proteins, antigens, small peptides or vitamins (Reddy et al. 2012). For instance, the arginine-glycine-aspartic acid (RGD) peptide have demonstrated high affinity for the $\alpha_v\beta_3$ integrins overexpressed by different cancer cell lines, thus MNPs can be functionalized with this biomolecule for the targeted drug delivery to breast tumors, malignant melanomas or squamous cell carcinomas. Generally speaking, it can be stated that all these active drug targeting strategies are preferable than the passive ones as they can be easily obtained by an enhanced cellular NP uptake through receptor-mediated endocytosis, hence leading to an efficient therapeutic outcome.

In a recent research report it was described that lectin-conjugated paclitaxel (PTX)-loaded MNPs showed a greater cellular uptake and a lower half maximum inhibitory concentration (IC_{50}) value in comparison with non-functionalized PTX-loaded MNPs and the native drug, thus suggesting the efficacy of the active targeted delivery strategy (Singh et al. 2011). Similarly, drug-loaded MNPs surface decorated with chlorotoxin (CTX) moieties (which are associated with the membrane-bound matrix metalloproteinase-2, MMP-2, protein complex) have shown a very promising therapeutic activity compared to controls in brain tumor cells (Deshane et al. 2003).

MAb-based targeting approach was the first ligand-based strategy to be exploited to deliver MNPs to non-healthy sites (Cerdan et al. 1989) and, given its high specificity, continues to be widely used. Such surface functionalized IO NPs have demonstrated their enhanced uptake by targeted cells compared to non-functionalized IO NPs. The formulation of MAb-functionalized IO NPs typically involves a preliminary stage consisting in the proper modification of IO surface to enable the attachment of the targeting moiety, i.e., by utilizing cleavable linkers or molecules that can develop electrostatic interactions with the MAb moieties.

Recently (Dilnawaz et al. 2010), MAbs against the human epidermal growth factor receptor 2 (HER2) were chemically conjugated to MNPs loaded with PTX and rapamycin. The antibody-conjugated MNPs demonstrated an enhanced *in vitro* cytotoxic activity against MCF-7 human breast carcinoma cell compared to unconjugated drug-loaded MNPs.

Iron Oxide Nanoparticles for Hyperthermia and Drug Delivery

Hyperthermia treatment is generally used against cancer, where the affected tissue is exposed to high temperatures (up to 113ºF) in order to damage and kill cancer cells. The therapeutic approach can also be used along with radiation/or and chemotherapy. IO NPs can create a magnetic induction hyperthermia when subjected to an Alternating Magnetic Field (AMF). This magnetic field is not absorbed by living tissues and, therefore, can be applied to deep regions in the living body. When IO NPs are subjected to an AMF, some heat is generated due to magnetic hysteresis loss. This phenomenon strongly depends on the strength and frequency of oscillation of the AMF.

In vivo experiments have demonstrated that cancer cells can be destroyed at temperatures > 43ºC (Luderer et al. 1983). For example, dextran magnetite (DM) NPs have been synthesized for oral cancer hyperthermia. DM NPs were locally injected to tumor (tongue carcinoma)-bearing hamsters, and then were heated up to 43–45ºC when exposed to an AMF (500 kHz). Experimental results demonstrated that the inhibition of the growth of cancer cells was significantly greater than that observed in the control group (Wada et al. 2003). In another study (Balivada et al. 2010), Fe/Fe_3O_4 core/shell MNPs were decorated with porphyrin before intratumor or intravenous administration to mice bearing B16-F10 melanomas. Hyperthermia activation (AMF of 366 kHz, applied thrice during 10 minutes) induced a significant decrease in tumor size. Finally, MNPs can be successfully used for both targeted hyperthermia and controlled drug delivery (Fig. 10.3) (Branca et al. 2008).

Gene therapy can also take advantage of MNP-based hyperthermia. In fact, it has been hypothesized that heat-induced gene expression is highly desirable to minimize the side effects associated to the conventional therapy. For instance, MNPs embedded in oligomannose-coated liposomes (OMLs) can successfully control tumor growth *in vivo* by developing a hyperthermia effect (Ikehara et al. 2006). MNP-based hyperthermia has further been suggested to induce an intense antitumor immunity in the body (heat immune-based therapy), thus determining an important tumor reduction as well as protection from future tumor development. This activity has been demonstrated in melanoma nodules (Suzuki et al. 2003) and mammary carcinoma cells (Sincai et al. 2005).

Finally, MNPs can also be used as bimodal anticancer agents for combined photodynamic therapy (PDT) and hyperthermia therapy. In this line, Gu et al. (2005) have reported the use of porphyrin-IO nanoparticulate conjugates to obtain an intense apoptotic effect against HeLa cancer cells.

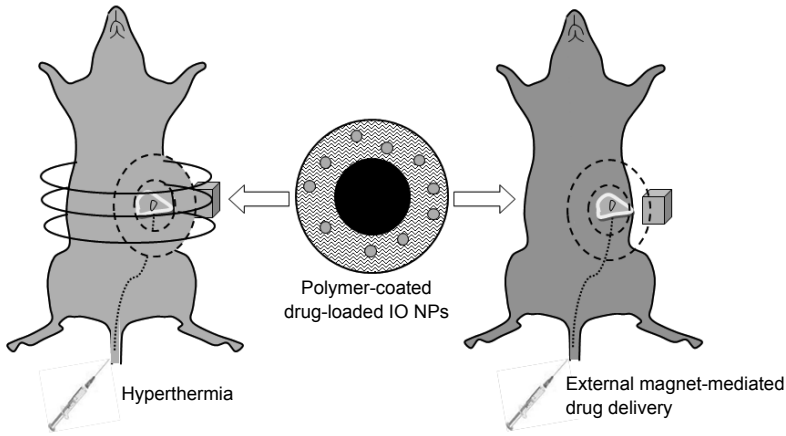

Figure 10.3. Polymer-coated drug-loaded IO NPs for both targeted hyperthermia and controlled drug delivery applications.

Hybrid Iron Oxide Nanoparticles and Drug Delivery

Metallic NPs, i.e., gold (Au), silver (Ag), and Pt, have fascinated scientists for several centuries, because of the colorful colloidal solutions that can be prepared with them, and because of their excellent optical properties, especially useful for biomedical applications (optical contrast agent, multimodal sensor combining optical and scattering imaging and photothermal therapy). Similar possibilities have been described for

silica NPs, especially in drug delivery. Of course, if the *in vivo* fate of all of these nanoparticulate systems could be magnetically controlled, a much better activity could be expected. This may be the most important reason for combining IO NPs with biocompatible metallic and silica shells. In addition, such hybrid nanoparticulate systems can be surface modified with various biological ligands for drug delivery, imaging and hyperthermia applications.

Gold-coated magnetic nanoparticles and drug delivery

Au-coated MNPs have attracted much attention in drug delivery because of their advantageous characteristics, such as, inertness, negligible toxicity, supermagneticity, ease detection in the human body, protection of the magnetic core against oxidation, ability to interact with biomolecules [e.g., polypeptides, deoxyribonucleic acid (DNA), and polysaccharides], facilitated bioconjugation and catalytic surface, thus having the potentiality for a variety of biological applications (Chen et al. 2003). For instance, Au-Fe_3O_4-biopolymer nanocomposites have attracted much attention in biotechnology and biomedicine, given their potential use for cancer treatment, drug delivery, biodetection and downstream processing (i.e., the purification and bioseparation of biomolecules).

Au-coated MNPs have been conjugated to the adenovirus (Ad) gene delivery vector for *in vitro* and *in vivo* gene transfer to Ad-resistant cells [those characterized by low coxsackievirus and adenovirus receptor (CAR) expression levels] (Kamei et al. 2009). The use of an external magnetic field permitted the penetration of the NPs into the targeted cells (B16BL6 mouse melanoma cells). Moreover, in this investigation, it was demonstrated that these NPs enhanced the expression levels of Enhanced Green Fluorescent Protein (EGFP) in the presence of a magnetic field, while poor expression levels were obtained with conventional Ad-EGFP, thus suggesting the importance of the NPs' magnetism to the cell type-independent penetration (and efficient gene expression).

Silica-coated magnetic nanoparticles and drug delivery

Silica is a biocompatible, non-toxic and chemically stable material suitable for preventing the degradation and agglomeration of MNPs in biological environments. In addition, the silica surface can be easily functionalized for bioconjugation purposes, favoring the capability of any given NP to interact with cells and tissues more effectively. In this way, silica-containing magnetic nanostructures show great promise for drug (and gene) delivery purposes (Li et al. 2011, Chen et al. 2012), hyperthermia (Chen et al. 2012) and as contrast agents for MRI (Chen et al. 2011).

For example, it has been recently demonstrated that magnetic silica NPs loaded with DNA fragments can be efficiently internalized by Caco-2 cells, reaching the endolysosomal compartments after 24 hours of incubation at 37ºC (Davila-Ibanez et al. 2012). In another study, magnetic silica nanotubes exhibited excellent possibilities as multifunctional drug carriers, and for applications in hyperthermia therapies (Chen et al. 2012). γ-Fe_2O_3 NPs served as templates for the fabrication of these nanotubes. Under exposure to an AMF, these magnetic silica NPs showed a significant heating effect. Apart from that, the NPs exhibited enhanced drug (rhodamine B) loading and sustained release capabilities. It has been proposed that the hollow inner space and the magnetic functionalization render the material promising for such biomedical applications.

In another investigation, Magnetic Mesoporous Silica Nanoparticles (MMSNPs) were synthesized for delivering drugs or biomolecules (*si*RNA or DNA) to non-healthy cells or tissues. In fact, these NPs exhibited a negligible cytotoxicity and excellent *si*RNA-loading capabilities and intracellular transfection efficiencies *in vitro*, thus being of interest for *si*RNA delivery and gene silencing. Briefly, *si*RNA was loaded to the poly(ethyleneimine) (PEI) shell onto the MMSNP surface. The PEI matrix protected *si*RNA from enzymatic degradation. It was shown that the NPs were internalized into A549 cancer cells, releasing *si*RNA in the cytoplasm. In gene silencing experiments, the NPs very efficiently mediated the knockdown of both the exogenous EGFP gene and the endogenous B-cell lymphoma 2 (Bcl-2) gene, upon successful *si*RNA release (Li et al. 2011).

Platinum-containing magnetic nanoparticles and drug delivery

Pt-containing magnetic nanostructures are promising platforms for biomedical applications, i.e., drug delivery.

For instance, iron platinum (FePt)/cobalt sulfide (CoS) yolk/shell nanocrystals have been proposed as potent agents to kill HeLa cells when loaded with cisplatin (Gao et al. 2007). In fact, the cytotoxicity activity of FePt/CoS NPs on HeLa cells showed lower IC_{50} values than that of native cisplatin. In this approach, FePt was used as seed to which there was sequential growth of CoS porous nanoshells thanks to the Kirkendall effect.

Conclusions

With the introduction of nanotechnology, it is possible to synthesize IO NPs with narrow size distribution along with superparamagnetic properties. IO NPs have become an important material for biomedical applications if they are properly coated by (principally) a polymeric matrix. Further,

metallic-based IO NPs are developed for delivering small biomolecules to the targeted site, thus permitting an effective therapy. With the advent of external magnetic fields, precise controlled delivery of drugs at the desired site of action can be achieved, hence leading to a rapid drug effect, a reduction in the drug dose and a minimization of side effects in healthy tissues. Thus, the IO-based (nano) approach opens very promising opportunities in therapy that can benefit patients.

Acknowledgements

F. Dilnawaz gratefully acknowledges the Department of Science and Technology, Government of India, for a women scientist fellowship (WOS-A). The authors are very thankful to Abhalaxmi Singh for reading the chapter.

Abbreviations

Ad	:	adenovirus
Ag	:	silver
AMF	:	alternating magnetic field
Au	:	gold
Bcl-2	:	B-cell lymphoma 2
CAR	:	coxsackievirus and adenovirus receptor
CoS	:	cobalt sulfide
CPT	:	camptothecin
CTAB	:	cetyltrimethylammonium bromide
CTX	:	chlorotoxin
Cup	:	*N*-nitrosophenylhydroxylamine
DM	:	dextran magnetite
DNA	:	deoxyribonucleic acid
EG	:	ethylene glycol
EGFP	:	enhanced green fluorescent protein
EPR	:	enhanced permeability and retention
Fe	:	iron
$FeCl_2$	:	iron(II) chloride
$FeCl_3$	:	iron(III) chloride
$FeCup_3$	:	iron cupferron complex
Fe_3O_4	:	magnetite
γ-Fe_2O_3	:	maghemite
FePt	:	iron platinum
HER2	:	human epidermal growth factor receptor 2
$H_2PtCl_6 \cdot (H_2O)_6$	:	chloroplatinic acid or hexachloroplatinic acid hexahydrate

IC_{50}	:	half maximum inhibitory concentration
IO	:	iron oxide
MAb	:	monoclonal antibody
MMP-2	:	matrix metalloproteinase-2
MNP	:	magnetic nanoparticle
MRI	:	magnetic resonance imaging
MTX	:	methotrexate
NaOH	:	sodium hydroxide
NP	:	nanoparticle
OML	:	oligomannose-coated liposome
PDT	:	photodynamic therapy
PEG	:	poly(ethylene glycol)
PEI	:	poly(ethyleneimine)
PLGA	:	poly(D,L-lactide-*co*-glycolide)
PMAA	:	poly(methylacrylic acid)
Pt	:	platinum
PTX	:	paclitaxel
PVA	:	polyvinyl alcohol
PVP	:	poly(*N*-vinyl-2-pyrrolidone)
RES	:	reticuloendothelial system
RGD	:	arginine-glycine-aspartic acid
RNA	:	ribonucleic acid
*si*RNA	:	small interfering ribonucleic acid
w/o	:	water-in-oil

References

Alexiou, C. and W. Arnold, R.J. Klein, F.G. Parak, P. Hulin, C. Bergemann, W. Erhardt, S. Wagenpfeil and A.S. Lübbe. 2000. Locoregional cancer treatment with magnetic drug targeting. Cancer Res. 60: 6641–6648.

Babes, L. and B. Denizot, G. Tanguy, J.J. Le Jeune and P. Jallet. 1999. Synthesis of iron oxide nanoparticles used as MRI contrast agents: a parametric study. J. Colloid Interface Sci. 212: 474–482.

Balivada, S. and R.S. Rachakatla, H. Wang, T.N. Samarakoon, R.K. Dani, M. Pyle, F.O. Kroh, B. Walker, X. Leaym, O.B. Koper, M. Tamura, V. Chikan, S.H. Bossmann and D.L. Troyer. 2010. A/C magnetic hyperthermia of melanoma mediated by iron(0)/iron oxide core/shell magnetic nanoparticles: a mouse study. BMC Cancer. 10: 119.

Branca, T. and C. Leuschner, C. Kumar, B. Fubara, W. Warren and B. Driehuys. 2008. Hyperpolarized ^{3}He MRI to detect lung metastases targeted by magnetic nanoparticles. Proc. Intl. Soc. Mag. Reson. Med. 16: 475.

Cerdan, S. and H.R. Lötscher, B. Künnecke and J. Seelig. 1989. Monoclonal antibody-coated magnetite particles as contrast agents in magnetic resonance imaging of tumors. Magn. Reson. Med. 12: 151–163.

Chen, M. and S. Yamamuro, D. Farrell and S.A. Majetich. 2003. Gold-coated iron nanoparticles for biomedical applications. J. Appl. Phys. 93: 7551–7553.

Chen, Y. and C. Chu, Y. Zhou, Y. Ru, H. Chen, F. Chen, Q. He, Y. Zhang, L. Zhang and J. Shi. 2011. Reversible pore-structure evolution in hollow silica nanocapsules: large pores for siRNA delivery and nanoparticle collecting. Small. 7: 2935–2944.

Chen, X. and R. Klingeler, M. Kath, A.A. El Gendy, K. Cendrowski, R.J. Kalenczuk and E. Borowiak-Palen. 2012. Magnetic silica nanotubes: synthesis, drug release, and feasibility for magnetic hyperthermia. ACS Appl. Mater. Interfaces. 4: 2303–2309.

Coey, J.M.D. 1971. Noncollinear spin arrangement in ultrafine ferrimagnetic crystallites. Phys. Rev. Lett. 27: 1140–1142.

Davila-Ibanez, A.B. and V. Salgueirino, V. Martinez-Zorzano, R. Mariño-Fernández, A. García-Lorenzo, M. Maceira-Campos, M. Muñoz-Ubeda, E. Junquera, E. Aicart, J. Rivas, F.J. Rodriguez-Berrocal and J.L. Legido. 2012. Magnetic silica nanoparticle cellular uptake and cytotoxicity regulated by electrostatic polyelectrolytes-DNA loading at their surface. ACS Nano. 6: 747–759.

Deshane, J. and C.C. Garner and H. Sontheimer. 2003. Chlorotoxin inhibits glioma cell invasion via matrix metalloproteinase-2. J. Biol. Chem. 278: 4135–4144.

Dilnawaz, F. and A. Singh, C. Mohanty and S.K. Sahoo. 2010. Dual drug loaded superparamagnetic iron oxide nanoparticles for targeted cancer therapy. Biomaterials. 31: 3694–3706.

Fievet, F. and J. Lagier, B. Blin, B. Beaudoin and M. Figlarz. 1989. Homogeneous and heterogeneous nucleations in the polyol process for the preparation of micron and submicron size metal particles. Solid State Ionics. 32: 198–205.

Gao, J. and G. Liang, B. Zhang, Y. Kuang, X. Zhang and B. Xu. 2007. FePt@CoS(2) yolk-shell nanocrystals as a potent agent to kill HeLa cells. J. Am. Chem. Soc. 129: 1428–1433.

Gu, H. and K. Xu, Z. Yang, C.K. Chang and B. Xu. 2005. Synthesis and cellular uptake of porphyrin decorated iron oxide nanoparticles-a potential candidate for bimodal anticancer therapy. Chem. Commun. (Camb.). 34: 4270–4272.

Gupta, A.K. and M. Gupta. 2005. Synthesis and surface engineering of iron oxide nanoparticles for biomedical applications. Biomaterials. 26: 3995–4021.

Ikehara, Y. and T. Niwa, L. Biao, S.K. Ikehara, N. Ohashi, T. Kobayashi, Y. Shimizu, N. Kojima and H. Nakanishi. 2006. A carbohydrate recognition-based drug delivery and controlled release system using intraperitoneal macrophages as a cellular vehicle. Cancer Res. 66: 8740–8748.

Jain, T.K. and M.A. Morales, S.K. Sahoo, D.L. Leslie-Pelecky and V. Labhasetwar. 2005. Iron oxide nanoparticles for sustained delivery of anticancer agents. Mol. Pharm. 2: 194–205.

Joseyphus, R.J. and D. Kodama, T. Matsumoto, Y. Sato, B. Jeyadevan and K. Tohji. 2007. Role of polyol in the synthesis of Fe particles. J. Magn. Magn. Mater. 310: 2393–2395.

Kamei, K. and Y. Mukai, H. Kojima, T. Yoshikawa, M. Yoshikawa, G. Kiyohara, T.A. Yamamoto, Y. Yoshioka, N. Okada, S. Seino and S. Nakagawa. 2009. Direct cell entry of gold/iron-oxide magnetic nanoparticles in adenovirus mediated gene delivery. Biomaterials. 30: 1809–1814.

Kohler, N. and C. Sun, A. Fichtenholtz, J. Gunn, C. Fang and M. Zhang. 2006. Methotrexate-immobilized poly(ethylene glycol) magnetic nanoparticles for MR imaging and drug delivery. Small. 2: 785–792.

Li, X. and Q.R. Xie, J. Zhang, W. Xia and H. Gu. 2011. The packaging of siRNA within the mesoporous structure of silica nanoparticles. Biomaterials. 32: 9546–9556.

López-Quintela, M.A. and J. Rivas. 1993. Chemical reactions in microemulsions: a powerful method to obtain ultrafine particles. J. Colloid Interface Sci. 158: 446–451.

Lübbe, A.S. and C. Alexiou and C. Bergemann. 2001. Clinical applications of magnetic drug targeting. J. Surg. Res. 95: 200–206.

Luderer, A.A. and N.F. Borrelli, J.N. Panzarino, G.R. Mansfield, D.M. Hess, J.L. Brown, E.H. Barnett and E.W. Hahn. 1983. Glass-ceramic-mediated, magnetic-field-induced localized hyperthermia: response of a murine mammary carcinoma. Radiat. Res. 94: 190–198.

Massart, R. 1981. Preparation of aqueous magnetic liquids in alkaline and acidic media. IEEE Trans. Magn. 17: 1247–1248.

Moghimi, S.M. and A.C. Hunter and J.C. Murray. 2001. Long-circulating and target-specific nanoparticles: theory to practice. Pharmacol. Rev. 53: 283–318.

Reddy, L.H. and J.L. Arias, J. Nicolas and P. Couvreur. 2012. Magnetic nanoparticles: design and characterization, toxicity and biocompatibility, pharmaceutical and biomedical applications. Chem. Rev. 112: 5818–5878.

Rockenberger, J. and E.C. Scher and A.P. Alivisatos. 1999. A new nonhydrolytic single-precursor approach to surfactant-capped nanocrystals of transition metal oxides. J. Am. Chem. Soc. 121: 11595–11596.

Sincai, M. and D. Ganga, M. Ganga, D. Argherie and D. Bica. 2005. Antitumor effect of magnetite nanoparticles in cat mammary adenocarcinoma. J. Magn. Magn. Mater. 293: 438–441.

Singh, A. and F. Dilnawaz and S.K. Sahoo. 2011. Long circulating lectin conjugated paclitaxel loaded magnetic nanoparticles: a new theranostic avenue for leukemia therapy. PLoS One. 6: e26803.

Stolnik, S. and L. Illum and S.S. Davis. 1995. Long circulating microparticulate drug carriers. Adv. Drug Deliv. Rev. 16: 195–214.

Sun, S. and H. Zeng. 2002. Size-controlled synthesis of magnetite nanoparticles. J. Am. Chem. Soc. 124: 8204–8205.

Suzuki, M. and M. Shinkai, H. Honda and T. Kobayashi. 2003. Anticancer effect and immune induction by hyperthermia of malignant melanoma using magnetite cationic liposomes. Melanoma Res. 13: 129–135.

Tepper, T. and F. Ilievski, C.A. Ross, T.R. Zaman, R.J. Ram, S.Y. Sung and B.J.H. Stadler. 2003. Magneto-optical properties of iron oxide films. J. Appl. Phys. 93: 6948–6950.

Wada, S. and K. Tazawa, I. Furuta and H. Nagae. 2003. Antitumor effect of new local hyperthermia using dextran magnetite complex in hamster tongue carcinoma. Oral Dis. 9: 218–223.

Weissleder, R. and D.D. Stark, B.L. Engelstad, B.R. Bacon, C.C. Compton, D.L. White, P. Jacobs and J. Lewis. 1989. Superparamagnetic iron oxide: pharmacokinetics and toxicity. AJR Am. J. Roentgenol. 152: 167–173.

Widder, K.J. and A.E. Senyel and G.D. Scarpelli. 1978. Magnetic microspheres: a model system of site specific drug delivery *in vivo*. Proc. Soc. Exp. Biol. Med. 158: 141–146.

Zhu, A. and L. Yuan, W. Jin, S. Dai, Q. Wang, Z. Xue and A. Qin. 2009. Polysaccharide surface modified Fe3O4 nanoparticles for camptothecin loading and release. Acta Biomater. 5: 1489–1498.

CHAPTER 11

Nanoengineered Magnetic Field-Induced Targeted Drug Delivery System with Stimuli-Responsive Release

R. Devesh K. Misra

ABSTRACT

The primary challenge in targeted drug delivery to a tumor site is having the anticancer drug specifically targeted into and around tumors at concentrations that will decrease their growth and/or viability. In this regard, the focus here is on the design of a nanocarrier to address issues that are critical to tune the functional aspects of the drug delivery system, which is characterized by a magnetic core surrounded by a shell that serves as a drug carrier. A unique system of fabricating a temperature- and pH-responsive magnetic drug nanocarrier that combines three approaches into one practical device (tumor targeting, carrier monitoring and controlled drug release) is elucidated. The magnetic nanoparticles offer the possibility of imaging the delivery process by magnetic resonance imaging and the ability to enhance drug efficacy by heat that results from the application of an external magnetic field. This localized and targeted heat, in conjunction with localized drug release, aids in the destruction of cancer cells. Thus, the combination of both chemotherapy and heat can be used for tumor

Center for Structural and Functional Materials, University of Louisiana at Lafayette. P.O. Box 44130, Lafayette, LA 70504-4130, USA.
Email: dmisra@louisiana.edu; rdm6853@louisiana.edu

List of abbreviations after the text.

therapy. An important aspect of the magnetic nanocarrier system is the combination of pH and thermal sensitivity of the drug-containing shell with magnetic properties of the core in a single unit. The magnetic system can be envisaged as using a focused magnetic field to concentrate anticancer drugs in and around tumors, and then allowing the novel core/shell design of the nanocarrier to trigger drug release specifically in the physiochemical environment prevailing at the tumor site.

Introduction, Design Perspective and Outlook

Diseases such as cancer continue to grow with urbanization and increasing age of the population. Despite the significant advances in medical science in recent decades, the cure for cancer is restricted. Globally, more than 7 million people died of cancer in recent years and the number is expected to increase many-fold in the coming years. In majority of the situations, the malignancy of tumors is diagnosed at advanced stages when chemotherapeutic drugs are toxic to healthy cells. In the effort, to bring improvement in this condition, early detection of cancer cells and targeted drug delivery are required. A tumor-targeting drug delivery system generally combines a tumor recognition moiety with a drug-loaded vesicle. Generally, the detection systems include invasive methods, such as, tissue biopsy and diagnostics tools including Magnetic Resonance Imaging (MRI). At present, we do not have a system that exhibits combined benefits of targeted drug delivery and simultaneous imaging to control the delivery process. Thus, there is a strong need for a magnetic nanoparticulate system that can act as a potential platform combining drug delivery and easy imaging by MRI.

The focus of this chapter is to revisit the concept of the combination of pH and thermal sensitivity of the drug-containing shell with magnetic properties of the core in a single unit or into one practical device. This is based on analysis of recent research by the author (Misra 2010, 2011). The application of an External Magnetic Field (EMF) will heat the Nanoparticles (NPs) and thus the NP-containing cells. The targeted heat will facilitate killing of tumor cells, besides the chemotherapeutic effect. The envisaged system consists of monodisperse magnetite (Fe_3O_4) nanocores, chemically functionalized to enable the loading of antitumor or other drugs. These NPs when encapsulated with a dual stimuli (pH and temperature)-responsive biodegradable polymer form the core/shell nanostructure. The important characteristics of the core/shell magnetic nanocarrier include: *i*) folic acid conjugation of the outer stimuli-responsive layer to target tumor cells; *ii*) transport of magnetic drug carrier by an EMF to the tumor site and retention; and, *iii*) drug release from the collapse of the temperature-sensitive polymer in response to the heat generated by an applied magnetic field (MF) and to the change in pH from physiological values (≈ 7.4) to the endosomal

values (≈ 5.3) of tumor cells, given the pH-sensitive nature of the polymer. The unique integration of these two release mechanisms has the potential to address important concerns in tumor therapy.

It is known that metastasis of malignant cells in the physiological system is a cancer-specific complication that creates serious risks besides the effect of the original tumor. Practically, the routes that are generally adopted to target tumor cells are surgical resection, radiation and chemotherapy. Despite development of new therapeutic drugs, there is a significant effort in improving the present non-invasive methods, such as, hyperthermia and photodynamic therapy (Jordan et al. 1999).

The fundamental challenge in drug delivery is the transfer of drugs to the targeted site (Orive et al. 2003). Chemotherapeutic drugs are cytotoxic to healthy cells and there is limited control on the rate of drug release. Site-specific drug delivery has the potential to increase the effectiveness of drugs, enhance local concentration, and thus minimize undesirable side effects and toxicity to healthy cells. A viable approach to accomplish these objectives is MF-induced targeted drug delivery. It was recently demonstrated that magnetic nanocrystals coated with a biocompatible polymer and loaded with anticancer agents via linking to functional groups are viable drug vesicles (Rana et al. 2007, Zhang et al. 2007). Drug-loaded nanoparticulate carriers can be injected into the blood stream and transported to the desired site using a high gradient MF. An advantage of utilizing Magnetic Nanoparticles (MNPs) is the use of an EMF gradient to attract the particles to the desired site, and hold them at the desired location until the therapy is completed, which is subsequently accompanied by removal of the MF.

Furthermore, to achieve an effective tumor-specific drug delivery, it is important that the vesicles distinguish malignant cells from healthy cells either morphologically or physiologically. Given the rapid growth rate of cancerous cells, they have a high metabolic rate and the intracellular pH is low (Weitman et al. 1992, Antony 1996, Lu and Low 2002, Orive et al. 2003). Thus, one strategy to deliver drugs to tumor cells is to conjugate drug-loaded vesicles with nutrients required for a specific tumor, so that tumor cells will associate with the drug carrier at a significantly faster rate than healthy cells. Using this methodology, the drug carrier is designed to release its drug cargo in response to the slightly acidic endosomal pH. To enhance the specificity of tumor targeting, receptor-specific groups can be conjugated to drug carriers. The folate receptor targets are considered appropriate for tumor-selective drug delivery for a number of reasons. Folic acid is stable, poorly immunogenic, and can preferentially target tumor cells because folate receptors are overexpressed on the surface of tumor cells (Weitman et al. 1992). The receptor binds folate to nourish the rapidly dividing tumor cells (Antony 1996, Maziarz et al. 1999, Lu and Low 2002).

When the drug carrier has reached the desired site, the drug can be released directly into the blood stream via a number of mechanisms including enzymatic biodegradation, by changes in temperature or pH or by direct cell uptake of biofunctionalized NPs (Grief and Richardson 2005). Drug release in response to a specific stimulus (i.e., triggered release) is an important characteristic of effective targeted drug delivery systems. In example, drug-loaded mesoporous silica nanorods capped with superparamagnetic Iron Oxide (IO) NPs through disulfide bonds, were proposed as a probable system for transport to the specific site with an external magnet and release of drug upon reducing the disulfide bonds (Giri et al. 2005). A simpler approach was the use of magnetic hydrogel, where drug release can be tuned "on" and "off" by an external magnet (Liu et al. 2006). The author believes that the magnetic drug-targeting carrier with triggered release is a new and effective delivery system and merits strong consideration for targeted and controlled drug delivery. The unique combination of localized transport of MNPs by an EMF and tumor targeting is promising. Thus, MNPs that respond to EMF, when loaded with drug and conjugated with folate receptor groups, provide a new and realistic approach to "selective and targeted" thermal ablation therapy of tumor cells, with little effect on normal tissues.

Stimuli-responsive polymers are a unique class of polymers that respond to changes in environmental conditions, notably pH, temperature and electric field (Qiu and Park 2001, Soppimath et al. 2002). A typical representative example of stimuli-responsive home polymer is poly(*N*-isopropylacrylamide) (PNiPAAm). It is characterized by Lower Critical Solution Temperature (LCST) in aqueous solution such that its volume and shape witness changes in a reversible manner in response to small changes in temperature in the vicinity of LCST. Moreover, the enzymatic degradation of PNiPAAm can be enhanced by grafting with water soluble and biodegradable dextran. Also, PNiPAAm with a molecular weight of less than 40,000 Da can be cleared or excreted by the physiological system (Grinberg et al. 2001, Huh et al. 2001). If we combine the stimuli-responsive or "smart" behavior of a polymer with the magnetic properties of NPs and tumor-targeting characteristic of folic acid, the system would serve as an effective drug delivery system with targeted accumulation and controlled drug release. Thus, stimuli-responsive properties of a polymer can be combined with MNPs to assemble a core/shell structure with triggered drug release. For instance, a temperature-responsive polymer having LCST can be "tuned" as desired by varying the hydrophilic or hydrophobic co-monomer content. The phase transition behavior is schematically illustrated in Figs. 11.1 and 11.2. Similarly, these polymers can be made sensitive to changes in pH (de Las Heras Alarcon et al. 2005, Wu et al. 2006). Thus, it is envisaged that these "smart" polymers play an important role in drug

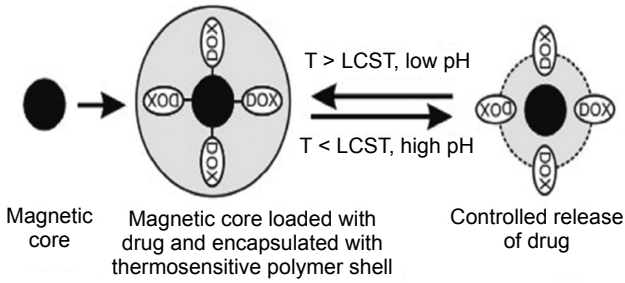

Figure 11.1. "Smart" polymer response with temperature and pH determining the release of the anticancer agent doxorubicin (DOX) from MNPs. Reprinted with permission from Misra (2011). Copyright John Wiley & Sons, Inc. (2011).

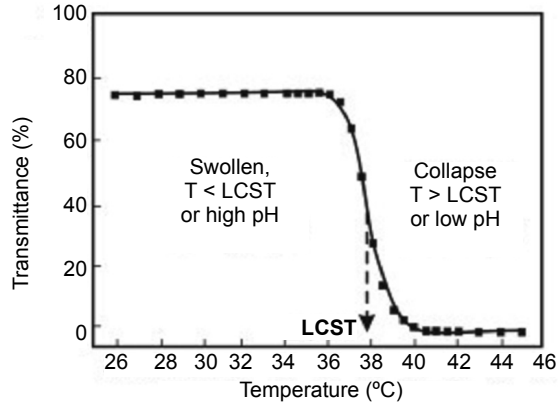

Figure 11.2. LCST of 5 wt% dextran-*g*-poly(NiPAAm-*co*-DMAAm) "smart" polymer in phosphate buffered saline (pH 7.4). Temperature and pH are expected to determine the drug release response. Reprinted with permission from Misra (2011). Copyright John Wiley & Sons, Inc. (2011).

delivery because they will not only dictate where the drug is to be delivered, but also guide when and how the drug is released.

Summarizing, the drug-loaded and polymer-coated magnetic drug carrier containing a target-specific payload is first transported to the desired site by an EMF. Upon removal of the MF, the magnetic nanocarrier detects tumor cells because of its tumor recognizing function. Then, the encapsulated drugs are released when the particles are taken up by cells because of change in pH from physiological to endosomal values. The system provides the feasibility of modulating the release rate of the drug using an oscillating sinusoidal MF, which is an external approach of accelerating drug release. During exposure to the MF, the nanocarrier will oscillate, alternately creating compressive and tensile forces. This in turn

will act as a pump providing an increased release of the drug. Furthermore, the oscillating relaxation of the particles' magnetic moments will locally heat the nanoparticulate carrier. The increase in temperature will shrink the shell and release the encapsulated drugs inside the tumor cells. In principle, both the release period and the amount of drug released can be controlled by the intensity and duration of the MF. It is expected that the carrier will stably retain the drug in the biological body until its release is induced. Also, the locally generated heat will have therapeutic effects and assist in destroying tumor cells (hyperthermia therapy).

A realistic approach in the aforementioned regard is to customize graft copolymers, consisting of a biodegradable polysaccharide and stimuli-responsive grafts, as building blocks for the new dual stimuli-responsive (pH- and temperature-sensitive) polymeric system. This is in contrast to most polymers that respond to a single stimulus. After drug release, the metabolism of IO crystals and their susceptibility to degradation will leach iron(II) (Fe^{2+}) and circulate in blood stream as micronutrient (Okon et al. 1994). It has been shown that Fe uptake decreases to 22% in a few days. Thus, the metabolic system cleans up the NPs, implying that the damage to healthy tissues is not a serious concern. Moreover, MNPs encapsulated with a "smart" polymer are suitable for site-specific transport and controlled release of drugs and represent effective drug carriers.

Magnetic Nanoparticulate Drug Carrier

Synthesis of magnetic nanocrystals

Chemical methods have been successfully developed to fabricate magnetic nanocrystals with uniform or narrow size distribution for medical (Rana et al. 2007, Zhang et al. 2007) and antimicrobial applications (Rana et al. 2005, 2006). Two important methods are a room temperature reverse micelle process (Kale et al. 2004, Misra et al. 2004, Nathani et al. 2005), and a relatively high temperature decomposition process to make NPs (Zhang et al. 2007). In the reverse micelle process, a water-in-oil microemulsion is used. These are nano-sized droplets of water sustained in a hydrocarbon bulk phase using surfactants, such as, sodium bis(2-ethylhexyl) sulfosuccinate (AOT, docusate sodium, or dioctyl sodium sulfosuccinate). Figure 11.3 is a generic flow sheet illustrating the steps in the chemical synthesis of Fe_3O_4 or ferrite (e.g., nickel ferrite) NPs done in an AOT reverse micelle system. Regarding the high temperature decomposition process, the reduction of Fe(III) salt to a Fe(II) intermediate occurs, followed by the decomposition of the intermediate at high temperature (260°C).

Transmission electron micrographs illustrating remarkably uniform-sized (average size: 3–5 nm) monodisperse NPs are presented in

Fig. 11.4. Uniform-sized NPs are an important requirement for drug delivery because it enhances the probability of uniform magnetic capture. At room temperature, these particles exhibited a superparamagnetic behavior (absence of hysteresis, immeasurable coercivity and remanence, Fig. 11.5) (Kale et al. 2004, Misra et al. 2004, Nathani et al. 2005). Superparamagnetism ensures that the NPs are not magnetic in the absence of an EMF. Additionally, superparamagnetic particles generate impressive levels of heating at low MF strength. The heat generated expressed in terms of specific absorption rate is ≈ 210 W/g at low field strength (≈ 15 kA/m). Such behavior is adequate for MNP hyperthermia, to induce the changes in temperature required for the collapse of a temperature-sensitive polymer (and triggered drug release).

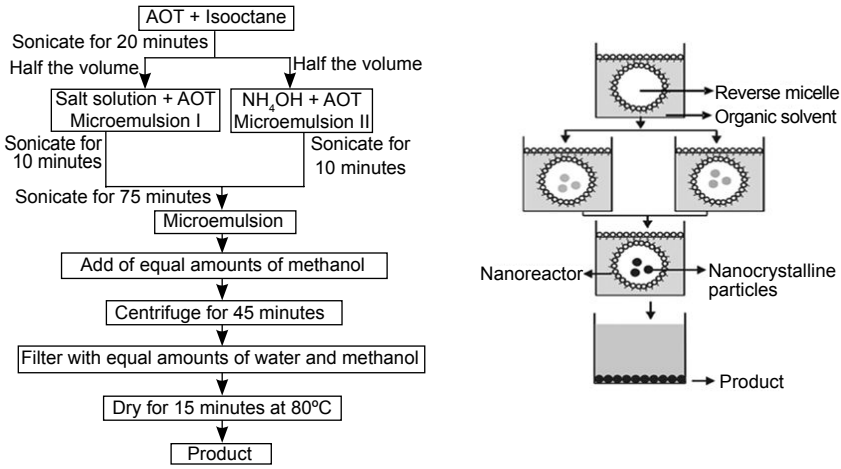

Figure 11.3. Reverse micelle process for the synthesis of MNPs. Reverse micelle is a colloidal aggregate of amphiphilic surfactant (AOT) molecules such that hydrophilic ends are in contact. It includes two (oil, and aqueous) microemulsions. The reaction takes place inside nanoreactors. Reprinted with permission from Misra (2011). Copyright John Wiley & Sons, Inc. (2011).

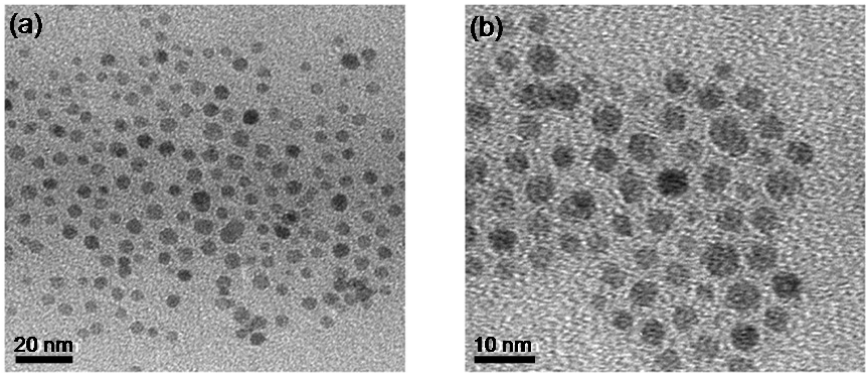

Figure 11.4. (a) Transmission electron micrograph of Fe_3O_4 NPs, and (b) detailed picture of the sample. Bar lengths: (a) 20 nm, and (b) 10 nm.

The magnetic nanocrystals were initially explored for encapsulation with poly(methylacrylic acid) (PMAA), polyvinyl alcohol (PVA) and poly(ethylene glycol) (PEG), while DOX was tethered to the ends of the polymer chains (Rana et al. 2007, Zhang et al. 2007, 2008). These synthetic polymers were considered because they degrade by hydrolytic cleavage of their backbone, thus achieving a sustained drug release (Etrych et al. 2001, Orive et al. 2003, Gupta and Wells 2004). *In vivo* studies conducted using a mouse model indicated that a temperature of 41ºC was obtained and magnetic accumulation of NPs occurred in the tumor (Fig. 11.6).

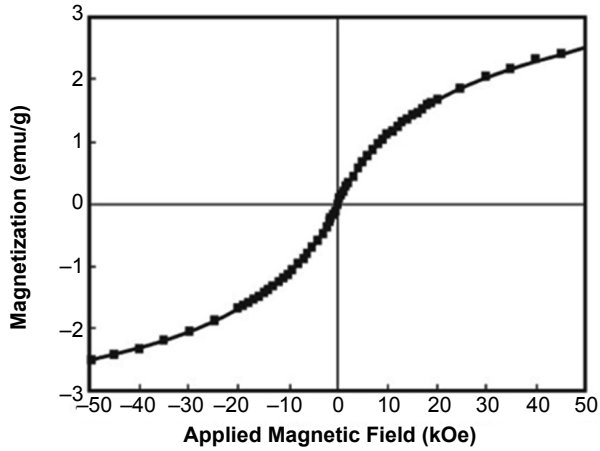

Figure 11.5. Variation of magnetization (emu/g) of superparamagnetic NPs with applied field (kOe) at room temperature.

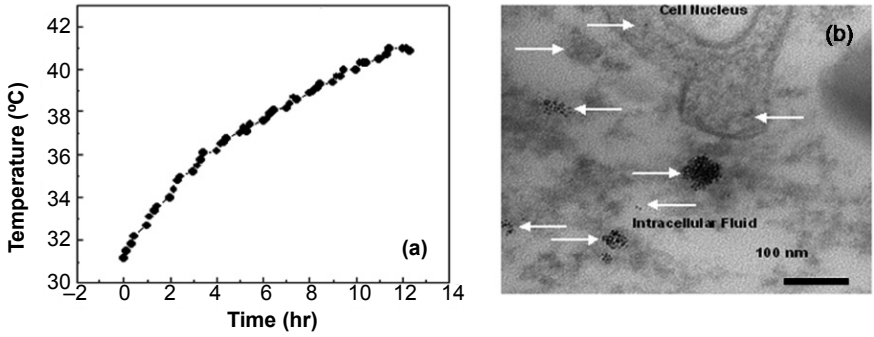

Figure 11.6. *In vivo* experiment on the administration of MNPs to tumor-bearing mice. (a) Increase in temperature (ºC) with time (hr) on injecting MNPs. (b) Transmission electron micrograph illustrating the localization of the MNPs inside the tumor tissue (white arrows). Bar length: 100 nm. A MF strength of 500 Oe and a Fe concentration of 7.5 mg/cm^3 were used in the study.

Surface functionalization of magnetite nanoparticles and conjugation with drug

The synthesized Fe_3O_4 NPs are generally hydrophobic and require surface functionalization to make them suitable for magnetic drug targeting. Bifunctional methyl 3-mercaptopropionate ($HSCH_2CH_2COOCH_3$) is one such surface functionalizing agent to chemically bond to the NP surface via Fe-S covalent bonds (Gupta and Wells 2004), which is also beneficial from the view point of the synthesis of stimuli-responsive polymers. To conjugate with the drug, the $–OCH_3$ functional group is converted to hydrazide ($–NHNH_2$) functional group by hydrazinolysis reaction, because the $–NHNH_2$ functional group facilitates subsequent conjugation with DOX. This group is more stable than the $–OCH_3$ group. Hydrazinolysis is required because the $–NHNH_2$ end groups that provide hydrazone linkage with DOX are acid-labile linkers. Hydrazones of this kind are stable at physiological pH (7.4), but the slightly acidic pH values (≈ 5–5.5) characteristic for endosomes/lysosomes of cancer cells hydrolyzes the hydrazone link, thus leading to DOX release (Willner et al. 1993, Firestone et al. 1996, Trail et al. 1997, King et al. 1999, Etrych et al. 2001, Christie and Grainger 2003). The hydrazinolysis reaction is confirmed by examining the product by Fourier transform infrared (FTIR) spectroscopy. The presence of the characteristic absorption band at 1655 cm^{-1} corresponding to a N=C bond and its intensity provides evidence of the hydrolytic cleavage of hydrazone. To accomplish the conjugation, a dispersion of hydrophobic Fe_3O_4 NPs in diphenyl ether is sonicated to form a colloidal solution. Then, $HSCH_2CH_2COOCH_3$ is added to the suspension and refluxed at ≈ 260ºC for 1 hour. Subsequently, the solution is cooled to 100ºC and hydrazine monohydrate ($N_2H_4 \cdot H_2O$) is added. The resulting NPs are then separated by centrifugation and washing with methanol, subsequently drying at ≈ 50ºC for 24 hours. This procedure functionalizes hydrophilic Fe_3O_4 NPs with $–NHNH_2$ groups (Zhang et al. 2007).

DOX is then chemically conjugated to the surface of functionalized Fe_3O_4 NPs by linking the hydrazone bond to the –C=O group of the drug (Fig. 11.7). To this aim, Fe_3O_4 NPs surface functionalized with $–NHNH_2$ are first dispersed by sonication in methanol containing a few drops of acetic acid (catalyst), thus obtaining a colloidal solution (Zhang et al. 2007). A similar approach can be used to conjugate other anticancer drugs, such as, tamoxifen and paclitaxel. The FTIR study of absorption bands associated with functional groups, such as, $–NHNH_2$ end group on Fe_3O_4 and carbonyl ($COCH_3$) group of DOX confirms the functionalization and conjugation of the drug to the NPs. The drug loading efficiency of functionalized Fe_3O_4 NPs can be quantified by fluorometric or absorbance measurements (Fig. 11.8).

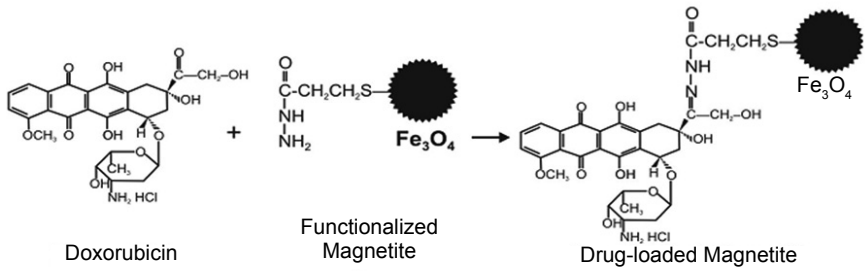

Figure 11.7. Chemical conjugation of DOX to the surface of functionalized Fe_3O_4 NPs. The reaction is carried out at room temperature for 48 hr.

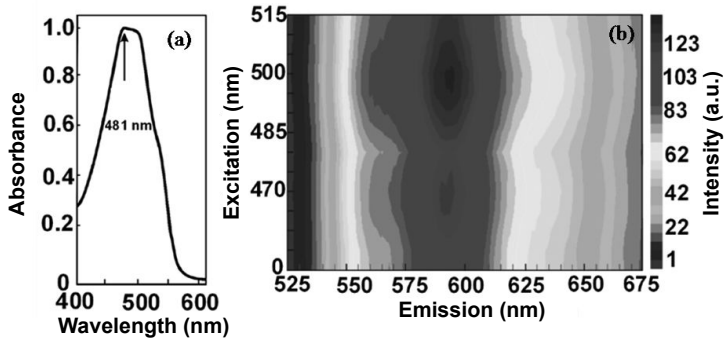

Figure 11.8. Ultraviolet-visible absorption (a) and fluorescence spectrum (b) of a DOX aqueous solution. Maximum absorption wavelength: 481 nm. The extinction coefficient of 17250 (OD/g) and the specific fluorescence (maximum excitation and emission wavelengths of 500 and 585 nm, respectively) allow the specific and sensitive detection of DOX concentrations < 5 μg/mL. Fluorescence measurements can detect < 50 ng drug. Reprinted with permission from Misra (2011). Copyright John Wiley & Sons, Inc. (2011).

Encapsulation of drug-loaded magnetic nanoparticles within a "smart" polymer

Temperature-sensitive polymer derived from *N*-isopropylacrylamide (NiPAAm) is a preferred material. The LCST of PNiPAAm can be tuned to 40–41°C to be at least 3–4°C above the physiological body temperature (37°C) by incorporating and optimizing the molecular weight of the co-monomer unit *N*,*N*-dimethylacrylamide (DMAAm). In fact, the LCST is expected to increase because of the hydrophilic contribution of DMAAm.

Furthermore, combining the biodegradable and stimuli-responsive polymer with tumor recognition of the nanocarrier for an efficient drug delivery to tumor cells is a challenging task. These requirements call for a new synthetic approach. In this line, the biodegradable natural

polysaccharide polymer dextran is appropriate. The introduction of a biodegradable lining helps the encapsulated temperature-responsive polymer to degrade under physiological conditions without harmful effect or significant changes in its hydration-dehydration. For instance, dextran-grafted poly(*N*-isopropylacrylamide-*co*-*N*,*N*-dimethylacrylamide) [dextran-*g*-poly(NiPAAm-*co*-DMAAm)] that is derived from NiPAAm and DMAAm includes the advantage of bio- and cyto-compatibility and exhibits "enzymatic degradation" upon temperature increase (Huh et al. 2001, Zhang and Misra 2007). A large decrease in viscosity occurs above LCST, because of steric hindrance of enzymatic accessibility by grafted chains (Zhang et al. 2007). Furthermore, PNiPAAm with a molecular weight of less than 40,000 Da is easily excreted. Thus, tailoring graft copolymers, consisting of a biodegradable polysaccharide and stimuli-responsive grafts as building blocks for new dual stimuli-responsive (pH- and temperature-sensitive) polymeric systems, is a necessity because most stimuli-responsive polymers are designed to respond to a single stimulus. For tumor-recognizing characteristics, folic acid conjugated dextran-*g*-poly(NiPAAm-*co*-DMAAm) is preferred to assure a targeted drug delivery. The different steps involved in the synthesis of a core/shell nanocarrier for targeted drug delivery are summarized in Fig. 11.9. An important aspect concerning the design of a drug nanocarrier is that it allows adequate binding strength to package drug and enables selective cellular internalization.

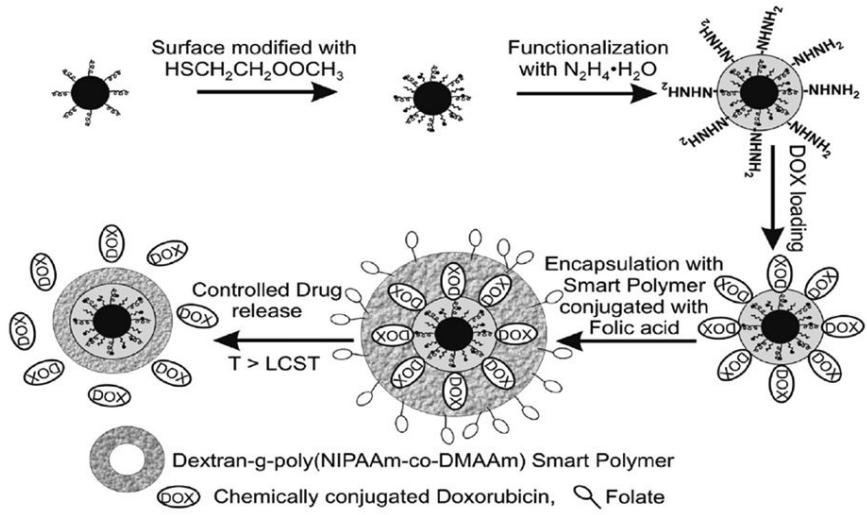

Figure 11.9. Steps involved in the synthesis of Fe_3O_4/folic acid-conjugated dextran-*g*-poly(NiPAAm-*co*-DMAAm) (core/shell) NPs for targeted DOX delivery (and controlled release). Reprinted with permission from Misra (2011). Copyright John Wiley & Sons, Inc. (2011).

Considering that dextran-*g*-poly(NiPAAm-*co*-DMAAm) is a temperature-sensitive polymer, drug release from the core/shell NPs can be easily regulated via response to temperature change in the vicinity of LCST by swelling and deswelling (Fig. 11.10). In fact, a more intensive (rapid and complete) DOX release is obtained at temperatures above 37ºC. Slightly acidic environments (pH 5.3) positively influence DOX release. Drug release during the first 10 hours corresponds to a burst release phase

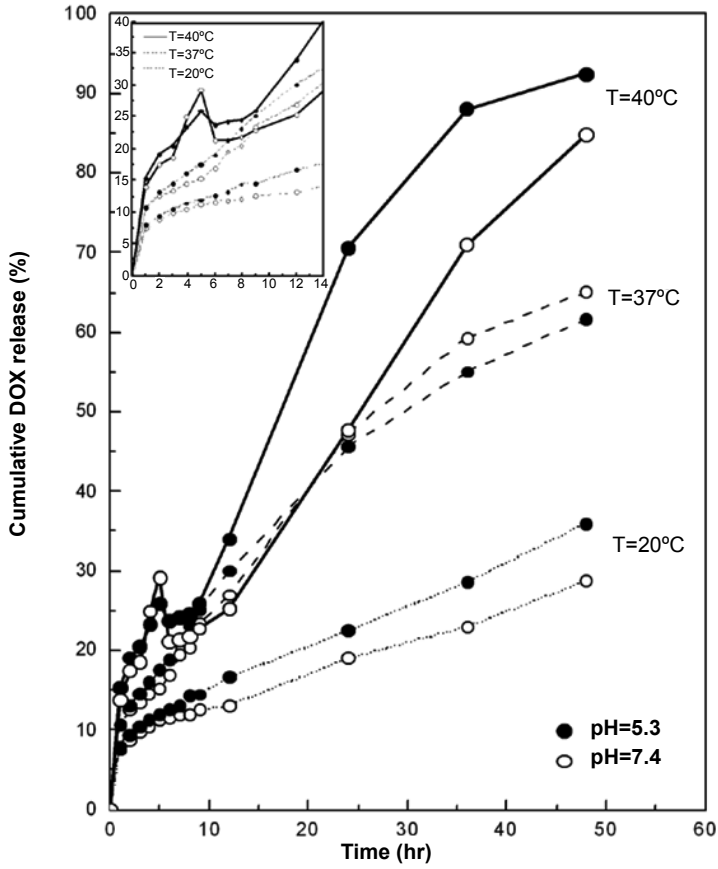

Figure 11.10. Cumulative DOX release (%) from Fe_3O_4/folic acid-conjugated dextran-*g*-poly(NiPAAm-*co*-DMAAm) (core/shell) NPs at 20, 37 and 40ºC, in phosphate buffered saline (pH 7.4) and at pH 5.3. Inset: detailed cumulative drug release (%) during the initial fast (burst) release phase. Data points are the average of at least three experiments. It can be said that the DOX release behavior from the Fe_3O_4 NPs encapsulated with the "smart" polymer is principally governed by the LCST of the "smart" polymer and by the binding affinity of the drug on the Fe_3O_4 cores, on the basis that degradation of the polymer in the absence of enzymes occurs at a very slow rate. Reprinted with permission from Zhang and Misra (2007). Copyright Elsevier (2007).

(Zhang and Misra 2007). Hence, the drug release response depends on temperature (and pH), temperature values greater than the LCST and mild acidic medium favors drug release. When the temperature is below the LCST, the drug carrier is stable and drug release is slow. However, when the temperature is greater than the LCST, the "smart" polymer shrinks or collapses such that the squeezing effect of the polymer leads to enhanced DOX release. Additionally, the acid-labile (hydrazone) linkage promotes drug release in the mild acidic medium of cancer cells as compared to the neutral medium under identical experimental conditions. The drug release behavior is further governed by factors including particle size, surface properties, degradation rate, interaction force between the drug and particle surface, and the rate of hydration and dehydration of the temperature-sensitive polymer. In addition, the drug release rate can be enhanced by using a MF. Another aspect that merits consideration is surface modification (i.e., PEGylation), which is expected to increase the circulation time for the drug nanocarrier.

An attractive alternative to dextran is chitosan (Yuan et al. 2008). Chitosan, a copolymer of *N*-acetyl glucosamine and D-glucosamine, is primarily obtained from renewable crustacean shells, such as, crab, shrimp and squid pen (Hu et al. 2013). Biological functions of chitosan depend on the acetyl content and molecular weight, in addition to other important physicochemical parameters. In a manner similar to dextran, this biodegradable polymer is a preferred alternative because chitosan-grafted PNiPAAm offers a means to improve biodegradability and the possibility to formulate pH-responsive hydrogels (Huh et al. 2001). This stimuli-response property is particularly beneficial for tumor drug targeting, where an external thermal stimuli is applied to control drug release, and the pH stimuli response occurs because of the change in pH values (from the physiological 7.4 to the acidic endosomal 5.5 in tumor cells). Some benefits of chitosan are (Ma et al. 2003, Brannon-Peppas and Blanchette 2004, Yamaura et al. 2004): *i*) it has the natural ability to bind (chelate) metal ions; *ii*) the presence of reactive amine groups provides an easier ligand attachment; *iii*) its solubility in mild acid (endosomal pH) will prevent untimely release of encapsulated drugs before the targeted site is arrived; *iv*) cationic chitosan can effectively adhere to the negatively charged phospholipid bilayer of cell membranes; and, *v*) the presence of lysozyme in cell endocytosis facilitates the biodegradation of the polymer and, thus, the release of encapsulated drugs.

Therefore, all the above outlined characteristics of chitosan are helpful in the development of stimuli-responsive targeted delivery systems, which provides high efficacy and low toxicity for treating primary and advanced metastatic tumors.

Conclusions

The magnetic nanoparticulate system described in this chapter addresses the challenge in the delivery of drugs to a tumor site at concentrations that will decrease their growth and/or viability. Some specific and important outcomes are: *i*) the structural and physicochemical aspects of the drug nanocarrier govern its potential therapeutic; *ii*) structural control [modulating the hydration-dehydration transition (LCST), and solubility in water] of temperature-responsive graft polymers allows for the design of a multistimuli polymer shell that assures controlled drug release properties; and, *iii*) the response of the nanoparticulate drug delivery nanodevice to changes in pH, temperature and MF provides an avenue for the control of drug release from tunable stimuli-responsive nanoplatforms that can respond to external and/or internal signals. Finally, the kinetic data coming from the *in vitro*/*in vivo* studies can be indicative of the factors that govern the drug release rate from these nanocarriers.

Abbreviations

AOT	:	sodium bis(2-ethylhexyl) sulfosuccinate, docusate sodium, or dioctyl sodium sulfosuccinate
$–COCH_3$	:	carbonyl
dextran-*g*-poly(NiPAAm-*co*-DMAAm)	:	dextran-grafted poly(*N*-isopropylacrylamide-*co*-*N*,*N*-dimethylacrylamide)
DMAAm	:	*N*,*N*-dimethylacrylamide
DOX	:	doxorubicin
EMF	:	external magnetic field
Fe	:	iron
Fe_3O_4	:	magnetite
FTIR	:	Fourier transform infrared
$HSCH_2CH_2COOCH_3$	:	methyl 3-mercaptopropionate
IO	:	iron oxide
LCST	:	lower critical solution temperature
MF	:	magnetic field
MNP	:	magnetic nanoparticle
MRI	:	magnetic resonance imaging
NiPAAm	:	*N*-isopropylacrylamide
$–NHNH_2$	:	hydrazide
$N_2H_4·H_2O$	:	hydrazine monohydrate
NP	:	nanoparticle
PEG	:	poly(ethylene glycol)

PMAA	:	poly(methylacrylic acid)
PNiPAAm	:	poly(*N*-isopropylacrylamide)
PVA	:	polyvinyl alcohol

References

Antony, A.C. 1996. Folate receptors. Annu. Rev. Nutr. 16: 501–521.

Brannon-Peppas, L. and J.O. Blanchette. 2004. Nanoparticle and targeted systems for cancer therapy. Adv. Drug Deliv. Rev. 56: 1649–1659.

Christie, R.J. and D.W. Grainger. 2003. Design strategies to improve soluble macromolecular delivery constructs. Adv. Drug Deliv. Rev. 55: 421–437.

de Las Heras Alarcon, C. and S. Pennadam and C. Alexander. 2005. Stimuli responsive polymers for biomedical applications. Chem. Soc. Rev. 34: 276–285.

Etrych, T. and M. Jelínková, B. Ríhová and K. Ulbrich. 2001. New HPMA copolymers containing doxorubicin bound via pH-sensitive linkage: synthesis and preliminary *in vitro* and *in vivo* biological properties. J. Control. Release. 73: 89–102.

Firestone, R.A. and D. Willner, S.J. Hofstead, H.D. King, T. Kaneko, G.R. Braslawsky, R.S. Greenfield, P.A. Trail, S.J. Lasch, A.J. Henderson, A.M. Casazza, I. Hellström and K.E. Hellström. 1996. Synthesis and antitumor activity of the immunoconjugate BR96-Dox. J. Control. Release. 39: 251–259.

Giri, S. and B.G. Trewyn, M.P. Stellmaker and V.S. Lin. 2005. Stimuli-responsive controlled-release delivery system based on mesoporous silica nanorods capped with magnetic nanoparticles. Angew. Chem. Int. Ed. Engl. 44: 5038–5044.

Grief, A.D. and G. Richardson. 2005. Mathematical modelling of magnetically targeted drug delivery. J. Magn. Magn. Mater. 293: 455–463.

Grinberg, V.Y. and N.V. Grinberg, A.I. Usov, N.P. Shusharina, A.R. Khokhlov and K.G. de Kruif. 2001. Thermodynamics of conformational ordering of iota-carrageenan in KCl solutions using high-sensitivity differential scanning calorimetry. Biomacromolecules. 2: 864–873.

Gupta, A.K. and S. Wells. 2004. Surface-modified superparamagnetic nanoparticles for drug delivery: preparation, characterization, and cytotoxicity studies. IEEE Trans. Nanobioscience. 3: 66–73.

Hu, L. and Y. Sun and Y. Wu. 2013. Advances in chitosan-based drug delivery vehicles. Nanoscale. 5: 3103–3111.

Huh, K.M. and Y. Kumashiro, T. Ooya and N. Yui. 2001. A new synthetic route for dextran graft copolymers containing thermo-responsive polymers. Polym. J. 33: 103–106.

Jordan, A. and R. Scholz, P. Wust, H. Fähling and R. Felix. 1999. Magnetic fluid hyperthermia (MFH): cancer treatment with AC magnetic field induced excitation of biocompatible superparamagnetic nanoparticles. J. Magn. Magn. Mater. 201: 413–419.

Kale, A. and S. Gubbala and R.D.K. Misra. 2004. Magnetic behavior of nanocrystalline nickel ferrite synthesized by the reverse micelle technique. J. Magn. Magn. Mater. 277: 350–358.

King, H.D. and D. Yurgaitis, D. Willner, R.A. Firestone, M.B. Yang, S.J. Lasch, K.E. Hellström and P.A. Trail. 1999. Monoclonal antibody conjugates of doxorubicin prepared with branched linkers: a novel method for increasing the potency of doxorubicin immunoconjugates. Bioconjug. Chem. 10: 279–288.

Liu, T.Y. and S.H. Hu, T.Y. Liu, D.M. Liu and S.Y. Chen. 2006. Magnetic-sensitive behavior of intelligent ferrogels for controlled release of drug. Langmuir. 22: 5974–5978.

Lu, Y. and P.S. Low. 2002. Folate-mediated delivery of macromolecular anticancer therapeutic agents. Adv. Drug Deliv. Rev. 54: 675–693.

Ma, M. and Y. Zhang, W. Yu, H.Y. Shen, H.Q. Zhang and N. Gu. 2003. Preparation and characterization of magnetite nanoparticles coated by amino silane. Colloids Surf. A Physicochem. Eng. Aspects. 212: 219–226.

Maziarz, K.M. and H.L. Monaco, F. Shen and M. Ratnam. 1999. Complete mapping of divergent amino acids responsible for differential ligand binding of folate receptors alpha and beta. J. Biol. Chem. 274: 11086–11091.

Misra, R.D.K. 2010. Core-shell magnetic nanoparticle carrier for targeted drug delivery: challenges and design. Mater. Technol. 25: 118–126.

Misra, R.D.K. Magnetic nanoparticle carrier for targeted drug delivery: perspective, outlook and design. pp. 709–724. *In*: X. Cheng [ed.]. 2011. Nanoplatform-Based Molecular Imaging. John Wiley & Sons, Inc., New Jersey, USA.

Misra, R.D.K. and S. Gubbala, A. Kale and W.F. Egelhoff, Jr. 2004. A comparison of the magnetic characteristics of nanocrystalline nickel, zinc, and manganese ferrites synthesized by reverse micelle technique. Mater. Sci. Eng. B. 111: 164–174.

Nathania, H. and S. Gubbala and R.D.K. Misra. 2005. Magnetic behavior of nanocrystalline nickel ferrite: part I. The effect of surface roughness. Mater. Sci. Eng. B. 121: 126–136.

Okon, E. and D. Pouliquen, P. Okon, Z.V. Kovaleva, T.P. Stepanova, S.G. Lavit, B.N. Kudryavtsev and P. Jallet. 1994. Biodegradation of magnetite dextran nanoparticles in the rat. A histologic and biophysical study. Lab. Invest. 71: 895–903.

Orive, G. and R.M. Hernández, A. Rodríguez Gascón, A. Domínguez-Gil and J.L. Pedraz. 2003. Drug delivery in biotechnology: present and future. Curr. Opin. Biotechnol. 14: 659–664.

Qiu, Y. and K. Park. 2001. Environment-sensitive hydrogels for drug delivery. Adv. Drug Deliv. Rev. 53: 321–339.

Rana, S. and J. Rawat and R.D. Misra. 2005. Anti-microbial active composite nanoparticles with magnetic core and photocatalytic shell: TiO2-NiFe2O4 biomaterial system. Acta Biomater. 1: 691–703.

Rana, S. and J. Rawat, M.M. Sorensson and R.D. Misra. 2006. Antimicrobial function of Nd3+-doped anatase titania-coated nickel ferrite composite nanoparticles: a biomaterial system. Acta Biomater. 2: 421–432.

Rana, S. and A. Gallo, R.S. Srivastava and R.D. Misra. 2007. On the suitability of nanocrystalline ferrites as a magnetic carrier for drug delivery: functionalization, conjugation and drug release kinetics. Acta Biomater. 3: 233–242.

Soppimath, K.S. and T.M. Aminabhavi, A.M. Dave, S.G. Kumbar and W.E. Rudzinski. 2002. Stimulus-responsive "smart" hydrogels as novel drug delivery systems. Drug Dev. Ind. Pharm. 28: 957–974.

Trail, P.A. and D. Willner, J. Knipe, A.J. Henderson, S.J. Lasch, M.E. Zoeckler, M.D. TrailSmith, T.W. Doyle, H.D. King, A.M. Casazza, G.R. Braslawsky, J. Brown, S.J. Hofstead, R.S. Greenfield, R.A. Firestone, K. Mosure, K.F. Kadow, M.B. Yang, K.E. Hellström and I. Hellström. 1997. Effect of linker variation on the stability, potency, and efficacy of carcinoma-reactive BR64-doxorubicin immunoconjugates. Cancer Res. 57: 100–105.

Weitman, S.D. and R.H. Lark, L.R. Coney, D.W. Fort, V. Frasca, V.R. Zurawski, Jr and B.A. Kamen. 1992. Distribution of the folate receptor GP38 in normal and malignant cell lines and tissues. Cancer Res. 52: 3396–3401.

Willner, D. and P.A. Trail, S.J. Hofstead, H.D. King, S.J. Lasch, G.R. Braslawsky, R.S. Greenfield, T. Kaneko and R.A. Firestone. 1993. (6-Maleimidocaproyl)hydrazone of doxorubicin—a new derivative for the preparation of immunoconjugates of doxorubicin. Bioconjug. Chem. 4: 521–527.

Wu, J. and Z.G. Su and G.H. Ma. 2006. A thermo- and pH-sensitive hydrogel composed of quaternized chitosan/glycerophosphate. Int. J. Pharm. 315: 1–11.

Yamaura, M. and R.L. Camilo, L.C. Sampaio, M.A. Macêdo, M. Nakamura and H.E. Toma. 2004. Preparation and characterization of (3-aminopropyl)triethoxysilane-coated magnetite nanoparticles. J. Magn. Magn. Mater. 279: 210–217.

Yuan, Q. and R. Venkatasubramanian, S. Hein and R.D. Misra. 2008. A stimulus-responsive magnetic nanoparticle drug carrier: magnetite encapsulated by chitosan-grafted-copolymer. Acta Biomater. 4: 1024–1037.

Zhang, J. and R.D. Misra. 2007. Magnetic drug-targeting carrier encapsulated with thermosensitive smart polymer: core-shell nanoparticle carrier and drug release response. Acta Biomater. 3: 838–850.

Zhang, J.L. and R.S. Srivastava and R.D. Misra. 2007. Core-shell magnetite nanoparticles surface encapsulated with smart stimuli-responsive polymer: synthesis, characterization, and LCST of viable drug-targeting delivery system. Langmuir. 23: 6342–6351.

Zhang, J. and S. Rana, R.S. Srivastava and R.D. Misra. 2008. On the chemical synthesis and drug delivery response of folate receptor-activated, polyethylene glycol-functionalized magnetite nanoparticles. Acta Biomater. 4: 40–48.

Color Plate Section

Chapter 4

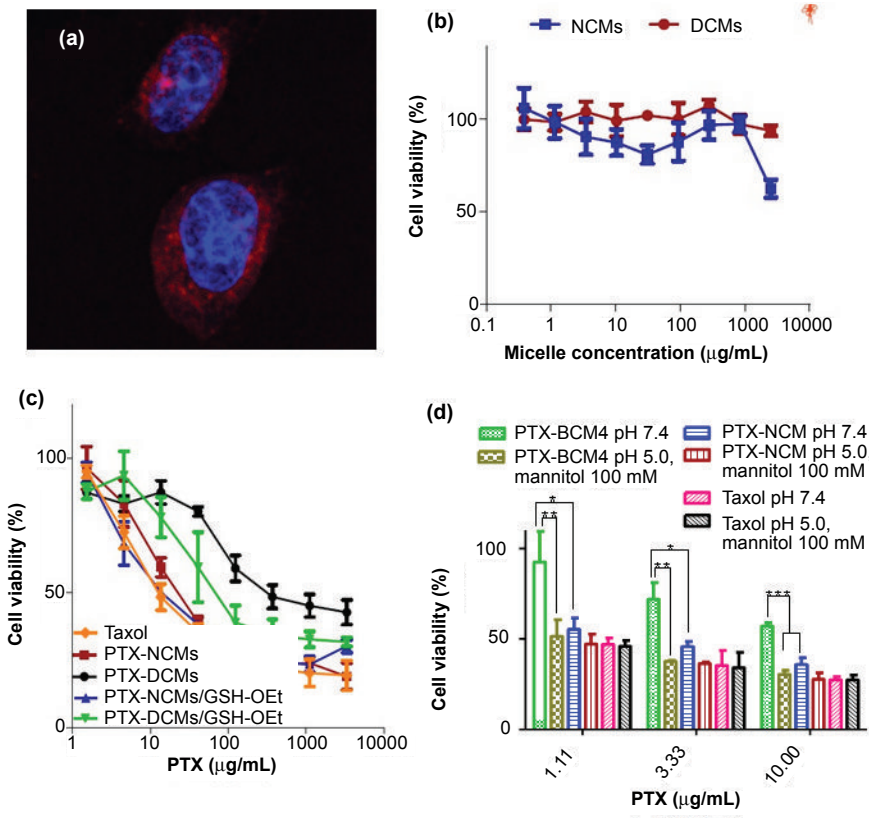

Figure 4.6. (a) Cellular uptake of DiD-labeled DCMs in SKOV-3 ovarian cancer cells after 3 hours incubation time, observed by confocal microscopy, and cell viability of SKOV-3 cells treated with, (b) different concentrations of blank NCMs and DCMs, (c) Taxol®, PTX-NCMs and PTX-DCMs with and without pre-treatment of 20 mM GSH-OEt, and (d) Taxol®, PTX-NCMs and PTX-BCM4 with or without treatment with 100 mM mannitol at pH 5.0. Adapted with permission from Li et al. (2011). Copyright Elsevier (2011).

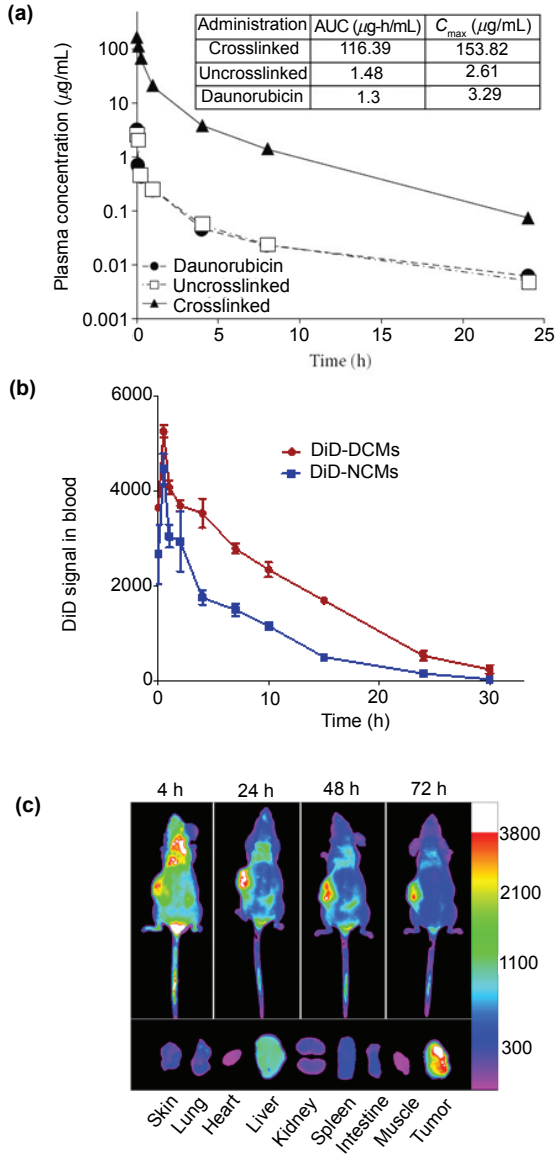

Figure 4.7. (a) Pharmacokinetics of daunorubicin-loaded micelles in Sprague-Dawley rats. The rats were given a single intravenous administration of cross-linked daunorubicin micelle, uncross-linked daunorubicin daunorubicin micelle or free daunorubicin at a 10 mg/Kg drug dose. *In vivo* pharmacokinetics (b) and biodistribution (c) of DiD-loaded DCMs and NCMs in nude mice bearing SKOV-3 ovarian cancer xenograft. Adapted with permission from Rios-Doria et al. (2012). Copyright Hindawi Publishing Corporation (2012).

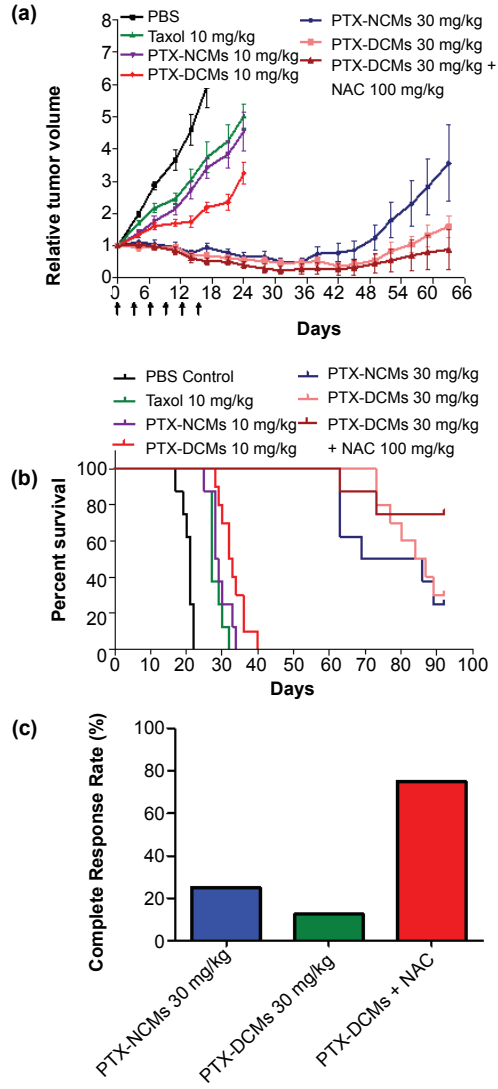

Figure 4.8. (a) *In vivo* antitumor efficacy after intravenous treatment of different PTX formulations in the subcutaneous mouse model of SKOV-3 ovarian cancer. Tumor bearing mice were administered intravenously with PBS (control) and PTX formulations (PTX-loaded NCMs: PTX-NCMs; and PTX-loaded DCMs: PTX-DCMs; equivalent dose of PTX: 10 mg/Kg) on days 0, 3, 6, 9, 12, 15 when tumor volume reached ≈ 100–200 mm^3 ($n = 8$). (b) Survival of mice in the treatment groups. (c) Complete tumor response rate (%) of mice treated with PTX-loaded NCMs, and PTX-loaded DCMs (equivalent dose of PTX: 30 mg/Kg) with or without the trigger release by NAC. Adapted with permission from Li et al. (2011). Copyright Elsevier (2011).

Chapter 5

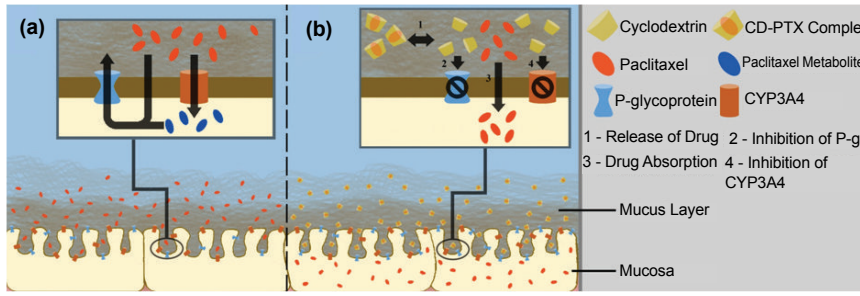

Figure 5.4. (a) Limited oral bioavailability of PTX conventional formulations due to *P*-gp efflux, and first-pass metabolism by cytochrome P_{450} 3A4 isoenzyme. (b) Mechanism by which the combination between CDs and poly(anhydride) nanoparticles would improve PTX absorption: (1) PTX release; (2 and 4) inhibition of *P*-gp and cytochrome P_{450} 3A4 by free CD, respectively; and, (3) PTX absorption.

Pharmacotherapy is often limited by the inefficient activity and severe toxicity of drug molecules. Nanotechnology offers a revolutionary and definitive approach for the efficient delivery of drug molecules to non-healthy tissues and cells. This first volume of a series of two volumes analyzes the basics in the development of drug-loaded nanoplatforms, the so-called nanomedicines. Special attention is given to physicochemical engineering, pharmacokinetics, biocompatibility and biodegradability, representative nanoplatforms (based on lipids, polymers, cyclodextrins, metals, carbon, silica, iron oxides, etc.), and advanced nano-engineering strategies for passive, ligand-mediated, and/or stimuli-sensitive drug delivery and release. The second volume will look at the applications of nanotechnology for oral, dental, topical and transdermal, pulmonary and nasal, ocular and otic, and brain drug delivery and targeting. The second volume will also cover the role of nanomedicines in the treatment of major health disorders such as, cancer, cardiovascular diseases, neurodegenerative disorders, infectious diseases, and metabolic diseases. This book will interest medical practitioners as well as researchers.

K20948

CRC Press
Taylor & Francis Group
an informa business
www.crcpress.com

6000 Broken Sound Parkway, NW
Suite 300, Boca Raton, FL 33487
711 Third Avenue
New York, NY 10017
2 Park Square, Milton Park
Abingdon, Oxon OX14 4RN, UK

9 781466 599475